Justus-Liebig-Universität Gießen
Fachbereich Veterinärmedizin

Institut für Veterinär-Physiologie und -Biochemie

„Mechanismen und Mediatoren der Kommunikationswege zwischen Immunsystem und Gehirn im Verlauf peripherer Entzündungsreaktionen“

HABILITATIONSSCHRIFT
zur Erlangung der Lehrbefähigung für das Fach Physiologie
im Fachbereich Veterinärmedizin
der Justus-Liebig-Universität Gießen

vorgelegt von

Dr. med. vet. Christoph Daniel Rummel

Gießen 2012

meinen Eltern und meiner Schwester

I. EINLEITUNG 5

1. Kommunikationswege zwischen Immunsystem und Gehirn bei systemischen Grunderkrankungen 5

1.1. Humorale Hypothese 6
1.2. Immunzell-Wanderung 7
1.3. Neuronale Hypothese 10

2. Biologische Relevanz 13

2.1. „Sensoren“ des angeborenen Immunsystems im Gehirn 13
2.2. Verständnis des Zusammenwirkens der Körperorgane mit dem ZNS bei Krankheiten 14
2.2.1. Wirkungen des Gehirns auf das Immunsystem 16
2.2.2. Wirkung des Immunsystems auf das Gehirn / im Gehirn 18
2.3. Einfluss systemischer Entzündungsreaktionen auf ZNS Erkrankungen 18

II. SCHRIFTTUM 20

1. „Sensoren“ des angeborenen Immunsystems 20

1.1. Pattern Recognition Rezeptoren (PRR) 20
1.2. Toll-like-Rezeptoren und deren Liganden 21
1.3. Zielzellen 24
1.4. Zelluläre Signalwege und therapeutisches Potenzial 24

2. Endogene Immunmediatoren - Zytokine 26

3. Transkriptionsfaktoren 28

3.1. NFκB 29
3.2. STAT3 30
3.3. NF-IL6 31

4. Zielgene 31

4.1. Zytokine 32
4.2. Prostaglandinsyntheseweg 32
4.3. Marker für Zellinvasion in das Gehirn 33
4.4. Oxidativer Stress 34

5. Krankheitssymptome 35

5.1. Fieber 36
5.2. Anorexie 38

6. Überernährung und Krankheit 39
6.1. Obesitas 40
6.2. Leptin 41

Fragestellung zur wissenschaftlichen Arbeit: 45

III. METHODEN 46

1. Tiermodelle 46
1.1. Meerschweinchen 46
1.2. Ratten 46
1.3. Mäuse 47
1.4. Stimulation der Versuchstiere; physiologische Parameter 47

2. Primäre Zellkultur 48

3. Analysemethoden des biologischen Materials 48

IV. ZUSAMMENFASSENDE DISKUSSION 49

1. Wirkung von TLR-Agonisten, IL6 und Leptin auf genomische Aktivierungen im Gehirn 49
1.1. STAT3 und NF-IL6-Aktivierung im Gehirn 49
1.1.1. TLR-Agonisten 50
1.1.1.1. STAT3 Aktivierung 50
1.1.1.2. NF-IL6 Aktivierung 52
1.1.1.3. Zeitliche Abfolge der Aktivierung von Transkriptionsfaktoren; Interaktionen 54
1.1.1.4. Hinweise für eine direkte Wirkung von TLR-Agonisten auf Zellen im Gehirn 56
1.1.2. STAT3-Aktivierung durch IL-6 57
1.1.3. STAT3-Aktivierung durch Leptin 59
1.2. Funktionen und relevante Gehirnstrukturen 60

2. Selektive Beteiligung von TLR Agonisten, IL-6 und Leptin an der Induktion des Prostaglandinsynthesewegs im Gehirn 65

3. Beteiligung von Leptin an der Kommunikation des Immunsystems mit dem Gehirn 69
3.1. Humorale Hypothese 70
3.2. Nervale Hypothese 72
3.3. Immunzell-vermittelt 73

4. TLR-Modelle, Therapiepotenzial und potentielle Nebenwirkungen 76
4.1. TLRs 76
4.2. Zytokine 80
4.3. Transkriptionsfaktoren 81

5. Thesenartige Zusammenfassung der Ergebnisse 85

6. Schlussfolgerung und Zukunftsperspektiven 86

V. VORGELEGTE VERÖFFENTLICHUNGEN 89

1. Begutachtete Veröffentlichungen 89
1.1. „Fever, sickness behavior and expression of inflammatory genes in the hypothalamus after systemic and localized subcutaneous stimulation of rats with the TLR 7 agonist imiquimod“ 89
1.2. „Fever induction by systemic stimulation with macrophage-activating lipopeptide-2 depends upon TLR2 but not CD36“ 108
1.3. „Parthenolide attenuates LPS-induced fever, circulating cytokines and markers of brain inflammation in rats“ 130
1.4. „Circulating IL-6 contributes to peripheral LPS-induced mPGES-1 expression in the rat brain“ 141
1.5. „Spatiotemporal nuclear factor interleukin 6 expression in the rat brain during LPS-induced fever is linked to sustained hypothalamic inflammatory target gene induction“ 149
1.6. „Peripheral and central cyclooxygenase (COX) products may contribute to the manifestation of brain controlled sickness responses during localized inflammation induced by macrophage-activating lipopeptide-2 (MALP-2)“ 179
1.7. „Leptin regulates neutrophil recruitment into the brain following severe systemic LPS-induced inflammation“ 185
1.8. „Molecular aspects of fever and hyperthermia“ 203
1.9. „Selective contribution of interleukin-6 and leptin to brain inflammatory signals induced by systemic LPS injection in mice“ 221
1.10. „The role of the vagus nerve in mediating the long-term anorectic effects of leptin“ 245
1.11. „STAT3 and COX-2 activation in the guinea-pig brain during fever induced by the Toll-like receptor-3 agonist polyinosinic:polycytidylic acid“ 258

1.12. „Circulating interleukin-6 induces fever through a STAT3-linked activation of COX-2 in the brain“ 272
1.13. „Fever and circulating cytokines induced by double-stranded RNA in guinea pigs: dependence on the route of administration and effects of repeated injections“ 284

2. Manuskripte in Vorbereitung 296
2.1. „AG490 potentiates LPS-induced fever while reversing LPS-induced lethargy and adipsia“ 296
2.2. „The role of IL-10 in the brain and periphery of LPS-induced septic like inflammation“ 296
2.3. “Intraperitoneal and subcutaneous injections of the TLR9 agonist ODN-1668 in rats: brain inflammatory responses are rather related to peripheral IL-6 than interferons” 296
2.4. „The inflammatory transcription factor NF-IL6 is linked to the activation of the hypothalamic-pituitary-adrenal stress axis in rats“.....296
2.5. “Age dependant effects of the PPAR-y agonist rosiglitazone on the brain and periphery during systemic LPS-induced inflammation in rats” 296

VI. ABKÜRZUNGEN 297

VII. LITERATURVERZEICHNIS 299

VIII. ANHANG 331

1. Publikationen 331
1.1. Begutachtete Veröffentlichungen: 331
1.2. Nicht begutachtete Veröffentlichungen: 333
1.3. Buchkapitel 336
1.4. Doktorarbeit 336

2. Danksagung.....337

3. Erklärung nach §6 der Habilitationsordnung.....339

I. EINLEITUNG

1. Kommunikationswege zwischen Immunsystem und Gehirn bei systemischen Grunderkrankungen

Bis noch vor etwa 30 Jahren wurde das Gehirn als vom Immunsystem isoliertes Organ im Körper angesehen (Barker and Billingham, 1977), welches über kein Lymphsystem verfügt. Seitdem und gerade in jüngster Vergangenheit sammeln bzw. verdichten sich Beobachtungen und Hinweise, die einen Zusammenhang zwischen dem Gesundheitsstatus des Körpers und des Gehirns aufzeigen. Eine ganzheitliche Vorstellung von Gesundheit des Körpers und des Geistes ist zwar nicht zuletzt seit der Zeit der alten Griechen bekannt (Sorabji, 1974), wird allerdings erst in den letzten Jahren zu einem wissenschaftlich belegten und ernst zu nehmenden Gesundheitskonzept (Kaplin and Bartner, 2005). So ist das Gehirn ein Organ mit einer selektiven und modifizierten Immunantwort, welches eben nicht vollständig vom Immunsystem isoliert ist. Beispielsweise besitzt es sehr wohl eine dem Lymphsystem ähnliche Drainage von interstitieller und zerebrospinaler Flüssigkeit, welche zum Beispiel entlang des *Bulbus Olfaktorius* bis zu 50% zu zervikalen lymphatischen Organen abgeleitet wird (Boulton *et al.*, 1999; Ransohoff *et al.*, 2003). Die Basis für das bessere Verständnis einer Interaktion bzw. Kommunikation zwischen Gehirn und dem aktivierten Immunsystem in peripheren Organen des Körpers bei Infektion und Krankheit wird mittlerweile in neuen sehr angesehenen Forschungsdisziplinen gebildet. Die Forschung in den übergreifenden Grenzdisziplinen wie der Psychoneuroimmunologie oder der Psychoneuroendokrinologie befasst sich hierbei mit bidirektionalen Eigenschaften solcher Signalwege, die vom Gleichgewicht der Körperfunktionen wie beispielsweise dem Ernährungszustand (Fantuzzi, 2009), Schlaf (Lorton *et al.*, 2006) oder Stress (Kaplin and Bartner, 2005) beeinflusst werden können. Die sehr interessante „Forschungsrichtung“ über Einflüsse des Gehirns auf das Immunsystem wird in einem kurzen Abschnitt entsprechend ihrer biologischen Relevanz in der hier vorliegenden Arbeit angesprochen. Der Fokus der hier dargelegten Forschungsarbeit liegt allerdings in der Untersuchung der unidirektionalen Signalübertragung vom Immunsystem zum Gehirn bei Infektion und Entzündung.

Bei systemischen Krankheitsgeschehen agiert das Immunsystem wie ein „Sensor“, leitet die „wahrgenommenen“ Informationen zum ZNS weiter und trägt nach zentralnervöser Verarbeitung zur Entstehung von Krankheitssymptomen wie Fieber, Anorexie und verringerter motorischer Aktivität bei (Wrona, 2006). In ihrer Gesamtheit werden diese

Symptome auch als „sickness behavior“ bezeichnet (Hart, 1988). Die Vielzahl von Analogien dieser Symptome zum Krankheitsbild der Depressionen und deren Zusammenhang zu chronischer Aktivierung des Immunsystems verdeutlichen die Bedeutung eines besseren Verständnisses der zugrundeliegenden Mechanismen und Signalwege (Dantzer and Kelley, 2007). Systemische Entzündungsreaktionen peripherer Organe beeinflussen dabei also auch die normalen Funktionen des Gehirns (Dantzer *et al.*, 2008) und können vor allem sogar bestehende Grunderkrankungen des zentralen Nervensystems verschlimmern (D'Mello et al., 2009; McColl et al., 2007; Perry et al., 2007; Riazi et al., 2008; Spencer et al., 2007b). Die molekularen Mechanismen und Signalwege, die hierbei eine Rolle spielen, sind demnach Grundlage für das Aufzeigen und Entwickeln möglicher Therapieansätze bzw. gleichzeitig Grundlage zur Prävention der sich summierenden Effekte zentraler und peripherer entzündlicher Prozesse auf das Gehirn. Nicht zuletzt sind neuropsychiatrische Erkrankungen wie Depressionen aber auch Tumor- bzw. Tumortherapie vermittelte Krankheitsbilder (Anorexie, Fieber, Lethargie…) durch immun-basierende Therapien zu behandeln und erfordern eine genaue Kenntnis der Wirkung und Nebenwirkung von Immunstimulantien, Mediatoren und Signalwegen, die auf das Gehirn wirken können (Capuron and Miller, 2011).

In Folgendem werden die verschiedenen Kommunikationswege vom peripheren Immunsystem zum Zentralnervensystem kurz dargestellt (Abbildung 1, Seite 12).

1.1. Humorale Hypothese

Der Signalweg über zirkulierende Botenstoffe und Immunzellen (humoraler Signalweg) ist am längsten bekannt und am besten erforscht (Kluger, 1991; Zeisberger, 1999). Das Prinzip dieser Kommunikation wird wie folgt beschrieben. Stimulation des angeborenen Immunsystems zum Beispiel durch Lipopolysaccharid (LPS), einem Bestandteil von gram negativen Bakterienzellwänden, führt zur Produktion endogener Immunmediatoren aus der Gruppe der Zytokine. Vor allem pro-inflammatorische Zytokine wie Interleukin (IL)-6, Tumor Nekrose Faktor (TNF)α und IL-1 wirken als humorale Botenstoffe direkt auf das Gehirn und führen zu einer genomischen und an bestimmten Strukturen auch elektrischen Aktivierung von Zellen. Die Blut-Hirn-Schranke (BBB), bestehend aus Endothelzellen mit Tight Junctions, dem perivaskulären Raum (in dem Monozyten, perivaskuläre Makrophagen und T-Lymphozyten zu finden sind) und der *Glia limitans perivascularis*, schützt in seiner Gesamtheit das Gehirn vor dem unkontrollierten Kontakt mit lipophoben Makromolekülen wie den Zytokinen aber auch Immunzellen (Bechmann *et al.*, 2007). Die vom Immunsystem in der Peripherie gebildeten humoralen Botenstoffe aber auch exogene Pathogen Assoziierte

Molekülstrukturen (PAMPS) gelangen über das Blut zum Gehirn und üben ihre Wirkung wahrscheinlich über mehrere Mechanismen gemeinsam aus:

1) Über die so genannten Zirkumventrikulären Organe, Gehirn-Strukturen mit einer unvollständigen BBB, ist eine direkte Detektion solcher Botenstoffe aus dem Blut möglich (Roth et al., 2004a).

2) Die zu vermittelnde Information erhält indirekten Zugang zum Gehirnparenchym durch Stimulation von Anteilen der BBB [Endothelzellen (Matsumura and Kobayashi, 2004) und perivaskuläre Makrophagen (Schiltz and Sawchenko, 2003)] zur Produktion einer zweiten Welle von in diesem Fall lipophilen Mediatoren wie Prostaglandinen oder Stickstoffmonoxid (NO). Die lipophilen Botenstoffe wiederum dringen ungehindert über kurze Distanzen in das Gehirngewebe ein und aktivieren dort Gliazellen und Neurone. Dies ist gefolgt von einer dritten Welle an abgegebenen Mediatoren bzw. Signalweiterleitungen, durch die die Information auch in die entsprechend weiter entfernten Gehirnstrukturen gelangen kann.

3) Außerdem ist für manche Zytokine ein limitierter Transport durch die BBB in das Gehirn beschrieben worden (Banks *et al.*, 2002). Es ist allerdings nicht davon auszugehen, dass in den meisten Fällen solch ein Transport ausreichende Mengen aller Mediatoren in das Gehirnkompartiment zu überführen vermag.

Zytokine und PAMPs wie LPS vermitteln Ihre Hauptwirkung über Rezeptor-vermittelte genomische Aktivierung von Zellen. Pro-inflammatorische Transkriptionsfaktoren wie Nuklear Faktor (NF)κB (Nadjar *et al.*, 2003) aktiviert durch IL-1β, TNFα und LPS und Signal Transducer und Aktivator von Transkription (STAT)3 unter anderem stimuliert durch IL-6 aber auch IL-10 (Gautron et al., 2002; Hübschle et al., 2001a) regulieren die *de novo* Expression inflammatorischer Gene, die schließlich zur Vermittlung und Verarbeitung der Information im Gehirn beitragen. Das genaue zeitliche Zusammenspiel der einzelnen Zytokine und Transkriptionsfaktoren und deren Bedeutung für die Expression verschiedener inflammatorischer Mediatoren sind allerdings weitgehend unklar. Zumindest wird dem Zytokin IL-1β und dem Transkriptionsfaktor NFκB eine Schlüsselrolle bei der Expression von zentralen Mediatoren und bei der Vermittlung von Krankheitssymptomen zugewiesen (Kozak et al., 2006; Nadjar et al., 2005b).

1.2. Immunzell-Wanderung

Die Vorstellung des Gehirns als ein immunprivilegiertes Organ rührt nicht zuletzt von Beobachtungen Mitte des letzten Jahrhunderts her, dass Implantationen von Fremdgewebe im Gehirn zu keinerlei Abstoßungsreaktionen geführt haben (Medawar, 1948). Perry und Gordon

charakterisierten in mehreren Studien die für das Zentralnervensystem lediglich limitierte und verzögerte Einwanderung von Immunzellen. Sie und Kollegen zeigten, dass neutrophile Granulozyten (NG) und Makrophagen nur in geringem Maße in das Gehirn bei Entzündungsreaktionen einwandern (Andersson et al., 1992a; b; Anthony et al., 1997). Diese Vorgänge entsprechen nicht annähernd der dramatischen Invasion von Immunzellen in peripheren Organen vor allem bei dem Schweregrad vergleichbaren Entzündungsprozessen. Neutrophile und Makrophagen werden dabei außerdem etwas verzögert zum Gehirn rekrutiert und binden an Endothelzellen (Bohatschek et al., 2001), ohne jedoch maßgeblich in das Parenchym einzuwandern. Die potentielle Einwanderung von Immunzellen in das Gehirn bei Entzündungsreaktionen ist außerdem altersabhängig; bei adulten Ratten war die Rekrutierung von NG im Vergleich zu jungen Ratten drastisch verringert (Lawson and Perry, 1995). So wurde lange Zeit angenommen, dass lediglich Stabverletzungen oder autoimmune Erkrankungen wie Multipler Sklerose (MS) mit einer signifikanten Einwanderung von Immunzellen in das Gehirngewebe einhergehen. In solchen Fällen wird nämlich die Blut-Hirn-Schranke (BBB) durchlässig, welche lange als eine für Immunzellen unüberwindliche Barriere angesehen wurde (Barker and Billingham, 1977). Es bleibt allerdings zu bemerken, dass Immunzellwanderungen nicht zwingend mit einer erhöhten BBB Durchlässigkeit korrelieren (Muller et al., 2005) und sogar transzellulär stattfinden und damit nicht direkt von einer veränderten Dichtigkeit von Tight Junctions der BBB abhängen (Engelhardt and Wolburg, 2004; Wolburg et al., 2005).

Kürzlich wurde von Rivest und Kollegen postuliert, dass zirkulierende Monozyten, also periphere Immunzellen aus dem Knochenmark, einen permanenten Ersatz und Austausch von Mikroglia im ZNS ermöglichen und damit das Gesamtverständnis des Zusammenwirkens von Immunsystem und Gehirn quasi revolutionär verändert wurde (Simard and Rivest, 2006). Dennoch scheinen neuere Ergebnisse eher darauf hinzuweisen, dass das gesunde Gehirn Erneuerungen von Mikroglia eher aus Gehirn intrinsischen Vorläuferzellen zu beziehen scheint und die Methode einer Bestrahlung bei den Versuchen von Rivest und Kollegen die BBB für Makrophagen durchlässig gemacht hatten (Lucin and Wyss-Coray, 2009). Alternativ zu einer Bestrahlung von Tieren und Transplantation von fluoreszenz-markierten Makrophagen konnte durch Parabiose (einer Technik, die einen Austausch über Gefäße zwischen zwei Tieren ermöglicht) ein Eindringen von markierten Makrophagen aus der Zirkulation in das Gehirn nicht beobachtet werden (Ajami et al., 2007). Trotzdem sind die Ergebnisse von Rivest und Kollegen interessant für Fälle von eingeschränkter BBB Funktion während Gehirnerkrankungen (Mildner *et al.*, 2007). Gerade neue Erkenntnisse über ein

Patrouillieren von T-Lymphozyten durch das gesunde oder kranke Gehirn als Bestandteil normaler physiologischer Prozesse (Engelhardt, 2006; Lucin and Wyss-Coray, 2009) haben das Konzept der Immunzellen vermittelten reziproken Kommunikation des Immunsystems mit dem Gehirn neuerdings zu einem zentralen Forschungsthema gemacht. So exprimieren verschiedene Gehirnzellen MHC1-Moleküle und sind sehr wohl in der Lage mit Lymphozyten zu kommunizieren (McAllister and van de Water, 2009). Außerdem konnte in zwei Studien gezeigt werden, dass nicht nur bei zentralen das Gehirn direkt betreffenden sondern auch bei peripheren Entzündungen von Organen wie der Leber, Monozyten in das Gehirn rekrutiert werden können (D'Mello et al., 2009; Kerfoot et al., 2006); ein wichtiger Hinweis auf die Bedeutung dieses zellulär getragenen Signalweges, auch wenn dies in weiteren Studien zu bestätigen ist und genauere Mechanismen zu untersuchen bleiben.

Den Mechanismus einer direkten Wirkung von Immunzellen auf das Gehirn kann man sich wie folgt vorstellen: Immunzellen aus der Peripherie wandern in das Gehirn und führen über gebundene oder von Immunzellen lokal (parakrin) gebildete Faktoren zu einer Modulation bestimmter Gehirnfunktionen (Capuron and Miller, 2011; Zeisberger, 1999). Entsprechend konnte gezeigt werden, dass solche Immunzellen pro-inflammatorische Eigenschaften haben und zum Beispiel das Zytokin IL-1β sowie die induzierbare NO-Synthase bilden (Proescholdt *et al.*, 2002) und damit zur Verschlimmerung ischämischer Hirnschädigungen beitragen. Folgerichtig führt die Hemmung der Invasion von NG zu neuroprotektiven Effekten (Jiang et al., 1995; Matsuo et al., 1994). Bei verschiedenen Krankheitsbildern wie Meningitis (Kim, 2003) oder viraler Enzephalitis (Andrews *et al.*, 1999) kommt es zu vermehrtem Einwandern von NG, was mit gravierenden Nebeneffekten auf den Gesundheitszustand in Zusammenhang gebracht wird. Aktivierte NG führen nämlich nicht nur zum Abtöten von potenziell gefährlichen Mikroorganismen, sondern auch zu Gewebeschäden (Lawson and Perry, 1995). Die Kontrolle der Einwanderung solcher Immunzellen stellt also ein mögliches Verfahren dar, solche Wirkungen des Immunsystems im Gehirn zu minimieren. Trotzdem sind NG natürlich wichtige Entzündungszellen und es bedarf einer kritischen Menge an NG, um erfolgreich Bakterien abtöten zu können (Li et al., 2002b). Über die Beteiligung dieses zellvermittelten Signalweges an der Entstehung zentralnervös kontrollierter Krankheitssymptome ist bisher noch sehr wenig bekannt und es bedarf weiterer Untersuchungen, zumal einwandernde Immunzellen höchst wahrscheinlich durch Aktivierung von Zytokin-Signalkaskaden bei verschiedenen Krankheitsbildern des ZNS wie Multipler Sklerose eine entscheidende Rolle spielen (Dantzer *et al.*, 2008).

1.3. Neuronale Hypothese

Neben den vom Blut getragenen Signalwegen, welche prinzipiell auf *de novo* Synthese von Mediatoren wie den Zytokinen in der Peripherie oder durch in das Gehirn einwandernde Immunzellen beruhen, wurde erkannt, dass es einen weiteren, schnelleren Kommunikationsweg geben müsse. Dieser konnte als so genannter neuronaler Signalweg identifizieren werden (Dantzer *et al.*, 2000). Die Hypothese dieses Signalweges rührt von Beobachtungen her, dass Vagotomie zu reduziertem Schmerz (Watkins et al., 1994a; Watkins et al., 1994b) oder Fieber führt (Sehic and Blatteis, 1996) wenn LPS oder Zytokine intraperitoneal appliziert worden waren. In weiteren Studien konnte eine Vermittlung einer Vielzahl anderer Symptome wie soziales Verhalten (Bluthé *et al.*, 1996; Luheshi *et al.*, 2000) oder Hypothalamus-Hypophysen-Nebennierenrinden (HPA)-Achsenaktivität (Gaykema *et al.*, 1995) durch Affarenzen des *Nervus vagus* gezeigt werden (Quan, 2008; Romanovsky, 2004). In Modellen lokaler, peripherer Inflammation wurde außerdem zu frühen Zeitpunkten bereits eine Induktion von Krankheitssymptomen und HPA-Achsenaktivierung beschrieben, obwohl noch keine humorale Mediatoren in der Zirkulation messbar waren (Campisi *et al.*, 2003) bzw. ohne eine Aktivierung von IL-1- und Zyklooxygenase 2 (COX2)-Expression im Gehirn (Zhang *et al.*, 2008), die typischer Weise über humorale Botenstoffe im Gehirn bei systemischen Entzündungsreaktionen exprimiert werden und maßgeblich an der Vermittlung der Krankheitssymptome beteiligt sind (Conti *et al.*, 2004).

Es gibt allerdings auch Hinweise, dass die Rolle des *N. Vagus* zum Beispiel für Fieber von begrenzter Bedeutung ist. Lediglich für mittel- bis geringgradige periphere Entzündungsreaktionen nach Stimulation mit niedrigen Dosierungen an LPS oder IL-1 konnte die Beteiligung des nervalen Signalweges an der Fieberentstehung belegt werden (Goldbach *et al.*, 1997; Rummel *et al.*, 2005a). Zur Erklärung wurde angenommen, dass bei zu großem Ausmaß einer humoralen Beteiligung von Mediatoren im Blut, neuronale Einflüsse überdeckt werden und deshalb nicht mehr nachweisbar sind. Auch die Bedeutung von vagalen Affarenzen bei der Vermittlung von Anorexie während Infektionen und Entzündungsreaktionen ist teilweise umstritten und bleibt im Weiteren noch näher zu untersuchen (Schwartz, 2002).

Funktionell kann man sich den neuronalen Signalweg folgendermaßen vorstellen: Als Sensor über den Aktivierungszustand des Immunsystems in den verschiedenen Kompartimenten des Körpers, führen lokale Entzündungsreaktionen vermittelt über die Produktion der inflammatorischen Mediatoren von zum Beispiel Zytokinen und

Prostaglandinen zu einer Stimulation der Nervenendigungen bzw. Zellen in der Nähe der Nervenendigungen, die Rezeptoren für die entsprechenden Faktoren besitzen und damit die Aktivität solcher Neurone beeinflussen (Ross et al., 2000; Roth and De Souza, 2001; Rummel et al., 2005a). Die Information wird dann über den *Nucleus tractus solitarius* als Eintrittsstelle des Vagus in den Hirnstamm über Konnektivitäten zu den autonomen Zentren des Hypothalamus wie den *Nucleus paraventricularis* (PVN) weiter geleitet. Mittels Untersuchungen von FOS-IR, einem relativ spezifischen Marker für neuronale Aktivierung, konnten solche Signalwege näher beschrieben werden (Dantzer *et al.*, 2000; Konsman *et al.*, 2000; Marvel *et al.*, 2004).

Zusätzlich zu solch einem vagalen Signalweg, gibt es weitere Studien, die eine Beteiligung von sensiblen afferenten Hautnerven an der Signalweiterleitung von peripheren Organen zum Gehirn belegen (Ross et al., 2000; Roth and De Souza, 2001; Rummel et al., 2005a). Eine kürzlich veröffentliche Studie konnte sogar zeigen, dass ein Monitoring peripherer Entzündungsreaktionen in lokalitätsspezifischer Art und Weise in bestimmten Gehirnregionen von statten geht (Belevych *et al.*, 2010). Eine lokale aseptische Entzündungsreaktion induziert durch Gabe des Milcheiweißes Kasein führte entsprechend im PVN zu FOS-Aktivierung in ähnlich lokalisierten Anteilen. Je nachdem ob die Entzündung das rechte oder linke, hintere oder vordere Bein betraf, war mehr der rechte, linke, vordere oder hintere Bereich dieser Gehirnstruktur aktiviert. Analog zum somatotopen Homunkulus der Großhirnrinde scheint es also eine zwar eingeschränkte aber dennoch spezifische Projektion der Information kodiert nach ihrem Grad und der Lokalisation ebenfalls im Hypothalamus zu geben. Dadurch könnte das Gehirn auf unterschiedlich lokalisierte Stimuli aus der Peripherie differenziert reagieren. Wenn also an einer Hand eine frische Wunde und am Bein eine abheilende Wunde zu beklagen wäre, könnte man annehmen, dass diese Information nach Schweregrad und Lokalisation abgestuft nicht nur im somatosensibles Kortex des *Gyrus postcentralis* abgebildet wird, sondern auch in Strukturen des Hypothalamus wie dem PVN. Entsprechend bleibt zu beweisen, ob solch ein Prozess auch von einer abgestuften Beeinflussung efferenter Anteile des vegetativen Nervensystems gefolgt ist, die wiederum die Heilung der Hand und des Fußes bzw. die lokale Immunantwort modulieren könnte. Ein immunologischer Homunkulus im Gehirn, der somatotopisch organisiert spezifische Immunfunktionen steuert, wurde zumindest bereits postuliert (Tracey, 2007).

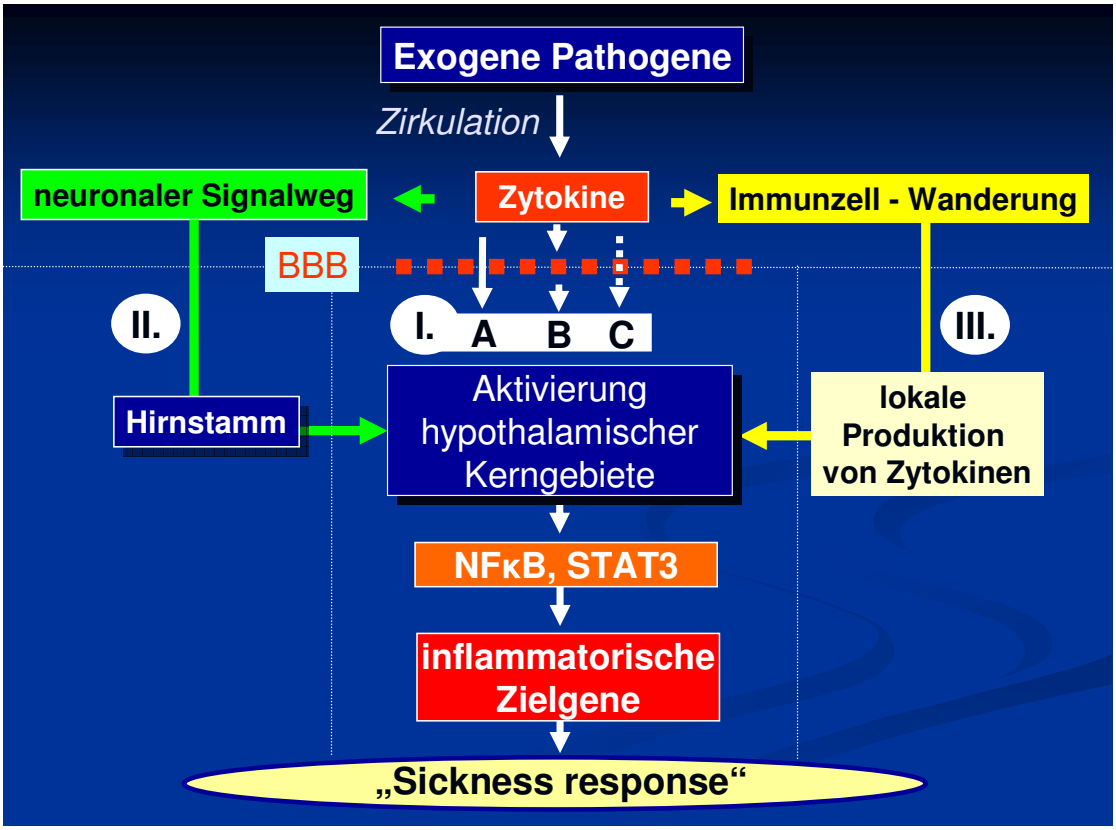


Abbildung 1

Schematische Darstellung der möglichen Signalwege vom Immunsystem zum Gehirn während systemischer Entzündungsreaktionen. In den Körper eindringende exogene Pathogene stimulieren die Bildung von endogenen Mediatoren, den so genannten Zytokinen, welche zusammen über drei Hauptsignalwege zu zentralnervös kontrollierten Krankheitssymptomen wie reduzierter Nahrungsaufnahme (Anorexie) oder erhöhter Körpertemperatur (Fieber) („sickness response“) führen: (I) Einem humoralen Signalweg bei dem Zytokine und Pathogen assoziierte Molekülstrukturen (PAMPS) (A) im Bereich von Gehirnstrukturen mit einer unvollständigen Blut-Hirn-Schranke (BBB) den so genannten Zirkumventrikulären Organen direkten Kontakt zu Gehirngewebe erlangen, (B) Endothelzellen zur Produktion von sekundären lipophilen Mediatoren stimulieren, welche durch die BBB zum Gehirnparenchym gelangen oder (C) über Transportprozesse durch die BBB ins Gehirn eindringen. (II) Darüber hinaus vermittelt eine neuronale Aktivierung durch PAMPS und Zytokine and andere Mediatoren (kutane Hautnerven, Nervus Vagus) inflammatorische Informationen von der Peripherie zum Gehirn. (III) Zusätzlich tragen in das Gehirn einwandernde Immunzellen über lokale Produktion vom Zytokinen als dritter Signalweg zur Informationsübertragung von der Peripherie zum Gehirn bei. Zytokine und PAMPS führen damit schließlich zu einer genomischen Aktivierung von Zellen hypothalamischer und extrahypothalamischer Gehirnstrukturen. Über den „signal transducer and activator of transcription“ (STAT3)- und dem Nuklear Faktor (NF)κB-Signalweg regulieren sie hierdurch die Expression spezifischer Zielgene, welche wiederum zur Entstehung der genannten Krankheitssymptome beitragen.

2. Biologische Relevanz

Untersuchungen am Modell von zentralnervös kontrollierten Krankheitssymptomen ermöglichen die Ermittlung mehrerer Zielparameter mit entsprechender Relevanz für ein besseres Verständnis der ablaufenden Prozesse bei Tier und Mensch bei der Kommunikation zwischen Immunsystem und Gehirn. Darüber hinaus können Mechanismen aufgeklärt und mögliche Zusammenhänge und Therapieansätze bei krankhaften Prozessen im Gehirn und des Gesamtorganismus ermittelt werden. Hierbei stellen sich folgende Fragen, deren Bedeutung und Hintergrund hier kurz dargestellt werden sollen.

- Wie erkennt das Gehirn, die Gefahren bei Infektion und Inflammation bzw. welche Sensoren finden sich im Gehirn, die solche Zustände detektieren können?
- Wie und wodurch wirkt das Gehirn auf die peripheren Organe bei solchen „Gefahrensituationen“ ein?
- Welche Funktionen hat das Immunsystem im Gehirn?
- Welche Folgen haben systemische Entzündungsreaktionen und ein aktiviertes Immunsystem für das Gehirn?

2.1. „Sensoren“ des angeborenen Immunsystems im Gehirn

Wie in vielen Studien von Rivest und Kollegen gezeigt, reagiert das Gehirn ausgesprochen sensibel auf akute Stimulation des angeborenen Immunsystems (Rivest, 2003; 2009). So finden sich eine Reihe von Rezeptoren, die so genannte PAMPs viralen oder bakteriellen Ursprungs erkennen können unter anderem auf Endothelzellen der BBB, perivaskulären Makrophagen sowie Mikrogliazellen. Über Kartierungen der Aktivierung und induzierten Expression dieser Rezeptoren und Mediatoren konnten einige wichtige Gehirnstrukturen näher definiert werden, welche besonders sensible auf exogene und endogene Stimulantien angeborener Immunität reagieren. Hierunter fallen die Zirkumventrikulären Organe (CVOs) sowie das Endothel selbst (Laflamme and Rivest, 1999; Lebel et al., 2000; Nadeau and Rivest, 1999; Rivest, 1999; Rummel et al., 2005b; Vallières and Rivest, 1997). Wir (Rummel *et al.*, 2005b) und andere (Konsman *et al.*, 2004) konnten dabei zeigen, dass die Reaktion von Endothelzellen nicht alle Gehirngefäßtypen betrifft, diese aber über das ganze Gehirn verteilt relativ gleichmäßig bei systemischer Entzündungsreaktion aktiviert werden. Trotz dieser umfangreichen Reaktion scheinen lediglich für Homeostase wichtige Gehirnstrukturen über die relevanten Rezeptoren für in der BBB gebildete sekundäre Mediatoren (z.B.

Prostaglandine) zu verfügen und damit die Information aufzunehmen und in neuronale Aktivierungsmuster umzusetzen. So ist der *Nucleus medianus praeopticus* (MnPO) eine zentrale Schalt-Struktur vieler homeostatischer Prozesse wie der Temperaturregulation und weist eine hohe Dichte an PG-Rezeptoren auf (Lazarus *et al.*, 2007). Über welche Mechanismen und mit welcher Funktion eine Aktivierung von Zellen der BBB das gesamte Gehirn beeinflusst und welche Bedeutung sie hat, bleibt noch zu untersuchen. Unter bestimmten Bedingungen ist aber davon auszugehen, dass solch potente Signalträger wie PGE2 in einer Reihe von Gehirnregionen regulatorisch wirken werden bzw. die Rezeptorexpression sicher eine gewisse Plastizität aufweist und sich dem Milieu anpassend ändern kann. Interessanter Weise scheinen perivaskuläre Makrophagen neben dem pro-inflammatorischen PGE2 sogar entzündungshemmende Faktoren freizusetzen, die eine ungehinderte Weiterleitung inflammatorischer Signale aus Endothelzellen begrenzen (Serrats *et al.*, 2010).

Insgesamt ermöglichen mikroneuroanatomische Untersuchungen in Kombination mit der Aufzeichnung von physiologischen Parametern nach Stimulation des angeborenen Immunsystems Aufschlüsse über beteiligte Mechanismen und Gehirnstrukturen. Die Stimulation mit verschiedenen PAMPs ist außerdem wichtig, um die differentielle Antwort des angeborenen Immunsystems im Gehirn bei verschiedenen Krankheitsprozessen besser zu verstehen. Möglicherweise sind protektive Funktionen solcher Reaktionen durch Gabe spezifischer synthetischer PAMPs für die Behandlung von Krankheiten nutzbar (Kong and Le, 2011). Ob eine Aktivierung des angeborenen Immunsystems positive oder negative Effekte auf das Gehirn hat, bleibt jeweils für den einzelnen Fall zu untersuchen und kann nicht generalisiert werden (Rivest, 2009).

2.2. Verständnis des Zusammenwirkens der Körperorgane mit dem ZNS bei Krankheiten

Die bidirektionale Kommunikation des Gehirns mit dem Immunsystem liegt in einer Balance, die über die bereits angesprochenen Signalwege vermittelt wird (Abbildung 2). Bei Krankheiten wird die Bedeutung einzelner Komponenten besonders deutlich, vor allem wenn einzelne Signalwege ausfallen und inflammatorische Prozesse außer Kontrolle des Immunsystems und des Gehirns geraten und folglich unbegrenzt zu chronischen Auswirkungen führen. Gerade das sich neu entwickelnde Verständnis, dass das vegetative Nervensystem nicht nur unter zentraler Kontrolle des Gehirns steht sondern auch in begrenztem Umfang bewusst trainiert bzw. gesteuert werden kann, bietet neue

„unkonventionelle“ therapiebegleitende Methoden wie Biofeedback oder Psychologische Betreuung, die maßgeblich zu einer verbesserten medizinischen Versorgung von Menschen beitragen kann.

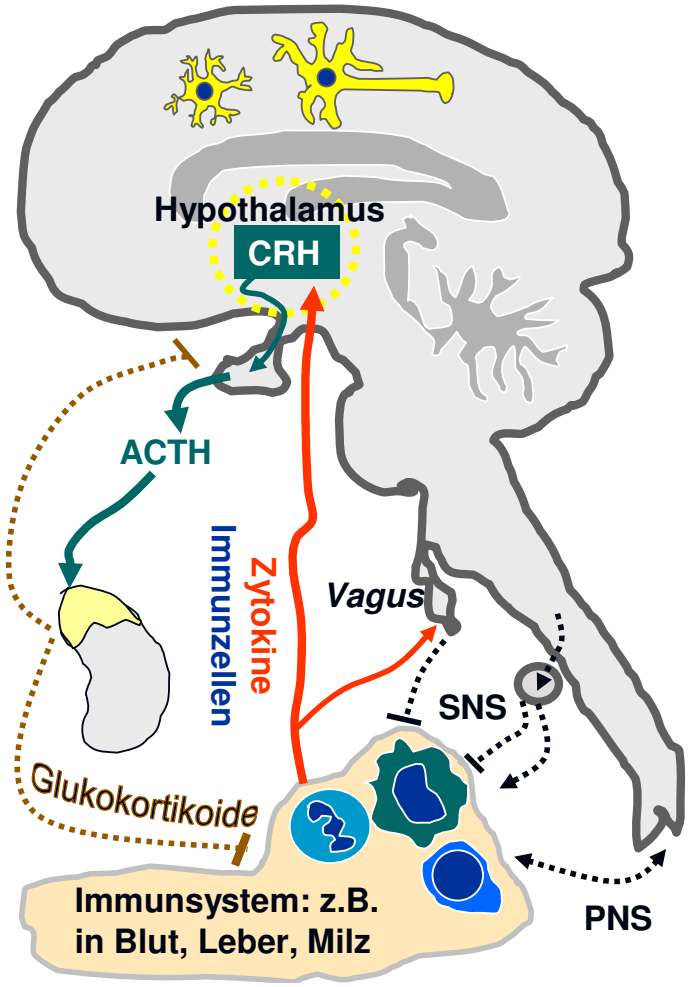


Abbildung 2

Die bidirektionale Kommunikation zwischen Immunsystem und Gehirn. Neben den drei Hauptwegen der Wirkung des aktivierten Immunsystems über Zytokine, Immunzellen dem Vagus und sensorischen Afferenzen auf das Gehirn kontrolliert wiederum das Gehirn über mehrere Wege die Aktivität des Immunsystems in seinen verschiedenen Kompartimenten in der Peripherie (z.B. Blut, Milz, Leber). Darunter fällt zunächst die Hypothalamus – Hypophysen - Nebennierenrinden – (HPA)Achse. Im *Nucleus paraventricularis* (PVN) wird Corticotropin Releasing Hormon (CRH) durch inflammatorische (z.B. Zytokine) oder psychologische Stressoren zur Freisetzung stimuliert und führt über den portalen Hypophysenkreislauf zur Freisetzung von andrenocorticotropem Hormon (ACTH) aus dem Hypophysenvorderlappen, welches schließlich aus der Nebennierenrinde Glukokortikoide (Cortisol bei Mensch, Corticosteron bei Ratte und Maus) in die Zirkulation absondern lässt. Glukokortikoide wirken vorwiegend immunsuppressiv. Das periphere Nervensystem (PNS, z.B. Substanz P) sowie teilweise der Sympathikus (SNS) können pro-inflammatorisch wirken. Allgemein wirken sowohl Parasympathikus als auch Sympathikus allerdings vorwiegend anti-inflammatorisch [abgewandelt nach (Sternberg, 2006)].

2.2.1. Wirkungen des Gehirns auf das Immunsystem

Die Wirkung des Gehirns auf das Immunsystem konnte in sehr anschaulichen Versuchen bei Sepsis gezeigt werden (Borovikova *et al.*, 2000). Eine Stimulation des Nervus Vagus führte zu einer verminderten Entzündungsreaktionen begleitet von niedrigeren TNFα Plasma Spiegeln. In einer anderen Studie reduzierte eine Vagusstimulation 50% der Anfälle sowie zirkulierende Zytokin- und Corticosteron-Konzentrationen bei Epilepsiepatienten (Majoie et al., 2011; Rijkers et al., 2010). Solch eine so genannte „hard wired" Verbindung über das vegetative Nervensystem genauer gesagt des Parasympathikus im Sinne des neuronalen Signalweges kann also über Neurotransmitter vermittelt anti-inflammatorisch auf Immunzellen wirken (Steinman, 2004a). Im Einzelnen konnte gezeigt werden, dass über nikotinerge Rezeptoren der typische parasympathische Transmitter Acetylcholin diesen Effekt vermittelt (Wang *et al.*, 2003). Es entstehen hierbei so genannte immunologische Synapsen, die allerdings noch weniger festgelegt sind, als man das für das Gehirn mit seinen plastischen Vorgängen herausgefunden hat. Kompliziert wird dieser Zusammenhang dadurch, dass auch Immunzellen Neurotransmitter bilden und freisetzen können und damit reziprok an solche Synapsen wirken könnten (Steinman, 2004b). Solch eine so genannte „autonomic neuroeffector junction" zwischen Neuronen und Immunzellen wird seit längerem diskutiert (Thayer and Sternberg, 2010). Obwohl eine Interaktion zwischen den zwei Systemen sicher ist, ist sie nicht statisch festgelegt und wahrscheinlich bidirektional. Gerade die Leber wird nach Gehirnverletzungen über den Vagusnerv stark aktiviert und scheint wahrscheinlich über eine ausgeprägte Chemokinproduktion zu systemischen Nebenwirkungen beizutragen (Campbell et al., 2008; Campbell et al., 2005). Es sind ebenfalls typischer Weise hauptsächlich anti-inflammatorische Einflüsse des Sympathikus zum Beispiel durch Noradrenalin über β_2 Rezeptoren (Le Tulzo et al., 1997) auf Immunzellen in der Milz (Straub, 2004) und sogar Einflüsse des somatischen Nervensystems auf Immunzellen und Inflammation beschrieben worden (Sternberg, 2006). Als Beispiel sei hier die neurogene Entzündung genannt, die in reflexartigen Bögen über antidrome Zurückleitung zur sensibel detektierten Entzündungsreaktion das Entzündungsgeschehen verstärken kann (Brain and Williams, 1988; Steinhoff et al., 2000; Sternberg, 2006). So wurde gezeigt, dass solche dünnen C-Fasern Substanz P freisetzen, welche im Gewebe zu einer Stimulation von Zytokinproduktion oder Rekrutierung von Immunzellen beizutragen scheint.

Ein Training der vegetativen Outputfunktion ist durch das so genannte Biofeedback möglich. Hier werden Programme und besonderes Monitoring von vegetativ beeinflussten Körperfunktionen verwendet, um die willentliche Beeinflussung zu trainieren und das Maß

der Regulation zu verbessern und zu stärken. Ein gut messbarer Parameter hierbei ist beispielsweise die Variabilität des Herzschlagrhythmus, der sehr einfach über ein Elektrokardiogramm (EKG) aufgezeichnet werden kann. Über die Atmung kommt es physiologisch durch periphere und zentrale Stimulationen des Sympathikus und Parasympathikus zur respiratorischen Arrhythmie. Durch gezielte Steuerung der Atemfrequenz kann also der Einfluss auf die Herzfrequenz mit Feedback trainiert werden (Lehrer et al., 2003). Eine große Breite an Herzschlagfrequenzänderungen ist hierbei ein guter Indikator für eine hohe ausgleichende Aktivität der Gegenspieler Sympathikus und Parasympathikus. Nach Biofeedback mit höherer Bandbreite dieser Herzschlagfrequenz konnten tatsächlich Symptome von Asthmas reduziert werden (Lehrer et al., 2004). Erste Versuche der Verwendung des Biofeedback bei LPS-induzierter Entzündungsreaktion beim Menschen waren allerdings nur teilweise erfolgreich, was in der Studie von Lehrer und Kollegen (2010) allerdings auch auf zu kurze Trainingszeiten für das Biofeedback zurück geführt wird (Lehrer *et al.*, 2010). Weitere Studien und Fortschritte in dieser interessanten, obgleich häufig nicht ernst genommenen Forschungssparte bleiben abzuwarten.

Interessant in diesem Zusammenhang sind auch der klassischen Pavlowschen Untersuchung ähnelnde Versuchsergebnisse. Mit einer Geschmackssinneswahrnehmung gekoppelt „erlernten“ Patienten hierbei eine Unterdrückung von Immunreaktionen. Menschen und Tieren wurde ein gesüßtes Getränk verabreicht und gleichzeitig ein immunsupprimierendes Medikament appliziert. Nach der Phase des Erlernens dieses Zusammenhangs zwischen Geschmack und Immunsuppression (Konditionierung), vermochte der Stimulus Geschmack, die Immunsuppression bereits ohne Gabe des entsprechenden Medikamentes verursachen (Goebel *et al.*, 2002). Diese erstaunlichen Effekte sind allerdings noch nicht genau verstanden, würden allerdings Möglichkeiten eröffnen, den Medikamenten-Einsatz zyklisch reduzieren zu können, wenn man solche intermittierende Lernphasen einsetzt. Die Hoffnung dabei liegt natürlich in der Umgehung unerwünschter Nebenwirkungen, falls diese nicht auch erlernt werden (Schedlowski and Pacheco-Lopez, 2010). Bekannt ist allerdings beispielsweise, dass Chemotherapie begleitende Symptome wie Übelkeit oder Müdigkeit alleine durch die geistige oder durch Bilder vermittelte Erinnerung an die Therapie bei den Patienten über Jahre hinweg zum Beispiel zu den regelmäßigen Nachkontrollen induziert werden können (Dadds et al., 1997; Redd et al., 1993). Es bleibt insgesamt zu bemerken, dass es umstritten ist, ob und inwiefern solch „konditioniertes Lernen“ tatsächlich therapeutisch bei verschiedenen Indikationen wie Immunsuppression einsetzbar sein wird.

2.2.2. Wirkung des Immunsystems auf das Gehirn / im Gehirn

Prinzipiell ist wie schon Eingehens erklärt, das Gehirn nicht immunprivilegiert sondern sollte eher als „immunspezialisiert“ bezeichnet werden (Anthony *et al.*, 2012). Mit Aufkommen der zwei Photonentechnologie wurde einer Studie von Nimmerjahn et al. (2005) besondere Aufmerksamkeit zu Teil, die mit faszinierenden Bildern *in vivo* filmisch zeigen konnten, wie ruhende kortikale Mikroglia permanent mit ihren sich verlängernden und verkürzenden Fortsätzen die unmittelbare Umgebung abtasten, „aufräumen“ und sofort auf Stressoren reagieren (Nimmerjahn *et al.*, 2005). Darüber hinaus spielen Immunzellen im Gehirn für die Homeostase und normale Funktion des Gehirns eine wichtige Rolle. 80% der migrierenden Immunzellen, die sich im Liquor, den Meningen oder im *Plexus choroideus* bei gesunden Menschen finden, sind interessanter Weise T-Gedächtniszellen (Ransohoff *et al.*, 2003). Eher zufällig entdeckte man, dass Immundefiziente Tiere Lerndefizite aufwiesen und tatsächlich ist von meningealen T-Zellen produziertes IL-4 für vom Hippocampus abhängiges Lernen physiologisch notwendig (Brynskikh et al., 2008; Derecki et al., 2010). Außerdem scheinen vor allem zirkulierende T-Zellen und Makrophagen von entscheidender Bedeutung zu sein, in einem regulierten kontinuierlichen „Dialog“ mit dem zentralen Nervensystem, lokale mikroglial vermittelte Entzündungsreaktionen abzudämpfen oder gar zu beenden (Ron-Harel et al., 2011; Shechter et al., 2009).

2.3. Einfluss systemischer Entzündungsreaktionen auf ZNS Erkrankungen

Mensch und Tier haben regelmäßig akute virale und bakterielle Infektionen oder zeigen chronische Zustände wie bei Obesitas (Könner and Bruning, 2011), die von systemischen Entzündungsreaktionen begleitet sind. In vielen Fällen werden bestehenden Gehirnpathologien wie Alzheimer, Hirntraumata, Parkinsonsche Krankheit, Depressionen oder Hirnentfarkte verstärkt bzw. der Verlauf negativ beeinflusst, wenn solche zusätzlichen systemische Entzündungsreaktionen auftreten (Perry *et al.*, 2007). So verschlimmern chronische systemische Entzündung bei Darminfektionen Schäden bei Gehirnischämie (Denes *et al.*, 2010). Ulcerative Kolitis erhöht LPS-induzierte Durchlässigkeit der Blut-Hirn-Schranke (BBB) und damit verbundene Verluste dopaminerger Neurone (Villaran *et al.*, 2010). Systemische Entzündung durch das Zytokin IL-1β oder LPS potenzieren traumatische Gehirnläsionen oder -Entfarkte (Denes et al., 2011; Denes et al., 2010; McColl et al., 2007; Spencer et al., 2007b; Utagawa et al., 2008). Insgesamt führen periphere Entzündungsreaktionen neben der bereits genannten Kolitis aber auch Osteoarthritis

(Kyrkanides *et al.*, 2011) oder Leberentzündungen (D'Mello *et al.*, 2009) über verschiedene nur zum Teil verstandene Mechanismen zu schwerwiegenden Folgen für das Gehirn und bestehende Gehirnpathologien. Nicht zuletzt sind wiederum akute systemische Entzündungsreaktionen wichtige Risikofaktoren für die Entwicklung von Gehirnpathologien wie beispielsweise von Hirnentfarkten (McColl *et al.*, 2009). Weitere Untersuchungen des Zusammenspiels und der Folgen unterschiedlichster Interaktionen zwischen dem aktivierten Immunsystem in der Peripherie und dem Gehirn sowie respektive Folgen für die Gesundheit sind folglich notwendig, um neue Therapien und präventive Maßnahmen entwickeln zu können. In der hier vorliegenden Arbeit werden einige grundsätzliche Mechanismen und Signalwege der Kommunikation des Immunsystems mit dem Gehirn bei Infektion und Inflammation näher charakterisiert und mögliche Einflussfaktoren bestimmt sowie potentielle Therapieansätze getestet.

.

II. SCHRIFTTUM

1. „Sensoren“ des angeborenen Immunsystems

Beim angeborenen Immunsystem handelt sich es um ein entwicklungsgeschichtlich sehr altes System (Beutler, 2004; Cooper and Alder, 2006) welches die Integrität des Organismus gegen möglicherweise schädigende Einwirkungen und eindringende Mikroorganismen ohne Zeitverzögerung verteidigt. Es ist perfekt in seinen Abläufen darauf abgestimmt, cirka 1000 verschiedene so genannte Pathogen und nicht Pathogen Assoziierte Molekülstrukturen exogenen oder sogar endogenen Ursprungs zu detektieren. Dabei sind die „Sensoren“ nicht nur auf spezialisierten Immunzellen der zellulären angeborenen Immunabwehr wie Beispielsweise Makrophagen oder neutrophilen Granulozyten zu finden sondern prinzipiell auf fast allen Körperzellen. Diese breit verstreute Suche nach möglicherweise schädlichen Zuständen ist sehr effektiv und überbrückt nicht nur die Zeit bis die erworbene Immunabwehr mit spezifischen Antikörpern gezielt und effektiv die Abwehr verstärkt, sondern sie moduliert und aktiviert sogar den erworbenen Teil der Abwehr entscheidend (Miyaji et al., 2011). So wird durch spezifische Zytokinmilieus die Differenzierung von T-Helfer Lymphozyten gesteuert bzw. moduliert und die Expression von Kontaktmolekülen beeinflusst. Die sich anschließenden nicht weniger wichtigen Mechanismen der Effektorfunktion nach erfolgter Erkennung eines potentiellen Pathogens durch das angeborene Immunsystem (Abwehrmechanismen) sowie Mechanismen der Toleranz auf körpereigene Substanzen sind nicht Gegenstand dieser Arbeit und sollen deshalb nicht genauer beschrieben werden.

1.1. Pattern Recognition Rezeptoren (PRR)

Man unterteilt die Vielzahl an Rezeptoren, die als „Sensoren“ des angeborenen Immunsystems fungieren nach ihrer Lokalisation, Funktion und ihrer charakteristischen Liganden bzw. Erkennungsstrukturen. Entsprechend der unterschiedlichen Möglichkeiten, wie Organismen oder Toxine auf Zellen wirken können, gibt es Rezeptoren für extrazellulär zu detektierende Stimuli in der Zellmembran, für phagozytierte Moleküle im Phagosom bzw. Endosom sowie im Zytoplasma. Das heißt sie erkennen eindringende Mikroorganismen im Extrazellularraum, sowie nach Phagozytose aber auch in die Zelle eingedrungene Mikroorganismen im Zytoplasma. In der Zellmembran finden sich neben Toll-like-Rezeptoren (TLR) auch C-Typ Lektin Rezeptoren. TLR3, TLR7, TLR8 und TLR9 sind endosomal lokalisiert. So genannte Retinoic acid-inducible gene (RIG-1), Sensoren für

doppelsträngige RNA, sowie nucleotide-binding domain and leucin-rich repeat containing Rezeptoren (NLRs) und andere DNA Sensoren sind zytoplasmatisch lokalisiert (Miyaji et al., 2011). Teilweise kooperieren die verschiedenen Rezeptortypen bei der Abwehr eines Mikroorganismus auf verschiedenen Ebenen der Zellkompartimente oder erkennen unterschiedliche Anteile des gleichen „Eindringlings“ auf seinem Weg in die Zelle, sei es aktiv oder durch Phagozytose (Akira et al., 2006). Gleichzeitig können mehrere unterschiedliche Rezeptortypen redundant die gleiche Molekülstruktur erkennen (Kawai and Akira, 2011; Miyaji et al., 2011). So werden beispielsweise virale Strukturproteine in der Zellmembran bzw. in Phagosomen und virale RNA zytoplasmatisch aber auch prozessiert in Endosomen durch unterschiedliche Rezeptorfamilien detektiert (Takeda and Akira, 2005). In der vorliegenden Arbeit wurden mehrere Liganden für TLRs zur Stimulation des angeborenen Immunsystems verwendet (Abbildung 3). Im Weiteren wird nun genauer auf diese Familie an PRR eingegangen.

1.2. Toll-like-Rezeptoren und deren Liganden

Insgesamt sind bisher 13 verschiedene TLRs mit unterschiedlichen extrazellulären Domänen für eine Reihe von Liganden identifiziert worden (siehe auch Abbildung 3). Sie sind etwa vor 600 Millionen Jahren entstanden und kommen vor allem bei Wirbeltieren und Insekten vor (Leulier and Lemaitre, 2008). TLR1-13 gibt es bei der Maus, wobei TLR10 nicht funktionell ist. TLR11-13 sind beim Menschen nicht mehr im Genom vorhanden und lediglich für TLR1-9 konnten bisher Liganden nachgewiesen werden. Manche Subtypen sind nur in einer Spezies beschrieben wie beispielsweise TLR15 bei Fischen. Außerdem sind teilweise funktionelle Redundanzen zwischen TLRs beschrieben worden. So konnte kürzlich nachgewiesen werden, dass das Hühneranalog zum TLR9 des Säugetiers TLR21 darstellt (Brownlie et al., 2009). Tabellarisch sind in mehreren ausführlichen Übersichtsartikeln die unterschiedlichen Liganden der einzelnen TLRs zusammengefasst und sollen hier nur exemplarisch aufgeführt werden (Akira et al., 2006; Kawai and Akira, 2011; Miyaji et al., 2011) (Abbildung 3).

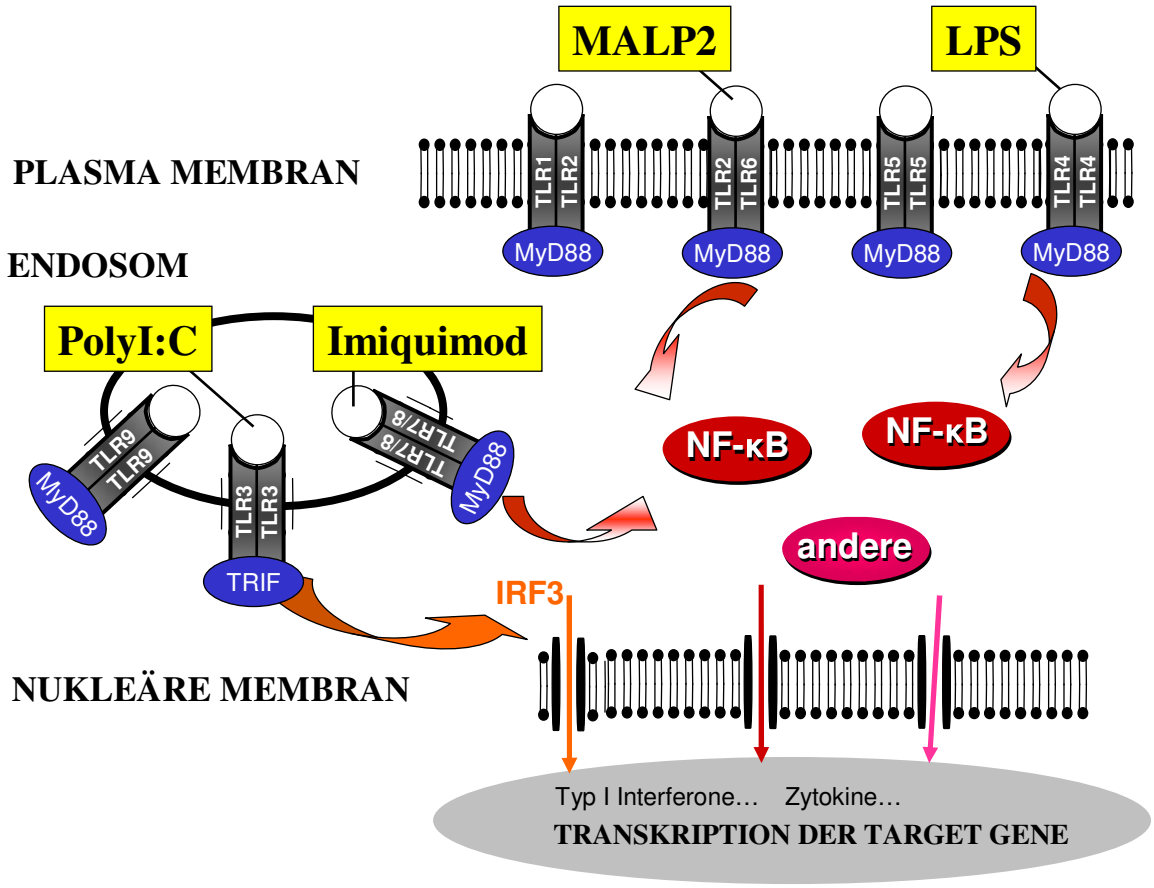


Abbildung 3
Vereinfachte schematische Darstellung der wichtigsten Toll-like-Rezeptoren (TLR) sowie die verwendeten Liganden in der vorliegenden Arbeit und Signalwege. TLR3, 7-9 liegen in Endosomen und die anderen Rezeptoren in der Zellmembran. Hauptsignalweg über das Adaptermolekül MyD88 (myeloid differentiation primary response gene 88) ist NFκB. Lediglich TLR3 besitzt kein MyD88 und reguliert über den interferon regulatory factor (IRF)3 die Expression von Typ I Interferonen. TLR4 kann ebenfalls über das Adaptermolekül TRIF [TIR damain-containing adapter inducing Interferon(INF)β] und andere Signalwege wirken [abgewandelt nach (Miyaji et al., 2011)]. andere = zum Beispiel STAT3 (signal tranducer and activator of transcription, indirekt) und NF-IL6 (nuclear factor interleukin-6, direkt)

TLR1, 2, 6 kommen als Heterodimere in unterschiedlichen Kombinationen vor. Je nach Kombination werden unterschiedliche, spezifische Molekülstrukturen wie unter anderem Lipoproteine erkannt. In der vorliegenden Arbeit wurde der TLR2/6 Ligand Makrophagen stimulierendes Lipoprotein 2 (MALP2) von *Mycoplasma fermentans* aus dieser Gruppe verwendet (Morr et al., 2002). TLR3 erkennt doppelsträngige RNA, ein Nebenprodukt bei der Replikation zahlreicher Viren. Das synthetische Analog Polyinosinic:polycytidylic acid (PIPC) solcher RNA ist ein häufig verwendetes Modell für virale Infektionen (Fortier et al., 2004) und wurde hier ebenfalls in zwei Teilstudien eingesetzt. TLR4 wird durch bakterielles Lipopolysaccharide (LPS) aktiviert und war bei Säugetieren als erster Rezeptor dieser Familie

charakterisiert worden (Rock et al., 1998). LPS stellt das am häufigsten verwendete und untersuchte PAMP dar und war deshalb auch ein wichtiger Stimulator des angeborenen Immunsystems in dieser Arbeit. Des Weiteren aktiviert bakterielles Flagellin TLR5 (Smith et al., 2003) und einzelsträngige RNA, wie sie bei RNA-Viren vermehrt vorkommt, bindet an TLR7 und 8 (Lee et al., 2003a). Unmethylierte CpG-DNA ist der spezifische Ligand für TLR9. Dieser wird nicht durch körpereigene DNA aktiviert, weil diese in der Regel hochgradig methyliert vorkommt, nicht endosomal lokalisiert ist und extrazellulär schnell enzymatisch degradiert wird (Takeda and Akira, 2005). Insgesamt kann also bis zu einem gewissen Maße garantiert werden, dass TLRs nur Körperfremdes erkennen und nicht auf körpereigene Molekülstrukturen reagieren. Trotzdem ist seit längerem bekannt, dass neben den PAMPs auch endogene so genannte Danger Associated Molecular Patterns (DAMPs) TLRs aktivieren können. Solche körpereigenen Substanzen werden zum Beispiel bei starken Gewebeschädigungen freigesetzt und geben das Alarmsignal an das Immunsystem weiter (Miyaji et al., 2011). Zu diesem Alarmsystem gehört beispielsweise high-mobility group box 1 (HMGB1), welches Zytokin ähnliche Funktionen hat und beispielsweise bei postischämischen Schäden im Gehirn freigesetzt wird (Kim et al., 2006). Viele potentielle endogene und exogene Liganden für TLRs sind allerdings gerade für das ZNS noch nicht bekannt (Kong and Le, 2011).

Vielschichtiger wird die Betrachtung der einzelnen Liganden dadurch, dass abhängig vom einzelnen Serotyp der Mirkoorganismen die zelluläre Antwort entsprechend variieren bzw. stärker oder schwächer ausfallen kann. Gerade das so häufig verwendete LPS ist in seiner Reaktion neben der Dosierung deutlich abhängig vom Serotyp (Akarsu and Mamuk, 2007; Dogan et al., 2000) und unter Umständen sogar von der einzelnen Charge (Reinheit) des Herstellers. Folglich sollte im Vergleich von unterschiedlichen Studien immer mit besonderer Vorsicht die jeweilige Dosierung nicht nur im Bezug auf die verwendete Tierspezies und Zuchtlinie sondern auch auf Grund der verwendeten Serotypen kritisch betrachtet werden. In der vorliegenden Arbeit wurden die Serotypen O111:B4 und O128:B12 verwendet. Schließlich ist bekannt, dass es zusätzlich mehrere Polymorphismen für einzelne TLR bei Tier und Mensch gibt, die nicht zuletzt für unterschiedliche Reaktivitäten und Anfälligkeiten für Krankheiten prädisponieren. So konnte gezeigt werden, dass ein solcher Polymorphismus für TLR5 mit erhöhter Anfälligkeit für Lungenentzündungen mit *Legionella pneumophila* darstellt (Hawn et al., 2003), Polymorphismen für TLR4 erhöhen das Risiko für bakterielle Infektionen und Sepsis, und für TLR2 sind sie assoziiert mit einer Prädisposition für Tuberkulose aber Schutz vor späten Stadien von Borreliose (Casanova et al., 2011). Einige

Unterschiede zwischen Zuchtlinien und Einzeltieren bei Ratten und Mäusen können hierdurch erklärt werden. Komplette Defizienzen solcher TLR Rezeptoren stellen beträchtliche gesundheitliche Einschränkungen dar und können das Immunsystem empfindlich in seiner Funktion einschränken. Insgesamt sind für Erkrankungen des ZNS sowohl protektive als auch schädliche Wirkungen durch TLRs beschrieben worden (Kong and Le, 2011).

1.3. Zielzellen

Zielzellen von TLR-Agonisten umfassen diverse Zellphänotypen im ganzen Körper. Prinzipiell werden neben allen großen inneren und äußeren Oberflächen auch im Gewebe TLRs exprimiert. Die Schutzfunktion von TLRs auf exponierten Stellen des Körpers wie dem Epithel liegt nahe. Auf Epithelzellen des Bronchial- und Magendarm-Traktes finden sich beispielsweise TLR2-5 aber auch andere Zellen wie Endothelzellen, Thrombozyten, Adipozyten, Muskel- oder Leber-Zellen exprimieren TLRs (Hopkins and Sriskandan, 2005; Kong and Le, 2011). Zellen des Immunsystems sind hierbei natürlich besonders hervorzuheben und zeigen einige Besonderheiten (McGettrick and O'Neill, 2007). So sind vor allem dendritische Zellen und Makrophagen wichtige Träger von TLR7 (Blasius and Beutler, 2010). Endothelzellen des Gehirns können TLR2-4 exprimieren, was allerdings auch je nach Aktivierungsstatus verschieden sein kann und wie bei anderen Zellen als dynamische Expression bezeichnet wird (Hopkins and Sriskandan, 2005). Im Gehirn konnte prinzipiell die Expression aller TLRs nachgewiesen aber nur teilweise zellphänotypisch charakterisiert / spezifiziert werden (Letiembre et al., 2007). Neben Speziesunterschieden zwischen Maus und Mensch exprimieren vor allem Mikroglia die komplette Vielfalt dieser Rezeptorfamilie (Kong and Le, 2011). Im Einzelfall sind neben der Expression Daten über die Funktionalität von TLRs im ZNS noch recht unvollständig. Dies liegt sicher auch daran, dass spezifische Antagonisten nicht immer erhältlich sind und eine immunhistochemische Detektion häufig wenig Erfolg verspricht. Der Nachweis per in situ Hybridisierung wurde häufiger durchgeführt, ist aber wesentlich weniger sensitiv (Laflamme and Rivest, 2001; Letiembre et al., 2007).

1.4. Zelluläre Signalwege und therapeutisches Potenzial

Nachdem ein Agonist an den entsprechenden Rezeptor gebunden hat, kommt es vermehrt zu Dimerisationen der Rezeptoren und anschließender Aktivierung einer zytoplasmatischen TIR-Domäne (Abbildung 3). Diese nachfolgende Signalkette hängt von den Toll-interleukin-1 receptor domain containing adaptor protein (TIRAP)-Domän-beinhaltenden

Adaptermolekülen ab. Prinzipiell haben alle TLRs außer TLR3 am TIRAP das MyD88 Adaptermolekül (myeloid differentiation primary response gene 88), welches schließlich ähnlich wie beim IL-1-Signalweg zur Aktivierung von NFκB führt. Klassischer Weise wird hierdurch die Expression von pro-inflammatorischen Zytokinen, Chemokinen, Adhäsionsmolekülen und Metalloproteinasen reguliert. Alternativ läuft die Signalweiterleitung von TLR3 aber auch von TLR4 über TIR domain-containing adapter inducing Interferon(INF)β (TRIF), welches über interferon regulating factor (IRF)3 zur Induktion von Typ I Interferonen führt. Diese Gruppe an Zielgenen beinhaltet INFα und INFβ. TLR4 besitzt mehrere Adaptermoleküle und kann weitere Signalwege aktivieren [zur Übersicht (Kawai and Akira, 2011; Miyaji et al., 2011; Takeda and Akira, 2005)]. So wurde gezeigt, dass unter gewissen Umständen LPS auch andere inflammatorische Transkriptionsfaktoren und zwar MyD88-abhängig indirekt STAT3-Aktivierung (Yamawaki et al., 2010) oder direkt NF-IL6 Expression regulieren kann (Lu et al., 2009). Eine detailliertere Beschreibung der Signalwege geht über den Rahmen dieser Arbeit hinaus und soll daher hier nicht weiter konkretisiert werden.

Als therapeutische Zielstrukturen sind TLRs von großem Interesse. Therapieansätze umfassen so genannte protektive Wirkungen nach Präkonditionierung bei Gehirnischämie mittels TLR2, 4 oder 9 Agonisten (Hua et al., 2008; Stevens et al., 2008; Tasaki et al., 1997), Behandlung von Leukämie (TLR7, 9) (McGettrick and O'Neill, 2007), subkutanen Melanomen (TLR7) (Ma et al., 2010) und Asthma (TLR2) (Patel et al., 2005). TLR3-Agonisten als Vorbehandlung auf eine Herpes simplex induzierte Virus-Enzephalitis erhöhte dramatisch die Überlebensraten (Boivin et al., 2008) aber auch TLR7/8-Agonisten wurden bereits als antivirale Strategien eingesetzt (Miller et al., 2008). Ein anderes wichtiges Einsatzgebiet für TLR-Agonisten liegt in Impftherapien bzw. als Bestandteil von Adjuvantien. Sie werden sowohl als Einzelzusätze oder sogar in Kombination verschiedener TLR-Agonisten verwendet. Potentielle Nebenwirkungen sind hierbei durch pro-inflammatorischen Reaktionen allerdings zu erwarten und stellen mögliche Gefahren für Mensch und Tier dar (McGettrick and O'Neill, 2007; Miyaji et al., 2011). Gerade deshalb sind detaillierte Studien über die Einflüsse solcher Stimulantien auf den Gesamtorganismen im Tiermodell wie in dieser Arbeit mehrfach durchgeführt von grundsätzlicher Bedeutung. Neben dem Wissensfortschritt über Kommunikationswege zwischen Immunsystem und Gehirn können Risikofaktoren zum möglichen therapeutischen Einsatz charakterisiert und abgeschätzt werden.

2. Endogene Immunmediatoren - Zytokine

Nach Stimulation mit PAMPs oder DAMPs werden wie bereits erwähnt eine Vielzahl von endogenen Immunmediatoren gebildet, welche lokal parakrin direkt im Gewebe am Entzündungsort oder als humorale Botenstoffe systemisch zum Beispiel auch auf das Gehirn wirken können. Viele dieser durch das Immunsystem gebildeten Botenstoffe werden übergreifend in der Gruppe der Zytokine zusammengefasst. Hierbei handelt es sich um hydrophile Makromoleküle mit Molekulargewichten zwischen 15-25 kDa, die sich dadurch auszeichnen, dass sie prinzipiell nach Stimulation durch *de novo* Synthese gebildet werden und außer TNFα nicht gespeichert werden. Man unterscheidet so genannte pro-inflammatorische Zytokine zu denen TNFα, IL-1β und IL-6 gehören von anti-inflammatorischen Zytokine wie beispielsweise IL-1 Rezeptor Antagonist (IL-1ra) oder IL-10 (Conti et al., 2004). Bei der Gruppe der Interferone (INFs), die ebenfalls zu den Zytokinen gezählt werden, fällt die Einteilung etwas schwerer. Prinzipiell haben INFs sowohl pro- als auch anti-inflammatorische Wirkungen. So konnte gezeigt werden, dass bei experimentell induzierter Influenzainfektion von Frettchen intranasale INFα-Gabe Fieber und Krankheitssymptome hemmt und die Viruslast reduziert (Kugel et al., 2009). INFγ hingegen induziert Fieber (Morimoto et al., 1987) und ist deutlich pro-inflammatorisch (Chen and Ivashkiv, 2010; Kluger, 1991). *In vivo* treten Zytokine nicht isoliert auf, sondern immer in einem so genannten Zytokinmilieu. Zusätzlich wird eine isolierte Betrachtung der Wirkung von Zytokinen erschwert, weil sie vielfach in ihrer Wirkung redundant sind, pleiotrop auf eine Vielzahl von Zielzellen wirken und nicht nur Rezeptoruntereinheiten zwischen einzelnen Zytokinen gleich sind, sondern auch wichtige intrazelluläre Signalwege von mehreren Zytokinen geteilt werden (Ozaki and Leonard, 2002). So wirken aus der Familie der Typ I Zytokine IL-6 (über das gp130 Signaltransduktionsmolekül) und das zytokinähnliche Hormon Leptin wie auch das anti-inflammatorische Zytokin IL-10, welches zur Interferon-Familie gezählt wird, unter anderem über den Janus Kinase (JAK)/STAT3-Signalweg (Kisseleva et al., 2002).

TNFα ist das erste Zytokin, welches gefolgt von Spuren von IL-1β und großen Mengen von IL-6 im Blut freigesetzt wird (Roth et al., 2006). Hervorzuheben bleibt, dass IL-6 als einziges Zytokin auch basal im Blut ohne jegliche Stimulation detektierbar ist. Es ist das wichtigste zirkulierende Zytokin, welches durchweg bei Fieber im Blut von Tier (Cartmell et al., 2001; Cartmell et al., 2000; Miller et al., 1997) und Mensch (Nijsten et al., 1987) detektierbar ist und in Dauer und Menge mit der Höhe der Fieberantwort korreliert (LeMay et al., 1990; Roth et al., 1993; Roth et al., 1994b; Roth, 2004). Obwohl IL-6 auch bei vielen

akuten und chronischen inflammatorischen Prozessen, wie beim Altern (Bruunsgaard and Pedersen, 2003; Kim et al., 2012; Stowe et al., 2010) oder Fettsucht (Eder et al., 2009) erhöht im Blut vorkommt und sogar als ein Risikofaktor zum Beispiel für Arteriosklerose diskutiert wird (Lee et al., 2007; Lobbes et al., 2006), ist seine tatsächliche Rolle für die Homeostase in Gesundheit oder Krankheit weitgehend unklar. Auch wenn die Rolle von IL-6 bei der Entstehung von Fieber durch neutralisierende Antikörper (Cartmell et al., 2000) und in IL-6 defizienten Mäusen (Chai et al., 1996; Kozak et al., 1998) eindeutig gezeigt werden konnte, gibt es auch andere Studien, bei denen eine eher moderate (Blatteis et al., 1990; Dinarello et al., 1991; Harré et al., 2002; Helle et al., 1988; Sakata et al., 1991) oder sogar gar keine Fieber-induzierende Wirkung nach Injektion von rekombinantem IL-6 in verschiedenen Tierspezies gezeigt werden konnte (Cartmell et al., 2000; LeMay et al., 1990; Wang et al., 1997a). Damit war vor allem die Rolle von IL-6 als im Blut zirkulierender, humoraler Mediator bisher weithin unklar. Prinzipiell wurden Kriterien zur Definition eines echten endogenen humoralen Fieber erzeugenden Stoffes (pyrogen) etwas modifiziert wie folgt aufgestellt (Kluger, 1991).

- Systemische Injektion eines endogenen Pyrogens sollte Fieber induzieren.
- Entzündliche Stressoren (LPS) sollten diese endogene Pyrogene induzieren.
- Die endogenen Pyrogene sollten bei solchen systemischen Entzündungsreaktionen als humorale Botenstoffe erhöht im Blut nachweisbar sein.
- Endogene Pyrogene sollten den Prostaglandin-Synthese-Weg bzw. COX2 induzieren.

Klassisch werden diese Kriterien durch IL-1β erfüllt, dieses Zytokin ist also ein endogenes Pyrogen (Conti et al., 2004; Dinarello, 1983; 2010; Kluger, 1991). Systemische IL-1β-Injektion induziert Fieber, IL-1β selbst wird durch LPS stimuliert und IL-1β aktiviert den PG-Syntheseweg im Gehirn (Nadjar et al., 2005b). Im Gegensatz zu IL-6 kommt allerdings IL-1β wenn überhaupt nur in geringen Mengen im Blut während Infektion und Inflammation vor (Kluger, 1991). Für IL-6 wurde die Induktion des PG-Synthesewegs bisher nicht gezeigt. Zusammen mit der eher moderat Fieber erzeugenden Wirkung war die Rolle von zirkulierendem IL-6 als Pyrogen demnach noch zu beweisen. Auch die Rolle von TNFα zum Beispiel in der Fieberentstehung ist nicht eindeutig geklärt. Ein Antiserum gegen TNFα verstärkte LPS-induziertes Fieber (Long et al., 1990) aber die Neutralisation des löslichen P55-TNFα Rezeptors führte zu einer verringerten Fieberantwort, vor allem zu späteren

Fieberphasen (Conti et al., 2004; Roth et al., 1998). Weitere Studien zur Rolle dieser Zytokine (vor allem IL-6, TNF und Interferone) bei der Kommunikation zwischen Immunsystem und dem Gehirn bei Infektion und Inflammation sind demnach noch notwendig und waren unter anderem Bestandteil der hier vorliegenden Arbeit.

3. Transkriptionsfaktoren

TLR-Agonisten und Zytokine regulieren die Expression von spezifischen Zielgenen über die Aktivierung von inflammatorischen Transkriptionsfaktoren. Zu den wichtigsten zählen wie bereits erwähnt (Kapitel I 1.1) nuclear factor kappa B (NFκB), signal transducer and activator of transcription 3 (STAT3), aber auch NF-IL6 (Synonym = CEBPβ) (Akira, 1992; Ramji and Foka, 2002). Sie wurden bereits in einer Vielzahl von Studien untersucht und tragen zur Expression von wichtigen inflammatorischen Zielgenen bei. Dazu gehören neben Zytokinen, die geschwindigkeitsbestimmenden Enzyme der Prostaglandin (PG)E2 Synthese nämlich Zyklooxygenase 2 (COX2) und mikrosomale Prostaglandin E Synthase (mPGES) aber auch Chemokine und Adhäsionsmoleküle (Kapitel II 4). Die Funktion scheint hierbei gewebespezifisch von der Ausstattung der respektiven Zellen abzuhängen und wird im Rahmen des Transkriptionskomplexes in seiner Funktion moduliert. Dabei handelt es sich beispielsweise um funktionelle Interaktionen der Transkriptionsfaktoren einem so genannten „crosstalk“, bei dem diese Faktoren physisch miteinander interagieren. Dies führt zu einer Stabilisierung der Bindung an die genomische DNA oder sogar an Promotoren, für die der einzelne Transkriptionsfaktor eigentlich gar keine Bindungsstelle im Promotor des Zielgens besitzt, was unter anderem in einer Studie für die Expression von C-reaktivem Protein in Leberzellen gezeigt werden konnte (Agrawal et al., 2003; Yoshida et al., 2004).

Immunhistochemische Detektion zumindest von NFκB und STAT3 wurde bereits mehrfach zum Nachweis einer Aktivierung von Zellen und damit bestimmter Gehirnstrukturen verwendet, um funktionelle Rückschlüsse auf die Rolle dieser Gehirnregionen bei Infektion und Inflammation zu gewinnen (Gautron et al., 2002; Hübschle et al., 2001a; Hübschle et al., 2001b; Nadjar et al., 2003; Rummel et al., 2004; Rummel et al., 2005b). Eine Akkumulation des Transkriptionsfaktors im Kern, also eine nukleäre Translokation, markiert hierbei eindeutig die Aktivierung der jeweiligen Zelle. Im unstimulierten Zustand ist die Immunreaktivität (IR) im Zytoplasma oder gar nicht detektierbar und daher deutlich von aktivierten Zellen zu unterscheiden (Abbildung 4). Außerdem fungiert die Analyse endogener Inhibitoren der einzelnen Signalwege mittels quantitativer PCR als Detektionsmethode ihrer Aktivierung. Dazu gehören supressor of

cytokine signaling 3 (SOCS3) für STAT3 (Lebel et al., 2000), der inhibitor of cytokine signaling (IκBα) für NFκB (Laflamme and Rivest, 1999) und der kürzlich entdeckte negative Regulator der NF-IL6-Aktivierung ein serin/threonin kinase like protein (Trib1) für NF-IL6 (Yamamoto et al., 2007). Die genaue funktionelle Rolle der Transkriptionsfaktoren für die Kommunikation zwischen dem Immunsystem und dem Gehirn wie auch für die Entstehung von zentralnervös kontrollierten Krankheitssymptomen (sickness behavior) oder der damit zusammenhängenden inflammatorischen Prozessen im Gehirn ist allerdings weiterhin weitgehend unklar und sollte im Rahmen dieser Arbeit näher untersucht werden.

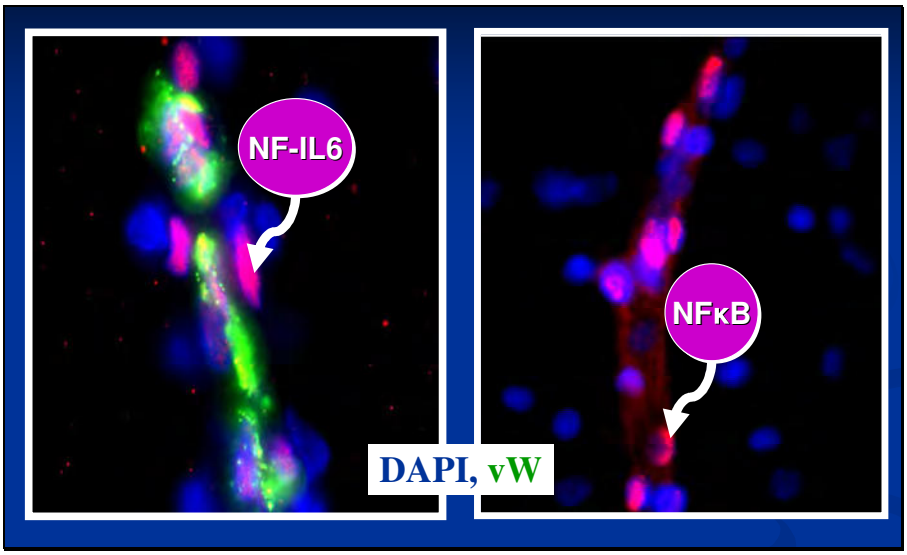


Abbildung 4
Exemplarische Darstellung zweier Immunfluoreszenzaufnahmen von Gefäßstrukturen des Rattengehirns. Nach LPS-Stimulation haben sich die Transkriptionsfaktoren NF-IL6 und NFκB (rot) im Kern (blau) akkumuliert. NF-IL6 befindet sich in von Willebrand Faktor (vW, grün) positiven Endothelzellen und anderen Zellphänotypen.

3.1. NFκB

NFκB ist der am besten bekannte und vielleicht auch wichtigste Transkriptionsfaktor bei Entzündungsreaktionen, der nicht zuletzt direkt durch die meisten TLR-Aktivatoren aber auch durch die wichtigen pro-inflammatorischen Zytokine IL-1β und TNFα aktiviert wird. Er ist der wichtigste Transkriptionsfaktor bei sickness behavior (Fieber, Anorexie und verringerte soziale Interaktion) (Kozak et al., 2006; Lee et al., 2003b; Nadjar et al., 2005a; Shao et al., 2004) und ist maßgeblich an der Induktion zum Beispiel des wichtigen Zielgens COX2 (Nadjar et al., 2005b) aber auch der Zytokine IL-6 und TNFα sowie IL-1β beteiligt. NFκB wird für die initiale Phase des Fiebers eine wichtige Bedeutung beigemessen (Nadjar et al., 2005a) und stellt ein wichtiges Ziel für therapeutische Strategien dar (Lee et al., 2003b). Die

frühe Aktivierung im Gehirn klingt allerdings bereits ca. 2 Stunden nach LPS/IL1β-Stimulation wieder ab (Laflamme and Rivest, 1999; Nadjar et al., 2003) und dürfte demnach nicht direkt für spätere Phasen der Entzündungsreaktion im Gehirn verantwortlich sein. Hinzu kommt, dass vor allem Zytokine wie IL-6, die nicht über den NFκB-Signalweg ihre Effekte vermitteln, vermehrt bei chronischen bzw. längeren Entzündungsprozessen im Blut vorkommen (Kapitel I 2) und große Bedeutung bei der Pathogenese von Krankheiten zu haben scheinen. Deshalb ist es wichtig die Rolle dieser anderen Signalwege und deren mögliche Interaktion mit dem NFκB-Weg zu untersuchen sowie das Potenzial für therapeutische Strategien zu analysieren und zu testen.

3.2. STAT3

Die potentielle Rolle von STAT3 im Gehirnendothel bei systemischer Inflammation wurde in einer Studie von Kano et al. (2003) mit Hilfe von konditionellen Knockout Mäusen untersucht und ergab dass STAT3 in diesem Zelltyp scheinbar anti-inflammatorische Funktion zu haben scheint und gegen LPS-induzierte Inflammation schützt (Kano et al., 2003). Im Gegensatz zu NFκB (Kozak et al., 2006) oder NF-IL6 (Liu et al., 1999) sind keine STAT3 defizienten Mäuse verfügbar, da diese embryonale Letalität zeigen (Takeda et al., 1997). Nicht zuletzt in Studien der eigenen Doktorarbeit konnte die zeitlich und räumlich differenzierte Aktivierung von STAT3 bei Meerschweinchen und Ratten untersucht werden, wobei eine besondere Rolle für Endothelzellaktivierung beobachtet wurde (Rummel et al., 2005b). Die Aktivierung von STAT3 kommt etwas versetzt aber auch teilweise (2-6h) überlappend zu NFκB in verschiedenen Gehirnstrukturen vor (Gautron et al., 2002; Rummel et al., 2004; Rummel et al., 2005b). Dabei scheint STAT3 für die Aufrechterhaltung von Fieber eine Rolle zu spielen (Rummel et al., 2004). Die genau funktionelle Bedeutung von STAT3 wurde im Rahmen einiger Teilstudien dieser Arbeit weiter untersucht. Dazu zählt auch die Untersuchung, welche über STAT3 wirkenden Mediatoren an der LPS-induzierten Aktivierung der einzelnen Gehirnregionen und Zelltypen sowie sickness behavior beteiligt sind. Damit kann also nicht nur die Bedeutung von STAT3-Aktivierungen an sich sondern auch der einzelnen Mediatoren näher untersucht werden. Einer dieser Faktoren ist neben dem Zytokin IL-6 das Appetit-hemmende und Energiehaushalt regulierende Hormon Leptin (Kapitel II 6.2) aber auch verschiedener TLR-Agonisten (Kapitel II 1.2.).

3.3. NF-IL6

NF-IL6 existiert in mehreren funktionell unterschiedlichen Isoformen: einem liver – enriched activating protein (LAP), einem liver-enriched inhibitory protein (LIP), dem die Aktivierungsdomäne fehlt und dem LAP, welches in voller Länge vorliegt (LAP*) (Descombes and Schibler, 1991; Ejarque-Ortiz et al., 2007). Obwohl NF-IL6 bereits als wichtiger inflammatorischer Transkriptionsfaktor seit mehr als 20 Jahren bekannt ist (Akira et al., 1990; Landschulz et al., 1988), sind erst in kürzlich publizierten Studien neue Erkenntnisse für die Bedeutung dieses Transkriptionsfaktors im Gehirn bekannt geworden. NF-IL6 ist ein Schlüsselfaktor bei Neuroinflammation (Perez-Capote et al., 2006; Straccia et al., 2011), bei excitotoxischen Gehirnläsionen (Cortes-Canteli et al., 2008), postischämischer Entzündung (Halterman et al., 2008; Kapadia et al., 2006; Yi et al., 2007), neuronalen (Nadeau et al., 2005) oder/ und mikroglial-vermittelten Gehirnläsionen (Cortes-Canteli et al., 2004; Straccia et al., 2011) und scheint eine wichtige Rolle bei der amyotrophen Lateralsklerose zu spielen (Valente et al., 2011). Neben einer Rolle in hippokampaler adulter Neurogenese (Cortes-Canteli et al., 2011) scheint NF-IL6 von Bedeutung für Hippocampus-abhängige Gedächtnis Konsolidierung zu spielen (Taubenfeld et al., 2001). Eine zeitlich und räumlich differenzierte Analyse der NF-IL6-Aktivierung im Gehirn nach systemischer Inflammation und seine Rolle für Gehirninflammation und sickness behavior fehlte bislang und war damit eines der Teilziele dieser Arbeit (Manuskripte Kapitel V 1.1, 1.3, 1.5).

4. Zielgene

De novo Synthese von Zielgenen über inflammatorische Transkriptionsfaktoren spielt eine wichtige Rolle zur Regulation der Expression der zweiten Welle an Zytokinen/Mediatoren im Gehirn nach systemischer Stimulation in der Peripherie. Vor allem die länger anhaltenden Entzündungsreaktionen im Gehirn bei LPS-vermittelten systemischen Reaktionen sind abhängig von direkter Wirkung des LPS auf das Gehirn (Chakravarty and Herkenham, 2005). Zirkulierende Botenstoffe gebildet von hämatopoetischen Zellen in der Peripherie spielen vor allem für die initiale Phasen der Entzündung im Gehirn und Fieber eine wichtige Rolle (Steiner et al., 2006a). Die Analyse der Expression solcher Gene ist ein guter Marker für den Grad des Entzündungsgeschehens im Gehirn. Darüber hinaus sind solche Mediatoren funktionell für die Entstehung von sickness behavior von großer Bedeutung. Dazu gehören neben Zytokinen selbst auch einer der wichtigsten terminalen Mediatoren für die Fieberentstehung und andere Krankheitssymptome nämlich PGE2 (Roth et al., 2009) sowie oxidativer Stress (Riedel et al., 2003). Im Zuge von Immunzellinvasion in das Gehirn als

zellulär gebundener Signalweg von der Peripherie zum Gehirn sind Chemokine, Adhäsionsmoleküle sowie Metalloproteasen entscheidend für die Attraktion, das Anheften und die Penetration/Extravasation von Immunzellen in das Gehirn und deshalb ebenfalls interessante und relevante Zielgene. Im Folgenden sollen solche Zielgene deshalb kurz näher erläutert werden, die bei der Untersuchung von Kommunikationswegen zwischen dem Immunsystem und dem Gehirn in der vorliegenden Arbeit von Bedeutung waren.

4.1. Zytokine

Zytokine kommen im gesunden Gehirn in niedrigen Konzentrationen vor (Pollmächer et al., 2002) und spielen zum Beispiel (IL-6 und IL-1β) für Gedächtniskonsolidierung eine wichtige Rolle bei normalen Gehirnfunktionen (Besedovsky and del Rey, 2011). Bei systemischen Entzündungsreaktionen kommt es zu einer zusätzlichen dramatischen Hochregulation und die entsprechenden Effekte zum Teil der gleichen Mediatoren wie IL-6, TNFα und IL-1β (Layé et al., 1994) führen zu völlig unterschiedlichen, in den meisten Fällen negativen Effekten (Besedovsky and del Rey, 2011; Pollmächer et al., 2002). Die meisten Zytokine zeigen also eine niedrige basale Expression im Gehirn, die akut nach Stimulation um ein Vielfaches erhöht werden kann und mittels quantitativer RT-PCR messbar ist. Die Detektion von Zytokinen auf der Proteinebene ist im Gehirn aufgrund der relativ gesehen immer noch niedrigen Konzentration immunhistochemisch oder per Western Blot häufig schwierig. Funktionell kann aber ihre Wirkung anhand einer Transkriptionsfaktoraktivierung dargestellt werden, auch wenn dies nicht unbedingt spezifisch für ein Zytokin sein muss. Alternativ kann in Überständen primärer Zellkulturen die Sekretion solcher Zytokine relativ unkompliziert bestimmt werden (Kapitel IV 1.2). Die Konzentrationen entsprechen dann allerdings nicht mehr den Verhältnissen *in vivo*. Anders als für periphere bzw. zirkulierende Zytokine nicht zuletzt mit Hilfe von Zytokin defizienten Mäusen, ist eine Fieber erzeugende Wirkung im Gehirn für IL-6, TNFα und IL-1β eindeutig bewiesen worden (Chai et al., 1996; Dinarello et al., 1991; Luheshi et al., 1993; Luheshi et al., 1997). Vor allem IL-1β im Gehirn ist ebenfalls ein wichtiger Mediator für die Entstehung von LPS-induzierter Anorexie (Bluthé et al., 2000; Laye et al., 2000).

4.2. Prostaglandinsyntheseweg

PGE2 spielt eine kritische Rolle für die Fieberentstehung (Ivanov and Romanovsky, 2004; Nilsberth et al., 2009b; Roth et al., 2006). Es induziert Fieber über Bindung an den EP3 Rezeptor(R) Subtyp im *Nucleus medianus praeopticus* (MnPO) (Lazarus et al., 2007).

Entsprechend ist die Konzentration des EP3R (Ek et al., 2000) und PG-Bindung (Matsumura et al., 1990) im MnPO besonders hoch. Prinzipiell stimmt die Literatur darin überein, dass im Gehirn gebildetes PGE2 zumindest für die späteren Phasen des Fiebers verantwortlich zu machen ist (Gaetano et al., 2010; Nakamura, 2011). Die initiale Phase der Fieberentstehung könnte Anteilig auch über PGE2 in Makrophagen der Lunge und Leber gebildet werden. Ein PGE2 Antiserum reduzierte beispielsweise die intitiale Fieberphase nach LPS-Stimulation (Steiner et al., 2006b). Eine kürzlich durchgeführte Studie konnte allerdings zeigen, dass die Aktivität der PG-produzierenden Enzyme bereits zu diesem Zeitpunkt aktiv ist und wahrscheinlich zentral gebildetes PGE2 wichtiger ist (Gaetano et al., 2010). Als Marker der Aktivierung des für die Entstehung von Krankheitssymptomen und der Kommunikation zwischen Immunsystem und Gehirn so wichtigen PG-Bildung kann die Sekretion von PGE2 im Blut oder der Zerebrospinalflüssigkeit bestimmt werden [Kapitel V 1.6, (Inoue et al., 2008)]. Die geschwindigkeitsbestimmenden Enzyme der PG-Synthese im Gehirn sind COX2 und die nachgeschaltete mPGES (Lacroix and Rivest, 1998; Nilsberth et al., 2009a; Oka et al., 2007; Turnbull et al., 2003; Vallières and Rivest, 1999). Dementsprechend wird die Detektion einer erhöhten Expression dieser beiden so wichtigen Enzyme ebenfalls als Marker der Aktivierung der PG-Synthese angesehen (Gaetano et al., 2010; Inoue et al., 2002; Lacroix and Rivest, 1998) und wurde auch in dieser hier vorliegenden Arbeit mit Hilfe von RT-PCR und Immunhistochemie (Kapitel V 1.1, 1.3, 1.4, 1.5, 1.6, 1.8, 1.9, 1.11, 1.12, 1.13) oder in situ Hybridisierung (Kapitel V 1.11) eingesetzt. Außerdem stellt die Verwendung von nicht steroidalen Entzündungshemmern aus der Gruppe der Zyklooxygenasehemmer eine Möglichkeit dar, physiologisch die Wirkung von PGE2 zu hemmen und die entsprechenden Effekte aufzuzeichnen. In der vorliegenden Arbeit wurde hierfür bei Meerschweinchen ein nicht selektiver Inhibitor (Diclofenac) und ein selektiver Inhibitor für COX2 (Nimesulid) verwendet (Kapitel V 1.11) sowie ein präferentieller COX2 Inhibitor bei Ratten (Meloxicam, Kapitel V 1.6).

4.3. Marker für Zellinvasion in das Gehirn

Es gibt eine Reihe von Chemokinen, die mehr oder weniger spezifisch für die Attraktion von Subtypen an Immunzellen zu sein scheinen. In der recht komplizierten Nomenklatur der Chemokine in 4 Subfamilien bestehen weiterhin die Originalnamen der Erstbeschreibung verschiedener wichtiger Chemokine (Thorpe, 2002). Das ersten Paar an Zysteinmolekülen (Gruppe C-C) kann durch eine (Gruppe C-x-C) oder drei Aminosäuren (Gruppe C-x_3-C) getrennt sein oder es fehlt ein Zystein (Gruppe C). In den vorliegenden Studien wurde das

Makrophagen spezifische Chemokin monocyte chemoattractant protein 1 (MCP1) oder auch CC Ligand (L)2 genannt sowie die für neutrophile Granulozyten der Maus relativ spezifischen Chemokine KC (CXCL1) und MIP2 (CXCL2) (Kielian et al., 2001) als Marker der aktivierten Attraktion von Immunzellen in das Gehirn untersucht (Kapitel V 1.7, 1.9). Für alle drei untersuchten Chemokine (KC, MIP2 und MCP1) konnte in früheren Studien eine erhöhte LPS/IL-1β induzierte Expression nachgewiesen werden (Rovai et al., 1998; Thibeault et al., 2001). Neben Chemokinen sind im nächsten Schritt der Extravasation von Immunzellen im Gehirn Adhäsionsmoleküle von großer Bedeutung. Zur Untersuchung der experimentell LPS-induzierten Invasion von neutrophilen Granulozyten war eine 50% Reduktion bei intercellular adhesion molecule (ICAM)1 defizienten Mäusen erzielt worden (Bohatschek et al., 2001). Dieses wurde deswegen auch hier als Markergen für die vorliegenden Untersuchungen verwendet. Schließlich ist eine gewisse Öffnung der Blut-Hirn-Schranke und Degradation extrazellulärer Matrix bei Extravasation notwendig, damit Zellen in das Gehirngewebe eindringen können (Rosenberg et al., 2007). Enzyme aus der Gruppe der Matrix-Metalloproteinasen (MMPs) spielen bei diesen Prozessen eine entscheidende Rolle und werden bei Infektion und Inflammation vermehrt gebildet und durch endogene tissue inhibitors of MMPs (TIMP) in ihrer Aktivität reguliert (Pagenstecher et al., 2000). TIMP1 scheint hierbei eine besondere Bedeutung zu haben und zum Beispiel eine kontrollierende Rolle bei experimenteller autoimmuner Enzephalitis (EAE) zu spielen (Crocker et al., 2006). In zwei Teilstudien wurden Hinweise einer Beteiligung von Leptin bei LPS-induzierter Invasion von Immunzellen in das Gehirn untersucht und deshalb Chemokine, Adhäsionsmoleküle und Metalloproteinasen als Zielgene untersucht (Manuskripte Kapitel V 1.7, 1.9).

4.4. Oxidativer Stress

Wie erwähnt ist oxidativer Stress auch als Mechanismus im Rahmen der Fieberentstehung beschrieben worden (Riedel et al., 2003). Proliferator-activated receptor (PPAR)γ coactivator (PGC)1α wird als der zentrale Regulator von oxidativem Stress bezeichnet, aktiviert nuclear respiratory factor (NRF)1 und erhöht die Expression von mitochondrial transcription factor A (TFAM). Dies führt schließlich zu einer vermehrten DNA-Synthese und gesteigerten Duplikation der Mitochondrien (Vina et al., 2009). Diese Marker von mitochondrialer Biosynthese / oxidativem Stress werden im Gehirn exprimiert (Cowell et al., 2007; Hertel et al., 2002). Einflüsse LPS-induzierter systemischer Entzündung auf die Expression dieser Moleküle im Gehirn sind allerdings bisher nicht bekannt. In einer Teilstudie wurde hier das

Potenzial eines möglichen NFκB-Inhibitors auf oxidativen Stress mit Hilfe dieser Marker im Gehirn getestet (Kapitel V 1.3).

5. Krankheitssymptome

Krankheitssymptome, die bei Mensch und Tier üblicher Weise bei systemischer Infektion und Inflammation mit Mikroben auftreten und mit Fieber einhergehen, werden als sickness behavior bezeichnet (Hart, 1988). Dies beinhaltet Lethargie (verringerte motorische Aktivität), Müdigkeit, Anorexie, Adipsie aber auch verändertes Schlafverhalten und verringerte Libido (Hart, 1988; Kent et al., 1992). Es handelt sich im Allgemeinen um eine präzise gesteuerte Reaktionen des Organismus, um die Infektion zu bekämpfen (Hart, 1988). Wichtig ist dabei, dass Mensch und Tier nicht als simple Konsequenz von Schwäche durch das Fieber eine Lethargie und verändertes Verhalten entwickeln. Sie sind vielmehr motiviert, sich krank zu verhalten (Holmes and Miller, 1963; Johnson, 2002). In Analogie zum Symptomkatalog, der zur Diagnose von Depressionen verwendet wird, wurde eine Parallele zwischen sickness behavior und Depression gezogen (Yirmiya et al., 1999). Depressionen könnten dabei einfach chronisch verlängerte Manifestationen von nicht kontrollierten unspezifischen Krankheitssymptomen darstellen; zumindest ist eine erhöhter Inzidenz von Depressionen unter anderem mit chronischen inflammatorischen Prozessen wie bei Immuntherapie und Altern assoziiert (Dantzer and Kelley, 2007). Ein besseres Verständnis der einzelnen Signalwege bei der Kommunikation des Immunsystems mit dem Gehirn bei Krankheiten dürfte auch hinsichtlich dieser Hypothese der Verbindung zwischen Depression und Inflammation neue Erkenntnisse bringen.

Neben diesen bei akuter Stimulation des angeborenen Immunsystems normaler Weise begrenzt andauernden Krankheitssymptomen können systemische Entzündungsreaktionen über besagten Signalweg bestehende krankhafte Prozesse im Gehirn zusätzlich verstärken und stellen deshalb ein großes Problem dar. In der vorliegenden Arbeit sind die hier stressfrei aufgezeichneten Krankheitssymptome Fieber, Anorexie, Adipsie und Lethargie außerdem als physiologische Endpunktparameter verwendet worden, um Mechanismen der Kommunikation wie betroffene Gehirnstrukturen (zum Beispiel CVOs oder das Gehirnendothel) und Mediatoren (IL-6, Leptin, PGE2) zu untersuchen und das Potenzial von Nebenwirkungen induziert durch verschiedene PAMPs zu definieren bzw. abzuschätzen (MALP2, PIPC, Imiquimod).

5.1. Fieber

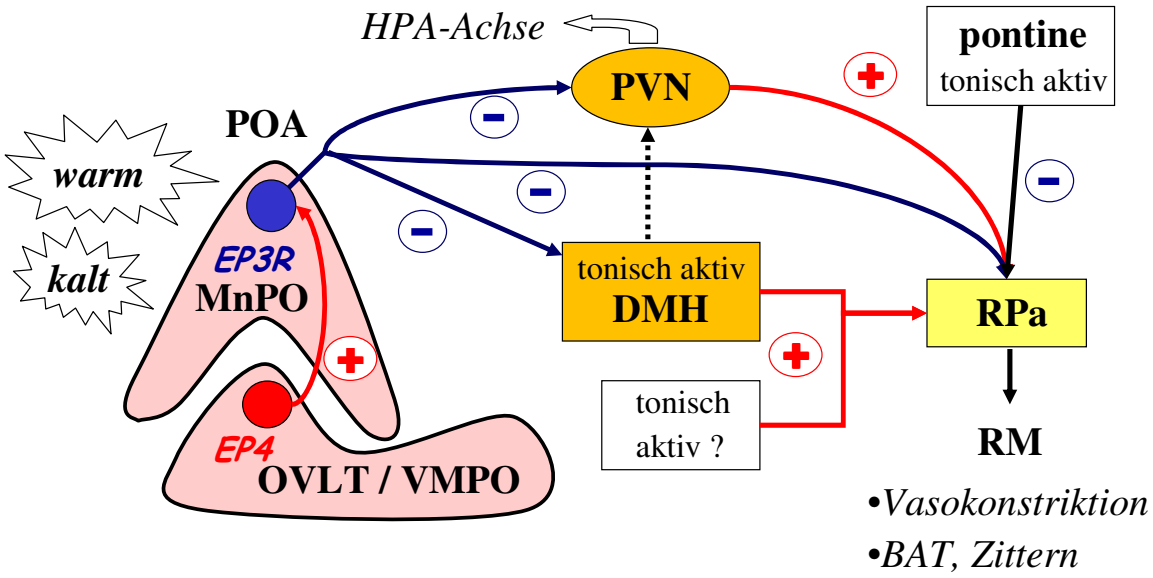


Abbildung 5
Vereinfachte schematische Darstellung der zentralen Verschaltungen bei der Fieberentstehung. Neurone aus der präoptischen Region (POA) steuern die zentralnervöse Fieberentstehung. Aus dem *Nucleus medianus praeopticus* (MnPO) aber auch teilweise aus der lateralen und medialen präoptischen Region (nicht dargestellt) inhibieren GABAerge Verbindungen tonisch den *Nucleus paraventricularis* (PVN) sowie den *Nucleus dorsomediales hypothalami* (DMH) und geben zusätzlich hemmende Bahnen an den *Nucleus raphe pallidus* (RPa) in den Hirnstamm. Der DMH und PVN hingegen besitzen tonisch aktivierende Verbindungen zum RPa, der Gehirnregion, wo präsympathische Neurone ihren Ursprung nehmen und zusammen mit den somatischen Efferenzen schließlich die Thermoeffektororgane ansteuern [Vasokonstriktion, Braune Fettgewebe (BAT), Zittern der Muskulatur (somatisch innerviert)]. Kältesignale aus der Peripherie sowie Prostaglandin E2 (PGE2) hemmen Neurone in der POA und vor allem im MnPO und führen dadurch zu einer Desinhibition der tonischen Aktivierung von Effektororganen und damit zu Hyperthermie bzw. Fieber. Zusätzlich gibt es in der pontinen Region eine tonische Inhibition des RPa, was wie eine zusätzliche „Bremse“ zu wirken scheint. PGE2 wirkt über den EP3R Fieber-induzierend durch Hemmung von MnPO (und OVLT) Neuronen. Eine PGE2 vermittelte EP4R-Aktivierung im *Organum vasculosum laminae terminalis* (OVLT) oder dem *Nucleus ventromedialis praeopticus* (VMPO) können die Inhibition des DMH verstärken. Fieberreaktionen gehen über den PVN ebenfalls mit einer Aktivierung der Hypothalamus-Hypophysen-Nebennierenrinden(HPA)-Achse einher. Modifiziert nach (Lazarus, 2006; Nakamura, 2011; Yoshida et al., 2009) sowie Kongressmitteilungen vom PPTR 2006 Symposium in Phoenix, Arizona.

Fieber wird prinzipiell als adaptiv betrachtet solange es nicht zu hoch ist und der Wirt nicht zu geschwächt ist (Blatteis, 1986). So wurde bei Mensch und Tier festgestellt, dass bei bakteriellen Infektionen die Überlebensraten höher lagen, wenn sich Fieber entwickeln konnte (Kluger and Vaughn, 1978; Mackowiak et al., 1980). Das Wachstum bestimmter Bakterien

kann reduziert werden, weil die höhere Temperatur (Miyamoto et al., 1995) und der Eisengehalt (Kluger and Rothenburg, 1979) ein Wachstum nicht mehr favorisieren. Außerdem steigt die Immunzellaktivität mit erhöhter Temperatur an (Rosenspire et al., 2002). Hier soll nun kurz der heutige Stand des zentralen neuronalen Netzwerkes skizziert werden, der für die vielfältigen mikroneuroanatomischen Untersuchungen in der hier vorliegenden Arbeit von besonderer Bedeutung ist (Abbildung 5).

Das Prinzip der zentralen Regulation der Abläufe bei der Entstehung von Fieber beruht auf einem Mechanismus der Disinhibition wie bereits 1870 durch Ott postuliert worden war (Bartfai and Conti, 2010). Fieber wird letztendlich durch PGE2 ausgelöst, welches im Endothel und durch perivaskulären Makrophagen gebildet wird (Matsumura and Kobayashi, 2004; Schiltz and Sawchenko, 2003) und als fettlöslicher Mediator im Bereich des MnPO durch die BBB zu den entsprechenden Neuronen gelangt. Dort hemmt es über den EP3 Rezeptor durch eine Erniedrigung der cAMP-Level Neurone, die zum *Nucleus dorsomediales hypothalami* (DMH) und zum *Nucleus raphe pallidus* (RPa) (Lazarus et al., 2007) projizieren. Damit wird die vegetative und somatische efferente Verschaltung vom DMH und RPa zu den thermoregulatorischen Effektoren disinhibiert und es kommt zu Wärmeeinsparung- (Vasokonstriktion) und Wärmebildung (zitterfreie Thermogenese, Zittern, erhöhter Stoffwechsel), also zu einer Erhöhung der Körperkerntemperatur; Fieber (Bartfai and Conti, 2010; Nakamura, 2011).

In den letzten 10 Jahren sind besonders viele neue Erkenntnisse über die zentrale Verschaltung der für Fieber bedeutenden Gehirnregionen mit neuen methodischen Ansätzen wie neuroanatomischen Untersuchungen, retrogradem transsynaptischen Tracing und chemischen und elektrischen Ablationsversuchen gewonnen worden (Manuskript Kapitel 1.8) (Nakamura, 2011). Hierbei sind nicht zuletzt einige für die Fieberentstehung zentrale Gehirnstrukturen zu nennen, die in der vorliegenden Arbeit ebenfalls neuroanatomisch anhand von Transkriptionsfaktoraktivierung sowie Expression wichtiger Zielgene (zum Beispiel COX2 und mPGES) untersucht worden sind. Dazu gehören das sensorische CVO *Organum vasculosum laminae terminalis* (OVLT), der *Nucleus ventromedialis praeopticus* (VMPO), der *Nucleus medianus praeopticus* (MnPO) und der *Nucleus raphe pallidus* (RPa). Ihre entsprechende Bedeutung in der Fieberentstehung geht aus Abbildung 5 hervor. Es bleibt zu bemerken, dass der vielfach postulierte Sollwert im Hypothalamus als Referenzwert des thermoregulatorischen Regelkreises bisher nicht gefunden wurde und höchst wahrscheinlich gar nicht existiert. Vielmehr gibt es eine so genannte Zwischenschwellenzone („balance

point“), die aus den vielen unabhängigen Regelkreisen der einzelnen Effektorsysteme mit unterschiedlichen Schwellenwerten gebildet wird (Romanovsky, 2007; Sessler, 1993).

5.2. Anorexie

Wie Fieber scheint akute Anorexie ein adaptiver Prozess als Antwort auf Infektion und Inflammation darzustellen. So sterben Tiere häufiger und früher, wenn sie bei Infektion einer Zwangsfütterung unterzogen werden und nicht „selbstmotiviert“ ihre Futteraufnahme reduzieren bzw. einstellen können (Murray and Murray, 1979). PAMPs und Zytokine (IL-1β, TNFα, IL-6 und INFγ) sind an der Vermittlung von Infektion bedingter Anorexie beteiligt (Arsenijevic et al., 2000; Langhans and Hrupka, 1999; Langhans et al., 1993; Laye et al., 2000; Moldawer et al., 1987). TNFα, welches klassisch auch zunächst als Cachexin bekannt wurde, ist einer der wichtigsten Mediatoren bei Krebs begleitender Anorexie (Oliff et al., 1987; Smith and Kluger, 1993; Tracey et al., 1988). Ob einiger synergistischer Wirkungen von Zytokinen (Sonti et al., 1996) und der Komplexizität der Mechanismen bei der Interaktion mit dem Immunsystem sowie endokrinen und metabolischen Einflüssen, sind die Signalwege der Anorexieentstehung zum Teil nicht geklärt (Asarian and Langhans, 2010). In einer Studie konnte gezeigt werden, dass LPS-induzierte Anorexie eher durch direkte Effekte von LPS auf das Gehirn vermittelt zu sein scheint. In knochenmarksupprimierten MyD88 KO Mäusen, die mit Wildtyp-Immunzellen substituiert worden waren, konnte keine nennenswerte Anorexie nach Gabe von LPS induziert werden (Wisse et al., 2007). Eine wichtige Wirkung von LPS direkt auf das Gehirn ist demnach anzunehmen, da ansonsten eine Immunzellsubstitution mit einer Wiederherstellung von LPS-induzierter Anorexie hätte einher gehen müssen. Dennoch konnte in anderen Studien durch Neutralisierungsstrategien gezeigt werden, dass zentrales IL-1β und zirkulierendes IL-6 eine wichtige Rolle bei LPS-induzierter Anorexie spielen (Bluthé et al., 2000; Harden et al., 2011; Laye et al., 2000). Hierbei scheinen vor allem eine Dosisabhängigkeit sowie eine unterschiedliche Sensitivität von Gehirnstrukturen auf die einzelnen Mediatoren (zum Beispiel IL-6, PGE2) von Bedeutung zu sein. Wie auch bei Fieber ist neben NO (Borner et al., 2012; Riediger et al., 2010) PGE2 einer der wichtigsten terminalen Mediatoren bei LPS-induzierter Anorexie (Asarian and Langhans, 2010; Pecchi et al., 2009). Dies hebt die Bedeutung eines besseren Verständnisses der Signalwege zur Bildung von PGE2 im Gehirn zusätzlich hervor; ein zentraler Bestandteil der hier vorliegenden Arbeit in mehreren Teilstudien (Manuskripte Kapitel V 1.1, 1.2, 1.3, 1.4, 1.5, 1.6, 1.9, 1.11, 1.12).

Neben dem humoralen Signalweg gibt es auch Hinweise für einen neuronalen Weg über den *N vagus* für IL-1β/LPS-induzierte Anorexie (Maier et al., 1998), da subdiaphragmale Vagotomie in einer Studie Anorexie zu vermindert vermochte (Bret-Dibat et al., 1995). Außerdem war eine direkte Aktivierung von vagalen Affarenzen durch IL-1β beschrieben worden (Goehler et al., 1998; Kurosawa et al., 1997). Trotzdem ist hier die Literatur recht uneinheitlich; andere Studien konnten keine vagale Beteiligung bei entzündungsbedingter Anorexie nachweisen (Porter et al., 1998; Schwartz et al., 1997). Interessanter Weise sind neben anderen gastrointestinalen Hormonen auch Rezeptoren für das Appetit regulierende Hormon Leptin auf dem Vagusnerv vorhanden und dieser kann sogar durch Leptin aktiviert werden (Gaige et al., 2002; Peters et al., 2006; Wang et al., 1997b). Injektion von Leptin in die Gefäßversorgung zum Magen reduzierte außerdem akut die Futteraufnahme in den ersten 24 Stunden nach Stimulation (Peters et al., 2005). Eine Beteiligung von Leptin an LPS-induzierter Anorexie konnte mit Hilfe eines spezifischen Antiserums, welches endogenes zirkulierendes Leptin neutralisiert, gezeigt werden (Harden et al., 2006; Sachot et al., 2004). Ob Leptin möglicherweise auch über den Vagusnerv an länger anhaltenden Effekten LPS-induzierter Anorexie beteiligt ist, war allerdings unklar und sollte in einer Teilstudie untersucht werden (Manuskript Kapitel V 1.10).

6. Überernährung und Krankheit

In einer Zeit, in der Überernährung und die damit verbundenen Krankheitsrisiken zu einem immer größeren Problem in den Industrienationen wird und Hunger weiterhin in anderen Teilen der Erde zu beklagen ist, sind Einflüsse des Ernährungszustandes auf die Gesundheit bzw. auf Krankheiten von großem Interesse (Könner and Bruning, 2011). Nicht zuletzt hat der Energiehaushalt, der natürlich bei der Thermoregulation eine wichtige Rolle spielt, Einflüsse auf den Gesundheitszustand (Engineer and Garcia, 2012). Beispielsweise sind in England ca. 25% aller Erwachsenen fettsüchtig (Rennie and Jebb, 2005) und für die USA wurde prognostiziert, dass bis 2015 41% aller Erwachsenen übergewichtig sein könnten (Wang and Beydoun, 2007). Auch bei Haustieren wie Hunden und Katzen steigt der Anteil übergewichtiger Tiere auf ca. 30% (German et al., 2010). In der vorliegenden Arbeit befassen sich drei Teilstudien mit dem Appetit hemmenden und Energiehaushalt regulierenden Hormon Leptin (Manuskripte Kapitel V 1.7, 1.9, 1.10), welches hauptsächlich im Fettgewebe gebildet wird und entsprechend dem Fettgehalt bei Fettsucht in größeren Mengen in der Zirkulation vorkommt (Considine et al., 1996b; Friedman, 2002; Maffei et al., 1995).

6.1. Obesitas

Zwei spontane Mutationen bei Mäusen von den Jackson Laboratories, einem Großzüchter für Versuchstiere in den USA, führten zu fettsüchtigen Phänotypen bei diesen Mäusen (Hummel et al., 1966; Ingalls et al., 1950). Dabei handelt es sich um die so genannten ob/ob Mäuse, denen das Hormon Leptin fehlt und so genannte db/db Mäuse die defizient in der langen Form des Leptin-Rezeptors (ObRb) sind. Im Gegensatz zu verschiedenen Tiermodellen für Obesitas, sind bei Menschen genetische Defekte im Leptin Rezeptor nicht bekannt (Considine et al., 1996a) und ein absoluter Leptinmangel mit weniger als ca. 20 bekannten Fällen weltweit (Farooqi et al., 2002; Ozata et al., 1999) ist ungewöhnlich selten (Maffei et al., 1996). Vielmehr ist Übergewicht bei Menschen mit erhöhten Konzentrationen von Plasma-Leptin-Spiegeln und damit einer so genannten Resistenz unter anderem durch verringerten Transport in das Gehirn (Banks, 2004) sowie veränderter Leptin-Signalkaskade (Myers et al., 2008) oder Insuffizienz von Leptin, die Nahrungsaufnahme zu hemmen und den Energieumsatz zu steigern, verbunden (Engineer and Garcia, 2012). Nur in den wenigen Ausnahmen einer Fettsucht durch Leptin-Defizienz konnten bisher beeindruckende Therapieerfolge mit Leptin bei Menschen erzielt werden (Farooqi et al., 2002).

Übergewicht bei Mensch und Tier wurde unter anderem mit erhöhter Anfälligkeit für Infektionen, Diabetes, Osteoarthritis oder Bluthochdruck in Zusammenhang gebracht (German, 2006; Kopelman, 2000; Matarese et al., 2005) und ist verbunden mit einer unterschwelligen leichten systemischen Entzündungsreaktion (Trayhurn, 2005). Dabei ist gerade das Fettgewebe nicht mehr nur als Energiespeicher sondern auch als endokrines Organ in den Fokus der Forschung gerückt. Fettgewebe sondert die so genannte Gruppe der Adipokine ab, zu denen neben Zytokinen (z.B. IL-6 und IL-10) auch Akute-Phase-Proteine und natürlich Leptin gehören. Diese Mediatoren können eine ganze Reihe von Einflüssen auf biologische Systeme wie Angiogenese, Appetit, Energiebalance aber auch Entzündungsreaktionen haben und treten vermehrt bei Fettsucht in der Zirkulation auf (Trayhurn and Wood, 2004). Für die erhöhte Bildung inflammatorischer Mediatoren werden verschiedene Ursachen in Betracht gezogen. Zum einen kann der Umstand, dass die wachsende Masse an Fettgewebe eine gewisse Hypoxie erfährt, zur erhöhten Inflammation beitragen (Trayhurn and Wood, 2004). Außerdem tritt eine erhöhte Einwanderung von Immunzellen wie Makrophagen in unterschiedlichste Gewebe wie dem Fettgewebe oder der Muskulatur bei Fettleibigkeit auf (Lumeng and Saltiel, 2011) und ist mit dem beobachteten Entzündungsgeschehen verbunden. Zum anderen scheinen gesättigte Fettsäuren als endogene

Liganden beispielsweise für TLR4 zu fungieren und dadurch die Verbindung von Fettsucht zu TLR4-vermittelter Inflammation herzustellen, obwohl auch eine Kontamination von Lipopeptiden möglicherweise in einigen Studien falsch positive Ergebnisse einer Beteiligung von Fettsäuren verursacht haben könnten (Könner and Bruning, 2011). Schließlich wurde auch in einigen Studien eine erhöhte Endotoxämie im Plasma von übergewichtigen Tieren oder Menschen festgestellt (Basu et al., 2011; Creely et al., 2007). Durch starke Fetteinlagerungen in der Darmbarriere erhöht sich die Durchlässigkeit für Bakterien (Brun et al., 2007) und dürfte zu der unterschwelligen Inflammation in fettsüchtigen Tieren und Menschen beitragen. Eine sich hieraus ergebende Hypothese besagt, dass erhöhte Spiegel des Adipokins Leptin bei Übergewicht assoziierten Erkrankungen eine wichtige Rolle spielen könnten.

6.2. Leptin

Leptin ist ein 16 kDa großes Peptid welches vor allem vom weißen Fettgewebe gebildet wird (Maffei et al., 1995) und 1994 als das verantwortliche Gen für die Fettsucht in ob/ob Mäusen identifiziert wurde (Halaas et al., 1995; Zhang et al., 1994). Dieses Hormone ist vor allem für seine Appetit hemmende und Energiehaushalt regulierende Funktion bekannt, spielt allerdings neben anderen Funktionen auch für das Immunsystem eine wichtige Rolle (La Cava and Matarese, 2004). Die Bedeutung von Leptin wurde nicht zuletzt durch viele Veränderungen in ob/ob und db/db Mäusen wie Immundefizienzen (Chandra, 1980; Fernandes et al., 1978), erhöhte Anfälligkeit für bakterielle Infektionen (Ikejima et al., 2005; Mancuso et al., 2002), oder Resistenz gegen autoimmune Erkrankungen (Busso et al., 2002; Matarese et al., 2001) in früheren Studien herausgearbeitet. Interessanter Weise können ähnliche Veränderungen ebenfalls durch Hungern bei Tieren induziert werden, ein komplexer physiologischer Zustand, der von einer dramatischen Verringerung an zirkulierendem Plasma-Leptin begleitet ist. Nach Leptinersatz in diesen Tieren sind die Veränderungen teilweise reversibel (Howard et al., 1999; Lord et al., 1998), was die Beteiligung von Leptin und nicht nur des veränderten physiologischen Zustands / Milieus bei Übergewicht an diesen Prozessen bestätigt (Myers et al., 2010). Leptin stellt also in gewisser Weise ein Verbindungsglied zwischen dem Ernährungszustand und Immunantworten auf pathogene Erreger dar (Friedman, 2002).

Leptin wirkt über sechs verschiedene Splicevarianten seines Rezeptors (ObRa-f) (Lee et al., 1996; Tartaglia, 1997; Tartaglia et al., 1995; Wang et al., 1996). Dabei besitzt nur die lange Form des Rezeptors nämlich ObRb zytosolische Bindungsstellen für mehrere

Signalwege. Der wichtigste hierbei ist ähnlich zu IL-6 der JAK/STAT3 Signalweg (Bjorbaek et al., 1997; Myers, 2004). Die genaue Funktion der kurzen Formen (ObRa) des Rezeptors sind nicht klar, obwohl eine Transportfunktion an der BBB oder eine Rolle beim Abbau von Leptin angenommen wird (Bjorbaek et al., 1998; Golden et al., 1997; Uotani et al., 1999). Zusätzlich gibt es noch eine lösliche Form des Rezeptors, der so genannte ObRe. ObRb und vor allem die kurzen Formen findet sich in vielen Geweben wie auch im Gehirn (Elmquist et al., 1998; Guan et al., 1997a) oder auf neutrophilen Granulozyten (Bruno et al., 2005). Ins Gehirn wird Leptin über spezifische Transportmechanismen aufgenommen und wirkt dort im *Nucleus arcuatus* (ARC) hemmend auf die Futteraufnahme und steigernd auf den Energieumsatz, nicht zuletzt über Aktivierung des vegetativen Nervensystems (Broberger, 2005; Friedman, 2002).

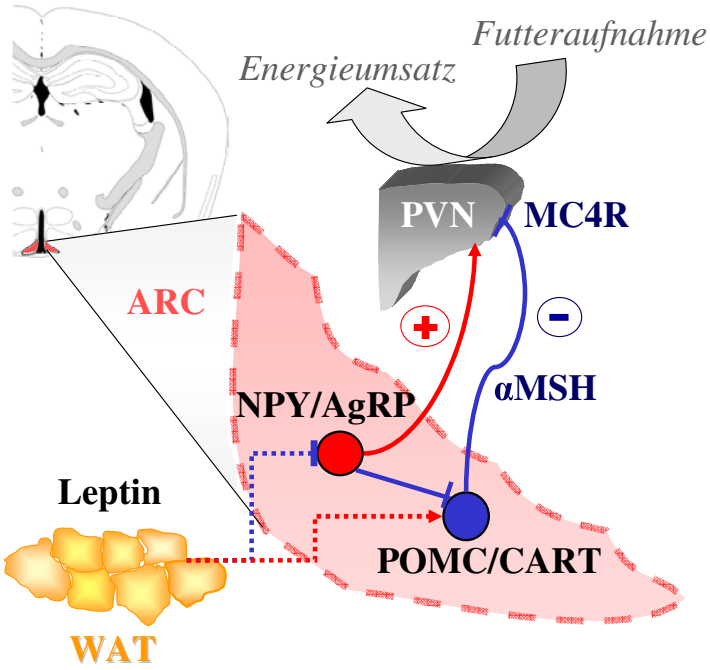


Abbildung 6

Schematische vereinfachte Skizze der Wirkung von Leptin auf das Melanocortin-System. Leptin wird entsprechend der Fettmenge im Körper in die Zirkulation abgegeben und gelangt über einen spezifischen Transport in den Hypothalamus und wirkt dort auf verschiedene Strukturen. Die wichtigste ist der *Nucleus arcuatus* (ARC), seitlich des dritten Ventrikels gelegen. Leptin hemmt dort Neuropeptid Y (NPY) / agouti-related peptide (AgRP) Neurone die ansonsten die Futteraufnahme fördern. Proopiomelanocortin (POMC) / cocain amphetamin related peptide (CART) Neurone werden gleichzeitig aktiviert und hemmen durch Abgabe von α Melanozyten stimulierendes Hormon (αMSH) über den Typ 4 Melanokortin Rezeptor (MC4R) ebenfalls die Futteraufnahme und fördern einen erhöhten Energieumsatz vor allem über den *Nucleus paraventricularis* (PVN). AgRP ist ein Antagonist des MC4R und NPY/AgRP Neurone hemmen POMC/CART Neurone. Modifiziert nach (Engineer and Garcia, 2012; Jovanovic and Yeo, 2010)

Die basalen Plasmakonzentrationen von Leptin liegen im Nanogrammbereich und zeigen einen ausgesprochenen zirkadianen, diurnalen Zyklus bei Ratten und Mäusen mit höchsten Konzentrationen am Ende der Nacht-Aktiv-Phase, nachdem entsprechend die meiste Futteraufnahme des Tages stattgefunden hat (Ahren, 2000; Ishihara et al., 2004; Sanchez et al., 2004).

Vereinfacht betrachtet (Abbildung 6), wird durch Leptin im ARC die Expression von Proopiomelanocortin (POMC) angeregt, was von einer Freisetzung der Folgeprodukte α Melanozyten stimulierendes Hormon (αMSH) und cocain amphetamin related peptide (CART) begleitet ist. αMSH bindet an den Typ 4 Melanokortin Rezeptor (MC4)-Rezeptor und vermittelt hierüber Anorexie und erhöhten Energieumsatz (Seeley et al., 2004). Gleichzeitig werden durch Leptin Futteraufnahme fördernde (orexigene) Neuropeptid Y (NPY) / agouti-related peptide (AgRP) Neurone gehemmt. Ein tonischer hemmender Feedback dieser Neurone wiederum auf POMC-Neurone favorisiert prinzipiell die Futteraufnahme (Engineer and Garcia, 2012). AgRP fungiert als endogener Antagonist des MCR4 (Lu et al., 1994). Die beiden Neuronengruppen des ARC stehen in Verbindung mit mehreren Gehirnstrukturen, zu denen auch der *Nucleus paraventricularis* (PVN) gehört. Neben dem Hirnstamm wirkt Leptin auch auf höhere Zentren des Gehirns und beeinflusst/hemmt dort unter anderem Belohnungssysteme, die mit Nahrungsaufnahme aktiviert werden (Jovanovic and Yeo, 2010). Über somatische (Trigeminus), vagale (zum Beispiel Magen) und sympathische (zum Beispiel Fettgewebe) Efferenzen werden schließlich die zentralen Wirkungen von Leptin in die Peripherie geleitet und regulieren unter anderem den Metabolismus (Gautron and Elmquist, 2011).

Neuere Erkenntnisse weisen darauf hin, dass Leptin allerdings auch als neuroimmuner Mediator wirken kann. Leptin wird einerseits bei LPS- oder Zytokin-stimulierter (IL-1β, TNFα) Entzündung in Mensch und Tier (Ratte, Hamster, Maus) vermehrt gebildet und die Zirkulation abgegeben (Berkowitz et al., 1998; Faggioni et al., 1998; Finck et al., 1998; Francis et al., 1999; Grunfeld et al., 1996; Landman et al., 2003; Sarraf et al., 1997). Andererseits stimuliert Leptin die Bildung verschiedener Zytokine durch Monozyten und Makrophagen (Gainsford et al., 1996; Loffreda et al., 1998). Im Gehirn konnte eine Leptin-induzierte Expression von IL-1β (Hosoi et al., 2002b; Luheshi et al., 1999; Wisse et al., 2004) zum Teil in perivaskulären Makrophagen (Inoue et al., 2006) und Mikroglia (Pinteaux et al., 2007) demonstriert werden. Die BBB überwindet Leptin anders als Zytokine wohl über einen spezifischen Transport (Banks et al., 1996) und kann dann auf hypothalamische Gehirnstrukturen (Hübschle et al., 2001b) und den Hirnstamm (Grill et al., 2002) wirken

(Münzberg et al., 2003; Mütze et al., 2007; Mütze et al., 2006). Entsprechend seiner Wirkung auf den Hypothalamus, konnte gezeigt werden, dass Leptin bei LPS-induzierter Anorexie aber auch bei Fieber eine Rolle zu spielen scheint (Harden et al., 2006; Sachot et al., 2004) und das wahrscheinlich über einen IL-1β- und Prostaglandin-abhängigen Mechanismus (Inoue et al., 2006; Luheshi et al., 1999). Die respektive Beteiligung und Bedeutung von Leptin an LPS-induzierter Aktivierung von Zellen im Gehirn ist allerdings unzureichend bekannt.

Die Rolle von Leptin als potentieller inflammatorischer Mediator bei Krankheiten ist nicht zuletzt für Zustände und Krankheiten von Bedeutung, die zum Beispiel bei Anorexie oder Essstörungen mit erhöhten (chronische Herzinsuffizienz- und Nierenerkrankungen, *Anorexia nervosa*) und erniedrigten Leptinkonzentrationen verbunden sind (Chronische obstruktive Lungenerkrankungen, Krebs, Esssucht) (Bluher and Mantzoros, 2004; Engineer and Garcia, 2012). Entsprechend wurde in drei Teilstudien dieser Arbeit auch die Rolle von Leptin als neuroimmuner Mediator bei der Kommunikation zwischen Immunsystem und Gehirn während Infektion und Inflammation näher untersucht.

Fragestellung zur wissenschaftlichen Arbeit:

„Mechanismen und Mediatoren der Kommunikationswege zwischen Immunsystem und Gehirn im Verlauf peripherer Entzündungsreaktionen“

Hier sollen kurz entsprechend des dargestellten Hintergrunds aus der Einleitung und des Schrifttums die wissenschaftlichen Fragestellungen zusammengefasst werden. Hieraus resultieren die entsprechenden Einzelprojekte der vorgelegten Arbeit.

A Mediatoren der Signalwege zur Kommunikation zwischen Immunsystem und Gehirn

- Welche Rolle spielen IL-6 und Leptin und TLR-Agonisten für den humoralen Signalweg und sind die Mediatoren an der Aktivierung des PG-Synthesewegs im Gehirn bei systemischer Entzündungsreaktion beteiligt?
- Spielt Leptin einer Rolle für den neuronalen Signalweg der Anorexieentstehung über den Vagusnerv bei systemischer LPS-induzierter Entzündung?
- Ist Leptin an einem über neutrophile Granulozyten vermittelten Immunzell-vermittelten Signalweg bei schweren systemischen Entzündungsreaktionen beteiligt?

B Genomische Aktivierung von Gehirnstrukturen / Zellphänotypen durch TLR-Agonisten, IL-6 und Leptin

- Welche räumlichen Aktivierungsmuster von Gehirnstrukturen gibt es?
- Wie ist der zeitliche Ablauf der Aktivierung von Gehirnzellen?
- Welche Zelltypen sind bei der Aktivierung beteiligt?
- Interagieren Mediatoren bei der Aktivierung von Zellen im Gehirn?
- Welche Stimuli führen zu einer Zellaktivierung?

C Welche Bedeutung haben aktivierte Transkriptionsfaktoren im Gehirn für:

- die Entstehung von Krankheitssymptomen?
- die Expression spezifischer Zielgene?
- die Entzündungsreaktion im Gehirn?
    - Aufrechterhaltung?
    - Hemmung?
- einen potentiellen therapeutischen Nutzen?

D Welche Bedeutung haben IL-6, Leptin und TLR-Agonisten als inflammatorische Mediatoren bei Krankheiten?

- Zirkulierendes IL-6; Leptin; TLR-Agonisten (Dosis, Applikationsweg)
- Therapieansätze

III. METHODEN

Untersuchungen von Veränderungen im Gehirn und deren Rolle im Gesamtorganismus; experimentelle Untersuchungen in Tiermodellen und Zellkultur. Die Einzelheiten können in den Manuskripten im Kapitel V entnommen werden.

1. Tiermodelle

Je nach wissenschaftlicher Fragestellung ist es notwendig unterschiedliche Versuchsmodelle zu verwenden. Für Untersuchungen der komplexen Interaktionen und Kommunikationswege des Gehirns mit dem Immunsystem können Daten zum Teil lediglich mit gezielter Versuchsanordnung *in vivo* ermittelt werden.

1.1. Meerschweinchen

In dieser Tierspezies wurden bereits einige wichtige Grundlagen für Kommunikationswege zwischen Immunsystem und Gehirn ermittelt (Goldbach et al., 1997; Ross et al., 2003; Ross, 2001; Ross et al., 2000; Rummel et al., 2004; Rummel et al., 2005b; Sachot et al., 2004). Über einen chronischen intraarteriellen Katheter können bei diesen Tieren stressfrei und wiederholt sowohl Substanzen appliziert als auch Blutproben gewonnen werden. Für zwei Teilstudien zur Charakterisierung des TLR3 Agonisten PIPC wurde deshalb diese Tierspezies verwendet (Manuskripte Kapitel V 1.11, 1.13).

1.2. Ratten

Ratten sind klassisch die Tierspezies der Wahl für neuroanatomische Untersuchungen und wurden in den meisten Teilstudien für unterschiedliche Untersuchungen verwendet. Darunter fallen zwei anspruchsvollere Versuchsanordnungen. In einer Studie wurde subdiaphragmale Vagotomie durchgeführt (Manuskripte Kapitel V 1.10). In fünf Teilstudien (Manuskripte Kapitel V 1.1, 1.4, 1.6, 1.12, 1.13) wurde als Stimulation die Injektion in eine präformierte subkutane Luftkammer als lokales Entzündungsmodell verwendet, welches auch Entnahmen von Proben (Lavage) aus diesem Kompartiment erlaubt. Die Vagotomie ermöglichte die Untersuchung der Beteiligung des neuronalen Signalwegs und beinhaltet einen besonders anspruchsvollen chirurgischen Eingriff und sorgfältige postoperative Nachsorge. In einer Teilstudie ist ein spontan hypertensiver Rattenstamm (SHR) sowie seine genetischer Kontrollstamm (Wistar Kyoto, WKY) verwendet worden, weil SHR-Ratten eine CD36-

Defizienz besitzen und zur Untersuchung der Rolle von CD36 als PRR verwendet wurden (Manuskript Kapitel V 1.2).

1.3. Mäuse

In drei Teilstudien wurden Mäuse als Tiermodell verwendet, weil genetisch modifizierte Tiere als „goldener Standard“ zur funktionellen Untersuchungen von Mediatoren und Mechanismen gelten. Hierunter fallen TLR2 defiziente Mäuse (Kapitel V 1.2), db/db (ObRb defizient) und ob/ob Mäuse (Leptin defizient, Manuskripte Kapitel V 1.7), sowie IL-6KO (IL-6 defizient) Mäuse (Kapitel V 1.9). Prinzipiell ist zu bedenken, dass kompensatorische Mechanismen bei diesen Mäusen den Phänotyp immer beeinflussen können und nicht unbedingt isoliert die Funktion des fehlenden Gens widerspiegeln müssen (siehe auch „Technical considerations“ Kapitel V 1.9). In ob/ob Mäusen wurde als Kontrollversuch Leptin mit Hilfe so genannter subkutan implantierter osmotischer Pumpen ersetzt. Außerdem wurde in dieser Studie ein 48-stündiges Fasten als Modell für Zustände dramatisch reduzierte Leptinwerte bei Hungern verwendet (Kapitel V1.10).

1.4. Stimulation der Versuchstiere; physiologische Parameter

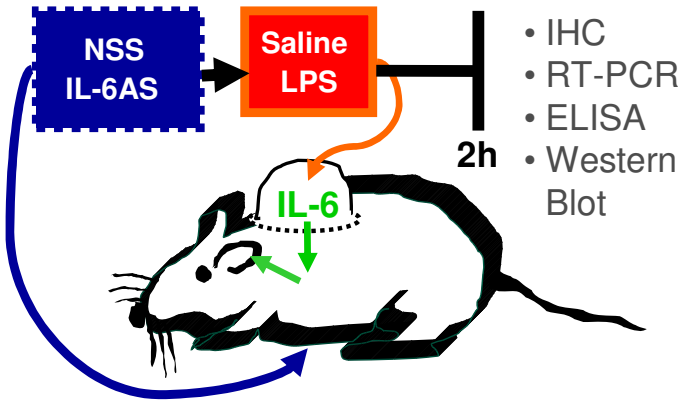


Abbildung 7

Schematische Darstellung eines Versuchsprotokolls hier beispielhaft für Manuskripte aus Kapitel V: 1.12 und 1.4. Ratten wurden mit IL-6-Antiserum (IL-6AS) oder Kontrollserum (normal sheep serum, NSS) 4 Stunden vor Stimulation mit LPS oder Lösungsmittel (physiologische Kochsalzlösung, Saline) vorbehandelt. Die Stimulation erfolgte in die subkutane Luftkammer, in der LPS-stimuliert eine große Menge an IL-6 gebildet wird, welches in die Zirkulation entweicht und auf das Gehirn wirken kann (grüne Pfeile). Das IL-6AS neutralisiert endogenes zirkulierendes IL-6. Damit kann der Beitrag von IL-6-vermittelter an LPS-induzierter Wirkung auf das Gehirn ermittelt werden. In diesem Fall wurden Tiere 2 Stunden nach Stimulation perfundiert und Gewebe (Gehirn, Leber, Milz, braunes, weißes Fettgewebe) sowie Lavage aus der Luftkammer und Blut für weitere Analysen entnommen (Immunhistochemie, IHC und weitere).

Bei der Stimulation bzw. Behandlung von Versuchtieren sind neben dem Applikationsweg, die gewählten Dosierungen von entscheidender Bedeutung und den einzelnen Publikationen mit jeweiliger Begründung zu entnehmen (Kapitel V). Für intraperitoneale (i.p.), intraarterieller (i.a.) und subkutane (s.c.) Applikation wurden neben der Injektion von Zytokinen (IL-6, Manuskripte Kapitel V 1.12), Leptin (Manuskripte Kapitel V 1.7, 1.10) und TLR-Agonisten (LPS, PIPC, MALP2 und Imiquimod; Manuskripte Kapitel V 1.1, 1.2, 1.3, 1.4, 1.5, 1.6, 1.7, 1.9, 1.10, 1.11, 1.12, 1.13) auch spezifische Zytokinantiseren gegen IL-6 (Manuskripte Kapitel V 1.12; Abbildung 7) und Leptin (Manuskripte Kapitel V 1.9, 1.7) und nicht steroidale Antiphlogistika (NSAIDs; Manuskripte Kapitel V 1.6, 1.11) verwendet. Wahrend der Stimulation wurde in den meisten Fällen mittels telemetrischer Systeme die Futter- und Wasseraufnahme, motorische Aktivität, und abdominale Körpertemperatur stressfrei und kontinuierlich aufgezeichnet. Neben diesen physiologischen Parametern sind weitere Analysen des nach Perfusion gewonnenen biologischen Materials (Blut / Plasma, Leber / Milz, Gehirne / Hypophyse und Fettgewebe) durchgeführt worden, um funktionelle Aussagen über die dazu korrelierenden physiologischen Effekte zu ermitteln.

2. Primäre Zellkultur

Zur direkten Analyse der Wirkung eines Naturhemmstoffs für NFκB auf Zellen des Gehirns wurden primäre neurogliale Kulturen des OVLT angefertigt und in den Überständen die Zytokinantwort auf LPS mit und ohne den Hemmstoff untersucht (Manuskript Kapitel V 1.3, Parthenolid). Außerdem wurde zur Bestätigung der *in vivo* Daten eine primäre Kultur von peritonealen Makrophagen hergestellt. Diese Kultur der beiden Rattenstämme SHR und WKY wurden mit LPS und MALP-2 stimuliert und die Zytokinantwort in den Überständen analysiert (Manuskript Kapitel V 1.2).

3. Analysemethoden des biologischen Materials

Neben den physiologischen Parametern, die mit Hilfe der Interventionsstudien im Tier gewonnen wurden, sind insbesondere detaillierte qualitative und quantitative mikroneuroanatomische Untersuchungen in den Gehirnen der verschiedenen Spezies durchgeführt worden. Folgende Analysemethoden sind zur Bearbeiten der einzelnen Teilstudien verwendet worden: IL-6-, TNFα-Bioassays; ELISAs; Immunhistologie / Immunfluoreszenz; Western Blot; konventionelle semiquantitative RT(reverse Transkription)-PCR und quantitative Real-Time PCR, in situ Hybridisierung.

IV. ZUSAMMENFASSENDE DISKUSSION

1. Wirkung von TLR-Agonisten, IL6 und Leptin auf genomische Aktivierungen im Gehirn

Verfügbares Wissen über das differenzierte Potenzial einer direkten Wirkung von PAMPs auf das Gehirn ist bisher unzureichend und bedarf weiterer Untersuchungen (Sternberg, 2006). In der vorliegenden Arbeit wurde die Wirkung der TLR-Agonisten LPS, PIPC, MALP2 und Imiquimod sowie speziell des Zytokins IL-6 und des Hormons Leptin *in vivo* auf genomische Aktivierung von Gehirnstrukturen und Zellen zunächst qualitativ und in ausgewählten Fällen auch semi-quantitativ und quantitativ immunhistologisch in mikroneuroanatomischen Untersuchungen analysiert. Unterstützend wurden die Ergebnisse auf Proteinebene auch mit Western Blot untersucht und die Expression spezifischer Marker der Aktivierung von inflammatorischen Transkriptionsfaktoren mittels RT-PCR relativ quantifiziert (SOCS3 für STAT3, IκBα für NFκB und Trib1/NF-IL6 für NF-IL6, siehe Kapitel II 3).

1.1. STAT3 und NF-IL6-Aktivierung im Gehirn

In früheren Studien wurden bereits exogene (z.B. LPS) und endogene (z. B. IL-1β, Leptin) Mediatoren/Pyrogene verwendet, um Aktivierungsprofile von einzelnen Gehirnstrukturen und Zellphänotypen mittels STAT3-Immunhistochmie (IHC) (Gautron et al., 2002; Gautron et al., 2003; Harré et al., 2003; Harré et al., 2002; Hübschle et al., 2001a; Hübschle et al., 2001b; Rummel et al., 2004; Rummel et al., 2005b) und NFκB-IHC (Nadjar et al., 2005b) sowie SOCS3- (Lebel et al., 2000) und IκBα- (Laflamme et al., 1999; Laflamme and Rivest, 1999) *in situ* Hybridisierung zu ermitteln. Dabei konnten bereits wichtige funktionelle Hinweise für die Bedeutung einzelner Gehirnregionen bei der Kommunikation des Immunsystems mit dem Gehirn gewonnen werden. Zwei besondere Zielstrukturen, die sich hierbei herauskristallisiert haben, liegen im Grenzbereich zwischen Gehirn und Peripherie nämlich die CVOs mit einer unvollständigen BBB und die BBB selbst. Drei Fragen sollen hier nun zur weiteren Aufklärung in der vorliegenden Arbeit beantwortet werden:

- Führen auch andere TLR-Agonisten als LPS wie PIPC, MALP2 und Imiquimod zu STAT3-Aktivierung und wie sieht das Aktivierungsmuster aus?

- Sind IL-6 und Leptin an LPS-induzierter STAT3-Aktivierung im Gehirn beteiligt; welche endogenen Mediatoren sind möglicherweise bei anderen TLR-Agonisten beteiligt?
- Ist eine IHC detektierte nukleäre NF-IL6-Translokation ein weiterer / alternativer Marker der Aktivierung von Zellen im Gehirn und wenn ja aktiviert durch welche Mediatoren?

1.1.1. TLR-Agonisten

1.1.1.1. STAT3 Aktivierung

Alle PRRs der untersuchten TLR-Agonisten werden im Gehirn exprimiert (Letiembre et al., 2007; Olson and Miller, 2004) und in bestimmten Regionen auch während inflammatorischen Stimuli in ihrer Expression hoch reguliert [TLR2, (Laflamme et al., 2001)] oder herunter reguliert [TLR4, (Laflamme and Rivest, 2001). Ihre funktionelle Rolle und zelluläre Verteilung ist allerdings vielfach noch unbekannt.

1) LPS induzierte in den hier vorliegenden Studien eine starke STAT3-Aktivierung in den sensorischen zirkumventrikulären Organen (sCVO), zu denen die *Area postrema* (AP) das OVLT und das *Organum subfornicale* (SFO) gehören, sowie im Gehirnendothel und einigen anderen hypothalamischen und extrahypothalamischen Gehirnstrukturen der Maus und Ratte (Manuskripte aus Kapitel V 1.9 und 1.12). Diese Ergebnisse bestätigen prinzipiell frühere Untersuchungen in Ratten und Meerschweinchen (Gautron et al., 2002; Harré et al., 2002; Rummel et al., 2004; Rummel et al., 2005b) und weisen auf ein Spezies konserviertes STAT3-Aktivierungsmuster nach LPS-Stimulation hin. Da LPS prinzipiell nicht über den STAT3-Signalweg wirkt und die LPS-induzierte STAT3-Aktivierung mit zirkulierenden IL-6-Plasmaspiegeln korreliert (Roth et al., 2004b), IL-6-Rezeptoren im Gehirn nach LPS-Stimulation unter anderem in den sCVOs exprimiert werden (Vallières and Rivest, 1997) und IL-6 ein ähnliches STAT3-Aktivierungsmuster erkennen lässt (Harré et al., 2003; Rummel et al., 2005b), ist eine Beteiligung von IL-6 an LPS-induzierter STAT3-Aktivierung postuliert worden (Gautron et al., 2002; Harré et al., 2002; Rummel et al., 2004). Bisher war auch für einen TLR9-Agonisten (Bakterielle DNA, **CpG-DNA**) ebenfalls ähnlich zu den Ergebnissen nach LPS-Stimulation eine Aktivierung in den sensorischen CVOs beschrieben (Sako et al., 2005) und eine Beteiligung von entweder zirkulierendem IL-6 oder im Gehirn gebildeten IL-6 an der STAT3-Aktivierung postuliert worden. Systemische CpG-DNA-Gabe erhöhte beispielsweise Plasma IL-6 und IL-10 Werte (Schwartz et al., 1999).

2) Zum ersten Mal wurde im Rahmen dieser hier vorliegenden Arbeit STAT3-IHC als Marker für Aktivierungen im Gehirn auch für weitere TLR-Agonisten getestet. Mit dem viralen Analog und TLR3-Agonisten **PIPC** konnte ebenfalls eine ähnliche Aktivierungsverteilung in den sCVOs, in Astrozyten und vor allem auch dem Gehirnendothel identifiziert werden (Kapitel V 1.11). Systemische Stimulation mit PIPC ist wiederum auch von erhöhten zirkulierenden Konzentrationen and IL-6 aber auch TNFα und Interferonen begleitet [(Alexopoulou et al., 2001; Fortier et al., 2004), Kapitel V 1.13], die ursächlich an der STAT3-Aktivierung beteiligt sein könnten.

3) Weiterhin konnten wir feststellen, dass der TLR2/6-Agonist **MALP2** eher zu einer moderaten STAT3-Aktivierung in gleichen Gehirnregionen führte (Kapitel V 1.2, 1.6), die i.p. etwas stärker ausfiel als s.c. und entsprechend wie in vorgehenden Studien ermittelt, von zirkulierenden Plasmakonzentrationen von IL-6 und Krankheitssymptomen begleitet war (Hubschle et al., 2006; Knorr et al., 2008). Dabei scheint MALP2 genauso wie LPS eine bestimmte Schwelle zu erreichen, die ähnlich starke STAT3-Aktivierungen induziert (Kapitel V 1.2).

4) Der TLR7-Agonist **Imiquimod** stimulierte lediglich einzelne STAT3-Aktivierungen in Endothelzellen und anderen Strukturen (Kapitel V 1.1) und war entsprechend von eher geringen IL-6 Konzentrationen begleitet.

Abkürzung	Substanz	Dosierungen	STAT3-Signale
LPS	Lipopolysaccharid von *Escherichia coli* (Stamm 0111:B4 und O128:B12)	50 , 100 µg/kg s.c. und i.p.	(+++) robust in Maus Ratte und Meerschwein, Peak bei ca. 2h
PIPC	in Saline	500 µg/kg i.a.	(+++) robust in Meerschweinchen bei 2h
MALP2	in 10% Cremophor® EL-90% Phoyphat gepufferte Saline (PBS)	100 µg/kg s.c. und i.p.	(++) moderat in Ratten bei 2h, 3h
Imiquimod	in sterilem Wasser	5 mg/kg i.p. und s.c.	(+) schwach in Ratten bei 2h und 6h
CpG-DNA	Saline ?	1 mg/kg i.p.	(++) moderat in Mäusen

Tabelle 1
Verwendete TLR-Agonisten und deren Potenzial zur Induktion einer STAT3-Aktivierung im Gehirn

Insgesamt konnte obgleich der unterschiedlichen Wirkung über verschiedene TLRs und Tierspezies (Maus, Ratte, Meerscheinchen) ein relativ einheitliches Aktivierungsmuster in allen Fällen bestätigt werden. Dies spricht für einen Spezies konservierten gemeinsamen Mechanismus der TLR-Agonisten über sekundäre zirkulierende oder zentrale Mediatoren wie

dem Zytokin IL-6, welches korrelierend der Stärke der STAT3-Aktivierung in der Zirkulation erhöht war (siehe auch Tabelle 1) aber auch im Gehirn gebildet wurde (LPS, Imiquimod Kapitel V 1.1,. 1.5). In einer früheren Studie war die Möglichkeit, dass solche Mediatoren wie IL-6 für die Aktivierung von STAT3 eine bestimmte Schwellenkonzentration erreichen müssen bereits diskutiert worden (Rummel et al., 2004), wofür es auch hier weitere Hinweise gab (Kapitel V 1.2).

1.1.1.2. NF-IL6 Aktivierung

Für NF-IL6 waren wir die ersten, die eine detaillierte zeitliche und räumliche Charakterisierung seiner Aktivierung nach LPS-Stimulation durchgeführt haben (Kapitel V 1.5). Bisher waren lediglich mikrogliale Aktivierungen ohne genaue Spezifizierung der implizierten Gehirnstrukturen durchgeführt worden (Ejarque-Ortiz et al., 2007). Ähnlich wie für STAT3 (Rummel et al., 2005b) waren in dieser hier vorliegenden Studie vor allem die sCVOs sowie Endothelzellen die Hauptzielstrukturen einer LPS-vermittelten NF-IL6-Aktivierung (Kapitel V 1.5). Insgesamt waren aber etwas weniger Zellen NF-IL6-aktiviert als bei STAT3 gezeigt worden war (ca. 20-30% versus 35-45%). Der Anteil an aktivierten Endothelzellen war sehr ähnlich ca. 20-30% (allerdings sogar 95% im MnPO) versus 20% für STAT3. Neben Astrozyten, aktivierten Mikroglia und Neuronen in der AP, dem SFO und der *Eminencia mediana* (ME) konnten nach LPS-Stimulation zum ersten Mal auch NF-IL6-aktivierte perivaskulären Makrophagen und Endothelzellen detektiert werden (Kapitel V 1.5). In früheren Studien waren lediglich LPS-induzierte NF-IL6-aktivierte Mikroglia und Astrozyten *in vitro* (Cortes-Canteli et al., 2008; Pahan et al., 2002) und für Mikroglia auch *in vivo* gezeigt worden (Ejarque-Ortiz et al., 2007). Schließlich konnte anders als für STAT3 (Rummel et al., 2005b) für NF-IL6 nach LPS-Stimulation im zeitlichen Verlauf keine Migration der Signale von den sCVOs in das umgebende Gewebe hinein beobachtet werden (Kapitel V 1.5). Solch ein Fortschreiten der Signale wurde mit einem humoralen Ausbreiten von Mediatoren wie IL-1β und IL-6 in Zusammenhang gebracht und als „volume transmission“ bezeichnet (Gautron et al., 2002; Konsman et al., 1999). Folglich könnte das Fehlen solch einer „volume transmission“ für NF-IL6 ein Hinweis darauf sein, dass NF-IL6 vielleicht gar kein unmittelbarer Marker einer Aktivierung darstellt, sondern vielmehr den im Verlauf sich verändernden Zustand der aktivierten Zellen widerspiegeln könnte. Tatsächlich war die NF-IL6-Aktivierung mit 4-10 Stunden wesentlich später als die von STAT3 [1,5-6 h, (Gautron et al., 2002; Rummel et al., 2005b)] oder NFκB [1-3 h, (Nadjar et al., 2003) Kapitel V 1.12; Abbildung 8]. In der vorliegenden Studie konnte mittels Western Blot bestätigt

werden, dass zum Peak der NF-IL6-Aktivierung (8h) LAP-Protein ebenfalls in erhöhter Konzentration vorlag und es sich deshalb bei der immunhistochemisch detektierten NF-IL6-Translokation um die aktivierende Form des Transkriptionsfaktors handelte (Kapitel V 1.5).

Eigene Untersuchungen (Kapitel V 1.5) und Ergebnisse von anderen (Ejarque-Ortiz et al., 2007; Kelicen and Tindberg, 2004; Perez-Capote et al., 2006) lassen vermuten, dass NF-IL6-Aktivierung direkt LPS-vermittelt sein könnte und dies wahrscheinlich über einen MyD88-abhängigen Mechanismus (Chakravarty and Herkenham, 2005; Lu et al., 2009). Gerade die verspätete Aktivierung und Expression von NF-IL6 könnte aber auch durch sekundäre endogene Mediatoren vermittelt worden sein. Hierfür bietet sich natürlich IL-6 an, welches in seinen Plasmakonzentrationen zum Peak der NF-IL6 Aktivierung ebenfalls höchste Werte zeigte (Kapitel V 1.5). Neben IL-6 stimulieren aber auch IL-1β und TNFα in peripheren Geweben die mRNA-Expression von NF-IL6 (Akira and Kishimoto, 1992). In Mäuseastrozyten konnte kürzlich ebenfalls eine erhöhte NF-IL6-Expression nach Stimulation mit diesen Zytokinen gezeigt werden (Cardinaux et al., 2000). Hinzu kommt, dass bei Stimulation mit Imiquimod in einer anderen Teilstudie nur spärliche STAT3- oder NFκB- aber robuste NF-IL6-Aktivierung beobachtet werden konnte (Kapitel V 1.1). Eine direkte Wirkung von Imiquimod auf NF-IL6-Aktivierung im Gehirn wäre hierbei denkbar, da nur moderate Plamsa-IL6 und TNFα-Werte gemessen wurden und TLR7 in Mikroglia, Astrozyten und mononukleären Makrophagen vorkommt (Butchi et al., 2010; Letiembre et al., 2007). Ob Imiquimod aus dem lokalen Entzündungskompartiment (s.c.-Stimulation) entweichen kann und über das Blut direkt auf das Gehirn wirkt ist nicht bekannt, aber aufgrund seiner Eigenschaft als eher kleines Molekül (Guanosinanalog) vielleicht möglich. Im Gegensatz zu der Situation in der Milz und Leber wurde allerdings keine erhöhte Expression von INFs im Hypothalamus dieser Tiere gemessen, was eine direkte Wirkung dieses viralen Mimetikums auf das Gehirn sehr unwahrscheinlich macht (Kapitel V 1.1). Als endogener Mediator kam in dieser Untersuchung neben IL-6 vor allem INFγ in Frage, welches in großen Mengen nach s.c. oder i.p. Gabe von Imiquimod in der Zirkulation zu messen war und prinzipiell mit dem zeitlichen Peak an INFγ-Plasmakonzentrationen korrelierte. Hingegen war bei s.c.-Stimulation die Aktivierung von NF-IL6 wesentlich stärker als nach i.p Stimulation obwohl die Plasma-INFγ-Werte nach i.p.-Gabe geringfügig höher gemessen waren. Dies weist darauf hin, dass andere Mediatoren wie beispielsweise lokal gebildete Chemokine oder sogar ein neuronaler Signalweg (Kapitel I 1.3) vom Ort der lokalen Inflammation aus die verstärkte NF-IL6-Aktivierung hervorgerufen hat. Als Chemokin kommt zum Beispiel CINC1 (CXCL1) in Frage (Iida et al., 1992). Solche Chemokine werden nämlich im Rahmen derartiger lokaler

Entzündungsreaktionen gebildet (Kukulski et al., 2010) und in die Zirkulation freigesetzt. Für CINC1 wurde sogar eine Fieber erzeugende Wirkung über den PG-Weg nachgewiesen (Soares et al., 2008).

Bisher wurden hier zur *in vivo* Untersuchung für NF-IL6 im Gehirn LPS und Imiquimod als Stimulantien verwendet und ähnliche Aktivierungsmuster wie auch für STAT3 ermittelt. Anders als für STAT3 korrelierten die Aktivierungen allerdings nicht in beiden Fällen mit zirkulierenden IL-6 Konzentrationen. Neben den vorgeschlagenen Kandidaten-Mediatoren CINC1 und INFγ, wurden in der Vergangenheit andere Stimuli wie Kainsäure-Trauma in Astrozyten, Mikroglia und Neuronen (Cortes-Canteli et al., 2008), KCl-induzierte Aktivität von Neuronen (Sun et al., 2007) oder Neurotransmitter-induzierte (Noradrenalin / vasoaktives intestinales Peptid) Aktivität von Astrozyten (Cardinaux and Magistretti, 1996) verwendet, um die NF-IL6-Expression und nukleare Translokation /-Aktivierung- zu induzieren. Folglich ist es möglich, dass NF-IL6-Aktivität eher ein allgemeiner Aktivitätsmarker darstellt, der nicht zwingend durch Zytokine sondern durch neuronale Aktivität oder sogar Traumen bedingt sein könnte.

1.1.1.3. Zeitliche Abfolge der Aktivierung von Transkriptionsfaktoren; Interaktionen

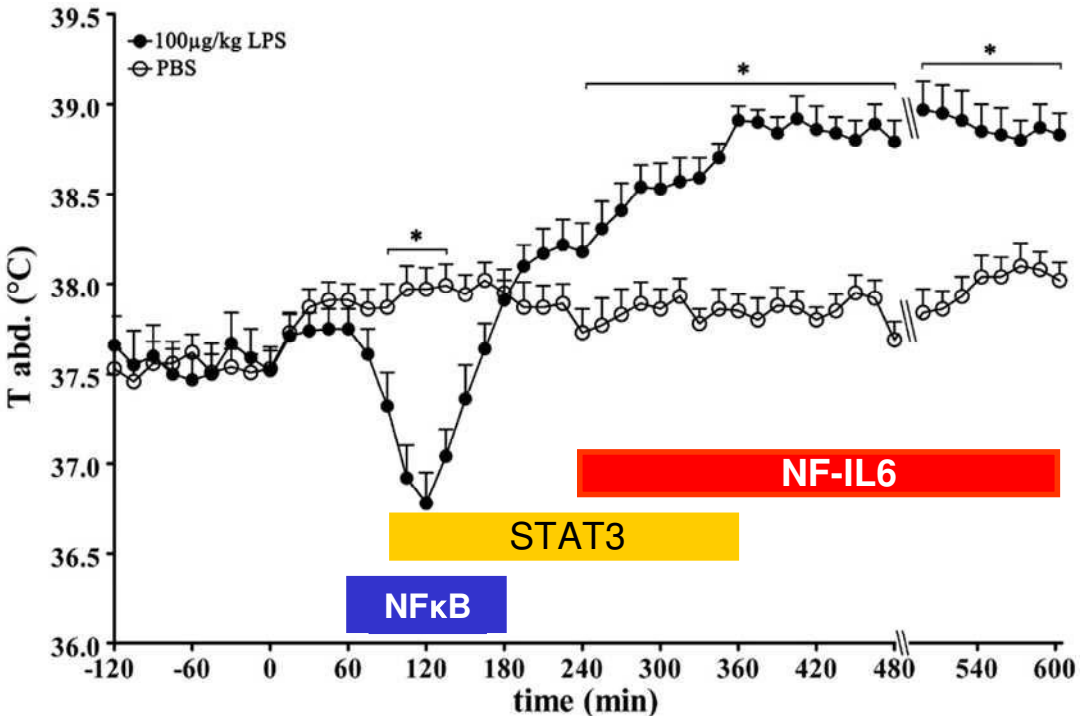


Abbildung 8
Schema zum zeitlichen Aktivierungsmuster inflammatorischer Transkriptionsfaktoren während einer typischen LPS-induzierten Fieberreaktion über 10 Stunden. Zusammengefasste Daten aus (Gautron et al., 2002; Laflamme and Rivest, 1999; Rummel et al., 2005b) und Kapitel V 1.5

Offensichtlich werden alle drei wichtigen inflammatorischen Transkriptionsfaktoren (NFκB, STAT3 und NF-IL6) in gleichen Gehirnstrukturen aktiviert und das in größten Teils den gleichen Zellphänotypen [(Ejarque-Ortiz et al., 2007; Gautron et al., 2002; Nadjar et al., 2003) Kapitel V 1.1, 1.3, 1.4, 1.5, 1.6, 1.9, 1.11, 1.12]; auch wenn mit unterschiedlichen Anteilen oder teilweise nicht umfassend identifiziert. Abhängig vom Untersuchungszeitpunkt fand STAT3- (Gautron et al., 2002) und NFκB-Aktivierung (Nadjar et al., 2003) zum großen Teil in Astrozyten statt und NF-IL6 eher in Endothelzellen (Kapitel V 1.5). Insgesamt waren aber Endothelzellen neben den sCVOs die wichtigsten Zielstrukturen. Allerdings bleibt zu bemerken, dass die aktivierten Zellphänotypen sich im Zeitverlauf der Entzündungsreaktion ändern und je nach Dosierung des TLR-Agonisten unterschiedlich sein können. So sind STAT3-aktivierte Astrozyten (Gautron et al., 2002) oder NF-IL6-aktivierte Mikroglia (Ejarque-Ortiz et al., 2007) vor allem bei späten Zeitpunkten (4h oder 16h) und hohen LPS-Dosierungen (250 µg/kg oder ~16mg/kg) nachgewiesen worden. Es bleibt hervorzuheben, dass solche hohen Dosierungen an LPS zu einem septischen Zustand führen und somit eine besondere Entzündungsform darstellen, die von einer Öffnung der BBB und direkten Effekten der TLR-Agonisten auf das Gehirn begleitet sind (Kiyatkin and Sharma, 2009; Tsao et al., 2001).

In einem Teilprojekt der hier vorliegenden Arbeit war eine Kolokalisation von nukleärer STAT3-IR mit nukleärer NFκB-IR beobachtet worden (Kapitel V 1.12), in einer anderen Teilstudie konnte allerdings nur wenig Kolokalisation von nukleärer NFκB-IR mit nukleärer NF-IL6-IR nachgewiesen werden (Kapitel V 1.3). Dies weist darauf hin, dass solche Aktivierungen von Transkriptionsfaktoren teils gleichzeitig in denselben Zellen aber auch zum Teil in unterschiedlichen Zellen oder sogar in zeitlicher Abfolge hintereinander stattfinden können. So wäre es denkbar, dass in einer Endothelzelle zunächst NFκB, dann STAT3 und schließlich NF-IL6 aktiviert werden könnte. Die physikalische Interaktion zwischen solchen Transkriptionsfaktoren über den so genannten „crosstalk“ (siehe Kapitel II 3) hat eine besondere Bedeutung und kann die Expression bestimmter Gene im Transkriptionskomplex verstärken, hemmen oder an völlig neue Bindungspartner im Genom führen. Damit könnten einige Eigenschaften der zum Teil redundanten Zytokinwirkungen erklärt und das Programm des Entzündungsgeschehens im Gehirn in seiner Form und Länge definiert werden. Dies dürfte folgerichtig dann auch die resultierenden Krankheitssymptome festlegen.

Bisher sind bereits die Hypothesen einer potentiellen Rolle von NFκB für die Initiierung und von STAT3 für die Aufrechterhaltung von Krankheitssymptomen und Inflammation im

Gehirn aufgestellt worden (siehe Kapitel II 3). Durch die vorliegende Studie konnte eine potentielle Rolle von NF-IL6 für die längerfristige Aufrechterhaltung bzw. sogar der Beendigung von Krankheitssymptomen und Inflammation im Gehirn ergänzt werden (Kapitel V 1.5). Dies ist von besonderer Bedeutung und weist NF-IL6 auch als verzögerten langfristigen Aktivierungsmarker für Untersuchungen inflammatorischer Prozesse im Gehirn aus. Bekannte Aktivitätsmarker wie c-FOS und auch STAT3 sind nicht nur auf kurze Zeiträume beschränkt sondern zum Teil auch auf bestimmte Zellphänotypen (c-FOS für Neurone) (Sako et al., 2005) und Stimulantien (Aktivatoren des STAT3-Signalwegs). Dies ist ein Vorteil von NF-IL6 und von großem Nutzen für weitere Untersuchungen. Die späte NF-IL6-Aktivierung bestärkt außerdem die bereits postulierte Rolle von NF-IL6 bei chronischen Entzündungsreaktionen wie der rheumatischen Arthritis (Pope et al., 1999).

1.1.1.4. Hinweise für eine direkte Wirkung von TLR-Agonisten auf Zellen im Gehirn

In wenigen Versuchen in primären Zellkulturexperimenten mit Hilfe des so genannten „Kalziumimaging“, bei dem die Aktivierung von einzelnen Zellen als Kalziumsignal direkt nach Stimulation aufgezeichnet werden kann, wurde beobachtet, dass in den sCVO, (für die AP und das OVLT) eine zeitnahe, direkte Aktivierung von Mikroglia, Astrozyten und Neuronen durch LPS-Stimulation stattfindet (Ott et al., 2010; Wuchert et al., 2008). Interessanter Weise reagierten hierbei 17% der Neurone im OVLT auf LPS und in der AP lediglich 2-4%. Demnach könnte das OVLT zumindest bei septischen Dosierungen von LPS direkt über neuronale Aktivierung die Information in die regulatorischen Zentren der präoptischen Region überleiten und dadurch zu Krankheitssymptomen beitragen. Auf Neuronen wurde TLR4 bereits nachgewiesen (Chakravarty and Herkenham, 2005), was ein solches Szenario unterstützt. Da jedoch Astrozyten oft mit einer kürzeren zeitlichen Latenz auf den PAMP-Stimulus reagierten, könnte die Reaktivität der Neurone zumindest zum Teil über „Gliotransmitter“ erfolgt sein. Gehirnstrukturen unterscheiden sich aber offensichtlich nicht nur in ihrer zellulären Zusammensetzung sondern auch in ihrem Antwortverhalten auf PAMPs. Prinzipiell sind vor allem Mikroglia und Astrozyten bekannt dafür, besonders stark auf eine TLR-Stimulation mit einer robusten Zytokinantwort zu reagieren (Hanisch, 2002; Kielian, 2006; Pinteaux et al., 2007; Wuchert et al., 2008). In einer Studie konnte so beispielsweise in Gehirnstrukturen mit hoher mikroglialer Dichte entsprechend eine stärkere inflammatorische Antwort auf LPS beobachtet werden (Pintado et al., 2011). Es gibt außerdem Hinweise, dass längerfristige Entzündungsreaktion durch TLR4 im Gehirn (Chakravarty and Herkenham, 2005) und die initiale Phase eher durch TLR4 auf

hämatopoetischen Zellen (Steiner et al., 2006b) bei systemischer LPS-Stimulation vermittelt wird. Obwohl der Haupteffekt von LPS über NFκB vermittelt wird und seine direkte Beteiligung an STAT3-Aktivierung zu vernachlässigen ist, gibt es in der Literatur insgesamt lediglich drei mir bekannte Studien, die eine direkte Wirkung von LPS zumindest über den JAK SAT/SOCS Signalweg postulieren (Bode et al., 1999; Dalpke et al., 2001; Shoenfelt and Fenton, 2006). Wahrscheinlich spielen aber zirkulierende Zytokine und in Gehirn gebildete Zytokine für die beobachtete STAT3 und NF-IL6-Aktivierung und entsprechend ihrem Auftreten in der Zirkulation für längerfristige Krankheitssymptome und Entzündungsgeschehen eine wichtige Rolle.

1.1.2. STAT3-Aktivierung durch IL-6

Neben den deutlichen Hinweisen bei der Verwendung von TLR-Agonisten, dass möglicherweise IL-6 an der STAT3-Aktivierung im Gehirn maßgeblich beteiligt ist (siehe Kapitel IV 1.1.1.1), sind in zwei Teilstudien in der vorliegenden Arbeit zum ersten Mal entscheidende Beweise für dessen tatsächliche Rolle bei lokalen (Kapitel V 1.12) und systemischen (Kapitel V 1.9) LPS-induzierten Entzündungsreaktionen ermittelt worden (Abbildung 9). Im subkutanen Luftkammermodell war LPS-induzierte STAT3-Aktivierung fast vollständig durch Vorbehandlung mit IL-6AS gehemmt worden. In einem Terpentin-induzierten lokalen Entzündungsmodell konnte die Rolle von IL-6 für die zentralenervöse STAT3-Aktivierung in einer späteren Studie bestätigt werden (Oka et al., 2007). In IL-6KO Mäusen hingegen wurde lediglich eine dramatische Reduzierung der Signale nach systemischer Stimulation der Tiere beobachtet [Abbildung 9; noch Signale in den Meningen, entlang großer Gefäße, Ependymzellen, den sCVOs, dem *Nucleus ventromediales praeopticus* (VMPO), dem *Nucleus supraopticus* (SON), *Nucleus periventricularis* (Pe), dem ARC und dem RPa].

Dies entsprach prinzipiell früheren Ergebnissen einer anderen Arbeitsgruppe, die mit Hilfe von SOCS3 *in situ* Hybridisierung ebenfalls in LPS-stimulierten IL-6KO eine anteilige und persistierende Aktivierung in den sCVOs und Ependymzellen ermittelt hatten (Lebel et al., 2000). Allerdings ist IHC eine sensitivere Methode und so konnte erst in der vorliegenden Arbeit ein differenzierteres Aktivierungsmuster ermittelt werden. Außerdem war die Dosis bei Lebel und Kollegen (2000) mit 2,5mg/kg (septisch) um ein vielfaches höher als in der hier vorliegenden Studie mit lediglich 50µg/kg (moderate Dosis). In einer Untersuchung von LPS-induzierter SOCS3-Aktivietung in der Leber von IL-6KO Mäusen ist ebenfalls ein Persisieren einiger Signale beschrieben worden (Yang et al., 2005). Prinzipiell liegt der Unterschied

zwischen dem lokalen und systemischen Entzündungsmodell darin, dass bei Applikation von der verwendeten LPS-Dosis in die Luftkammer nur IL-6 aber kein LPS oder TNFα in die Zirkulation entweicht (Cartmell et al., 2001; Cartmell et al., 2000; Ross et al., 2003). Diese beiden Mediatoren könnten mit der persistierenden STAT3-Aktivierung im systemischen Entzündungsmodell in Verbindung stehen. Neben IL-6 könnte in diesen Fällen aber auch ein anderer über STAT3-Wirkender Mediator hier eine Rolle spielen. Dazu gehören nicht zuletzt Zytokine aus der gp130 Rezeptorfamilie wie „leukemia inhibiting factor“ (LIF), „ciliary neurotrophic factor“ (LIF) aber auch „oncostatin“ (OSM) und IL-11, die durch LPS oder LPS-stimulierbare Zytokine induziert werden können (Heinrich et al., 1998). So konnte beispielsweise eine CNTF induzierte SOCS3-Expression im ARC, SFO, in Ependymzellen und in der ME dokumentiert werden (Bjorbaek et al., 1999). In der vorliegenden Arbeit wurde die Beteiligung von Leptin als potentieller Kandidat weiter untersucht (siehe nächster Abschnitt).

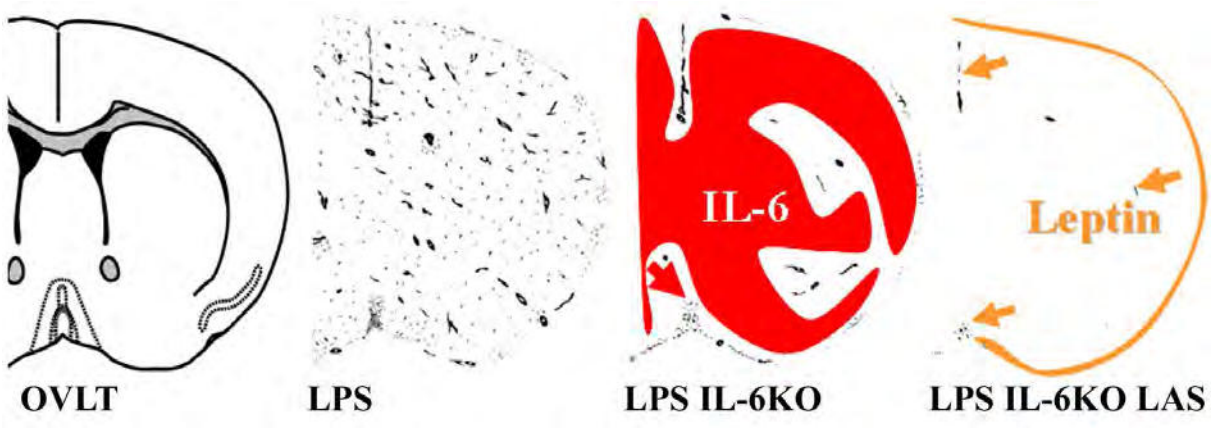


Abbildung 9
Schematische Darstellung der Beteiligung von IL-6 und Leptin an LPS-induzierter STAT3-Aktivierung im Gehirn der Maus. Schwarze Striche stellen STAT3-Aktivierungen in Endothelzellen und hypothalamischen Gehirnstrukturen wie dem *Organum vasculosum laminae terminalis* (OVLT) 3h nach LPS-Stimulation (50µg/kg) dar. Von links nach rechts: Überblick, Wildtyp-Maus, IL-6KO-Maus, IL-6KO-Maus mit Leptin Antiserum (LAS) behandelt. In Rot ist der Bereich der IL-6-vermittelten LPS-induzierten STAT3-Aktivierung (Gefäßassoziiert und im OVLT) sowie in Orange der Leptin-vermittelte Anteil (in großen Gefäßen und im OVLT) der verbleibenden STAT3-Aktivierung in IL-6KO Mäusen gekennzeichnet. Die IL-6- und Leptin-vermittelte LPS-induzierte STAT3-Aktvierung ist jeweils in farbiger Fläche hervorgehoben; Pfeile weisen auf eine Beteiligung von STAT3-Aktivierung entlang großer Gefäßstrukturen und / oder im OVLT hin.

1.1.3. STAT3-Aktivierung durch Leptin

Anders als für IL-6-induzierte STAT3-Aktivierung im Gehirn (Harré et al., 2003; Hübschle et al., 2001a; Rummel et al., 2005b) ist nach zentraler oder peripherer Gabe von Leptin ein deutlich anderes aber teilweise ähnliches Aktivierungsmuster als nach LPS-Stimulation beschrieben worden und betrifft neben dem Hypothalamus auch den Hirnstamm [(Hosoi et al., 2002a; Hübschle et al., 2001b; Münzberg et al., 2003; Mütze et al., 2006; Stepanyan et al., 2003) Kapitel V 1.10]. In der vorliegenden Teilstudie wurde zum ersten Mal gezeigt, dass endogenes Leptin über STAT3 besonders auf große Gehirngefäße, Meningen, Ependymzellen und einige spezifische Gehirnstrukturen nämlich den VMPO, den *Nucleus supraopticus* (SON), den ARC, das OVLT und den RPa während moderater LPS-induzierter systemischer Entzündungsreaktion einwirken kann. Diese Signale waren nämlich nach Vorbehandlung mit LAS, also in Abwesenheit von zirkulierendem endogenen Leptin, von den verbleibenden LPS-stimulierten STAT3-Signalen in IL-6KO Mäusen fast völlig verschwunden (Abbildung 9). Auf alle diese Strukturen außer dem VMPO scheinen IL-6 und Leptin gemeinsam zu wirken. Die akute Leptin-Neutralisation hatte den Vorteil, dass die relativ geringe Beteiligung von Leptin an LPS-induzierter STAT3-Aktivierung detektierbar war. In ob/ob Mäusen (Leptin-defizient) wäre die Differenz dieser Effekte Aufgrund der Vielzahl an IL-6-STAT3-Signalen schwer zu detektieren gewesen. Zudem zeigten diese Mäuse (ob/ob) in einer anderen Teilstudie eine verstärkte IL-6-Antwort auf LPS (Kapitel 1.7), was auf einen kompensatorischen Mechanismus hinweist und die Ergebnisse hätte beeinflusst können.

Die Diskrepanz, dass Leptin-aktivierte Gehirnstrukturen nur nach LPS-Stimulation in der vorliegenden Arbeit zu beobachten waren und nicht in früheren Studien, die exogenes Leptin als Stimulus verwendeten, könnte mit einer veränderten Ansprechbarkeit von Zellen durch den LPS-Stimulus zusammenhängen. Eine Hochregulation des IL-6R war durch LPS beschrieben worden (Vallières and Rivest, 1997), wir konnten allerdings keine veränderte ObRb-Expression auf mRNA Ebene nachweisen. Alternativ gibt es Hinweise dafür, dass auch andere Substanzen, beispielweise Amylin, die Sensitivität von endogenem Leptin auf das Gehirn verändern können und dadurch zu erhöhten STAT3-Aktivierungen beitragen (Lutz, 2010; Turek et al., 2010). Besonders die Wirkung von Leptin auch auf Endothelzellen bei LPS-Stimulation war unerwartet. Vorher war allerdings schon die Expression des ObRb (Bjorbaek et al., 1998) und STAT3-IR in Gehirnendothelzellen nach Leptin-Stimulation demonstriert worden (Mütze et al., 2006). Interessanter Weise war in einigen frühen Studien eine Leptin-Bindung und eine Expression des ObR (vornämlich kurze Formen)(Baskin et al.,

1999; Carlo et al., 2007; Corp et al., 1998; Guan et al., 1997b; Schwartz et al., 1996) mit einem unerwartet ähnlichen Verteilungsmuster wie in der eigenen Studie zu beobachten, was die Relevanz unsere Beobachtung weiter unterstützt (Abbildung 10). Die Verteilung um den ventralen Hypothalamus, die Ventrikel, große Gefäße und die Meningen an der Grenzfläche zwischen Gehirn und Peripherie war so auffallend, dass wir die Hypothese entwickelten, dass Leptin vielleicht bei LPS-induzierter Invasion/Rekrutierung von Immunzellen an dieser wichtigen Schnittstelle eine Rolle spielen könnte. Tatsächlich konnte sowohl in dieser Studie (Kapitel V 1.9) als auch in der Folgestudie (Kapitel V 1.7) gezeigt werden, dass die Expression von essentiellen Zielgenen hierfür (Chemokine, Adhäsionsmoleküle, Regulatoren von Metalloproteinasen) durch Leptin beeinflusst wird und Leptin an der LPS-induzierten Rekrutierung von neutrophilen Granulozyten beteiligt ist (Abbildung 10).

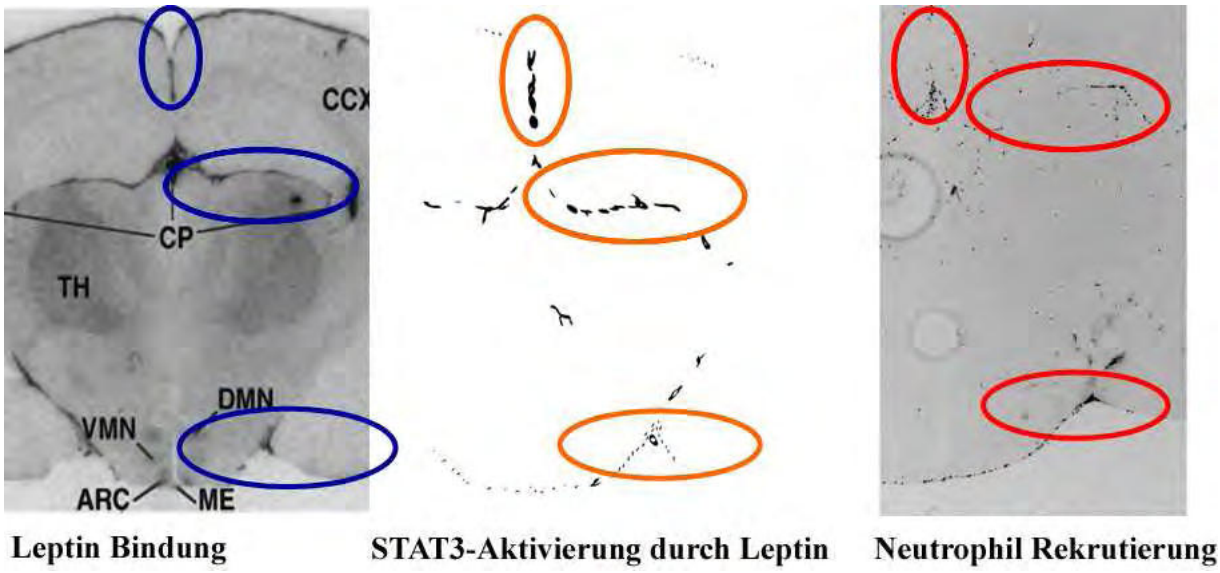


Abbildung 10
Beispielhafter Vergleich einer typischen Leptin-Bindungsstudie (Baskin et al., 1999) mit Leptin vermittelter STAT3-Aktvierung (Kapitel V 1.9) und Leptin-vermittelter Rekrutierung von neutrophilen Granulozyten in das Gehirn (ob/ob Maus + Leptin; Kapitel V 1.7) bei LPS-induzierter systemischer Entzündung. Respektive Wirkungsmuster sind durch korrespondierende farbige Kreise jeweils hervorgehoben.

1.2. Funktionen und relevante Gehirnstrukturen

Ein Vorteil von neuroanatomischen Untersuchungen ist, dass nach dem einfachen wissenschaftlichen Prinzip der Beobachtung und Interpretation funktionieren. Die Aktivierungsmuster im Zusammenhang mit den Konnektivitäten zu anderen Gehirnstrukturen sowie physiologischen und biochemischen Parametern bieten Hinweise auf die mögliche Funktion der Gehirnstruktur und des untersuchten Stimulus. Dementsprechend sind in der

vorliegenden Arbeit vor allem in zwei sehr ausführlichen neuroanatomischen Charakterisierungen von LPS-induzierter NF-IL6-IR sowie IL-6- und Leptin-vermittelter STAT3-IR (Kapitel V 1.5, 1.9) mehrere Hypothesen zur Funktion einzelner Gehirnstrukturen entwickelt bzw. bestätigt worden.

1) Fieber: Die im Schrifttum (Kapitel II 5.1) und in einer Übersichtsarbeit (Kapitel V 1.8) beschriebenen wichtigen Gehirnstrukturen der zentralnervösen Verschaltung zur Fieberentstehung sind nach LPS-Stimulation immunhistologisch sowohl über STAT3- als auch über NF-IL6-aktiviert worden [OVLT, SFO, VMPO, MnPO, RPa, *Nucleus tractus solitarius* (NTS)]. Damit stellen beide Transkriptionsfaktoren interessante Aktivitätsmarker für Untersuchungen der Fieberentstehung dar und wurden hierfür in mehreren Studien verwendet (Kapitel V 1.1, 1.3, 1.4, 1.6, 1.11, 1.12). Die Rolle der CVOs wurde in früheren Übersichtarbeiten genau beschrieben (Roth et al., 2004a); die Rolle des OVLT und des SFO wurde unter anderen durch Läsionsstudien erstmalig eindeutig bestätigt (Hashimoto et al., 1994; Takahashi et al., 1997). In unmittelbarer Nähe zum OVLT liegt der VMPO. Ihm wurde für die Entstehung von Fieber ebenfalls eine wichtige Rolle zugewiesen (Elmquist et al., 1996; Scammell et al., 1996). Der MnPO und der RPa sind in die vegetative Weiterleitung an die Fieber-induzierenden Effektororgane beteiligt [(Lazarus et al., 2007; Nakamura, 2011) Kapitel II 5.1]. In den meisten dieser Regionen scheint Leptin also potentiell seine beschriebene Beteiligung an LPS-induziertem Fieber zu vermitteln (Harden et al., 2006; Sachot et al., 2004). Rezeptoren für Leptin (ObR-IR) sind zumindest für das OVLT (Meister and Hakansson, 2001) und den RPa (Hay-Schmidt et al., 2001) beschrieben worden. In allen diesen Regionen und zusätzlich im NTS waren STAT3-Signale auch anteilig IL-6-vermittelt. Da IL-6KO-Mäuse bei der gleichen Dosierung an LPS kein Fieber bekommen (Chai et al., 1996; Kozak et al., 1998), könnte die respektive Beteiligung von IL-6 in diesen Gehirnstrukturen die Resistenz dieser Tiere Fieber zu entwickeln erklären. Dies schließt vor allem auch die Rolle des Endothels an sich als wichtige Zielstruktur für zirkulierende Mediatoren ein [(Rummel et al., 2005b)(Kapitel V 1.5, 1.12, 1.9)]. Interessanter Weise wurde für NF-IL6 allerdings keine Aktivierung im NTS beobachtet, einer Gehirnstruktur, in der vagale Affarenzen aus dem Bauchraum enden. Eine direkte Stimulation mit Leptin induziert in diesem Gehirngebiet zwar STAT3 (Kapitel V 1.10), dies scheint aber nach LPS-Stimulation lediglich IL-6 vermittelt zu sein (Kapitel V 1.9). Ob es sich hierbei um die Wirkung von IL-6 über die Aktivierung des Vagusnervs oder eine direkte Wirkung des Zytokins über die AP mit seiner unvollständigen BBB handelt ist nicht klar. Von besonderem Interesse war die Beobachtung, dass Leptin und IL-6 im Hirnstamm direkt auf die RPa

möglicherweise auf dortige präsympathische Neurone zu wirken scheinen. In früheren Studien hatten beide Mediatoren nach intrazerebroventrikulärer Injektion zu einer Aktivierung von braunem Fettgewebe (BAT) geführt, wissend dass BAT eines der wichtigsten Effektororgane zur Thermogenese bei Nagetieren darstellt (Li et al., 2002a; Morrison, 2004). Eine Aktivierung serotonerger Neurone in der RPa hemmte diesen Effekt von Leptin wieder. In einer kürzlich durchgeführten Studie gab es tatsächlich neue Hinweise für die Möglichkeit, dass Leptin die sympathische Aktivierung von BAT über Modulation der Aktivität des RPa bewirken könnte (Barnes et al., 2010).

2) Adipsie: Das SFO und der SON, zwei Gehirnstrukturen, die für die Wasseraufnahme eine wichtige Rolle spielen, zeigten in den vorliegenden Studien (Kapitel V 1.1, 1.3, 1.5) NF-IL6- (SFO) und oder STAT3-IR (SFO und SON, Kapitel V 1.6, 1.9, 1.11, 1.12). In einer früheren Arbeit war eine STAT3-Aktivierung nach systemischer LPS- und IL-6-Stimulation in diesen Strukturen bereits beobachtet worden (Harré et al., 2002; Rummel et al., 2004). LPS-induzierte IL-6 und Leptin-vermittelte STAT3-Aktivierung im SON war bisher allerdings noch nicht beschrieben worden. Eine Rolle für das SFO in der Regulation des Wasserhaushalts ist seit längerem bekannt (Ferguson and Li, 1996; McKinley et al., 1998). In der vorliegenden Studie wurde eine Wirkung von IL-6 auf das SFO bei LPS-induzierter systemischer Inflammation bestätigt (Lebel et al., 2000). Dies könnte neben einer Funktion bei der Fieberentstehung auch eine Beteiligung von IL-6 bei Adipsie begleitenden Wasserretention widerspiegeln (Palin et al., 2008). Obwohl Leptin in einer Studie nach systemischer Gabe die Wasseraufnahme reduzierte (Bojanowska and Nowak, 2007), konnte in der vorliegenden Studie eine Beteiligung von Leptin im SFO bei LPS-Stimulation über STAT3-IR nicht festgestellt werden (Kapitel V 1.9). Auch ein anderes die Futteraufnahme hemmendes Peptid, nämlich Amylin, wirkt direkt auf das SFO und ist an der Regulation der Wasseraufnahme beteiligt (Riediger et al., 1999; Riediger et al., 2001). Amylin aktiviert aber nicht den STAT3-Signalweg sondern eine NO-abhängige cGMP-Bildung im SFO (Riediger et al., 2001) und dürfte demnach nicht an der verbliebenen STAT3-Aktivierung beteiligt sein. Dennoch könnte dieses Peptidhormon zu der beobachteten LPS-induzierten Adipsie über NO-vermittelte Mechanismen beitragen (Riediger et al., 2010). Außerdem könnte Amylin wie bereits angedeutet die Sensitivität anderer Mediatoren zur STAT3-Aktivierung beeinflussen (Turek et al., 2010) und sollte in Zukunft in diesem Zusammenhang weiter untersucht werden.

Im SON aktiviert LPS im Allgemeinen oxytocinerge und vasopressinerge (AVP) Neurone (Matsunaga et al., 2000) und beeinflusst den Wasserhaushalt durch AVP-Freisetzung und die damit verringerte Wasserausscheidung (Giusti-Paiva et al., 2003). In der vorliegenden Studie

wurde solch eine Aktivierung des SON lediglich durch STAT3 aber interessanter Weise nicht mittels NF-IL6 nachgewiesen (Kapitel V 1.5, 1.9). Da IL-6 und Leptin im SON zwar STAT3 aktivieren aber nicht NF-IL6, könnte das möglicherweise bedeuten, dass diese zwei Mediatoren auch in anderen Gehirnstrukturen nicht direkt zur NF-IL6-Aktivierungen beitragen. Untersuchungen in IL-6KO- und ob/ob-Mäusen sollten zur Klärung dieses Zusammenhangs in Zukunft beitragen. Die Wirkung von Leptin über STAT3 auf den SON wird durch frühere Studien unterstützt, die zeigen konnten, dass OBR-IR dort exprimiert wird (Hakansson et al., 1998; Meister and Hakansson, 2001) und Leptin-Stimulation zu nukleärer STAT5-IR führt (Mütze et al., 2007). Zudem induzierte sowohl zentral appliziertes Leptin (Yamamoto et al., 1999) und systemisch appliziertes IL-6 (Mastorakos et al., 1994) bzw. LPS-induziertes IL-6 (Palin et al., 2008) die Freisetzung von AVP, was auf eine funktionelle Rolle dieser beiden Mediatoren für den Wasserhaushalt bestätigt.

3) Anorexie: Wie bereits ausführlich im Kapitel II 5.2 und 6.2 beschrieben, spielt der ARC eine Schlüsselrolle für die Vermittlung von Anorexie (Asarian and Langhans, 2010). Zu bemerken bleibt allerdings, dass auch der Hirnstamm ein wichtige Rolle für Futteraufnahme hemmende Substanzen wie Leptin (Hayes et al., 2010) oder Amylin spielt (Potes and Lutz, 2010). Hier konnten wir aber im Hirnstamm mittels STAT3-IHC keine Hinweise für die Beteiligung von Leptin und IL-6 an LPS-induzierter Anorexie nachweisen. Die eindeutig belegte Wirkung von Leptin auf den ARC (Elias et al., 2000; Faouzi et al., 2007) wurde allerdings unter LPS-stimulierter Bedingung in der vorliegenden Studie bestätigt (Kapitel V 1.9). Diese Beobachtung ist im Einklang mit der Beteiligung von zirkulierendem Leptin an LPS-induzierter Anorexie (Harden et al., 2006; Sachot et al., 2004). Erstaunlich war die sogar tendenziell größere Beteiligung von IL-6 an der Aktivierung von STAT3 im ARC. Unterstützt wird eine Rolle für IL-6 bei Anorexie durch Studien von Terpentin-induzierter lokaler Entzündung (Fattori et al., 1994; Kozak et al., 1997) und dadurch, dass IL-6KO Mäuse im Alter übergewichtig werden (Wallenius et al., 2002). Die Tatsache, dass nach LPS-Stimulation mit einer hohen Dosis an LPS in IL-6KO Mäusen keine Beteiligung für IL-6 bei der entstehenden Anorexie beobachtet wurde, hängt wahrscheinlich mit der hohen Dosierung im Vergleich zur moderaten hier verwendeten LPS-Dosis zusammen. Solch eine Dosis hatte selbst in IL-6KO Mäusen Fieber erzeugt (Kozak et al., 1997). Wie bereits erwähnt könnte bei solch einer septischen Entzündungsreaktionen möglicherweise LPS direkt auf das Gehirn wirken und dann die (in diesem Fall nicht vorhandene) Wirkung von zirkulierenden Zytokinen auf die Futteraufnahme durch den LPS-Effekt überdeckt haben.

4) Gedächtnis: Die hohe Aktivität von NF-IL6-IR im Hippocamus wurde bereits in früheren Studien beschrieben (Nadeau et al., 2005; Sterneck and Johnson, 1998) und mit einer Rolle von Hippocampus-abhängiger Gedächtniskonsolidierung in Verbindung gebracht (Taubenfeld et al., 2001). Bereits basale NF-IL6-Aktivierungen in dieser Gehirnstruktur könnten hierbei bei der Expression von Zytokinen wie IL-1β eine wichtige Rolle spielen, die für die normale Funktion des Hippocampus von Bedeutung sind (Kapitel II 4.1) und LPS-induziert vermehrt exprimiert werden (Layé et al., 1994).

5) Stress-Achse: Schließlich gab es deutliche Hinweise einer Beteiligung von NF-IL6- und STAT3-aktivierten Gehirnstrukturen an der Beeinflussung der HPA-Achse. Eine nukleäre STAT3- und NF-IL6-IR wurde in der AP, ME, dem *Nucleus paraventricularis* PVN und der Hypophyse festgestellt [(Gautron et al., 2003) (Kapitel V 1.5, 1.9)]. Corticotropin Releasing Hormon (CRH) wird in Neuronen des PVN gebildet, welche zur ME projizieren, dort CRH abgeben und zur Ausschüttung von adrenokortikotropen Hormon (ACTH) aus dem Hypophysenvorderlappen ins Blut führen. ACTH induziert schließlich die Freisetzung von Corticosteron (Ratten) aus der Nebennierenrinde (Papadimitriou and Priftis, 2009). Eine direkte Beteiligung von IL-6 über STAT3 und NF-IL6 an der ACTH-Bildung in der Hypophyse aber auch an der CRH-Freisetzung in der ME bei LPS-induzierter Aktivierung der Stressachse erscheint möglich. In der ME war LPS-induzierte STAT3-Aktivierung in IL-6KO Mäusen zwar nicht verringert und für die Hypophyse nicht untersucht worden aber eine Beteiligung von IL-6 an ACTH-Freisetzung konnte in anderen Studien eindeutig gezeigt worden (Perlstein et al., 1993; van Enckevort et al., 2001). So ist IL-6 ein wichtiger Faktor; für Leptin gab es keine Hinweise in der vorliegenden Studie. Nach Literaturangaben ist die Regulation der HPA-Achse über Leptin vielschichtig und wohl eher als negativer Feedback zu verstehen (Roubos et al., 2012). STAT3 wurde mit der Expression von ACTH in POMC-Neuronen in Verbindung gebracht (Gautron et al., 2003) und NF-IL6 ist an der Bildung von CRH und POMC-Expression beteiligt (Abbud et al., 2004; Stephanou et al., 1997). Die genaue Rolle beider Transkriptionsfaktoren für die Kontrolle der HPA-Achse und mögliche therapeutische Interventionsmöglichkeit sind Teil laufender weiterführender Untersuchungen. Eine Beteiligung der AP an der HPA-Achsen-Aktivierung besteht vor allem über aufsteigende noradrenerge Verbindungen zum PVN und könnte nach LPS-Stimulation ebenfalls eine Rolle spielen (Buller, 2001). LPS-induzierte STAT3 und NF-IL6-Aktivierung konnten in den hier vorliegenden Studien für die AP zwar festgestellt werden, aber waren den endogenen Mediatoren IL-6 oder Leptin nicht eindeutig zuzuordnen.

2. Selektive Beteiligung von TLR Agonisten, IL-6 und Leptin an der Induktion des Prostaglandinsynthesewegs im Gehirn.

Wie bereits im Schrifttum dargestellt (Kapitel II 4.2) und in einem Übersichtsartikel ausgeführt (Kapitel V 1.8), ist PGE2 einer der wichtigsten terminalen Fiebermediatoren, wobei sowohl zentral im Gehirn gebildetes PGE2 als auch peripher in die Zirkulation abgegebenes PGE2 bei der Fieberentstehung eine gewisse Rolle spielen. Vor allem Untersuchungen mit selektiven COX2-Inhibitoren (Cao et al., 1997; Steiner et al., 2009; Steiner et al., 2001; Zhang et al., 2003) und die Verwendung von COX2- (Li et al., 1999; Steiner et al., 2005b) und mPGES-defizienten Mäusen (Nilsberth et al., 2009b; Saha et al., 2005), konnten die Rolle dieser zwei geschwindigkeitsbestimmenden Enzyme bei der PGE2 Synthese unter inflammatorischen Bedingungen und der Fieberentstehung nachweisen. In eigenen Untersuchungen der vorliegenden Arbeit wurde ebenfalls die Rolle von PGE2 für PIPC und MALP2-induziertes (zentral und peripher gebildet) Fieber mittels COX-Inhibitoren bestätigt bzw. erweitert (Kapitel V 1.6, 1.11). Die Bildung von PGE2 kann indirekt auch durch eine erhöhte Expression der anatomisch und funktionell gekoppelten (Yamagata et al., 2001) Enzyme COX2 und mPGES im Gehirn untersucht werden. Die erhöhte Expression beider Enzyme im Hypothalamus von Imiquimod-stimulierten Tieren zeichnet auch diesen TLR-Agonisten höchstwahrscheinlich als ein exogenes PGE2-abhängiges Pyrogen aus (Kapitel V 1.1). Dies ist von Bedeutung, da doch auch PGE2-unabhängige endogene Pyrogene bekannt sind (Davatelis et al., 1989) und manche Antipyretika über einen PGE2-unabhängigen Weg zu wirken scheinen (Machado et al., 2007; Malvar Ddo et al., 2011). Sogar die obligatorische Rolle von PGE2 wurde dadurch ergänzt, dass nach Läsion der präoptischen Region LPS-induziert auch über Verhaltensänderungen (in einem Temperaturgradientenkäfig) trotzdem Fieber induziert werden kann (Almeida et al., 2006). Insgesamt konnte in der vorliegenden Arbeit zumindest für die untersuchten TLR-Agonisten, ein konservierter, PG-abhängiger Mechanismus der Fieberentstehung dokumentiert werden.

Neben TLR-Agonisten wurde in drei hier vorliegenden Studien die Rolle von IL-6 und Leptin als zirkulierende (humorale) neuroimmune Mediatoren näher untersucht (Kapitel V 1.4, 1.9, 1.12). Entsprechend der großen Bedeutung dieser zwei Mediatoren zum Beispiel bei Obesitas und Altern (sieh Kapitel II 2, 6.2) sollte untersucht werden, ob IL-6 und Leptin als zirkulierende Pyrogene tatsächlich an der Aktivierung des PG-Syntheseweg im Gehirn bei lokalen und oder systemischen Entzündungsreaktionen beteiligt sind. In dem Modell einer lokalen Entzündung (Luftkammer, s.c.) konnten wir hier zum ersten Mal eindeutig zeigen, dass zirkulierendes IL-6 tatsächlich an der s.c.-LPS-stimulierten COX2 und mPGES-

Expression in Endothelzellen [zum Teil auch in perivaskulären Makrophagen, (Schiltz and Sawchenko, 2003; Serrats et al., 2010)] und damit Fieber beteiligt ist (Kapitel V 1.4, 1.12). Lediglich in einer früheren Studie war berichtet worden, dass in IL-6KO Mäusen nach lokaler Terpentin-Stimulation ebenfalls COX2-IR verringert war (Turnbull et al., 2003). Hier konnten wir aber durch Neutralisation von LPS-induziertem, zirkulierenden IL-6 und durch direkte Stimulation mit einer pyrogenen IL-6-Dosis, eine IL-6-vermittelte Induktion von COX2 und mPGES-Expression und respektiver IR nachweisen. Zusätzlich war nachfolgend in einem Carageenan-induziertem Schmerzmodell von einem japanischen Kollegen unser Ergebnis auch für COX2- und mPGES-Induktion im Rückenmark bestätigt worden (Oka et al., 2007). Im Modell einer systemischen LPS-induzierten Entzündung war allerdings dieser IL-6-vermittelte Effekt lediglich anteilig auf mRNA-Ebene aber nicht auf Proteinebene bei IL-6KO Mäusen zu beobachten (Kapitel V 1.9).

In der Vergangenheit war die mit der PG-Synthese zusammenhängende Pyrogenität von IL-6 mehrfach in Frage gestellt worden. So konnte Spezies spezifisch eine Fieber erzeugende Wirkung für zirkulierendes IL-6 in Kaninchen als stark (Helle et al., 1988), in Ratten eher moderat (Cartmell et al., 2000; Harré et al., 2002)(Kapitel V 1.12) oder in Mäusen sogar als abwesend (Chai et al., 1996; LeMay et al., 1990; Nilsberth et al., 2009a; Wang et al., 1997a) festgestellt werden. Dabei sind Kaninchen insgesamt besonders empfindlich gegenüber exogenen Pyrogenen wie LPS, Ratten sind weniger empfindlich und Mäuse weisen z.B. eine sehr geringe Sensitivität für Endotoxinschock auf, eine Reaktionen, die nach Stimulation mit hohen LPS-Dosen entsteht (Kluger, 1991; Romanovsky et al., 1996; Rudaya et al., 2005). Hinzu kommt, dass entsprechend sehr hohe Mengen an IL-6 gerade in weniger LPS-sensitiven Tierspezies benötigt werden dürften, um eine früher bereits postulierte Schwelle an zirkulierendem IL-6 zu erreichen, die pyrogen wirkt, bzw. STAT3 und den PG-Syntheseweg im Gehirn aktivieren kann (Rummel et al., 2004). Gerade in den Studien, in denen keine Pyrogenität von zirkulierendem IL-6 in Mäusen ermittelt werden konnte, waren deutlich geringere IL-6-Mengen appliziert worden als in der vorliegenden Studie und in einer früheren Studie bei Ratten [(Harré et al., 2002)(Kapitel V 1.4, 1.12)].

Die teilweise unterschiedlichen Ergebnisse im Falle LPS-induzierter systemischer Entzündung durch Nilsberth und Kollegen (2009) sind allerdings nicht ganz klar. Sie hatten im Gegensatz zu unseren Ergebnissen (Kapitel V 1.9) keine veränderte Expression von mPGES und COX2 in LPS-stimulierten IL-6KO Mäusen detektiert. Relativ hohe Variationen in beiden Studien und methodische Unterschiede (PCR und genetischer Hintergrund der wildtyp Tiere) könnten diese Diskrepanz erklären. Die Wirkung von IL-6 auf den PG-Weg

wurde kürzlich allerdings nochmal in einer Kultur von Astrozyten bestätigt (Chikuma et al., 2009).

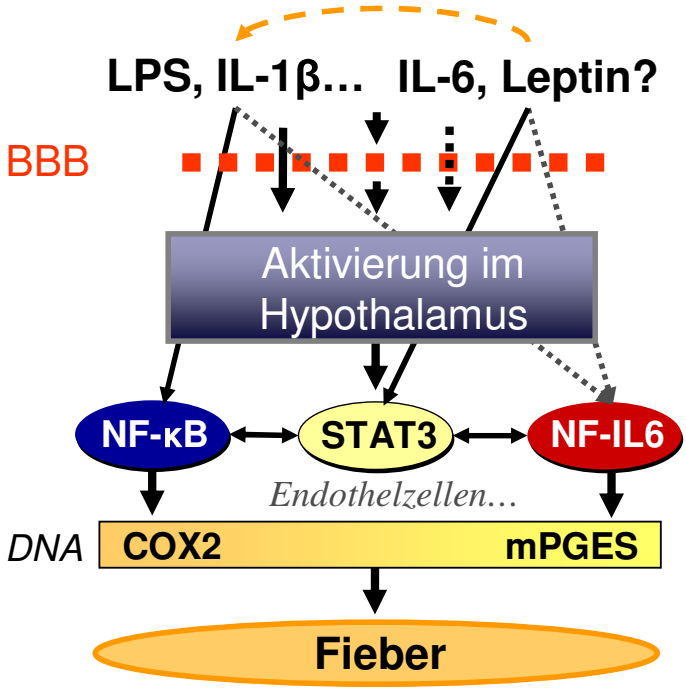


Abbildung 11
Schematische Darstellung der potentiellen Wirkung von zirkulierendem IL-6 über STAT3 und potentiell über NF-IL6 und zirkulierendem IL-1β (LPS, und andere TLR-Agonisten) über NFκB und potentiell über NF-IL6 auf die Regulation der Expression von COX2 und mPGES in Endothelzellen und perivaskulären Makrophagen. Leptin scheint hier indirekt über Modulation von IL-1β zu wirken.

Insgesamt bleibt trotzdem zu bemerken, dass IL-6 alleine offensichtlich im Gegensatz zu anderen Mediatoren wie IL-1β (Conti et al., 2004) ein eher schwacher Aktivator des PG-Synthesewegs darstellt. Es ist zu vermuten, dass IL-6 vielmehr in Kooperation mit kleinen Konzentrationen anderer Mediatoren wie IL-1β oder auch dem vorher genannten Chemokin CINC1, erst seine ganze Wirkung auf PGE2-Bildung entfaltet. Das heißt, IL-6 könnte ein permissiver Faktor sein, die PGE2-Produktion zu verstärken und zu fördern. Dies könnte physiologische mindestens genauso bedeutsam sein wie eine direkte Wirkung, da zum einen IL-6 gehäuft in höheren Konzentrationen im Blut vorkommt und zum anderen immer im Zytokinmilieu also zusammen mit anderen eben genannten Faktoren auftritt (Kapitel II 2). Außerdem bleibt zu bemerken, dass diese Funktion von IL-6, die COX2 und mPGES-Expression besonders zu fördern, vor allem für das Gehirn gilt. In der Leber war IL-6 zwar notwendig aber nicht ausreichend, um eine mPGES-Expression zu induzieren (Kapitel V 1.4). Interessanter Weise korrelierte außerdem neben COX2 gerade die Expression von mPGES mit den IL-6-Konzentrationen im Blut und der STAT3-Aktivierung (SOCS3) im Gehirn. Dies

ist von besonderer Bedeutung, da Inhibitoren von mPGES als neue therapeutische Alternative zu COX-Inhibitoren mit weniger kardiovaskulären Nebenwirkungen im Fokus der klinischen Forschung stehen (Guerrero et al., 2009; Samuelsson et al., 2007).

Den Mechanismus betreffend, wie IL-6 über seine STAT3-Signalkaskade die COX2 und mPGES-Expression beeinflussen könnte, sind in den hier vorliegenden Arbeiten zwei Hypothesen vorgeschlagen worden (Abbildung 11).

1) Da STAT3 keine Bindungsstelle im Promotor für COX2 besitzt, ist davon auszugehen, dass es zu einem „crosstalk" zwischen STAT3 und NFκB kommt. Dieser Mechanismus wurde bereits im Schrifttum beschrieben (Kapitel II 3) und könnte erklären, wie STAT3 durch diese Interaktion den Transkriptionskomplex in seiner Funktion zur COX2-Expression fördert (Abbildung 11). Über den NFκB-Signalweg war bereits eine COX2-Induktion in Endothelzellen des Gehirns belegt (Nadjar et al., 2005b). Da dieser Signalweg in der vorgelegten Studie im lokalen LPS-induzierten Entzündungsmodell aktiviert, aber nicht signifikant zusammen mit COX2- und mPGES-Expression durch IL-6AS beeinflusst worden war, ist solch eine Interaktion zwischen STAT3 und NFκB wahrscheinlich. Eine hier gezeigte Kolokalisation von aktivierter STAT3-IR mit aktivierter NFκB-IR in Endothelzellen belegt, dass solch eine Interaktion stattfinden könnte (Kapitel V 1.12). Tatsächlich wurde in einem Modell myokardialer Präkonditionierung eine STAT3- und NFκB-abhängige COX2-Expression bereits im Herzen nachgewiesen (Bolli et al., 2003). Ein solcher sich verstärkender „crosstalk" zwischen STAT3 und NFκB würde auch erklären, warum eine Kombination von IL-6 mit subpyrogenen Dosierungen an IL-1β zu Fieber führt, auch wenn jeder Mediator einzeln in dieser Studie keine Pyrogenität aufwies (Cartmell et al., 2000).

2) NF-IL6 könnte die Expression von mPGES und COX2 vermitteln. Tatsächlich konnte in peripheren Endothelzellen und Makrophagen gezeigt werden, dass auch NF-IL6 und NFκB synergistisch an COX2-Expression beteiligt sein können (Billack et al., 2002) und NF-IL6 auch bei der LPS-induzierten Expression von mPGES von großer Bedeutung ist (Uematsu et al., 2002; Walters et al., 2012). Zu dem untersuchten recht frühen Zeitpunkt im IL-6AS-Experiment (Kapitel V 1.4, 1.12) nach LPS-Stimulation (2h), war eine Aktivierung von NF-IL6 jedoch noch nicht detektiert worden. Zu einem späteren Zeitpunkt (4h) nach LPS-Stimulation war allerdings in einer hier vorgelegten Folgestudie (Kapitel V 1.5), auch eine Kolokalisation von NF-IL6-IR mit STAT3-IR nachgewiesen worden, was für eine wichtige Rolle für NF-IL6 bei der längerfristigen COX2 und aber auch mPGES-Expression spricht. Zumal NFκB zu diesem Zeitpunkt nicht mehr aktiv ist, erscheint dieses Szenario als sinnvoll und folgerichtig (Abbildung 8).

Obwohl in eine ähnliche Rolle auch für Leptin bei der Induktion von COX2 beschrieben wurde, so ist diese wohl eher indirekt über IL-1β vermittelt (Inoue et al., 2006). Wir konnten in der vorliegenden Arbeit, eine Beteiligung von Leptin für IL-1β-Expression bestätigen (Kapitel V 1.7), aber keine direkte Beteiligung von Leptin bei LPS-induzierte COX2 und mPGES-Expression (Kapitel V 1.9).

Die Verwendung des NFκB-Inhibitors Parthenolid bei LPS-induzierter systemischer Entzündung ergab in einer hier vorliegenden Studie bezüglich der Expression von COX2 und mPGES eine interessante Beobachtung. Wir fanden Hinweise dafür, dass beide Enzyme nicht immer in gleicher Weise reguliert sein müssen bzw. durch leicht unterschiedliche Mechanismen reguliert zu sein scheinen (Kapitel V 1.3). Tatsächlich scheint für mPGES Expression auch der Transkriptionsfaktor early growth response 1 (Egr1) beteiligt zu sein (Walters et al., 2012). Auch andere Studien bestätigen, dass unter gewissen Bedingungen beide Enzyme differenziert reguliert werden können (de Oliveira et al., 2008; Samuelsson et al., 2007). Die zeitlich divergierenden Expressionsprofile beider Enzyme lassen ebenfalls Unterschiede in der Regulation vermuten (Inoue et al., 1995; Ivanov and Romanovsky, 2004). Aufgrund der therapeutischen Bedeutung beider Enzyme sind solche Mechanismen weiter zu untersuchen. Hier konnte gezeigt werden, dass zirkulierendes IL-6 einer der Faktoren sein könnte, die dazu beisteuern; IL-6 scheint an der mPGES-Regulation eine größere Rolle als für die COX2-Induktion zu spielen.

3. Beteiligung von Leptin an der Kommunikation des Immunsystems mit dem Gehirn

In der vorliegenden Arbeit wurden drei Untersuchungen zur Rolle von Leptin als inflammatorischer Mediator bei Krankheiten durchgeführt, die alle drei Signalwege der Kommunikation des Immunsystems mit dem Gehirn abdecken (Kapitel V 1.7, 1.9, 1.10): den humoralen, den nervalen und den Immunzell-vermittelten. Dabei ist zu beachten, dass je nach Versuchsmodell direkte und indirekte Effekte von Leptin von denen zu unterscheiden sind, die mit Übergewicht einhergehen. So wurde tatsächlich in einer kürzlich veröffentlichten Studie nachgewiesen, dass Diät induzierte Obesitas, einer neuronalen Verletzung im Gehirn gleichkommt und mit einer Inflammation einhergeht (Thaler et al., 2012). Neben den im Schrifttum bereits genannten Einflüssen auf das Immunsystem (Kapitel II 6), gilt es nun die Bedeutung von Leptin auch in solchen Prozessen als pro- oder anti-inflammatorischer Modulator für das zentrale Nervensystem (ZNS) aufzuklären; also auch die tatsächlich Leptin-vermittelten Effekte bei Erkrankungen zu analysieren, die mit Übergewicht

einhergehen. Bisher war eine pro-inflammatorische Rolle für Leptin beispielweise bei neuropathischem Schmerz (Lim et al., 2009; Maeda et al., 2009) aber auch eine anti-inflammatorische Rolle bei experimentellen Rückenmarksschäden gezeigt worden (Fernandez-Martos et al., 2012). Letztere Beobachtung stimmt übrigens mit eigenen nicht publizierten Beobachtungen aus einer Teilstudie in Montreal überein, dass eine Leptin Antiserum (LAS)-Behandlung den klinischen Verlauf einer solchen experimentell induzierten Rückenmarksverletzung signifikant verschlimmern kann. Das zeigt, wie unterschiedlich die Wirkung von Leptin sein kann und wie genau man die einzelnen betrachteten / verwendeten Systeme und Krankheitsmodelle hierbei zur Beurteilung berücksichtigen muss. Interessanter Weise wird Leptin sogar eine wichtige Rolle für Langlebigkeit zugeschrieben. Seit langem weiß man, dass unter anderem Futterrestriktion bei Mäusen maßgeblich die Lebensdauer verlängert (Fernandes et al., 1976). Zum Beispiel zeigten Mäuse, deren verfügbares Futter auf 60% ihrer normalen Aufnahme reduziert worden war, eine längere Lebensspanne, da solche Mäuse eine reduziertes aber dennoch intaktes Leptin-System besitzen (Dagon et al., 2005). Außerdem führt eine experimentell induziert erhöhte Expression von Leptin im Hypothalamus von ob/ob Mäusen zu verlängerter Lebensdauer dieser Tiere (Boghossian et al., 2007). Offensichtlich sind also weitere Untersuchungen über die Rolle von Leptin für das Immunsystem und die Homeostase nicht nur im Bezug zu verlängerter Lebensdauer weiterhin notwendig.

3.1. Humorale Hypothese

In zwei aufeinander folgenden Studien (Kapitel V 1.9, 1.7) konnten wir, wie bereits in Abbildung 10 dargestellt, die bekannte Wirkung von Leptin als humoraler neuroimmuner Mediator auf das Gehirn (Kapitel II 6.2) bei LPS-induzierter Inflammation um neue Erkenntnisse erweitern. Leptin wirkt offensichtlich in solchen Situationen der Inflammation direkt auf Gefäßstrukturen, den ventralen Hypothalamus und einzelne andere Gehirnregionen, was anhand einer STAT3-Aktivierung nachgewiesen werden konnte (Kapitel IV 1.1.3). Eine kürzlich durchgeführte Studie im Mäusegehirn bestätigte das Vorhandensein von ObRb in den Regionen, wo wir Leptin-induzierte STAT3-Aktivität bei systemischer Inflammation beobachten konnten (Scott et al., 2009). Die neuen Erkenntnisse werden zusätzlich dadurch unterstützt, dass Mütze und Kollegen (2006) eine direkte Aktivierung von Endothelzellen durch Leptin zeigen konnten (Mütze et al., 2006) und Inoue und Kollegen (2006) auch eine indirekte Wirkung von Leptin auf IL-1β-Expression in perivaskuläre Makrophagen beschrieben. Darüber hinaus kann Leptin sogar modulatorisch eine LPS-induzierte Expression

von IL-1β und Chemokinen in Mikrogliazellen erhöhen (Lafrance et al., 2010). In diesen drei Zelltypen (Endothelzellen, perivaskuläre Makrophagen und Mikroglia) könnte Leptin demnach modulatorisch im Bereich der Schnittstelle zwischen Peripherie und Gehirn bei systemischer Inflammation zusätzlich zu den bereits bekannten Strukturen (ARC, Hirnstamm) wirken.

Allerdings bleibt hervorzuheben, dass anders als bei anderen Zytokinen wie IL-6, Leptin auch unter basalen [(Luheshi and Rummel, 2007), starved animals] Bedingungen in hohen Konzentrationen (ng Bereich für Leptin versus pg-Bereich für IL-6) im Blut zirkuliert. Damit verhält sich dieser Mediator grundsätzlich völlig anders als ein Zytokin. Ein humoraler Mediator sollte außerdem eigentlich durch exogene Stimulation des Immunsystems wie LPS bzw. bei systemischer Inflammation erhöht in der Zirkulation messbar sein. Bei Zytokinen kommt es unter diesen Bedingungen zu einer bis zu 10.000-fachen Erhöhung (Pollmächer et al., 2002). In den hier vorlegenden Studien ist in Mäusen, einmal eine zweifache Erhöhung (Kapitel V 1.9) und in der anderen Studie gar keine Erhöhung zirkulierender Leptin-Konzentrationen nachgewiesen worden (Kapitel V 1.7). Bei Ratten hatten wir sogar in vorhergehenden Studien ebenfalls keine LPS-induzierte Plasmaleptin-Erhöhung nachweisen können (Luheshi and Rummel, 2007). In drei weiteren Studien bei Ratten konnte ebenfalls keine Erhöhung von Leptin nach inflammatorischen Stimuli (LPS, Zytokine) nachgewiesen werden (Gautron et al., 2005; Inoue et al., 2008; Spencer et al., 2007a). Dies widerspricht der vielfach zitierten Meinung, dass Leptin als neuroimmuner Mediator im Blut erhöht bei Infektion und Inflammation vorkommt. Bei genauerer Betrachtung eines Großteils der Studien, die eine solche Erhöhung nachgewiesen haben, fällt allerdings auf, dass die Leptinkonzentrationen dabei nicht wirklich höhere Werte annehmen wie sie auch im normalen zirkadianen Tagesrhythmus auftreten (Kapitel II 6.2). Außerdem wurden Tiere (Möglichkeit von Speziesunterschieden zwischen Hamster, Maus und Ratte) vor der Stimulation vielfach gehungert, was die basalen Konzentrationen von Leptin dramatisch absinken lässt und damit eine relative „Erhöhung“ von Leptin hierzu erst sichtbar macht (Berkowitz et al., 1998; Faggioni et al., 1998; Gomez-Ambrosi et al., 2004; Sarraf et al., 1997). Ob eine 2-fache, wie hier beobachtet, bis vielleicht 10-fache Erhöhung der Plasma-Leptin Konzentrationen tatsächlich einen physiologischen Unterschied in seiner Wirkung ausmacht, bleibt zu beweisen, ist aber unwahrscheinlich. Vielmehr ist Leptin eher als ein Modulator von Entzündungsreaktionen zu sehen (Lafrance et al., 2010). Damit muss Leptin nicht zwingend in seiner Plasmakonzentration ansteigen sondern erst durch seine

Abwesenheit / Reduktion bzw. Unwirksamkeit (zentrale oder periphere Resistenz) werden über Leptin das Immunsystem und die Homeostase maßgeblich beeinflusst.

3.2. Nervale Hypothese

Bei Versuchsreihen in denen Leptin als Stimulation verwendet wurde, wie auch in einer Teilstudie der vorliegenden Arbeit (2,5 mg/kg, Kapitel V 1.10), sind vielfach sehr hohe Mengen appliziert worden, um eine längerfristige Wirkung zu untersuchen (1-5mg/kg)(Ahima et al., 1996; Campfield et al., 1995; Halaas et al., 1995; Harris et al., 1998). Es konnte hier allerdings keine maßgebliche Rolle des Vagusnerven an der Vermittlung längerfristiger Appetit-hemmender Effekte unter physiologischen bzw. inflammatorischen Bedingungen nachgewiesen werden. Leptin scheint lediglich an der Beendigung von individuellen Mahlzeiten beteiligt zu sein (Peters et al., 2005). Vielmehr konnten wir mittels Vagotomie und Leptin-Stimulation zeigen, dass vagale Affarenzen wahrscheinlich auch Hunger-vermittelnde Signale zum Gehirn weiterleiten, wie bereits in einer früheren Studie vorgeschlagen wurde (Furness et al., 2001). Wir konnten nämlich feststellen, dass vagotomierte Tiere reduzierte Futteraufnahme zeigten, obwohl im Hypothalamus die Expression vom orexigen wirkenden AgRP erhöht war und von POMC ein Trend zur Erniedrigung festgestellt wurde (Abbildung 6). Obwohl die Tiere also mehr fressen sollten, fehlte ihnen offensichtlich der Stimulus dazu, so dass sie auch nach langer Rekonvaleszenz nach der chirurgischen Prozedur (Vagotomie) immer noch weniger wogen als die scheinoperierten Kontrolltiere. Letztendlich konnte vielleicht auch wegen der verwendeten relativ hohen Dosis an Leptin keine vagale Beteiligung an der Leptin-reduzierten Futteraufnahme nachgewiesen werden. Eine starke Aktivierung humoraler Signalwege im Hypothalamus (phophoSTAT3 im ARC) und Hirnstamm (STAT3-Signale im NTS) trat nämlich in dieser Studie in Erscheinung. Tatsächlich aktiviert Leptin wohl parallel zum Hypothalamus auch den Hirnstamm und induziert die entsprechenden Effekte Anorexie und erhöhten Energieumsatz (Grill et al., 2002; Skibicka and Grill, 2009). Damit wirkt Leptin nicht nur auf thermoregulatorische Effektorbahnen (Kapitel IV 1.2), sondern auch auf das Herz-Kreislauf-System sowie die Atmung (Inyushkin et al., 2009; Skibicka and Grill, 2009). Die zentrale Wirkung von Leptin über das autonome Nervensystem könnte zudem einige seiner Effekte auf das Immunsystem erklären. In einer Untersuchung bei dem ein septisches Modell von lebenden Bakterien durch Punktion des Caecum verwendet wurde, schlagen die Autoren vor, dass eine Wirkung von Leptin im ZNS, die Überlebensrate der Mäuse durch

solche anti-inflammatorischen Signalwege des vegetativen Nervensystems vermitteln könnte (Tschöp et al., 2010).

3.3. Immunzell-vermittelt

In einer Teilstudie konnten wir zum ersten Mal zeigen, dass Leptin an der LPS-stimulierten Rekrutierung von neutrophilen Granulozyten in das Gehirn beteiligt ist. Anders als bei Tschöp und Kollegen (2010), haben wir eine hohe fast septische Dosierung von LPS (2.5mg/kg) verwendet, die die Mäuse in jedem Fall aber überleben. Das hier verwendete Entzündungsmodell unterscheidet sich auch dadurch von der Caecumpunktion, dass keine bakterielle Abwehr stattfinden muss. Tatsächlich konnten wir zeigen, dass Leptin wahrscheinlich über die Modulation der Expression von LPS-induziertem IL-1β, Chemokinen (KC, MIP2) und ICAM1 die LPS-induzierte Rekrutierung von neutrophilen Granulozyten vermittelt (Kapitel V 1.7, Abbildung 12). Das heißt, die Rekrutierung dieser Immunzellen zum Gehirn war in ob/ob sowie db/db Mäusen sowie im physiologischen Modell einer natürlichen Leptin-Defizienz durch 48-stündiges Hungern dramatisch reduziert. Schließlich konnten wir auch zeigen, dass eine pharmakologische Reduzierung von endogenem zirkulierenden Leptin mittels LAS, zu einer reduzierten Rekrutierung von Neutrophilen führt. In diesem Fall könnte man also Leptin eher als einen inflammatorischen Mediator bezeichnen. Wie schon erwähnt ist abhängig von dem Entzündungsmodell die Wirkung von Leptin offensichtlich unterschiedlich.

Die Beteiligung von Leptin an der Induktion von IL-1β (z.B. in perivaskulären Makrophagen, und Mikroglia) wird durch mehrere schon erwähnte Studien unterstützt (Hosoi et al., 2002b; Inoue et al., 2006; Lafrance et al., 2010; Lim et al., 2009; Luheshi et al., 1999; Pinteaux et al., 2007; Sachot et al., 2004). Außerdem ist bekannt, dass IL-1β die Rekrutierung von Neutrophilen in das Gehirn induzieren kann (Anthony et al., 1998; Anthony et al., 1997; Proescholdt et al., 2002; Shaftel et al., 2007). In der vorliegenden Studie war der Effekt von Leptin auf die Rekrutierung von Neutrophilen also wahrscheinlich indirekt über Modulation der IL-1β-Expression vermittelt und nicht direkt durch die bekannte Wirkung von Leptin auf neutrophile Granulozyten. Solche Leptin-vermittelten Effekte auf Chemotaxis und Apoptose sind über die kurze Form des OBR auf Neutrophilen vermittelt (Bruno et al., 2005; Montecucco et al., 2006). Da in db/db Mäusen ebenfalls eine reduzierte Rekrutierung von Neutrophilen beobachtet worden war, obwohl diese Mäuse noch die kurzen Formen des OBR besitzen (welche auf diesen Immunzellen lediglich vorkommen), ist eine direkte Beteiligung von Leptin deshalb auszuschließen. Vielmehr übte Leptin seine Wirkung also wahrscheinlich

direkt auf das Gehirn aus. Dort war auch die Expression und IR des für die Rekrutierung von Neutrophilen so wichtigen Adhäsionsmoleküls ICAM1 dramatisch in ob/ob, db/db und im Hungermodell verringert. Dieser Faktor ist sehr wichtig für den Prozess der Rekrutierung; es konnte nämlich gezeigt werden, dass in ICAM-defizienten Mäusen die LPS-induzierte Rekrutierung von Neutrophilen um 50% reduziert ist (Bohatschek et al., 2001). Die pharmakologische Strategie der Reduktion endogenen Leptins mit LAS hatte allerdings keinen Effekt auf ICAM1-Expression aber auf die Expression von Chemokinen. Dies deutet darauf hin, dass die drei verwendeten Versuchsmodelle (Hunger, ob/ob – db/db und LAS) zwar prinzipiell ähnlich, aber die zugrundeliegenden Mechanismen einer verringerten Rekrutierung von neutrophilen Granulozyten leicht unterschiedlich sind. Es könnte auch sein, dass nicht die akute Leptin-Neutralisation, sondern längerfristige indirekte Effekte eine Rolle spielen. Dennoch war in allen drei Modellen auch die Expression der für Neutrophile wichtigsten Chemokine nämlich KC und MIP2 (Kielian et al., 2001) stark reduziert. Neben IL-1β (McColl et al., 2007; Shaftel et al., 2007) ist sogar eine direkte Wirkung von Leptin für die Regulation der Expression dieser Zielgene möglich. In peripheren Organen (Kolon) war eine Leptin-vermittelte Induktion von KC und MIP2 beschrieben worden (Fenton et al., 2007). Da ICAM1 durch STAT3 induziert werden kann, ist auch hier eine direkte Wirkung durch Leptin denkbar (Wung et al., 2005), aber ein indirekter IL-1β-vermittelter Weg wahrscheinlicher (Cao et al., 1996).

Die Tatsache, dass LPS-induzierte Rekrutierung von neutrophilen Granulozyten Leptin vermittelt ist, könnte von großer Bedeutung für Individuen sein, die veränderte Leptinkonzentrationen aufweisen, wie bei Essstörungen oder Übergewicht (Bluher and Mantzoros, 2004). Bei vorhandenen Pathologien, die mit einer erhöhten Rekrutierung von Neutrophilen einhergehen (Bohatschek et al., 2001; McColl et al., 2007; Perry et al., 2007), könnte LAS eine therapeutische Strategie darstellen, um mögliche negative Auswirkungen zu minimieren. Gerade bei Ischämien im Gehirn, in deren Rahmen Rekrutierung von neutrophilen Granulozyten und systemische Inflammation mit negativen Auswirkungen verbunden sind, wäre dies sinnvoll (McColl et al., 2007; Spencer et al., 2007b).

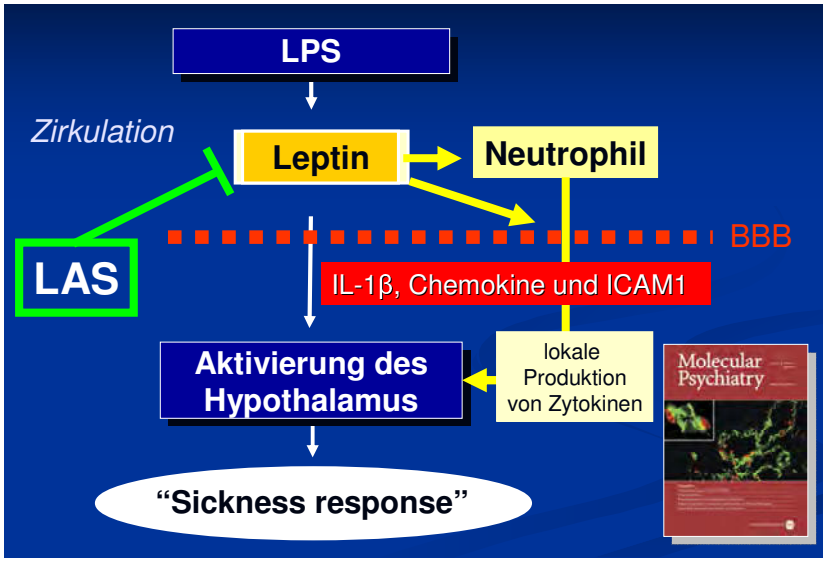


Abbildung 12
Schematische Darstellung der Beteiligung von Leptin an LPS-induzierter Rekrutierung von neutrophilen Granulozyten (Neutrophile) in das Gehirn von Mäusen. Leptin wirkt prinzipiell direkt auf Strukturen der Blut-Hirn-Schranke (BBB) und kann außerdem bei Neutrophilen die Chemotaxis beeinflussen. Während LPS-induzierter Entzündung vermittelt Leptin die Rekrutierung der Neutrophilen über die Expression von IL-1β, neutrophil spezifischen Chemokinen (KC und MIP2) sowie dem interzellulären Adhäsionsmolekül ICAM1. Durch eine Neutralisation von zirkulierendem Leptin mit einem spezifischen Antiserum (LAS) kann die Rekrutierung pharmakologisch reduziert werden (Kapitel V 1.7).

Trotzdem bleibt anzumerken, dass wiederum das Entzündungsmodell und der Entzündungsstatus differenziert betrachtet werden müssen, wenn solche Therapien angewendet werden sollen. Neutrophile Granulozyten können dabei sowohl negative also auch positive Effekte vermitteln. Sie können neurotoxisch wirken und unter anderem die BBB durch Bildung von freien Radikalen und proteolytischen Enzymen beschädigen (Dinkel et al., 2004; Emerich et al., 2002). So wurde die Hemmung der Invasion von Neutrophilen in einigen Studien mit neuroprotektiven Effekten in Zusammenhang gebracht. Es finden sich aber auch Untersuchungen zur zerebralen Ischämie, in der eine Depletion von Neutrophilen wenige bis keine protektiven Effekte zeigten (Beray-Berthat et al., 2003; Harris et al., 2005) oder sogar eine chronische Rekrutierung von Neutrophilen keine Zeichen an Neurodegeneration induzierte (Shaftel et al., 2007).

Ob der beobachtete Effekt einer reduzierten Rekrutierung von neutrophilen Granulozyten in das Gehirn bei den 48-stündig gehungerten Tieren auch etwas mit der Langlebigkeit zu tun hat, die durch restringierte Futteraufnahme beschrieben worden ist (Kapitel V 3), bleibt unklar, lässt aber Raum für Spekulationen. Futterrestriktion geht mit einer Reduzierung der

zirkulierenden Leptin-Konzentrationen einher (Guevara et al., 2008; Moyse et al., 2012). Folglich könnte damit verbunden auch die Rekrutierung von Immunzellen bei vorliegenden Pathologien gedämpft werden. Dies wiederum könnte die Gesundheit und Langlebigkeit fördern. Da Futterrestriktion nicht zu einer Defizienz des Leptin-Systems führt, wäre eine übermäßige Beeinträchtigung der Immunabwehr gleichzeitig nicht zu erwarten. Vielmehr könnten reduzierte Leptin-Konzentrationen beim Altern mögliche Überreaktionen einschränken und sich insgesamt positiv (vielleicht Lebensspannen verlängernd) auswirken.

4. TLR-Modelle, Therapiepotenzial und potentielle Nebenwirkungen

Um TLR-Agonisten, Zytokine und Leptin therapeutisch verwenden zu können, ist es notwendig, die Signalwege möglichst genau zu kennen und mögliche Nebenwirkungen zu determinieren und mit dem therapeutischen Nutzen in Relation zu setzten. In der vorliegenden Arbeit wurden zum einen Untersuchungen zur Aufklärung von Mechanismen (neuronal, humoral, Immunzell-vermittelt) und Signalwegen (LPS, PIPC, MALP2, Imiquimod, IL-6, Leptin, COX2, mPGES) und zum anderen zur Charakterisierung von Nebenwirkungen (MALP2, Imiquimod; in Form von Krankheitssymptomen) bei verschiedenen Applikationswegen durchgeführt. Das zusammenfassende überarbeitete Modell der Mechanismen und Signalwege ist in Abbildung 13 dargestellt.

4.1. TLRs

LPS: Für verschiedenste Untersuchungen stellt LPS das klassische Modell einer akuten Entzündungsreaktion dar. Neben den hier aufgeführten Applikationsformen (i.a., i.p., s.c., i.m.) ist beispielsweise aber auch die LPS-Inhalation ein gutes Versuchsmodell und wird sogar bei Menschen zur Charakterisierung von chronisch inflammatorischen Prozessen (Kitz et al., 2008) oder zur Untersuchung von neuen anti-inflammatorischen Signalwegen in der Lunge verwendet (Mayer et al., 2009). Bei systemischer Gabe von LPS ist allerdings zu beachten, dass es bei hohen Dosen auch zu langfristigen Effekten kommen kann, die im Gehirn noch über Monate nachweisbar sein können (Qin et al., 2007). Ein weiterer Punkt, der bei der Verwendung solcher Modelle zu bedenken bleibt, ist, dass LPS nicht mit einer echten bakteriellen Infektion gleichgesetzt werden kann. So ist LPS zwar sehr gut dosierbar, ist in der Regel aber bereits nach einer Stunde wieder aus dem Blut verschwunden. In Studien, die lebende Bakterien zur Stimulation verwenden, kann hingegen einer länger andauernde, kontinuierliche Stimulation des Immunsystems untersucht werden (Campisi et al., 2003; Soares et al., 2012). Allerdings ist hier keine ganz isolierte Betrachtung der TLR4-

Aktivierung mehr möglich, da beispielsweise auch TLR2 zum Beispiel durch enthaltene Peptidoglykane vermehrt aktiviert werden dürfte (Soares et al., 2012).

PIPC: Dieser spezifische TLR3-Agonist wurde bereits vielfach als Modell für virale Infektionen verwendet (Fortier et al., 2004; Katafuchi et al., 2003) wie auch für virale Infektionen des Respirationstraktes über intratracheale Applikation (Traynor et al., 2004). Für das Gehirn konnte beispielsweise unter Verwendung des viralen Mimetikums PIPC eine erhöhte Empfindlichkeit für Anfallsleiden nach intrazerebroventrikulärer Injektion detektiert werden (Galic et al., 2009). In der vorliegenden Arbeit konnten wir die Erkenntnisse über die bekannte Fieber induzierende Wirkung in Ratten erweitern (Chuang et al., 1990; Fortier et al., 2004). Neben seiner PG-induzierenden Wirkung konnten wir zum ersten Mal zeigen, dass bei subkutaner Applikation von PIPC kein Fieber induziert werden kann (Kapitel V 1.11, 1.13). Anscheinend sind keine oder eine nicht ausreichende Zahl an TLR3-Rezeptoren im subkutanen Gewebe aktiviert worden oder dort gar nicht vorhanden, um solch eine Reaktion hervorzurufen. Lediglich nach subkutaner Stimulation mit *Staphyloccocus aureus* Zellwandbestandteilen war solch eine fehlende stimulierende Wirkung für einen TLR-Agonisten bisher beschrieben worden (Cartmell et al., 2002). Die funktionelle Aufklärung der Verteilung an TLRs ist sehr wichtig, um die Mechanismen der Wirkung besser verstehen zu können und konnte in der vorliegenden Studie supplementiert werden (Kapitel V 1.13). Außerdem konnten wir nachweisen, dass sich im Gegensatz zu LPS, gegenüber PIPC nur eine partielle Toleranz entwickelt. Bei mehrmaliger Applikation von LPS, aber auch einem Analog für MALP2 (FSL1) kommt es nämlich zu einer graduellen fast völligen Abnahme der Fieber erzeugenden Wirkung und sogar zu einer Kreuztoleranz zwischen den beiden TLR-Agonisten (Greis et al., 2009; Roth et al., 1997; Roth et al., 1994a). Für den Toleranzeffekt gibt es verschiedene Erklärungen. Sie beinhalten beispielweise Änderungen in der NFκB Zusammensetzung aus zwei P50 Untereinheiten anstelle des Heterodimers von P50 und P65, was schließlich mit niedrigeren Zytokinantworten und Fieber einhergeht (Zeisberger and Roth, 1998). In der vorliegenden Arbeit wäre ein mögliche Erklärung der fehlenden Toleranzentwicklung gegenüber PIPC durch eine kürzlich durchgeführte Studie zu ergänzen, die besagt, dass über PIPC-induziertes INFγ möglicherweise Toleranzentwicklung gehemmt werden kann (Chen and Ivashkiv, 2010).

MALP2: Dieser TLR2/6-Agonist ist therapeutisch von größerem Interesse. So wurde MALP2 als mukosales Adjuvanz für intranasal applizierte Impfstoffe verwendet (Borsutzky et al., 2003; Rharbaoui et al., 2002) und eine topische Anwendung konnte die Heilung von Hautwunden in diabetischen Mäusen beschleunigen (Deiters et al., 2004). In einer Studie

konnten sogar positive Effekte durch Injektion von MALP2 in Pankreastumore für die Patienten erzielt werden (Schmidt et al., 2007). In dieser Studie kam es allerdings auch zu systemischen adversen Effekten mit Sepsis artigen Ausmaßen. Folglich waren weitere Untersuchungen mit MALP2 notwendig, um potentielle Nebenwirkung besser abschätzen zu können. In der vorliegenden Arbeit konnten wir die Mechanismen der MALP2-Wirkung näher aufklären. Zum einen fanden wir heraus, dass s.c. appliziertes MALP2 über periphere und zentrale PG-abhängige Mechanismen an der Fieberentstehung beteiligt ist und eher ein moderates Fieber erzeugendes Potenzial besitzt [(Knorr et al., 2008) Kapitel V 1.6]. Zum anderen konnten wir in einem anderen Teilprojekt feststellen, dass entgegen früheren Studien mit anderen Lipoproteinen (Ozinsky et al., 2000), MALP2 *in vivo* wohl maßgeblich über den dimeren Rezeptor TLR2/6 wirkt und TLR6 allein nicht ausreichend für seine Erkennung ist (Kapitel V 1.2). Dies hängt wohl damit zusammen, dass MALP2 nur zwei Fettsäuren besitzt und zur Erkennung eine Ko-Expression von TLR2/6 notwenig ist (Morr et al., 2002). Außerdem waren die Krankheitssymptome nach LPS-Gabe in TLR2KO-Mäusen abgeschwächt, was darauf hinweist, dass TLR2 auch einen gewissen Beitrag zu LPS-induzierter Inflammation leistet. Hierzu gibt es frühere Studien, die das bestätigen (Kirschning et al., 1998) aber auch andere Publikationen, die eine Kontamination mit Lipoproteinen für die Beteiligung von TLR2 an LPS-induzierten Reaktionen verantwortlich machen (Steiner et al., 2005a). Des Weiteren war durch die Verwendung von SHR-Ratten (sind CD36 defizient) keine Beteiligung des Rezeptors CD36 bei MALP2-stimulierter, systemischer Entzündungsreaktion und damit verbundenen Krankheitssymptomen nachgewiesen worden. Anders als in früheren Studien, konnte also die Beteiligung von CD36 an der MALP2-Erkennung nicht bestätigt werden (Hoebe et al., 2005). Vielmehr war sogar die LPS-stimulierte Aktivierung von isolierten Makrophagen sowie LPS-induzierte Krankheitssymptome bei dieser Rattenlinie im Vergleich zum Kontrollstamm (WKY) stärker beeinträchtigt worden als in den SHR-Tieren. Dies weist auf einen generellen Einfluss von CD36 unabhängig von MALP2 auf Entzündungsreaktionen nach Stimulation mit TLR-Agonisten hin.

Imiquimod: Dieser TLR7-Agonist hat sich bisher durch sein antitumorösen Eigenschaften ausgezeichnet (Broomfield et al., 2009; Lu et al., 2010) und wurde vor allem beim subkutanen Melanom eingesetzt (Ma et al., 2010). Die Applikationsweise für solche Tumortherapiestrategien beschränkt sich für diese Substanz hauptsächlich auf topische Behandlungen, beispielsweise durch intraepitheliale Gabe auf mukosale oder kutane Oberflächen (Kapitel V 1.1). *In vivo* wurde Imiquimod bisher lediglich auf seine Krankheit

erzeugenden Effekte nach intranasaler Gabe getestet, was zu keinem Fieber aber zu Anorexie geführt hatte (Hayashi et al., 2008). Hier konnten wir zum ersten Mal zeigen, dass Imiquimod im moderaten Ausmaß Fieber und Anorexie führte und zwar sogar eine stärkere Fieberreaktion nach s.c.-Stimulation als nach i.p.-Applikation. Zudem war erst eine sehr hohe Dosis von 5 mg/kg überhaupt pyrogen wirksam, was darauf hinweist, dass diese Substanz bei seiner Anwendung lediglich ein sehr moderates Potenzial für Nebenwirkungen zu haben scheint. Die kürzlich vorgeschlagene Anwendung zur Behandlung von ovarialen Mikrometastasen durch i.p. Bauchspülung (Lavage) mit Imiquimod, lässt relativ wenige negative Nebenwirkungen erwarten. In der vorliegenden Arbeit war die Wirkung von Imiquimod von einer robusten Induktion von INF vor allem in der Milz aber auch von INFγ im Plasma begleitet. Diese Mediatoren waren wahrscheinlich zumindest anteilig an den vermittelten Effekten beteiligt. Genauere Analysen der Beteiligung der einzelnen INF-Typen an Krankheitssymptomen und dem therapeutischen Potenzial erfordern weiterführende Untersuchungen. Es bleibt aber zu bemerken, dass Imiquimod ein vielversprechender Kandidat für therapeutische Ansätze bleibt, wozu unsere Ergebnisse für die zukünftigen Untersuchungen beitragen.

Abkürzung	Rezeptor	Lokalisation Maus	STAT3-Signale	PG	Fieberantwort	
					s.c.	i.p./i.a.
LPS	TLR4 (TLR2)	ubiquitär (Neurone, Mikroglia, Endothel)	(+++) robust in Maus Ratte und Meerschwein, Peak bei ca. 2h	+++	++	+++
PIPC	TLR3	nicht s.c.? (ZNS)	(+++) robust in Meerschweinchen bei 2h	+++	-	+++
MALP2	TLR2/6 (nicht CD36)	(ZNS)	(++) moderat in Ratten bei 2h, 3h	++	+	++
Imiquimod	TLR7	Makrophagen dendritische Zellen, besonders s.c.? (ZNS)	(+) schwach in Ratten bei 2h und 6h	+(?)	++	+

Tabelle 2

Zusammenstellung des Antwortverhaltens der untersuchten TLR-Agonisten: deren Rezeptoren, Rezeptorverteilung, STAT3-Signalintensität, PG-Bildungspotenzial / Abhängigkeit und Fieberantwort aufgeteilt nach Applikationsweg [Kapitel V 1.1, 1.2, 1.3, 1.4, 1.5, 1.6, 1.9, 1.11, 1.12, 1.13; (Kong and Le, 2011)].

Zusammenfassend sind die verwendeten TLR-Agonisten in Tabelle 2 mit ihren respektiven Eigenschaften und diskutierten Wirksamkeiten aufgeführt.

4.2. Zytokine

Neben den Ergebnissen aus der hier vorliegenden Arbeit (Kapitel V 1.1, 1.2, 1.3, 1.4, 1.5, 1.6, 1.8, 1.9, 1.11, 1.12, 1.13) gibt es noch weitere Studien, die eine Beteilung von IL-6, anderen Zytokinen und Leptin als humorale Mediatoren für die Entstehung von Fieber und Krankheitssymptomen bestätigen. Dabei wurden prinzipielle Mechanismen der Kommunikation zwischen Immunsystem und Gehirn bestätigt, die auch bei anderen Prozessen wie chronischen Erkrankungen von Bedeutung sind.

Während LPS-induzierter systemischer Entzündung konnte in einer Studie gezeigt werden, dass zirkulierendes Leptin und IL-6 an LPS-induziertem Fieber und sickness behavior beteiligt ist; TNFα reduzierte lediglich die frühe Phase des Fiebers und zirkulierendes IL-1β hatte keine signifikanten Effekte (Harden et al., 2006). Eine Beteiligung von zirkulierendem IL-6 und zentralem IL-1β an LPS-induzierter Anorexie und Lethargie sowie für Fieber konnte kürzlich zusätzlich durch Harden und Kollegen (2011) bestätigt werden (Harden et al., 2011). Diese Zytokine können ihrerseits Neurone und andere Zellen in den CVOs aktivieren (Elektrophysiologie, Kaziumimaging) und die Information an andere Gehirnstrukturen weiter leiten (Desson and Ferguson, 2003; Ott et al., 2010; Wuchert et al., 2009). Auch zentral gebildete Zytokine IL-6 (Chai et al., 1996; Soares et al., 2012), TNFα (Palin et al., 2007) und IL-1β (Fortier et al., 2004; Harden et al., 2011) scheinen bei der Entstehung von Fieber und Anorexie beteiligt zu sein.

Ausgehend nicht zuletzt von den zahlreichen Erkenntnissen der Fieberforschung und der Analyse der Kommunikationswege zwischen Immunsystem und Gehirn, werden anti-Zytokinstrategien oder Zytokine selbst heute in der Klinik eingesetzt. Bisher werden therapeutisch beispielsweise IL-6R-Antikörper (Navarro-Millan et al., 2012; Tanaka and Kishimoto, 2012) und anti-TNFα (Tocilizumab) bei rheumatoider Arthritis relativ erfolgreich angewendet (Alves et al., 2011). Auch die Blockade von IL-1β durch IL-1ra (Anakinra) wird häufiger bei relativ seltenen „autoinflammatorischen“ Krankheiten verwendet (Dinarello, 2009; 2010). Interferone sind vielfach in Gebrauch, unter anderem bei Multipler Sklerose (Meuth et al., 2012) und Hepatitis C (Casey and Lee, 2012) oder bei Katzen zur Behandlung des felinen Leukämievirus (Interferon omega) (Domenech et al., 2011).

Hervorgehend aus der vorliegenden Arbeit könnte die Neutralisation von Leptin (LAS), wie bereits beschrieben, bei Pathologien, die mit erhöhter Rekrutierung von neutrophilen

Granulozyten einhergehen, von Nutzen sein (Kapitel IV 3.3). Therapeutisch ist eine Neutralisation von IL-6 potentiell durch das auch hier verwendete IL-6AS eine Möglichkeit, um neben mechanistischen Untersuchungen in den beschriebenen Situationen, die mit erhöhten zirkulierenden IL-6-Konzentrationen einhergehen, positive Effekte zu erzielen. Entsprechend den hier dargestellten Ergebnissen, könnte damit indirekt auch der PG-Syntheseweg anteilig gehemmt werden, ein Konzept, welches in vieler Hinsicht von großem Interesse ist, da PGE2 (bzw. beispielweise mPGES) an vielen Krankheitsprozessen beteiligt ist (Samuelsson et al., 2007). Einige Fragen bleiben bisher allerdings noch unbeantwortet und bedürfen weiteren Untersuchungen, bevor solch ein therapeutischer Einsatz in Frage kommt.

Die Vielzahl an über STAT3-wirkenden Zytokinen nicht zuletzt aus der gp130-Rezeptorfamile und des anti-inflammatorischen Zytokins IL-10 oder der pro-inflammatorischen Interferone des Typs I werfen die Frage auf, wie STAT3 sowohl anti- als auch pro-inflammatorische Effekte erzielen kann (Greenhill et al., 2011). Greenhill und Kollegen (2011) konnten mit Hilfe genetisch modifizierter Mäuselinien mit Bezug zu gp130 zeigen, dass so genanntes IL-6 Trans-Signaling über lösliche IL-6-Rezeptoren(R) vor allem die pro-inflammatorische Wirkung von IL-6 während Endotoxämien erklärt. In anderen kürzlich durchgeführten Studien konnte zudem gezeigt werden, dass eine Hemmung von IL-6 Trans-Signaling zu einer schnelleren Genesung von LPS-induziertem sickness behavior beiträgt (Burton et al., 2011) und altersbedingte Infekt begleitende kognitive Defekte reduzieren kann (Burton and Johnson, 2011). Der klassische Signalweg über den IL-6-Rezeptor wäre in diesem Fall eher anti-inflammatorisch und würde die beobachteten protektiven Funktionen von IL-6 bei starken Krankheitsstadien erklären (Roth et al., 2004b; Xing et al., 1998). IL-6 hemmt nämlich unter anderem die Produktion von IL-1 und TNFα und ist an der Stimulation von anti-inflammatorischen Mediatoren wie IL-10 beteiligt (Roth et al., 2004b). In der eigenen Studie traten auch Hinweise für solch einer möglicherweise anti-inflammatorische Wirkung anhand einer verstärkten LPS-induzierten Expression von inflammatorischen Markerproteinen (ICAM1, MCP1, MIP2) in IL-6KO Mäusen zu Tage (Kapitel V 1.9). In Zukunft bleibt abzuwarten, ob IL-6 mit seinen pro- und anti-inflammatorischen Wirkungen gehemmt werden kann, ohne starke Nebenwirkungen zu erzielen.

4.3. Transkriptionsfaktoren

Prinzipiell sind Transkriptionsfaktoren als Zielstrukturen für anti-inflammatorische Therapien schon lange bekannt. In dieser so kritischen Position der *de novo* Synthese von

Entzündungsmediatoren kann hier logischer Weise sehr effektvoll eingegriffen werden, um die Bildung von Zytokinen oder PG einzudämmen. In der Tat sind viele anti-inflammatorischen Wirkungen durch eine Hemmung von inflammatorischen Transkriptionsfaktoren vermittelt. Interessanter Weise hat sich gerade dieses Prinzip in der Natur bereits sehr bewährt. Nicht zuletzt üben Glucocorticoide ihre Hauptwirkung über eine Hemmung von inflammatorischen Transkriptionsfaktoren aus (Franchimont et al., 2003). Dazu gehörend vor allem NFκB aber auch STATs, die teilweise über eine Protein-Protein-Interaktion (crosstalk) gehemmt werden (McKay and Cidlowski, 1999). Im Gehirn wirken Glucocorticoide beispielsweise aber auch hemmend über die erhöhte Transkription des negativen NFκB-Regulators IκBα (Quan et al., 1997). NF-IL6-scheint dagegen sogar in der Expression durch Glucocorticoide erhöht oder erniedrigt zu werden (Eastman et al., 1996; McKay and Cidlowski, 1999). Die Entwicklung von mehr spezifischen Glucocorticoid Derivaten, die lediglich einen dieser Signalwege hemmen, stellt eine der Herausforderungen der relevanten Forschung in diesem Feld dar (Franchimont et al., 2003). Neben endogenen Mediatoren werden viele Natursubstanzen aufgrund ihrer bekannten anti-inflammatorischen Wirkung eingesetzt (Yuan et al., 2006). Dazu gehört auch Curcumin, welches unter anderem den NFκB-Signalweg hemmt (Aggarwal, 2010). NFκB-Inhibition ist außerdem eine bewährte Strategie, Fieber zu hemmen (Lee et al., 2003b). Parthenolid (P) ein weiterer Naturstoff wurde in der hier vorliegenden Arbeit als NFκB-Inhibitor eingesetzt. Dieses sesquiterpene Lactone ist die hauptaktive Substanz von Heilpflanzen, welche mexikanische Indianer beispielsweise bei Hautinfektionen einsetzten (Yuan et al., 2006). Es wurde unter anderen aber auch bereits als Therapeutikum bei Migräne und zur Krebsbehandlung verwendet (Anderson and Bejcek, 2008; Kawasaki et al., 2009; Tassorelli et al., 2005). Bisher gab es allerdings keine Daten darüber, ob P tatsächlich auch direkt auf das Gehirn wirken kann, obwohl eine gute BBB-Permeabilität aufgrund des lipophilen Charakters zu erwarten ist (Pandey et al., 2008; Tassorelli et al., 2005). Tatsächlich konnten wir zum ersten Mal zeigen, dass P auch im Gehirn den NFκB-Signalweg und Fieber reduzieren kann. Außerdem war auch die NF-IL6-Expression signifikant verringert; nicht aber der STAT3-Signalweg, obwohl eine hemmende Wirkung von P für STAT3 in früheren Studien gezeigt werden konnte (Sobota et al., 2000). Die direkte Wirkung von P auf Zellen im Gehirn konnten wir zusätzlich in Experimenten an primären neuroglialen Kulturen des OVLT bestätigen. Da in dieser Gehirnstruktur eine unvollständige BBB vorliegt, sind die Zellen direkt P ausgesetzt. LPS-induzierte Konzentrationen von IL-6 und TNFα wurden sowohl im Plasma als auch in den Überständen der Kultur signifikant gehemmt. Neben einer Reduktion der Schlüsselenzyme

der PG-Synthese (COX2, mPGES) hatte P auch signifikante Effekte auf die Expression von Markern für mitochondrialen Stress im Gehirn, nämlich PGC1α und NRF1. Insgesamt scheint also P über eine Hemmung peripherer und zentraler Zytokine und vielleicht der Reduktion von oxidativem Stress sowie des PG-Wegs moderate positive Effekte auf Fieber und Krankheitssymptome zu bewirken. Peripher appliziertes P hat unseren Untersuchungen nach therapeutisches Potenzial für die Behandlung von inflammatorischen Prozessen im Gehirn.

In einer anderen hier vorliegenden Teilstudie konnten wir die Hypothese aufstellen, dass der negative NF-IL6-Regulator Trib1 möglicherweise als so genanntes „Stopsignal“ der Entzündungsreaktion im Gehirn fungieren könnte (Kapitel V 1.5). Seine hemmende Wirkung auf die NF-IL6-Aktivität war in einer früheren Studie eindeutig gezeigt worden (Yamamoto et al., 2007). Wir fanden heraus, dass Trib1 am Ende der Entzündungsreaktion im Gehirn parallel zum Abklingen des Fiebers signifikant in seiner Expression ansteigt. Demzufolge wäre Trib1 ein gutes Ziel für weitere Untersuchungen, um eventuell seine Funktion gezielt nutzbar zu machen. Zusätzlich ist bei der möglichen Rolle von NF-IL6 für die Aufrechterhaltung der Entzündungsreaktion im Gehirn noch zu bemerken, dass wohl Zytokine wie IL-10 und INF zellspezifisch das Verhältnis von aktivierendem LAP zu inhibierendem LIP verschieben könnte (Tanaka et al., 2005). Die Aufklärung der Regulation und Rolle dieser Veränderungen ist ebenfalls für weitere Ansätze zur potentiellen Therapie von Bedeutung. Nicht zuletzt ist NF-IL6 auch bei viraler Replikation im Gehirn von Bedeutung und deshalb ein interessante Zielstruktur in dieser Hinsicht (Dudaronek et al., 2007; Lee et al., 2001). Inhibitionsstrategien für STAT3 sind unter anderem Ziel laufender Arbeiten und werden im Ausblick kurz erläutert.

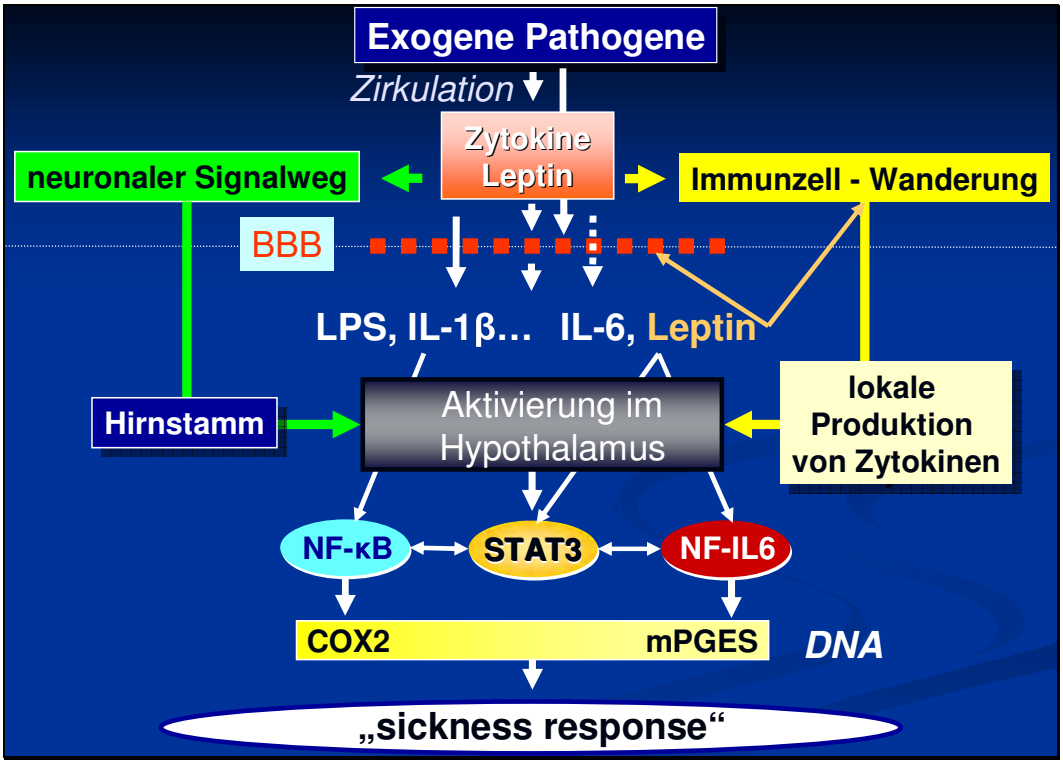


Abbildung 13

Schematische Darstellung der Kommunikationswege zwischen Immunsystem und Gehirn aus dem Schrifttum (Kapitel I 1, Abbildung 1) entsprechend ergänzt um die neuen Ergebnisse dieser Arbeit. Speziell wurde unter anderem die Rolle von zirkulierendem IL-6, Leptin und TLR-Agonisten für den PG-Syntheseweg und genomische Aktivierungen (inflammatorische Transkriptionsfaktoren) untersucht, sowie in zwei Teilprojekten die Rolle von Leptin beim zellulären und beim neuronalen Signalweg.

5. Thesenartige Zusammenfassung der Ergebnisse

A TLR-Agonisten besitzen therapeutisches Potenzial und sind wichtige Versuchsmodelle

- LPS ist das älteste und am besten untersuchte Versuchsmodell systemischer Inflammation
- PIPC ist ein wichtiges virales Mimetikum
- MALP2 hat Potenzial zur Therapie von Wunden und Tumoren
- Imiquimod ist der beste Kandidat zur lokalen Behandlung für INF-abhängige Prozesse
- *Diesen TLRs liegen konservierte Mechanismen zugrunde*

B Zytokine bestimmen Physiologie und Pathophysiologie von Krankheiten

- Die Wirkung hängt von der Zusammensetzung, dem Zytokinmilieu ab
- IL-6 ist das wichtigste zirkulierende Zytokin, Leptin ist eher als Modulator inflammatorischer Prozesse zu verstehen
- *Interaktionen zwischen den einzelnen Mediatoren machen den Effekt aus*

C Transkriptionsfaktoren

C_1 STAT3 ist ein guter akuter Aktivitätsmarker im Gehirn für viele JAK/STAT stimulierenden Mediatoren

- Gehirnstrukturen / Zellphänotypen sind differenziert zu betrachten
- *STAT3 ist wichtig für die Aufrechterhaltung der Entzündungsreaktion*

C_2 NFκB

- - kommt ubiquitär vor und ist essentiell für die Induktion inflammatorische Prozesse
- *Interaktion mit STAT3 und NF-IL6 bestimmen die Wirkung*

C_3 NF-IL6

- - besitzt ähnliche Zielstrukturen wie STAT3
- - kolokalisiert nur teilweise mit STAT3 und NFκB
- *Es gibt komplexe Interaktion mit STAT3 und NFκB; NF-IL6 ist durch diverse Stimuli aktivierbar bzw. als unspezifischer langfristiger Aktivierungsmarker zu sehen; NF-IL6 spielt eine Rolle bei der Aktivierung der Stress-Achse*

6. Schlussfolgerung und Zukunftsperspektiven

Das Wissen über Stimulantien des angeborenen Immunsystems wie den TLR-Agonisten ist noch immer lückenhaft. Gerade Tier-spezifische Unterschiede, wie hier zumindest für Ratten, Mäuse und Meerschweinchen (beispielsweise STAT3 oder der PG-Weg) in Auszügen untersucht, sind zum Teil völlig unbekannt. Dabei sollten solche Unterschiede nicht zuletzt eine große Rolle im Rahmen des „One Health Konzeptes“ spielen (Currier and Steele, 2011). Hinzu kommt, dass Speziesbarrieren bei Zoonosen überwunden werden und gerade hier die Unterschiede der Immunantwort ermittelt werden sollten und zwar unter standardisierten, vergleichbaren Bedingungen. Für solche Untersuchungen bietet sich die Verwendung der gut dosierbaren TLR-Agonisten natürlich an. Neben den hier untersuchten exogenen TLR-Agonisten sind aber dabei auch endogene Agonisten neuerdings von größerem Interesse. Dazu gehört unter anderem high-mobility group box 1 (HMGB1), welches über TLR4 vermittelt systemische Inflammation bei Organtrauma (Levy et al., 2007) und bei ischämischem Trauma im Gehirn am Entzündungsgeschehen beteiligt ist (Kim et al., 2006; Muhammad et al., 2008). Auch die Befunde aus der vorliegenden Arbeit, dass Spezies spezifisch IL-6 offensichtlich unterschiedliche Schwellenkonzentrationen benötigt, um Fieber zu erzeugen und die LPS-Sensitivität ebenfalls je nach Tierart unterschiedlich ist, sollten weiter untersucht werden (Kapitel IV 2). Dies sind Faktoren, die die Kommunikationswege zwischen Immunsystem und Gehirn in den einzelnen Tierarten beeinflussen. Dazu kommt, dass das Wissen um die Wirkung von psychischem und physischem Stress sowie Einflüssen der Ernährung auf neuro-immune Interaktionen lückenhaft ist und in Zukunft auch in eigenen weiterführenden Projekten untersucht werden soll. Weitere Stressoren wie Altern und Obesitas sowie sportliche Aktivitäten und deren Wirkung auf Inflammation im Gehirn gehören zu den zentralen Eckpunkten solcher geplanten Untersuchungen. In Teilen liegen bereits erste Ergebnisse vor und sollen hier zumindest zum Teil in Auszügen als Zukunftsperspektive skizziert werden.

1) Strategien zur Inhibition von Transkriptionsfaktoren: Zur weiteren Untersuchung des JAK-STAT und des NF-IL6-Signalweges wurde AG490 verwendet, um die Rolle dieser zwei Transkriptionsfaktoren für Fieber und Krankheitssymptome näher zu analysieren. Die Ergebnisse zeigen, dass die intrazerebroventrikuläre Gabe von AG490 bei LPS-induzierter systemischer Entzündung zu einer Dissoziation der Krankheitssymptome führt. Unter dem Einfluss dieser Substanzen wurde das Fieber verstärkt aber gleichzeitig die begleitende

Adipsie und Lethargie reduziert bzw. aufgehoben, ohne dass die Anorexie beeinflusst worden wäre. Diese Veränderungen waren von einem abgeschwächten PG-Syntheseweg im Gehirn und verringerter hypothalamischer Expression des anti-inflammatorischen Zytokins IL-10 begleitet. Die Befunde zeigen bereits, dass Adipsie und Anorexie offensichtlich unterschiedlich reguliert werden. Insgesamt könnte der Einsatz von AG490 als therapeutische Strategie interessant sein, weil es die als protektiv anzusehende Fieberwirkung verstärkt aber Lethargie und Adipsie abschwächen kann. Untersuchungen mit NF-IL6KO Mäusen sollen schließlich weitere Erkenntnisse über die Bedeutung dieses so wichtigen Transkriptionsfaktors bringen und sind in Bearbeitung.

2) Psychischer Stress im Vergleich zu TLR-Stimulation: Aufbauend auf den Beobachtungen, dass NF-IL6 in Strukturen der HPA-Achse aktiviert wurde, erfolgten präzise immunhistologische Analysen der Aktivierungsmuster von inflammatorischen Transkriptionsfaktoren in eben diesen Strukturen. Neben einer Kolokalisation von NF-IL6 in ACTH-positiven Zellen, konnten wir in Primärkulturen des Hypophysenvorderlappens diese Ergebnisse einer LPS-induzierten Stimulation bestätigen und fanden außerdem Hinweise auf eine Beteiligung von NF-IL6 an der LPS-stimulierten TNFα-Produktion in *Folliculo-stellatae*-Zellen. Interessanter Weise konnten wir nach einem psychischen Stimulus in Form eines Käfigwechsels („novel environment“), der ebenfalls mit Fieber einhergeht, ebenfalls eine zeitlich koordinierte Aktivierung von NF-IL6 in Gehirnstrukturen der HPA-Achse detektieren (PVN, Hypophyse). NF-IL6 scheint also eine Rolle für verschiedene Formen von Stress zu spielen. Dies ist Bestandteil weiterer Untersuchungen.

3) Einflüsse von Altern und Obesitas auf die Kommunikation zwischen Immunsystem und Gehirn: Als physiologische Stressoren sind sowohl Altern wie auch das damit zunächst einhergehende Übergewicht bekannt dafür, die Kommunikation zwischen Immunsystem und Gehirn zu beeinflussen. Bisherige Ergebnisse konnten hier keine Beteiligung von oxidativem Stress für die verstärkten Krankheitssymptome, wie sie bei alten Menschen und Tieren auftreten, verantwortlich gemacht werden. Des Weiteren scheint anders als bei jungen Ratten bei alten Ratten aber die verstärkte inflammatorische Antwort im Gehirn und Blut (zirkulierenden Zytokine) von erhöhten LPS-induzierten Leptin-Spiegeln begleitet zu sein. Dies könnte ein bisher übersehener wichtiger Faktor sein, zumal in vorhergehenden Studien eine Rolle für Leptin bei der Kommunikation des Immunsystems mit dem Gehirn eindeutig gezeigt wurde (Kapitel V 3). Mit Hilfe des LAS und Kulturen von Fettgewebe junger und

alter Ratten, sollen die Ursachen und Mechanismen dieser Prozesse weiterhin genauer aufgeklärt werden.

4) Sport als anti-inflammatorische Strategie bei Übergewicht: In Kooperation mit dem Institut für Sportmedizin der Justus-Liebig-Universität Giessen werden Analysen von Gehirnen von Mäusen durchgeführt, die entweder Diät-induziert fettleibig oder normalgewichtig sind und verschiedenen chronischen Trainingseinheiten unterzogen werden (Krafttraining, Ausdauertraining, Kontrollen). Diese Untersuchungen sollen Aufschluss darüber geben, ob und in welchem Umfang Sport die Ausbildung von entzündlichen Veränderungen im Gehirn beeinflussen kann.

V. VORGELEGTE VERÖFFENTLICHUNGEN

Impakt Faktoren sind jeweils nach Thomas und Reuters 2010 angegeben

1. Begutachtete Veröffentlichungen

1.1. „Fever, sickness behavior and expression of inflammatory genes in the hypothalamus after systemic and localized subcutaneous stimulation of rats with the TLR 7 agonist imiquimod“

Damm J., Wiegand F., Harden LM, Gerstberger R., **Rummel C**. and Roth J.
Neuroscience (2012) 201: 166-83

Impakt Faktor: 3,215

Eigener Anteil an der Publikation:

- Initiative: unterstützend (20 %)
- Projektplanung: wesentlich (50 %)
- Durchführung der Versuche: unterstützend (20 %)
- Auswertung der Experimente: unterstützend (30 %)
- Erstellung der Publikation: unterstützend (30 %)

Neuroscience 201 (2012) 166–183

FEVER, SICKNESS BEHAVIOR, AND EXPRESSION OF INFLAMMATORY GENES IN THE HYPOTHALAMUS AFTER SYSTEMIC AND LOCALIZED SUBCUTANEOUS STIMULATION OF RATS WITH THE TOLL-LIKE RECEPTOR 7 AGONIST IMIQUIMOD

J. DAMM,[a1] F. WIEGAND,[a1] L. M. HARDEN,[a,b] R. GERSTBERGER,[a] C. RUMMEL[a] AND J. ROTH[a*]

[a]*Institut für Veterinär-Physiologie und -Biochemie, Justus-Liebig-Universität Giessen, Frankfurter Strasse 100, D-35392 Giessen, Germany*

[b]*Brain Function Research Group, School of Physiology, Faculty of Health Sciences, University of the Witwatersrand, 7 York Road, Parktown, Johannesburg, South Africa*

Abstract—The Toll-like receptor 7 (TLR7) agonist imiquimod is used for topical treatment of skin cancers. We studied the consequences of injections of imiquimod into a subcutaneous (s.c.) air pouch or of intraperitoneal (i.p.) injections on the manifestation of fever, sickness behavior, and the peripheral and brain-intrinsic induction of a variety of inflammatory molecules. Rats were given imiqimod s.c. or i.p. (1 or 5 mg/kg). Body temperature, motor activity, and food and water intake were recorded by telemetric devices. Peripheral and brain-intrinsic induction of inflammatory mediators was analyzed by real-time polymerase chain reaction (RT-PCR), bioassays, enzyme-linked immunosorbent assays (ELISAs), and immunohistochemistry. Imiquimod is the first TLR-agonist to produce more potent effects with s.c. than i.p. administration. Peripheral induction of interferons (IFNs) and putative circulating pyrogens corresponded to the magnitude of the illness responses. In the brain, an expression of cytokines (TNFα, IL-1β, and IL-6) and inducible forms of enzymes for prostaglandin E2 synthesis (COX-2 and mPGES) occurred, which was accompanied by a moderate activation of the transcription factors NFκB and STAT3, and a strong activation of the transcription factor NF-IL6, in cells of specific areas with an open blood–brain barrier. These inflammatory responses noted within the brain were more marked after s.c. administration, than i.p. administration of imiquimod. At a dose of 5 mg/kg, imiquimod causes rather moderate brain-inflammatory responses, which are related to peripheral IFN-expression and possibly mediated by brain-intrinsic activation of NF-IL6 and induction of a proinflammatory cocktail. The lack of a septic-like state in imiquimod-treated rats reinforces the therapeutic use of this drug. © 2011 IBRO. Published by Elsevier Ltd. All rights reserved.

Key words: fever, Toll-like receptors, immune to brain signaling, nuclear factor-IL6, interferons, cytokines.

Innate immune recognition is mediated by a system of germline-encoded receptors that recognize conserved molecular patterns associated with microbial pathogens. These so-called Toll-like receptors (TLRs) are coupled to signal transduction pathways that control expression of a variety of inducible immune-response genes (Uematsu and Akira, 2006; Beutler, 2009). The ability of TLRs to initiate and propagate inflammation makes them attractive therapeutic targets. Distinct TLR agonists have thus been used as agents for cancer treatment (Schmidt et al., 2007; Adams, 2009), as adjuvants for improved elimination of intracellular pathogens (Borsutzki et al., 2003; Rajagopal et al., 2010), and as inducers of endogenous mediators that might accelerate wound healing (Deiters et al., 2004) or reduce the severity of autoimmune diseases (O'Brian et al., 2010). Depending on the route of administration of a given TLR agonist, a marked systemic or local inflammatory response will develop that may affect multiple organs including the brain. Some TLR agonists even have the capacity to cause a life-threatening septic shock-like state and may contribute to organ dysfunction remote from the site where beneficial effects are desired (Levy et al., 2007; Schmidt et al., 2007; Steiner et al., 2011).

With special emphasis on the manifestation of brain-controlled illness responses, including fever or anorexia, data from several studies have shown that agonists of distinct TLRs differ in their capacities to induce a localized versus a systemic inflammatory response *in vivo*. Systemic inflammation can be mimicked by intraperitoneal injections of a given TLR agonist, whereas injections of such substances into a subcutaneous air pouch have been used as a model of a local inflammatory response (Miller et al., 1997; Zhang et al., 2008). Such a property of the air pouch is based on the observations that virtually all of the injected lipopolysaccharide (LPS) was recovered from the pouch, and that LPS was undetectable in plasma at any time after its intrapouch administration (Cartmell et al., 2001).

Clearly, the TLR4 agonist LPS is the most potent inducer of brain-controlled sickness-type responses after i.p. or intrapouch administration, even at moderate doses

[1] These authors contributed equally to this work.

*Corresponding author. Tel: +49-641-99-38850; fax: +49-641-99-38159.
E-mail address: Joachim.Roth@vetmed.uni-giessen.de (J. Roth).

Abbreviations: AP, *area postrema*; COX-2, cyclooxygenase-2; CVOs, circumventricular organs; DAPI, 4,6-diamidino-2-phenylindole; ELISA, enzyme-linked immuno-sorbent assay; FSL-1, fibroblast-stimulating lipopeptide-1; IFN, interferon; IHC, immunohistochemistry; IL, interleukin; LPS, lipopolysaccharide; MALP-2, macrophage-activating lipopeptide-2; mPGES, microsomal prostaglandin E synthase; NF-IL6, nuclear factor IL6; NFκB, nuclear factor kappaB; OVLT, *organum vasculosum laminae terminalis*; PBS, phosphate buffered saline; PGE2, prostaglandin E2; Poly I:C, polyinosinic:polycytidylic acid; RT, room temperature; RT-PCR, real-time polymerase chain reaction; SE, standard error; SOCS3, suppressor of cytokine signaling 3; STAT3, signal transducer and activator of transcription 3; T_{abdi}, abdominal temperature; TLR, Toll-like receptor; TNF, tumor necrosis factor; vWF, van Willebrand factor.

0306-4522/12 $36.00 © 2011 IBRO. Published by Elsevier Ltd. All rights reserved.
doi:10.1016/j.neuroscience.2011.11.013

(Ross et al., 2003; Rummel et al., 2004). TLR2/6 agonists show similar, perhaps less pronounced, effects when compared with LPS (Galanos et al., 2000; Hübschle et al., 2006; Knorr et al., 2008; Greis et al., 2007, 2009). TLR3 agonists, such as polyinosinic:polycytidylic acid (Poly I:C), however, induce fever, sickness behavior, and cytokine synthesis when injected systemically, but not when injected s.c. (Cartmell et al., 2002; Fortier et al., 2004; Voss et al., 2006). In terms of TLR7 agonists, there is only one study in mice which has investigated its effects on brain-controlled sickness responses. Intranasal administration of a TLR7 ligand (9-benzyl-8-hydroxy-2-[2-methoxy-ethoxy]adenine) failed to induce fever but caused anorexia (Hayashi et al., 2008).

Originally, guanosin-rich single-stranded RNA was identified as a ligand for TLR7 (Heil et al., 2004), and it has been suggested that innate antiviral responses are achieved via TLR7-mediated recognition of single-stranded RNA and subsequent induction of interferons (IFNs) (Diebold et al., 2004). Activation of TLR7 occurs intracellularly, namely in the endosomal compartments of dendritic cells and macrophages (Blasius and Beutler, 2010).

The guanosin analog imiquimod proved to be a specific activator of TLR7, and thus this substance represents an excellent tool to study the role of TLR7 under various pathophysiological conditions (Lee et al., 2003). Several beneficial effects of imiquimod have been reported, including antitumor effects (Broomfield et al., 2009; Lu et al., 2010; Ma et al., 2010) and antiviral activities (Miller et al., 2008). Interestingly, strong beneficial effects of imiquimod on subcutaneous melanoma cells were observed (Ma et al., 2010), and topical treatments with this drug focused on intraepithelial neoplasms of cutaneous and mucosal surfaces (Hengge and Stark, 2001; Green et al., 2008; Broomfield et al., 2009). Thus far imiquimod has not yet been tested with regard to its capacity to induce inflammatory responses within the brain or brain-controlled signs of illness after i.p. or s.c. treatments *in vivo*. Given, that imiquimod is most effective within a local cutaneous/subcutaneous compartment, systemic investigations on its afferent signaling to the brain and on putative subsequent brain-mediated inflammatory responses seem warranted. The primary goal of this study was therefore to compare the induction of inflammatory mediators in the periphery and in the brain of rats in response to i.p. or s.c. (intrapouch) injections of imiquimod and to analyze the manifestation of brain-controlled illness responses. We demonstrate that imiquimod is the first TLR-agonist investigated to date, which induces more potent inflammatory responses when administered into the pouch to that noted when administered into the abdominal cavity. We further show that even when given at a comparably high dose, this drug does not induce severe sickness responses or even shock-like states, but rather produces a moderate activation of inflammation-related transcription factors in brain sites with an incomplete blood–brain barrier and fever-related genes in the hypothalamus.

EXPERIMENTAL PROCEDURES

Animals

The study was performed in male Wistar rats with body weights in the range of 170–185 g. Experiments were carried out in accordance with the local Ethics committee (ethics approval number GI 18/2—Nr. 43/2009). Every effort was made to reduce the number of animals used and to minimize animal suffering (analgesic treatment pre- and post-surgery with 2mg/kg meloxicam, Boehringer, Ingelheim, Germany). After surgery animals were housed individually in a temperature- and humidity-controlled climatic chamber (Weiss Umwelttechnik GmbH, Typ 10'US/+5 - +40 DU, Reiskirchen, Germany), which was adjusted to 25 °C and 50% humidity. The rats had constant access to water and were fed with powdered standard laboratory chow *ad libitum*. The use of special cages with water bottles and food supply dishes placed on balances (AccuScan Instruments, Columbus, OH, USA) allowed continuous monitoring of food and water intake. Artificial lights were on from 7:00 AM to 7:00 PM. Body weight was determined once per day (~9:00 to 9:30 AM). Surgery was performed on animals to implant biotelemetry transmitters (mentioned later in the article) at least one week before the experiment.

Measurement of body temperature and motor activity

Abdominal temperature of rats was measured using biotelemetry transmitters (model PTD-4000 E-Mitter; Mini-Mitter, Sunriver, OR, USA) implanted into the abdominal cavity at least one week before the experiment. Before the surgery, rats were anesthetized with 100 mg/kg ketamine hydrochloride (Albrecht, Aulendorf, Germany) and 5 mg/kg xylazine (Bayer Vital, Leverkusen, Germany). The output (frequency in Hz) was monitored by a receiver placed under each cage (model ER-4000 radio receivers; Mini-Mitter). A data acquisition system (Vital View; Mini-Mitter) was used for automatic control of data collection and analysis. Body temperature was continuously recorded at 5-min intervals. For analysis and graphical documentation, temperature data at time intervals of 15 min were used. Motor activity of rats was measured using the same biotelemetry system described before. Changes in activity were detected by changes in the position of the implanted transmitter over the receiver board. This resulted in a change of the signal strength, which was detected by the receiver and recorded as a pulse of activity. Activity pulses were counted every 5 min and calculated as a cumulative measure of daytime or nighttime activity (activity counts per 12 h).

Measurement of food and water intake

Food intake and drinking behavior were monitored telemetrically, at 5-min intervals, using special cages equipped with water bottles and food supply dishes placed on balances, which in turn were connected via a Diet Scan analyzer to a personal computer (AccuScan Instruments, Columbus, USA). The AccuDiet software package was used to record the data used for graphical and statistical analysis. Cumulative food and water intake over 5 min were combined into cumulative measures of food and water intake over a 24-h period. Therefore, the final data shown represent the cumulative food and water intake in grams per 24 h.

Drugs

Lyophilized imiquimod (R837; InvivoGen, San Diego, CA, USA) was reconstituted in sterile endotoxin-free water at a concentration of 1 mg/ml according to the manufacturer's instructions. Doses of 1 mg/kg or 5 mg/kg were used for i.p. or intrapouch injections. Imiquimod has been shown to activate only TLR7, but not TLR8 or other TLRs (Lee et al., 2003).

Treatments and experimental protocols

Experiment 1: Fever and sickness behavior responses to systemic (i.p.) or subcutaneous (air pouch) injections of imiquimod. Immediately after placement of a biotelemetry transmitter into the

abdominal cavity (aforementioned in the article), a subcutaneous air pouch was formed in about 50% of the rats used for this study. A volume of 20 ml of air, sterilized by passing through a 0.7 μm filter (BD Plastipak; Bechton-Dickinson, Heidelberg, Germany), was injected into the subcutaneous tissue of the dorsal midline, caudal to the scapulae. Three or two days before the experiment, the air pouch was reinflated with another 10 ml of sterile air. This model has been used previously by us (Knorr et al., 2008, 2010) and by others (Miller et al., 1997; Cartmell et al., 2000; Zhang et al., 2008) to induce a localized inflammatory response in rats. One week after surgery, imiquimod was injected i.p. or into the air pouch at a dose of 1 or 5 mg/kg. To achieve a good distribution of the substance within the abdominal cavity or the air pouch, the injection volume was adjusted to 1 ml. Control rats were injected with 1 ml solvent (Ampuva *aqua ad injectionem*, Fresenius, Bad Homburg, Germany). All injections were performed at 9:00 AM, 2 h after the start of the "light on" period. Groups of six to eight rats were used for these experiments. Body weight and food and water intake were determined immediately before the respective injection (day 0) to obtain the basal values of these parameters cumulated over the previous 24 h. Further measurements of these parameters were performed 24 h and 48 h after the injections of imiquimod or solvent (days 1–2). Body temperature and motor activity were continuously recorded over the experimental period (days 1–2) starting 2 h before the respective injections.

Experiment 2: Concentrations of cytokines in plasma and lavage from the site of localized subcutaneous inflammation. Separate groups of rats (n=3–5 per group and time point) were treated with imiquimod or solvent as described in the protocol for experiment 1. At selected time intervals of 60 min, 120 min, and for the high dose of imiquimod also 360 min, after the injection of imiquimod or vehicle, blood from the systemic circulation was taken from all rats. In addition, lavage fluid from rats equipped with a subcutaneous air pouch was collected. Briefly, the rats were anesthetized about 5 min before the respective sampling time with sodium pentobarbital (0.5 ml i.p., Narcoren; Merial, Hallbergmos, Germany). Blood was collected by cardiac puncture, and sampling of the inflammatory exudate within the pouch was achieved by rinsing the pouch with 1 ml of sterile phosphate buffered saline (PBS). Blood and lavage fluid were immediately centrifuged. Plasma and supernatant were stored at −70 °C for later determination of TNFα, IL-6, and IFNγ.

Experiment 3: Preparation and processing of liver, spleen, and brain tissue for immunohistochemistry (IHC) and real-time polymerase chain reaction (RT-PCR). Two or six hours after an i.p. or intrapouch injection of imiquimod or solvent (n=3–4 per group and time point), animals were deeply anesthetized with sodium pentobarbital (0.5 ml i.p., Narcoren; Merial, Hallbergmos, Germany) and transcardially perfused with 200 ml ice-cold 0.9% saline, and their brains, livers, and spleens were quickly removed, frozen in powdered dry ice, and stored at −70 °C.

For IHC, coronal 20 μm brain sections were cut on a cryostat (model HM 500; Microm, Walldorf, Germany) and thaw-mounted onto poly-L-lysine-coated glass slides. Sections (nine per animal and brain area) were prepared from the *organum vasculosum laminae terminalis* (OVLT), located rostrally from the preoptic-anterior hypothalamus and from the *area postrema* (AP), located in the brainstem as a component of the dorsal vagal complex according to the stereotactic atlas of the rat brain (Paxinos and Watson, 1998). To perform IHC and RT-PCR from the same brains, another remaining 25 consecutive frozen 80 μm sections of each hypothalamus [bregma −0.26 at the beginning of median preoptic nucleus to bregma −2.30 mm at the beginning of arcuate nucleus according to Paxinos and Watson (1998)] were stapled and also thaw-mounted on glass slides, the hypothalamus dissected and used for RNA-extraction. From the liver and spleen samples, 10–15 consecutive frozen 80 μm sections were prepared, like the sections prepared for the hypothalamic tissue, and used later for extraction of RNA.

Real-time PCR

Total RNA of the collected tissue sections from spleen, liver, and hypothalamus was isolated using TRIzol (Invitrogen, CA, USA) according to the manufacturer's protocol. One microgram of total RNA was transcribed into DNA, using 50 units of murine Leukemia virus [MULV] Reverse Transcriptase, 50 μM of random hexamers, and 10 mM of dNTP mix (Applied Biosystems, Foster City, CA, USA), in a total reaction volume of 20 μl. After reverse transcription, quantitative real-time PCR was performed in duplicate using preoptimized primer/probe mixture (TaqMan Gene Expression Assay; Applied Biosystems) and TaqMan Universal PCR Master Mix (Applied Biosystems) on a StepOne™ Real-Time PCR System (Applied Biosystems). The cDNA quantities between different reactions were normalized by measurement of the housekeeping gene β-actin (cat: 4352340E, Applied Biosystems) as a reference. The sample values represent x-fold differences from a control sample (given as a designated value of 1) within the same experiment. Assay IDs for the analyzed genes are as follows: IFNα (Rn02395770_g1), IFNβ (Rn00569434_s1), IFNγ (Rn00594078_m1), TNFα (Rn99999017_m1), IL-1β (Rn00580432_m1), IL-6 (Rn01410330_m1), IκBα (Rn01473658_g1), SOCS3 (Rn00585674_s1), NF-IL6 (Rn00824635_s1), COX2 (Rn00568225_m1), and mPGES1 (Rn00572047_m1). Each sample was run in duplicate.

Measurement of cytokines

Cytokine analysis was performed with plasma and subcutaneous lavage samples from rats stimulated either with imiquimod or sterile water. Determination of TNFα was achieved by a bioassay based on the cytotoxic effect of TNFα on the mouse fibrosarcoma cell line WEHI 164 subclone 13 (Espevic and Nissen-Meyer, 1986). The assay was performed in sterile, 96-well microtiter plates. Serial dilutions of biological samples or different concentrations of a murine TNFα standard (code 88/532; National Institute for Biological Standards and Control, South Mimms, UK) were incubated for 24 h in wells that had been seeded with 50,000 actinomycin D-treated WEHI cells. The number of surviving cells after 24 h was measured by use of the dimethylthiazol-diphenyl tetrazolium bromide (MTT) colorimetric assay (Holt et al., 1991). Plasma samples were prediluted so that serial dilution of samples and standard dilution curves were parallel. The detection limit of the assay, after considering the dilution of samples into the assays, was 6 pg/ml TNF.

Determination of IL-6 was achieved by a bioassay based on the dose-dependent growth stimulation of IL-6 on the B9 hybridoma cell line (Aarden et al., 1987). The assay was performed in sterile, 96-well microtiter plates. In each well, 5000 B9 cells were incubated for 72 h with serial dilutions of biological samples or with different concentrations of a human IL-6 standard (code 89/548; National Institute for Biological Standards and Control). Plasma samples were prediluted so that serial dilution of samples and standard dilution curves were parallel. The number of cells in each well was measured by use of the MTT assay (as described before in the article). The detection limit of the assay, after considering the dilution of samples into the assays, was 3 international units (IU) IL-6/ml.

Rat IFN-γ was measured by an enzyme-linked immunosorbent assay (ELISA) kit (Hölzel Diagnostika; Köln, Germany), which recognizes both natural and recombinant rat IFNγ. The assay was performed according to the manufacturer's instructions. The minimum detectable dose of rat IFN-γ was about 10 pg/ml.

Immunohistochemistry

On the day of the experiment, the frozen brain sections were briefly air dried at room temperature for 7 min and then immersion-fixed in

2% paraformaldehyde (Merck, Darmstadt, Germany) diluted in PBS for 10 min at room temperature (RT). After three consecutive washes in PBS, the sections were treated for 1 h at RT with a blocking solution consisting of PBS, containing 10% normal donkey serum (NDS; Biozol, Eching, Germany) and 0.3% triton X-100. The sections were incubated with the primary rabbit anti NF-IL6 polyclonal IgG (1:5000; cat. sc-150; Santa Cruz Biotechnology, CA, USA), the rabbit anti-STAT3-antibody (1:2000; cat no. sc-482; Santa Cruz Biotechnology), the goat anti NFκB polyclonal IgG (1:500; cat no. sc-372; Santa Cruz Biotechnology), and the sheep anti von Willebrand (vW) polyclonal IgG (1:3000; cat no. A 008202; Dako GmbH, Hamburg, Germany) for 20–22 h at 4 °C, followed by three consecutive washes in PBS, and visualization with Cy3-anti goat IgG (cat. 705-165-147; Jackson ImmunoResearch, West Grove, PA, USA) and Alexa-488-conjugated anti rabbit IgG (cat. AZA11055; MoBiTec GmbH, Göttingen, Germany), after a 2-h incubation at RT and a 1:500 dilution in blocking solution for each secondary antibody. Sections were counterstained with the nuclear 4,6-diamidino-2-phenylindole (DAPI) stain (Mobitec GmbH, Göttingen, Germany) for 10 min, using a 1:1.000 dilution in PBS to clearly visualize the tissue surrounding the signal and to demonstrate the nuclear localization of NF-IL6-, STAT3-, and NFκB-immunoreactivity. Finally, all sections were coverslipped (glass coverslips) using a glycerol/PBS solution (Citifluor LTD, London, UK) and stored at 4 °C until microscopic analysis was performed. These antibodies have been used previously, and respective control preabsorbtion experiments have confirmed the specificity of the signals observed (Hübschle et al., 2001; Nadjar et al., 2003; Rummel et al., 2006; Damm et al., 2011).

Sections were analyzed using a conventional light/fluorescent Olympus BX50 microscope (Olympus Optical, Hamburg, Germany) equipped with the appropriate filter sets to detect the fluorescent conjugates Cy3, Alexa-488, and DAPI. Images were taken with a black and white Spot Insight camera (Diagnostic Instruments, Visitron Systems, Puchheim, Germany) using the MetaMorph 5.05 software. Image editing software was used to combine

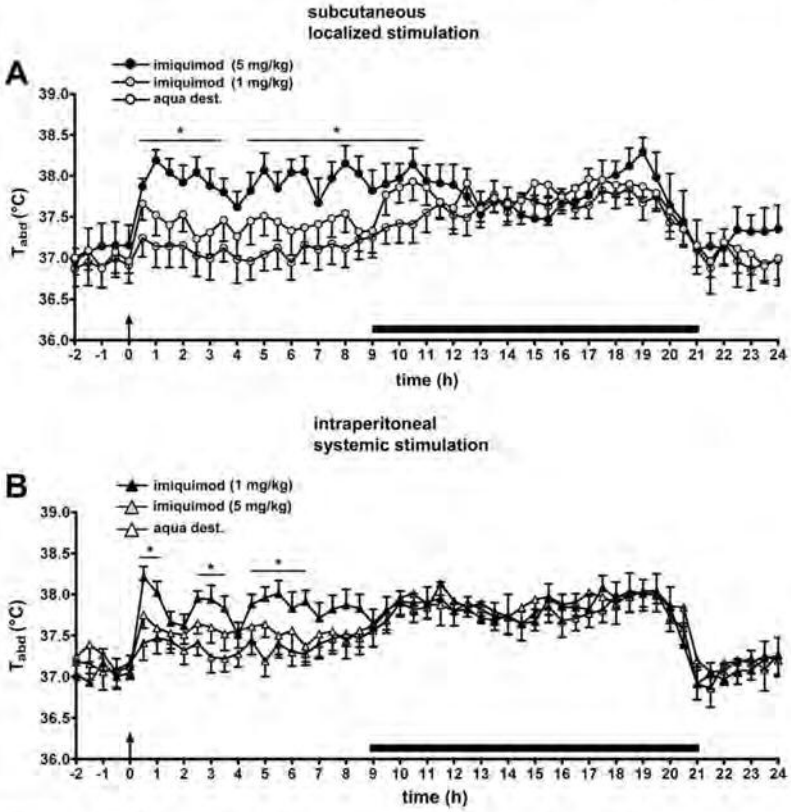


Fig. 1. Abdominal temperature of rats in response to injections of a low (1 mg/kg) or a high dose (5 mg/kg) of imiquimod into a subcutaneous air pouch (A) or *via* the intraperitoneal route of administration (B). Control animals were injected with an equivalent volume of aqua dest (solvent for imiquimod). The thick horizontal bar at the bottom of each graph indicates the "lights off" period; the arrow at time "0" marks the time of injection. Above the recorded body temperatures, the horizontal bars and a star (*) indicate the time intervals during which the tested dose of imiquimod caused a significant elevation of abdominal temperature (T_{abd}) compared with rats treated with solvent ($P<0.05$; 2-way repeated ANOVA followed by an all pairwise Bonferroni's multiple comparison post hoc test). Only the high dose of imiquimod caused significant elevations of body core temperature on the day of the injection. This effect was greater when the subcutaneous route of administration was used.

the individual images into the red/green/blue color figure plates (MetaMorph 5.05), to adjust brightness and contrast, and to store the images as TIFF files (Adobe Photoshop 5.5).

Evaluation and statistics

In graphs of the thermal responses of rats to injections of imiquimod or solvent, the mean abdominal temperatures were plotted against time and expressed as means±SE at each time point. Abdominal temperatures were compared between different groups over time by 2-way repeated-measures ANOVA followed by an all pairwise Bonferroni's multiple comparison post hoc test. A statistical significance was accepted for $P<0.05$.

Concentrations of bioactive cytokines in blood, relative expression of inflammatory marker molecules, and cumulative data on food and water intake were compared between imiquimod-treated and control animals by 1-way ANOVA followed by Scheffe's post hoc test. Because the values for bioactive cytokine concentrations are not normally distributed, a log transformation of the TNF- and IL-6-values was performed before the statistical calculation. All data were analyzed using StatView software 4.57 (Abacus Concepts, Berkeley, CA, USA).

RESULTS

Imiquimod induces brain-controlled illness responses of moderate potency

In the first experiment, we evaluated the putative manifestation of fever and other sickness responses after subcutaneous (s.c.) intrapouch administration or after systemic (i.p.) injection of imiquimod at doses of 1 or 5 mg/kg as well as solvent (aqua dest.). Abdominal temperature (T_{abd}) was continuously recorded and evaluated from 2 h before until 24 h after the respective injection (Fig. 1).

In control groups treated with solvent s.c. (A) or i.p. (B), the normal circadian rhythm of rats' body temperature with higher nighttime temperatures remained undisturbed. Injections of 1 mg/kg imiquimod caused a slight but, not significant, elevation of T_{abd} during the day of injection (A, B). Rats treated with 5 mg/kg imiquimod s.c. or i.p. developed a fever over the day of injection, which showed some fluctuations. The imiquimod-induced febrile response was more pronounced when the drug was injected s.c., but irrespective of the route of administration, T_{abd} marginally exceeded 38 °C, so the observed fever can be categorized as moderate. Before (i.p. injections, B) or during (s.c. injections, A) the subsequent night, body temperature of both imiquimod-treated groups reached values that could no longer be discriminated from those of control rats.

Cumulative motor activity of rats followed a characteristic pattern with lower daytime (1000–2000 activity counts per day) when compared with nighttime activity (4000–5000 activity counts per night). This activity rhythm was not disturbed or impaired by treatment with imiquimod, even at the high dose of 5 mg/kg (not shown).

Within the 24 h before the respective injections, rats consumed 17.5–19 g of powdered laboratory chow. Only in rats treated with the high dose of imiquimod, the amount of

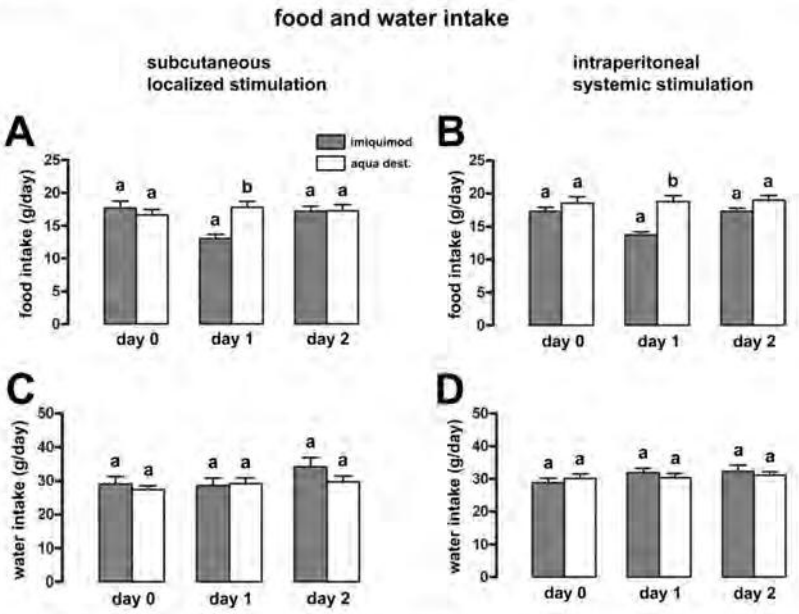


Fig. 2. Cumulative food (A, B) and water intake (C, D) of rats injected with 5 mg/kg imiquimod or solvent into a subcutaneous air pouch (A, C) or *via* the intraperitoneal route of administration (B, D). The values were recorded over 24 h periods before (day 0) and after (days 1 and 2) the respective injections. On a given day, any pair of columns with the same letter are not significantly different from each other, whereas any pair of columns with different letters are significantly different from each other ($P<0.05$; 1-way ANOVA followed by Scheffe's post hoc test). Columns represent means±SE.

consumed food significantly decreased to about 13 g (Fig. 2A, B) within the 24 h when the drug was administered. On the following day (day 2), food intake normalized and was again identical to that of rats injected with solvent. S.c. or i.p. injections of 5 mg/kg imiquimod did not induce adipsia (Fig. 2C, D), irrespective of the route of its administration. According to the results of this experiment, all further experiments were performed with only the high dose of imiquimod (5 mg/kg).

Imiquimod induces expression of interferons in spleen and liver

Because TLR7 signaling is thought to be coupled with production of type-1 IFNs (Diebold et al., 2004; Blasius and Beutler, 2010), we first compared the effectiveness of s.c. and i.p. stimulations of rats with 5 mg/kg imiquimod or solvent on the expression of IFNs in spleen and liver using specific RT-PCR assays. The results of these measurements are summarized in Figs. 3 and 4.

In the spleen, injections of 5 mg/kg imiquimod into the subcutaneous air pouch caused a significant elevation of IFNα, IFNβ, and IFNγ mRNA expression 2 h after stimulation compared with the corresponding values of control rats. The drug had a greater effect on the expression of IFNγ (about 10,000-fold increase of expression) when compared with IFNα (almost 100-fold increase) or IFNβ (280-fold increase). Another 4 h later, expression of IFNα and IFNβ fell below the level of that observed in control

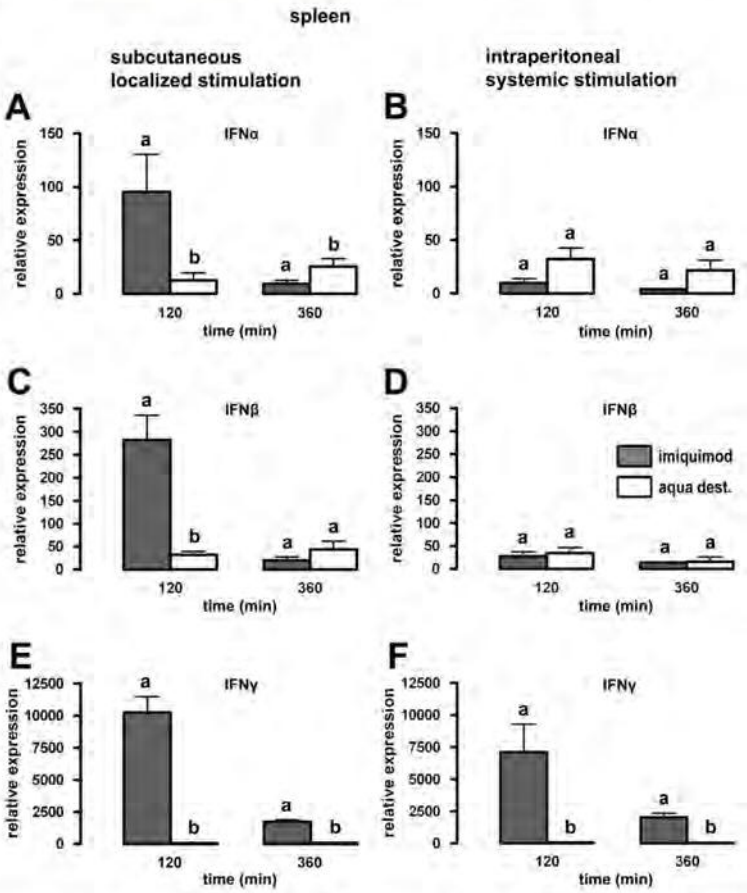


Fig. 3. mRNA expression of IFNs α, β, and γ in the rat spleen, using quantitative RT-PCR, at 2 h and 6 h after s.c. (A, C, E) or i.p. (B, D, F) injections of 5 mg/kg imiquimod or solvent. At a given time point, any pair of columns with the same letter are not significantly different from each other, whereas any pair of columns with different letters are significantly different from each other ($P<0.05$; 1-way ANOVA followed by Scheffe's post hoc test). Columns represent means ± SE.

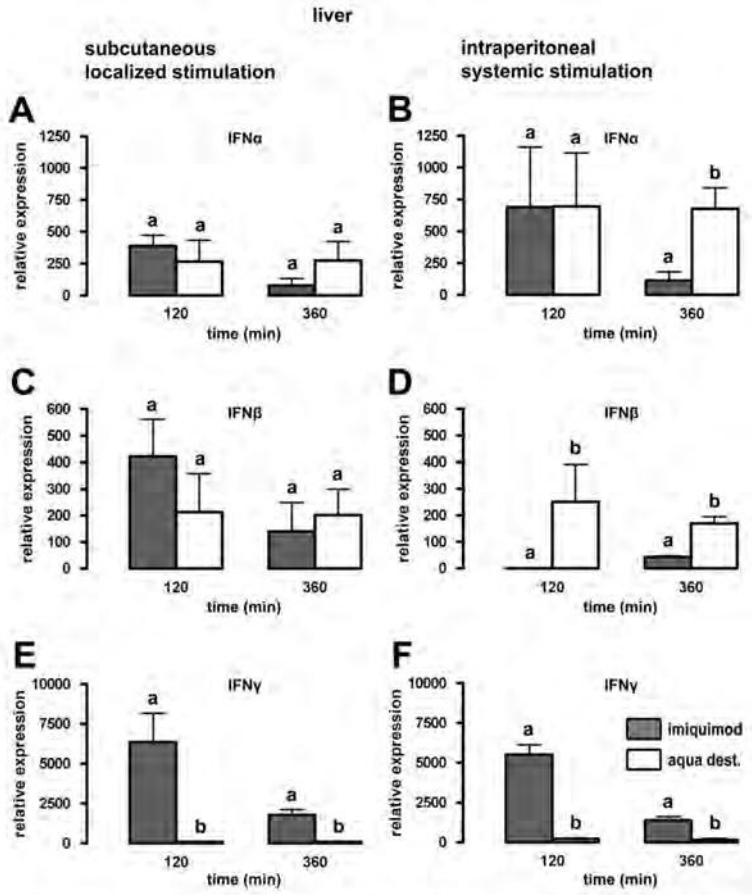


Fig. 4. mRNA expression of IFNs α, β, and γ in the rat liver, using quantitative RT-PCR, at 2 h and 6 h after s.c. (A, C, E) or i.p. (B, D, F) injections of 5 mg/kg imiquimod or solvent. At a given time point, any pair of columns with the same letter are not significantly different from each other, whereas any pair of columns with different letters are significantly different from each other ($P < 0.05$; 1-way ANOVA followed by Scheffe's post hoc test). Columns represent means ± SE.

rats, whereas there was still a 1800-fold higher expression of IFNγ in rats treated s.c. with imiquimod. Interestingly, the pattern of imiquimod-induced expression of IFNs in the spleen was much different when the drug was administered via the i.p. route. There was no increase in mRNA expression for IFNα and IFNβ in imiquimod-treated rats, whereas a 7000-fold (2 h) or more than 2000-fold (6 h) elevation of IFNγ expression was measured (Fig. 3F). In the liver s.c. and i.p. injections of imiquimod failed to cause increased levels of IFNα or IFNβ mRNA (Fig. 4). However, a pronounced (more than 5000-fold) elevation of relative expression of IFNγ was measured in liver tissue of imiquimod-treated rats, irrespective of the route of administration.

Putative imiquimod-induced circulating humoral signals for the manifestation of fever and sickness behavior

TNFα and IL-6 are regarded as afferent humoral signals for the induction of brain-mediated illness responses because of the fact that both cytokines are detected in the blood in increased amounts under various inflammatory conditions (Ross et al., 2003; Hübschle et al., 2006; Oka et al., 2007; Harden et al., 2011; Soares et al., in press). We therefore tested the capacity of imiquimod to synthesize bioactive TNFα and IL-6. Owing to the pronounced expression of IFNγ in spleen and liver (Figs. 3 and 4), we further tried to detect this cytokine at the protein level in the blood

and within the site of subcutaneous inflammation. The results of these measurements are summarized in Fig. 5.

Intrapouch injection of imiquimod induced a significant increase of IL-6 in the air pouch lavage fluid at all time points investigated (1, 2, and 6 h after injection; Fig. 5A). This pattern preceded the first significant rise in plasma at 6 h. Concentrations of bioactive IL-6 were higher in lavage fluid (several 1000 IU/ml) when compared with those in plasma (less than 100 to several 100 IU/ml at 6 h) of imiquimod-treated rats. In rats injected with solvent just basal levels of IL-6 were detected. I.p. injections of imiquimod caused a significant increase of circulating IL-6 from less than 100 to about 475 (2 h) and 1650 (6 h) IU/ml (Fig. 5B). Bioactive TNFα, which was never detected in the plasma of control animals, increased significantly in the lavage fluid from the pouch and became detectable in plasma at 1 and 2 h after the respective injection of imiquimod. I.p. treatment with the TLR7 agonist significantly increased the biological activity of TNFα in plasma (Fig. 5D). When compared with the effects of other agonists of TLRs on the biological activity of IL-6 and TNF (Ross et al., 2003; Hübschle et al., 2006; Voss et al., 2006; Knorr et al., 2008), the rise in bioactive IL-6 and TNF in plasma and/or lavage fluid following administration of imiquimod can be categorized as moderate.

S.c. as well as i.p. injections of 5 mg/kg imiquimod induced a significant increase in immunoreactive IFNγ in blood plasma when compared with the respective controls (Fig. 5E, F). The increase in circulating IFNγ started at 2 h after injection, but was much more pronounced 6 h after injection, when concentrations of 500 (s.c. injection) or even 750 (i.p. injec-

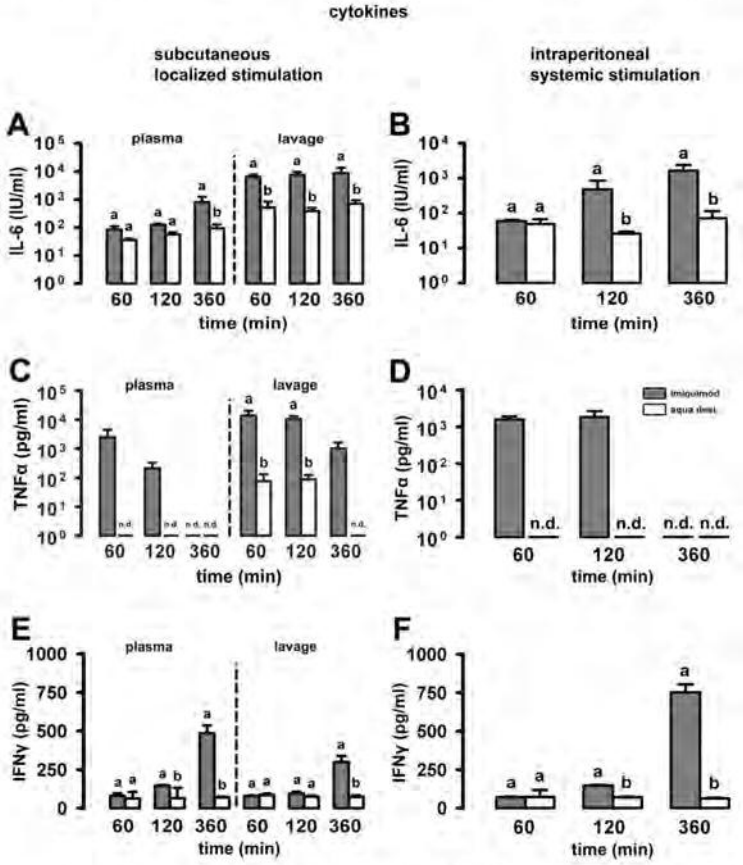


Fig. 5. Levels of bioactive IL-6 (A, B), bioactive TNFα (C, D), and immunoreactive IFNγ (E, F) in plasma and lavage from the air pouch of rats injected s.c. with 5 mg/kg imiquimod or solvent (A, C, E) and in plasma of rats injected i.p. with 5 mg/kg imiquimod or solvent (B, D, F). Samples were collected 1, 2, and 6 h after the respective injections. At a given time point, any pair of columns with the same letter are not significantly different from each other, whereas any pair of columns with different letters are significantly different from each other ($P<0.05$; 1-way ANOVA followed by Scheffe's post hoc test). Columns represent means ± SE.

tion) pg/ml INFγ were measured. At 6 h after injection, an increased concentration of IFNγ was also measured in the lavage fluid collected from the injection site in the pouch (Fig. 5E). Thus, the imiquimod-induced increase in peripheral IFNγ at 6 h followed the peak of its mRNA expression in the spleen and liver at 2 h (Figs. 3 and 4).

Imiquimod induces expression of inflammatory genes in the hypothalamus

The inflammatory activation of transcription factors and the subsequent expression of inflammatory molecules, namely cytokines and prostaglandins, within the hypothalamus are regarded as critical at least for the maintenance of the full spectrum of physiological or behavioral signs of illness (Dantzer et al., 2008). We therefore investigated the hypothalamic expression of a broad spectrum of putative endogenous mediators involved in the manifestation of sickness responses, that is, transcription factors or related molecules (Fig. 6), cytokines (Figs. 7 and 8), and the inducible forms of enzymes responsible for prostaglandin synthesis (Fig. 9). Inhibitor of kappa B (IκB) and suppressor of cytokine signaling 3 (SOCS3) are negative regulators proteins of the transcription factors NFκB and STAT3 and represent markers of their activation (Damm et al., 2011). For both molecules, an increased expression was detected in hypothalamic tissue, which was more pronounced for SOCS3. Six hours after s.c. stimulation with imiquimod, the mRNA expression of the transcription factor NF-IL-6 was significantly elevated, whereas there was only a tendency for such an increase in rats treated via the i.p. route (Fig. 6).

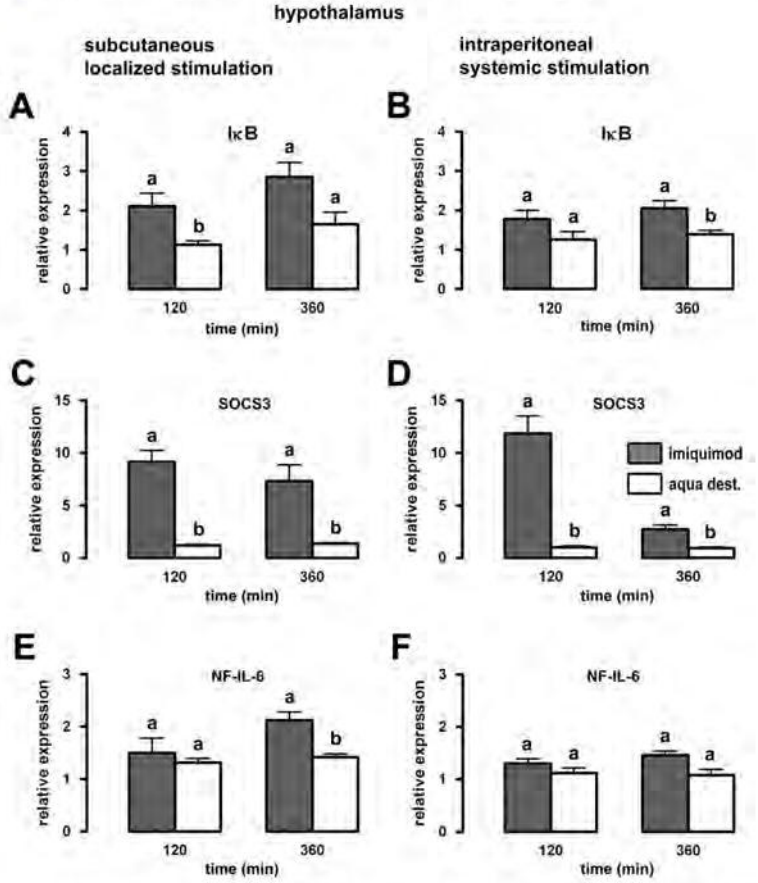


Fig. 6. mRNA expression of inflammatory transcription factor-related molecules (IκB, SOCS3, NF-IL6) in the rat hypothalamus, using quantitative RT-PCR, at 2 h and 6 h after s.c. (A, C, E) or i.p. (B, D, F) injections of 5 mg/kg imiquimod or solvent. At a given time point, any pair of columns with the same letter are not significantly different from each other, whereas any pair of columns with different letters are significantly different from each other ($P<0.05$; 1-way ANOVA followed by Scheffe's post hoc test). Columns represent means ± SE.

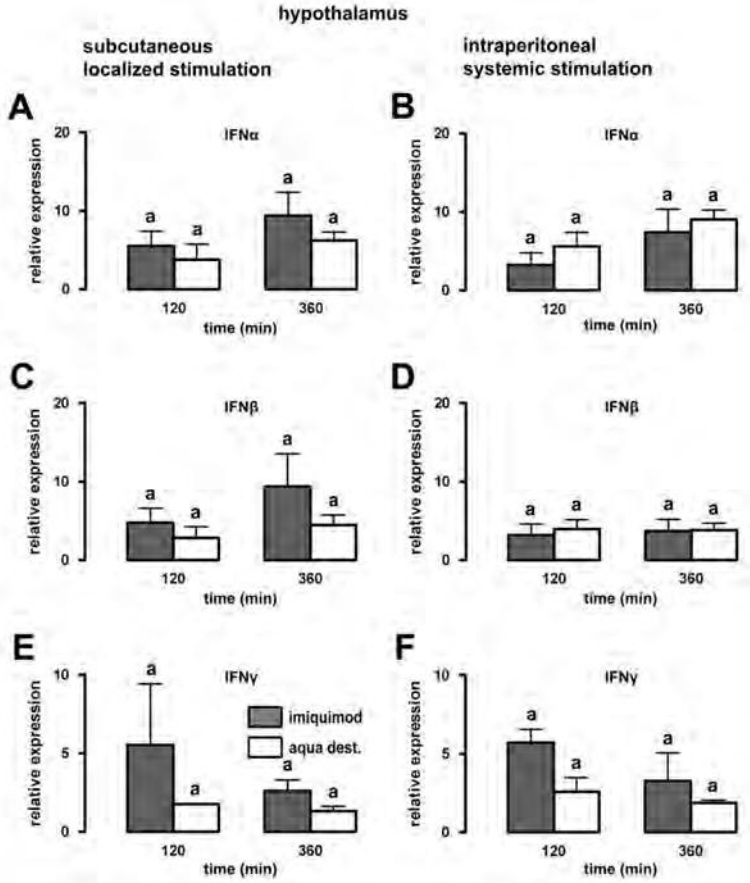


Fig. 7. mRNA expression of IFNs α, β, and γ in the rat hypothalamus, using quantitative RT-PCR, at 2 h and 6 h after s.c. (A, C, E) or i.p. (B, D, F) injections of 5 mg/kg imiquimod or solvent. At a given time point, any pair of columns with the same letter are not significantly different from each other, whereas any pair of columns with different letters are significantly different from each other ($P<0.05$; 1-way ANOVA followed by Scheffe's post hoc test). Columns represent means ± SE.

In contrast to the situation in the peripheral organs (liver and spleen), no expression of IFNs could be detected in the hypothalamus of rats receiving imiquimod (Fig. 7).

The hypothalamic expression of other cytokines implicated in fever and sickness behavior, that is, TNFα, IL-1, and IL-6, was significantly increased in rats injected s.c. with imiquimod and, to a lesser extent, also in i.p.-injected animals, with the exception of IL-1 (Fig. 8). Moreover, we measured an increased expression of the inducible forms of the enzymes involved in the synthesis of prostaglandin E2 (PGE2) in the hypothalamus under conditions of infection or inflammation, that is, cycloxygenase-2 (COX-2) and microsomal PGE synthase (mPGES; Fig. 9).

Imiquimod causes activation of inflammatory transcription factors in brain sites with an incomplete blood–brain barrier

Sensory circumventricular organs (CVOs), such as the OVLT and AP, are brain sites with an incomplete blood–brain barrier, and thus represent putative ports of entry for circulating molecules to signal the brain. Namely, the OVLT is involved in the manifestation of fever (Roth et al., 2004), whereas the AP plays an important role in the control of ingestive behavior (Fry and Ferguson, 2007). Demonstration of an activation of transcription factors (described before in the text) within these specialized brain sites is therefore a useful tool to evaluate inflammatory activation of the brain to a given insult. Owing to the fact

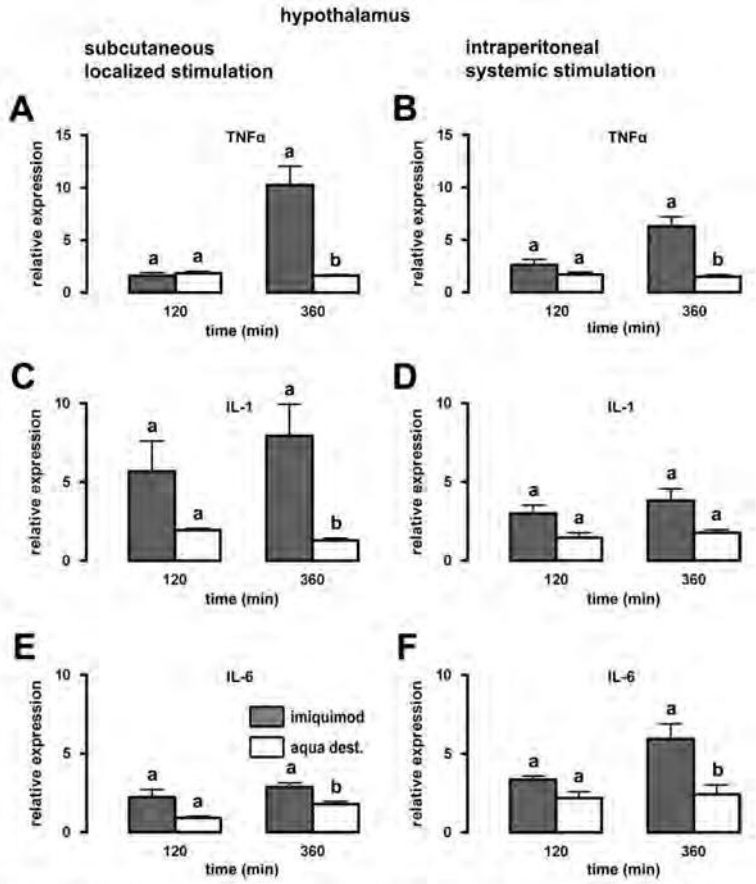


Fig. 8. mRNA expression of the cytokines TNFα, IL-1β, and IL-6 in the rat hypothalamus, using quantitative RT-PCR, at 2 h and 6 h after s.c. (A, C, E) or i.p. (B, D, F) injections of 5 mg/kg imiquimod or solvent. At a given time point, any pair of columns with the same letter are not significantly different from each other, whereas any pair of columns with different letters are significantly different from each other ($P<0.05$; 1-way ANOVA followed by Scheffe's post hoc test). Columns represent means±SE.

that these transcription factors are constitutively present in the cytoplasm and migrate and accumulate in the nucleus of a stimulated cell, the activation of NFκB, STAT3, or NF-IL6 within specific brain sites can be analyzed by means of immunohistochemistry. Because of the observed fever (Fig. 1) and moderate anorexia (Fig. 2), we focused on the OVLT and AP. In control rats treated with solvent s.c. or i.p., nuclear NFκB and STAT3 signals were not detected in both brain sites, whereas a few NFκB- and STAT3-positive cell nuclei appeared in endothelial and other cells within OVLT and AP, as well as in endothelial cells of cortical blood vessels in imiquimod-injected animals (not shown). Compared with treatments with other TLR-agonists, the inflammatory activation of both transcription factors could be categorized as rather moderate.

In contrast, we observed activation of the transcription factor NF-IL6 in imiquimod-treated rats, the strength of which depended on the time and on the route of imiquimod administration (Fig. 10).

NF-IL6 immunoreactivity was almost absent in the OVLT and AP of rats injected with solvent. At 2 h after s.c. or i.p. injection of 5 mg/kg imiquimod, NF-IL6 signals already appeared in both CVOs investigated, and NF-IL6 immunoreactivity increased strongly at the 6-h time point. The strength of the signals was substantially greater in rats treated s.c. with the TLR7 agonist, corresponding to the greater fevers measured in these animals. Triple staining with antibodies against NF-IL6 and vWF, plus nuclear DAPI staining, revealed that the brain vasculature represents an important component of

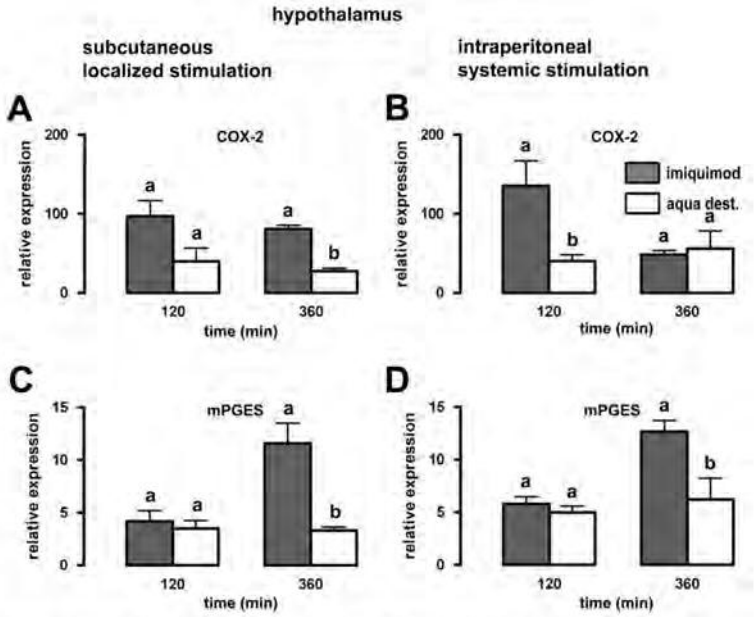


Fig. 9. mRNA expression of inducible forms of enzymes for prostaglandin (PG) E2 synthesis (COX-2 and mPGES1) in the rat hypothalamus, using quantitative RT-PCR, 2 h and 6 h after s.c. (A, C) or i.p. (B, D) injections of 5 mg/kg imiquimod or solvent. At a given time point, any pair of columns with the same letter are not significantly different from each other, whereas any pair of columns with different letters are significantly different from each other ($P<0.05$; 1-way ANOVA followed by Scheffe's post hoc test). Columns represent means ± SE.

immune-to-brain communication in imiquimod-treated rats (Fig. 11).

Numerous endothelial (vWF-positive) cells showed nuclear NF-IL-6 signals not only in the OVLT and AP, but also in cortical blood vessels. However, in both of the sensory CVOs investigated, NF-IL6 immunoreactivity also appeared in cells of nonendothelial origin, the putative phenotypes of which have been analyzed in a previous study on LPS-treated rats (Damm et al., 2011). These cell types included astrocytes, microglial cells, perivascular macrophages, and even a few neurons (Damm et al., 2011). In summary, from the three transcription factors, which are known to be recruited in the brain during inflammation (NFκB, STAT3, and NF-IL6), only NF-IL6 showed a pronounced activation in response to imiquimod. The magnitude of the response was greater following s.c., than i.p. administration, and it was also greater at 6 h compared with 2 h after the respective injection.

DISCUSSION

Brain-controlled illness responses after s.c. or i.p. treatments with imiquimod

The TLR7 agonist imiquimod has been used for topical treatments of neoplasms within cutaneous or subcutaneous tissues. Moreover, it has also been suggested to use intraperitoneal lavage with imiquimod to eliminate epithelial ovarian cancer micrometastases (Kast and Altschuler, 2008). In this study, we characterized the effects of s.c. intrapouch and systemic (i.p.) treatments with imiquimod on some vital homeostatic functions, which are known to be influenced by other TLR-agonists, such as LPS, or diacylated lipopeptides. The TLR4 agonist LPS and the TLR2/6 agonists macrophage-activating lipopeptide-2 (MALP-2) or fibroblast-stimulating lipopeptide-1 (FSL-1) induce fever, anorexia, adipsia, and reduced voluntary locomotor activity in experimental animals, when injected locally or systemically at doses in the range of 10–100 μg/kg, with more potent effects noted with systemic routes of administration (Ross et al., 2003; Rummel et al., 2004; Steiner et al., 2005, 2006a; Hübschle et al., 2006; Knorr et al., 2008, 2010). Subcutaenous administration of the TLR3 agonist Poly I:C has even failed to induce sickness-type responses (Voss et al., 2006).

Here, we show for the first time, that a given TLR-agonist (imiquimod) has greater effects when it is injected subcutaneously, than when it is injected peripherally. The results of our study correspond to data from another study showing that intranasal administration of the synthetic TLR7 ligand, 1V136, caused hypothermia and pronounced anorexia in mice only when a local intranasal administration was performed (Hayashi et al., 2008). At the doses, which we tested in our experiments, the observed illness responses were comparatively moderate. A dose of 1

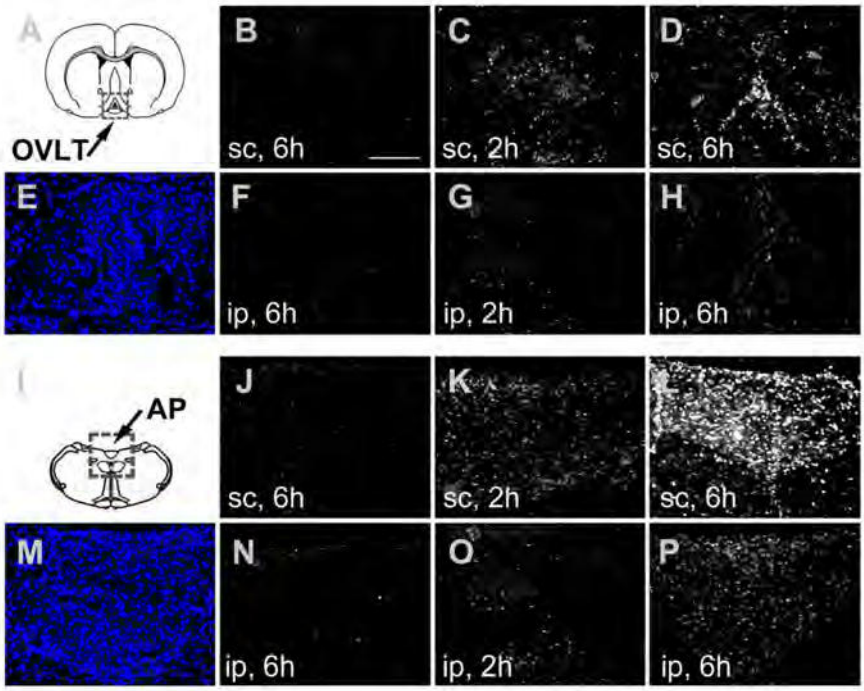


Fig. 10. Nuclear NF-IL6 immunoreactivity in the OVLT (B, C, D, F, G, H) and the AP (J, K, L, N, O, P) 2 h (C, G, K, O) and 6 h (D, H, L, P) after s.c. (C, D and K, L) or i.p. (G, H and O, P) injections of 5 mg/kg imiquimod. Schematic line drawings (A, I) and microphotographs (E, M) showing DAPI-counterstained coronal brain sections at the level of the OVLT (E) and AP (M) are shown for visualization of the surrounding tissue. White, spot-like nuclear NF-IL6 emerges in these regions 2 h and to a greater degree 6 h after the respective challenge with imiquimod. (B, F, J, N) show the corresponding staining 6 h after s.c. (B, J) or i.p. (F, N) injections of solvent. Note that nuclear NF-IL6 immunoreactivity is stronger in s.c. compared with i.p.-stimulated rats and stronger at 6 h after the respective injection of imiquimod than at 2 h. Scale bar = 100 μm. For interpretation of the references to color in this figure legend, the reader is referred to the Web version of this article.

mg/kg imiquimod (s.c. or i.p.) did not induce anorexia or fever. The higher dose of 5 mg/kg of the TLR agonist caused a moderate fever and a slight reduction in food intake on the day of injection only. Both of these responses are mediated within the brain, in particular by the hypothalamus. We therefore tried to characterize putative mediators within the signaling pathways from the periphery to the brain, which might have been induced by s.c. or i.p. injections of imiquimod.

Peripheral induction of cytokines after s.c. or i.p. treatment with imiquimod

TLR7 belongs to the group of intracellular TLRs, which are present in endosomes of macrophages and dendritic cells. They are responsible for intracellular sensing of foreign nucleic acids of viruses and certain bacteria (Blasius and Beutler, 2010). TLR7 activation by nucleic acids within endolysosomes leads to transcriptional activation of the nucleus and as a consequence to the production of type I IFNs, namely IFNα (Rajagopal et al., 2010) or IFNβ (O'Brian et al., 2010). Another study demonstrated the capacity of topical treatment with imiquimod cream to induce the expression of IFNγ in mammary tumors (Lu et al., 2010). We therefore measured the expression of IFNs α, β, and γ in the liver and spleen of rats injected s.c. or i.p. with imiquimod and the respective control. Indeed, s.c. injections of imiquimod caused a pronounced elevation in the expression of all three IFNs in the spleen within two hours after the s.c. treatment. A possible explanation for this observation may be related to the fact that imiquimod is a rather small molecule, and may therefore have escaped from the site of injection (i.e. the subcutaneous air pouch) into the systemic circulation and been transported to the spleen, where it caused the observed effect. However, the fact that the expression of IFNγ showed a much greater relative stimulation, when compared with IFNs α/β was surprising and important for our study for the following reason. We were interested in possible side effects of putative treatments with TLR7 agonists and observed a moderate fever. With regard to endogenous mediators and signaling pathways for fever induction, IFNs have been shown to have both antipyretic and pyretic effects. In an

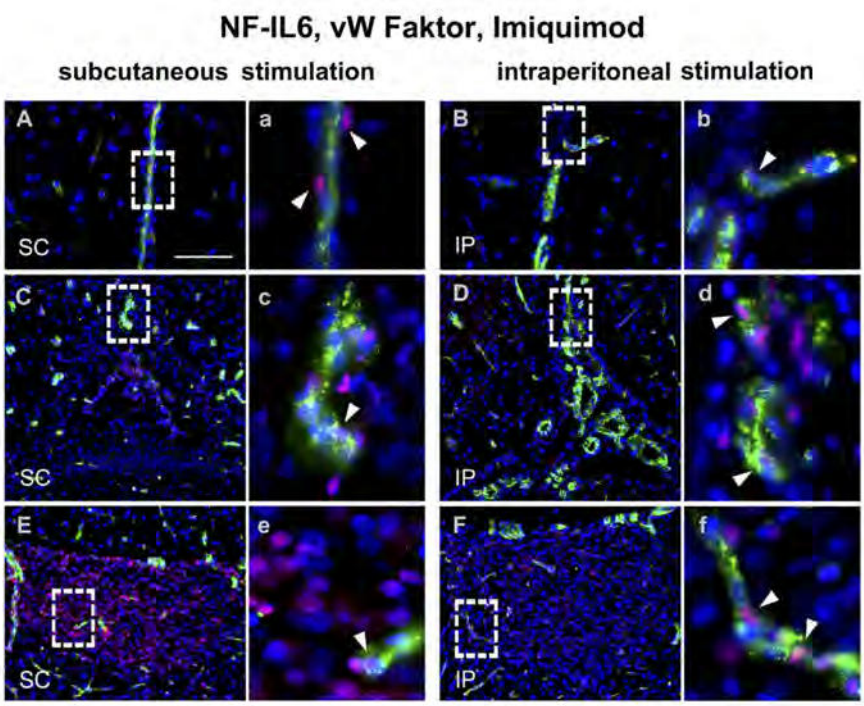


Fig. 11. Fluorescent immunohistochemical colocalization study of NF-IL6 signals (red) with the nuclear DAPI stain (blue) and the endothelial cell marker vWF (green). The figure shows coronal brain sections of the cortex (A, B), the OVLT (C, D), and the AP (E, F) 6 h after s.c. (A, C, E) or i.p. (B, D, F) stimulation with 5 mg/kg imiquimod. Dashed squares are shown at higher magnification (a–f). These magnified insets document colocalization of NF-IL6 with the nuclear DAPI stain (white arrowheads) surrounded by vWF (green) indicative of the endothelial cellular phenotype. Note that nuclear NF-IL6 immunoreactivity is greater in s.c. compared with i.p.-stimulated rats. The horizontal scale (shown in A) corresponds to 50 μm in (A) and (B), to 100 μm in (C–F), and to 20 μm in (a–f). For interpretation of the references to color in this figure legend, the reader is referred to the Web version of this article.

experimentally induced influenza infection, which was accompanied by fever, intranasal administration of IFNα caused a complete suppression of the febrile response (Kugel et al., 2009). This study indicates antipyretic properties of IFNα. IFNγ, on the other hand, has proinflammatory capacities (Chen and Ivashki, 2010) and pyrogenic properties (Morimoto et al., 1987; Kluger, 1991). We therefore tried to detect IFNγ at the protein level to investigate its potential role as a candidate molecule to transfer a fever-inducing signal to the brain. Indeed, we observed elevated levels of immunoreactive IFNγ, not only in the lavage collected from the injection site in the air pouch, but also in the systemic circulation of rats injected s.c. and i.p. with imiquimod. IFNγ might therefore represent one of the humoral signals participating in the manifestation of brain-controlled unspecific illness responses after treatment with the TLR7 agonist. The IFNγ, which we detected in the lavage collected from the pouch, might be derived from the dendritic cells located within this compartment. These cells were exposed to high concentrations of the TLR7 agonist, at least temporarily, and therefore they could provide a significant contribution to the amount of circulating IFN-γ, which we measured.

Traditionally, TNFα and particularly IL-6 are regarded as the most important circulating signals, which influence the brain during a peripheral inflammatory process (Kluger, 1991; Roth and de Souza, 2001; Conti et al., 2004; Oka et al., 2007). The postulated role for both of these cytokines is based on the repeated observations that TNFα and IL-6 are elevated in the blood under various experimental and clinical conditions of systemic inflammation. Our data revealed that imiquimod induces the appearance of bioactive TNFα and IL-6 in the circulation. Thus, a role for these cytokines in mediating fever or anorexia cannot be ruled out. However, the concentrations of both cytokines in the lavage of the pouch and in the blood were rather low, when compared with other TLR agonists (Miller et al., 1997; Rummel et al., 2004; Hübschle et al., 2006; Knorr et al., 2008). A detailed analysis of inflammatory activation of brain sites involved in the manifestation of fever and anorexia, such as the hypothalamus, OVLT, and AP, were therefore performed in imiquimod-treated rats to obtain

information about mechanisms (i.e. activation of transcription factors) and putative endogenous mediators of the moderate imiquimod-induced illness responses.

Induction of inflammatory markers in the brain after s.c. or i.p. treatment with imiquimod

There are several possible options to explain how the brain senses a given inflammatory process taking place somewhere in the periphery. One possibility relates to TLRs present on macrophage-like cells in the CVOs, or on brain endothelial and perivascular cells, which can directly monitor circulating pathogen-associated molecular patterns (Dantzer et al., 2008). As a consequence, cytokines and prostaglandins are produced in the brain area involved in the generation of illness responses, namely the anterior hypothalamus. Although TLR7 seems to be present in endosomal compartments of brain microglia and astrocytes (Butchi et al., 2010), a direct contribution of circulating imiquimod on hypothalamic formation of cytokines seems questionable, because of the fact that we did not observe any significant increase in the expression of IFNs in the hypothalamus (Fig. 7). Other inflammatory mediators (i.e. the cytokines which we detected in the circulation) could also cause an increased expression of hypothalamic cytokines. Indeed, the expression of these cytokines, which are traditionally regarded as brain-intrinsic mediators of illness responses (Layé et al., 2000), was elevated in the hypothalamus of rats injected with imiquimod; the s.c. route of administration being more potent than the i.p. route of administration (Fig. 8). There is evidence that central TNFα (Palin et al., 2007), IL-6 (Chai et al., 1996; Soares et al., in press), and IL-1 (Fortier et al., 2004; Harden et al., 2011) are involved in the manifestation of fever and anorexia. The increased expression of a cocktail of all three of these cytokines, which we observed after peripheral TLR7 stimulation, could thus readily contribute to the moderate signs of illness in imiquimod-treated rats.

The formation of PGE2, by the inducible enzymes COX-2 and mPGES1, within the hypothalamus is regarded as critical by some authors for the manifestation of a febrile response (Yamagata et al., 2001; Gaetano et al., 2010). Others have shown that peripherally derived PGE2 seems to be crucial at least for the early stages of fever (Steiner et al., 2006b), and not all fevers seem to be dependent on PGE2 synthesis in the hypothalamus (Malvar et al., 2011). An obligatory role for intrahypothalamic formation of PGE2 has even been questioned for the model of LPS-induced systemic inflammation (Almeida et al., 2006). In this study, injections of low or high LPS doses caused normal febrile or hypothermic responses in rats with complete lesions of the preoptic-anterior hypothalamus. These animals used behavioral means to develop fever or hypothermia, which thus seem to operate without intrahypothalamic formation of PGE2.

It is currently not known, whether an increased formation of PGE2 within the anterior hypothalamus is critical for the fever, which we observed in response to s.c. or i.p. injections of imiquimod. In this case, the increased expression of COX-2 and mPGES1 in the hypothalamus of imiquimod-treated rats provides the molecular prerequisite for the fever, which we observed after s.c. or i.p. stimulation with imiquimod. The transcription profiles for PGE2-synthesizing enzymes have been carefully studied in rats treated with a fever-inducing dose of LPS (Ivanov et al., 2002). Compared with this study, we detected a similar time course of the expression of COX-2 and mPGES1 with an earlier induction of COX-2 and a later induction of mPGES1 in imiquimod-treated rats, irrespective of the route of its administration. Also the decrease of COX-2 expression at the later stage of our experiment corresponded to the observations, which were made in LPS-treated rats. This phenomenon has been discussed as the reason for a reported lack of correlation between tissue levels of COX-2 and concentrations of PGE2 (Ivanov and Romanovsky, 2004). The authors of this review further suggested that enzymes, such as mPGES1, that are upregulated when COX-2 is downregulated may be better candidate targets for antiinflammatory drugs. Our measurements in imiquimod-treated rats (Fig. 9) with mPGES1 being upregulated when COX-2 starts getting downregulated support such a view.

The activation of inflammatory transcription factors within the brain is a step which occurs before the expression of target genes, which trigger the brain-intrinsic responses. This phenomenon can be assessed by measurements of the expression of markers of their activation, which showed moderate increases after the respective injections of imiquimod (Fig. 6). At the protein level, inflammatory transcription factors are present in the cytoplasma of cells in the CVOs, brain endothelial cells, and other cells and move into the nucleus after inflammatory stimulation. This process of activation is called nuclear translocation and can be visualized by means of immunohistochemistry. NFκB and STAT3 are early markers of an inflammatory activation of the brain, and their nuclear translocation can be induced by TNF/IL-1 (NFκB) and IL-6 (STAT3) as shown in previous studies (Harré et al., 2002; Nadjar et al., 2003; Rummel et al., 2008). Corresponding to the rather moderate levels of IL-6 and TNF in the blood, we detected only a few nuclear STAT3 and NFκB signals in the brains of imiquimod-treated animals. These signals were located in CVOs and endothelial cells of other brain sites (i.e. the cortex). To our surprise, the situation was markedly different for the transcription factor NF-IL6 (synonym: C/EBPβ), which is regarded as a novel marker of brain inflammation (Damm et al., 2011). The activation of NF-IL6 in the brains of imiquimod-injected rats showed a clear spatiotemporal pattern (Figs. 10 and 11), starting quite early after stimulation with the TLR7 agonist and showing a further increase during the time course of fever. A role for NF-IL6 has been suggested in the TLR-mediated induction of proinflammatory cytokines (Lu et al., 2009). However, it has to be defined which signal caused the pronounced activation of this transcription factor in the brains of imiquimod-treated rats. A possible explanation for our observation comes from recent studies on viral replication in macrophages (Dudaronek et al., 2007) and within the CNS (Witwer et al., 2009). In these studies it was shown that

IFN signaling, which occurs along with the innate immune response to viral pathogens, causes activation of NF-IL6. It might thus be the case that the increase in circulating IFNγ, which we observed after injection of imiquimod, is related to the activation of NF-IL6 in brain sites with an incomplete blood–brain barrier or brain endothelial cells also exposed to circulating IFNs. An argument against this hypothesis is that NF-IL6 activation in the brain, but not circulating levels of IFNγ, was stronger in rats injected via the s.c. route with the TLR7 agonist. Further studies using neutralizing antibodies to IFNγ, or experiments on NF-IL6- and/or IFNγ-deficient mice will be required to elaborate, whether there are causal relationships between circulating IFNγ, the activation of NF-IL6 in the brain, and the hypothalamic expression of proinflammatory cytokines (TNF, IL-1, IL-6) in mediating fever and anorexia following imiquimod administration.

CONCLUSIONS

Topical administration of immunomodulators such as imiquimod has therapeutic capacities with regard to treatments of skin cancers, cutaneous viral infections, autoimmune or allergic disorders. A locally generated cytokine milieu at the site of treatment can influence distant organs, including the brain, where unspecific illness responses are generated. According to our data the inflammatory response within the brain and its consequences to s.c. or i.p. administration of imiquimod are moderate, compared with the effects of other TLR agonists. The fever, which develops after injections of imiquimod, may even be beneficial because of an accelerated and enhanced immune response at febrile temperatures (Kluger, 1991). By understanding TLR-induced systemic effects and their underlying mechanisms, the therapeutic potential of TLR agonists in a variety of disorders may be improved.

Acknowledgments—The authors are grateful to Jolanta Murgott, Doreen Marks, and Daniela Ott for their expert technical assistance. J Damm and C Rummel are supported by the Emmy Noether Program of the German Research Foundation [DFG project RU 1397/2-1]. LM Harden was supported by a research fellowship from the Alexander von Humboldt Foundation.

REFERENCES

Aarden LA, DeGroot ER, Schaap OL, Landsdorp PM (1987) Production of hybridome growth factors by human monocytes. Eur J Immunol 17:1411–1416.

Adams S (2009) Toll-like receptor agonists in cancer therapy. J Immunother 1:949–964.

Almeida MC, Steiner AA, Branco LG, Romanovsky AA (2006) Neural substrate of cold-seeking behavior in endotoxin shock. PLoS One 1: e1.

Beutler BA (2009) TLRs and innate immunity. Blood 113:1399–1407.

Blasius AL, Beutler B (2010) Intracellular Toll-like receptors. Immunity 32:305–315.

Borsutzki S, Fiorelli V, Ebensen T, Tripiciano A, Rharbaoui F, Scoglio A, Link C, Nappi F, Morr M, Buttó S, Cafaro A, Mühlradt PF, Ensoli B, Guzmán CA (2003) Efficient mucosal delivery of the HIV-1 Tat protein using the synthetic lipopeptide MALP-2 as adjuvant. Eur J Immunol 33:1548–1556.

Broomfield SA, van der Most RG, Prosser AC, Mahendran S, Tovey MG, Smyth MJ, Robinson BW, Currie AJ (2009) Locally administered TLR7 agonists drive systemic antitumor immune responses that are enhanced by anti-CD40 immunotherapy. J Immunol 182:5217–5224.

Butchi NB, Du M, Peterson KE (2010) Interactions between TLR7 and TLR9 agonists and receptors regulate innate immune responses by astrocytes and microglia. Glia 58:650–664.

Cartmell T, Luheshi GN, Hopkins SJ, Rothwell NJ, Poole S (2001) Role of endogenous intetrleukin-1 receptor antagonist in regulating fever induced by localised inflammation in the rat. J Physiol 531 (Pt 1):171–180.

Cartmell T, Mitchell D, Lamond FJ, Laburn HP (2002) Route of administration differentially affects fevers induced by Gram-negative and Gram-positive pyrogens in rabbits. Exp Physiol 87(3):391–399.

Cartmell T, Poole S, Turnbull AV, Rothwell NJ, Luheshi GN (2000) Circulating interleukin-6 mediates the febrile response to localised inflammation in rats. J Physiol 526:653–661.

Chai Z, Gatti S, Toniatti C, Poli V, Bartfai T (1996) Interleukin (IL)-6 gene expression in the central nervous system is necessary for fever response to lipopolysaccharide or IL-1 beta: a study on IL-6-deficient mice. J Exp Med 183:311–316.

Chen J, Ivashkiv LB (2010) IFN-γ abrogates endotoxin tolerance by facilitating Toll-like receptor-induced chromatin remodeling. Proc Natl Acad Sci U S A 107:19438–19443.

Conti B, Tabarean I, Andrei C, Bartfai T (2004) Cytokines and fever. Front Biosci 9:1433–1449.

Damm J, Luheshi GN, Gerstberger R, Roth J, Rummel C (2011) Spatiotemporal nuclear factor interleukin-6 expression in the rat brain during lipopolysaccharide-induced fever is linked to sustained hypothalamic inflammatory target gene induction. J Comp Neurol 519:480–505.

Dantzer R, O'Connor JC, Freund GG, Johnson RW, Kelley KW (2008) From inflammation to sickness and depression: when the immune system subjugates the brain. Nat Rev Neurosci 9:46–56.

Deiters U, Barsig J, Tawil B, Mühlradt PF (2004) The macrophage-activating lipopeptide-2 accelerates wound healing in diabetic mice. Exp Dermatol 13:731–739.

Diebold SS, Kaisho T, Hemmi H, Akira S, Reis e Sousa C (2004) Innate antiviral responses by means of TLR7-mediated recognition of single-stranded RNA. Science 303:1529–1531.

Dudaronek JM, Barber SA, Clements JE (2007) CUGBP1 is required for IFNβ-mediated induction of dominant-negative CEBPb and suppression of SIV replication in macrophages. J Immunol 179: 7262–7269.

Espevic T, Nissen-Meyer J (1986) A highly sensitive cell line, WEHI 164 clone 13, for measuring cytotoxic factor/tumor necrosis factor from human monocytes. J Immunol Methods 95:99–105.

Fortier ME, Kent S, Ashdown H, Poole S, Boksa P, Luheshi GN (2004) The viral mimic, polyinosinic: polycytidylic acid, induces fever in rats via an interleukin-1-dependent mechanism. Am J Physiol Regul Integr Comp Physiol 287: R759–R766.

Fry M, Ferguson AV (2007) The sensory circumventricular organs: brain targets for circulating signals controlling ingestive behavior. Physiol Behav 91:413–423.

Gaetano L, Watanabe K, Barogi S, Coceani F (2010) Cyclooxygenase-2/microsomal prostaglandin E synthase-1 complex in the preoptic-anterior hypothalamus of the mouse: involvement through fever to intravenous lipopolysaccharide. Acta Physiol (Oxf) 200: 315–324.

Galanos C, Gumenschneider M, Mühlradt PF, Jirillo E, Freudenberg MA (2000) MALP-2, a mycoplasma lipopeptide with classical endotoxic properties: end of an era of LPS monopoly? J Endotoxin Res 6:471–476.

Green DS, Dalgleish AG, Belonwu N, Fischer MD, Bodman-Smith MD (2008) Topical imiquimod and intralesional interleukin-2 increase

activated lymphocytes and restore the Th1/Th2 balance in patients with metastatic melanoma. Br J Dermatol 159:606–614.
Greis A, Murgott J, Gerstberger R, Hübschle T, Roth J (2009) Effects of repeated injections of fibroblast-stimulating lipopeptide-1 on fever, formation of cytokines, and on the responsiveness to endotoxin in guinea pigs. Acta Physiol (Oxf) 197:35–45.
Greis A, Murgott J, Rafalzik S, Gerstberger R, Hübschle T, Roth J (2007) Characterization of the febrile response induced by fibroblast-stimulating lipopeptide-1 in guinea pigs. Am J Physiol Regul Integr Comp Physiol 293: R152–R161.
Harden LM, du Plessis I, Roth J, Loram LC, Poole S, Laburn HP (2011) Differences in the relative involvement of peripherally released interleukin (IL)-6, brain IL-1β and prostanoids in mediating lipopolysaccharide-induced fever and sickness behaviour. Psychoneuroendocrinology 36:608–622.
Harré EM, Roth J, Pehl U, Kueth M, Gerstberger R, Hübschle T (2002) Selected contribution: role of IL-6 in LPS-induced nuclear STAT3 translocation in sensory circumventricular organs during fever in rats. J Appl Physiol 92:2657–2666.
Hayashi T, Cottam HB, Chan M, Jin G, Tawatao RI, Crain B, Ronacher L, Messer K, Carson DA, Corr M (2008) Mast cell-dependent anorexia and hypothermia induced by mucosal activation of Toll-like receptor 7. Am J Physiol Regul Integr Comp Physiol 295: R123–R132.
Heil F, Hemmi H, Hochrein H, Ampenberger F, Kirschning C, Akira S, Lipford G, Wagner H, Bauer S (2004) Species-specific recognition of single-stranded RNA via Toll-like receptor 7 and 8. Science 303:1526–1529.
Hengge UR, Stark R (2001) Topical imiquimod to treat intraepidermal carcinoma. Arch Dermatol 137:709–711.
Holt I, Cooper RG, Hopkins SJ (1991) Relationship between local inflammation, interleukin-6 concentration and the acute phase response in arthritic patients. Eur J Clin Invest 21:479–484.
Hübschle T, Mütze J, Mühlradt PF, Korte S, Gerstberger R, Roth J (2006) Pyrexia, anorexia, adipsia, and depressed motor activity in rats during systemic inflammation induced by the Toll-like receptors-2 and -6 agonists MALP-2 and FSL-1. Am J Physiol Regul Integr Comp Physiol 290: R180–R187.
Hübschle T, Thom E, Watson A, Roth J, Klaus S, Meyerhoff W (2001) Leptin-induced nuclear translocation of STAT3 immunoreactivity in hypothalamic nuclei involved in body weight regulation. J Neurosci 21:2413–2424.
Ivanov AI, Pero RS, Scheck AC, Romanovsky AA (2002) Prostaglandin E2-synthesizing enzymes in fever: differential transcriptional regulation. Am J Physiol Regul Integr Comp Physiol 283: R1104–R1117.
Ivanov AI, Romanovsky AA (2004) Prostaglandin E2 as a mediator of fever: synthesis and catabolism. Front Biosci 9:1977–1993.
Kast RE, Altschuler EL (2008) Intraperitoneal lavage with imiquimod to eliminate epithelial ovarian cancer micro metastases. Med Hypoth 70:1223–1224.
Kluger MJ (1991) Fever: role of pyrogens and cryogens. Physiol Rev 71:93–127.
Knorr C, Hübschle T, Murgott J, Mühlradt PF, Gerstberger R, Roth J (2008) Macrophage-activating lipopeptide-2 (MALP-2) induces a localized inflammatory response in rats resulting in activation of brain sites implicated in fever. Brain Res 1205:36–46.
Knorr C, Marks D, Gerstberger R, Mühlradt PF, Roth J, Rummel C (2010) Peripheral and central cyclooxygenase (COX) products may contribute to the manifestation of brain-controlled sickness responses during localized inflammation induced by macrophage-activating lipopeptide-2 (MALP-2). Neurosci Lett 479:107–111.
Kugel D, Kochs G, Obojes K, Roth J, Kobasa D, Gray M, Haller O, Staeheli P, von Messling V (2009) Intranasal administration of interferon-alpha reduces seasonal influenza A virus morbidity in ferrets. J Virol 83:3843–3851.
Layé S, Gheusi G, Cremona S, Combe C, Kelley K, Dantzer R, Parnet P (2000) Endogenous brain IL-1 mediates LPS-induced anorexia and hypothalamic cytokine expression. Am J Physiol Regul Integr Comp Physiol 279: R93–R98.
Lee J, Chuang TH, Redecke V, She L, Pitha PM, Carson DA, Raz E, Cottam HB (2003) Molecular basis for the immunostimulatory activity of guanine nucleoside analogs: activation of Toll-like receptor 7. Proc Natl Acad Sci U S A 100:6646–6651.
Levy RM, Mollen KP, Prince JM, Kaczorowski DJ, Vallabhaneni R, Liu S, Tracey KJ, Lotze MT, Hackam DJ, Fink MP, Vodovotz Y, Billiar TR (2007) Systemic inflammation and remote organ injury following trauma require HMGB1. Am J Physiol Regul Integr Comp Physiol 293: R1538–R1544.
Lu H, Wagner WM, Gad E, Yang Y, Duan H, Amon LM, Van Denend N, Larson ER, Chang A, Tufvesson H, Disis ML (2010) Treatment failure of a TLR-7 agonist occurs due to self-regulation of acute inflammation and can be overcome by IL-10 blockade. J Immunol 184:5360–5367.
Lu YC, Kim I, Lye E, Shen F, Suzuki N, Suzuki S, Gerondakis S, Akira S, Gaffen SL, Yeh WC, Ohashi PS (2009) Differential role for c-Rel and C/EBPbeta/delta in TLR-mediated induction of proinflammatory cytokines. J Immunol 182:7212–7221.
Ma F, Zhang JH, Zhang JA, Zhang C (2010) The TLR7 agonists imiquimod and gardiquimod improve DC-based immunotherapy for melanoma in mice. Cell Mol Immunol 7:381–388.
Malvar DC, Soares DM, Fabrício ASC, Kanashiro A, Machado RR, Figueiredo MJ, Rae GA, de Souza GE (2011) The antipyretic effect of dipyrone is unrelated to inhibition of PGE2 synthesis in the hypothalamus. Br J Pharmacol 162:1401–1409.
Miller AJ, Luheshi GN, Rothwell NJ, Hopkins SJ (1997) Local cytokine induction by LPS in the rat air pouch and its relationship to the febrile response. Am J Physiol Regul Integr Comp Physiol 272: R857–R861.
Miller RL, Meng TC, Tomai MA (2008) The antiviral activity of Toll-like receptor 7 and 7/8 agonists. Drug News Perspect 21:69–87.
Morimoto A, Murakami N, Takada M, Teshirogi S, Watanabe T (1987) Fever and acute phase response induced in rabbits by human recombinant interferon-γ. J Physiol 391:209–218.
Nadjar A, Combe C, Laýe S, Tridon V, Dantzer R, Amédée T, Parnet P (2003) Nuclear factor κB nuclear translocation as a crucial marker of brain response to interleukin-1. A study in rat and interleukin-1 type I deficient mouse. J Neurochem 87:1024–1036.
O'Brian K, Fitzgerald D, Rostami A, Gran B (2010) The TLR7 agonist, imiquimod, increases IFN-beta production and reduces the severity of experimental autoimmune encephalomyelitis. J Neuroimmunol 221:107–111.
Oka Y, Ibuki T, Matsumura K, Namba M, Yamazaki Y, Poole S, Tanaka Y, Kobayashi S (2007) Interleukin-6 is a candidate molecule that transmits inflammatory information to the CNS. Neuroscience 145:530–538.
Palin K, Bluthé RM, McCusker RH, Moos F, Dantzer R, Kelley KW (2007) TNF alpha-induced sickness behavior in mice with functional 55 kD TNF receptors is blocked by central IGF-1. J Neuroimmunol 187:55–60.
Paxinos G, Watson C (1998) The rat brain in stereotaxic coordinates. 4th ed. San Diego: Academic Press.
Rajagopal D, Paturel C, Morel Y, Uematsu S, Akira S, Diebold SS (2010) Plasmacytoid dendritic cell-derived type I interferon is crucial for the adjuvant activity of Toll-like receptor 7 agonists. Blood 115:1949–1957.
Ross G, Hübschle T, Pehl U, Braun HA, Voigt K, Gerstberger R, Roth J (2003) Fever induction by localized subcutaneous inflammation in guinea pigs: the role of cytokines and prostaglandins. J Appl Physiol 94:1395–1402.
Roth J, de Souza GE (2001) Fever induction pathways: evidence from responses to systemic or local cytokine formation. Braz J Med Biol Res 34:301–314.
Roth J, Harré EM, Rummel C, Gerstberger R, Hübschle T (2004) Signaling the brain in systemic inflammation: role of sensory circumventricular organs. Front Biosci 9:290–300.

Rummel C, Hübschle T, Gerstberger R, Roth J (2004) Nuclear translocation of the transcription factor STAT3 in the guinea pig brain during systemic or localized inflammation. J Physiol 557(2):671–687.

Rummel C, Inoue W, Sachot C, Poole S, Hübschle T, Luheshi GN (2008) Selective contribution of interleukin-6 and leptin to brain inflammatory signals induced by systemic LPS injection in mice. J Comp Neurol 511:373–395.

Rummel C, Sachot C, Poole S, Luheshi GN (2006) Circulating interleukin-6 induces fever through a STAT3-linked activation of COX-2 in the brain. Am J Physiol Regul Integr Comp Physiol 291: R1316–R1326.

Schmidt J, Welsch T, Jäger D, Mühlradt PF, Büchler MW, Märten A (2007) Intratumoural injection of the Toll-like receptor-2/6 agonist macrophage-activating lipopeptide-2 in patients with pancreatic carcinoma: a phase I/II trial. Br J Cancer 97:598–604.

Soares DM, Figueiredo MJ, Martins JM, Machado RR, Sorgi C, Faciolli LH, Alves-Filho JC, Cunha FQ, Souza GEP (in press) A crucial role for IL-6 in the CNS of rats during fever induced by injection of life E. coli. Med Microbiol Immunol, in press.

Steiner AA, Chakravarty S, Robbins JR, Dragic AS, Pan J, Herkenham M, Romanovsky AA (2005) Thermoregulatory responses of rats to conventional preparations of lipopolysaccharide are caused by lipopolysaccharide per se—not by lipoprotein contaminants. Am J Physiol Regul Integr Comp Physiol 289: R348–R352.

Steiner AA, Chakravarty S, Rudaya AY, Herkenham M, Romanovsky AA (2006a) Bacterial lipopolysaccharide fever is initiated via Toll-like receptor 4 on hematopoietic cells. Blood 107:4000–4002.

Steiner AA, Ivanov AI, Serrats J, Hosokawa H, Phayre AN, Robbins JR, Roberts JL, Kobayashi S, Matsumura K, Sawchenko PE, Romanovsky AA (2006b) Cellular and molecular basis of the initiation of fever. PLoS Biol 4:1517–1524.

Steiner AA, Molchanova AY, Dogan MD, Patel S, Pétervári E, Balaskó M, Wanner SP, Eales J, Oliveira DL, Gawa NR, Almeida MC, Székely M, Romanovsky AA (2011) The hypothermic response to bacterial lipopolysaccharide critically depends on brain CB1, but not CB2 or TRPV1, receptors. J Physiol 589:2415–2431.

Uematsu S, Akira S (2006) Toll-like receptors and innate immunity. J Mol Med 84:712–725.

Voss T, Rummel C, Gerstberger R, Hübschle T, Roth J (2006) Fever and circulating cytokines induced by double stranded RNA in guinea pigs: dependence on the route of administration and effects of repeated injections. Acta Physiol (Oxf) 187:379–389.

Witwer KW, Gama L, Li M, Bartizal CM, Queen SE, Varrone JJ, Brice AK, Graham DR, Tarwater PM, Mankowski JL, Zink MC, Clements JE (2009) Coordinated regulation of SIV replication and immune responses in the CNS. PLoS One 4:1–11.

Yamagata K, Matsumura K, Inoue W, Shiraki T, Suzuki K, Yasuda S, Sugiura H, Cao C, Watanabe Y, Kobayashi S (2001) Coexpression of microsomal-type prostaglandin E synthase with cyclooxygenase-2 in brain endothelial cells of rats during endotoxin-induced fever. J Neurosci 21:2669–2677.

Zhang H, Ching S, Chen Q, Li Q, An Y, Quan N (2008) Localized inflammation in peripheral tissue signals the CNS for sickness response in the absence of interleukin-1 and cyclooxygenase-2 in the blood and brain. Neuroscience 157:895–907.

(Accepted 4 November 2011)
(Available online 12 November 2011)

1.2. „Fever induction by systemic stimulation with macrophage-activating lipopeptide-2 depends upon TLR2 but not CD36“

Welsch J., Hübschle T., Murgott J., Kirschning C., **Rummel C.**, Gerstberger R., Roth J. *Innate Immun* (2012) 18: 541-559

Impakt Faktor: 3,283

Eigener Anteil an der Publikation:

- Initiative: unterstützend (20 %)
- Projektplanung: wenig beteiligt (10 %)
- Durchführung der Versuche: unterstützend (30 %)
- Auswertung der Experimente: unterstützend (30 %)
- Erstellung der Publikation: unterstützend (30 %)

Original Article

Innate Immunity

Innate Immunity
18(3) 541–559
© The Author(s) 2011
Reprints and permissions:
sagepub.co.uk/journalsPermissions.nav
DOI: 10.1177/1753425911426892
ini.sagepub.com

SAGE

Fever induction by systemic stimulation with macrophage-activating lipopeptide-2 depends upon TLR2 but not CD36

Janina Welsch[1]*, Thomas Hübschle[1]*, Jolanta Murgott[1], Carsten Kirschning[2], Christoph Rummel[1], Rüdiger Gerstberger[1] and Joachim Roth[1]

Abstract

This study was designed to test the responses of TLR2-knockout mice (TLR2-KO) and wild- type mice (C57/BL-6), and of CD36 deficient spontaneously hypertensive rats (SHR) and their genetic controls [Wistar Kyoto (WKY) rats] to systemic stimulations with the TLR2/6 agonist MALP-2 and the TLR4 agonist LPS. Fever and formation of TNF-α and IL-6 induced by intraperitoneal injections of MALP-2 (1000 μg/kg) were completely blunted in TLR2-KO, while LPS (100 μg/kg)-induced responses were not abolished in these animals. In SHR lacking CD36, a reduction of fever was observed in response to MALP-2 (100 μg/kg), but LPS-fever was even more attenuated in SHR when compared with WKY controls. Concentrations of circulating IL-6 tended to be lower in SHR after stimulation with both pyrogens. However, the IL-6-mediated activation of the transcription factor STAT3 in the brain was identical in both strains, indicating that the brain-controlled inflammatory response to MALP-2 (and LPS) is not impaired in the absence of CD36. In addition, stimulation of peritoneal macrophages with LPS and MALP-2 (10 μg/ml) caused the appearance of similar concentrations of bioactive cytokines in the supernatants from cells of both rat strains. These results demonstrate that TLR2 is essential for the manifestation of MALP-2, but not LPS-induced inflammatory responses. A moderate participation of CD36 in MALP-2-induced sickness- and cytokine-responses can not be ruled out but is unlikely as LPS-induced inflammatory responses were also attenuated in SHR.

Keywords

Febrile response, sickness behavior, Toll-like receptors, TNF-α, IL-6

Date received: 5 May 2011; revised: 5 August 2011; 5 September 2011; accepted: 26 September 2011

Introduction

TLRs recognize conserved pathogen-associated molecular patterns (PAMPs) from diverse microorganisms.[1] For example, LPS from Gram-negative bacteria, the most frequently used agent to induce experimental fever, is recognized by TLR4,[2,3] and it has recently been shown that all phases of LPS-induced fever depend on TLR4 signaling.[4] Bacterial lipopeptides, on the other hand, are recognized via TLRs 1, 2 and 6, which can form functional pairs for pattern recognition to evoke a full cellular response to such molecules including MALP-2, which is the natural component of the wall-less bacterium *Mycoplasma fermentans*.[5–9] Within the last few years, evidence for substantial therapeutic capacities of MALP-2 has accumulated. The substance is useful as a mucosal adjuvant, especially for intranasally administered vaccines.[10,11] It further accelerates the healing of skin wounds,[12] and injections of MALP-2 into pancreatic tumors appear to have beneficial effects in human patients.[13] A detailed analysis of how a treatment with MALP-2 affects the organism is

[1]Institut für Veterinär-Physiologie und -Biochemie, Justus-Liebig-Universität Giessen, Giessen, Germany
[2]Institut für Medizinische Mikrobiologie, Universitätsklinikum Essen, Germany

*These authors contributed equally to this work.

Corresponding author:
Joachim Roth, Institut für Veterinär-Physiologie und -Biochemie, Justus-Liebig-Universität Giessen, Frankfurter Strasse 100, D-35392 Giessen, Germany.
Email: Joachim.Roth@vetmed.uni-giessen.de

Downloaded from ini.sagepub.com at Bibliotheksystem der Universitaet Giessen on May 28, 2012

therefore warranted, especially because of the fact that treatment of human patients with this substance caused septic shock-like states with cardiac arrest or hypovolemia in single individuals.[13] In previous studies, we investigated the manifestation of brain-controlled non-specific illness responses of rats injected systemically,[14] or locally,[15,16] with MALP-2 to characterize possible side-effects of therapeutic treatments. With regard to the cellular mechanisms responsible for the observed responses *in vivo*, some interesting data have been published within the last years. On the one hand, the formation of heterodimers of TLR2 with TLRs 1 or 6 appears to be involved in the discrimination between diacyl and triacyl lipopeptides by the innate immune system.[1] In addition, it was shown that a mutation, and thereby inactivation, of the scavenger receptor CD36 made murine macrophages much less sensitive to a stimulation with MALP-2.[17] The authors of this, and of another, study[18] suggested a critical role for CD36 as a sensor of diacylglycerides, such as MALP-2, which associates with the respective TLRs and may be required for the MALP-2-induced signal transduction.

Based on these observations, the specific goals of this study can be summarized as follows: (i) using TLR2-deficient mice, we aimed to prove whether TLR2 is essential for a full manifestation of brain-controlled illness responses (i.e. fever) after stimulation with MALP-2; (ii) using CD36-deficient, spontaneously hypertensive rats (SHRs),[19,20] we tried to characterize the postulated role for CD36 in the manifestation of MALP-2-induced responses *in vivo*; And, (iii) we further tested the responses of TLR2-KO mice and SHRs and their respective genetic controls to systemic stimulation with LPS, as LPS-induced fever has not yet been investigated in these strains of experimental animals. We show that MALP-2-induced responses *in vivo* are completely abolished by TLR2-deficiency. On the other hand, the *in vitro* observation that MALP-2-mediated cellular activation strongly depends on CD36[17] could not be confirmed *in vivo*. Surprisingly, the LPS-induced responses of SHRs were more attenuated than MALP-2-induced fever or cytokine formation in the CD36-deficient animals.

Materials and methods

Animals

The first series of experiments was performed in wild-type (C57/BL-6, purchased from Charles River Laboratories, Sulzfeld, Germany) and TLR2-deficient (TLR2-KO) mice ninefold backcrossed towards the C57/BL-6 genetic background.[21] Male mice with a body weight of 23–28 g were used for the experiments. After surgery (see below), the mice were individually housed in a temperature- and humidity-controlled climate chamber (Typ 10'US/+5 – +40 DU, Weiss Umwelttechnik GmbH, Reiskirchen, Germany) at an ambient temperature of 30°C and 50% humidity. Animals had constant access to water and were fed with standard lab chow *ad libitum*.

The second series of experiments were performed in CD36-deficient, SHRs (obtained from an in-house breeding colony in the Department of Physiology, University of Giessen, Faculty of Medicine) and their genetic controls [Wistar Kyoto (WKY) rats obtained from Charles River Laboratories]. Male rats with a body weight of 200–230 g on the day of surgery (see below) were used for the experiments. Again, the animals were individually housed in the climatic chamber (Weiss Umwelttechnik GmbH), which was adjusted to 25°C and 50% humidity for this species. The rats had constant access to water and were fed with powdered, standard lab chow *ad libitum*, which was required for telemetric measurement of cumulative food intake (see below).

Artificial lights were on from 07:00 to 19:00. Body weight was determined once on a day (~09:00 to 09:30). The animals were surgically prepared for telemetric measurement of body temperature (see below) at least one week before the experiment. The experiments were carried out in accordance with the local ethics committee (ethics approval number GI 18/2 – Nr. 15/2007).

Substances

The biologically active R stereoisomer of MALP-2 was kindly provided by Prof. Mühlradt. It was synthesized and purified by HPLC as previously described.[8] MALP-2 was donated as a sterile, lyophilized, endotoxin- and pyrogen-free powder, which was then diluted in 10% Cremophor® EL—90% sterile PBS. Cremophor® EL is a non-ionic solubilizer and emulsifier designed for *in vivo* use in the human and veterinary pharmaceutical industry. Cremophor® EL was a kind gift from BASF Aktiengesellschaft (Ludwigshafen, Germany). For rats, MALP-2 was used at a dose of 100 µg/kg body weight, as described in a previous study.[14] Control experiments were performed with 10% Cremophor® EL in 90% PBS (solvent). For mice, pilot experiments were performed to find a pyrogenic dose of MALP-2. Tests with doses of 10, 100 and 1000 µg/kg MALP-2 revealed that a dose of 1000 µg/kg was required to induce a significant elevation of body temperature in mice.

LPS derived from *Escherichia coli* (serotype O111:B4, Sigma Chemicals, Deisenhofen, Germany) was suspended in sterile PBS. For mice and rats, a dose of 100 µg/kg LPS was used, which is a fever-inducing dose in both species investigated.[22,23]

Downloaded from ini.sagepub.com at Bibliotheksystem der Universitaet Giessen on May 28, 2012

Measurement of body temperature

The abdominal temperature of rats was measured using biotelemetry transmitters (battery powered VM-FH-discs for rats and XM-FH-discs for mice; Mini-Mitter, Bend, OR, USA) implanted into the abdominal cavity at least one week before the experiment. Before the surgery, mice and rats were anesthetized with 100 mg/kg ketamine hydrochloride (Albrecht, Aulendorf, Germany) and 5 mg/kg xylazin (Bayer Vital, Leverkusen, Germany). The output (frequency in Hz) was monitored by a receiver placed under each cage (RA 1000, Mini-Mitter). A data acquisition system (Vital View, Mini-Mitter) was used for automatic control of data collection and analysis. Body temperature was continuously recorded at 5-min intervals. For analysis and graphical documentation, temperature data at time intervals of 15 min were used.

Measurement of food and water intake

In rats, food intake and drinking behavior was telemetrically monitored at 5 min intervals by use of special cages equipped with water bottles and food supply dishes placed on balances, which, in turn, were connected via a DietScan analyzer to a personal computer (AccuScan Instruments, Columbus, OH, USA). The AccuDiet software package (AccuScan Instruments) was used to record, and later to transfer, the data for graphical and statistical analysis. Cumulative food and water intake per 5 min were combined into cumulative measures of food and water intake over a 24-h period.[14] Therefore, the final data represent cumulative food and water intake in grams per 24 h. The equipment for recording food and water intake was not applicable for the experiments performed with mice.

Measurement of blood pressure

In two groups of SH and WKY rats, systolic arterial blood pressure and heart rate were measured by use of a computerized microprocessor-based non-invasive blood pressure monitoring system on the tail of the conscious rat with the aid of a pressure cuff (TSE-Systems Inc., Midland, MI, USA; courtesy of Prof. K.D. Schlüter, Department of Physiology, Justus-Liebig-University of Giessen, Faculty of Medicine). The TSE system consisted of pulse transducers, pressure cuffs with pressure tubing, an animal restraining device and a control unit with integrated temperature control. All rats were repeatedly accustomed to the measurement procedure for 5–6 consecutive days prior to the final measurement.

Cytokine bioassays

Cytokine analysis was performed with plasma samples from mice or rats or supernatants from peritoneal macrophages stimulated either with MALP-2, LPS or the respective control vehicles (10% Cremophor® EL in 90% PBS for MALP-2, PBS for LPS). Determination of TNF-α was achieved by a bioassay based on the cytotoxic effect of TNF-α on the mouse fibrosarcoma cell line, WEHI 164 subclone 13.[24] The assay was performed in sterile, 96-well microtiter plates. Serial dilutions of biologic samples or different concentrations of a murine TNF-α standard (code 88/532, National Institute for Biological Standards and Control, South Mimms, UK) were incubated for 24 h in wells that had been seeded with 50,000 actinomycin D-treated WEHI cells. The number of surviving cells after 24 h was measured by use of the dimethylthiazol-diphenyl tetrazolium bromide (MTT) colorimetric assay.[25] Plasma samples were pre-diluted so that serial dilution of samples and standard dilution curves were parallel. The detection limit of the assay, after considering the dilution of samples into the assays, was 6 pg/ml TNF-α.

Determination of IL-6 was achieved by a bioassay based on the dose-dependent growth stimulation of IL-6 on the B9 hybridoma cell line.[26] The assay was performed in sterile, 96-well microtiter plates. In each well, 5000 B9 cells were incubated for 72 h with serial dilutions of biologic samples or with different concentrations of a human IL-6 standard (code 89/548, National Institute for Biological Standards and Control). Plasma samples were pre-diluted so that serial dilution of samples and standard dilution curves were parallel. The number of cells in each well was measured by use of the MTT assay (see above). The detection limit of the assay, after considering the dilution of samples into the assays, was three international units (I.U.) IL-6/ml.

PGE_2-ELISA

PGE_2 was determined by use of a commercially-available enzyme immunoassay (Assay Designs, Ann Arbor, MI, USA). The assay is based on the competitive-binding technique in which PGE_2 in a sample competes with a fixed amount of alkaline phosphatase-labeled PGE_2 for sites on a mouse mAb. During incubation, the mouse mAb was bound to a goat anti-mouse Ab that coated the wells of a microplate. After the sample was washed once to remove excess conjugate and unbound sample, a substrate solution was added to the wells for determination of the bound enzyme activity. Immediately after color development, absorbance was read at 405 nm on a microplate reader (Digiscan, Asys Hightech, Eugendorf, Austria). The color intensity inversely correlated with the PGE_2 concentration in the sample. According to the manufacturer's product information, the sensitivity of the PGE_2 assay was 8.3 pg/ml.

Downloaded from ini.sagepub.com at Bibliothekssystem der Universitaet Giessen on May 28, 2012

STAT3 immunohistochemistry

In order to obtain information about the MALP-2/LPS-induced and IL-6 mediated inflammatory brain activation in SHRs and WKY rats, we analyzed the nuclear translocation of the transcription factor 'signal transducer and activator of transcription 3' (STAT3) in brain sites with an incomplete blood-brain-barrier, i.e. the *organum vasculosum laminae terminalis* (OVLT), the subfornical organ (SFO), the median eminence (ME) and the *area postrema* (AP). To detect STAT3 signals in the brain, free-floating brain sections were incubated with a rabbit anti-STAT3 Ab (sc-482, Santa Cruz Biotechnology, Heidelberg, Germany). Coronal 40-µm brain sections were cut on a freezing microtome (model 1205, Jung, Heidelberg, Germany). Tyramide amplification was performed with a commercial amplification kit (NEL700, NEN Life Science Products, Cologne, Germany). Sections were placed into 10% normal horse serum containing 0.3% Triton X-100 for 1 h at room temperature (22°C). Sections were then transferred into 0.5% blocking powder to block the unspecific tyramine binding sites. Primary STAT3 Ab incubation (dilution 1:12000) was performed for 36–48 h at 4°C. The STAT3 Ab was then detected with a secondary biotinylated anti-rabbit Ab (1:200, Vector BA-1000, Linaris Biologische Produkte, Mannheim, Germany) for 1 h at room temperature. After amplification, the immunohistochemical processing was finished with an avidin biotin HRP complex (Vector Elite Kit, Linaris Biologische Produkte), which was visualized by diaminobenzidine hydrochloride (DAB, Sigma Chemicals) reaction in the presence of hydrogen peroxide. Finally, sections were counterstained with cresyl violet and cover-slipped with Entellan (Merck, Darmstadt, Germany) for light microscopic analysis. Controls for STAT3 immunoreactivity included processing sections without the primary Ab, or incubating sections with rabbit preimmune serum instead of rabbit anti-STAT3 antiserum. In both cases, no STAT3 immunoreactivity was found in any brain area. Finally, the specificity of the STAT3 immunohistochemistry was proven by pre-adsorbing the primary Abs with the antigen.[27,28] Sections were analyzed by use of an Olympus BX50 light microscope (Olympus Optical, Hamburg, Germany). Digital images were taken with an Olympus Camedia C-3030 camera and the Olympus Camedia Master 2.0 software package.

The numbers of STAT3-immunoreactive cell nuclei were quantitatively evaluated in both rat strains for the aforementioned structures (the OVLT, the SFO, the ME and the AP), 120 min after systemic intraperitoneal treatment with MALP-2 or cremophor, LPS or PBS, respectively. This time point was chosen according to previous studies in which LPS- or MALP-2-induced nuclear STAT3 translocation in brain cells reached maximal values 2 h after the respective stimulation.[15,23] For each investigated animal, three sections of each brain structure were evaluated. A microscopic counting grid (200 µm × 200 µm) was used at × 400 magnification to determine the number of STAT3-positive cell nuclei per section within the OVLT, the SFO, the ME and the AP. Therefore, the quantitative data finally represent the means (three sections from each structure per individual animal) of the means (animals of a given group; $n = 3$ for each group).

Preparation and cultivation of peritoneal macrophages

SHR and WKY were deeply anesthetized with a mixture of ketamin/xylazin (see above). Peritoneal macrophages were harvested by injecting 20 ml of sterile PBS into the abdominal cavity, which was gently massaged for 15 min thereafter. Then, the abdominal cavity was opened, the lavage solution collected with a syringe and immediately centrifuged for 5 min at 4°C. The pellet was incubated for 2 min with red blood cell lysis-buffer (160 mM NH_4Cl, 12 mM $NaHCO_3$, 100 µM EDTA, pH 7.3) to remove traces of erythrocytes. The cells were then washed twice with 10 ml PBS and re-suspended in 5 ml RPMI medium containing 10% fetal calf serum, 200 nM glutamine, 100 U/ml penicillin and 0.1 mg/ml streptomycin. This solution was centrifuged once more and the cells were re-suspended in 1 ml RPMI medium. After cell counting, a solution of 10^6 cells/ml was adjusted with medium, and 350 µl of this solution was put into each well of sterile, 24-well microplates according to data from several series of pilot experiments. Until the evening, the cells adhered and the medium was changed. On the following day, the wells were exposed to fresh medium containing LPS, MALP-2 or the respective solvents (see *'Substances'*, above).

Experimental protocols

Experiment 1 (mice). Four groups of TLR2-KO and another four groups of C57/BL-6 mice ($n = 7$–10 per group) were injected i.p. at ~09:00–09:30 (at least 2 h after start of the 'light on' period) with 1000 µg/kg MALP-2, 100 µg/kg LPS, or the respective solvent (Cremophor or PBS). Abdominal body temperature (T_b) was recorded and evaluated from 07:00 on the day of injection until the end of the 'light on' period.

Experiment 2 (mice). Separate groups of mice ($n = 5$ per group) were treated as described in the protocol for Experiment 1. Ninety minutes after the respective injection, blood from the systemic circulation was collected. Briefly, the mice were anesthetized about 5 min prior to the scheduled sampling time with ketamine/xylazine (see above). Blood was collected by cardiac puncture

Downloaded from ini.sagepub.com at Bibliotheksystem der Universitaet Giessen on May 28, 2012

and immediately centrifuged. Plasma was stored at −70°C for later determination of TNF-α and IL-6. Pilot experiments had shown that both cytokines are present in the circulation in high amounts at the selected time for collection of blood.

Experiment 3 (rats). Four groups of SHRs and another four groups of WKY rats ($n=9$–12 per group) were injected i.p. at ~09:00–09:30 (at least 2 h after start of the 'light on' period) with 100 µg/kg MALP-2, 100 µg/kg LPS or the respective solvent (Cremophor or PBS). T_b, food and water intake, as well as changes in body weight, were recorded and evaluated from 07:00 on the day of injection for the following 48 h. Values for body weight, food and water intake were also measured for the 24-h period prior to the respective injection.

Experiment 4 (rats). Separate groups of rats ($n=4$–5 per group) were treated as described in the protocol for Experiment 3. At selected time intervals (60, 120 and 180 min after injection of LPS or PBS, and 60 and 120 min after injection of MALP-2 or cremophor), blood from the systemic circulation was collected as described above and later analyzed for bioactive cytokines.

Experiment 5 (rats). Separate groups of SHRs and WKY rats ($n=3$ per group) were treated as described in Experiment 3. The brains of all animals were prepared for STAT3 immunohistochemistry 2 h after injection. The rats were deeply anesthetized with sodium pentobarbital (60–100 mg/kg, Narcoren, Merial GmbH, Hallbergmoos, Germany) and transcardially perfused with 400 ml 0.9% NaCl solution followed by 500 ml of fixative containing 4% paraformaldehyde in 0.1 M phosphate buffer (pH 7.2). The brains were removed and post-fixed in the same fixative for 1 h at room temperature. The tissue was cryoprotected in 20% sucrose in phosphate buffer overnight at 4°C. Brain tissue was cut the following day.

Experiment 6 (rats). Peritoneal macrophages were prepared from separate groups of SHRs and WKY rats ($n=5$ per group). Macrophages from each rat were exposed to medium containing LPS or MALP-2, at concentrations of 10 µg/ml, or the respective solvent. These doses were chosen according to pilot experiments in which different doses and cell numbers were tested for their capacity to release bioactive TNF-α and IL-6 into the supernatant. The dose, which we used to evaluate the capacity of peritoneal macrophages of SHRs and WKY rats to release cytokines into the supernatants, did not represent threshold doses, but rather corresponded to the concentrations of LPS or MALP-2 to which we exposed the abdominal cavity of rats in our *in vivo* experiments. Supernatants were collected 1 h and 2 h after the start of the exposure to the respective stimuli (LPS, MALP-2 or the respective vehicles).

Evaluation and statistics

In graphs of the thermal responses of mice or rats to injections of MALP-2, LPS or the respective solvent, the mean abdominal temperatures were plotted against time and expressed as means ± SEM at each time point. Abdominal temperatures were compared between different groups over time by two-way repeated-measures ANOVA followed by an all pairwise Bonferroni's multiple comparison *post hoc* test. A statistical significance was accepted for $P<0.05$. For a detailed analysis of the febrile responses of mice, the body temperature changes (relative changes to the pre-injection temperatures) were calculated owing to differences in the baseline temperatures between some groups of mice to be compared. In addition to the comparison of temperature data points, we also evaluated the integrated time curves—the fever index (F.I.). The mean F.Is. the integrated areas between thermal responses of febrile and normothermic animals, were expressed as a product of degrees Celsius and hour (for 9 h after the respective injection). The mean of all temperatures, measured at 15-min intervals over the 2-h period before the injection, was calculated as the baseline temperature. Concentrations of bioactive cytokines in blood or supernatants and data on food and water intake, heart rate and systolic blood pressure, as well as the numbers of nuclear STAT3 signals within a given brain structure were compared by one-way ANOVA followed by Scheffe's *post hoc* test. Because the values for circulating cytokine concentrations are not normally distributed, a log-transformation of the cytokine values was performed prior to the statistical calculation. All data were analyzed using StatView software 4.57 (Abacus Concepts, Berkeley, CA, USA).

Results

Experiments with TLR2-KO and C57/BL-6 mice

TLR2-KO and C57/BL-6 mice were injected i.p. with 1000 µg/kg MALP-2 or cremophor (solvent). The injection caused a transient elevation of T_b in all groups of mice for 60–75 min. Thereafter, T_b of MALP-2-treated TLR2-KO mice returned to its baseline value (Figure 1A), while C57/BL-6 mice developed a moderate fever (Figure 1B). Both groups of mice injected with cremophor showed the stress-induced increase of T_b and returned to their baseline temperature thereafter. A detailed analysis revealed that the MALP-2-induced increase of T_b in C57/BL-6 mice was significant from 90–330 min after the injection when compared with the respective values of TLR2-KO mice ($F=11.1$; $P=0.0037$; Figure 1C).

Downloaded from ini.sagepub.com at Bibliotheksystem der Universitaet Giessen on May 28, 2012

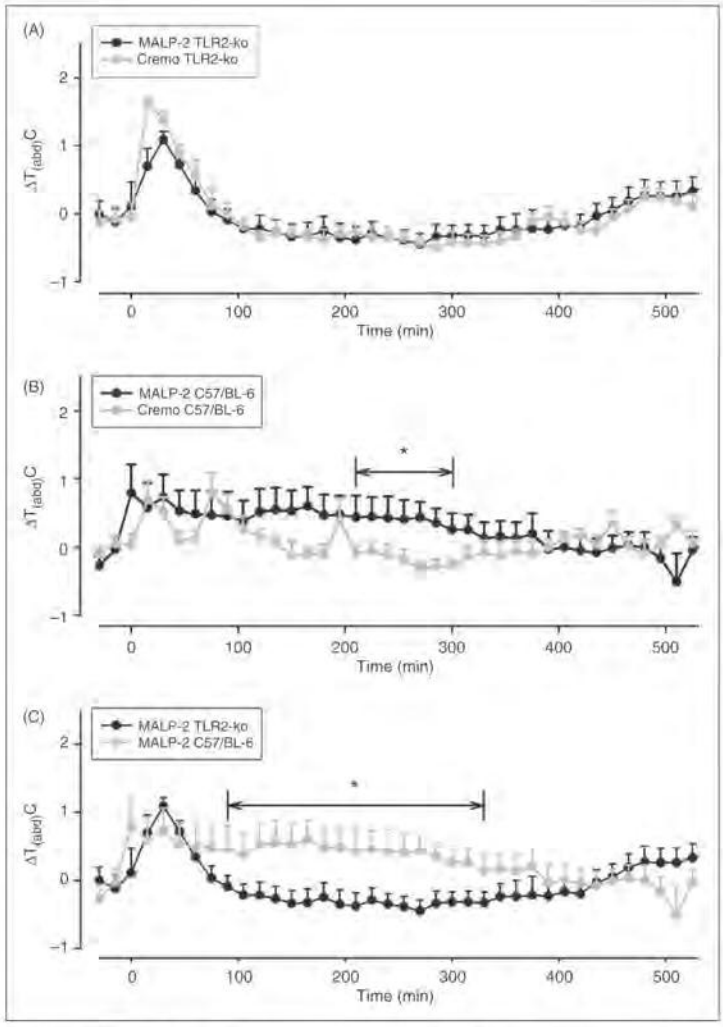


Figure 1. MALP-2-induced changes of T_{abd} in TLR2-KO and C57/BL-6 mice. Mice were injected i.p. with 1000 μg/kg MALP-2 or vehicle (Cremo) at time '0'. Abdominal body temperature changes (ΔT_{abd}) in response to the respective injections are shown as means ± SEM. Those time intervals are labeled with horizontal significance bars at which the tested dose of MALP-2 caused a significant elevation of ΔT_{abd} ($P < 0.05$) in comparison with mice treated with solvent (B), or at which differences between TLR2-KO and C57/BL-6 mice were observed (C). MALP-2 did not evoke any increase of ΔT_{abd} in TLR2-KO mice (A). The mean absolute values of T_{abd} prior to the time of injection were 36.8°C in TLR2-KO mice treated with MALP-2 ($n = 10$), 36.75°C in TLR2-KO mice treated with vehicle ($n = 9$), 36.52°C in C57/BL-6 mice treated with MALP-2 ($n = 9$) and 36.3°C in C57/BL-6 mice treated with vehicle ($n = 7$).

Plasma levels of TNF-α and IL-6 were measured 90 min after injection of MALP-2 or cremophor. Bioactive TNF-α was exclusively present in the plasma of MALP-2-treated C57/BL-6 mice with a mean value of 71.2 ± 17.3 ng/ml (not shown). In mice of both strains injected with cremophor, and in TLR2-KO mice stimulated with MALP-2, bioactive TNF-α could not be detected in blood plasma. Bioactive IL-6 was detected in all groups of mice (Figure 2). Injection of MALP-2 caused a significant elevation of IL-6 in the plasma of C57/BL-6 mice (2300 ± 1050 I.U./ml; $P = 0.0015$: MALP-2 vs vehicle in C57/BL-6 mice), while the corresponding levels measured in TLR2-KO mice remained at the baseline (90–190 I.U./ml), which

Downloaded from ini.sagepub.com at Bibliotheksystem der Universitaet Giessen on May 28, 2012

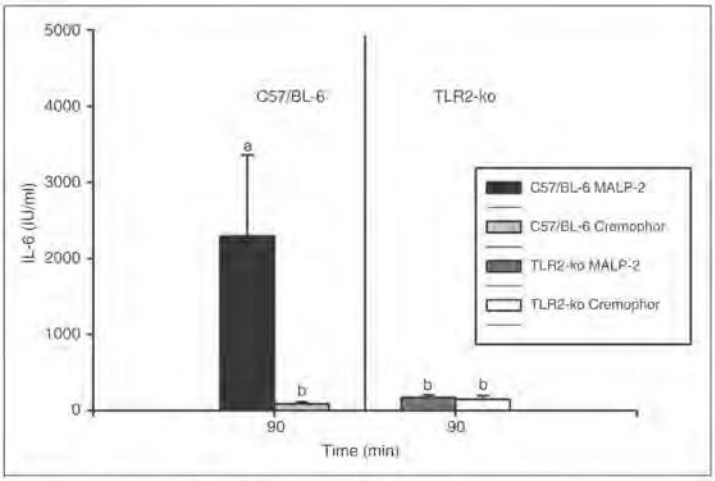


Figure 2. MALP-2-induced circulating IL-6 in TLR2-KO and C57/BL-6 mice. Mice were injected i.p. with 1000 μg/kg MALP-2 or vehicle (Cremo) and plasma samples were collected and analyzed 90 min after the respective injections. All columns are means ± SEM ($n = 5$ in each group). Any columns with the same letter are not significantly different from each other, while any columns with different letters are significantly different ($P < 0.05$; differences between groups). MALP-2 did not evoke any increase of circulating IL-6 in TLR2-KO mice.

was observed in both strains of mice 90 min after injection of cremophor. The MALP-2-induced amount of IL-6 in plasma was significantly higher in C57/BL-6 compared with TLR2-KO mice ($P = 0.0005$).

In the next experiment, we tested the responses of TLR2-KO and C57/BL-6 mice to i.p. injections of 100 μg/kg LPS. During the day of LPS injection, both strains of mice developed a moderate fever, while T_b of mice treated with solvent (PBS) returned to the baseline levels after its transient stress-induced rise (Figure 3A, B).

The febrile response of the C57/BL-6 mice developed a bit later, but was longer lasting than in TLR2-KO mice. A detailed analysis revealed that the LPS-induced increase of T_b in C57/BL-6 mice was significantly higher from 330–440 min after the injection when compared with the respective values of TLR2-KO mice ($F = 13.4$; $P = 0.0024$; Figure 3C).

Ninety minutes after injection of 100 μg/kg LPS, 84.2 ± 29.9 ng/ml TNF-α were measured in the plasma of TLR2-KO mice; 107.1 ± 31.1 ng/ml were detected in C57/BL-6 mice with no significant difference between both strains (not shown). In no case was bioactive TNF-α observed after the injection of solvent. The LPS-induced increase of bioactive IL-6 in plasma was almost identical in both mice strains (14350 ± 3900 I.U./ml in TLR2-KO vs 13470 ± 5430 I.U./ml in C57/BL-6 mice; Figure 4).

The integrated fever responses, i.e. the areas under the respective thermal response curves, were calculated for each experiment performed with TLR2-KO and C57/BL-6 mice. The results of these calculations are summarized in the Supplementary Figure S1 (A, B). The TLR2-KO mice showed a smaller stress-induced rise in body temperature owing to the injection procedure when compared with the stress response of the C57/BL6 mice. Over the daytime, the abdominal temperature of mice is at its minimum. Both of these reasons, and the lack of response to MALP-2, caused the negative fever- or thermal-response indexes of TLR2-KO mice in response to injections of MALP-2, cremophor and PBS. Interestingly, the integrated fever response to LPS was also lower in TLR2-KO compared with C57/BL-6-mice, although circulating cytokines were as high as in the control animals. The high thermal response of C57/BL-6 mice to the injection procedure compensated the low daytime temperatures so that the thermal-response index of these mice to cremophor and PBS reached positive values, which were not different from each other.

In summary, with regard to fever and the formation of cytokines, both strains of mice could respond to LPS, with higher fever in the C57/BL-6 controls. In contrast, all these responses were completely abolished in TLR2-deficient animals after stimulation with MALP-2, showing that TLR2 is essential for any kind of reactivity to this PAMP.

Experiments with SHRs and WKY rats

The systolic blood pressure of SHRs was, on average, 175 mmHg and significantly higher than in their genetic

Downloaded from ini.sagepub.com at Bibliotheksystem der Universitaet Giessen on May 28, 2012

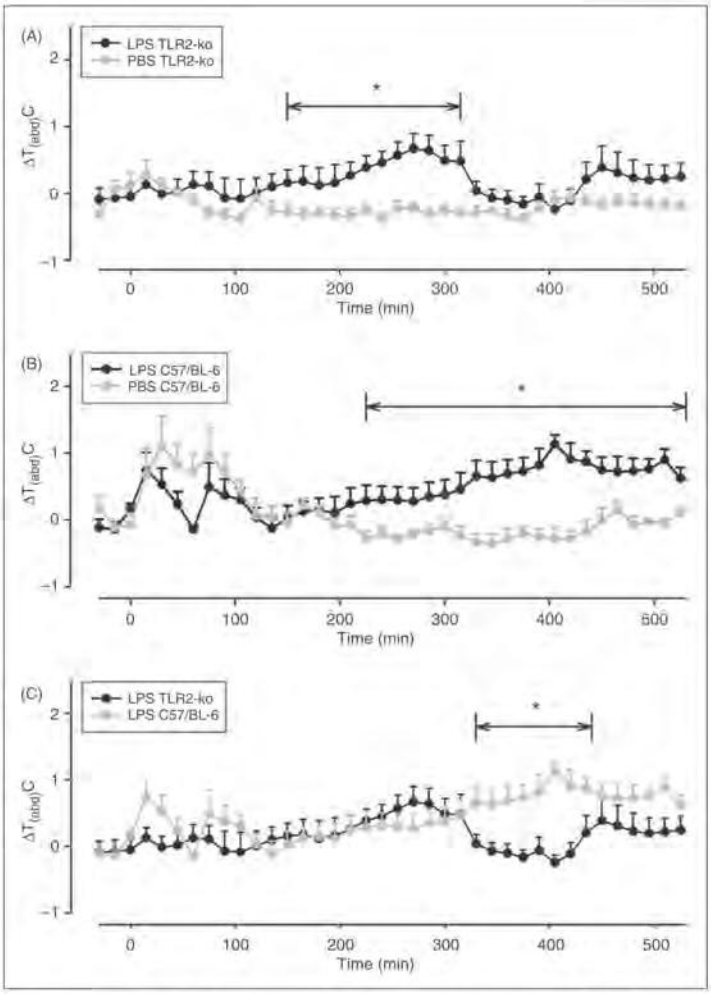


Figure 3. LPS-induced changes of T_{abd} in TLR2-KO and C57/BL-6 mice. Mice were injected i.p. with 100 µg/kg LPS or vehicle (PBS) at time '0'. Abdominal body temperature changes (ΔT_{abd}) in response to the respective injections are shown as means ± SEM Those time intervals are labeled with horizontal significance bars at which the tested dose of LPS caused a significant elevation of ΔT_{abd} ($P < 0.05$) in comparison with mice treated with the vehicle (A, B) or at which differences between TLR2-KO and C57/BL-6 mice were observed (C). LPS evoked a moderate increase of ΔT_{abd} in both TLR2-KO and C57/BL-6 mice. The absolute values of T_{abd} prior to the time of injection were 36.62°C in TLR2-KO mice treated with LPS ($n = 10$), 36.95°C in TLR2-KO mice treated with vehicle ($n = 8$), 36.5°C in C57/BL-6 treated mice with LPS ($n = 9$) and 36.4°C in C57/BL-6 mice treated with vehicle ($n = 7$).

controls, the WKY rats (138 mmHg; $F = 72.6$; $P < 0.0001$), while both strains showed almost identical heart rates (342 vs 346 beats per min, $n = 8$ in both groups).

Intraperitoneal injections of 100 µg/kg MALP-2 induced fever in SHRs and WKY rats (Figure 5A, B), with the response of SHR being significantly smaller from 165 to 435 min after administration of the pyrogen ($F = 7.4$; $P = 0.0121$; Figure 5C). Also, the mean F.I. was significantly lower in MALP-2-treated SHRs compared with WKY rats (4.94 ± 0.22 vs 5.95 ± 0.25°C x h; $P < 0.05$; see Supplementary Figure S1C).

Within the 24 h before the respective injections, the mean food intake was almost identical in all four groups of rats (19–22 g/d, no significant differences between groups). MALP-2 caused a strong, and

Downloaded from ini.sagepub.com at Bibliotheksystem der Universitaet Giessen on May 28, 2012

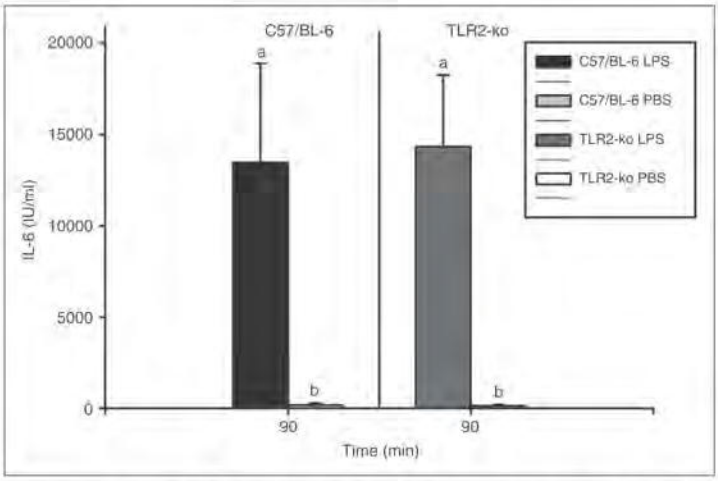


Figure 4. LPS-induced circulating IL-6 in TLR2-KO and C57/BL-6 mice. Mice were injected i.p. with 100 µg/kg LPS or vehicle (PBS) and plasma samples were collected and analyzed 90 min after the respective injections. All columns are means ± SEM ($n = 5$ in each group). Any columns with the same letter are not significantly different from each other, while any columns with different letters are significantly different ($P < 0.05$; differences between groups). LPS evoked almost identical increases of circulating IL-6 in TLR2-KO and C57/BL-6 mice.

significant, reduction in the consumption of food on the day of injection in both rat strains (10 ± 1.5 g/d in SHRs *vs* 6 ± 1.4 g/d in WKY rats, no significant difference). On the second day, food intake in SHRs returned to normal (19 ± 1.2 g/d), while WKY rats still showed signs of anorexia (12 ± 0.7 g/d; $P = 0.0015$, SHRs *vs* WKY rats). Injections of MALP-2 further caused a reduced consumption of drinking water from 25 ± 14 g/d to 13 ± 1.6 g/d in SHRs and from 26 ± 0.8 to 11 ± 2.0 in WKY rats (no significant difference between both strains). On the second day, consumption of drinking water was completely normalized in both rat strains.

One hour after injection of MALP-2, about 25–30 ng/ml TNF-α were measured in the plasma of SHRs and WKY rats with no significant difference between both strains (Figure 6A). Also, the decrease to about 4–5 ng/ml TNF-α within the following hour was similar in SHRs and WKY rats. In no case was bioactive TNF-α observed after injection of solvent.

In both strains, IL-6 in plasma rose from about 1500 I.U./ml to 4000 ± 360 I.U./ml in SHRs and even to 6220 ± 1900 I.U./ml in WKY rats (Figure 6B). This tendency to a reduction in MALP-2-induced circulating IL-6 in SHRs was not significant statistically.

In the next set of experiments, we tested the responses of SHRs and WKY rats to LPS. Intraperitoneal injections of 100 µg/kg LPS caused fever in both rat strains (Figure 7A, B). The response of SHRs was significantly smaller from 270–510 min after administration of the pyrogen ($F = 7.0$; $P = 0.0163$; Figure 7C). In agreement with the temperature data, the F.I. of LPS-injected SHRs was also significantly lower compared with the integrated fever response of WKY rats (3.72 ± 0.3 vs 6.1 ± 0.87°C x h; $P < 0.05$; see: Supplementary Figure S1D).

The LPS-induced reduction of food intake from 21.6 ± 0.75 to 8.2 ± 1.8 g/d was more pronounced in WKY rats when compared with SHRs (24 ± 1 to 16 ± 1.6 g/d), within the first 24 h after LPS-injection ($P = 0.0013$, SHRs vs WKY rats). On the second day, no significant differences in food consumption between both strains were calculated—the absolute values being normalized to almost 20 g/d. Measurements of consumed amounts of drinking water provided similar results: a significant decrease on the day of LPS-injection, which was stronger in WKY rats ($P = 0.0085$), and a complete normalization on the second day.

The kinetics of circulating TNF-α was similar in both rat strains with a peak of about 65 (SHRs) or 97 (WKY rats) ng/ml occurring 1 h after the administration of LPS (Figure 8A).

Thereafter, we observed a rapid decline of TNF-α in plasma which was very similar in SHRs and WKY rats. There was, however, a difference in the IL-6-response to LPS-treatment between SHRs and WKY rats (Figure 8B). In both strains, circulating IL-6 rose to about 2700 I.U./ml within 1 h. The subsequent increase during the following 2 h was much stronger in WKY rats compared with SHRs. At 180 min from the time of LPS-injection, the level of IL-6 in plasma was significantly higher in WKY rats when compared with SHRs

Downloaded from ini.sagepub.com at Bibliotheksystem der Universitaet Giessen on May 28, 2012

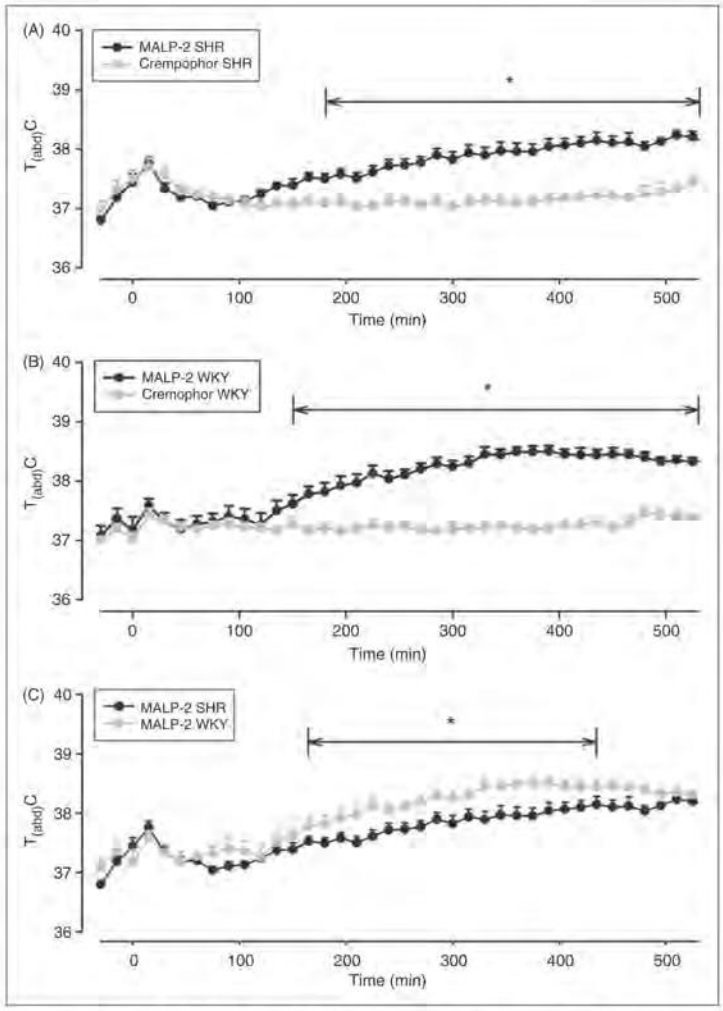


Figure 5. MALP-2-induced changes of T_{abd} in SHRs and WKY rats. Rats were injected i.p. with 100 µg/kg MALP-2 (SHRs: $n = 12$; WKY rats: $n = 12$) or vehicle (Cremophor; SHRs: $n = 11$; WKY rats: $n = 10$) at time '0'. Mean abdominal body temperature in response to the respective injections is shown as mean ± SEM Those time intervals are labeled with horizontal significance bars at which the tested dose of MALP-2 caused a significant elevation of T_{abd} ($P < 0.05$) in comparison with rats treated with solvent (A, B) or at which differences between SHRs and WKY rats were observed (C). MALP-2 evoked fever in both rat strains—the response of WKY rats being significantly higher from 170–435 min after injection.

(13,500 vs 4100 I.U./ml; $F = 8.0$; $P = 0.0297$). To test whether the reduced fever of SHRs was related to circulating PGE2, we measured PGE2 in plasma.

Basal levels of PGE2 in the range of 40–100 pg/ml were detected in both rat strains. Injections of MALP-2 and LPS caused a two- to fourfold increase of PGE2 concentrations in the blood. These values tended to be higher in WKY rats (compared with SHRs) and in response to LPS (compared with MALP-2), but, because of individual variations, these differences were not significant (not shown).

This observation, that IL-6 was the only putative circulating mediator of fever, for which we observed a significant difference between SHRs and WKY rats, at least in response to LPS (Figure 8B), provided the rationale for the next experiment.

Downloaded from ini.sagepub.com at Bibliothekssystem der Universitaet Giessen on May 28, 2012

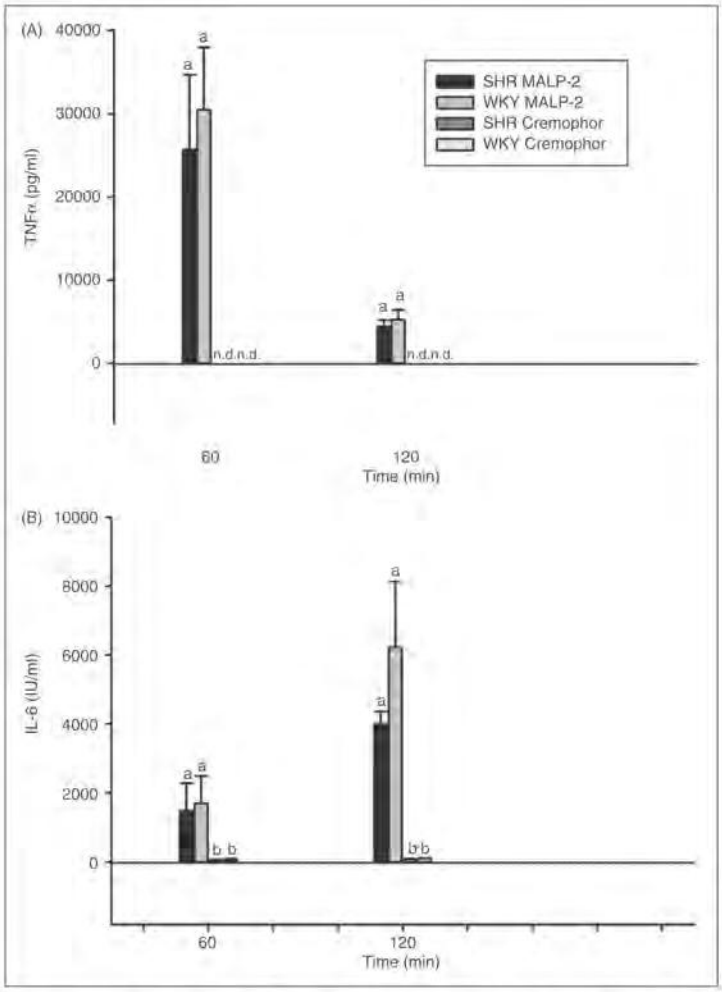


Figure 6. MALP-2-induced circulating cytokines in SHRs and WKY rats. Rats were injected i.p. with 100 µg/kg MALP-2 or vehicle (Cremo) and plasma samples were collected and analyzed for bioactive TNF-α (A) or IL-6 (B) 60 and 120 min after the respective injections. All columns are means ± SEM ($n = 4–5$ in each group). At a given time, any columns with the same letter are not significantly different from each other, while any columns with different letters are significantly different ($P < 0.05$; differences between groups; n.d.: not detectable, below the detection limit of the assay).

In this experiment, we therefore tested whether there were differences in the IL-6-mediated inflammatory activation of brain sites without a tight blood-brain-barrier. For that purpose, we quantified the degree of nuclear translocation of the transcription factor STAT3 within these brain areas by counting nuclear STAT3 signals. The results of this evaluation are summarized in Figure 9.

Hardly any nuclear STAT3 signal was observed in brain sections from OVLT, SFO, ME and AP in both control groups (i.p. injections of cremophor or PBS; see Supplementary Figure S2, showing examples of STAT3 immunohistochemistry performed in this study). In none of the four investigated brain sites prepared from MALP-2 (Figure 9A) or LPS-treated animals (Figure 9B), could we detect any significant differences in numbers of STAT3- positive cell nuclei between the two rat strains (see the brown reaction product as a result of diaminobenzidine hydrochloride conversion in Supplementary Figure S2). In OVLT and SFO,

Downloaded from ini.sagepub.com at Bibliotheksystem der Universitaet Giessen on May 28, 2012

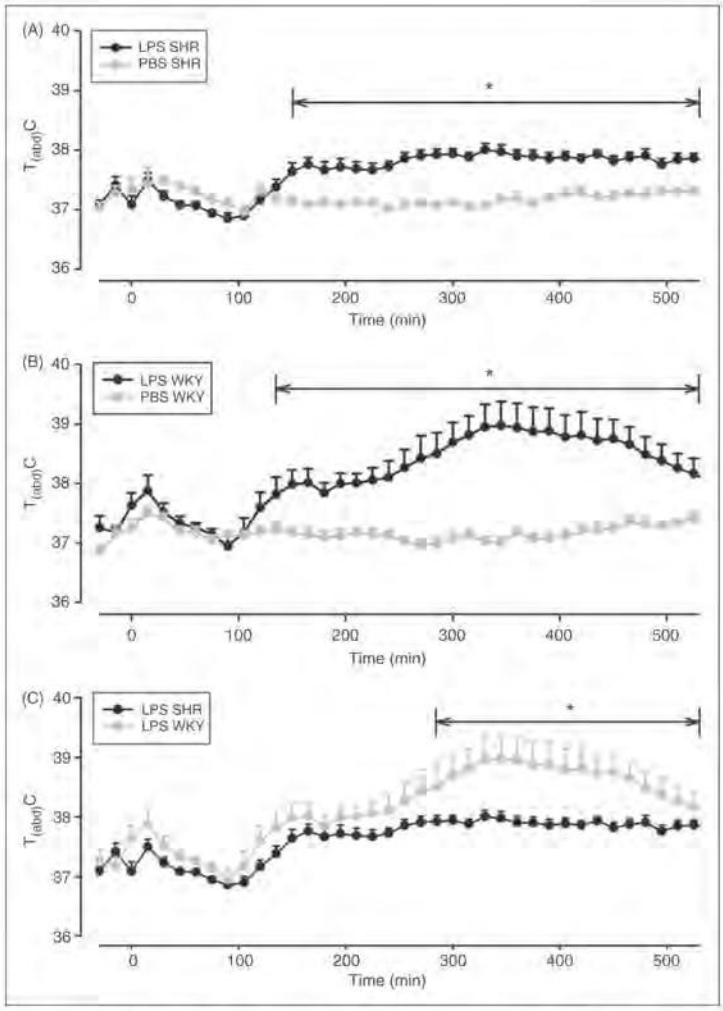


Figure 7. LPS-induced changes of T_{abd} in SHRs and WKY rats. Rats were injected i.p. with 100 μg/kg LPS (SHRs: $n = 11$; WKY rats: $n = 10$) or the vehicle (PBS; SHRs: $n = 10$; WKY rats: $n = 9$) at time '0'. Mean abdominal body temperature in response to the respective injections is shown as mean ± SEM Those time intervals are labeled with horizontal significance bars at which the tested dose of LPS caused a significant elevation of T_{abd} ($P < 0.05$) in comparison with rats treated with PBS (A, B), or at which differences between SHRs and WKY rats were observed (C). LPS evoked fever in both rat strains—the response of WKY rats being significantly higher from 270–510 min after injection.

mean numbers of STAT3 positive cell nuclei ranged from 80 to 180 per section. Nuclear STAT3 activation in ME and AP was less pronounced (20–40 STAT3 positive nuclei per section). The strength of nuclear STAT3 activation was similar, irrespective of the injected pyrogen, suggesting that a threshold level of IL-6 sufficient to cause comparable brain activation was reached in all pyrogen-treated SHR and WKY rats. The observed differences between SHR and WKY with regard to fever, anorexia or adipsia can thus not fully be explained by impaired formation of cytokines (i.e. IL-6) in the SHR strain. In addition, our data suggest that the CD36 deficiency of SHR does not blunt the responses of these animals to MALP-2, as it has been observed under *in vitro* conditions in cultured cells.[17,18]

Downloaded from ini.sagepub.com at Bibliotheksystem der Universitaet Giessen on May 28, 2012

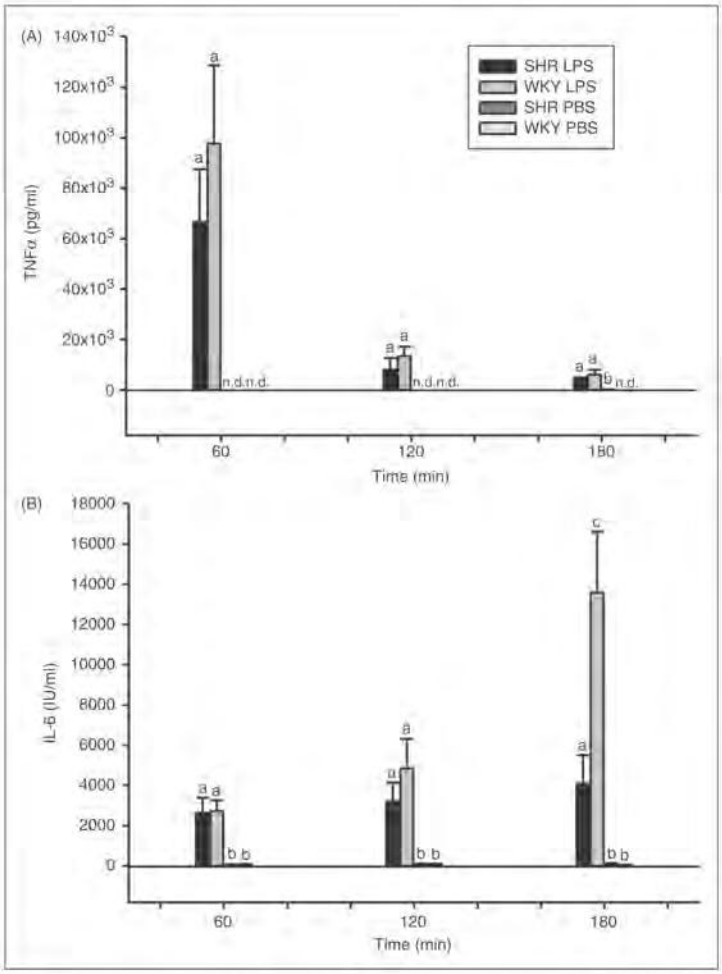


Figure 8. LPS-induced circulating cytokines in SHRs and WKY rats. Rats were injected i.p. with 100 µg/kg LPS or vehicle (PBS) and plasma samples were collected and analyzed for bioactive TNF-α (A) or IL-6 (B) 60, 120 or 180 min after the respective injections. All columns are means ± SEM ($n = 4$–5 in each group). At a given time, any columns with the same letter are not significantly different from each other, while any columns with different letters are significantly different ($P < 0.05$; differences between groups; n.d.: not detectable, below the detection limit of the assay).

Experiments with peritoneal macrophages from SHR and WKY rats

In the final experiment, we tested the capacity of peritoneal macrophages collected from SHRs and WKY rats to respond to stimulations with LPS and MALP-2 with the release of bioactive cytokines into the culture medium. The results of these measurements can be summarized as follows (Figure 10).

At a dose of 10 µg/ml, LPS (Figure 10C, D) caused a 15 (TNF-α) or 2–4 times (IL-6) stronger release of bioactive cytokines into the supernatant when compared with MALP-2 (Figure 10A,B). At both time points investigated, the concentrations of IL-6 and TNF-α in the medium of LPS- or MALP-2-treated cells were significantly higher than in the supernatants of macrophages stimulated with PBS or cremophor. The respective values tended to be higher for cells from WKY rats, but there was no significant difference for both cytokines at any time point. Interestingly, the

Downloaded from ini.sagepub.com at Bibliothekssystem der Universitaet Giessen on May 28, 2012

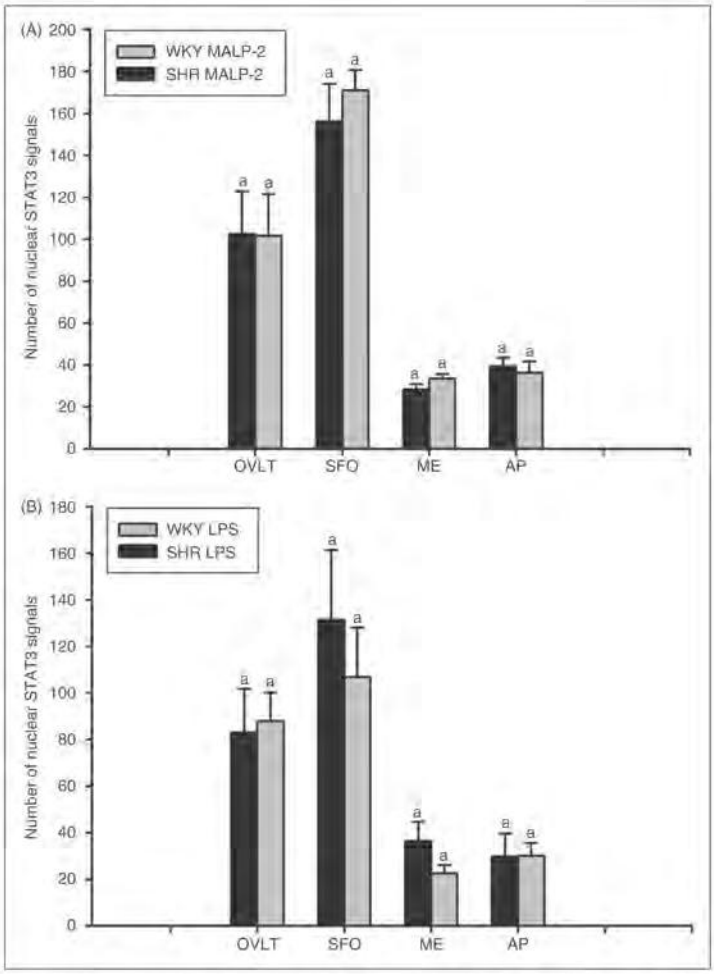


Figure 9. Numbers of STAT3-positive cell nuclei in selected brain structures of MALP-2- or LPS-treated SHRs and WKY rats. Two hours after i.p. injections of 100 μg/kg MALP-2 (A), 100 μg/kg LPS (B) or the respective solvent (cermophor or PBS), the numbers of STAT3-immunoreactive cell nuclei were counted in the *organum vasculosum laminae terminalis* (OVLT), the subfornical organ (SFO), the median eminence (ME) and the *area postrema* (AP) prepared from SHRs and WKY rats. The columns represent means of the means ± SEM ($n = 3$ in each group, 3 brain section from each animal and each brain structure). In rats treated with cremophor or PBS, hardly any nuclear STAT3 signal was detected (see Supplementary Figure as a representative example). The identical letters above the columns indicate that there were no significant differences in MALP-2 or LPS-induced nuclear STAT3 activation between both rat strains in any brain structure investigated.

exposure of peritoneal macrophages to cremophor had a significant effect ($P < 0.05$) on the concentrations of TNF-α or IL-6 in the supernatants when compared with the respective stimulation with PBS. A moderate inflammatory effect of the vehicle, cremophor, is thus likely, but it was not significant under *in vivo* conditions.

Discussion

Responses of TLR2 KO and C57/BL-6 mice to MALP-2 and LPS

The capacity of MALP-2 to induced fever in mice has not yet been tested. In the first part of the present study,

Downloaded from ini.sagepub.com at Bibliothekssystem der Universitaet Giessen on May 28, 2012

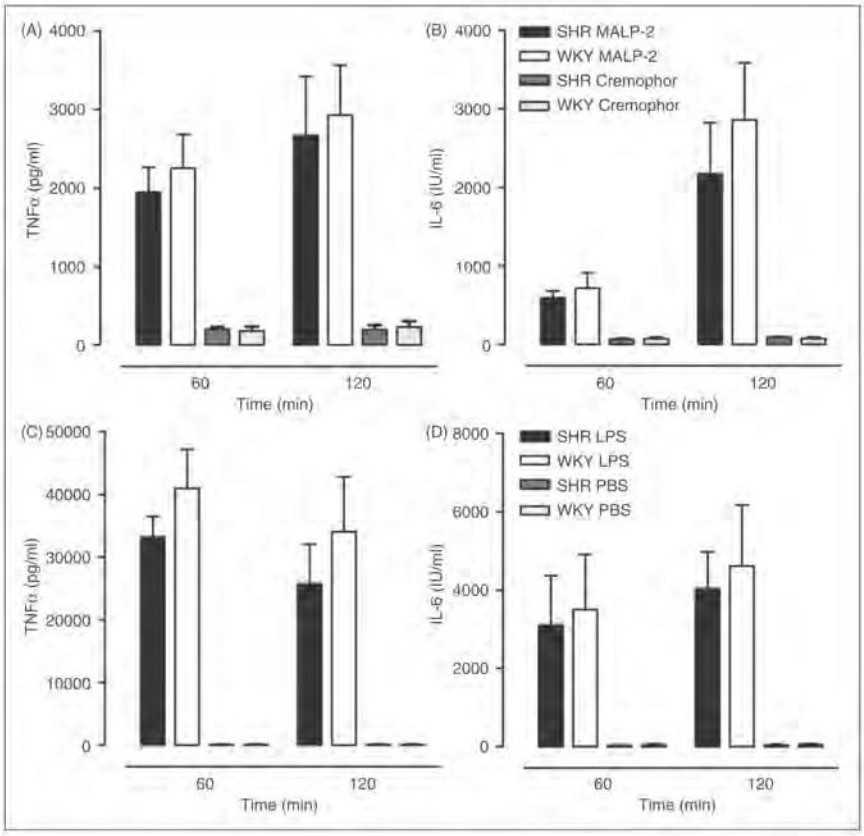


Figure 10. MALP-2- and LPS-induced cytokines in supernatants of peritoneal macrophages from SHRs and WKY rats. Peritoneal macrophages (five cell preparations from different SHRs or WKY rats; 350,000 cells per well) were stimulated with MALP-2 or LPS at concentrations of 10 μg/ml or the respective solvent (cermophor or PBS) and bioactive cytokines were measured in the supernatants. All columns are means ± SEM; there were no significant differences at any time point between the two rat strains.

we demonstrated that MALP-2 fails to induce fever in TLR2 KO mice as opposed to C57/BL-6 mice. This indicates that TLR2 is essential for MALP-2-mediated fever and that TLR6 alone is not able to induce a functionally-relevant MALP-2-induced signal transduction *in vivo*. Corresponding to these observations, TLR2-deficiency is accompanied with non-responsiveness to MALP-2 challenge in respect to TNF-α and IL-6 release. The results of our experiments are not natural *per se* owing to the fact that TLR2 alone is sufficient to recognize other bacterial lipopeptides *in vitro*, meaning that a functional pair formed by two TLRs is not required for all bacterial lipopeptides.[6] The structural details responsible for this discrepancy have been elaborated and it has been shown that recognition of microbial lipopeptides carrying only two fatty acids, such as MALP-2, requires co-expression of TLRs 2 and 6.[8]

In our experiments, MALP-2 caused a rather moderate fever of about 6 h that followed the rise of deep body temperature caused by the injection procedure. The failure of TLR2-KO mice to produce fever in response to MALP-2 cannot be explained by a general lack of capacity to develop a fever-response because of the fact that they readily become febrile after an appropriate LPS-challenge. The shape and duration of LPS-fever in mice depend on the dose and ambient temperature.[29] At the ambient temperature of 30°C, which is close to thermoneutral in this species,[29] the febrile responses to LPS were significantly lower in TLR2-KO mice compared with C57/BL-6 mice, despite of the fact that the LPS-induced concentrations of circulating TNF-α and IL-6 were almost identical in both mouse strains. This observation is of interest in so far as it has previously been argued that TLR2 can confer responsiveness to

Downloaded from ini.sagepub.com at Bibliotheksystem der Universitaet Giessen on May 28, 2012

LPS, at least under *in vitro* conditions,[30] although the expression of TLR2 is not essential for mammalian responses to endotoxin.[31] Not only LPS-fever, but also the rise of body temperature caused by the injection procedure was diminished in TLR-KO mice so that they developed a negative FI in response to administration of cremophor or PBS. One way of explaining this observation is that TLR2-KO mice display reduced thermogenesis, at least under stimulated conditions. This question requires further investigation. A second way of possibly explaining the reduced febrile response to LPS in TLR2-KO mice relates to the aforementioned presence of TLR2-activity in the LPS-preparation that we used for our experiments. Our data on reduced LPS-fever in these mice are in agreement with earlier observations that TLR2 confers responsiveness to LPS,[30,31] although it has also been reported that all components of the febrile and thermoregulatory responses to LPS are mediated via TLR4 signaling and not by lipoprotein contaminants that might signal through TLR2.[32]

In conclusion, it is thus likely that fever and cytokines induced by i.p. injections of LPS were, at least, predominantly mediated via stimulation of TLR4 not only in TLR2-KO mice but also in C57/BL-6 mice, while a significant contribution of TLR2 activity to LPS-fever cannot be ruled out.

Responses of SHRs and WKY rats to MALP-2 and LPS

Hoebe et al.[17] transfected HEK-293 cells to express CD36 in combination with TLR2 and/or TLR6, as well as NF-κB and stimulated the distinct cell populations with MALP-2. In these experiments, MALP-2 caused NF-κB activation when cells expressed TLR2, whereas transfection with either CD36 or TLR6 alone did not support activation by MALP-2. Interestingly, the response to MALP-2 was highly augmented when either CD36 or TLR6 were co-expressed with TLR2. In the same study, it was shown that a mutation of the CD36 caused an immunodeficiency in mice with reduced responsiveness of the animals' macrophages to MALP-2.[17] The authors of this study concluded that CD36 acts as a sensor of microbial diacylglycerides that signal via TLR2 or the TLR2/6 heterodimer. Another study on human monocytes and transfected HEK-cells demonstrated that secretion of TNF-α in response to MALP-2 was strongest in presence of TLRs 2 and 6 in combination with CD36.[18]

One of the diverse abnormalities of the SHR is a chromosomal deletion event that occurred at the CD36 locus during the evolution of this rat strain.[19] Interestingly, it has been reported that the deficiency of CD36, which participates in outer segment phagocytosis by the retinal pigment epithelium, leads to age-related photoreceptor degeneration and chorodial involution via down regulation of cyclooxygenase-2 (COX-2) in SHR and CD36-KO mice.[20] This study indicates that the induction of pro-inflammatory genes, including COX-2, may be impaired in the CD36-deficient SHR. Thus, the SHRs seemed to represent an appropriate animal model to investigate a possible reduced *in vivo* responsiveness to MALP-2 caused by a lack of CD36. With regard to fever, the response of SHR was significantly lower from 170–435 min after injection of MALP-2 when compared with their genetic controls, the WKY rats. However, the reduction of the febrile response was not dramatic. Differences in MALP-2-induced formation of cytokines were even less pronounced between SHRs and WKY rats; circulating IL-6 just tended to be lower in SHR at 2 h after the MALP-2 was administered. In the case that these small differences were caused by the lack of CD36, one would expect that LPS-induced responses were not impaired in the SHR strain. However, we obtained the opposite results. The reduction of LPS-induced fever and LPS-induced release of cytokines (i.e. IL-6) in SHRs was even more pronounced when compared with the respective MALP-2-induced responses. A significant contribution of CD36 in MALP-2-induced fever and cytokine responses is, thus, rather unlikely. Some support for our finding is given by a recent study in CD36-KO mice.[33] In this study, activators of TLR2/6 [fibroblast-stimulating lipopeptide-1 (FSL-1)], TLR2/1 [palmitoyl-*S*-dipalmitoylglyceryl (Pam3)] or LPS were injected intracerebroventricularly into wild-type or CD36-KO mice, and inflammatory gene expression was assessed in the brain. Interestingly, only the inflammatory response to Pam3, but not to FSL-1 or LPS, was suppressed in CD36-KO mice.[33] FSL-1 is a substance that shares many properties with MALP-2 and both evoke similar responses *in vivo*.[14–16,34,35] Thus, it seems that the impaired effects of MALP-2 on special CD36-deficient cells[17,18] cannot fully be transferred to *in vivo* conditions. We thus tried to obtain information about the responsiveness of peritoneal macrophages of SHRs and WKY rats to stimulations with MALP-2 or LPS. Although there was a tendency for reduced formation of MALP-2-induced cytokines in macrophages from SHRs, this effect was not significant and it also occurred in response to LPS (Figure 10). Our observation may be related to the doses of MALP-2, which we tested to obtain pronounced effects in our *in vitro* experiment. In addition, a moderate participation of the solubilizer cremophor in the MALP-2-induced activation of macrophages cannot be ruled out because of to the fact that cremophor alone had a small, but significant, stimulatory effect on the formation of cytokines *in vitro*. However, at least for the *in vivo* experiments with MALP-2 reported in our study, additive effects of cremophor on the parameters, which we investigated, were small-to-negligible. We cannot exclude the possibility that there are synergistic effects of cremophor with LPS or the water-soluble diacylated

Downloaded from ini.sagepub.com at Bibliotheksystem der Universitaet Giessen on May 28, 2012

lipopeptide, FSL-1. A detailed investigation of interactions of cremophor with LPS or FSL-1 may merit another study on this question.

We further wondered whether the observed reduction of MALP-2-, and especially of LPS-, induced production of IL-6 in SHRs may have had any impact at all on the inflammatory activation of the brain. Circulating IL-6 is regarded as an afferent signal to the brain that contributes to the manifestation of fever.[23,36–38] The inflammatory activation of the brain by circulating IL-6 and some other cytokines can be quantified by the degree of the nuclear translocation of the transcription factor STAT3 in brain sites with an incomplete blood-brain-barrier and it has been shown that LPS-induced activation of STAT3 in the brain depends, to a very high degree, on circulating IL-6.[39] The numbers of nuclear STAT3 signals were almost identical in both rat strains in response to both pyrogens. Our interpretation of this finding is that a critical threshold of IL-6, sufficient for an appropriate nuclear STAT3 activation in brain sites with an open blood-brain-barrier, was reached in both rat strains after stimulation with MALP-2 or LPS. Given that the afferent pyrogenic signaling via IL-6 or other mediators was strong enough to cause similar, or even identical, inflammatory activation of the brain, then the question of why the febrile response to MALP-2 and LPS was smaller in SHRs when compared with WKY rats arises. One possible way of explaining this phenomenon relates to the fact that we used i.p. injections of MALP-2 or LPS to induce fever in SHRs and WKY rats. Intraperitoneal injections of LPS, and possibly also of MALP-2, may cause a localized formation of inflammatory mediators in the abdominal cavity, for example IL-1β. It is known that IL-1β has the capacity to stimulate afferent fibers of the vagus nerve via their receptors on glomus cells of vagal paraganglia.[40] Such an inflammatory stimulation of vagal nerve fibers contributes to the manifestation of fever, as long as the i.p. route of administration is used.[40] Thus, it will be worthwhile investigating whether local formation of IL-1β within the abdominal cavity is impaired in the SHR strain. On the other hand, it was reported that CD36 deficiency can be accompanied by down-regulation of COX-expression.[20] In the hypothalamus, expression of COX-2 after appropriate peripheral inflammatory stimulation is regarded as a crucial step in the manifestation of fever,[38,40] although there are some fever pathways that are independent of intrahypothalamic formation of prostaglandins.[41] An analysis of intrahypothalamic expression of COX-2 in MALP-2- and LPS-treated SHRs and WKY rats would thus merit further study on this subject.

Physiologic situations that are accompanied by reduced fever despite similar afferent pyrogenic signaling to the brain are known.[37] Intrahypothalamic injections of prostaglandin E2 also result in smaller fevers in SHRs compared with WKY rats[42] and this experimental fever model does not depend on peripherally-derived pyrogenic signals. The strength of fever strongly depends on the balance between endogenous pyrogenic and antipyretic systems.[43,44] There are some endogenous antipyretic substances of which the formation and/or secretion seem to be higher in SHRs than in WKY rats, including vasopressin and adrenocorticotropic hormone (ACTH).[45,46] It was also reported that the expression of IL-10, which is an antipyretic cytokine,[22] is stronger in bacterially-infected SHRs compared with WKY rats.[47] Taken together, these data from literature suggest that there are several possibilities to explain the reduced fever of SHRs seen in our experiments, in addition to the moderate reduction of circulating IL-6. We are unable to decide which one of the proposed mechanisms is the strongest operator for the attenuation of fever in SHR, but a significant participation of the lack of CD36 is, in our eyes, rather unlikely.

Final conclusions

The ability of TLRs to initiate and propagate inflammation makes them attractive therapeutic targets. TLR2, for example, is required for innate host defense to infections with pathogens carrying numerous lipopeptides.[48] TLR2 alone can be activated by some of these microbial ligands, or heterodimers with TLR1 and TLR6 are formed for effective cellular stimulation. Although CD36 can act as a sensor of microbial lipopeptides, the quantitative role of this scavenger receptor in the manifestation of responses to diacylated lipopeptides, such as MALP-2 seems to depend on the respective experimental model and situation.[17,18,33] Our data show that CD36-deficiency of SHRs has a merely insignificant inhibitory effect on MALP-2 driven inflammation *in vivo*. The observation that LPS-induced effects are more attenuated than MALP-2-induced effects in SHRs compared with WKY rats suggests that the complex SHR-sickness syndrome can not solely be explained by CD36-deficiency in this rat strain. Our results indicate TLR2 and TLR4 as target candidates for therapeutic interference with inflammatory pathology and neurologic malfunction upon infection and disqualify CD36 as such.

Acknowledgements

The authors thank Dr Peter F. Mühlradt for providing MALP-2 and for his helpful comments on the manuscript. Skilful and expert technical assistance from Daniela Ott with the preparation and cultivation of peritoneal macrophages is gratefully acknowledged.

Funding

This research received no specific grant from any funding agency in the public, commercial, or not-for-profit sectors.

Downloaded from ini.sagepub.com at Bibliotheksystem der Universitaet Giessen on May 28, 2012

References

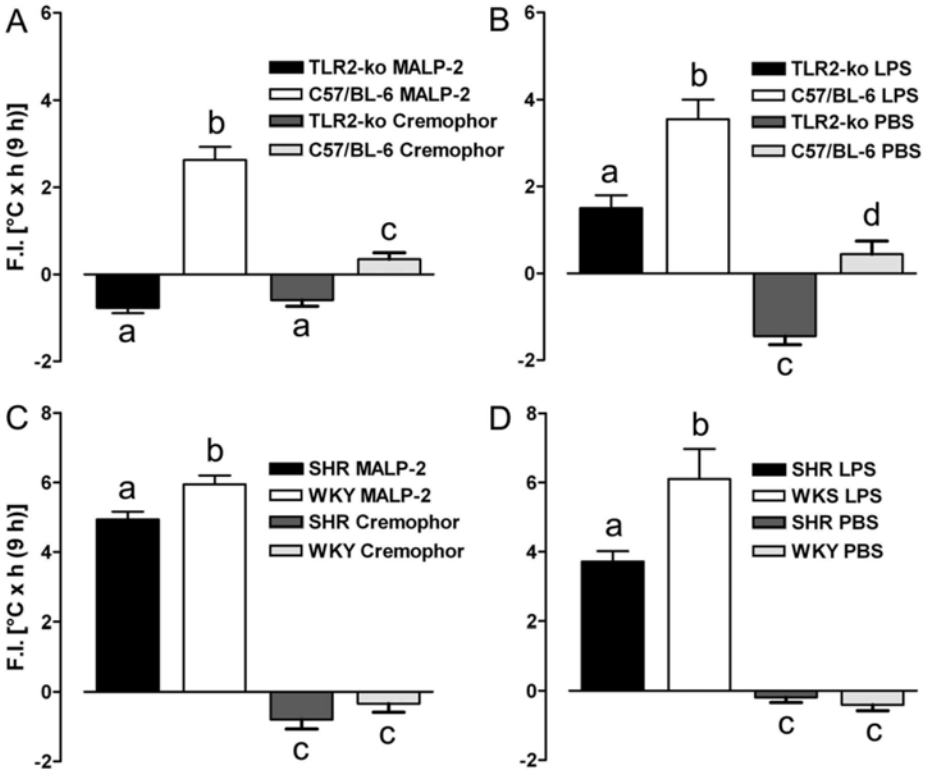
1. Uematsu S and Akira S. Toll-like receptors and innate immunity. *J Mol Med* 2006; 84: 712–725.
2. Chow JC, Young DW, Golenbock DT, Christ WJ and Gusovsky F. Toll-like receptor-4 mediates lipopolysaccharide-induced signal transduction. *J Biol Chem* 1998; 274: 10689–10692.
3. Poltorak A, He X, Smirnova I, Liu MY, Van Huffel C, Du X, et al. Defective LPS signalling in C3H/HeJ and C57BL/10ScCr mice: mutations in Tlr4 gene. *Science* 1998; 282: 2085–2088.
4. Steiner AA, Chakravarty S, Rudaya AY, Herkenham M and Romanovsky AA. Bacterial lipopolysaccharide fever is initiated via toll-like receptor 4 on hematopoietic cells. *Blood* 2006; 107: 4000–4002.
5. Galanos C, Gumenschneider M, Mühlradt PF, Jirillo E and Freudenberg MA. MALP-2, a Mycoplasma lipopeptide with classical endotoxic properties: end of an era of LPS monopoly? *J Endotoxin Res* 2000; 6: 471–476.
6. Ozinsky A, Underhill DM, Fontenot JD, Hajjar AM, Smith KD, Wilson CB, et al. The repertoire for pattern recognition of pathogens by the innate immune system is defined by cooperation between Toll-like receptors. *Proc Natl Acad Sci USA* 2000; 97: 13766–13771.
7. Takeuchi O, Kawai T, Mühlradt PF, Morr M, Radolf JD, Zychlinsky A, et al. Discrimination of bacterial lipoproteins by Toll-like receptor 6. *Int Immunol* 2001; 13: 933–940.
8. Morr M, Takeuchi O, Akira S, Simon MM and Mühlradt PF. Differential recognition of structural details of bacterial lipopeptides by toll-like receptors. *Eur J Immunol* 2002; 32: 3337–3347.
9. Okusawa T, Fujita M, Nakamura J-I, Into T, Yasuda M, Yoshimura A, et al. Relationship between structures and biological activities of mycoplasmal diacylated lipopeptides and their recognition by Toll-like receptors 2 and 6. *Infect Immun* 2004; 72: 1657–1665.
10. Rharbaoui F, Drabner B, Borsutzki S, Winckler U, Morr M, Ensoli B, et al. The Mycoplasma-derived lipopeptide MALP-2 is a potent mucosal adjuvant. *Eur J Immunol* 2002; 32: 2857–2865.
11. Borsutzki S, Fiorelli V, Ebensen T, Tripiciano A, Rharbaoui F, Scoglio A, et al. Efficient mucosal delivery of the HIV-1 Tat protein using the synthetic lipopeptide MALP-2 as adjuvant. *Eur J Immunol* 2003; 33: 1548–1556.
12. Deiters U, Barsig J, Tawil B and Mühlradt PF. The macrophage-activating lipopeptide-2 accelerates wound healing in diabetic mice. *Exp Dermatol* 2004; 13: 731–739.
13. Schmidt J, Welsch T, Jäger D, Mühlradt PF, Büchler MW and Märten A. Intratumoural injection of the toll-like receptor-2/6 agonist macrophage-activating lipopeptide-2 in patients with pancreatic carcinoma: a phase I/II trial. *Br J Cancer* 2007; 97: 598–604.
14. Hübschle T, Mütze J, Mühlradt PF, Korte S, Gerstberger R and Roth J. Pyrexia, anorexia, adipsia, and depressed motor activity in rats during systemic inflammation induced by the Toll-like receptors-2 and -6 agonists MALP-2 and FSL-1. *Am J Physiol Regul Integr Comp Physiol* 2006; 290: R180–R187.
15. Knorr C, Hübschle T, Murgott J, Mühlradt PF, Gerstberger R and Roth J. Macrophage-activating lipopeptide-2 (MALP-2) induces a localized inflammatory response in rats resulting in activation of brain sites implicated in fever. *Brain Res* 2008; 1205: 36–46.
16. Knorr C, Marks D, Gerstberger R, Mühlradt PF, Roth J and Rummel C. Peripheral and central cyclooxygenase (COX) products may contribute to the manifestation of brain-controlled sickness responses during localized inflammation induced by macrophage-activating lipopeptide-2 (MALP-2). *Neurosci Lett* 2010; 479: 107–111.
17. Hoebe K, Georgel P, Rutschmann S, Du X, Mudd S, Crozat K, et al. CD36 is a sensor of diacylglycerides. *Nature* 2005; 433: 523–527.
18. Triantafilou M, Gamper FGJ, Haston RM, Mouratis MA, Morath S, Hartung T and Triantafilou K. Membrane sorting of Toll-like receptor (TLR)-2/6 and TLR2/1 heterodimers at the cell surface determines heterotypic associations with CD36 and intracellular targeting. *J Biol Chem* 2006; 281: 31002–31011.
19. Glazier AM, Scott J and Aitman TJ. Molecular basis of the Cd36 chromosomal deletion underlying SHR defects in insulin action and fatty acid metabolism. *Mammalian Genome* 2002; 3: 1108–1113.
20. Houssier M, Raoul W, Lavalette S, Keller N, Guillonneau X, Baragatti B, et al. CD36 deficiency leads to choroidal involution via COX2 down-regulation in rodents. *PLoS Medicine* 2008; 5: 323–330.
21. Spiller S, Dreher S, Meng G, Grabiec A, Thomas W, Hartung T, et al. Cellular recognition of trimyristoylated peptide or enterobacterial lipopolysaccharide via both TLR2 and TLR4. *J Biol Chem* 2007; 282: 13190–13198.
22. Léon LR, Kozak W, Rudolph K and Kluger MJ. An antipyretic role for interleukin-10 in LPS fever in mice. *Am J Physiol Regul Integr Comp Physiol* 1999; 276: R81–R89.
23. Harré EM, Roth J, Pehl U, Kueth M, Gerstberger R and Hübschle T. Selected contribution: Role of IL-6 in LPS-induced nuclear STAT3 translocation in sensory circumventricular organs during fever in rats. *J Appl Physiol* 2002; 92: 2657–2666.
24. Espevic T and Nissen-Meyer J. A highly sensitive cell line, WEHI 164 clone 13, for measuring cytotoxic factor/tumor necrosis factor from human monocytes. *J Immunol Methods* 1986; 95: 99–105.
25. Holt I, Cooper RG and Hopkins SJ. Relationship between local inflammation, interleukin-6 concentration and the acute phase response in arthritic patients. *Eur J Clin Invest* 119; 21: 479–484.
26. Aarden LA, DeGroot ER, Schaap OL and Landsdorp PM. Production of hybridome growth factors by human monocytes. *Eur J Immunol* 1987; 17: 1411–1416.
27. Hübschle T, Thom E, Watson A, Roth J, Klaus S and Meyerhoff W. Leptin-induced nuclear translocation of STAT3 immunoreactivity in hypothalamic nuclei involved in body weight regulation. *J Neurosci* 2001; 21: 2413–2424.
28. Rummel C, Hübschle T, Gerstberger R and Roth J. Nuclear translocation of the transcription factor STAT3 in the guinea pig brain during systemic or localized inflammation. *J Physiol* 2004; 557.2: 671–687.
29. Rudaya AY, Steiner AA, Robbins JR, Dragic AS and Romanovsky AA. Thermoregulatory responses to lipopolysaccharide in the mouse: dependence on the dose and ambient temperature. *Am J Physiol Regul Integr Comp Physiol* 2005; 289: R1244–R1252.
30. Kirschning CJ, Wesche H, Merrill Ayres T and Rothe M. Human toll-like receptor 2 confers responsiveness to bacterial lipolysaccharide. *J Exp Med* 1998; 188: 2091–2097.
31. Heine H, Kirschning CJ, Lien E, Monks BG and Golenbock DT. Cutting edge: Cells that carry a null mutation for toll-like receptor 2 are capable of responding to endotoxin. *J Immunol* 1999; 162: 6971–6975.
32. Steiner AA, Chakravarty S, Robbins JR, Dragic AS, Pan J, Herkenham M and Romanovsky AA. Thermoregulatory responses of rats to conventional preparations of lipopolysaccharide are caused by lipopolysaccharide per se – not by lipoprotein contaminants. *Am J Physiol Regul Integr Comp Physiol* 2005; 289: R348–R352.
33. Abe T, Shimamura M, Jackman K, Kurinami H, Anrather J, Zhou P and Iadecola C. Key role of CD36 in toll-like receptor 2 signaling in cerebral ischemia. *Stroke* 2010; 41: 898–904.
34. Greis A, Murgott J, Gerstberger R, Hübschle T and Roth J. Effects of repeated injections of fibroblast-stimulating

Downloaded from ini.sagepub.com at Bibliothekssystem der Universitaet Giessen on May 28, 2012

lipopeptide-1 on fever, formation of cytokines, and on the responsiveness to endotoxin in guinea pigs. *Acta Physiol* 2009; 197: 35–45.
35. Greis A, Murgott J, Rafalzik S, Gersiberger R, Hübschle T and Roth J. Characterization of the febrile response induced by fibroblast-stimulating lipopeptide-1 in guinea pigs. *Am J Physiol Regul Integr Comp Physiol* 2007; 293: R152–R161.
36. Cartmell T, Poole S, Turnbull AV, Rothwell NJ and Luheshi GN. Circulating interleukin-6 mediates the febrile response to localised inflammation in rats. *J Physiol* 2000; 526: 653–661.
37. Harré EM, Mouihate A and Pittman QJ. Attenuation of fever at near term: is interleukin-6-STAT3 signalling altered? *J Neuroendocrinol* 2006; 18: 57–63.
38. Rummel C, Sachot C, Poole S and Luheshi GN. Circulating interleukin-6 induces fever through a STAT3-linked activation of COX-2 in the brain. *Am J Physiol Regul Integr Comp Physiol* 2006; 291: R1316–R1326.
39. Rummel C, Inoue W, Sachot C, Poole S, Hübschle T and Luheshi GN. Selective contribution of interleukin-6 and leptin to brain inflammatory signals induced by systemic LPS injection in mice. *J Comp Neurol* 2008; 511: 373–395.
40. Roth J and de Souza GEP. Fever induction pathways: evidence from responses to systemic or local cytokine formation. *Braz J Med Biol Res* 2001; 34: 301–314.
41. Malvar DC, Soares DM, Fabricio ACS, Kanashiro A, Machado RR, Figueiredo MJ, et al. The antipyretic effect of dipyrone is unrelated to inhibition of PGE2 synthesis in the hypothalamus. *Br J Pharmacol* 2011; 162: 1401–1409.
42. Bhatnagar S, Meaney MJ and Amir S. The effects of prostaglandin E2 injected into the paraventricular nucleus of the hypothalamus on brown adipose tissue thermogenesis in spontaneously hypertensive rats. *Brain Res* 1993; 613: 285–287.
43. Kluger MJ. Fever: role of pyrogens and cryogens. *Physiol Rev* 1991; 71: 93–127.
44. Roth J. Endogenous antipyretics. *Clin Chim Acta* 2006; 371: 13–24.
45. Ichida T and Kuriyama K. Age-related development of γ-aminobutyric acid $(GABA)_B$ receptor functions in various brain regions of spontaneously hypertensive rats. *Neurochem Res* 1998; 23: 89–95.
46. Negro-Vilar A and Saavedra JM. Changes in brain somatostatin and vasopressin levels after stress in spontaneously hypertensive and Wistar-Kyoto rats. *Brain Res Bull* 1980; 5: 353–358.
47. Bauhofer A, Tischer B, Middeke M, Plaul U, Lorenz W and Torossian A. The genetic background of hypertensive, septic rats determines outcome improvement with antibiotic and G-CSF prophylaxis. *Shock* 2003; 20: 326–331.
48. Wooten RM, Ma Y, Yoder RA, Brown JP, Weis JH, Zachary JF, et al. Toll-like receptor 2 is required for innate, but not acquired, host defense to *Borrelia burgdorferi*. *J Immunol* 2002; 168: 348–355.

Downloaded from ini.sagepub.com at Bibliothekssystem der Universitaet Giessen on May 28, 2012

Supplementary Figure 1



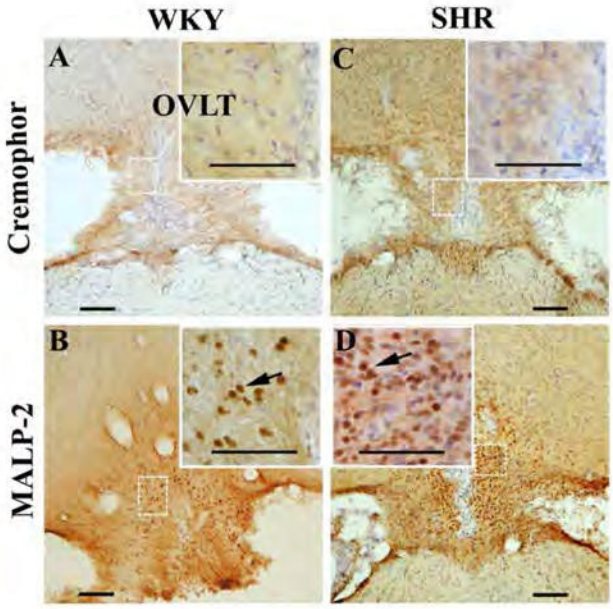
Supplementary Figure 1: The integrated time curves, the fever index (F.I.). From all groups of experimental animals investigated in this study. The mean fever indexes, the integrated areas between thermal responses of febrile and normothermic animals were expressed as a product of degrees celcius and hour (for 9 h after the respective injection). The mean of all temperatures measured at 15-min intervals over the 2 h period before the injection was calculated as the baseline temperature.

A, B: F.I.s from TLR2-ko and C57/BL-6 mice injected with MALP-2 or cremophor (A) or with LPS or PBS (B).

C, D: F.I.s from SHR and WKY rats injected with MALP-2 or cremophor (C) or with LPS or PBS (B).

Columns represent means ± S.E.M. In a given panel of this figure, any columns with the same letter are not significantly different from each other, while any columns with different letters are significantly different ($p < 0.05$; differences between groups). Note, that TLR2-ko mice show no response to MALP-2 and reduced responses to LPS or the vehicles. The F.I.s calculated from MALP-2- or LPS-treated SHR are significantly lower compared to those of WKY rats.

Supplementary Figure 2



Supplementary Figure 2: Representative photomicrographs of the OVLT of a WKY (A, B) and SHR (C, D) after i.p. injection of vehicle (cremophor, A, C) or 100 µg/kg MALP-2 (B, D). Note that specific STAT3 immunoreactivity is shown by the brown reaction product as a result of diaminobenzidine hydrochloride conversion. Cresyl violet counterstaining was used to label cell nuclei and general neuroanatomy. Specific MALP-2-induced nuclear STAT3 labeling, which is absent in rats of both strains treated with the vehicle, is shown at higher magnification in the insets (arrows in B and D). Bars in the overviews correspond to 100 µm, bars in the insets correspond to 25 µm.

1.3. „Parthenolide attenuates LPS-induced fever, circulating cytokines and markers of brain inflammation in rats“

Rummel C., Gerstberger R., Roth J., Hübschle H.
Cytokine (2011) 56: 739-48

Impakt Faktor: 3,537

Eigener Anteil an der Publikation:

- Initiative: wesentlich (40 %)
- Projektplanung: wesentlich (50 %)
- Durchführung der Versuche: wesentlich (40 %)
- Auswertung der Experimente: wesentlich (40 %)
- Erstellung der Publikation: weitgehend eigenständig (90 %)

Cytokine 56 (2011) 739–748

Contents lists available at SciVerse ScienceDirect

Cytokine

journal homepage: www.elsevier.com/locate/issn/10434666

Parthenolide attenuates LPS-induced fever, circulating cytokines and markers of brain inflammation in rats

Christoph Rummel *, Rüdiger Gerstberger, Joachim Roth, Thomas Hübschle

Institute of Veterinary-Physiology and -Biochemistry, Justus-Liebig-University Giessen, Frankfurter Strasse 100, D-35392 Giessen, Germany

ARTICLE INFO

Article history:
Received 13 July 2011
Received in revised form 23 September 2011
Accepted 25 September 2011
Available online 17 October 2011

Keywords:
Systemic inflammation
Immune-to-brain communication
Cyclooxygenase 2
Circumventricular organs
Nuclear factor kappa B

ABSTRACT

Parthenolide, a sesquiterpene lactone, has been reported to exhibit a variety of anti-inflammatory and immunomodulatory effects. To test the effect of parthenolide on brain inflammatory responses, brain oxidative stress and fever, we treated rats with parthenolide (1 mg/kg), simultaneously or 1 h prior to a systemic (i.p.) challenge with a moderate dose (100 μg/kg) of lipopolysaccharide (LPS). The initial hypothermia was exaggerated; the second phase of the biphasic LPS-induced fever and circulating interleukin-6 (IL-6) and tumor necrosis factor α (TNFα) were significantly attenuated only in parthenolide-pretreated animals. In the hypothalamus, markers of NFκB/NF-IL6 pathway activation (inhibitor κBα, NF-IL6 and the serin/threonin kinase-like protein mRNA expression) and markers of oxidative stress (including nuclear respiratory factor 1) and NFκB immunoreactivity were significantly reduced while NF-IL6 immunoreactivity and suppressor of cytokine signaling 3 mRNA expression remained unaltered, 8 h after LPS-stimulation with parthenolide-pretreatment. Importantly, this response was accompanied by decreased mRNA expression of the rate limiting enzyme in prostaglandin synthesis, cyclooxygenase 2 (COX2), known for its critical role in fever induction pathways. A direct action of parthenolide on brain cells was also confirmed in a primary neuro-glial cell culture of the vascular organ of the lamina terminalis a pivotal brain structure for fever manifestation with a leaky blood–brain barrier. In summary, pretreatment with parthenolide attenuates the febrile response during LPS-induced systemic inflammation by reducing circulating IL-6 and TNFα and decreasing hypothalamic NFκB/NF-IL6 activation, oxidative stress and expression of COX2. Thus parthenolide appears to have the potential to reduce brain inflammation.

© 2011 Elsevier Ltd. All rights reserved.

1. Introduction

Endotoxemia is accompanied by brain controlled sickness type responses, including fever [1], a hallmark of the acute phase response. Experimentally, fever and its accompanying brain inflammatory response can be mimicked by systemic injection of lipopolysaccharide (LPS), a compound derived from Gram negative bacterial cell walls. During the systemic inflammatory response humoral mediators such as interleukin (IL)-6 and tumor necrosis factor (TNF)α, increase in the circulation [2]. Subsequently, these cytokines act on brain structures with a leaky blood–brain barrier (BBB), the so-called circumventricular organs (CVOs) [3] or on the BBB itself [4], to modulate hypothalamic activity and contribute to the induction of brain controlled sickness responses via transcriptional regulation of inflammatory target genes. Spatiotemporal stimulation of brain signaling pathways, activated by LPS or cytokines, which are implicated in this response involve the transcription factors nuclear factor (NF)κB [5], signal transducer and activator of transcription (STAT3) [6,7] and NF-IL6 [8]. Target genes for these transcription factors include the two rate limiting, functionally coupled enzymes within the prostaglandin (PG)E2 synthesis pathway, namely cyclooxygenase (COX)2 and microsomal PGE synthase (mPGES) [5–7]. PGE2 is known as the critical terminal mediator in fever generation [9]. In addition to these inflammatory mediators, LPS is also known to increase oxidative stress in the brain. Previously, it was even proposed that this oxidative stress is also involved in fever induction after peripheral LPS-stimulation [10].

Parthenolide is a sesquiterpene lactone, derived from Mexican India medicinal plants and feverfew (*Tanacetum parthenium*),

Abbreviations: BBB, blood–brain barrier; CD, cluster of differentiation; COX2, cyclooxygenase 2; CVOs, circumventricular organs; DAPI, 4′,6-diamidino-2-phenylindole dilactate; IκBα, inhibitor kappa B alpha; IL, interleukin; IR, immunoreactivity; LPS, lipopolysaccharide; mPGES, microsomal PGE2 synthase; NFκB, nuclear factor kappa B; NF-IL6, nuclear factor IL-6; NRF1, nuclear respiratory factor; OVLT, vascular organ of the lamina terminalis; PBS, phosphate buffered saline; PG, prostaglandin; PGC1α, peroxisome proliferator-activated receptor γ coactivator 1 α; RT, room temperature; RT-PCR, reverse transcription polymerase chain reaction; SOCS3, suppressor of cytokine signaling 3; STAT3, signal transducer and activator of transcription 3; SFO, subfornical organ; TFAM, mitochondrial transcription factor A; TNFα, tumor necrosis factor alpha; Trib1, the serin/threonin kinase-like protein.

* Corresponding author. Tel.: +49 641 99 38155; fax: +49 641 99 38159.
E-mail address: Christoph.D.Rummel@vetmed.uni-giessen.de (C. Rummel).

1043-4666/$ - see front matter © 2011 Elsevier Ltd. All rights reserved.
doi:10.1016/j.cyto.2011.09.022

which belongs to a variety of natural products that have been used for their potential anti-inflammatory [11] and anti-oxidative [12] properties. Importantly, related to its inhibitory properties and its lipophilic character that favors a good BBB-permeability [13], parthenolide seems to be effective in models of migraine therapy [14] and emerges to be a therapeutic agent for cancer treatment including glioblastomas [15,16]. *In vitro* studies revealed that parthenolide inhibits the NFκB pathway by targeting the inhibitor (I)κB kinase activation [17] or IκBα degradation [18]. Among other effects (for review see also [19]), parthenolide was reported to also inhibit STAT3 [20]. Its influence on NF-IL6 remains to be determined.

The pivotal role of NFκB in fever is supported by the fact that NFκB-deficient mice do not develop fever in response to LPS or bacterial DNA, another stimulant of the innate immunity [21]. However, Kozak et al. (2006) did not show attenuated LPS-induced fever by pretreatment with parthenolide in mice and did not reveal an effect of parthenolide on LPS-induced plasma cytokine levels as previously shown by others [22,23]. Nonetheless, *in vitro* experiments performed by others have shown that parthenolide-treatment significantly decreases LPS-induced IL-6 and TNFα [23] and COX2 and mPGES expression derived from several macrophage populations [24,25].

LPS, which alters the activity of these transcription factors [7,8], is known to mediate its main effects by the nuclear factor (NF)κB signaling pathway [21] and to induce oxidative stress [10]. Therefore, LPS is a good model to investigate the effect of parthenolide on the brain and the periphery *in vivo*. The molecular mechanisms for parthenolide acting on the brain *in vivo* during infection and inflammation are still to be determined though.

Thus, the purpose of the present study was to investigate the effects of i.p. injected parthenolide on the LPS-induced (moderate dose, 100 μg/kg) febrile- and accompanying brain inflammatory and brain oxidative stress responses in rats. The systemic LPS-stimulated reaction was monitored by measuring plasma IL-6 and TNFα bioactivity. As a measure for the brain inflammatory response, hypothalamic activation of the inflammatory signaling pathways was determined by RT-PCR analyses of IκB, the suppressor of cytokine signaling (SOCS)3, the serin/threonin kinase-like protein, Trib1 (inhibitory regulators of STAT3/NFκB/NF-IL6 that are broadly used markers for their activation [8]) and NF-IL6 mRNA expression. The RT-PCR measurements were combined with immunohistochemistry for NF-IL6 and NFκB. To investigate if parthenolide also alters the PG synthesis pathway in the brain, the hypothalamic expression of COX2 and mPGES mRNA was analyzed. As markers of LPS-induced brain oxidative stress we decided to investigate the expression of pivotal genes implicated in mitochondrial biogenesis, namely peroxisome proliferator-activated receptor γ (PPARγ) coactivator (PGC)1 α, nuclear respiratory factor (NRF)1 and mitochondrial transcription factor A (TFAM) [26]. Finally we investigated the direct action of parthenolide on brain cells using primary neuroglial cell cultures of a sensory CVO, namely the vascular organ of the lamina terminalis (OVLT). The pivotal role of this brain structure for fever induction pathways is well accepted [3,27]. Thus, the OVLT with its leaky BBB is a good model to use to investigate the direct action of parthenolide on brain cells. Bioactivity of IL-6 and TNFα in the culture supernatant was used as a functional readout.

2. Materials and methods

2.1. Animals

Male Wistar rats (*Rattus* sp.) with a body weight of 275 ± 30 g originating from an in-house breeding colony with parent animals obtained from Charles River WIGA (Sulzfeld, Germany), were used in the present study. Animals were housed individually at an ambient temperature of 25 °C and 50% humidity on an 12:12 h light–dark cycle (lights off at 7:00 PM) with constant access to water and standard lab chow (Altromin1311; Altromin Spezialfutter GmbH & Co KG, Lage, Germany). Seven days before the experiment animals were implanted with intra-abdominal radiotransmitters (VM-FR PDT-4000, Mini-Mitter, Sunriver OR) for measurement of body core temperature. Output (frequency in Hz) from the radiotransmitter was monitored at 5 min intervals by an antenna placed under the cage (ER-4000 radio receivers, Mini-Mitter), which was connected to a data acquisition system (Vital View, Mini-Mitter). Data at time intervals of 15 min were used for analyses and graphical documentation. The rats were handled extensively for at least 3 days prior to the injections for habituation. Animal care, breeding and experimental procedures were conducted according to the national guidelines for experiments with vertebrate animals and Ethics committee approval was obtained from the regional government for the experimental protocols (ethics approval numbers GI 18/2–51/2008; GI 18/2–1/2011; cell culture experiments V 54-19 c20/15 c GI 18/2).

2.2. Treatment and experimental protocols

Rats were injected i.p. with a moderate (100 μg/kg) dose of LPS (derived from *Escherichia coli, serotype 0128:B12*, Sigma Chemicals, Deisenhofen, Germany) or with an equal volume of the pyrogen-free vehicle saline (NaCl, 0.9%, 1 ml/kg). LPS-treatment was further combined with i.p. treatment of 1 mg/kg parthenolide (Sigma Chemicals, Deisenhofen, Germany) or an equal volume of solvent (0.05% Tween 80 in saline, 0.9% NaCl at 1 ml/kg) together or 1 h prior to the systemic (i.p.) challenge with LPS or saline. The dose

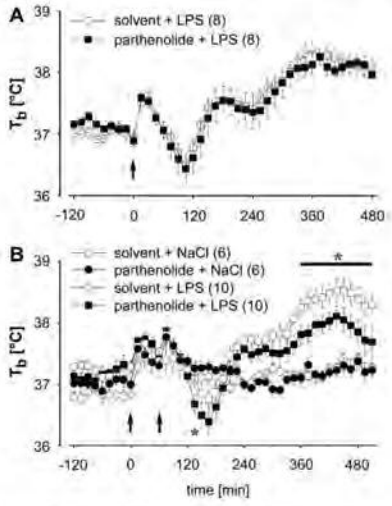


Fig. 1. Changes in abdominal temperature (T_b) of rats in response to intraperitoneal injections of LPS (100 μg/kg) or solvent (0.9% NaCl) combined with parthenolide (1 mg/kg; filled symbols; $t = 0$) or solvent (0.05% Tween 80, open symbols; at $t = 0$). In panel A all injections were done at $t = 0$; in panel B only LPS or 0.9% NaCl were injected at $t = 60$ min. At those time points indicated by significance bar and/or asterisk a significant LPS-induced pathenolide-mediated change of abdominal body temperature (T_b) compared with rats treated with LPS and solvent was observed (solvent + LPS versus parthenolide + LPS, $P < 0.05$). The number of animals for each experimental treatment group is indicated with brackets in the figure legend.

and solvent we used was based on results obtained by Sheehan et al. (2002), who effectively used parthenolide in a septic-like model of endotoxic shock. As simultaneous injection of parthenolide with LPS did not show any effect, the respective control groups treated with saline and solvent or parthenolide were omitted from the present manuscript (Fig. 1A). For all further experiments rats were pretreated 1 h before LPS-injection with parthenolide or solvent. Another group of animals was sacrificed 1, 2, 4 and 8 h after stimulation for measurements of IL-6 and TNFα bioactivity. Radiotransmitters were not implanted in animals of this particular set of experiments. All injections were performed between 9 and 10 AM. Body temperature was evaluated from 2 h before until ~8 h after the i.p. stimulation. This time interval was chosen because it ended prior to the start of the "light-off" period. The 15 min intervals values were shifted to the actual time point of injection. At the given time points, animals were deeply anesthetized with sodium pentobarbital (0.5 ml i.p.; Narcoren, Merial, Hallbergmos, Germany) and blood samples were collected via cardiac puncture using a sterile heparinized syringe.

Previously, we suggested that NF-IL6 might play a role in the maintenance of LPS-induced fever as its activation peaked 8 h after LPS-administration [8], at the same time, when fever was attenuated by parthenolide-treatment in the present study (Fig. 1B). Thus, using the same does and serotype of LPS we used in our previous study, we decided to look at the molecular mechanisms of parthenolide action on the brain at the peak of the NF-IL6 activation (8 h). Subsequently, rats for the time point at 8 h were transcardially perfused with 200 ml ice-cold 0.9% saline, their brains quickly removed, frozen in powdered dry ice, and stored at −55 °C until analysis.

2.3. Tissue processing

Coronal 20 μm brain sections were cut on a cryostat (model HM 500, Microm, Walldorf, Germany) and thaw-mounted on poly-L-lysine-coated glass slides. Sections (9 per animal and brain area) were prepared from several brain areas encompassing the hypothalamus (including the vascular organ of the lamina terminalis, OVLT and the subfornical organ, SFO) according to the stereotactic atlas of the rat brain [28]. In order to perform immunohistochemistry (IHC) and RT-PCR from the same brains, another remaining 10–15 consecutive frozen 80 μm sections of each hypothalamus (bregma 0.50 to −3.5 mm) were also thaw-mounted on glass slides, the hypothalamus (containing rostral to caudal portions) dissected and used for RNA-extraction.

2.4. Immunohistochemistry

On the day of the experiment the frozen brain sections were briefly air dried at room temperature for 7 min and then immersion-fixed in 2% paraformaldehyde (Merck, Darmstadt, Germany) diluted in PBS for 10 min at room temperature (RT). Following three successive washes in PBS, the sections were treated for 1 h at RT with a blocking solution consisting of PBS, containing 10% normal donkey serum (NDS; Biozol, Eching, Germany) and 0.3% triton X-100. The sections were incubated with the primary rabbit anti NF-IL6 polyclonal IgG (cat. sc-150; Santa Cruz Biotechnology, CA, USA) and the goat anti NFκB polyclonal IgG (p65, cat. sc-372 G; Santa Cruz Biotechnology, CA, USA) for 20–22 h at 4 °C followed by three successive washes in PBS and visualization with CY3-anti goat (cat. 705-165-147; Jackson ImmunoResearch, West Grove, PA) and Alexa-488-conjugated anti rabbit IgG (cat. AZA11055; MoBiTec GmbH, Goettingen, Germany) after a 2 h incubation at RT and a 1:500 dilution in blocking solution for each secondary antibody. Sections were counterstained with the nuclear 4,6-diamidino-2-phenylindole (DAPI) stain (Mobitec GmbH, Göttingen, Germany) for 10 min, using a 1:1000 dilution in PBS in order to clearly visualize the tissue surrounding the signal and to demonstrate the nuclear localization of NF-IL6- and NFκB IR. Finally, all sections were cover slipped (glass cover slips) using a glycerol/PBS solution (Citifluor LTD, London, UK) and stored at 4 °C until microscopic analysis was performed. Both antibodies have been used previously and respective control preabsorbtion experiments have confirmed the specificity of the observed signals [7,8].

2.5. Microscopical analysis

Sections were analyzed using a conventional light/fluorescent Olympus BX50 microscope (Olympus Optical, Hamburg, Germany) equipped with the appropriate filter sets to detect the fluorescent conjugates Cy3, Alexa Fluor 488 and DAPI. Images were taken with a black and white Spot Insight camera (Diagnostic Instruments, Visitron Systems, Puchheim, Germany) using the MetaMorph 5.05 software. Image editing software was used to combine the individual images into the red/green/blue color figure plates (MetaMorph 5.05), to adjust brightness and contrast and to store the images as TIFF files (Adobe Photoshop 5.5).

2.6. Real-time PCR

Total RNA of the collected hypothalamic tissue was isolated using TRIzol (Invitrogen, CA, USA) according to the manufacturer's protocol. One microgram of total RNA was transcribed into DNA, using 50 units of Murine Leukemia Virus [MULV] Reverse Transcriptase, 50 μM of random hexamers, and 10 mM of dNTP mix (Applied Biosystems), in a total reaction volume of 20 μl. Following reverse transcription, quantitative real time PCR was performed in duplicate using preoptimized primer/probe mixture (TaqMan Gene Expression Assay; Applied Biosystems, Foster City, CA, USA) and TaqMan universal PCR Master Mix (Applied Biosystems) on a StepOne™ Real-Time PCR System (Applied Biosystems). The cDNA quantities between different reactions were normalized by measurement of the housekeeping gene β-actin (cat: 4352340E, Applied Biosystems) as a reference. The sample values represent x-fold differences from a control sample (given as a designated value of 1) within the same experiment. Assay IDs for the analyzed genes are as follows: IκBα (Rn01473658_g1), SOCS3 (Rn00585674_s1), NF-IL6 (Rn00824635_s1), Trib1 (Rn01505060_m1), COX2 (Rn00568225_m1) and mPGES (Rn00572047_m1), CD163 (Rn01492520_m1), PGC-1α (Rn 00580241-m1), NRF1 (Rn01455958_m1), TFAM (Rn00580051_m1).

2.7. Isolation and cultivation of OVLT primary cell cultures

As previously described [27] primary microcultures of the rat OVLT were established from topographically excised brain tissue of 4–6 days old Wistar rat pups. Therefore, 5–6 animals per preparation were quickly decapitated with sharp scissors and the heads immersed (<20 s) in cold 70% ethanol. Each brain was immediately removed from the skull under aseptic conditions, fixed onto a Teflon®-block with Histoacryl® tissue glue (Braun, Melsungen, Germany) and rapidly transferred to a chamber containing ice-cold oxygenated Gey's Balanced Salt Solution (GBSS; Biotrend, Cologne, Germany) enriched with 5% D-glucose (Sigma–Aldrich, Munich, Germany). The chamber was fixed to a vibratome (752M Vibroslice; WPI, Berlin, Germany) equipped with fiber optics (1500 KL; Schott, Mainz, Germany), and serial coronal brain slices (400 μm) were cut at the level of the anterior hypothalamus. Using the anterior commissure and optic chiasm as main neuroanatomical landmarks [28], the section containing the OVLT was selected and the OVLT region dissected under stereomicroscopic control (SMZ-U; Nikon, Düsseldorf, Germany) from the surrounding anterior third ventricular region using fine eye scissors. It should be noted that

the 400 μm slice, which we used might as well contain some tissue anterior or posterior to the OVLT and is not represented by just one coronal plane from the representative stereotaxic atlas of the rat brain [28].

The isolated OVLT tissue fragments of 5–6 rat pups were collected in small Petri dishes filled with ice-cold, oxygenated Hanks Balanced Salt Solution (HBSS) without Ca2+ and Mg2+ (Biochrom, Berlin, Germany), but supplemented with 20 mM/L HEPES (Sigma–Aldrich), pH 7.4. The supernatant was removed, and the OVLT fragments were treated with 2 ml dispase-1 (1.0 U/ml; Roche Diagnostics, Mannheim, Germany) in oxygenated HBSS with 20 mM/L HEPES, pH 7.4, for 30 min at 37.0 °C. After enzymatic treatment, the OVLT fragments were washed with HBSS containing 1.0 mM/L EDTA (Sigma–Aldrich) to inactivate the enzyme. Then the tissue was washed three times with 3.0 ml complete medium, consisting of Neurobasal medium A supplemented with 2.0% B 27 (Invitrogen, Karlsruhe, Germany), penicillin (100 U/ml), streptomycin (0.1 mg/ml) and 2.0 mM/L L-glutamine (Biochrom). Finally, 2.0 ml complete medium were added to each tube and the tissue was dissociated by repeated trituration with a fire-polished pasteur pipette. The dissociated OVLT cells were plated onto prewarmed, poly-L-lysine (1.0 mg/ml H_2O; Sigma Aldrich) coated glass coverslips (Eppendorf, Hamburg, Germany) forming the bottom of a reusable Flexiperm-micro-12 well (6 mm diameter; Greiner Bio-One GmbH, Solingen, Germany) to ensure sufficient cell density despite limited absolute cell number. Cells were cultured in a humidified atmosphere of 5% CO_2 and 95% air at 37.0 °C. The medium was exchanged the next day to remove cellular debris and thereafter every 2 days during the culture period. After 4–6 days cultivation on glass coverslips, the OVLT cells were incubated with LPS (100 μg/ml) in complete medium for 360 min in a humidified atmosphere of 5% CO_2 and 95% air at 37.0 °C. In addition, cells were pretreated either with parthenolide (100 μg/ml) or solvent. Some wells were only pretreated with parthenolide or solvent to control for their effects under non-stimulated conditions. In pilot experiments we tested several doses of parthenolide (10, 100, 300 μg/ml) and determined 100 μg/ml to be most effective. The dose of 10 μg/ml was not sufficient to cause a significant reduction of LPS-induced release of bioactive cytokines into the supernatants of neuro-glial OVLT primary cell cultures. High doses of parthenolide on its own induced death and detachment of the cultured cells and TNFα induction in the supernatant (data not shown). Others have also shown that parthenolide causes oxidative stress-mediated apoptosis when administered at high concentrations [12], confirming our observation. The time interval and dose of LPS we used, has previously been shown to induce a robust increase in IL-6 and TNFα in the supernatant, compared to counterpart controls [27]. Overall, 10–100 μg/ml parthenolide have been previously shown to abolish TNFα *de novo* synthesis in macrophages when stimulated with 10 μg/ml of LPS [24]. Here, we used the maximal dose of parthenolide e.g. 100 μg/ml with a 10 times higher dose of LPS (100 μg/ml) to show its inhibitory effects on neuro-glial cell cultures after this potent LPS-stimulation. In this regard, we have to acknowledge that we are at the upper level of the normal range of parthenolide that has been used previously. The supernatants were removed from the cells, transferred and stored at −45 °C for later determination of cytokines.

2.8. Plasma and supernatant IL-6 and TNFα measurements

Determination of IL-6 and TNFα was performed by bioassay based on a dose-dependent growth stimulation of IL-6 on the B9 hybridoma cell line and on a cytotoxic effect of TNF on a mouse fibrosarcoma cell line WEHI 164 subclone 13 as described previously [29]. The detection limit of the assay, after considering the dilution of samples for the assays, proved to be three international units (IU) for IL-6/ml and 6 pg/ml for TNF.

2.9. Data analysis

All data are given as means ± SEM. Statistical calculations were carried out with the SigmaPlot/SigmaStat analysis software (SPSS Science Software GmbH, Erkrath, Germany) for abdominal temperatures, which were compared between the two different groups (solvent + LPS versus parthenolide + LPS) over time by a two-way repeated-measures ANOVA, followed by an all pairwise Tukey multiple comparison post hoc test. Levels of bioactive IL-6 or TNFα, semiquantitative data on relative expression of IκB-, SOCS3-, NF-IL6-, Trib1-, COX2- and mPGES mRNA in the hypothalamus were compared separately between the experimental groups (solvent + NaCl, parthenolide + NaCl, solvent + LPS and parthenolide + LPS) by ANOVA, followed by a Newman–Keuls multiple comparison post hoc test (GraphPad Prism 5 software; San Diego, CA, USA). A log transformation of the individual plasma cytokine values was performed prior to the statistical calculation, because the values for cytokines are not normally distributed. For IL-6 and TNFα levels in supernatants we calculated the mean ($n = 1–3$ wells) of the mean from five independent experiments. *P*-values less than 5% were deemed significant. All data are presented as means ± SEM.

3. Results

3.1. Pretreatment with parthenolide attenuates LPS-induced fever

As a physiological readout of the brain controlled sickness response after systemic LPS-stimulation (100 μg/kg, i.p.), we investigated changes in body core temperature. LPS induced an initial thermoregulatory stress peak at 15 min after injection (37.6 °C) followed by a hypothermic response which lasted until 120 min (~36.4 °C). Thereafter a biphasic fever developed, which peaked at 180 (~37.4 °C), respectively and 360 min (~38.4 °C). Simultaneous administration of parthenolide and LPS did not alter this response (Fig. 1A). However, in animals pretreated with parthenolide 1 h prior to LPS injection, the second phase of the biphasic LPS-induced fever was significantly attenuated (360–510 min) and the hypothermic response significantly enhanced (135 min). Parthenolide administration alone did not have any significant effect on basal temperature in NaCl injected control animals (Fig. 1B).

3.2. LPS-induced IL-6 and TNFα plasma bioactivity is partially decreased by parthenolide pretreatment

To determine the magnitude of the systemic inflammation induced by LPS administration and the effect of parthenolide on this response, we measured the most prominent pro-inflammatory humoral mediators, namely IL-6 and TNFα. Circulating IL-6 bioactivity dramatically increased in a time-dependant manner after i.p. LPS-stimulation (100 μg/kg) and peaked at 240 min with values ~12.000 IU compared to basal NaCl treated counterpart controls with values ~50 IU, as reported previously [30]. This response was significantly attenuated for the time points 240 and 480 min by pretreatment with parthenolide. Basal levels of NaCl-injected animals were not altered (Fig. 2A) by parthenolide pretreatment. TNFα peaked at 60 min with ~59 ng/ml after LPS-stimulation and was undetectable at the 480 time point like in all control counterpart animals. Parthenolide did not affect LPS-induced TNFα levels 60 and 120 min after stimulation, while TNFα was not

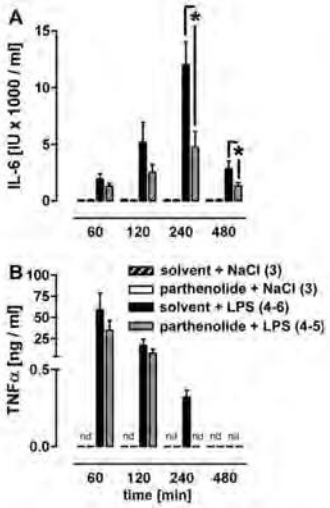


Fig. 2. Changes in plasma IL-6 (A) and TNFα (B) bioactivity of rats in response to intraperitoneal injections of LPS (100 μg/kg) or solvent (0.9% NaCl) combined with parthenolide (1 mg/kg; at $t = -1$ h) or solvent (0.05% Tween 80; at $t = -1$ h). IL-6 bioactivity remains at basal values and TNFα levels were not detectable (nd) in NaCl-treated control animals. The number of animals for each experimental treatment group is indicated with brackets. All data are presented as means ± SEM and statistical significance was considered as $P < 0.05$; *differences between groups solvent + LPS versus parthenolide + LPS.

detectable at 240 min, indicating an abolished TNFα-induction by parthenolide pretreatment (Fig. 2B) only at this time point.

3.3. Parthenolide alters LPS-induced mRNA expression of markers for hypothalamic inflammation e.g. the NFκB/STAT3/NF-IL6 signaling pathways and COX2/mPGES

To study the potential beneficial effect of parthenolide on reducing brain inflammatory markers during the systemic inflammatory response, we analyzed the pro-inflammatory signaling pathways for STAT3/NFkB, and we decided to investigate if the recently described LPS-activated brain inflammatory transcription factor NF-IL6 [8] was changed by parthenolide. Using RT-PCR we revealed that LPS (100 μg/kg, i.p.) drastically increased the mRNA expression of markers of NFκB/STAT3/NF-IL6 activation, namely IkBα and SOCS3 as well as NF-IL6 expression and its negative regulator Trib1, in the hypothalamus at 8 h after LPS-stimulation (Fig. 3A–D). Pretreatment with parthenolide, 1 h before LPS-injection, significantly attenuated the NFκB and NF-IL6 pathway, while SOCS3 mRNA expression was not altered, suggesting that LPS-induced STAT3-activation remained unchanged by parthenolide.

We also measured hypothalamic mRNA expression of the rate limiting enzymes in PGE2 induction, namely COX2 and mPGES; PGE2 being the most prominent terminal fever inducing mediator. The expression of these enzymes was significantly increased 8 h after LPS-administration (Fig. 3E and F). Injection of parthenolide 1 h before LPS-stimulation significantly decreased relative COX2 mRNA expression, while mPGES mRNA expression was significantly elevated.

An important cell phenotype that has been shown to be implicated in brain COX2 expression, during systemic inflammation, is perivascular macrophages [31]. To test if the observed reduced

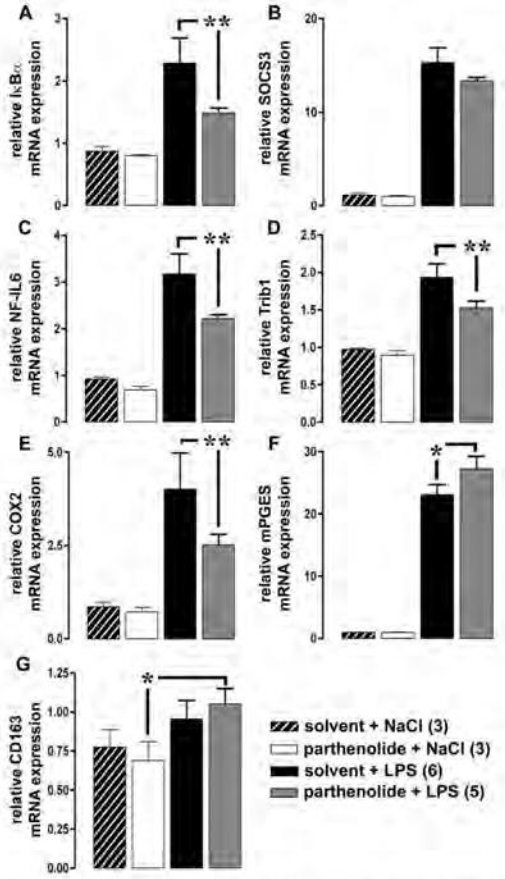


Fig. 3. mRNA expression of inflammatory mediators and activity markers of signaling pathways in the rat hypothalamus 8 h following systemic injection of LPS (100 μg/kg i.p.) compared to vehicle (0.9% NaCl)-treated animals combined with parthenolide (1 mg/kg; at $t = -1$ h) or solvent (0.05% Tween 80; at $t = -1$ h) using quantitative RT-PCR. The number of animals for each experimental treatment group is indicated with brackets. Columns represent means ± SEM; inhibitor of kappa B alpha (IκBα), suppressor of cytokine signaling 3 (SOCS3), nuclear factor interleukin 6 (NF-IL6), tribbles-1 (Trib1), cyclooxygenase 2 (COX2), microsomal prostaglandin E synthase (mPGES); *<0.05; **<0.01.

COX2 mRNA expression was due to decreased numbers of perivascular macrophages in the LPS-stimulated and parthenolide pretreated brains, we studied hypothalamic mRNA expression of the perivascular macrophage specific marker CD163 [32]. However, parthenolide did not significantly alter CD163 mRNA expression suggesting that rather reduced COX2 expression in the brain than reduced numbers of these cells were responsible for the observed decrease of hypothalamic COX2 mRNA expression.

3.4. LPS-induced nuclear NFκB but not NF-IL6 immunoreactivity is almost abolished 8h after stimulation

Brain inflammation was also monitored at the protein level using immunohistochemistry for NFκB and NF-IL6 at the 8 h time

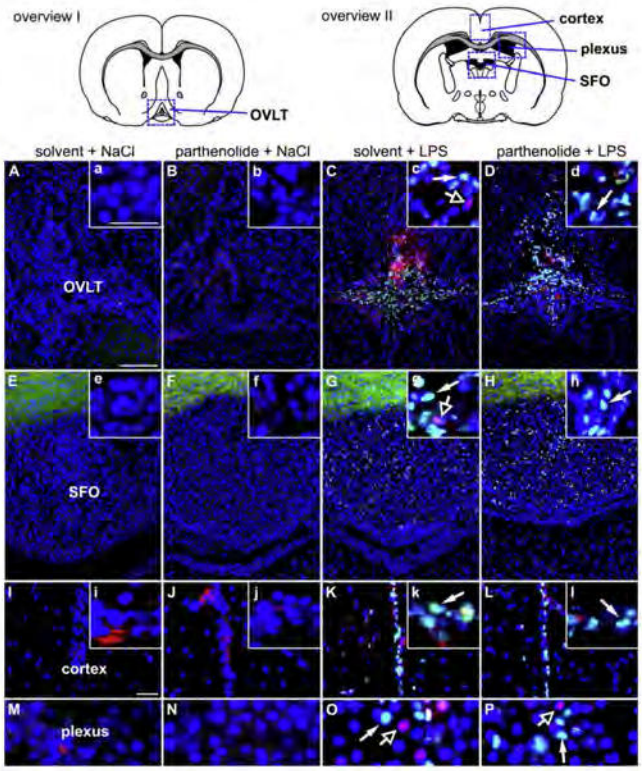


Fig. 4. LPS-induced (100 μg/kg, i.p.) nuclear NF-IL6 (green, filled white arrows) and NFκB (red, open white arrows) staining was observed in multiple brain structures including the vascular organ of the lamina terminalis (OVLT, C), the subfornical organ (SFO, G), blood vessel like structures in the bifurcation of the cortical hemispheres (K, only nuclear NF-IL6) and the choroid plexus (O) compared to vehicle (0.9% NaCl)-treated counterpart controls (A, E, I, M). This response was partially reduced for nuclear NFκB IR in parthenolide pretreated animals (1 mg/kg, at $t = -1$ h; D, H, P) but not visually affected for NF-IL6 staining. Co-localization of green/red NF-IL6/NFκB signals with the nuclear DAPI stain (blue) indicates the nuclear localization of the signals, which can be clearly depicted at high magnifications (insets of C, D, G, H, K, I, O and P). Almost no nuclear but some cytoplasmatic staining was observed in vehicle injected and solvent (0.05% Tween 80; at $t = -1$ h) pretreated animals (solvent + NaCl, parthenolide + NaCl). Scale bars = 100 μm in A (applies to A–H); 25 μm in insets (each applies to the following high magnifications) and M–P; 25 μm in I (applies to I–L). (For interpretation of the references to color in this figure legend, the reader is referred to the web version of this article.)

point after LPS-stimulation (100 μg/kg). As predicted, LPS induced a dramatic increase in nuclear NF-IL6 IR (IR; Fig. 4C, G, K and O), but only a couple of nuclear NFκB signals (Fig. 4C, G and O) within the CVOs of the OVLT and the SFO, in the choroid plexus and along blood vessels distributed all over the brain such as the cortex (Fig. 4K, primarily NF-IL6). This LPS-induced increase in nuclear NFκB and NF-IL6 IR was decreased for nuclear NFκB staining with only very few single cells showing nuclear NFκB IR for example in the choroid plexus after LPS-stimulation and parthenolide pretreatment (Fig. 4P). An obvious change in LPS-induced nuclear NF-IL6 IR by parthenolide pretreatment could not, however, be observed (Fig. 4D, H, L and P) when compared to LPS and vehicle treated counterpart control animals suggesting that this signaling pathway might not have been significantly altered by parthenolide at the protein level. In NaCl-injected control animals cytoplasmatic, but hardly any nuclear NF-IL6 and NFκB staining was observed (Fig. 4A, B, E, F, I, J, M and N). Interestingly, nuclear NF-IL6 and NFκB staining predominantly did not co-localize in the brain of LPS-treated animals (Fig. 4, white arrows) indicating that they are activated in distinct populations of brain cells at this time point.

3.5. Parthenolide alters LPS-induced mRNA expression of markers for hypothalamic oxidative stress and mitochondrial biogenesis e.g. PGC1α/NFR1/TFAM

As parthenolide was previously reported to have anti-oxidative properties *in vitro* [12] we decided to look at hypothalamic mRNA-expression of PGC1α/NFR1/TFAM, pivotal genes involved in oxidative stress (for review [26]) in our *in vivo* model (Fig. 5). These genes are master regulators of mitochondrial biogenesis and known to be induced/modulated by oxidative stress [33]. However, in the present study, LPS (100 μg/kg) did not significantly alter any of the respective genes 8 h after stimulation. While the LPS-induced increase for PGC1α and NRF1 mRNA levels did not reach significance compared to the controls, parthenolide treatment significantly reduced mRNA levels compared to LPS-stimu-

lated solvent counterparts, suggesting anti-oxidative effects of parthenolide on the hypothalamus *in vivo*.

3.6. LPS-induced IL-6 and TNFα levels in supernatants of primary neuro-glial OVLT cell cultures are inhibited by parthenolide pretreatment

To test for the direct action of parthenolide on brain cells we used primary neuro-glial OVLT cell cultures. This brain structure belongs to the sensory CVOs and, therefore, cells have direct contact to parthenolide also *in vivo*. Cultures incubated with LPS (100 μg/ml) for 6 h and pretreated 1 h before with solvent showed a pronounced increase in supernatant IL-6 and TNFα levels (Fig. 6). For both cytokines this response was significantly decreased with parthenolide pretreatment (100 μg/ml), confirming that parthenolide can directly act on brain cells. At the dose used, parthenolide alone did not alter IL-6 nor TNFα levels in the supernatants of non-stimulated NaCl treated cell cultures.

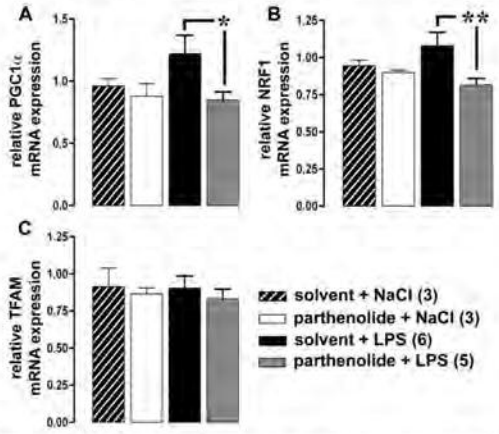


Fig. 5. mRNA expression of oxidative stress markers namely genes involved in mitochondrial biogenesis in the rat hypothalamus 8 h following systemic injection of LPS (100 μg/kg i.p.) compared to vehicle (0.9% NaCl)-treated animals combined with parthenolide (1 mg/kg; at $t = -1$ h) or solvent (0.05% Tween 80; at $t = -1$ h) using quantitative RT-PCR. The number of animals for each experimental treatment group is indicated with brackets. Columns represent means ± SEM; peroxisome proliferator-activated receptor γ coactivator 1 α (PGC1α), nuclear respiratory factor (NRF1), mitochondrial transcription factor A (TFAM); *<0.05; **<0.01.

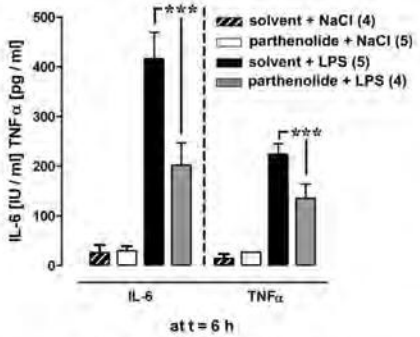


Fig. 6. Changes in IL-6 and TNFα bioactivity in supernatants of primary neuro-glial cell cultures of the vascular organ of the lamina terminalis (OVLT) 6 h following stimulation with LPS (100 μg/ml) compared to vehicle (0.9% NaCl)-treatment combined with parthenolide (100 μg/ml; at $t = -1$ h) or solvent (0.05% Tween 80; at $t = -1$ h). Please note that in several experiments with NaCl-stimulation cytokine bioactivity remained undetectable. The number of independent experiments for each treatment group is indicated with brackets. Each experiment consisted of 1–3 wells. Columns represent means ± SEM; ***<0.001.

4. Discussion

In the present study, we have shown for the first time that parthenolide attenuates LPS-induced fever, brain inflammation and brain oxidative stress when injected 1 h before LPS-stimulation, but not when administered simultaneously with LPS. The decreased febrile was most likely due to the reduction of circulating IL-6 and TNFα levels, as well as the direct central actions of parthenolide on brain cells. The partially enhanced hypothermic response was not reflected by significant changes in plasma IL-6 or altered TNFα levels at this early time point (120 min). In more detail, parthenolide action was accompanied by attenuated hypothalamic IκBα, NF-IL6 and Trib1, COX2, PGC1α and NRF1, but increased mPGES mRNA expression and reduced nuclear NFκB IR. Parthenolide pretreatment did not affect hypothalamic CD163 or the mitochondrial transcription factor TFAM mRNA expression.

In the periphery, cytokines are released as humoral mediators and transmit the inflammatory challenge to the brain. As opposed to the results obtained after *in vitro* parthenolide-treatment of stimulated macrophages [23,34] previous *in vivo* studies have shown moderate [35] or even no significant inhibitory effects of parthenolide on plasma cytokines [21–23]. In our study, we found that parthenolide-pretreatment attenuated LPS-induced IL-6 and TNFα plasma levels. Pretreatment with parthenolide might therefore have targeted the production of these humoral mediators in peripheral circulating monocytes and other organ-resident macrophages (e.g. kupfer cells in the liver). In support of a peripheral action of parthenolide, we observed decreased cytokine levels, two hours later an attenuated fever and a subsequent reduction of nuclear NFκB activation in critical pyrogen sensitive brain structures including the OVLT. This is also in line with a proposed IL-6 and TNFα mediated *de novo* synthesis of COX2 and subsequent production of the terminal pyrogen, PGE2, in these brain structures e.g. the CVOs and endothelial cells [2,7]. We did not find any evidence for parthenolide inhibiting the number of perivascular macrophages, another cell phenotype also been implicated in increasing COX2 expression in the brain during systemic inflammation [31] as shown by unchanged hypothalamic expression of its specific marker protein CD163.

The exact reason for the moderate enhancement of hypothermia by parthenolide is not clear. Although circulating TNFα has been proposed to be a potential mediator of LPS-induced hypothermia, plasma levels were not altered in our present study. In addition, TNFα has also been shown to induce fever and, therefore, its role in fever and hypothermia is still controversial [2]. Opposed to circulating TNFα levels, brain TNFα might be the potential mediator to explain LPS-induced hypothermia as previously suggested [36], however, remains to be confirmed for our *in vivo* and the *in vitro* experiments in future studies. Another explanation for LPS-induced hypothermia are known to be hypotonic cardiovascular effects that quickly decrease body core temperature by redistribution of central and peripheral blood compartments. Nonetheless, the study by Sheehan et al. (2003) shows some improvement i.e. an increase in blood pressure by parthenolide-treatment during septic inflammation indicating that hypothermia might not be related to hypotonic cardiovascular effects in our present study.

A role for NFκB activation in fever induction in the periphery [21] or the brain [5] is well accepted. Different NFκB-inhibitors

have been shown to block fever induced by LPS [37], bacterial DNA [21] or staphylococcal enterotoxin A [38]. However, Kozak et al. (2006) did not find any effect of parthenolide on LPS-induced fever, when injecting it (2 mg/kg i.p.) 30 min before an i.v. injection of a similar dose of LPS (50 μg/kg in mice) to that used in the present study. Differences in animal species (mice versus rats) the solvent used for the preparation of this lipophilic substance (0.01 M anhydrous sodium carbonate versus 0.05% Tween in PBS) or the route of LPS-application (i.a. versus i.p.) might account for this discrepancy. Another explanation might be related to the timing of parthenolide and LPS administration. In the present study, we found no effect of parthenolide when injection simultaneously with LPS. Pretreatment with parthenolide 1 h before the LPS-challenge did, however, have a significant affect, indicating that the timing of parthenolide administration might be an important factor, at least when using a moderate dose of LPS in rats. Previously, parthenolide has been administered at various different time intervals including 15 min before, simultaneous and 3 h after in models of septic like inflammation with either beneficial or even detrimental effects [22,39].

In addition to the peripheral action of parthenolide inhibiting circulating cytokines and subsequent hypothalamic activation of the NF-IL6-/NFkB-signaling pathway and COX2 expression, the effect of parthenolide on brain inflammation might also be due to a direct action of this substance. Notably, a central action of parthenolide has previously been proposed for inhibiting Fos activation in various brain nuclei in a model of nitroglycerine-induced migraine [14] possibly also by reducing inducible nitride oxide synthase expression in the dura mater [40] or acting on 5HT2A receptors [41]. Nonetheless, the expression of inflammatory genes in the brain under the influence of parthenolide has not been investigated. In the present study, we report for the first time the inhibitory effects of parthenolide on hypothalamic NFκB activation by showing reduced nuclear IR and attenuated IκBα mRNA expression. Moreover, we present evidence for a direct action of parthenolide on brain cells in a primary neuro-glial cell culture of a sensory CVO, namely the OVLT. Parthenolide-pretreatment decreased LPS-induced IL-6 and TNFα levels in the supernatant. Importantly, parthenolide has direct access to this brain structure, with its leaky BBB, *in vivo* confirming a central action of parthenolide on the brain in inhibiting cytokines, the prostaglandin pathway, oxidative stress and subsequently fever.

Unlike for NFκB, we were not able to detect parthenolide-induced decreases in the JAK-STAT3 signaling pathway, as shown by unchanged hypothalamic SOCS3 mRNA expression, although it has been suggested previously that parthenolide inhibits IL-6 induced activation of this signaling pathway in a human hepatoma cell line [20]. Such a parthenolide-inhibitory action on STAT3 was reported to be mediated by increased reactive oxygen species in a culture of cardiomyocytes and was prevented by antioxidant pretreatment [14]. Thus, the redox-sensitive STAT3-signaling pathway might not have been challenged enough by the low dose of parthenolide in our model of a moderate LPS-stimulation *in vivo* and furthermore may have been protected by basic anti-oxidative mechanisms. Apparently only high doses of parthenolide seem to increase oxidative stress and lower doses actually are anti-oxidative [12], which might explain discrepancies between studies. Interestingly, another study even revealed increased SOCS3 mRNA expression in a culture of hypothalamic neurons after parthenolide-treatment [42]. The mechanism for this increase has yet to be determined. Overall, our data suggest that the STAT3-signaling pathway was not significantly altered by parthenolide-treatment. An inhibitory effect of parthenolide on hypothalamic STAT3-signaling at earlier time points than those investigated in the present study, cannot however be ruled out.

As opposed to the effects on STAT3, we are the first to show that hypothalamic NF-IL6 activation might have been altered by parthenolide pretreatment, as the mRNA expression of both NF-IL6 and its negative feedback regulator Trib1 were significantly reduced in the hypothalamus. Increased mRNA *de novo* expression of NF-IL6 has been suggested to be an important mechanism of its own activation [8]. Nonetheless, at the protein level we did not detect an obvious decrease in nuclear NF-IL6 IR in several brain structures suggesting that the effect of parthenolide on this signaling pathway might not have been very strong or that sufficient amounts of pre-formed cytoplasmatic NF-IL6 might already have been present in the hypothalamus. Interestingly, NF-IL6 and NFκB predominantly did not co-localize in the same cells 8 h after LPS-stimulation. In detail, during inflammation NFκB is known to be the first transcription factor activated throughout the brain [7,43] followed by or partially overlapping with STAT3- [44,45] and NF-IL6- [8] activation and hence might explain why we did not observe any co-localization. The significance of this concerted time-dependent distribution pattern of brain cell activation in the induction of brain derived sickness responses remains to be determined, but a role for NFκB in the initiation and for STAT3 (first phase) and NF-IL6 (second phase) in the maintenance of these responses has been suggested [8,46].

The way transcription factors like NFκB, STAT3 and NF-IL6 contribute to fever induction pathways seems to involve the two rate limiting enzymes for the PGE2 synthesis pathway, namely COX2 [5,7,8] and mPGES [6,47]. The present study further substantiates the link between NF-IL6/NFκB and COX2-induction. The small, but significant increase in mPGES expression is however puzzling, as a predominant functional and anatomical coupling of these two enzymes has been reported in several previous investigations [48,49]. However, COX2 IR in the brain precedes mPGES IR in time course experiments [50] and a recent report by Geatano et al. (2010) revealed mPGES activity to be already very high in the hypothalamus of non-stimulated animals, suggesting that the observed moderate increase of mRNA in the present study might not be of functional significance. Moreover, as the transcription factor early growth response 1 (Erg1) seems to be a key factor regulating the inducible mPGES mRNA expression [51], which so far has not been reported to be affected by parthenolide treatment, a more complex regulated expression of these two important enzymes COX2 and mPGES during brain inflammation is indicated. The reason why mPGES mRNA expression might have been increased when NFκB, and possibly NF-IL6 activation were attenuated, remains to be clarified.

LPS-induced brain oxidative stress has been proposed to be a component of an alternative fever inducing pathway [10]. Indeed, in the present study we revealed that parthenolide inhibiting hypothalamic oxidative stress might also have contributed to the observed reduction of the febrile response. Our results are in line with previous results by Li-Weber et al. (2005) showing anti-oxidative action of parthenolide using an *in vitro* model. PGC1α was proposed to be a master regulator of oxidative stress [26] and low protein levels have previously been detected in the rat hypothalamus using immunohistochemistry [52]. Others did not detect any PGC1α mRNA in the hypothalamus using in situ hybridisation in the mouse brain under basal and stimulated conditions [53], probably due to a lack of sensitivity of this method as opposed to real-time PCR used in our study. PGC1α activates the production of NRF1, which itself has also been shown to be expressed in brain tissue [54]. In addition, NRF1 has been shown to be induced by LPS-induced oxidative stress 6 h after stimulation in the liver [33]. Although we could not detect increased PGC1α or NRF1 expression 8 h after LPS-stimulation, parthenolide significantly reduced their mRNA expression levels to values comparable to those noted in the unstimulated counterpart controls. Thus, our data indicate that parthenolide might have had anti-oxidative effects on the brains of these animals. However, TFAM e.g. mitochondrial

DNA replication was not significantly altered and LPS did not significantly induce TFAM nor PGC1α or NRF1. Therefore, the effect of parthenolide on oxidative stress in the brain *in vivo* is partially speculative and should be confirmed in future experiments. Moreover, spatiotemporal changes in the expression of these genes during the complete time course of LPS-induced brain inflammation remain to be determined.

In summary, we are the first to show, that parthenolide, a substance which was recently found to be the main active component of plant extracts used for their anti-inflammatory effects on fever, migraine and arthritis [11], exerts some moderately beneficial effects *in vivo* on LPS-induced fever. We propose parthenolides' fever reducing action to be most likely due to peripheral inhibition of circulating IL-6 and TNFα activity and to its direct central action on brain cells via partial inhibition of oxidative stress, the NFκB and NF-IL6 but not the STAT3 signaling pathway and the brain-intrinsic formation of cytokines at brain cites with an incomplete BBB. Future studies are needed to confirm these observations and to reveal the potential therapeutic benefit of this substance. Still, our observations suggest that parthenolide can be a useful tool to reduce the effects of oxidative and inflammatory processes taking place within the brain.

Conflict of interest

None declared.

Acknowledgments

We would like to thank Doreen Marks, Jolanta Murgott and Daniela Ott for excellent technical assistance and Dr. Tina Wenz for her advice on genes implicated in mitochondrial biogenesis. This study was supported by the Emmy Noether Program of the German Research Foundation [DFG Project RU 1397/2-1].

References

[1] Dantzer R, O'Connor JC, Freund GG, Johnson RW, Kelley KW. From inflammation to sickness and depression: when the immune system subjugates the brain. Nat Rev Neurosci 2008;9:46–56.
[2] Conti B, Tabarean I, Andrei C, Bartfai T. Cytokines and fever. Front Biosci 2004;9:1433–49.
[3] Roth J, Harré EM, Rummel C, Gerstberger R, Hübschle T. Signaling the brain in systemic inflammation: role of sensory circumventricular organs. Front Biosci 2004;9:290–300.
[4] Matsumura K, Kobayashi S. Signaling the brain in inflammation: the role of endothelial cells. Front Biosci 2004;9:2819–26.
[5] Nadjar A, Tridon V, May MJ, Ghosh S, Dantzer R, Amedee T, et al. NFkappaB activates in vivo the synthesis of inducible Cox-2 in the brain. J Cereb Blood Flow Metab 2005;25:1047–59.
[6] Oka Y, Ibuki T, Matsumura K, Namba M, Yamazaki Y, Poole S, et al. Interleukin-6 is a candidate molecule that transmits inflammatory information to the CNS. Neuroscience 2007;145:530–8.
[7] Rummel C, Sachot C, Poole S, Luheshi GN. Circulating interleukin-6 induces fever through a STAT3-linked activation of COX-2 in the brain. Am J Physiol Regul Integr Comp Physiol 2006;291:R1316–26.
[8] Damm J, Luheshi GN, Gerstberger R, Roth J, Rummel C. Spatiotemporal nuclear factor interleukin-6 expression in the rat brain during lipopolysaccharide-induced fever is linked to sustained hypothalamic inflammatory target gene induction. J Comp Neurol 2011;519:480–505.
[9] Lazarus M, Yoshida K, Coppari R, Bass CE, Mochizuki T, Lowell BB, et al. EP3 prostaglandin receptors in the median preoptic nucleus are critical for fever responses. Nat Neurosci 2007;10:1131–3.
[10] Riedel W, Lang U, Oetjen U, Schlapp U, Shibata M. Inhibition of oxygen radical formation by methylene blue, aspirin, or alpha-lipoic acid, prevents bacterial-lipopolysaccharide-induced fever. Mol Cell Biochem 2003;247:83–94.
[11] Yuan G, Wahlqvist ML, He G, Yang M, Li D. Natural products and anti-inflammatory activity. Asia Pac J Clin Nutr 2006;15:143–52.
[12] Li-Weber M, Palfi K, Giaisi M, Krammer PH. Dual role of the anti-inflammatory sesquiterpene lactone: regulation of life and death by parthenolide. Cell Death Differ 2005;12:408–9.
[13] Pandey DK, Rajkumar R, Mahesh R, Radha R. Depressant-like effects of parthenolide in a rodent behavioural antidepressant test battery. J Pharm Pharmacol 2008;60:1643–50.
[14] Tassorelli C, Greco R, Morazzoni P, Riva A, Sandrini G, Nappi G. Parthenolide is the component of tanacetum parthenium that inhibits nitroglycerin-induced Fos activation: studies in an animal model of migraine. Cephalalgia 2005;25:612–21.
[15] Kawasaki BT, Hurt EM, Kalathur M, Duhagon MA, Milner JA, Kim YS, et al. Effects of the sesquiterpene lactone parthenolide on prostate tumor-initiating cells: an integrated molecular profiling approach. Prostate 2009;69:827–37.
[16] Anderson KN, Bejcek BE. Parthenolide induces apoptosis in glioblastomas without affecting NF-kappaB. J Pharmacol Sci 2008;106:318–20.
[17] Kwok BH, Koh B, Ndubuisi MI, Elofsson M, Crews CM. The anti-inflammatory natural product parthenolide from the medicinal herb Feverfew directly binds to and inhibits IkappaB kinase. Chem Biol 2001;8:759–66.
[18] Hehner SP, Heinrich M, Bork PM, Vogt M, Ratter F, Lehmann V, et al. Sesquiterpene lactones specifically inhibit activation of NF-kappa B by preventing the degradation of I kappa B-alpha and I kappa B-beta. J Biol Chem 1998;273:1288–97.
[19] Mathema VB, Koh YS, Thakuri BC, Sillanpaa M. Parthenolide, a sesquiterpene lactone, expresses multiple anti-cancer and anti-inflammatory activities. Inflammation 2011.
[20] Sobota R, Szwed M, Kasza A, Bugno M, Kordula T. Parthenolide inhibits activation of signal transducers and activators of transcription (STATs) induced by cytokines of the IL-6 family. Biochem Biophys Res Commun 2000;267:329–33.
[21] Kozak W, Wrotek S, Kozak A. Pyrogenicity of CpG-DNA in mice: role of interleukin-6, cyclooxygenases, and nuclear factor-kappaB. Am J Physiol Regul Integr Comp Physiol 2006;290:R871–80.
[22] Li X, Cui X, Li Y, Fitz Y, Hsu L, Eichacker PQ. Parthenolide has limited effects on nuclear factor-kappa beta increases and worsens survival in lipopolysaccharide-challenged C57BL/6J mice. Cytokine 2006;33:299–308.
[23] Smolinski AT, Pestka JJ. Modulation of lipopolysaccharide-induced proinflammatory cytokine production in vitro and in vivo by the herbal constituents apigenin (chamomile), ginsenoside Rb(1) (ginseng) and parthenolide (feverfew). Food Chem Toxicol 2003;41:1381–90.
[24] Hwang D, Fischer NH, Jang BC, Tak H, Kim JK, Lee W. Inhibition of the expression of inducible cyclooxygenase and proinflammatory cytokines by sesquiterpene lactones in macrophages correlates with the inhibition of MAP kinases. Biochem Biophys Res Commun 1996;226:810–8.
[25] Gomez-Hernandez A, Martin-Ventura JL, Sanchez-Galan E, Vidal C, Ortego M, Blanco-Colio LM, et al. Overexpression of COX-2, prostaglandin E synthase-1 and prostaglandin E receptors in blood mononuclear cells and plaque of patients with carotid atherosclerosis: regulation by nuclear factor-kappaB. Atherosclerosis 2006;187:139–49.
[26] Vina J, Gomez-Cabrera MC, Borras C, Froio T, Sanchis-Gomar F, Martinez-Bello VE, et al. Mitochondrial biogenesis in exercise and in ageing. Adv Drug Deliv Rev 2009;61:1369–74.
[27] Ott D, Murgott J, Rafalzik S, Wuchert F, Schmalenbeck B, Roth J, et al. Neurons and glial cells of the rat organum vasculosum laminae terminalis directly respond to lipopolysaccharide and pyrogenic cytokines. Brain Res 2010;1363:93–106.
[28] Paxinos G, Watson C. The rat brain in stereotaxic coordinates. 4th ed. San Diego: Academic Press; 1998.
[29] Knorr C, Hubschle T, Murgott J, Muhlradt P, Gerstberger R, Roth J. Macrophage-activating lipopeptide-2 (MALP-2) induces a localized inflammatory response in rats resulting in activation of brain sites implicated in fever. Brain Res 2008;1205:36–46.
[30] Harré EM, Roth J, Pehl U, Kueth M, Gerstberger R, Hubschle T. Selected contribution: role of IL-6 in LPS-induced nuclear STAT3 translocation in sensory circumventricular organs during fever in rats. J Appl Physiol 2002;92:2657–66.
[31] Schiltz JC, Sawchenko PE. Distinct brain vascular cell types manifest inducible cyclooxygenase expression as a function of the strength and nature of immune insults. J Neurosci 2002;22:5606–18.
[32] Polfliet MM, Fabriek BO, Daniels WP, Dijkstra CD, van den Berg TK. The rat macrophage scavenger receptor CD163: expression, regulation and role in inflammatory mediator production. Immunobiology 2006;211:419–25.
[33] Suliman HB, Carraway MS, Welty-Wolf KE, Whorton AR, Piantadosi CA. Lipopolysaccharide stimulates mitochondrial biogenesis via activation of nuclear respiratory factor-1. J Biol Chem 2003;278:41510–8.
[34] Shah VO, Ferguson JE, Hunsaker LA, Deck LM, Vander Jagt DL. Natural products inhibit LPS-induced activation of pro-inflammatory cytokines in peripheral blood mononuclear cells. Nat Prod Res 2010;24:1177–88.
[35] Sheehan M, Wong HR, Hake PW, Zingarelli B. Parthenolide improves systemic hemodynamics and decreases tissue leukosequestration in rats with polymicrobial sepsis. Crit Care Med 2003;31:2263–70.
[36] Nautiyal KM, McKellar H, Silverman AJ, Silver R. Mast cells are necessary for the hypothermic response to LPS-induced sepsis. Am J Physiol Regul Integr Comp Physiol 2009;296:R595–602.
[37] Lee JJ, Huang WT, Shao DZ, Liao JF, Lin MT. Blocking NF-kappaB activation may be an effective strategy in the fever therapy. Jpn J Physiol 2003;53:367–75.
[38] Shao DZ, Lee JJ, Huang WT, Liao JF, Lin MT. Inhibition of nuclear factor-kappa B prevents staphylococcal enterotoxin A-induced fever. Mol Cell Biochem 2004;262:177–85.
[39] Sheehan M, Wong HR, Hake PW, Malhotra V, O'Connor M, Zingarelli B. Parthenolide, an inhibitor of the nuclear factor-kappaB pathway, ameliorates cardiovascular derangement and outcome in endotoxic shock in rodents. Mol Pharmacol 2002;61:953–63.

[40] Reuter U, Chiarugi A, Bolay H, Moskowitz MA. Nuclear factor-kappaB as a molecular target for migraine therapy. Ann Neurol 2002;51: 507–16.
[41] Weber JT, O'Connor MF, Hayataka K, Colson N, Medora R, Russo EB, et al. Activity of parthenolide at 5HT2A receptors. J Nat Prod 1997; 60:651–3.
[42] Brown R, Imran SA, Wilkinson M. Lipopolysaccharide (LPS) stimulates adipokine and socs3 gene expression in mouse brain and pituitary gland in vivo, and in N-1 hypothalamic neurons in vitro. J Neuroimmunol 2009;209:96–103.
[43] Nadjar A, Combe C, Layé S, Tridon V, Dantzer R, Amedee T, et al. Nuclear factor kB nuclear translocation as a crucial marker of brain response to interleukin-1. A study in rat and interleukin-1 type I deficient mouse. J Neurochem 2003;87:1024–36.
[44] Gautron L, Lafon P, Chaigniau M, Tramu G, Laye S. Spatiotemporal analysis of signal transducer and activator of transcription 3 activation in rat brain astrocytes and pituitary following peripheral immune challenge. Neuroscience 2002;112:717–29.
[45] Rummel C, Voss T, Matsumura K, Korte S, Gerstberger R, Roth J, et al. Nuclear STAT3 translocation in guinea pig and rat brain endothelium during systemic challenge with lipopolysaccharide and interleukin-6. J Comp Neurol 2005;491:1–14.
[46] Rummel C, Hübschle T, Gerstberger R, Roth J. Nuclear translocation of the transcription factor STAT3 in the guinea pig brain during systemic or localised inflammation. J Physiol 2004;557:671–87.
[47] Uematsu S, Matsumoto M, Takeda K, Akira S. Lipopolysaccharide-dependent prostaglandin E(2) production is regulated by the glutathione-dependent prostaglandin E(2) synthase gene induced by the Toll-like receptor 4/MyD88/NF-IL6 pathway. J Immunol 2002;168:5811–6.
[48] Yamagata K, Matsumura K, Inoue W, Shiraki T, Suzuki K, Yasuda S, et al. Coexpression of microsomal-type prostaglandin E synthase with cyclooxygenase-2 in brain endothelial cells of rats during endotoxin-induced fever. J Neurosci 2001;21:2669–77.
[49] Gaetano L, Watanabe K, Barogi S, Coceani F. Cyclooxygenase-2/microsomal prostaglandin E synthase-1 complex in the preoptic-anterior hypothalamus of the mouse: involvement through fever to intravenous lipopolysaccharide. Acta Physiol (Oxf) 2010;200:315–24.
[50] Inoue W, Matsumura K, Yamagata K, Takemiya T, Shiraki T, Kobayashi S. Brain-specific endothelial induction of prostaglandin E(2) synthesis enzymes and its temporal relation to fever. Neurosci Res 2002;44:51–61.
[51] Naraba H, Yokoyama C, Tago N, Murakami M, Kudo I, Fueki M, et al. Transcriptional regulation of the membrane-associated prostaglandin E2 synthase gene. Essential role of the transcription factor Egr-1. J Biol Chem 2002;277:28601–8.
[52] Cowell RM, Blake KR, Russell JW. Localization of the transcriptional coactivator PGC-1alpha to GABAergic neurons during maturation of the rat brain. J Comp Neurol 2007;502:1–18.
[53] Tritos NA, Mastaitis JW, Kokkotou EG, Puigserver P, Spiegelman BM, Maratos-Flier E. Characterization of the peroxisome proliferator activated receptor coactivator 1 alpha (PGC 1alpha) expression in the murine brain. Brain Res 2003;961:255–60.
[54] Hertel M, Braun S, Durka S, Alzheimer C, Werner S. Upregulation and activation of the Nrf-1 transcription factor in the lesioned hippocampus. Eur J Neurosci 2002;15:1707–11.

1.4. „Circulating IL-6 contributes to peripheral LPS-induced mPGES-1 expression in the rat brain“

Rummel C., Matsumura K., Luheshi GN.

Brain Res Bull (2011) 86: 319-25

Impakt Faktor: 2,498

Eigener Anteil an der Publikation:

- Initiative: eigenständig (95 %)
- Projektplanung: weitgehend eigenständig (75 %)
- Durchführung der Versuche: eigenständig (95 %)
- Auswertung der Experimente: eigenständig (95 %)
- Erstellung der Publikation: weitgehend eigenständig (75 %)

Brain Research Bulletin 86 (2011) 319–325

Contents lists available at SciVerse ScienceDirect

Brain Research Bulletin

journal homepage: www.elsevier.com/locate/brainresbull

Research report

Circulating IL-6 contributes to peripheral LPS-induced mPGES-1 expression in the rat brain

Christoph Rummel [a,*], Kiyoshi Matsumura [b], Giamal N. Luheshi [a]

[a] Douglas Mental Health University Institute, Department of Psychiatry, McGill University, Montreal, Quebec H4H 1R3, Canada
[b] Department of Information Science and Technology, Osaka Institute of Technology, 1-79-1 Kitayama, Hirakata-City, Osaka 573-0196, Japan

ARTICLE INFO

Article history:
Received 27 June 2011
Received in revised form 24 August 2011
Accepted 10 September 2011
Available online 16 September 2011

Keywords:
Immune-to-brain communication
Prostaglandins
fever
STAT3
COX2
Localized inflammation

ABSTRACT

Interleukin-(IL)6 is the most prominent circulating cytokine induced by systemic infection and inflammation, and the main humoral mediator to the brain in fever. We have previously demonstrated that the PG-pathway, the ultimate step in fever generation, is activated by circulating IL-6 by triggering the expression of the rate limiting enzyme cyclooxygenase (COX)2 in the brain. Downstream of COX2, another enzyme, microsomal PG synthase (mPGES)-1 has also been implicated in the inflammatory response but relatively little is known about its role in cytokine mediated inflammation. Here, we investigated for the first time the direct role of circulating IL-6 in brain and peripheral mPGES-1-expression. Rats were either treated with LPS into a subcutaneous air pouch combined with intraperitoneal injection of a rat specific IL-6 antiserum (AS) or received a single intraperitoneal injection of IL-6. LPS increased the expression of mPGES-1 mRNA in the brain, liver and brown adipose tissue (BAT) but not epididymal white (eW) adipose tissue. This response was reversed by IL-6AS in LPS-injected animals for the brain and liver. IL-6-treatment only induced mPGES-1-expression in the brain and its immunoreactivity co-localized with phosphorylated signal transducer and activator of transcription (STAT)3 the main transcription factor activated by IL-6. Moreover, circulating IL-6 levels and the suppressor of cytokine signaling (SOCS)-3, a broadly used marker of STAT3-activation, strongly correlated with mPGES-1 expression in the brain. In summary, we have clearly shown that circulating IL-6 can directly induce mPGES-1 linked to STAT3-activation in the brain but not peripheral tissues of rats during localised peripheral inflammation.

© 2011 Elsevier Inc. All rights reserved.

1. Introduction

Circulating levels of the pro-inflammatory cytokine interleukin (IL)-6 dramatically increase during infection and inflammation and correlate with a rise in core body temperature [41]. Moreover, plasma IL-6 is consistently increased in a variety of chronic low grade inflammatory conditions such as in obese individuals [11] or during aging [3,21,52], and appears to be a strong risk factor for inflammatory disease including atherosclerosis [15,18]. Interestingly, the precise role of circulating IL-6 in health and disease has not been extensively studied and remains relatively unknown. It has been shown that depending on the dose and route of peripheral administration, fever inducing capacities of recombinant IL-6 are strong in rabbits [16], rather moderate in rats [6,15,46] or even absent in mice [7,28,33,56]. Thus, unlike other pro-inflammatory cytokines such as IL-1β [9], circulating IL-6 shows diverse pyrogenic capacities. Some studies question the involvement of IL-6 in the induction of the rate limiting enzymes of the prostaglandin (PG)E2-synthesis pathway namely cyclooxygenase (COX)2 and microsomal PGE2 synthase (mPGES)-1 [25,33,34,45,46,54,55]; both of which lead to the production of PGE2, the pivotal terminal mediator in fever and inflammation [49]. Previously, we, and others have demonstrated unequivocally that circulating IL-6 participates in brain COX2-induction during inflammation using the injection of turpentine into the hind limb [54] or LPS into a subcutaneous airpouch [46]. In the present study we sought to investigate the role of circulating IL-6 in mPGES-1 expression. A previous study using a model of localized carageenan-induced inflammation demonstrated that circulating IL-6 most likely participates in the induction of both mPGES-1 and COX2 in

Abbreviations: BBB, blood–brain barrier; BAT, brown adipose tissue; COX2, cyclooxygenase 2; CVOs, circumventricular organs; DAPI, 4′,6-diamidino-2-phenyl-indole dilactate; eW, epididymal white; IL-1β, interleukin-1 beta; IL-6, interleukin-6; IR, immunoreactivity; LPS, lipopolysaccharide; mPGES, microsomal PGE2 synthase; NFκB, nuclear factor kappa B; NF-IL6, nuclear factor IL-6; OVLT, vascular organ of the lamina terminalis; PBS, phosphate buffered saline; PG, prostaglandin; RT, room temperature; RT-PCR, reverse transcription polymerase chain reaction; SOCS3, suppressor of cytokine signaling 3; STAT3, signal transducer and activator of transcription 3.

* Corresponding author. Present address: Institute of Veterinary-Physiology and -Biochemistry, Justus-Liebig-University Giessen, Frankfurter Strasse 100, D-35392 Giessen, Germany. Tel.: +49 641 99 38850; fax: +49 641 99 38159.
E-mail address: Christoph.D.Rummel@vetmed.uni-giessen.de (C. Rummel).

0361-9230/$ – see front matter © 2011 Elsevier Inc. All rights reserved.
doi:10.1016/j.brainresbull.2011.09.006

Author's personal copy

the spinal cord of rats [34]. Interestingly, there is increasing evidence of differential regulation of COX2 and mPGES-1 [49]. This is quite a surprising observation as it was clearly demonstrated that these two enzymes are functionally and microanatomically coupled [57]. Nonetheless, differences in kinetics of the induction of these enzymes in the brain after LPS-stimulation in vivo have been observed [19]. Moreover, in vitro studies using several signaling pathway inhibitors in cell cultures of rat microglia [10] and human fibroblasts [58] have revealed partially uncoupled regulation of COX2 and mPGES-1. Thus, we decided to test whether circulating IL-6 directly participates in mPGES-1 expression in the brain and peripheral organs of rats in a similar way as previously shown for COX2 [46]. For peripheral tissues we chose to investigate the liver as a known important source of PGE2 production during systemic inflammation [2] and adipose tissue as this was previously described to express the highest levels of mPGES-1 relative to other tissue samples [17].

2. Materials and methods

Male Sprague-Dawley rats (Charles River, Saint Constant, Canada) with body weights (BW) in the range of 290–320 g were used for this study. After surgery animals were housed individually in a controlled environment at 21 ± 2 °C under a 12:12 h day–night cycle with lights on from 7:00 a.m. to 7:00 p.m. with free access to standard laboratory chow and water. Anesthetized animals (ketamine/xylazine/acepromazine (50, 5, and 0.5 mg/kg, respectively) received 20 ml of sterile air injected into the subcutaneous tissue of the dorsal midline at the level of the scapulae to form an 'air-pouch' for administering the inflammatory agent, as previously described [12,46]. Injections were performed between 1:00 and 2:00 p.m. directly into the subcutaneous air pouches (ipo) in lightly restrained (hand held), conscious animals. The Animal Care Committee of McGill University pursuant to the Canadian Council of Animal Care guidelines approved all experimental procedures.

IL-6AS experiment: One group of animals including controls were pre-treated (−4 h) either intraperitoneally (i.p.) with 1.8 ml normal sheep serum ($n = 10$; NSS; Sigma) or 1.8 ml of sheep anti-rat IL-6 serum ($n = 5$; IL-6AS; National Institute for Biological Standards and Control; NIBSC, Potters Bar, UK). Some animals (for NSS and IL-6AS; $n = 5$ each) were injected ipo with bacterial LPS (derived from *Escherichia coli*, suspended in sterile pyrogen-free 0.9% saline; 0111:B4, Lot 42k4120; L-2630, Sigma) at 100 μg/kg (prepared as 100 μg/ml solution, 1 ml/kg). *IL-6 experiment*: A different group of rats ($n = 4$) received an i.p. injection of rrIL-6 (*E. coli*-derived, non-glycolysated, specific activity 2,500,000 IU/μg as measured in a B9 mouse hybridoma bioassay, NIBSC) at a dose of 45 μg/kg and a volume of 1 ml/kg diluted in sterile 0.9% saline. Equivalent volumes of the vehicle (0.9% saline, 1 ml/kg, each $n = 5$) were injected ipo or i.p. respectively in control groups. The animals were euthanized 2 h after treatment by using terminal anesthesia (ketamine/xylazine/acepromazine; 100, 10, and 1 mg/kg, respectively via i.p. injection), blood samples were collected via cardiac puncture, rats transcardially perfused with 150 ml ice-cold 0.9% NaCl solution, their brains, liver, epididymal white adipose tissue (eWAT) and interscapular brown (B)AT (from the site of localized inflammation in the airpouch model) quickly removed, frozen in powdered dry ice and kept at −80 °C until analysis as previously described [47].

To determine IL-6 concentration, heparinized (10 IU/ml) blood was centrifuged (5300 g, 10 min, 4 °C), the supernatant was collected and stored at −80 °C until assays were performed. IL-6 levels were measured in duplicates using a two sites, rat-specific ELISA (NIBSC, Potters Bar, UK) as reported previously [36].

Immunohistochemistry was performed on coronal cryostat sections (20 μm, CM 3050 S cryostat, Leica Microsystems, Nussloch, Germany), which were prepared as described elsewhere [46]. In order to perform RT-PCR and immunohistochemistry from the same brain, every third consecutive frozen section was thaw-mounted on poly L-lysine coated glass slides for immunohistochemistry and stored at −80 °C until processing. The remainder of the serial whole brain sections were collected for RNA extraction and stored in a cryotube at −80 °C for mRNA extraction.

Total RNA was extracted using Trizol (Invitrogen, Burlington, Ontario) according to the manufacturer's instructions and reverse transcription was performed as reported previously [46] using the same procedure, controls and design of primers. The gene accession numbers, primer sequences, annealing temperatures and cycle numbers used are listed as follows: mPGES-1 (NM_022415) sense 5′-TTTCTGCTCTGCAGCACACT-3′, anti-sense 5′-CATGGAGAAACAGGTGAACT-3′, 57 °C, 36 cycles; SOCS3 (NM_053565) sense 5′-CCAGCGCCACTTCTTCAC-3′, anti-sense 5′-GTGGAGCATCATACTGGTCC-3′, 60 °C, 40 cycles; β-actin (NM_031144) sense 5′-GCCGTCTTCCCCTCCATCGTG-3′, anti-sense 5′-TACGACCAGAGGCATACAGGGACAAC-3′, 60 °C, 20 cycles. PCR products were separated by 2% agarose gel electrophoresis and visualized with ethidium bromide staining. The band density was obtained for quantification using GeneTool image analysis software (Syngene, Frederick, MD). To normalize the expression level of genes between different samples, the levels were estimated as the ratio of geneX/β-actin.

Rabbit polyclonal anti-mPGES-1 IgG (1:500; cat: 160140; Cayman Chemical, Ann Arbor, MI), sheep polyclonal anti-von Willebrand factor (vW) IgG (1:3000; cat: SARTW-1G; Affinity Biologicals, Ancaster, Ontario) and mouse monoclonal anti-posphoSTAT3 IgG (1:200; cat: sc-8059; Santa Cruz Biotechnology, CA) were used to detect the respective molecules. Specificity of each antibody was shown previously [45,46,50,57]. On the day of the experiment, the frozen brain sections were air-dried at room temperature for 10 min and then immersion fixed in 0.1% sodium metaperiodate (only NaIO4 for co-localization of mPGES-1 with vW) and in 2% paraformaldehyde (for co-localization of mPGES-1 with pSTAT3) diluted in 0.1 M phosphate buffered saline (PBS, pH 7.4) for 10 min at room temperature (RT) each. Following 3 successive washes in PBS the sections were treated for 1 h at RT with a blocking solution consisting of PBS, containing 10% normal donkey serum (NDS; Chemicon International Inc., Temecula) and depending on the type of applied antibodies, 0.1% (mPGES-1/pSTAT3) or 0.5% (mPGES-1/vW) Triton-X100. The sections were incubated with the primary antibodies for 36–48 h at 4 °C followed by visualization with CY3 or FITC-conjugated donkey anti-rabbit IgG (mPGES-1; 1:500 dilution; cat: 711-165-152, 711-095-152) or FITC-conjugated donkey anti-sheep IgG (vW, 1:500 dilution; cat: 713-095-147) or CY3-conjugated donkey anti-mouse IgG (PSTAT3, 1:500 dilution; cat: 715-165-150). All secondary antibodies were raised in donkey and all were multiple labeling-grade (Jackson Immuno Reaserch, West Grove, PA). Sections were counterstained with the nuclear DAPI stain (Molecular Probes, Eugene, OR) for 15 min, using a 1:4000 dilution in PBS to judge for the perinuclear localization of mPGES-1, nuclear localization of pSTAT3 signals and to give better visualization of the tissue surrounding the signal. Finally all sections were cover slipped using an equal mix of glycerol/phosphate buffer solution and stored at 4 °C until microscopic analysis was performed.

One-way ANOVA followed by Newman–Keuls multiple comparisons post hoc test was used to compare relative mPGES-1 expression; a parametric unpaired two tailed t-test was used to compare IL-6- and vehicle-treated groups. We also investigated potential correlations between individual values of plasma IL-6 and SOCS3 mRNA expression with the respective relative density of mPGES-1 mRNA signals in the forebrain and brainstem with a two tailed *P*-value and Pearson correlation coefficient. Graph Pad Prism (GraphPad Prism, GraphPath Software Inc.) was used for the statistical analysis. Values (p value) less than 5% were deemed significant. Data in Fig. 1 are presented as mean values ±SEM.

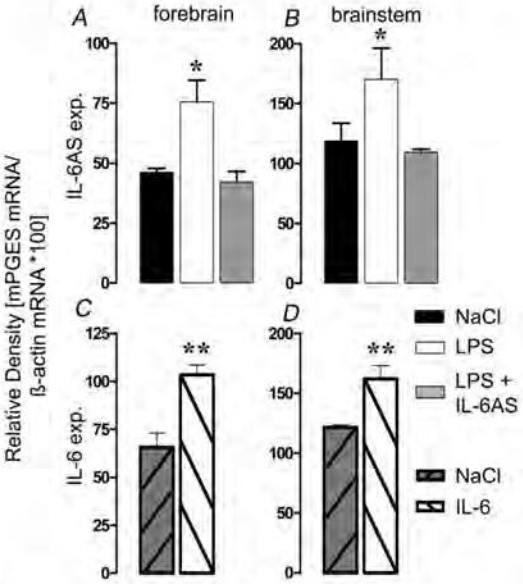


Fig. 1. IL-6 induces mPGES-1 mRNA expression in the rat brain. Injection of LPS (100 μg/kg ipo) induces a significant increase of mPGES-1 mRNA expression in the forebrain (A) and the brainstem (B) of rats 2 h after the injection (IL-6AS exp.). These responses were significantly attenuated by administration of IL-6AS (1.8 ml/kg i.p.). In addition, rrIL-6 treatment (45 μg/kg, i.p.; IL-6 exp.) induced a rise of mPGES-1 mRNA expression in the forebrain (C) and the brainstem (D) of rats 2 h after the injection. $^{*}P < 0.05$, $^{**}P < 0.01$; exp. = experiment.

author's personal copy

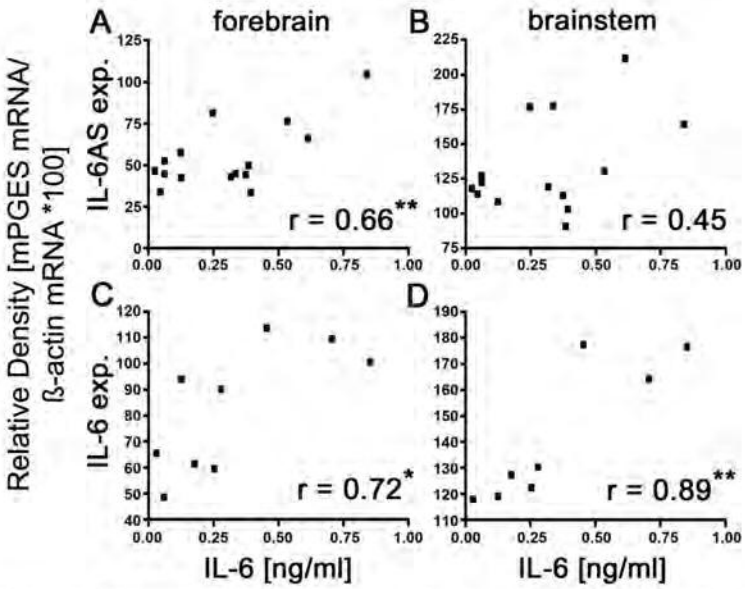


Fig. 2. Correlation analysis of circulating IL-6 levels with mPGES-1 mRNA expression in the rat brain. In LPS (100 μg/kg ipo) and NSS, LPS and IL-6AS (1.8 ml/kg i.p.) and NaCl and NSS treated animals circulating IL-6 levels significantly correlate to mPGES-1 mRNA expression in the forebrain (A) but not the brainstem (B) of rats 2 h after the injection from all individual pairs of values (black squares). In addition, circulating IL-6 levels of animals treated with rrIL-6 (45 μg/kg, i.p.) or NaCl significantly correlate to mPGES-1 mRNA expression in the forebrain (C) and the brainstem (D) from all individual pairs of values (black squares) of rats 2 h after the injection. *$P < 0.05$, **$P < 0.01$; r = Pearson correlation coefficient; exp. = experiment.

3. Results and discussion

Injection of LPS (100 μg/kg) ipo induced a significant increase of mPGES-1 expression in the forebrain and brainstem 2 h after stimulation, a response that was abolished by IL-6AS pretreatment (Fig. 1A and B). In addition, systemic treatment with a physiological dose of IL-6 [14,15] also increased mPGES-1 expression in the same areas (Fig. 1C and D). Interestingly, with the exception of the brainstem in the IL-6AS experiment, mPGES-1 mRNA expression shows high correlation to circulating IL-6 levels for the forebrain and the brainstem in both experimental models of either systemic injection of rat recombinant (rr)IL-6 or localized LPS-induced inflammation (Fig. 2).

Inflammation in the preformed airpouch results in the induction of IL-6, TNFα, IL-1β and chemokine of which only IL-6 and some chemokines leak into the circulation [4–6,24,31,53]. Moreover, mPGES-1 mRNA expression showed even higher correlation (Person $r = 0.6$ up to 0.94) to SOCS3 mRNA expression in the brains of these animals (Fig. 3). As a marker of STAT3-activation, which is involved in an inhibitory autoregulatory feedback [26], this correlation and SOCS3 expression itself suggest that IL-6 is directly involved in mPGES-1 expression via its main signaling pathway. Moreover, in support of this hypothesis we are able to demonstrate for the first time that LPS-activated phosphoSTAT3-immunoreactivity (IR) co-localizes with mPGES-1 IR in blood vessels (Fig. 4B and C) of the vascular organ of the lamina terminalis (Fig. 4A), a brain structure with a 'leaky' blood brain barrier, which is critically involved in sensing circulating mediators such as IL-6 [35,41] and is implicated in fever induction pathways [40]. Finally, we confirm that systemic injection of rrIL-6 at a dose which induces physiologically comparable plasma IL-6 concentrations to that injected with ipo LPS [14,46] not only increases mPGES-1 mRNA expression but also mPGES-1 IR in vW positive endothelial cells of the hypothalamus, when compared to NaCl treated controls (Fig. 4D and E). In the periphery (Fig. 5), LPS-injection induced mPGES-1 mRNA expression in the liver, a response that was abolished by IL-6AS to undetectable levels. In NaCl-injected counterpart controls mPGES-1 mRNA expression in the liver was also undetectable, as previously shown by others [20]. While LPS did not affect eWAT, it significantly increased mPGES-1 mRNA expression in BAT that was derived from the local inflammatory side of the air pouch situated in the interscapular region. However, this response was not altered by IL-6AS-treatment. Moreover, i.p. IL-6-administration did not influence mPGES-1 mRNA expression in any of the peripheral tissues investigated suggesting that circulating IL-6 alone does not play a significant role in mPGES-1-expression in peripheral organs. Interestingly, IL-6 was required to induced mPGES-1 expression in the liver during localized LPS-induced inflammation but was not sufficient to increase mPGES-1 mRNA expression when injected i.p. Thus an additional factor to IL-6 might be needed for mPGES-expression in the liver.

Chemokines might be important candidates for this role. These mediators are known to be induced in the airpouch fluid after LPS-stimulation and importantly can be also detected in the circulation of these animals [24]. In particular, the neutrophil chemoattractant, CINC1 an CXCL1 chemokine, is known to be rapidly increased at 2 h and reaching a peak at 4 h after stimulation [18]. This chemokine also induces a prostaglandin dependant fever when injected intracerebroventricularly in rats [51]. The capacity of chemokines to induce mPGES-1 expression is a question that will be explored in future studies. IL-1β or TNFα might also play an important role but they were reported not to leak into the circulation from the "air pouch" [4,31].

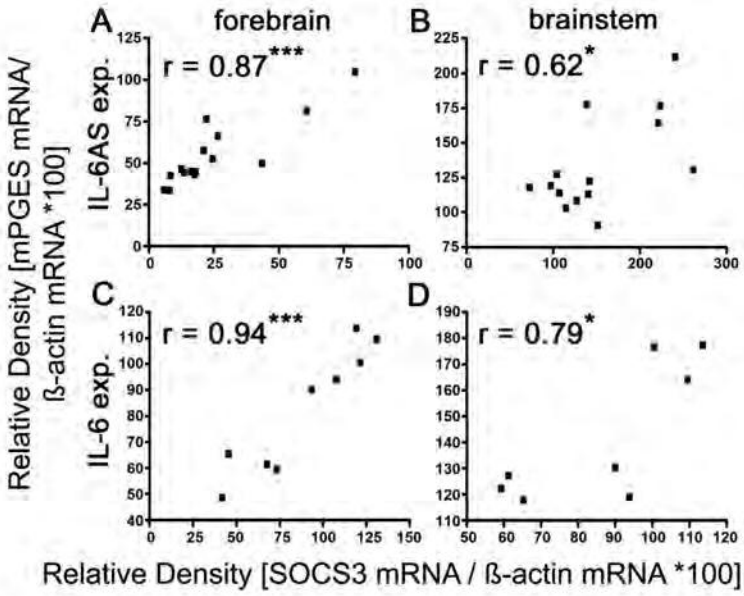


Fig. 3. Correlation analysis of mPGES-1 mRNA with SOCS3 mRNA expression in the rat brain. In LPS (100 μg/kg ipo) NSS, LPS IL-6AS (1.8 ml/kg i.p.) and NaCl NSS or rrIL-6 (45 μg/kg, i.p.) and NaCl treated animals mPGES-1 mRNA expression significantly correlates with SOCS3 mRNA expression in the forebrain (A, C) and the brainstem (B, D) of rats 2 h after treatment from all individual pairs of values (black squares). $^{*}P < 0.05$, $^{**}P < 0.01$, $^{***}P = 0.001$; r = Pearson correlation coefficient; exp. = experiment.

An alternative to the humoral mediators like IL-6 and chemokines is another route of immune-to brain communication involved in fever induction pathways during localized inflammation namely afferent sensory signals (for review [39]). Recently, it was even suggested that localized inflammation leads to a site-specific activation of neurons in the paraventricular nucleus, dependant on the localization of the inflammatory site (i.e. left or right and front or back limb [1]). Thus, it can be considered that during localized inflammation in the "air pouch" this neuronal pathway might have contributed to brain or peripheral (liver/BAT) mPGES-1 induction. However, the moderate fever inducing effects of neuronal activation were also shown to be undetectable when using the same dose of LPS as employed in the present study where humoral mediators like IL-6 reach a critical level [38,43,44]. The neuronal pathway seems to be overwritten by humoral pathways in these cases. The possible contribution of the neuronal pathway to mPGES-1 induction will be further investigated in future studies. However, we believe that this contribution will be minimal given the data supporting the role of the humoral signal [43,44,46].

The observations made in the present study contradict previous findings showing that circulating IL-6 lacks the capacity to induce COX2 and mPGES-1 [25,33,55]. This may be due to differences in sensitivity of the species that were investigated. Amongst rabbits [16], rats [6,15,46] and mice [7,28,33,56], it is known that rabbits are the most sensitive to the administration of the exogenous pyrogen LPS, followed by rats and subsequently by mice, which are less prone to high LPS-induced responses such as fever or endotoxin shock [22,37,42]. Thus, even higher amounts of the most prominent circulating cytokine (i.e. IL-6) might have been needed to achieve a potential critical threshold in mice as opposed to rats or rabbits to activate the PG-synthesis pathway. Notably, such a threshold for circulating IL-6-induced brain STAT3-activation was previously suggested in the guinea pig [44]. However, the studies showing no pyrogenic activity of systemic IL-6 treatment in mice [7,28,33,56] actually injected lower amounts of IL-6 than used for the present study in rats (45 μg/kg), which might account for the observed discrepancies in pyrogenic activity.

The reason why Nilsberth et al. [33] did not show any changes in COX2 and mPGES-1 expression in LPS-treated mice opposed to our previous findings [45] is not clear but might pertain to large variance in both studies or methodological differences (PCR, background of wild type animals used). Nonetheless, another recent study was able to show that mouse astrocytes produce PGE2 via an IL-6 dependent mechanism supporting our finding that IL-6 contributes to the induction of the rate limiting enzymes for PG-synthesis [8].

Overall, our observations strongly support the notion that circulating IL-6 acting on endothelial cells in the brain is able to induce mPGES-1 expression, the most important enzyme for PGE2 induction downstream of COX2. Therefore, knowing that IL-6 exhibits clear, but rather moderate capacities in COX2-induction [45,46], its pro-inflammatory capacities might primarily or complementary/supplementary be due to a more prominent mPGES-1 induction. This would also explain why we and others previously observed a permissive effect of systemic IL-6 injection when combined with low subpyrogenic doses of IL-1β [6,33]. A pivotal role of IL-1β in COX2-induction via the nuclear factor kappa B pathway [32] in brain endothelial cells [23] is well known. This strong effect of IL-1β on COX2 mRNA expression might be even enhanced by IL-6 action. Our current finding that LPS-induced mPGES-1 expression in the liver was IL-6 dependent while IL-6 was not sufficient to induce mPGES-1 expression alone (Fig. 5A and D) also suggests a permissive role of IL-6 for mPGES in this peripheral organ. Interestingly, the brain seems to be unique in its capacity to directly respond to IL-6 by induction of both COX2 and mPGES-1 by circulating IL-6 alone. Opposed to eWAT, BAT was directly

Author's personal copy

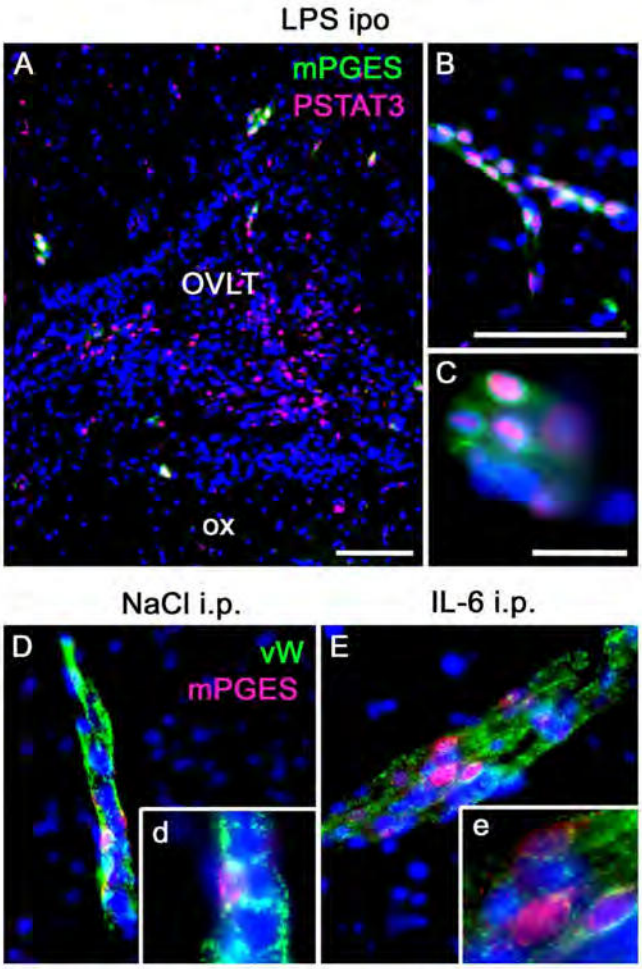


Fig. 4. LPS-induced mPGES-1-IR co-localizes with PSTAT-IR and systemic rrIL-6 injection induces mPGES-1-IR in rat brain endothelial cells. LPS (100 μg/kg ipo) treatment leads to induction of mPGES-1-IR (green) 2 h after the injection in the cranial portion of the rat vascular organ of the lamina terminalis (OVLT, A–C) and co-localizes with PSTAT3-IR (red) along blood vessels (B and C). Treatment with rrIL-6 (D and E; 45 μg/kg i.p.) induces increased mPGES-1-IR (red) within von Willebrand factor (vW, green) positive endothelial cells compared to NaCl i.p. injected controls. The perinuclear (blue nucleus, DAPI) staining of mPGES-1 can be clearly identified at high magnification (B and C, d–e). Scale bar in (A) and (B) represents 100 μm (B also applies to D and E); 25 μm in C and also applies to inserts (d–e); ox, optic chiasm. (For interpretation of the references to color in this figure legend, the reader is referred to the web version of the article.)

exposed to LPS in the local inflammatory site. Therefore, BAT might have shown this strong induction of mPGES-1 mRNA expression that was not altered by IL-6AS, which was injected systemically and might not have entered to the local site of inflammation in the preformed airpouch. In addition, the observed differences might be due to the divergent nature between BAT and WAT [48].

Given the emerging importance of mPGES-1 as a potential alternative therapeutic target to COX2 under a variety of inflammatory conditions including artherosclerosis and the fact that inhibitory drugs for mPGES-1 have less cardiovascular side effects [13,49], our observation support a potential beneficial effect of those drugs in common diseases related to increased circulating IL-6 levels. However, it needs to be clarified in future studies whether IL-6 is capable of activating one of the pathways, which are relevant for the uncoupled expression of COX2 and mPGES-1 as previously reported by others [10,58]. In general, other than for COX2, mPGES-1 expression seems to be primarily regulated by the transcription factors NF-IL6 and early growth response 1 (Egr1) both of which can be activated by IL-6 [30,57]. However, we did not previously detect NF-IL6 activation in the brain of rats injected with IL-6 or ipo LPS at the early 2 h time point [46] and the relevance of Egr1 activated by IL-6 or other cytokines in mPGES-1-induction in the brain remains to be clarified. Finally, a functional "crosstalk" between transcription

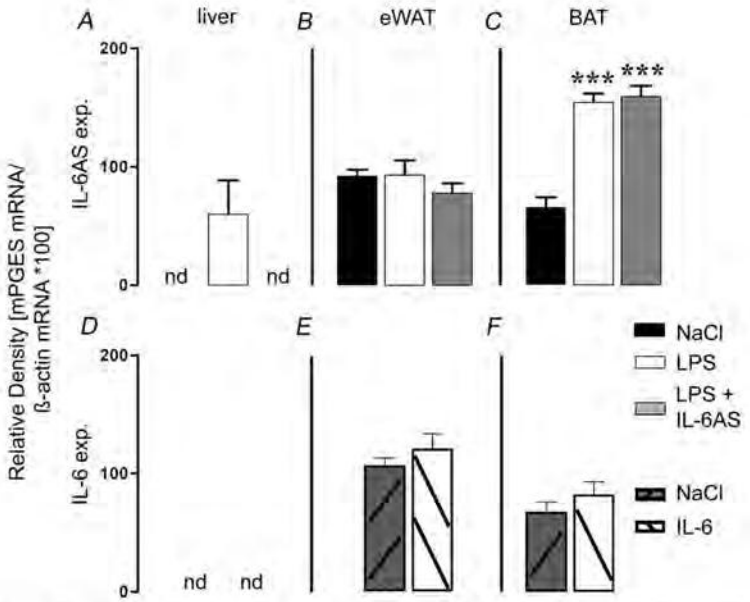


Fig. 5. IL-6 does not induce mPGES-1 mRNA expression in eWAT and BAT but might contributes to mPGES-1 mRNA expression in the liver. Injection of LPS (100 μg/kg ipo) induces a significant increase of mPGES-1 mRNA expression in the liver (A) and brown adipose tissue (BAT, C) but not epididymal adipose tissue (eWAT, B) of rats 2 h after the injection. This response was significantly attenuated by administration of IL-6AS (1.8 ml/kg i.p.) in the liver. In addition, rrIL-6 treatment (45 μg/kg, i.p.) did not induce any rise of mPGES-1 mRNA expression in the liver (D), eWAT (E) and BAT (F) of rats 2 h after the injection. $^{*}P < 0.05$, $^{**}P < 0.01$; exp. = experiment, nd = not detectable.

factors including STAT3 might explain the potential participation of IL-6 in mPGES-1 induction as previously suggested for COX2 [46]. In support of this hypothesis we observed co-localization of mPGES-1 with activated STAT3-IR and a robust correlation of SOCS3 with mPGES-1 mRNA-expression. Overall, a role for circulating IL-6 to the differential regulation of both rate-limiting enzymes for PGE2-induction might be even more exhaustive/potent for mPGES-1 than for COX2.

In conclusion, we provide critical evidence for a direct contribution of circulating IL-6 in mPGES-1 induction in the brain but not the periphery (liver, eWAT or BAT), possibly linked to STAT3-activation and fever. We further propose that the amplitude of IL-6 action on fever and inflammation might additionally depend on sufficient concentrations of other mediators, such as IL-1β or chemokines, that possess stronger capacities to induce COX2 (brain) or co-stimulate mPGES (liver). This observation has marked implications for a variety of inflammatory conditions that are accompanied with elevated circulating IL-6 levels including obesity [11], aging [3,21,52] or atherosclerosis [27,29].

Conflict of interest

None.

Acknowledgements

This work was supported by the Canadian Institutes of Health Research and Natural Sciences, the Engineering Research Council of Canada and C. Rummel by a scholarship from the Deutsche Forschungsgemeinschaft, Grant number: DFG project RU 1397/1-1. We thank Ms. G. Somay for excellent technical assistance

References

[1] N. Belevych, K. Buchanan, Q. Chen, M. Bailey, N. Quan, Location-specific activation of the paraventricular nucleus of the hypothalamus by localized inflammation, Brain Behav. Immun. 24 (2010) 1137–1147.
[2] C.M. Blatteis, Endotoxic fever: new concepts of its regulation suggest new approaches to its management, Pharmacol. Ther. 111 (2006) 194–223.
[3] H. Brüünsgaard, B.K. Pedersen, Age-related inflammatory cytokines and disease, Immunol. Allergy Clin. North Am. 23 (2003) 15–39.
[4] T. Cartmell, G.N. Luheshi, S.J. Hopkins, N.J. Rothwell, S. Poole, Role of endogenous interleukin-1 receptor antagonist in regulating fever induced by localised inflammation in the rat, J. Physiol. 531 (2001) 171–180.
[5] T. Cartmell, A.J. Miller, Y. Mistry, N.J. Rothwell, G.N. Luheshi, Circulating IL-6 is derived from the site of inflammation in response to a localized injection of lipopolysaccharide in the rat, J. Physiol. (1998) 146–513.
[6] T. Cartmell, S. Poole, A.V. Turnbull, N.J. Rothwell, G.N. Luheshi, Circulating interleukin-6 mediates the febrile response to localised inflammation in rats, J. Physiol. 526 (Pt 3) (2000) 653–661.
[7] Z. Chai, S. Gatti, C. Toniatti, V. Poli, T. Bartfai, Interleukin, (IL)-6 gene expression in the central nervous system is necessary for fever response to lipopolysaccharide or IL-1 beta: a study on IL-6-deficient mice, J. Exp. Med. 183 (1996) 311–316.
[8] T. Chikuma, T. Yoshimoto, M. Ohba, M. Sawada, T. Kato, T. Sakamoto, Y. Hiyama, H. Hojo, Interleukin-6 induces prostaglandin E(2) synthesis in mouse astrocytes, J. Mol. Neurosci. 39 (2009) 175–184.
[9] B. Conti, I. Tabarean, C. Andrei, T. Bartfai, Cytokines and fever, Front Biosci. 9 (2004) 1433–1449.
[10] A.C. de Oliveira, E. Candelario-Jalil, H.S. Bhatia, K. Lieb, M. Hull, B.L. Fiebich, Regulation of prostaglandin E2 synthase expression in activated primary rat microglia: evidence for uncoupled regulation of mPGES-1 and COX-2, Glia 56 (2008) 844–855.
[11] K. Eder, N. Baffy, A. Falus, A.K. Fulop, The major inflammatory mediator interleukin-6 and obesity, Inflamm. Res. 58 (2009) 727–736.
[12] J.C. Edwards, A.D. Sedgwick, D.A. Willoughby, The formation of a structure with the features of synovial lining by subcutaneous injection of air: an in vivo tissue culture system, J. Pathol. 134 (1981) 147–156.
[13] M.D. Guerrero, M. Aquino, I. Bruno, R. Riccio, M.C. Terencio, M. Paya, Anti-inflammatory and analgesic activity of a novel inhibitor of microsomal prostaglandin E synthase-1 expression, Eur. J. Pharmacol. 620 (2009) 112–119.
[14] E.M. Harré, J. Roth, R. Gerstberger, T. Hübschle, Interleukin-6 mediates lipopolysaccharide-induced nuclear STAT3 translocation in astrocytes of rat sensory circumventricular organs, Brain Res. 980 (2003) 151–155.

Author's personal copy

[15] E.M. Harré, J. Roth, U. Pehl, M. Kueth, R. Gerstberger, T. Hubschle, Selected contribution: role of IL-6 in LPS-induced nuclear STAT3 translocation in sensory circumventricular organs during fever in rats, J. Appl. Physiol. 92 (2002) 2657–2666.
[16] M. Helle, J.P. Brakenhoff, E.R. De Groot, L.A. Aarden, Interleukin 6 is involved in interleukin 1-induced activities, Eur. J. Immunol. 18 (1988) 957–959.
[17] P.O. Hetu, D. Riendeau, Down-regulation of microsomal prostaglandin E2 synthase-1 in adipose tissue by high-fat feeding, Obesity (Silver Spring) 15 (2007) 60–68.
[18] M. Iida, K. Watanabe, M. Tsurufuji, K. Takaishi, Y. Iizuka, S. Tsurufuji, Level of neutrophil chemotactic factor CINC/gro, a member of the interleukin-8 family, associated with lipopolysaccharide-induced inflammation in rats, Infect Immun. 60 (1992) 1268–1272.
[19] W. Inoue, K. Matsumura, K. Yamagata, T. Takemiya, T. Shiraki, S. Kobayashi, Brain-specific endothelial induction of prostaglandin E(2) synthesis enzymes and its temporal relation to fever, Neurosci. Res. 44 (2002) 51–61.
[20] A.I. Ivanov, R.S. Pero, A.C. Scheck, A.A. Romanovsky, Prostaglandin E(2)-synthesizing enzymes in fever: differential transcriptional regulation, Am. J. Physiol. Regul. Integr. Comp. Physiol. 283 (2002) R1104–R1117.
[21] O.Y. Kim, J.S. Chae, J.K. Paik, H.S. Seo, Y. Jang, J.M. Cavaillon, J.H. Lee, Effects of aging and menopause on serum interleukin-6 levels and peripheral blood mononuclear cell cytokine production in healthy nonobese women, Age (Dordr) (2011).
[22] M.J. Kluger, Fever: role of pyrogens and cryogens, Physiol. Rev. 71 (1991) 93–127.
[23] J.P. Konsman, S. Vigues, L. Mackerlova, A. Bristow, A. Blomqvist, Rat brain vascular distribution of interleukin-1 type-1 receptor immunoreactivity: relationship to patterns of inducible cyclooxygenase expression by peripheral inflammatory stimuli, J. Comp. Neurol. 472 (2004) 113–129.
[24] F. Kukulski, F. Ben Yebdri, F. Bahrami, S.A. Levesque, M. Martin-Satue, J. Sevigny, The P2 receptor antagonist PPADS abrogates LPS-induced neutrophil migration in the murine air pouch via inhibition of MIP-2 and KC production, Mol. Immunol. 47 (2010) 833–839.
[25] S. Lacroix, S. Rivest, Effect of acute systemic inflammatory response and cytokines on the transcription of the genes encoding cyclooxygenase enzymes (COX-1 and COX-2) in the rat brain, J. Neurochem. 70 (1998) 452–466.
[26] E. Lebel, L. Vallieres, S. Rivest, Selective involvement of interleukin-6 in the transcriptional activation of the suppressor of cytokine signaling-3 in the brain during systemic immune challenges, Endocrinology 141 (2000) 3749–3763.
[27] W.Y. Lee, M.A. Allison, D.J. Kim, C.H. Song, E. Barrett-Connor, Association of interleukin-6 and C-reactive protein with subclinical carotid atherosclerosis (the Rancho Bernardo Study), Am. J. Cardiol. 99 (2007) 99–102.
[28] L.G. LeMay, A.J. Vander, M.J. Kluger, Role of interleukin 6 in fever in rats, Am. J. Physiol. Regul. Integr. Comp. Physiol. 258 (1990) R798–R803.
[29] M.B. Lobbes, E. Lutgens, S. Heeneman, K.B. Cleutjens, M.E. Kooi, J.M. van Engelshoven, M.J. Daemen, P.J. Nelemans, Is there more than C-reactive protein and fibrinogen? The prognostic value of soluble CD40 ligand, interleukin-6 and oxidized low-density lipoprotein with respect to coronary and cerebral vascular disease, Atherosclerosis 187 (2006) 18–25.
[30] T. Maekawa, N. Takahashi, T. Honda, D. Yonezawa, H. Miyashita, T. Okui, K. Tabeta, K. Yamazaki, Porphyromonas gingivalis antigens and interleukin-6 stimulate the production of monocyte chemoattractant protein-1 via the upregulation of early growth response-1 transcription in human coronary artery endothelial cells, J. Vasc. Res. 47 (2010) 346–354.
[31] A.J. Miller, G.N. Luheshi, N.J. Rothwell, S.J. Hopkins, Local cytokine induction by LPS in the rat air pouch and its relationship to the febrile response, Am. J. Physiol. 272 (1997) R857–R861.
[32] A. Nadjar, V. Tridon, M.J. May, S. Ghosh, R. Dantzer, T. Amedee, P. Parnet, NFkappaB activates in vivo the synthesis of inducible Cox-2 in the brain, J. Cereb. Blood Flow Metab. 25 (2005) 1047–1059.
[33] C. Nilsberth, L. Elander, N. Hamzic, M. Norell, J. Lonn, L. Engstrom, A. Blomqvist, The role of interleukin-6 in lipopolysaccharide-induced fever by mechanisms independent of prostaglandin E2, Endocrinology 150 (2009) 1850–1860.
[34] Y. Oka, T. Ibuki, K. Matsumura, M. Namba, Y. Yamazaki, S. Poole, Y. Tanaka, S. Kobayashi, Interleukin-6 is a candidate molecule that transmits inflammatory information to the CNS, Neuroscience 145 (2007) 530–538.
[35] D. Ott, J. Murgott, S. Rafalzik, F. Wuchert, B. Schmalenbeck, J. Roth, R. Gerstberger, Neurons and glial cells of the rat organum vasculosum laminae terminalis directly respond to lipopolysaccharide and pyrogenic cytokines, Brain Res. 1363 (2010) 93–106.
[36] G.S. Rees, C. Ball, H.L. Ward, C.K. Gee, G. Tarrant, Y. Mistry, S. Poole, A.F. Bristow, Rat interleukin 6: expression in recombinant *Escherichia coli*, purification and development of a novel ELISA, Cytokine 11 (1999) 95–103.
[37] A.A. Romanovsky, O. Shido, S. Sakurada, N. Sugimoto, T. Nagasaka, Endotoxin shock: thermoregulatory mechanisms, Am. J. Physiol. 270 (1996) R693–R703.
[38] G. Ross, J. Roth, B. Storr, K. Voigt, E. Zeisberger, Afferent nerves are involved in the febrile response to injection of LPS into artificial subcutaneous chambers in guinea pigs, Physiol. Behav. 71 (2000) 305–313.
[39] J. Roth, G.E. De Souza, Fever induction pathways: evidence from responses to systemic or local cytokine formation, Braz. J. Med. Biol. Res. 34 (2001) 301–314.
[40] J. Roth, E.M. Harré, C. Rummel, R. Gerstberger, T. Hübschle, Signaling the brain in systemic inflammation: role of sensory circumventricular organs, Front Biosci. 9 (2004) 290–300.
[41] J. Roth, C. Rummel, E.M. Harré, T. Voss, J. Mütze, R. Gerstberger, T. Hübschle, Is interleukin-6 the necessary pyrogenic cytokine? J. Therm. Biol. 29 (2004) 383–389.
[42] A.Y. Rudaya, A.A. Steiner, J.R. Robbins, A.S. Dragic, A.A. Romanovsky, Thermoregulatory responses to lipopolysaccharide in the mouse: dependence on the dose and ambient temperature, Am. J. Physiol. Regul. Integr. Comp. Physiol. 289 (2005) R1244–R1252.
[43] C. Rummel, S.W. Barth, T. Voss, S. Korte, R. Gerstberger, T. Hubschle, J. Roth, Localized vs. systemic inflammation in guinea pigs: a role for prostaglandins at distinct points of the fever induction pathways? Am. J. Physiol. Regul. Integr. Comp. Physiol. 289 (2005) R340–R347.
[44] C. Rummel, T. Hübschle, R. Gerstberger, J. Roth, Nuclear translocation of the transcription factor STAT3 in the guinea pig brain during systemic or localised inflammation, J. Physiol. 557 (2004) 671–687.
[45] C. Rummel, W. Inoue, C. Sachot, S. Poole, T. Hubschle, G.N. Luheshi, Selective contribution of interleukin-6 and leptin to brain inflammatory signals induced by systemic LPS injection in mice, J. Comp. Neurol. 511 (2008) 373–395.
[46] C. Rummel, C. Sachot, S. Poole, G.N. Luheshi, Circulating interleukin-6 induces fever through a STAT3-linked activation of COX-2 in the brain, Am. J. Physiol. Regul. Integr. Comp. Physiol. 291 (2006) R1316–R1326.
[47] C. Rummel, T. Voss, K. Matsumura, S. Korte, R. Gerstberger, J. Roth, T. Hübschle, Nuclear STAT3 translocation in guinea pig and rat brain endothelium during systemic challenge with lipopolysaccharide and interleukin-6, J. Comp. Neurol. 491 (2005) 1–14.
[48] C.H. Saely, K. Geiger, H. Drexel, Brown versus white adipose tissue: a mini-review, Gerontology (2010).
[49] B. Samuelsson, R. Morgenstern, P.J. Jakobsson, Membrane prostaglandin E synthase-1: a novel therapeutic target, Pharmacol. Rev. 59 (2007) 207–224.
[50] A.P. Santos-Silva, E.G. Moura, C.R. Pinheiro, A.S. Rios, Y. Abreu-Villaca, M.C. Passos, E. Oliveira, P.C. Lisboa, Neonatal nicotine exposure alters leptin signaling in the hypothalamus–pituitary–thyroid axis in the late postnatal period and adulthood in rats, Life Sci. 87 (2010) 187–195.
[51] D.M. Soares, R.R. Machado, L.H. Yamashiro, M.C. Melo, G.E. Souza, Cytokine-induced neutrophil chemoattractant (CINC)-1 induces fever by a prostaglandin-dependent mechanism in rats, Brain Res. 1233 (2008) 79–88.
[52] R.P. Stowe, M.K. Peek, M.P. Cutchin, J.S. Goodwin, Plasma cytokine levels in a population-based study: relation to age and ethnicity, J. Gerontol. A Biol. Sci. Med. Sci. 65 (2010) 429–433.
[53] P.A. Tessier, P.H. Naccache, I. Clark-Lewis, R.P. Gladue, K.S. Neote, S.R. McColl, Chemokine networks in vivo: involvement of C–X–C and C–C chemokines in neutrophil extravasation in vivo in response to TNF-alpha, J. Immunol. 159 (1997) 3595–3602.
[54] A.V. Turnbull, S. Prehar, A.R. Kennedy, R.A. Little, S.J. Hopkins, Interleukin-6 is an afferent signal to the hypothalamo–pituitary–adrenal axis during local inflammation in mice, Endocrinology 144 (2003) 1894–1906.
[55] L. Vallières, S. Rivest, Interleukin-6 is a needed proinflammatory cytokine in the prolonged neural activity and transcriptional activation of corticotropin-releasing factor during endotoxemia, Endocrinology 140 (1999) 3890–3903.
[56] J. Wang, T. Ando, A.J. Dunn, Effect of homologous interleukin-1, interleukin-6 and tumor necrosis factor-alpha on the core body temperature of mice, Neuroimmunomodulation 4 (1997) 230–236.
[57] K. Yamagata, K. Matsumura, W. Inoue, T. Shiraki, K. Suzuki, S. Yasuda, H. Sugiura, C. Cao, Y. Watanabe, S. Kobayashi, Coexpression of microsomal-type prostaglandin E synthase with cyclooxygenase-2 in brain endothelial cells of rats during endotoxin-induced fever, J. Neurosci. 21 (2001) 2669–2677.
[58] T. Yucel-Lindberg, T. Olsson, T. Kawakami, Signal pathways involved in the regulation of prostaglandin E synthase-1 in human gingival fibroblasts, Cell Signal 18 (2006) 2131–2142.

1.5. „Spatiotemporal nuclear factor interleukin 6 expression in the rat brain during LPS-induced fever is linked to sustained hypothalamic inflammatory target gene induction“

Damm J., Luheshi GN., Gerstberger R., Roth J., **Rummel C.**

J Comp Neurol (2011) 519: 480-505

Impakt Faktor: 3,774

Eigener Anteil an der Publikation:

- Initiative: eigenständig (95 %)
- Projektplanung: weitgehend eigenständig (75 %)
- Durchführung der Versuche: unterstützend (30 %)
- Auswertung der Experimente: wesentlich (40 %)
- Erstellung der Publikation: weitgehend eigenständig (70 %)

RESEARCH ARTICLE

Spatiotemporal Nuclear Factor Interleukin-6 Expression in the Rat Brain During Lipopolysaccharide-Induced Fever Is Linked to Sustained Hypothalamic Inflammatory Target Gene Induction

Jelena Damm,[1] Giamal N. Luheshi,[2] Rüdiger Gerstberger,[1] Joachim Roth,[1] and Christoph Rummel[1]*

[1]Department of Veterinary-Physiology, Justus-Liebig-University Giessen, D-35392 Giessen, Germany
[2]Douglas Mental Health University Institute, Department of Psychiatry, McGill University, Montreal, Quebec, H4H 1R3 Canada

ABSTRACT

Rats injected with lipopolysaccharide (LPS) show brain-controlled sickness symptoms, including fever. In these animals, early genomic activation of brain cells was previously monitored by immunohistochemical detection of transcription factors such as nuclear factor (NF)-κB or signal transducer and activator of transcription (STAT)3 and was linked to the initiation or maintenance of the febrile response. To investigate whether NF-IL6 might be another important transcription factor implicated in this kind of immune-to-brain signaling, rats were injected with LPS (100 μg/kg, intraperitoneally) or phosphate-buffered saline, and brains were analyzed by immunohistochemistry, real-time PCR, or Western blot 4, 6, 8, and 10 hours later. Moderate to strong LPS-induced nuclear NF-IL6 immunoreactivity (IR) occurred in a time-dependent manner within circumventricular organs, namely, the vascular organ of the lamina terminalis, the subfornical organ, the area postrema, and the median eminence, brain structures with a leaky blood-brain barrier. Furthermore, nuclear NF-IL6-IR was observed in the pituitary gland, the choroid plexus, and the meninges as well as blood vessels throughout the entire brain. Endothelial, microglial, and ependymal cells, astrocytes, perivascular macrophages, and neurons exhibited LPS-induced nuclear NF-IL6-IR; mRNA levels of NF-IL6, responsive inflammatory genes, and NF-IL6 protein levels were significantly elevated. As opposed to observations on STAT3 or NFκB, the percentage of NF-IL6-reactive cells increased in parallel to late phases of the febrile response. In conclusion, these results suggest a potential role for NF-IL6 in the maintenance or possibly the termination of LPS-induced fever. Moreover, we propose NF-IL6 to be a delayed brain cell activation marker. J. Comp. Neurol. 519:480–505, 2011.

© 2010 Wiley-Liss, Inc.

INDEXING TERMS: systemic inflammation; immune-to-brain communication; cytokines; circumventricular organs; endothelial cells; brain cell activation marker

Research on immune-to-brain communication has provided valuable insight on mechanisms regulating the host's response to infection (Quan and Banks, 2007). In particular, a number of advances have recently been made in our understanding of how systemic inflammatory insults can impact the innate immune response in the brain (D'Mello et al., 2009; Dantzer et al., 2008; Rivest, 2009; Rummel et al., 2009). Fever, a hallmark of a brain controlled "sickness" response following systemic inflammation (Kluger, 1991), has been widely used as an experimental model for studying immune-to-brain interactions. Indeed, much of what we now know about the neuroimmune axis emerged from studies using bacterial lipopolysaccharide (LPS) to induce fever in rodents, which

© 2010 Wiley-Liss, Inc.

Additional Supporting Information may be found in the online version of this article.

Grant sponsor: Emmy Noether Program of the German Research Foundation (DFG); Grant number: RU 1397/2-1.

*CORRESPONDENCE TO: Dr. Christoph Rummel, Department of Veterinary-Physiology, Justus-Liebig-University Giessen, Frankfurter Strasse 100, D-35392 Giessen, Germany.
E-mail: christoph.d.rummel@vetmed.uni-giessen.de

Received March 11, 2010; Revised September 20, 2010; Accepted September 22, 2010
DOI 10.1002/cne.22529
Published online October 28, 2010 in Wiley Online Library (wileyonlinelibrary.com)

increases the production of cytokines in the periphery and the brain.

Subsequently, both cytokines and LPS mediate their effects on the brain via de novo synthesis of a characteristic subset of target gene proteins, including the rate-limiting enzymes for PGE2 synthesis, cycloocygenase 2 (COX2; Konsman et al., 2004; Rummel et al., 2006) and microsomal PG synthase (mPGES; Oka et al., 2007), which are believed to contribute to the manifestation of fever (Cao et al., 1997; Saha et al., 2005). The expression of these target gene proteins is increased through proinflammatory transcription factors, including the signal transducer and activator of transcription 3 (STAT3) and nuclear factor-κB (NFκB). Recently, we and others have used immunohistochemical detection of STAT3 or NFκB to determine IL6 (STAT3)- or LPS/IL1β-induced (NFκB) genomic activation of specific cell types and brain structures during inflammation and have revealed several hypothalamic nuclei that are implicated in the induction of "sickness" responses such as fever (Gautron et al., 2002; Harré et al., 2002, 2003; Nadjar et al., 2003; Rummel et al., 2004, 2005, 2006, 2008).

NF-IL6, another important inflammatory transcription factor belonging to the CCAAT/enhancer-binding protein (C/EBP) family, has recently emerged as a key factor for neuroinflammation (Perez-Capote et al., 2006) following excitotoxic injury (Cortes-Canteli et al., 2008), postischemic inflammation (Halterman et al., 2008; Kapadia et al., 2006; Yi et al., 2007), or neuronal/brain injury (Cortes-Canteli et al., 2004; Nadeau et al., 2005). There are six known family members (C/EBPα–C/EBPζ) of these basic leucine zipper class transcription factors that can bind to the DNA as homo- or heterodimers (Ramji and Foka, 2002). NF-IL6 (C/EBPβ) can be found in several functionally distinct isoforms; a liver-enriched activating protein (LAP) of about 32–36 kDa; a liver-enriched inhibitory protein (LIP; 20 kDa), which lacks the activation domain; and a full-length protein called LAP* of about 35–39 kDa (Descombes and Schibler, 1991; Ejarque-Ortiz et al., 2007). To date, NF-IL6 has been implicated among other factors in the control of proliferation (Nerlov, 2007), differentiation, long-term memory consolidation (Taubenfeld et al., 2001), and inflammation (Ramji and Foka, 2002). As such, mice deficient in NF-IL6 are more susceptible to listeria, salmonella, and mycobacterial infection (Sugawara et al., 2001; Tanaka et al., 1995). In the unstimulated adult mouse brain, NF-IL6 is, for example, strongly expressed in the hippocampus (Kuo et al., 1990), but only low levels of NF-IL6 mRNA could be detected in the sensory circumventricular organs (sCVOs), brain structures with a leaky blood–brain barrier, by in situ hybridization (Nadeau et al., 2005). Notably, LPS and cytokines such as IL6 induce NF-IL6 activation (Ramji and Foka, 2002) and subsequently NF-IL6-responsive target gene expression, including COX2 (Chun and Surh, 2004), mPGES (Uematsu et al., 2002) and IL6 or IL1β (Akira, 1997; Akira and Kishimoto, 1992). However, although NF-IL6 was described more than 20 years ago (Akira et al., 1990; Landschulz et al., 1988), a comprehensive characterization of NF-IL6 expression in conjunction with its target genes in the brain during systemic inflammation has not yet been performed.

Thus, in the present study, we wanted to investigate the contribution of NF-IL6 to the genomic activation of cells in the brain and to gain insights into its putative role for immune-to-brain communication. To this end, we injected rats with LPS (100 μg/kg) at a dose that has previously been shown to induce a robust and well-characterized febrile response, and animals were killed at different time points along the fever trajectory, for collection of brain tissue and blood. In these animals, plasma IL6 bioactivity was measured, because this cytokine is one of the recognized main circulating pyrogens (Cartmell et al., 2000; Miller et al., 1997; Roth et al., 1993) and might contribute to NF-IL6 activation in the brain. To determine the exact time course, distribution pattern, and cellular phenotype of NF-IL6 activation in the brain, immunohistochemical detection of NF-IL6 was combined with visualization of specific cell marker proteins, and the results were quantified by counting of immunoreactive cells in selected responsive brain areas. In addition, by using real-time (RT)-PCR, we sought to investigate possible NF-IL6-responsive target gene mRNA expression, including COX2, mPGES, IL1β, IL6, and the antiinflammatory cytokine IL10, as well as NF-IL6 mRNA itself. To determine the possible contribution of the NF-IL6 signaling pathway to that of STAT3 and NFκB, we analyzed the gene expression of their negative regulatory proteins, which represent markers of their activation and include the suppressor of cytokine signaling (SOCS3) for STAT3 (Lebel et al., 2000), the inhibitor (I)κB for NFκB (Laflamme and Rivest, 1999), and the recently identified negative regulator of NF-IL6, a serine/threonin kinase-like protein called Trib1 (Yamamoto et al., 2007). Finally, we used Western blot analyses at the determined peak of NF-IL6 activation to identify the LPS-induced NF-IL6 isoforms in the rat brain.

MATERIALS AND METHODS

Animals

The present study was performed in male Wistar rats (*Rattus* sp.) with a body weight (BW) of 275 ± 30 g originating from an in-house breeding colony with parent animals obtained from Charles River WIGA (Sulzfeld, Germany). For the duration of the experiment, animals were housed individually in a temperature- and humidity-

TABLE 1.
Conditions for the Primary Antibodies Used for Immunohistochemistry

Antigen	Immunogen	Species, type	Dilution used	Catalog No., manufacturer
NF-IL6	Corresponding to aa 258–276, C-terminus, rat origin	Goat polyclonal IgG	1:250	sc-150-G; Santa Cruz Biotechnology, Santa Cruz, CA
NF-IL6	Corresponding to aa 258–276, C-terminus, rat origin	Rabbit polyclonal IgG	1:5,000	sc-150; Santa Cruz Biotechnology
vWF	Purified human plasma von Willebrand factor	Rabbit polyclonal IgG	1:2,000	008202, Dako Deutschland GmbH, Hamburg, Germany
vWF	Purified rat plasma von Willebrand factor	Sheep polyclonal IgG	1:3,000	SARTW-IG, Affinity Biologicals, Ancaster, Ontario, Canada
GFAP	Purified porcine spinal cord glial filament	Mouse monoclonal IgG	1:2,000	MAB3402; Millipore, Billerica, MA
CD68	Rat spleen cells	Mouse monoclonal IgG	1:1,000	MCA341R; AbD Serotec; Oxford, United Kingdom
CD163	Rat spleen cell homogenate	Mouse monoclonal IgG	1:500	MCA342R; AbD Serotec
NOS1	Corresponding to aa 1400–1419, C-terminus, rat origin	Rabbit polyclonal IgG	1:500	sc-648; Santa Cruz Biotechnology
COX2	Peptide SRLDDINPTVLIKRR	goat polyclonal IgG	1:2,000	sc-1747; Santa Cruz Biotechnology

controlled climate chamber (Weiss Umwelttechnik GmbH, Typ 10'US/+5–+40 DU, Germany) at an ambient temperature of 25°C and 50% humidity on a 12:12-hour light-dark cycle (lights off at 7:00 PM), with constant access to water and powdered standard lab chow (Altromin1311; Altromin Spezialfutter GmbH & Co KG, Lage, Germany). About 8 days before the experiment, the animals were implanted with intraabdominal radiotransmitters (VM-FR TR-3000; Mini-Mitter, Sunriver, OR) for measurement of body core temperature. Output (frequency in Hz) was monitored at 5-minute intervals by an antenna placed under the cage (RA-1000 radio receivers; Mini-Mitter). A data-acquisition system (Vital View; Mini-Mitter) was used for automatic control of data collection and analysis. The rats were handled extensively for at least 3 days prior to the injections for habituation. Animal care, breeding, and experimental procedures were conducted according to guidelines approved by the local Ethics committee (ethics approval No. GI 18/2-51/2008).

Treatment and experimental protocols

Rats were intraperitoneally (i.p.) injected with LPS (100 µg/kg BW; derived from *Escherichia coli*, serotype 0128:B12; Sigma, Deisenhofen, Germany) suspended in sterile pyrogen-free 0.9% PBS (Dulbecco's phosphate-buffered saline; PAA, D-Cölbe) at a total injection volume of 1 ml per animal. Control animals received the equivalent volume of PBS (0.1 M, pH 7.4). All injections were performed between 9 and 10 AM.

In a previous study, NF-IL6 IR was not detected in brains of rats 2 hours after LPS stimulation into a subcutaneous air pouch, which is a model of localized inflammation (Rummel et al., 2006). Subsequently, we performed a pilot experiment in separate groups of rats to test the induction of NF-IL6 immunoreactivity (IR) in the rat brain at 2, 4, 6, 8, 10, or 24 hours after systemic LPS stimulation (data not shown; see also Figs. 2, 3). In this experiment, NF-IL6 IR was induced 4, 6, 8, and 10 hours after LPS and was undetectable at 2 and 24 hours. Therefore, the two time points 2 and 24 hours were omitted from the experimental groups of LPS or PBS treatment for the present study ($n = 5$ for 8 hours; $n = 3$ for the time points 4, 6, and 10 hours). At the given time points, animals were deeply anesthetized with sodium pentobarbital (0.5 ml i.p., Narcoren; Merial, Hallbergmos, Germany), and blood samples were collected via cardiac puncture using a sterile, heparinized syringe. Subsequently, rats were transcardially perfused with 200 ml ice-cold 0.9% saline, and their brains were quickly removed, frozen in powdered dry ice, and stored at −55°C until analysis.

Tissue processing

Coronal 20-µm brain sections were cut on a cryostat (model HM 500; Microm, Walldorf, Germany) and thaw-mounted onto poly-L-lysine-coated glass slides. Sections were prepared from several brain areas encompassing the hypothalamus (including the vascular organ of the lamina terminalis, OVLT; the median preoptic nucleus, MnPO; the subfornical organ, SFO; the arcuate nucleus, ARC; and the median eminence, ME; bregma 0.50 to −3.5 mm) and the brainstem (area postrema, AP; raphe pallidus, RPa; bregma −14.28 to −12.28 mm) according to the stereotactic atlas of the rat brain (Paxinos and Watson, 1998). To perform immunohistochemistry (IHC) and RT-PCR from the same brains, 10–15 consecutive frozen 80-µm sections were also thaw-mounted onto glass slides, and the hypothalamus was dissected and used for RNA extraction. As determined in the preliminary experiments, the cortex was shown to be highly responsive in LPS-induced NF-IL6 IR in blood vessel-like structures, with a peak at 8 hours after stimulation. Therefore, the

cortex of these sections was used for protein extraction and subsequent Western blot analyses of NF-IL6 protein content. Samples were stored at −55°C until processing.

Immunohistochemistry

General procedure

On the day of the experiment, the frozen brain sections were briefly air dried at room temperature for 7 minutes and then immersion fixed in 2% paraformaldehyde (Merck, Darmstadt, Germany) diluted in PBS for 10 minutes at room temperature (RT). After three successive washes in PBS, the sections were treated for 1 hour at RT with a blocking solution consisting of PBS, containing 10% normal donkey serum (NDS; Biozol, Eching, Germany) and 0.3% Triton X-100 (only for goat COX2 and rabbit NF-IL6). Details of the primary antibody concentrations are shown in Table 1. The sections were incubated with the primary antibodies for 20–22 hours at 4°C, followed by three successive washes in PBS and visualization with Cy3- or Alexa-488-conjugated IgG (for details see under Colocalization studies). Sections were counterstained with the nuclear 4.6-diamidino-2-phenylindole (DAPI) stain (Mobitec GmbH, Göttingen, Germany) for 10 minutes, using a 1:1,000 dilution in PBS to visualize clearly the tissue surrounding the signal and to demonstrate the nuclear localization of NF-IL6 IR. Finally, all sections were coverslipped (glass coverslips) with a glycerol/PBS solution (Citifluor, London, United Kingdom) and stored at 4°C until microscopic analysis was performed.

NF-IL6

A goat and a rabbit antibody were used to detect nuclear NF-IL6 signals in the rat brain and showed almost identical results, with some differences in staining intensity (see Fig. 9). Specificity of the rabbit and goat antibody was confirmed by preabsorption with the blocking peptide (sc-150 P; Fig. 9). Notably, we were able to use the rabbit antibody at a very high dilution (Table 1) compared with the goat antibody to obtain similar specific immunohistochemical staining. Both antibodies were raised against the C-terminus of the protein (see Table 1 for sequence; Kitami et al., 1999). In mouse mixed glial cultures, the rabbit antiserum recognizes three bands: full (~35 kD), LAP (~32–33 kDa), and LIP (~20 kDa; Ejarque-Ortiz et al., 2007). In our study, Western blot analysis of rat cortex samples revealed a single band at 35 kDa corresponding to the LAP isoform of NF-IL6. The antibody shows specific staining in mouse brain sections and primary mouse cultures (microglia, astrocytes), which is absent in NF-IL6-deficient animals (Ejarque-Ortiz et al., 2007). Furthermore, it was found to specifically stain MAP2-positive hippocampal neurons in *Aplysia* (Yukawa et al., 1998). The characteristic but low basal staining pattern in unstimulated PBS-injected control animals that we observed in several structures of the rat brain by IHC in the present study confirms previous results by others using in situ hybridization of NF-IL6 mRNA expression in the mouse brain (Nadeau et al., 2005).

von Willebrand factor

The antibodies were raised in rabbit or sheep against human or rat von Willebrand factor (vWF) specifically to stain endothelial cells and are known to produce a typical cytoplasmatic staining pattern. Visualizing the characteristic morphology and distribution of brain endothelial cells, these antibodies have been extensively used for characterization of endothelial cell phenotypes in mice, guinea pigs, and rats (Konsman et al., 2004; Rummel et al., 2005, 2008; Yamamoto et al., 1998). The same vW IR could be observed in the present study. The results of IHC were confirmed by in situ hybridization of vW mRNA expression in the mouse brain (Yamamoto et al., 1998). The antiserum A 0082 (Dako, Carpinteria, CA) shows one precipitate by crossed immunoelectrophoresis against human plasma and cross-reacts with the mouse equivalent of vW by IHC (manufacturer's data sheet).

Glial fibrillary acidic protein

The cytoplasmatic class III intermediate filament glial fibrillary acidic protein (GFAP) is a cell-specific marker that distinguishes astrocytes from other glial cells during the development of the central nervous system (manufacturer's data sheet). In tissue sections, the antibody raised against this protein stains astrocytes and Bergman glia cells (Debus et al., 1983). Species reactivity encompasses human, rat, mouse, pig, chicken, cow, and rabbit. Immunoblotting reveals a single band at 51 kDa in Westerns of total brain lysates (manufacturer's data sheet). The antiserum reveals a characteristic staining pattern as previously shown in rat and guinea pig brain sections (Harré et al., 2003; Kim et al., 2008; Rummel et al., 2005) or in another study using a different GFAP specific antibody (Gautron et al., 2002).

Cluster of differentiation 68 (CD68/ED1)

A monoclonal mouse antibody raised against rat spleen cells has been used to detect activated microglia. The antigen CD68, a glycosylated protein of 90–110 kD, is expressed on the membranes of cytoplasmatic granules, such as phagolysosomes, as well as on the cell surface (manufacturer's data sheet). The amount of CD68 expression in a single cell can be correlated to its phagocytic activity. As such, activated microglial cells show de novo synthesis of the respective antigen (Bauer et al., 1994; Damoiseaux et al., 1994). The antibody recognizes a single-chain glycoprotein of 110 kDa (manufacturer's data

sheet) and has been used specifically to stain microglia in rat or mouse brain sections as well as primary glial cultures (Bauer et al., 1994; Hughes et al., 2002; Wuchert et al., 2009). Moreover, the anti-CD68 antibody (synonym: ED1) recognizes perivascular cells other than activated microglia (Graeber et al., 1989; see also CD163/ED2). In general, immunoreactivity can be detected in the cytosol of phagocytosing macrophages (Bauer et al., 1994; Satriotomo et al., 2006).

Cluster of differentiation 163 (CD163/ED2)

To detect perivascular macrophages in the brain, we used a monoclonal mouse antibody against CD163 (synonym: ED2). It has been raised against rat spleen cell homogenate and recognizes a rat 175-kDa glycoprotein (manufacturer's data sheet) of a surface protein on resident macrophages that consists of three protein chains of 175, 160, and 95 kDa (Barbe et al., 1990). Macrophages in most tissues express the cell surface glycoprotein, but it is not expressed by monocytes, alveolar macrophages, or microglial cells (manufacturer's data sheet). The antiserum allows discrimination between distinct subpopulations of macrophages, localized in characteristic compartments of lymphoid organs (Dijkstra et al., 1985). In immunohistochemical studies, ED2-positive cells have been detected within the basal membrane of blood vessels in the CNS that differed both immunologically and morphologically from resting parenchymal microglia. These ED2- and coincidentally ED1-positive macrophages were detected mostly perivascularly, whereas perivascularly located and ramified microglia did not show ED2 immunoreactivity (Graeber et al., 1989). The same antibody has recently been thoroughly characterized by using immunperoxidase histochemistry, immunfluorescence, and electron microscopy (Galea et al., 2008; Goehler et al., 2006).

Neuronal nitric oxide synthase

Neuronal nitric oxide synthase (NOS1, or nNOS) is one of two constitutive Ca^{2+}/CaM-dependent forms of nitric oxide synthase, and its activity was first identified in neurons. The NOS1 antibody, raised against a peptide of 155 kDa, mapping near the C-terminus of NOS1 of rat origin, was used to determine immunoreactive neurons in the analyzed brain structures. The antiserum detects NOS1 (nNOS) of mouse, rat, and human origin (manufacturer's data sheet). Western blot analysis of rat brain tissue or primary rat hippocampal neurons reveals a single band at about 160 kDa (Atamna et al., 2002; Hashida-Okumura et al., 1999). Specific staining of neurons has been demonstrated in primary cultures of fetal rat brain neuronal cells (Hashida-Okumura et al., 1999) as well as in neurons located in the cerebral cortex, hippocampus, cerebellum, and brainstem (Alm et al., 2000). NOS1 immunoreactivity in the rostral ventrolateral medulla of the rat brain colocalized with cells that were additionally positive for the neuronal marker NeuN (Chang et al., 2003).

Cyclooxygenase 2

This antibody was raised in goat (Table 1) and shows the characteristic perinuclear COX2 staining that is absent in PBS-treated animals but is induced by LPS treatment in rat brain vessels (see Fig. 9) as previously observed by us using a different antibody in mice (Rummel et al., 2008) or others using the same antibody in rats (Summy-Long and Hu, 2009) and by in situ hybridization (Cao et al., 2001). Specificity of staining in the rat brain was confirmed by preabsoption with the respective blocking peptide provided by the manufacturer (data not shown; Summy-Long and Hu, 2009). The antiserum recognizes a single band on Western blot of LPS-treated mouse leukemic monocyte macrophage cell line whole-cell lysates (manufacturer's data sheet).

Colocalization studies

Double IHC was performed to determine the contribution of endothelial cells, astrocytes, activated microglia, perivascular macrophages, and neurons to the NF-IL6 immunoreactive cell population. The antibodies for NF-IL6 were mixed with the cell marker antibody (dilutions given in Table 1) prior to the first incubation (20–22 hours). NF-IL6 was visualized with Cy3-conjugated anti-goat or anti-rabbit IgG (catalog Nos. 705-165-147, 711-165-152; Jackson ImmunoResearch, West Grove, PA), cell markers with Alexa-488-conjugated anti-rabbit, anti-mouse, or anti-sheep IgG (catalog Nos. AZA11055, AZA21202, AZA11015; MoBiTec GmbH, Goettingen, Germany) as secondary antibodies (1:500 dilution each). In control experiments, the sections were incubated with the primary antibody mixture in which one of the primary antibodies was substituted with nonimmunized animal IgG (goat IgG for COX2, rabbit IgG for NF-IL6). Inappropriate cross-reaction between antibodies was confirmed to be negligible.

Microscopic analysis

Sections were analyzed using a conventional light/fluorescent Olympus BX50 microscope (Olympus Optical, Hamburg, Germany) equipped with the appropriate filter sets to detect the fluorescent conjugates Cy3, Alexa Fluor 488, and DAPI. Images were taken with a black-and-white Spot Insight camera (Diagnostic Instruments, Visitron Systems, Puchheim, Germany). Digital rat brain maps were arranged by the adjustment of corresponding rat brain levels taken from the digital brain map atlas of Paxinos and Watson (1998).

Cell counts were performed on photomicrographs of the middle parts of each brain region with a similar

TABLE 2.
Quantitative Analysis of the Mean Horizontal Nuclear Diameter per Selected Brain Structure and Cell Phenotype[1]

	Approximate horizontal mean nuclear diameter per selected brain structure or cell phenotype (μm)				
Nuclei that show IR for	OVLT	SFO	MnPO	ME	AP
DAPI	5.3 ± 2.1	7.6 ± 2.5	7.4 ± 2.4	5.0 ± 1.9	6.5 ± 2.1
DAPI + NF-IL6	4.8 ± 1.5	6.6 ± 1.8	6.2 ± 1.8	4.6 ± 1.4	6.7 ± 1.8
	vWF	GFAP	nNOS	CD68	CD163
DAPI + NF-IL6	4.8 ± 1.7	5.6 ± 1.3	7.4 ± 1.8	5.5 ± 1.5	5.8 ± 1.5

[1]The mean diameter of more than 290 DAPI IR nuclei and more than 100 DAPI/NF-IL6 IR nuclei was measured in the horizontal axes of high resolution images taken with a ×100 objective and immersion oil for each selected brain structures (OVLT, vascular organ of the lamina terminalis; SFO subfornical organ; MnPO, median preoptic nucleus; ME, median eminence and the AP, area postrema) using MetaMorph 5.05 analysing software. In addition, the mean horizontal diameter of more than 100 DAPI/NF-IL6 IR nuclei for each colocalizing specific cell marker protein (vWF, endothelial cells; GFAP, astrocytes; nNOS, neurons; CD68, activated microglia; CD163, perivascular macrophages) are displayed. Values are presented as mean ± standard error.

coronal level (see also Figs. 2, 5, 9 at lower magnification; OVLT, bregma 0.40 to 0.60 mm; SFO, bregma −0.80 to −1.10 mm; AP, bregma −13.70 to −14.20 mm; ME, bregma −2.80 to −3.20 mm; MnPO, bregma 0.00 to −0.20 mm) and the same size.

1. For the time-course experiment (see Figs. 2, 3), microphotographs were taken with a ×40 objective lens (UPlanFl; numeric aperture, NA = 0.75; Olympus Optical). Obviously damaged sections were omitted from counting. Two to ten sections per animal were analyzed for each of the LPS-treated groups. For each section, two pictures (×40 objective lens) were taken to cover the whole brain area, with some overlap in a very small portion in the middle part of the brain structure (Supp. Info. Fig. 1A), one picture of the right and one of the left brain hemisphere (Supp. Info. Fig. 1B,C). First, we started counting NF-IL6-positive dots, which were automatically labeled with "1" [as seen in Supp. Info. Fig. 1a; here (a), we only show a small fraction of the picture (C) for more clarity]. In a second step, we added the blue color channel of DAPI staining and counted all the cells marked with "1" that also showed a clear nuclear DAPI staining (labeled with "2"; Supp. Info. Fig. 1b) to avoid counting red dots that were actually staining artifacts (Supp. Info. Fig. 1a,b, open arrow). We calculated the mean of all values for the pictures (×40 objective lens) in one animal and the mean for each group at a given time point, and cell counts were adjusted to the volume (surface × depth of field of the microphotograph) in cubic millimeters to obtain densities of NF-IL6 IR cells for these brain structures. According to Berek (1927), the depth of field was calculated for the wave length used (565 nm) and the NA of 0.75 to be 12,17 μm [0,565 μm/2 × NA^2 + 350 μm (microscope specific value provided by the manufacturer)/NA × 40 (total magnification)]. Thus, we used the mean density of this portion for each brain structure as a measure of its NF-IL6 activation. Densities of NF-IL6 IR cells represent means (n = 2–10 sections times 2 pictures) of the means (n = 3 per LPS-treated group; n = 5 for 8 hours).
2. Percentages of reactive cell phenotypes were quantified on photomicrographs that were taken with a ×100 objective (UPlanFl oil; NA = 1.30; Olympus Optical) lens (2–5 sections, 2–4 pictures per section, n = 5 animals) using immersion oil (refractive index, 1,51; Olympus Optical), which were as well taken at similar levels evenly spaced on coronal sections of the middle part of each brain structure (Supp. Info. Fig. 2A–D). First, DAPI-stained nuclei were counted and labeled with "2" (Supp. Info. Fig. 2a); second, NF-IL6-positive nuclei were counted and labeled with "1" (Supp. Info. Fig. 2b); third, NF-IL6-positive nuclei, that colocalized with the green cell marker protein (here vWF for endothelial cells) were counted (Supp. Info. Fig. 2c). All values were used to reveal some information about the percentage of NF-IL6-responsive cells of all DAPI-stained cells and the percentage of cell phenotype-specific NF-IL6 activation (see Fig. 6). Notably, in the ME, obvious ependymal cells were omitted, and a small part of the ventral, medial arcuate nucleus was included into the counting area. The final data on NF-IL6 IR cell phenotypes represent means (n = 2–5 sections times 2–4 pictures) of the means (LPS-treated group; n = 5 for 8 hours).
3. To correct for overcounts of large cell nuclei, Abercrombie's formula (Abercrombie, 1946; Guillery, 2002) was used for both counting procedures (1 and 2). Depending on the nuclear diameter of the cells counted, a correction factor was calculated, and cell counts were corrected for oversampling. The correction was thus calculated as follows: CV = T/T + h (CV, correction value; T, the thickness of the section; h, mean diameter of the counted nuclei). Overestimates of counted cells were then corrected by dividing actual counts by the correction factor [CF = 100/

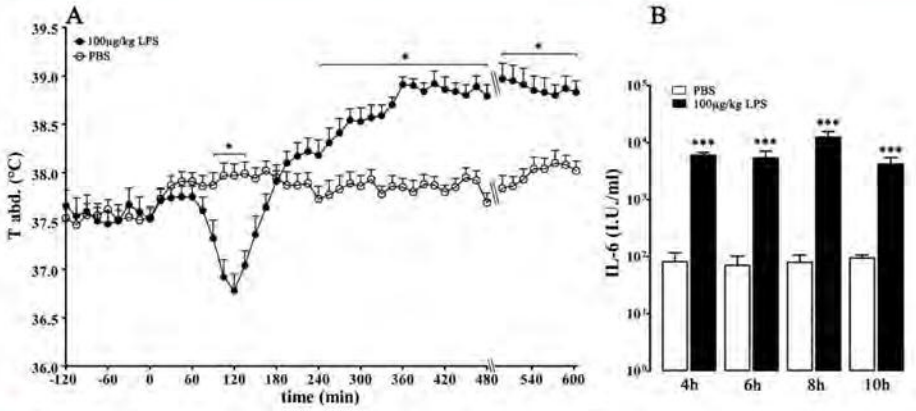


Figure 1. Intraperitoneal injection of a moderate dose (100 µg/kg) of lipopolysaccharide (LPS) into rats induced a characteristic febrile response and strongly elevated plasma IL6 levels. **A:** After the injection (time = 0), LPS induced an initial hypothermia, followed by a typical fever that did not decline over a period of 10 hours compared with control animals that were injected with an equivalent volume of pyrogen-free phosphate-buffered saline [PBS; n = 11 (n = 5 for 8 hours + n = 3 for 10 hours + n = 3 for 24 hours) from −120 minutes to 480 minutes; n = 6 (n = 3 for 10h + n = 3 for 24 hours) from 495 minutes to 600 minutes for both groups]. **B:** LPS stimulation caused strongly elevated levels of bioactive plasma interleukin-6 (IL6) at time points 4, 6, 8, and 10 hours after intraperitoneal injections. IL6 bioactivity remained at basal values in counterpart control animals (each n = 3–5), similarly to untreated animals, as previously shown (Harré et al., 2002). All data are presented as means ± SEM, and statistical significance was considered as $^{*}P < 0.05$ differences between groups, $^{***}P < 0.001$. T_{abd}, body temperature.

(CV × 100)]. To obtain the mean diameter (h; Table 2) in the time course experiment (Fig. 3), the diameter for a minimum of 290 DAPI-stained nuclei (a cutout is shown as an example in Supp. Info. Fig. 2d) as well as the nuclear diameter for more than 100 NF-IL6 IR cell nuclei (a cutout is shown as an example in Supp. Info. Fig. 2e) were measured for each brain structure in the horizontal axis of high-resolution pictures (×100 objective and immersion oil). The horizontal mean diameter of at least 100 nuclei that colocalized with the cell marker protein was measured (h; Table 2; a cutout is shown as an example in Supp. Info. Fig. 2f) for cell phenotyping (Fig. 6). As expected, the mean nuclear size differed among different brain structures or cellular phenotypes and was used for correction of cell overcounts in the present paper.

Microphotographs were taken in MetaMorph 5.05 software. Image editing software was used to combine the individual images into the RGB color figure plates (MetaMorph 5.05), to adjust brightness and contrast, and to store the images as TIFF files (Adobe Photoshop 5.5). All measurements were done with the distance measurement and manual counting tool of MetaMorph 5.05 software on microphotographs before adjusting brightness and contrast.

Real-time PCR

Total RNA of the collected hypothalamic tissue was isolated with Trizol (Invitrogen, Carlsbad, CA) according to the manufacturer's protocol. One microgram of total RNA was transcribed into DNA, by using 50 U murine leukemia virus (MULV) reverse transcriptase, 50 µM random hexamers, and 10 mM dNTP mix (Applied Biosystems, Foster City, CA), in a total reaction volume of 20 µl. After reverse transcription, quantitative real-time PCR was performed in duplicate using preoptimized primer/probe mixture (TaqMan Gene Expression Assay; Applied Biosystems) and TaqMan universal PCR Master Mix (Applied Biosystems) on a StepOne Real-Time PCR System (Applied Biosystems). The cDNA quantities between different reactions were normalized by measurement of the housekeeping gene β-actin (catalog No. 4352340E; Applied Biosystems) as a reference. The sample values represent x-fold differences from a control sample (given as a designated value of 1) within the same experiment. Assay IDs for the analyzed genes are as follows: NF-IL6 (Rn00824635_s1), SOCS3 (Rn00585674_s1), IκBα (Rn01473658_g1), IL6 (Rn01410330_m1), IL1β (Rn00580432_m1), IL10 (Rn99999012_m1), COX2 (Rn00568225_m1), mPGES (Rn00572047_m1), and Trib1 (Rn01505060_m1).

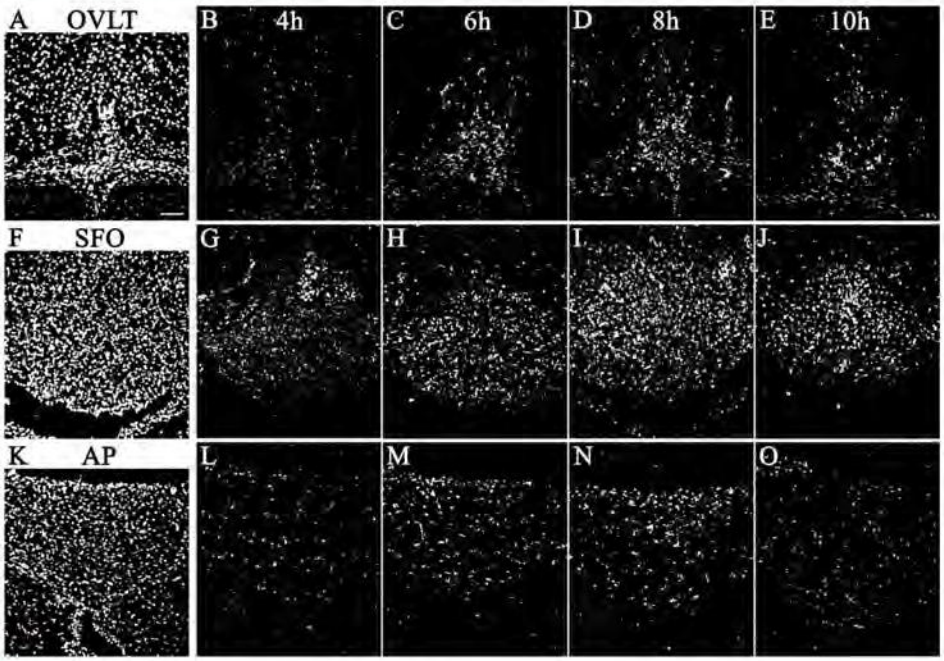


Figure 2. Time-dependent nuclear NF-IL6 immunoreactivity (IR) in the sensory circumventricular organs (CVOs) after a systemic LPS challenge (100 μg/kg, i.p.). Microphotographs **A,F,K** illustrate representative DAPI-counterstained coronal brain sections at the level of the vascular organ of the lamina terminalis (OVLT), subfornical organ (SFO), and area postrema (AP) for a better visualization of the surrounding tissue. White, spot-like nuclear NF-IL6-IR emerges in these regions 4 hours following LPS injection (**B,G,L**), increases by 6 hours (**C,H,M**), peaks at 8 hours (**D,I,N**), and decreases again 10 hours after stimulation (**E,J,O**). Note that in the SFO a primarily robust reaction masks the characterized peak to some extent. Scale bar = 50 μm.

Western blot analysis

The cortical tissue was disaggregated in lysis buffer (50 mM Tris-HCl, 2 mM EDTA, and 1% Nonidet) that contained a protease inhibitor cocktail for general use and a phosphatase inhibitor (catalog No. P2714, P5726; Sigma-Aldrich, St. Louis, MO). Protein concentration was determined by using Bradford's reagent (catalog No. B6916; Sigma-Aldrich), following the manufacturer's instructions; proteins then were aliquoted and stored at −55°C until the next step.

On the day of the analytical procedure, the protein was mixed (1:1) with Laemmli sample buffer mixed with β-mercaptoethanol (50 μl β-mercaptoethanol; catalog No. 161-0710; Bio-Rad, Munich, Germany) per 1 ml Laemmli buffer (catalog No. 161-0737; Bio-Rad) and incubated at 95°C for 5 minutes. Fifty micrograms of protein was then loaded onto 10% acrylamide gels and electrophoresed for 2 hours at 120 V. The protein was then transferred (3 mA/cm^2, 50 minutes) to nitrocellulose membranes (catalog No. 162-0150;p Bio-Rad), following the manufacturer's instructions for semidry transfer and washed for 3 × 5 minutes with 0.1% Tween 20 in 1× Tris-buffered saline (catalog No. 170-6435, Bio-Rad; TBS-T). For immunodetection, membranes were blocked with 10% nonfat dry milk (Bio-Rad) in TBS-T for 2 hours at room temperature. Membranes were then incubated overnight (at 4°C) with a mixture of antibodies (rabbit NF-IL6/β-actin; catalog No. 2066; Sigma-Aldrich) diluted in TBS-T and 5% milk for 2 hours at room temperature. Antibody excess was washed out (1× for 15 minutes and for 4 × 5 minutes) with TBS-T, and membranes were incubated with a detection antibody (1:1,000; donkey anti-rabbit IgG-HRP, catalog No. sc-2313; Santa Cruz Biotechnology, Santa Cruz, CA), diluted in TBS and 5% milk for 1 hour at ambient temperature. After a similar series of washing steps, the membranes were incubated with Luminol/enhancer/peroxide buffer solution (0,125 ml/cm^2; catalog No. 170-5070; Bio-Rad) for 1 minute, and then chemoluminiscence was detected with the Molecular Imager (Chemi-Doc XRS Imaging System; Bio-Rad) for 5–10 minutes using

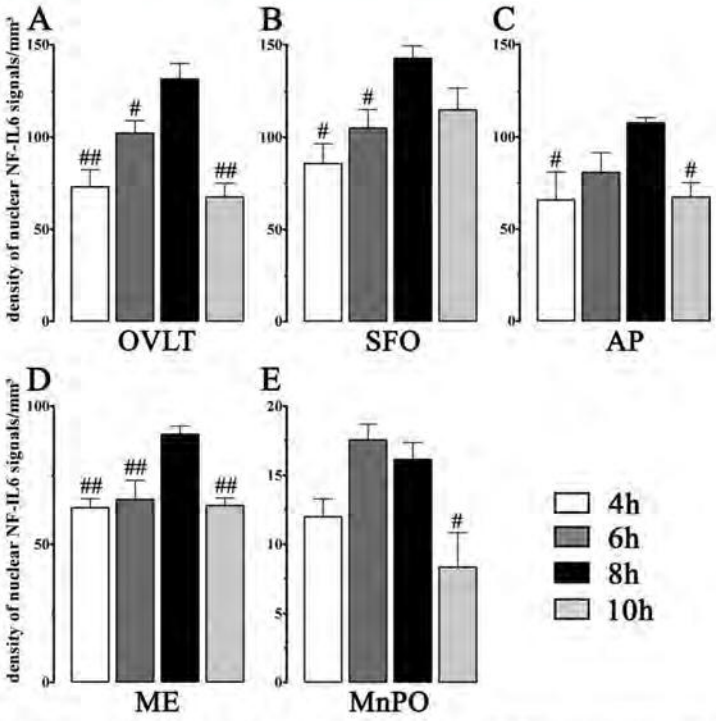


Figure 3. Quantification of nuclear NF-IL6 IR in the sensory CVOs (OVLT, vascular organ of the lamina terminalis; SFO, subfornical organ; and AP, area postrema), the median preoptic nucleus (MnPO), and the median eminence (ME) 4, 6, 8, and 10 hours after LPS injection (100 μg/kg, i.p.) by counting of NF-IL6 IR cells on photomicrographs of the middle parts of each brain region as cell densities per cubic millimeter. Cell densities confirmed the visually defined maximum of NF-IL6 IR at time point 8 hours in the sensory CVOs (A–C), except for the SFO, where the cell density did not significantly decrease at 10 hours compared with the 8-hour time point. In the ME, a quite similar time course with a peak at 8 hours was detected (D), but quantitative analysis in the MnPO revealed a less well defined peak 6–8 hours following LPS stimulation (E). Two to ten sections per animal were analyzed for each group ($n = 5$ for 8 hours, $n = 3$ for other groups). Basal levels of nuclear NF-IL6 IR in these brain structures were uniformly nil. Data represent means of the means ± SEM. Different from LPS-treated group after 8 hours: $^{\#}P < 0.05$, $^{\#\#}P < 0.01$.

Quantity One software. Two bands were detected, one at approximately 42 kDa corresponding to actin and another at 35 kDa corresponding to the NF-IL6 isoform LAP. Levels of NF-IL6 expression were expressed as a ratio of the β-actin signal to that of the NF-IL6 signal.

Plasma IL6 measurement

Determination of IL6 was performed by bioassay based on a dose-dependent growth stimulation of IL6 on the B9 hybridoma cell line (Aarden et al., 1987). The assay was carried out in sterile, 96-well microtiter plates. In each well, 5,000 B9 cells were incubated for 72 hours with serial dilutions of biological samples or with different concentrations of human IL6 standard (code 89/548; National Institute of Standards and Control, South Mimms, United Kingdom). The number of cells in each well after 24 hours was measured by use of the dimethylthiazol-diphenyl tetrazolium bromide (MTT) colorimetric assay (Holt et al., 1991). The detection limit of the assay, after considering the dilution of samples for the assays, proved to be 3 IU IL6/ml.

Data analysis

Abdominal temperatures were compared by repeated-measures analysis of variance (ANOVA), followed by Scheffe's post hoc test (StatView; Abacus Concepts, Berkeley, CA). Relative density of NF-IL6 protein in the Western blot was analyzed by using a parametric

TABLE 3.
Qualitative Analysis of Nuclear NF-IL6 Immunoreactivity in the Rat Brain[1]

	Nuclear NF-IL6 immunoreactivity				
Selected brain stuctures	PBS 4–10 hours	LPS 4 hours	LPS 6 hours	LPS 8 hours	LPS 10 hours
Forebrain					
Cortex	–	++	++	+++	+
Hippocampus	+++	+++	+++	+++	+++
Hypothalamus and preoptic area					
Ventromedial preotic nucleus	–	++	++	++	+
Supraoptic nucleus	–	±	–	–	–
Median preoptic nucleus	–	+	+	++	±
Pituitary gland	+	++	+++	+++	++
Circumventricular organs					
Vascular organ of the lamina terminalis	–	++	++	+++	++
Subfornical organ	–	++	++	+++	++
Median eminence	–	++	++	++	+
Area postrema	–	++	++	++	+
Brainstem					
Raphe pallidus	–	+	++	++	+
Nucleus of the solitary tract	–	–	–	–	–
Others					
Choroid plexus	–	+++	+++	+++	++
Ependymal lining of all ventricles	±	±	+	++	++
Meninges	–	++	+++	+++	++
Endothelial cells throughout the brain					
Capillaries	–	++	+++	++	++
Large vessels	–	++	++	+++	+

[1]Relative values of nuclear NF-IL6 immunoreactivity are given as estimates for the density of their labeling. Analyses of the rat brains were performed 4, 6, 8, and 10 hours after i.p. injection of LPS (100 μg/kg) or saline (n = 5 for 8 hours, n = 3 for other groups). A five-point scale was used to rate the data: +++ = high density of nuclear signals, ++ = moderate density, + = low density, ± = single nuclear signals in some cases, – = no nuclear signals.

unpaired two-tailed Student's *t*-test. Circulating levels of bioactive IL6; semiquantitative data on nuclear NF-IL6 IR; and relative expression of NF-IL6-, SOCS3-, IκB-, IL6-, IL1β-, IL10-, COX2-, mPGES-, and Trib1 mRNA in the hypothalamus were compared separately among the experimental groups (PBS, LPS; 4 hours, 6 hours, 8 hours, and 10 hours) by ANOVA, followed by Newman-Keuls multiple-comparisons post hoc test (Prism 5 software; GraphPad, San Diego, CA). A log transformation of the individual cytokine values was performed prior to the statistical calculation, because the values for cytokines are not normally distributed. *P* values less than 5% were deemed significant. All data are presented as mean ± SEM.

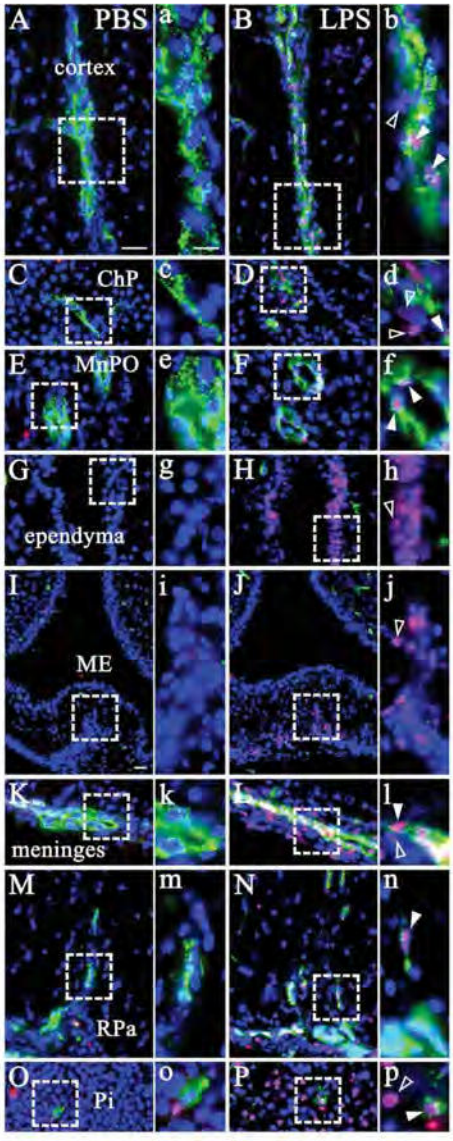
RESULTS

LPS treatment induces nuclear NF-IL6 IR in the circumventricular organs (CVO) in a time-dependent manner that corresponds to the late phase of the febrile response

LPS injection (100 μg/kg, i.p.) in rats induced a characteristic systemic inflammatory response that was accompanied by an initial hypothermia (105–135 min; minimum t = 120 minutes, 36.6 ± 0.16°C), followed by a typical fever, which progressively increased starting from 240 minutes, reached a plateau at 360 minutes (240–600 minutes; maximum t = 485 minutes, 38.97 ± 0.16°C), and tended to decline at the endpoint of the measurements (10 hours; Fig. 1). Plasma IL6 bioactivity was dramatically increased 4, 6, and 8 hours after LPS stimulation and, though not statistically significant, tended to decrease again at 10 hours (LPS 8 hours, 12,441 ± 3,165 IU vs. LPS 10 hours, 4,199 ± 1,262 IU). In PBS-injected animals, core body temperature (~37.5°C) and IL6 levels (~100 IU) remained at basal throughout the time course of experiment similar to basal IL6 activity (Harré et al., 2002).

NF-IL6 IR appeared in the brain of rats 4 hours after stimulation and peaked at 8 hours, reflecting a time course similar to that shown for the febrile response and plasma IL6 bioactivity. In particular, strong LPS-induced NF-IL6 IR occurred in the sensory circumventricular organs (sCVOs), namely, the vascular organ of the lamina terminalis (OVLT), the subfornical organ (SFO), and the area postrema (AP; Fig. 2). These qualitative results were confirmed by quantification of nuclear NF-IL6 IR cells within the sCVOs. The highest NF-IL6-positive cell densities were found in the OVLT and SFO, with about 132 or 143 cells/mm^3 (Fig. 3), and lowest NF-IL6-positive cell

densities were found in the median eminence (ME) that were similar to the AP with ~90 or 108 cells/mm^3. With the exception of the SFO, the amount of NF-IL6 IR cells significantly declined 10 hours after LPS stimulation compared with the 8-hours time point.



NF-IL6 IR following LPS challenge is expressed in a distinct distribution pattern linked to brain blood vessels throughout the brain

LPS-induced NF-IL6 IR was observed throughout the whole rat brain (Table 3, Fig. 4). In contrast to the data shown for the CVOs, the amount of NF-IL6 IR cells peaked earlier in other brain areas, and most of these brain structures showed less pronounced increases in NF-IL6 signals. As a representative example, although there were some exceptions, for the overall picture documented for NF-IL6 IR in the brain we chose to quantify nuclear NF-IL6 IR in the median preoptic area because of its involvement in the regulation of the febrile response (Lazarus et al., 2007). As such, the MnPO exhibited six to 14 times fewer cells with LPS-induced nuclear NF-IL6 IR (Fig. 3E) than observed in the CVOs, with a peak already at 6 hours that was maintained until 8 hours and significantly decreased 10 hours after stimulation. In addition, a qualitative assessment of LPS-induced nuclear NF-IL6 IR (Table 3) revealed strong signals in blood vessels throughout the brain, the cortex, the meninges, the pituitary gland, and the choroid plexus that peaked at 6 hours, 8 hours, 6 hours, and 8 hours (meninges and pituitary gland) or 4 hours, 6 hours, and 8 hours after stimulation, respectively. Moderate NF-IL6 IR occurred in the ventromedial preoptic nucleus and ependymal linings of all ventricles, in particular the third ventricle, which increased at 6 hours and was maintained until 8/10 hours after the LPS challenge. In PBS-

Figure 4. LPS-induced (100 μg/kg, i.p.) nuclear NF-IL6 staining was observed in multiple brain structures other than the sensory CVOs. Nuclear NF-IL6 signals (pink) occurred in distinct large and small blood vessels and diferent cell types of the cerebral cortex (**B**), the choroid plexus (ChP; **D**), the ventral part of the median preoptic nucleus below the anterior part of the anterior commissure (MnPO; **F**), the ependyma of all ventricles (**H**), the median eminence (ME, **J**), the meninges (**L**), the raphe pallidus (Rpa; **N**), and the pituitary gland (Pi; **P**). Colocalization of red NF-IL6 signals with the nuclear DAPI stain (blue) indicates the nuclear localization of the signals, which can be clearly depicted at high magnifications (insets **b,d,f,h,j,l,n,p**). The location of areas used for high magnification are indicated by a dashed square in the overviews. Some of the responding cells were identified to be endothelial cells, because they additionally displayed von Willebrand factor (vW) IR (green). White arrowheads indicate NF-IL6-positive endothelial cells; NF-IL6 IR in other cell phenotypes is highlighted by open arrowheads. Except for the pituitary gland (**O,o**) almost no nuclear NF-IL6 IR can be observed in the brain structures of PBS-injected control animals (**A,a,C,c,E,e,G,g,I,i,K,k,M,m**). Scale bars = 25 μm in A (applies to A-H,K-O); 25 μm in I (applies to I,J); 10 μm in insets.

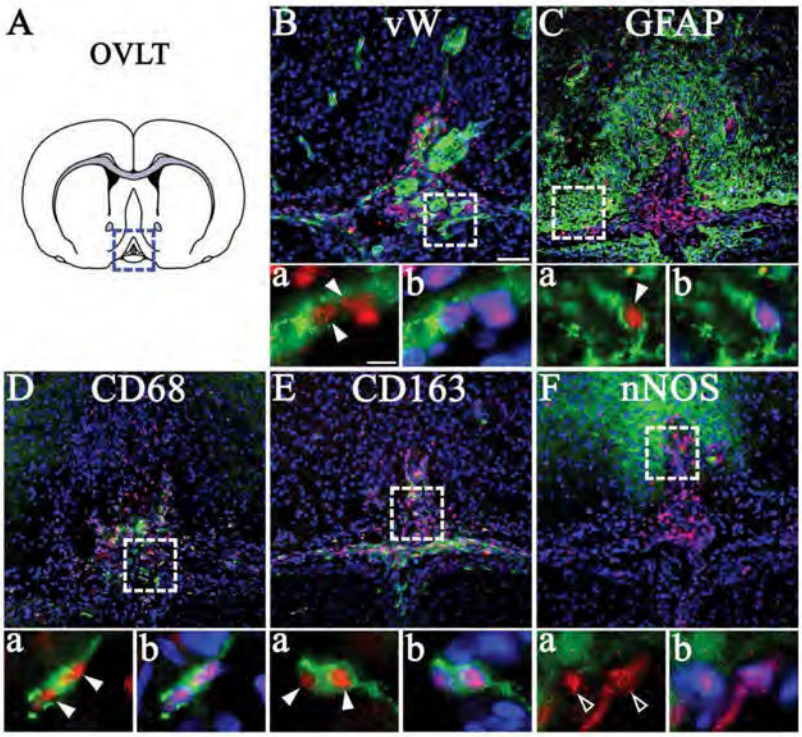


Figure 5. Fluorescent immunohistochemical colocalization studies in the vascular organ of the lamina terminalis (OVLT, A–F), the subfornical organ (SFO, G–L) and the area postrema (AP, M–R) of coronal rat brain sections 8 hours after an LPS (100 μg/kg, i.p.) challenge. **A–F:** Colocalization studies in the OVLT (B–F) identified at least five different phenotypes of NF-IL6-immunoreactive cells (red) by the use of specific cell marker proteins (green). The analyzed levels of coronal sections used for the study are schematically illustrated in the overview; a blue dashed square indicates the OVLT (A). Von Willebrand factor (vWF)-positive NF-IL6-immunoreactive endothelial cells are labeled in the analyzed structures (B); colocalization of NF-IL6 IR with glial fibrillary acidic protein (GFAP) is used to detect astrocytes (C), and cluster of differentiation 68 (CD68) IR identifies NF-IL6-positive activated microglia (D). To visualize perivascular macrophages and neurons displaying nuclear NF-IL6 IR, cluster of differentiation 163 (CD163; E) and neuronal nitric oxide synthase (nNOS; F) are used as cell marker proteins. Except for NF-IL6-immunoreactive neurons that were not found in the OVLT, all the analyzed cell types turned out to contribute to the population of NF-IL6-positive cells in the sensory CVOs of coronal rat brain sections 8 hours after the LPS challenge. The displayed microphotographs F and insets were taken 4 hours after LPS injection. High magnifications in insets for every photograph show colocalization of NF-IL6-positive nuclei (red) with several specific cell marker proteins (green) in dual overlays of the red with the green individual color channel for better visualization of the phenotype of responsive cells (a). In addition, nuclear localization of NF-IL6 signals can be clearly depicted in triple overlays, including the nuclear DAPI stain (blue, b). White arrowheads indicate nuclear NF-IL6 IR colocalizing with the cell marker protein; open arrowheads highlight NF-IL6 signals in nuclei of other cell phenotypes. Areas of high magnifications are indicated with a dashed white square in B–F. **G–L:** NF-IL6-immunoreactive (red) cellular phenotypes in coronal rat brain sections of the subfornical organ (SFO), 8 hours after an LPS (100 μg/kg, i.p.) challenge, identified by the use of specific cell marker proteins (green) and nuclear DAPI stain (blue). Again, the analyzed level of coronal sections is schematically illustrated in an overview, with a blue dashed square indicating the SFO (G). Von Willebrand (vW), endothelial cells (H); glial fibrillary acidic protein (GFAP), astrocytes (I); cluster of differentiation 68 (CD68), activated microglia (J); cluster of differentiation 163 (CD163) perivascular macrophages (K); neuronal nitric oxide synthase (nNOS), neurons (L). White arrowheads indicate nuclear NF-IL6 IR colocalizing with the respective cell marker protein; open arrowheads highlight NF-IL6 signals in nuclei of other cell phenotypes. Areas of high magnifications are indicated with a dashed white square in H–L. **M–R:** Fluorescent immunohistochemical analysis of the area postrema (AP) in coronal rat brain sections 8 hours after an LPS (100 μg/kg, i.p.) challenge. A blue dashed square schematically illustrates the analyzed level of coronal sections in an overview, indicating the AP (M). Cell marker proteins (green) and nuclear DAPI stain (blue) were used to identify NF-IL6-immunoreactive (red) cell phenotypes. Von Willebrand (vW), endothelial cells (N); glial fibrillary acidic protein (GFAP), astrocytes (O); cluster of differentiation 68 (CD68), activated microglia (P); cluster of differentiation 163 (CD163) perivascular macrophages (Q); neuronal nitric oxide synthase (nNOS), neurons (R). White arrowheads indicate nuclear NF-IL6 IR colocalizing with the respective cell marker protein; open arrowheads highlight NF-IL6 signals in nuclei of other cell phenotypes. Areas of high magnification are indicated with a dashed white square in N–R. Scale bars = 25 μm in B (applies to B–F); 25 μm in H (applies to H–L); 25 μm in N (applies to N–R); 10 μm in insets.

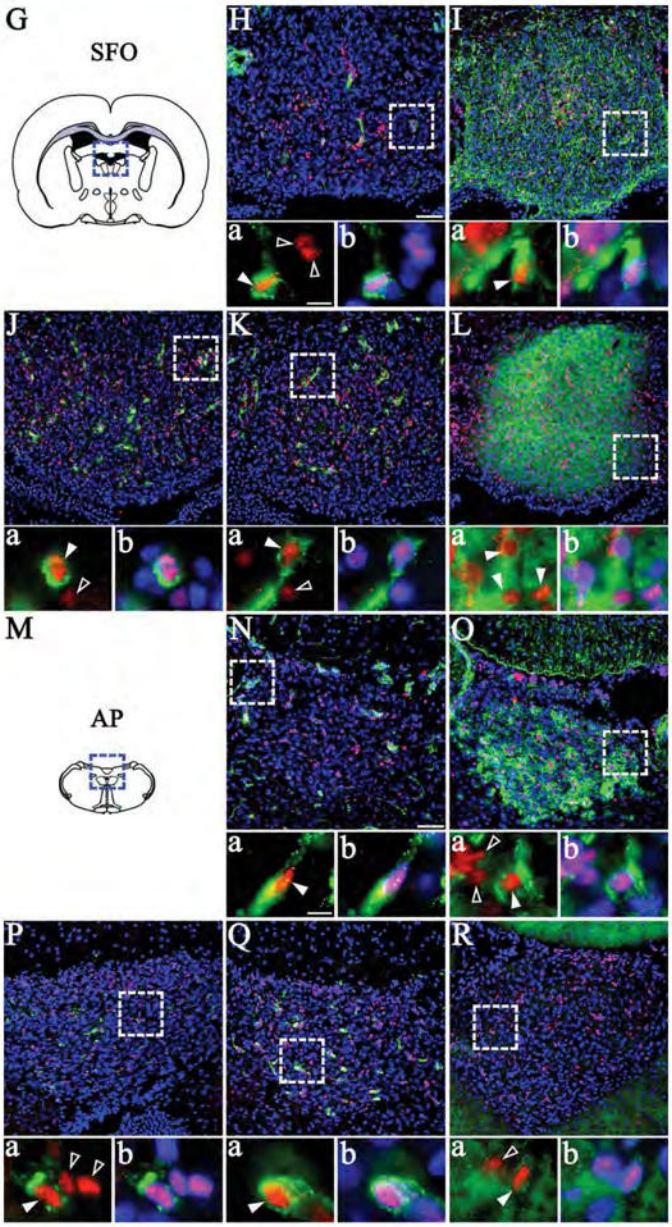


Figure 5. (Continued).

treated animals almost no NF-IL6 IR was observed, with the exception of the hippocampus, which always showed strong nuclear NF-IL6 IR (data not shown), as previously demonstrated by others (Nadeau et al., 2005; Sterneck and Johnson, 1998). Low to moderate basal NF-IL6 IR was also detected in the pituitary gland, the ependymal linings of ventricles, and the raphe pallidus (RPa). Interestingly, no NF-IL6 IR was detected in the supraoptic nucleus or the nucleus of the solitary tract.

As previously shown for STAT3 and NFκB, brain vasculature appears to be very important in immune-to-brain communication during inflammation (Nadjar et al., 2003; Rummel et al., 2005, 2008). Therefore, we tested whether LPS-induced NF-IL6 IR could also be detected along blood vessels. Indeed, in almost all brain structures, NF-IL6 signals were found to colocalize with the endothelial cell marker protein vWF (Fig. 4B,D,F,L,N,P). However, it became clear that, depending on the brain structure investigated, a distinct population of NF-IL6 IR cells appeared to be of a phenotype different from that of endothelial cells. For instance, in the cortex, the choroid plexus, the ependyma, the ME, the meninges, the RPa, and the pituitary gland, NF-IL6 signals occurred in vWF-negative cells (Fig. 4b,d,h,j,l,p). Notably, the ependyma and the ME contained hardly any vWF-positive cells, whereas almost all NF-IL6-positive cells within the MnPO colocalized with vWF IR.

The phenotype of LPS-induced NF-IL6 IR cells includes neurons, astrocytes, microglia, and perivascular macrophages in addition to endothelial cells

To investigate the contributions of different phenotypes to LPS-induced NF-IL6 IR-positive cells, NF-IL6 immunohistochemistry was combined with colabeling of the cell marker proteins for endothelial cells (vW), astrocytes (GFAP), activated microglia (CD68), perivascular macrophages (CD163), and nitrergic neurons (nNOS). At the peak of NF-IL6 signals, which was 8 hours after the LPS challenge, the sCVOs, the ME, and the MnPO were analyzed in consecutive brain sections of five animals (Figs. 5, 6). All analyzed brain structures contained NF-IL6 IR cells of each phenotype to some degree, except for the OVLT and the MnPO, where NF-IL6 immunoreactive nNOS positive neurons were totally absent (Figs. 5F, 6A,E).

When quantifying these results for two to five sections per animal and cellular phenotype overall, about 20% (AP), 25% (SFO), and 30% (OVLT and ME) of all cells responded to LPS injection with nuclear NF-IL6 IR in the CVOs and only ~10% in the MnPO (Fig. 6). The majority of NF-IL6-positive cells in the OVLT, AP, and MnPO could be identified as endothelial cells, with approximately 30%, 20%, or even 95%, respectively, whereas NF-IL6-immunoreactive neurons predominated in the SFO (~30%). Astrocytes also exhibited nuclear NF-IL6 IR primarily in the SFO (~15%), whereas the percentages of activated microglia and perivascular macrophages showing NF-IL6 staining seemed to be highest in the MnPO and AP, corresponding to ~20% and ~13% of all NF-IL6-positive cells. Collectively, ~35% (ME), ~60% (OVLT), ~65 (AP), or even ~75% (SFO) of all LPS-induced NF-IL6 IR cell phenotypes could be identified in the brain structures investigated, indicating that a distinct population of these cells remains to be phenotypically identified. Solely for the MnPO, which contained NF-IL6 IR almost exclusively in endothelial cells (together with a few microglial cells, perivascular macrophages, and astrocytes), the relative contribution of all LPS-induced NF-IL6-positive cell phenotypes could be determined almost completely, although the total number of NF-IL6-positive cells exceeded the amount (~40% higher) that was expected (100%).

LPS-induced time-dependent expression of proinflammatory, NF-IL6-responsive target genes shows sustained induction for IL6, IL1β, IL10, and mPGES in parallel to spatiotemporal NF-IL6 IR in the rat brain

As expected, LPS-induced NF-IL6 mRNA expression in the hypothalamus was significantly elevated 4 hours after LPS injection compared with PBS-treated control animals preceding the peak of NF-IL6 IR in the rat brain, which was found to occur at 6 or 8 hours after stimulation (Fig. 7A). SOCS3 and IκBα mRNA expression were also significantly up-regulated at 4 hours (Fig. 7B,C), even though these two marker proteins of the STAT3 and NFκB signaling pathway are negative regulators and downstream of activation (Laflamme et al., 1999; Laflamme and Rivest, 1999; Lebel et al., 2000). Similarly to STAT3 and NFκB, NF-IL6 is a transcription factor that has previously been shown to participate in the induction of several important inflammatory target genes, which are implicated in fever induction (Akira, 1997). Therefore, the mRNA expression of the proinflammatory cytokines IL6 and IL1β as well as the antiinflammatory cytokine IL10 and the rate-limiting enzymes of the prostaglandin (PG) synthesis pathway, namely, COX2 and mPGES, were investigated by using RT-PCR (Fig. 7D–H). At the beginning of the observed time course of LPS-induced NF-IL6 IR in the rat brain, mRNA levels of all investigated target genes were significantly elevated compared with their counterpart controls 4 hours after stimulation. In parallel to the late peak of NF-IL6 IR observed in the present study, significantly elevated mRNA expression was sustained for IL6 until 6 hours, for IL10 and mPGES until 8 hours, and for IL1β

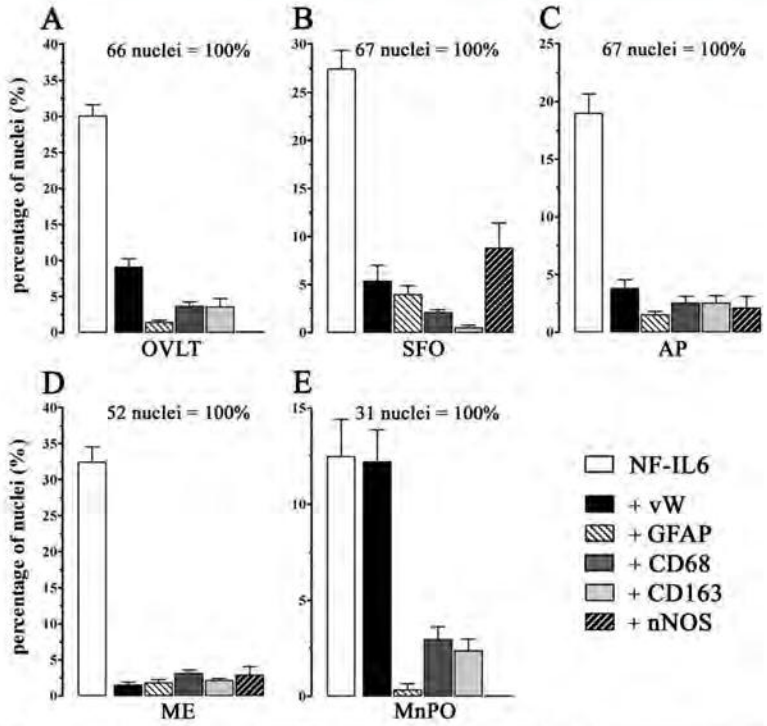


Figure 6. A–E: Quantitative analysis of NF-IL6-immunoreactive cell phenotypes in the sensory CVOs, i.e., vascular organ of the lamina terminalis, OVLT; subfornical organ, SFO; area postrema AP; the median eminence, ME; and in addition the median preoptic nucleus (MnPO) of two to five sections per animal ($n = 5$) 8 hours after systemic LPS (100 μg/kg, i.p.) stimulation. The average number of all nuclei counted in each structure is given on the top of each panel. White bars represent the total percentage of NF-IL6 immunoreactive nuclei in the respective brain structure. Note that the MnPO shows the smallest amount of NF-IL6 positive nuclei (E). Portions of endothelial cells predominate in both the sensory CVOs and the MnPO (A–C,E), whereas astrocytes exhibit nuclear NF-IL6 IR primarily in the SFO, which additionally contains by far the highest level of NF-IL6-positive neurons of all the analyzed structures (B). Similar to the OVLT, no nuclear NF-IL6 IR can be detected in MnPO neurons (E). NF-IL6 signals in activated microglia and macrophages are present in all analyzed brain structures. Please note that a small number of reacting cells could not be identified. Data are presented as means of means ± SEM.

until 10 hours after the LPS challenge. The recently identified negative regulator of NF-IL6 expression Trib1 that modulates NF-IL6-responsive target gene expression was the only putative target gene investigated (Fig. 7I) and showed an LPS-induced significant increase in mRNA expression only at 10 hours after stimulation, in general confirming previous results for elevated Trib1 mRNA levels after LPS or IL1β in various cell culture systems (Sung et al., 2006). LPS-induced Trib1 mRNA levels might also show an additional early inflammation-induced peak of expression such as at the 4-hour time point, which did not reach significance in the present study but remains to be determined.

NF-IL6 protein levels are significantly increased in the rat brain 8 hours after LPS treatment

NF-IL6 protein can be found in three functionally distinct isoforms. Neither immunohistochemical staining nor the detection of NF-IL6 mRNA expression can help to distinguish LAP*, LAP, and LIP from each other, because alternative initiation sites or posttranslational proteolysis might be the underlying mechanisms for isoform generation (Ramji and Foka, 2002). Ejarque-Ortiz et al. (2007) revealed an increase of LAP in the mouse brain 16 hours after LPS stimulation using Western blot. To confirm these results for our experiments, Western blot analyses

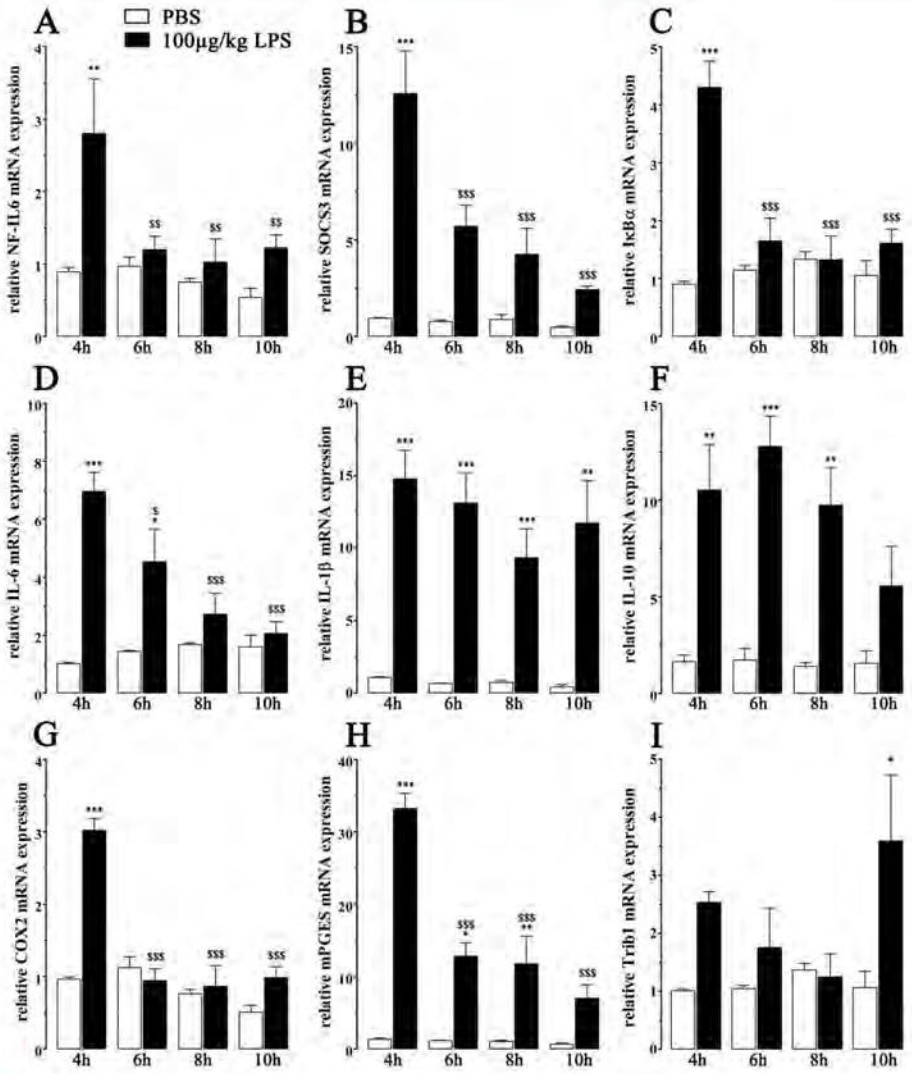


Figure 7. mRNA expression of innate inflammatory mediators in the rat hypothalamus 4, 6, 8, and 10 hours following systemic injection of LPS (100 µg/kg i.p.) compared with PBS-treated animals using quantitative RT-PCR. NF-IL6, suppressor of cytokine signaling 3 (SOCS3), inhibitor of kappa B alpha (IκBα), interleukin (IL)-6, IL1β, cyclooxygenase 2 (COX2), and microsomal prostaglandin E synthase (mPGES) mRNA levels peaked in the early phase of the febrile response (4 hours) following LPS challenge, whereas IL10 mRNA levels did not peak until 6 hours after LPS stimulation. In addition, IL6, IL1β, and mPGES levels were still significantly elevated in comparison with the control animals at 6 hours, whereas a significant difference from controls at 8 hours was detected only for IL10, mPGES, and IL1β mRNA levels, the latter of which were still elevated after 10 hours. Note that tribbles-1 (Trib1) mRNA expression was significantly increased exclusively at the time point 10 hours. Colums represent means ± SEM (n = 5 for 8 hours, n = 3 for other groups). An analysis of basal expression of mRNA levels was omitted from the present experiment because nuclear NF-IL6 IR was almost undetectable in the rat hypothalamus in untreated animals. *Different from respective control; $different from 4 hours; $P^{*,\$}P < 0.05$, $^{**,\$\$}P < 0.01$, $^{***,\$\$\$}P < 0.001$.



Figure 8. Protein levels of the active form of NF-IL6 (liver-enriched activating protein; LAP) were significantly elevated in the rat brain cortex (A,B) 8 hours after LPS (100 μg/kg, i.p.) compared with PBS stimulation. To normalize the protein levels between different samples, the levels were estimated as ratio of protein X/β-actin (PBS, n = 3; LPS, n = 4). The average molecular weight of the detected protein (35 kDa) was characteristic for LAP (molecular ladder in the middle lane). *$P < 0.05$.

of protein extracted from the rat brain cortex, a brain area that was highly responsive for NF-IL6 IR, was performed for animals 8 hours after LPS stimulation (n = 4) or PBS treatment (n = 3). This revealed a significant increase of NF-IL6 protein content when normalized with the housekeeping gene actin (Fig. 8). Moreover, the molecular weight of the only determined NF-IL6-stained band appeared to be 35 kDa, characteristic of the long and active form of this transcription factor (LAP, LAP*).

NF-IL6 IR staining colocalizes with COX2 IR

To verify the specificity of our NF-IL6 IR in the present study, we used two different antibodies raised against the same immunogen from two different species, namely, rabbit and goat, and preincubated with the blocking peptide (Fig. 9). Indeed, both antisera showed an almost equal staining pattern in the rat brain of animals 8 hours after LPS treatment, as shown for the AP, which was abolished after preincubation with the blocking peptide. NF-IL6 IR was absent in PBS-injected control animals.

In addition to our RT-PCR results, we wanted to know whether NF-IL6-responsive target genes such as COX2 were induced in cells that show NF-IL6 IR. In fact, we revealed a colocalization of perinuclear COX2 IR with nuclear NF-IL6 IR throughout the rat brain (data not shown), including the MnPO along blood vessel-like structures (Fig. 9) 4 hours after LPS treatment. Previously, we have demonstrated a link between STAT3 and COX2 in this brain structure that is crucial for fever induction, but at an earlier time point (2 hours) and during localized LPS-induced inflammation (Rummel et al., 2006). Here, we show for the first time that the NF-IL6 that colocalizes with COX2 IR might be another participant implicated in PG synthesis in the hypothalamus, but at later stages during the febrile response.

DISCUSSION

This study is the first to perform detailed spatiotemporal characterization of NF-IL6 protein and mRNA expression in the rat brain during LPS-induced systemic inflammation. We provide experimental evidence for the potential role of NF-IL6 in the induction of several important brain inflammation markers during the late phase of systemic LPS-mediated inflammation, including COX2, and NF-IL6 activation itself appears to be a new delayed brain cell activation marker during infection and inflammation. Notably, the colocalization of NF-IL6 IR with COX2 IR shown in the present study provides strong evidence for a role of this transcription factor in the induction of the PG synthesis pathway in the brain during systemic inflammation. Moreover, we are also the first to demonstrate that the expression of a potential inflammatory "stop" signal, namely, the negative regulator of NF-IL6, Trib1, is significantly induced in the hypothalamus 10 hours after LPS stimulation, at the time point of the beginning of the dark phase when fever tends to decline. Overall, although this remains speculative, we propose that NF-IL6 might be involved in the maintenance or even termination of the febrile response.

Technical considerations

The present study used profile counts to obtain quantitative data on the time course of NF-IL6 activation in several brain structures and for the determination of NF-IL6 IR cell phenotypes. The counting procedure used has some limitations, in that large objects counted in relatively thin sections (20 μm) will produce overcounts (Abercrombie, 1946; Guillery, 2002). Therefore, we used Abercrombie's formula to correct cell counts for oversampling. Accuracy for counting the cells was limited by the fact that coronal brain sections were postfixed on glass slides, which alters the thickness of the sections (T), but in a consistent way throughout all sections. Overall, the obtained results have the required accuracy to support the conclusions we have drawn from our data.

Another technical consideration pertains to the use of a conventional microscope for colocalization of NF-IL6-positive cell nuclei with IR of specific cell marker proteins. Although we used a ×100 objective with oil immersion to obtain the best resolution and focus for determining cell phenotypes, we have to acknowledge that the possibility remains that cellular elements could have been sitting atop each other instead of in the same focal plane. As a result, we were rather conservative when identifying cell phenotypes and included only cells that, in our hand, showed obvious colocalization, as demonstrated for example in Figure 5 using the channel function of the image analyzing program MetaMorph to omit a single

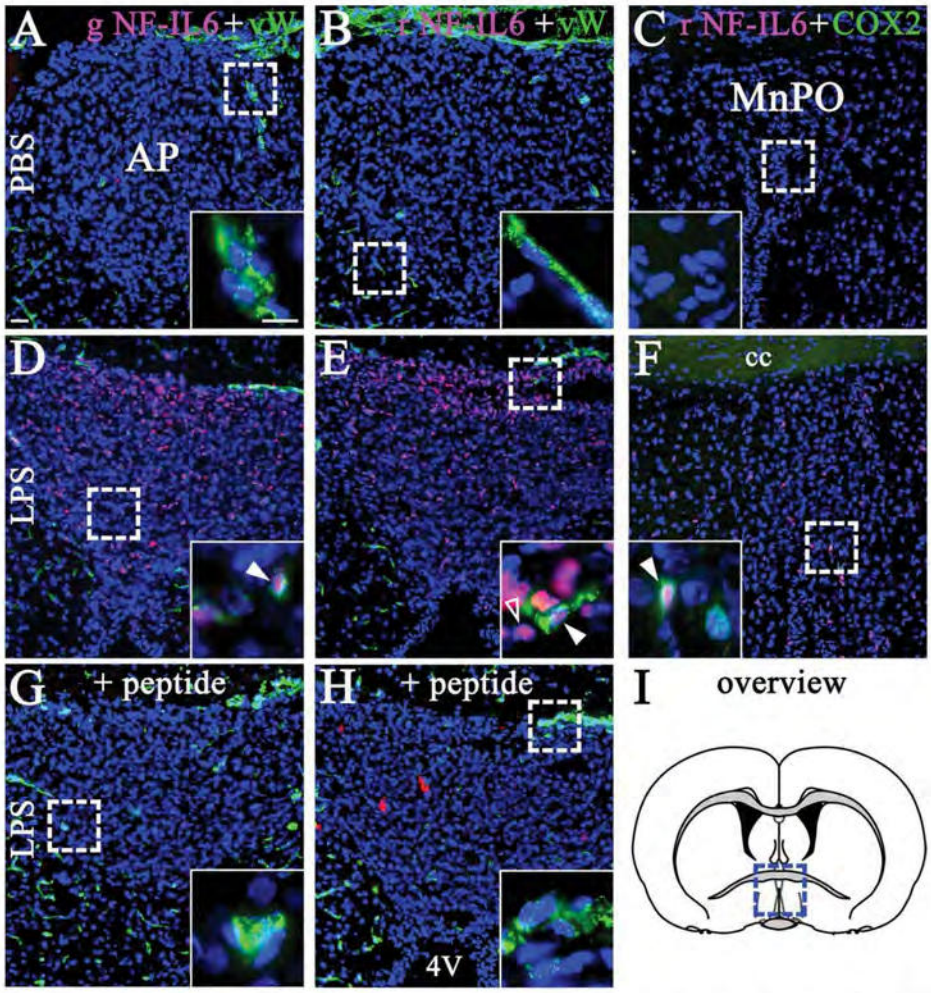


Figure 9. Identical staining pattern of nuclear NF-IL6 signals in LPS-injected rats (100 µg/kg) using a goat (g) or a rabbit (r) antibody against NF-IL6 (red) in the area postrema (AP; **D,E**) was completely abolished after preincubation of both antibodies with the blocking peptide (**G,H**). NF-IL6 staining was absent in the PBS-treated controls (**A,B**). Immunohistochemical detection of perinuclear COX2 revealed a colocalization with nuclear NF-IL6 signals 4 hours after LPS treatment throughout the rat brain, among others, in the median preoptic nucleus (green, MnPO; **F**). PBS injection caused neither NF-IL6 nor COX2 IR (**C**). White arrowheads indicate nuclear NF-IL6 IR colocalizing with endothelial von Willebrand factor IR (green; vW; A,B,D,E,G,H) or perinuclear COX2 IR (green; C,F); open arrowheads highlight NF-IL6 signals in nuclei of other cell phenotypes. Nuclear DAPI counterstain (blue) visualizes the microanatomy of the surrounding tissue and nuclear localization of NF-IL6 IR. Areas of high magnifications are indicated with a dashed white square. The overview in **I** schematically illustrates the localization of the ventral, caudal MnPO (blue dashed square) on a coronal section that was shown in the present study (C,F; see also Fig. 4E,F). 4V, fourth ventricle. Scale bars = 25 µm in A (applies to B–H); 10 µm in insets.

color from the RGB coded image. In this manner, we were able to depict the typical nuclear recess that is formed by the cell marker IR for the colocalization.

Anatomical and functional implications of LPS-induced spatiotemporal NF-IL6 IR in the rat brain

Recently, Ejarque-Ortiz et al. (2007) reported an increase of NF-IL6 protein by means of Western blot and immunofluorescence in an in vivo model of septic- like inflammation using two different high doses of LPS (~4 or ~16 mg/kg, i.p.) in the mouse brain 16 hours after stimulation. In this study, the authors did not specify any results for particular brain structures and reported NF-IL6 IR only in microglia. A potential function of activated microglia in neurotoxic effects was discussed, but for characterization of this cell phenotype a detection marker protein for resting microglia was used. Here, we present for the first time experimental evidence of a dramatic time- and brain structure-dependent increase of NF-IL6 IR in the rat brain during systemic inflammation induced by a physiologically more relevant moderate dose of LPS (100 μg/kg). In addition, we opted to use a marker for activated microglia for NF-IL6 IR-positive cells as opposed to a marker for resting microglia used by Ejarque-Ortitz et al. (2007). Consistently with previous results (Nadeau et al., 2005), obtained by in situ hybridization of NF-IL6 mRNA in the mouse brain, PBS-treated animals did not show any or at most very weak NF-IL6 IR within most brain structures, including the CVOs (OVLT, SFO, AP, and ME). However, some weak staining was detected in ependymal cells or the pituitary of these animals. Strong NF-IL6 IR occurred only in the hippocampus, an observation that is well supported by several other studies using in situ hybridization or IHC in mice (Ejarque-Ortiz et al., 2007; Kuo et al., 1990; Nadeau et al., 2005) and is in line with its proposed role in hippocampus-dependent memory consolidation (Taubenfeld et al., 2001).

Possible relevance of NF-IL6 IR in selected brain structures

Systemic LPS treatment increased NF-IL6 IR in several brain structures and most prominently in the sensory CVOs, namely, the OVLT, SFO, and AP, known to be key sites for immune-to-brain communication during infection and inflammation (Roth et al., 2004). For instance, lesion studies support a role for the OVLT (Hashimoto et al., 1994) and the SFO (Takahashi et al., 1997) in fever generation and for the AP in the activation of the hypothalamo-pituitary adrenal axis (HPA; Buller, 2001). Moreover, the ventromedial preoptic nucleus, the MnPO, and the RPa, three NF-IL6-responsive brain structures residing within the blood-brain barrier, have been proposed to activate/be part of fever-inducing autonomic pathways at distinct levels (Lazarus et al., 2007; Nakamura et al., 2002, 2004; Scammell et al., 1996).

A role for NF-IL6 in long-term memory consolidation (Taubenfeld et al., 2001) is well established. Interestingly, the hippocampus is as well known to respond with increased cytokine expression after peripheral LPS stimulation (Henry et al., 2008; Layé et al., 1994), and the transcription factor NF-IL6 represents a good candidate that might be involved in this process. In the present study, we did not detect a qualitative increase in LPS-induced NF-IL6 IR cells in this brain structure (Table 3), so the high basal NF-IL6 expression as reported previously (Nadeau et al., 2005; Sterneck and Johnson, 1998) might already be sufficient for inflammation-induced transcriptional regulation. However, a possible increase in NF-IL6 mRNA expression or a moderate elevated NF-IL6 protein content in this brain structure cannot be excluded for the present study in the hippocampus and remains to be investigated.

LPS-induced NF-IL6 IR in the ME and pituitary gland might be of functional significance for LPS-stimulated HPA axis activation. Corticotropin-releasing hormone (CRH) is derived from paraventricular nucleus neurons projecting to the ME, where CRH is released to trigger in turn adrenocorticotropic hormone (ACTH) release by corticotropic cells of the pituitary gland into the circulation, which subsequently induces cortisol release from the adrenal cortex, (Papadimitriou and Priftis, 2009). NF-IL6 is known to activate the promoter of CRH (Stephanou et al., 1997), and overexpression of NF-IL6 in rat pituitary adenoma cells increased proopiomelanocortin (POMC) transcription, supporting a possible role for LPS-induced NF-IL6 in the control of activity of the HPA axis (Abbud et al., 2004). Although a possible colocalization of NF-IL6 IR with POMC has not been investigated in the present study, LPS-induced IL6-mediated STAT3 activation in pituitary corticotropes has been shown previously (Gautron et al., 2003), suggesting NF-IL6 as another participant in this process. For the ME, CRH release appears to be controlled by PG and nitric oxide (NO), both of which can be activated and induced by NF-IL6 via transcription of the inducible nitric oxide synthase (iNOS) and the rate-limiting enzyme for PG synthesis, COX2 (Chun and Suh, 2004; Kolyada and Madias, 2001). Therefore, NF-IL6 might contribute to HPA axis activation by CRH, POMC, and the expression of factors that control CRH release, with possible important implications for NF-IL6 in toning down immune-to-brain communication in the course of systemic inflammation.

NF-IL6 IR cell phenotypes

We observed LPS-induced NF-IL6 IR in astrocytes, microglia, neurons, perivascular macrophages, and endothelial

cells. In this context, it is important to note that antibodies against CD163 and CD68 that were used in the present study do not stain exclusively perivascular macrophages (CD163) or activated microglia (CD68), respectively. For instance, these antibodies are reported also to detect neutrophil granulocytes (Matsumoto et al., 2007; Saito et al., 1991; Wu et al., 2003). However, with the dose of LPS (100 μg/kg) at the time points investigated, neutrophils should be hardly detectable in the brain, as previously shown in a time-course experiment in mice (Rummel et al., 2009), and CD68/CD163-positive cells did not show a segmented nuclear DAPI stain that is characteristic for neutrophils. In addition, Dijkstra et al. (1985) and Graeber et al. (1989) reported that perivascular cells are as well detected by the antibody raised against CD68 that stains activated microglia although with a much weaker staining intensity. Therefore, we have to consider that in the present study a significant portion of CD68 cells might have also been stained by CD163, which may account for the results in the MnPO, where we observed a total number of determined cell phenotypes that was greater than 100%. Some cells might have been counted for both phenotypes, namely, activated microglia and perivascular macrophages.

In astrocytes, microglia, and neurons, NF-IL6 IR has previously been detected in several cell culture models after LPS and cytokine stimulation (Ejarque-Ortiz et al., 2007; Pahan et al., 2002) or hypoxia (Halterman et al., 2008) or in vivo during excitotoxic and LPS-induced brain inflammation (Cortes-Canteli et al., 2008; Ejarque-Ortiz et al., 2007), respectively. Among other substances, vasoactive intestinal peptide, noradrenaline, and glutamate have been reported to induce NF-IL6 in astrocytes (Cardinaux and Magistretti, 1996) or neurons (Cortes-Canteli et al., 2008), supporting the role of NF-IL6 as an activation-dependent marker, as previously suggested for NF-IL6 in rat cortical neurons stimulated with KCl (Sun et al., 2007). However, we are the first to perform a detailed neuroanatomical characterization of NF-IL6 IR cell phenotypes in an in vivo model of systemic inflammation.

Our present results also are the first to show NF-IL6 IR in perivascular macrophages and brain endothelial cells of LPS-injected animals. Endothelial cells in the periphery, e.g., in the lung, however, have already been shown to express NF-IL6 (Kolyada and Madias, 2001). We are not aware of any report of NF-IL6 IR in perivascular macrophages, but macrophages in general are known to express NF-IL6 constitutively (Akira, 1997; Tanaka et al., 1995). Tanaka et al. (1995) reported an LPS-induced activation of NF-IL6 in peritoneal macrophages. Perivascular macrophages and brain endothelial cells express COX2 and are supposed to be the main source for PGE_2 synthesis in the brain. The importance of these two cell types at the interface of the periphery to the brain is well established (Matsumura and Kobayashi, 2004; Schiltz and Sawchenko, 2003) and might be of particular interest in the case of immune cell trafficking during infection and inflammation (Rummel et al., 2009). Nonetheless, other potentially NF-IL6-positive cell phenotypes remain to be identified. For example, the neuronal marker nNOS that we used in the present study does not stain all neurons, which might explain why we did not detect any (OVLT or MnPO) or very few (AP) LPS-induced NF-IL6-positive neurons in the sCVOs.

Previous observations on LPS-induced STAT3 activation in the rat and mouse brain revealed very similar results on responsive brain structures compared with our present results on LPS-induced NF-IL6-IR in the rat brain. However, a few differences were revealed for responsive cell phenotypes when comparing STAT3 and NF-IL6 IR. For instance, astrocytes appeared to be the main phenotype that showed LPS-induced STAT3 activation in the CVOs of the rat or guinea pig brain (Gautron et al., 2002; Rummel et al., 2005), but only 3–13% of astrocytes exhibited NF-IL6 IR in the present study, and endothelial cells appeared to be the most important cellular phenotype in almost all of the brain structures stained for NF-IL6. Nonetheless, the brain endothelium was also highly responsive for STAT3 activation in mice, rats, and guinea pigs (Rummel et al., 2005, 2008). Previously, we detected a time-dependent migration of STAT3 activation during LPS-induced systemic inflammation from the CVOs into the brain parenchyma (Rummel et al., 2005); however, LPS-induced NF-IL6 IR did not show this effect, which might be due to the early STAT3 and the delayed NF-IL6 activation.

NF-IL6 activation

The LPS-induced NF-IL6 IR and protein content in the rat brain that we observed might have been directly induced by LPS as suggested by others using astroglial cell cultures (Ejarque-Ortiz et al., 2007; Kelicen and Tindberg, 2004; Perez-Capote et al., 2006). LPS, after binding to CD14 and its specific receptor, namely, toll-like receptor (TLR)4, was shown to activate cells subsequently via NFκB and to increase the transcription of a variety of inflammatory mediators in the sCVOs and brain vasculature (Rivest, 2003). In the present study, NF-IL6 IR was detected in these LPS-responsive brain structures with a distribution pattern similar to that previously reported for LPS-induced STAT3 activation (Rummel et al., 2005, 2008) or SOCS3/IκB/CEBPδ expression (Laflamme and Rivest, 1999; Lebel et al., 2000; Reyes et al., 2003) but with a later onset, supporting a direct but delayed action of LPS on NF-IL6 induction probably via an MyD88-dependent pathway (Lu et al., 2009). Alternatively, or additionally, secondary inflammatory mediators such as cytokines might have contributed to increased NF-IL6 expression. This could explain why NF-IL6 IR peaked at a

late time point (6–8 hours), at which de novo production of these cytokines preceded NF-IL6 induction. For instance, circulating IL6 might be a good candidate, which reached its highest plasma bioactivity at the peak of brain NF-IL6 IR in the present study. Moreover, IL6 (Rummel et al., 2006, 2008) but also IL1β (Nadjar et al., 2003) and tumor necrosis factor (TNF)α (Laflamme and Rivest, 1999) were previously demonstrated to act on the CVOs and blood vessels during LPS-induced inflammation and have been shown to increase NF-IL6 mRNA in a Northern blot within several tissues, including the liver and the lung (Akira and Kishimoto, 1992), although a significant increase for the brain was not detected in that study. However, a more recent study presents experimental evidence for an IL1β- and TNFα-induced increase in NF-IL6 expression in mouse primary astrocyte cultures (Cardinaux et al., 2000). Thus, significantly increased NF-IL6 mRNA expression in the hypothalamus and protein content in the rat cortex after LPS stimulation, which were revealed by our present results, might have been caused by LPS as well as circulating or brain-derived cytokines. The possible contribution of each of these mediators in NF-IL6 expression remains to be determined.

Several mechanisms of NF-IL6 activation have been proposed. These are related mostly to increased NF-IL6 expression, phosphorylation, and/or nuclear translocation (Akira, 1997; Akira and Kishimoto, 1992). Collectively, our data and results by Ejarque-Ortiz et al. (2007) generally do not support nuclear translocation of an existing pool of NF-IL6 protein (cytoplasmatic staining in PBS-treated control animals was absent or very weak) as shown for NFκB or STAT3 but rather an activation of NF-IL6 by increased expression via acute de novo synthesis. However, a role for different phosphorylation sites in the activation process of NF-IL6 has been documented by others (Poli, 1998), and its specific role for regulation of NF-IL6 activity still has to be elucidated. Another complication in interpreting the functional role of NF-IL6 in inflammation is its appearance in different isoforms, which cannot be distinguished by immunohistochemistry but by Western blot. Interestingly, posttranscriptional modifications may transform the activating forms into the shorter, inhibiting-form LIP, in particular after stimulation with antiinflammatiory mediators. The cytokine IL10 has been shown to inhibit viral replication in HIV-infected macrophages by this mechanism (Tanaka et al., 2005). Overall, our results confirm previous results by others on increased NF-IL6 protein content in the mouse brain after systemic LPS stimulation (Ejarque-Ortiz et al., 2007) and provide evidence for the existence and an increase in the activating-form LAP at 8 hours after LPS stimulation in the rat brain, although changes or even a switch from LAP to LIP in the course of the inflammatory response cannot be excluded and might be of great interest for future studies.

Putative NF-IL6-responsive target genes

NF-IL6 binding sites and/or a role for NF-IL6 in the transcriptional regulation of IL6 (Matsusaka et al., 1993), IL1β (Zhang and Rom, 1993), IL10 (Liu et al., 2003), COX2 (Billack et al., 2002; Tazawa et al., 1994), and mPGES (Uematsu et al., 2002) have been previously demonstrated. In addition, it has been shown that LPS treatment increases mRNA expression of IL6, IL1β, IL10, COX2, or mPGES (Rivest, 2003) confirming the RT-PCR results on hypothalamic expression of these inflammatory mediators in the present study. By using in situ hybridization, several authors have demonstrated the expression of these NF-IL6-responsive target genes among others within brain blood vessels and/or the CVOs during systemic inflammation (Lacroix and Rivest, 1998; Laflamme and Rivest, 1999; Vallières and Rivest, 1997; Wong et al., 1997; Yamagata et al., 2001) in a distribution pattern similar to that observed for LPS-induced NF-IL6 IR here. Collectively, these observations support the idea that indeed NF-IL6 is involved in the induction of these very important inflammatory target genes (e.g., COX2) in the rat brain during systemic LPS-induced inflammation but also including antiinflammatory cytokines such as IL10, which might be important for the termination of the brain inflammatory response and subsequently brain-controlled sickness symptoms such as fever (Cartmell et al., 2003; Ledeboer et al., 2002; Leon et al., 1998).

Possible functional significance of delayed NF-IL6 brain cell activation

As opposed to the early LPS/IL1β-induced NFκB (1–2 hours; Nadjar et al., 2003; Rummel et al., 2006) or the LPS/IL6-induced STAT3 activation (3–4 hours; Gautron et al., 2002; Rummel et al., 2005), brain NF-IL6 IR detection peaked very late at about 6–8 hours during the systemic inflammatory response, confirming previous results showing that NF-IL6 occurs relatively late during inflammation (Poli, 1998) and therefore might be involved in the late induction of acute-phase genes in the liver or chronic inflammation in rheumatoid arthritis (Pope et al., 1999). Our observation in the present study that mRNA expression of IκBα and SOCS3, the negative regulators of NFκB and STAT3, peaks at 4 hours after LPS stimulation at the same time as NF-IL6 (as an activating signal) is in line with this time course of protein levels revealed by immunohistochemistry. Functionally, the successive time-dependent activation of NFκB followed by STAT3 and finally NF-IL6 might be a mechanism to explain changes in target gene expression. Notably, these transcription factors have been shown to interact with each other, enhancing or even inhibiting their transcriptional activity. For instance, NF-IL6 and NFκB synergistically activate the transcription of IL6 and COX2 (Billack et al., 2002; Matsusaka et al., 1993), and

STAT3 contributes to NF-IL6 transcription by a so-called tethering mechanism (Niehof et al., 2001), or NF-IL6 controls NFκB-associated signaling by inhibiting IκBα (Cappello et al., 2009). Previously, we have shown that nuclear phosphorylated (p)STAT3 IR colocalized with NFκB and with COX2 2 hours after LPS treatment, whereas NF-IL6 IR did not colocalize with COX2 IR at this time point, suggesting a STAT3/NFκB-linked activation of COX2 in the rat brain during early LPS-induced localized peripheral inflammation (Rummel et al., 2006). However, there is no consensus region described for STAT3 in the COX2 promotor, although NFκB (Nadjar et al., 2005) and NF-IL6 (Kirtikara et al., 2000) are known to induce COX2 expression in endothelial cells. Here, by using a systemic stimulation with LPS, we were able to demonstrate for the first time that COX2 indeed colocalizes with NF-IL6 IR but only at later time points starting 4 hours after the LPS challenge, pointing to a possible time-dependent role of these transcription factors. Notably, the time course of LPS-induced NF-IL6 IR in the brain occurred in parallel to both the late phase of the LPS-induced febrile response and the sustained increased expression of other potentially NF-IL6 responsive target genes besides COX2, namely, IL1, IL10, and mPGES. mPGES is the second rate-limiting enzyme for PGE2 synthesis, the most important terminal mediator in fever induction (Nilsberth et al., 2009).

Potential regulatory role for Trib1 in NF-IL6 signaling

Members of the tribbles family of proteins are known to regulate or modulate various important signaling pathways involving NF-IL6 among others (Hegedus et al., 2006). Notably, we were able to show for the first time significantly increased Trib1 mRNA expression in the rat hypothalamus at 10 hours after LPS stimulation, although others have already demonstrated that Trib1 expression is increased after IL1β treatment in several cell lines, including endothelial or macrophage cultures (Sung et al., 2006). In *Drosophila* and in mouse macrophages, Trib1 inhibited NF-IL6 mRNA as well as protein expression, and Yamamoto et al. (2007) even demonstrated a Trib1-mediated modulation of NF-IL6 target gene expression. For instance, the authors revealed unequivocally that Trib1 represses NF-IL6-mediated expression of IL10 and mPGES by using Trib1-deficient or -overexpressing cells, an observation that matches our findings that mPGES and IL10 expression in the hypothalamus was no longer significantly elevated 10 hours after LPS stimulation, the time point of significantly increased Trib1 expression. Thus, Trib1 might be an important inflammatory stop signal that inhibits NF-IL6 and target gene expression. Overall, these observations in conjunction with the aforementioned interactions of STAT3/NFκB-NF-IL6 allow the assumption, though speculative, that STAT3 and NFκB contribute to the first phase, whereas NF-IL6, which is potentially modulated by Trib1, might be responsible for the maintenance of sickness type symptoms such as fever by transcriptional regulation of inflammatory target genes (Poli, 1998).

In conclusion, we propose a novel role for NF-IL6 as a delayed brain cell activation marker that is associated with a prolonged transcriptional activation after systemic inflammation in microglia, astrocytes, neurons, perivascular macrophages, and endothelial cells in several brain structures, including the circumventricular organs (CVOs) and the MnPO, that are pivotal for immune-to-brain communication (Lazarus et al., 2007; Roth et al., 2004). A role for NF-IL6 in the maintenance or even the termination of the febrile response is suggested. The definite physiological significance of NF-IL6 activation and its participation in the manifestation or termination of brain-controlled sickness type responses remains speculative and should be elucidated at a functional level.

ACKNOWLEDGMENTS

We thank Daniela Ott, Doreen Marks, and Jolanta Murgott for excellent technical assistance.

LITERATURE CITED

Aarden LA, De Groot ER, Schaap OL, Lansdorp PM. 1987. Production of hybridoma growth factor by human monocytes. Eur J Immunol 17:1411–1416.

Abbud RA, Kelleher R, Melmed S. 2004. Cell-specific pituitary gene expression profiles after treatment with leukemia inhibitory factor reveal novel modulators for proopiomelanocortin expression. Endocrinology 145:867–880.

Abercrombie M. 1946. Estimation of nuclear population from microtome sections. Anat Rec 94:239–247.

Akira S. 1997. IL-6-regulated transcription factors. Int J Biochem Cell Biol 29:1401–1418.

Akira S, Kishimoto T. 1992. IL-6 and NF-IL6 in acute-phase response and viral infection. Immunol Rev 127:25–50.

Akira S, Isshiki H, Sugita T, Tanabe O, Kinoshita S, Nishio Y, Nakajima T, Hirano T, Kishimoto T. 1990. A nuclear factor for IL-6 expression (NF-IL6) is a member of a C/EBP family. EMBO J 9:1897–1906.

Alm P, Sharma HS, Sjoquist PO, Westman J. 2000. A new antioxidant compound H-290/51 attenuates nitric oxide synthase and heme oxygenase expression following hyperthermic brain injury. An experimental study using immunohistochemistry in the rat. Amino Acids 19:383–394.

Atamna H, Killilea DW, Killilea AN, Ames BN. 2002. Heme deficiency may be a factor in the mitochondrial and neuronal decay of aging. Proc Natl Acad Sci U S A 99:14807–14812.

Barbe E, Damoiseaux JG, Dopp EA, Dijkstra CD. 1990. Characterization and expression of the antigen present on resident rat macrophages recognized by monoclonal antibody ED2. Immunobiology 182:88–99.

Bauer J, Sminia T, Wouterlood FG, Dijkstra CD. 1994. Phagocytic activity of macrophages and microglial cells during the course of acute and chronic relapsing experimental

autoimmune encephalomyelitis. J Neurosci Res 38: 365–375.
Berek M. 1927. Grundlagen der Tiefenwahrnehmung im Mikroskop. Marburg Sitzungsber 62:189–223.
Billack B, Heck DE, Mariano TM, Gardner CR, Sur R, Laskin DL, Laskin JD. 2002. Induction of cyclooxygenase-2 by heat shock protein 60 in macrophages and endothelial cells. Am J Physiol Cell Physiol 283:C1267–C1277.
Buller KM. 2001. Role of circumventricular organs in proinflammatory cytokine-induced activation of the hypothalamic-pituitary-adrenal axis. Clin Exp Pharmacol Physiol 28: 581–589.
Cao C, Matsumura K, Yamagata K, Watanabe Y. 1997. Involvement of cyclooxygenase-2 in LPS-induced fever and regulation of its mRNA by LPS in the rat brain. Am J Physiol Regul Integr Comp Physiol 272:R1712–R1725.
Cao C, Matsumura K, Shirakawa N, Maeda M, Jikihara I, Kobayashi S, Watanabe Y. 2001. Pyrogenic cytokines injected into the rat cerebral ventricle induce cyclooxygenase-2 in brain endothelial cells and also upregulate their receptors. Eur J Neurosci 13:1781–1790.
Cappello C, Zwergal A, Kanclerski S, Haas SC, Kandemir JD, Huber R, Page S, Brand K. 2009. C/EBPbeta enhances NF-kappaB-associated signalling by reducing the level of IkappaB-alpha. Cell Signal 21:1918–1924.
Cardinaux JR, Magistretti PJ. 1996. Vasoactive intestinal peptide, pituitary adenylate cyclase-activating peptide, and noradrenaline induce the transcription factors CCAAT/enhancer binding protein (C/EBP)-beta and C/EBP delta in mouse cortical astrocytes: involvement in cAMP-regulated glycogen metabolism. J Neurosci 16:919–929.
Cardinaux JR, Allaman I, Magistretti PJ. 2000. Proinflammatory cytokines induce the transcription factors C/EBPbeta and C/EBPdelta in astrocytes. Glia 29:91–97.
Cartmell T, Poole S, Turnbull AV, Rothwell NJ, Luheshi GN. 2000. Circulating interleukin-6 mediates the febrile response to localised inflammation in rats. J Physiol 526: 653–661.
Cartmell T, Ball C, Bristow AF, Mitchell D, Poole S. 2003. Endogenous interleukin-10 is required for the defervescence of fever evoked by local lipopolysaccharide-induced and Staphylococcus aureus-induced inflammation in rats. J Physiol 549:653–664.
Chang AY, Chan JY, Chan SH. 2003. Differential distribution of nitric oxide synthase isoforms in the rostral ventrolateral medulla of the rat. J Biomed Sci 10:285–291.
Chun KS, Surh YJ. 2004. Signal transduction pathways regulating cyclooxygenase-2 expression: potential molecular targets for chemoprevention. Biochem Pharmacol 68: 1089–1100.
Cortes-Canteli M, Wagner M, Ansorge W, Perez-Castillo A. 2004. Microarray analysis supports a role for ccaat/enhancer-binding protein-beta in brain injury. J Biol Chem 279:14409–14417.
Cortes-Canteli M, Luna-Medina R, Sanz-Sancristobal M, Alvarez-Barrientos A, Santos A, Perez-Castillo A. 2008. CCAAT/enhancer binding protein beta deficiency provides cerebral protection following excitotoxic injury. J Cell Sci 121:1224–1234.
D'Mello C, Le T, Swain MG. 2009. Cerebral microglia recruit monocytes into the brain in response to tumor necrosis factoralpha signaling during peripheral organ inflammation. J Neurosci 29:2089–2102.
Damoiseaux JG, Dopp EA, Calame W, Chao D, MacPherson GG, Dijkstra CD. 1994. Rat macrophage lysosomal membrane antigen recognized by monoclonal antibody ED1. Immunology 83:140–147.
Dantzer R, O'Connor JC, Freund GG, Johnson RW, Kelley KW. 2008. From inflammation to sickness and depression: when the immune system subjugates the brain. Nat Rev Neurosci 9:46–56.
Debus E, Weber K, Osborn M. 1983. Monoclonal antibodies specific for glial fibrillary acidic (GFA) protein and for each of the neurofilament triplet polypeptides. Differentiation 25:193–203.
Descombes P, Schibler U. 1991. A liver-enriched transcriptional activator protein, LAP, and a transcriptional inhibitory protein, LIP, are translated from the same mRNA. Cell 67(3):569–579.
Dijkstra CD, Dopp EA, Joling P, Kraal G. 1985. The heterogeneity of mononuclear phagocytes in lymphoid organs: distinct macrophage subpopulations in rat recognized by monoclonal antibodies ED1, ED2 and ED3. Adv Exp Med Biol 186:409–419.
Ejarque-Ortiz A, Medina MG, Tusell JM, Perez-Gonzalez AP, Serratosa J, Saura J. 2007. Upregulation of CCAAT/enhancer binding protein beta in activated astrocytes and microglia. Glia 55:178–188.
Galea I, Felton LM, Waters S, van Rooijen N, Perry VH, Newman TA. 2008. Immune-to-brain signalling: the role of cerebral CD163-positive macrophages. Neurosci Lett 448:41–46.
Gautron L, Lafon P, Chaigniau M, Tramu G, Laye S. 2002. Spatiotemporal analysis of signal transducer and activator of transcription 3 activation in rat brain astrocytes and pituitary following peripheral immune challenge. Neuroscience 112:717–729.
Gautron L, Lafon P, Tramu G, Laye S. 2003. In vivo activation of the interleukin-6 receptor/gp130 signaling pathway in pituitary corticotropes of lipopolysaccharide-treated rats. Neuroendocrinology 77:32–43.
Goehler LE, Erisir A, Gaykema RP. 2006. Neural-immune interface in the rat area postrema. Neuroscience 140: 1415–1434.
Graeber MB, Streit WJ, Kreutzberg GW. 1989. Identity of ED2-positive perivascular cells in rat brain. J Neurosci Res 22: 103–106.
Guillery RW. 2002. On counting and counting errors. J Comp Neurol 447:1–7.
Halterman MW, De Jesus C, Rempe DA, Schor NF, Federoff HJ. 2008. Loss of c/EBP-beta activity promotes the adaptive to apoptotic switch in hypoxic cortical neurons. Mol Cell Neurosci 38:125–137.
Harré EM, Roth J, Pehl U, Kueth M, Gerstberger R, Hubschle T. 2002. Selected contribution: role of IL-6 in LPS-induced nuclear STAT3 translocation in sensory circumventricular organs during fever in rats. J Appl Physiol 92:2657–2666.
Harré EM, Roth J, Gerstberger R, Hübschle T. 2003. Interleukin-6 mediates lipopolysaccharide-induced nuclear STAT3 translocation in astrocytes of rat sensory circumventricular organs. Brain Res 980:151–155.
Hashida-Okumura A, Okumura N, Iwamatsu A, Buijs RM, Romijn HJ, Nagai K. 1999. Interaction of neuronal nitric-oxide synthase with alpha1-syntrophin in rat brain. J Biol Chem 274:11736–11741.
Hashimoto M, Ueno T, Iriki M. 1994. What roles does the organum vasculosum laminae terminalis play in fever in rabbits? Pflugers Arch 429:50–57.
Hegedus Z, Czibula A, Kiss-Toth E. 2006. Tribbles: novel regulators of cell function; evolutionary aspects. Cell Mol Life Sci 63:1632–1641.
Henry CJ, Huang Y, Wynne A, Hanke M, Himler J, Bailey MT, Sheridan JF, Godbout JP. 2008. Minocycline attenuates lipopolysaccharide (LPS)-induced neuroinflammation, sickness behavior, and anhedonia. J Neuroinflammation 5:15.

Holt I, Cooper RG, Hopkins SJ. 1991. Relationships between local inflammation, interleukin-6 concentration and the acute phase protein response in arthritis patients. Eur J Clin Invest 21:479–484.

Hughes PM, Botham MS, Frentzel S, Mir A, Perry VH. 2002. Expression of fractalkine (CX3CL1) and its receptor, CX3CR1, during acute and chronic inflammation in the rodent CNS. Glia 37:314–327.

Kapadia R, Tureyen K, Bowen KK, Kalluri H, Johnson PF, Vemuganti R. 2006. Decreased brain damage and curtailed inflammation in transcription factor CCAAT/enhancer binding protein beta knockout mice following transient focal cerebral ischemia. J Neurochem 98:1718–1731.

Kelicen P, Tindberg N. 2004. Lipopolysaccharide induces CYP2E1 in astrocytes through MAP kinase kinase-3 and C/EBPbeta and -delta. J Biol Chem 279:15734–15742.

Kim JE, Kwak SE, Choi SY, Kang TC. 2008. Region-specific alterations in astroglial TWIK-related acid-sensitive K^+-1 channel immunoreactivity in the rat hippocampal complex following pilocarpine-induced status epilepticus. J Comp Neurol 510:463–474.

Kirtikara K, Raghow R, Laulederkind SJ, Goorha S, Kanekura T, Ballou LR. 2000. Transcriptional regulation of cyclooxygenase-2 in the human microvascular endothelial cell line, HMEC-1: control by the combinatorial actions of AP2, NF-IL-6 and CRE elements. Mol Cell Biochem 203:41–51.

Kitami Y, Fukuoka T, Hiwada K, Inagami T. 1999. A high level of CCAAT-enhancer binding protein-delta expression is a major determinant for markedly elevated differential gene expression of the platelet-derived growth factor-alpha receptor in vascular smooth muscle cells of genetically hypertensive rats. Circ Res 84:64–73.

Kluger MJ. 1991. Fever: role of pyrogens and cryogens. Physiol Rev 71:93–127.

Kolyada AY, Madias NE. 2001. Transcriptional regulation of the human iNOS gene by IL-1beta in endothelial cells. Mol Med 7:329–343.

Konsman JP, Vigues S, Mackerlova L, Bristow A, Blomqvist A. 2004. Rat brain vascular distribution of interleukin-1 type-1 receptor immunoreactivity: relationship to patterns of inducible cyclooxygenase expression by peripheral inflammatory stimuli. J Comp Neurol 472:113–129.

Kuo CF, Xanthopoulos KG, Darnell JE Jr. 1990. Fetal and adult localization of C/EBP: evidence for combinatorial action of transcription factors in cell-specific gene expression. Development 109:473–481.

Lacroix S, Rivest S. 1998. Effect of acute systemic inflammatory response and cytokines on the transcription of the genes encoding cyclooxygenase enzymes (COX-1 and COX-2) in the rat brain. J Neurochem 70:452–466.

Laflamme N, Rivest S. 1999. Effects of systemic immunogenic insults and circulating proinflammatory cytokines on the transcription of the inhibitory factor kappaB alpha within specific cellular populations of the rat brain. J Neurochem 73:309–321.

Laflamme N, Lacroix S, Rivest S. 1999. An essential role of interleukin-1beta in mediating NF-kappaB activity and COX-2 transcription in cells of the blood-brain barrier in response to a systemic and localized inflammation but not during endotoxemia. J Neurosci 19:10923–10930.

Landschulz WH, Johnson PF, Adashi EY, Graves BJ, McKnight SL. 1988. Isolation of a recombinant copy of the gene encoding C/EBP. Genes Dev 2:786–800.

Layé S, Parnet P, Goujon E, Dantzer R. 1994. Peripheral administration of lipopolysaccharide induces the expression of cytokine transcripts in the brain and pituitary of mice. Brain Res Mol Brain Res 27:157–162.

Lazarus M, Yoshida K, Coppari R, Bass CE, Mochizuki T, Lowell BB, Saper CB. 2007. EP3 prostaglandin receptors in the median preoptic nucleus are critical for fever responses. Nat Neurosci 10:1131–1133.

Lebel E, Vallieres L, Rivest S. 2000. Selective involvement of interleukin-6 in the transcriptional activation of the suppressor of cytokine signaling-3 in the brain during systemic immune challenges. Endocrinology 141:3749–3763.

Ledeboer A, Binnekade R, Breve JJ, Bol JG, Tilders FJ, Van Dam AM. 2002. Site-specific modulation of LPS-induced fever and interleukin-1 beta expression in rats by interleukin-10. Am J Physiol Regul Integr Comp Physiol 282:R1762–R1772.

Leon LR, Kozak W, Kluger MJ. 1998. Role of IL-10 in inflammation. Studies using cytokine knockout mice. Ann N Y Acad Sci 856:69–75.

Liu YW, Tseng HP, Chen LC, Chen BK, Chang WC. 2003. Functional cooperation of simian virus 40 promoter factor 1 and CCAAT/enhancer-binding protein beta and delta in lipopolysaccharide-induced gene activation of IL-10 in mouse macrophages. J Immunol 171:821–828.

Lu YC, Kim I, Lye E, Shen F, Suzuki N, Suzuki S, Gerondakis S, Akira S, Gaffen SL, Yeh WC, Ohashi PS. 2009. Differential role for c-Rel and C/EBPbeta/delta in TLR-mediated induction of proinflammatory cytokines. J Immunol 182:7212–7221.

Matsumoto H, Kumon Y, Watanabe H, Ohnishi T, Shudou M, Ii C, Takahashi H, Imai Y, Tanaka J. 2007. Antibodies to CD11b, CD68, and lectin label neutrophils rather than microglia in traumatic and ischemic brain lesions. J Neurosci Res 85:994–1009.

Matsumura K, Kobayashi S. 2004. Signaling the brain in inflammation: the role of endothelial cells. Front Biosci 9:2819–2826.

Matsusaka T, Fujikawa K, Nishio Y, Mukaida N, Matsushima K, Kishimoto T, Akira S. 1993. Transcription factors NF-IL6 and NF-kappa B synergistically activate transcription of the inflammatory cytokines, interleukin 6 and interleukin 8. Proc Natl Acad Sci U S A 90:10193–10197.

Miller AJ, Luheshi GN, Rothwell NJ, Hopkins SJ. 1997. Local cytokine induction by LPS in the rat air pouch and its relationship to the febrile response. Am J Physiol 272:R857–R861.

Nadeau S, Hein P, Fernandes KJ, Peterson AC, Miller FD. 2005. A transcriptional role for C/EBP beta in the neuronal response to axonal injury. Mol Cell Neurosci 29:525–535.

Nadjar A, Combe C, Layé S, Tridon V, Dantzer R, Amedee T, Parnet P. 2003. Nuclear factor κB nuclear translocation as a crucial marker of brain response to interleukin-1. A study in rat and interleukin-1 type I deficient mouse. J Neurochem 87:1024–1036.

Nadjar A, Tridon V, May MJ, Ghosh S, Dantzer R, Amedee T, Parnet P. 2005. NFkappaB activates in vivo the synthesis of inducible Cox-2 in the brain. J Cereb Blood Flow Metab 25:1047–1059.

Nakamura K, Matsumura K, Kaneko T, Kobayashi S, Katoh H, Negishi M. 2002. The rostral raphe pallidus nucleus mediates pyrogenic transmission from the preoptic area. J Neurosci 22:4600–4610.

Nakamura K, Matsumura K, Hubschle T, Nakamura Y, Hioki H, Fujiyama F, Boldogkoi Z, Konig M, Thiel HJ, Gerstberger R, Kobayashi S, Kaneko T. 2004. Identification of sympathetic premotor neurons in medullary raphe regions mediating fever and other thermoregulatory functions. J Neurosci 24:5370–5380.

Nerlov C. 2007. The C/EBP family of transcription factors: a paradigm for interaction between gene expression and proliferation control. Trends Cell Biol 17:318–324.

Niehof M, Streetz K, Rakemann T, Bischoff SC, Manns MP, Horn F, Trautwein C. 2001. Interleukin-6-induced tethering of STAT3 to the LAP/C/EBPbeta promoter suggests a new mechanism of transcriptional regulation by STAT3. J Biol Chem 276:9016-9027.

Nilsberth C, Hamzic N, Norell M, Blomqvist A. 2009. Peripheral lipopolysaccharide administration induces cytokine mRNA expression in the viscera and brain of fever-refractory mice lacking microsomal prostaglandin E synthase-1. J Neuroendocrinol 21:715-721.

Oka Y, Ibuki T, Matsumura K, Namba M, Yamazaki Y, Poole S, Tanaka Y, Kobayashi S. 2007. Interleukin-6 is a candidate molecule that transmits inflammatory information to the CNS. Neuroscience 145:530-538.

Pahan K, Jana M, Liu X, Taylor BS, Wood C, Fischer SM. 2002. Gemfibrozil, a lipid-lowering drug, inhibits the induction of nitric-oxide synthase in human astrocytes. J Biol Chem 277:45984-45991.

Papadimitriou A, Priftis KN. 2009. Regulation of the hypothalamic-pituitary-adrenal axis. Neuroimmunomodulation 16: 265-271.

Paxinos G, Watson C. 1998. The rat brain in stereotaxic coordinates, 4th ed. San Diego: Academic Press.

Perez-Capote K, Saura J, Serratosa J, Sola C. 2006. Expression of C/EBPalpha and C/EBPbeta in glial cells in vitro after inducing glial activation by different stimuli. Neurosci Lett 410:25-30.

Poli V. 1998. The role of C/EBP isoforms in the control of inflammatory and native immunity functions. J Biol Chem 273:29279-29282.

Pope RM, Lovis R, Mungre S, Perlman H, Koch AE, Haines GK 3rd. 1999. C/EBP beta in rheumatoid arthritis: correlation with inflammation, not disease specificity. Clin Immunol 91:271-282.

Quan N, Banks WA. 2007. Brain-immune communication pathways. Brain Behav Immun 21:727-735.

Ramji DP, Foka P. 2002. CCAAT/enhancer-binding proteins: structure, function and regulation. Biochem J 365: 561-575.

Reyes TM, Walker JR, DeGino C, Hogenesch JB, Sawchenko PE. 2003. Categorically distinct acute stressors elicit dissimilar transcriptional profiles in the paraventricular nucleus of the hypothalamus. J Neurosci 23:5607-5616.

Rivest S. 2003. Molecular insights on the cerebral innate immune system. Brain Behav Immun 17:13-19.

Rivest S. 2009. Regulation of innate immune responses in the brain. Nat Rev Immunol 9:429-439.

Roth J, Conn CA, Kluger MJ, Zeisberger E. 1993. Kinetics of systemic and intrahypothalamic IL-6 and tumor necrosis factor during endotoxin fever in guinea pigs. Am J Physiol 265:R653-R658.

Roth J, Harré EM, Rummel C, Gerstberger R, Hübschle T. 2004. Signaling the brain in systemic inflammation: role of sensory circumventricular organs. Front Biosci 9:290-300.

Rummel C, Hübschle T, Gerstberger R, Roth J. 2004. Nuclear translocation of the transcription factor STAT3 in the guinea pig brain during systemic or localised inflammation. J Physiol 557:671-687.

Rummel C, Voss T, Matsumura K, Korte S, Gerstberger R, Roth J, Hübschle T. 2005. Nuclear STAT3 translocation in guinea pig and rat brain endothelium during systemic challenge with lipopolysaccharide and interleukin-6. J Comp Neurol 491:1-14.

Rummel C, Sachot C, Poole S, Luheshi GN. 2006. Circulating interleukin-6 induces fever through a STAT3-linked activation of COX-2 in the brain. Am J Physiol Regul Integr Comp Physiol 291:R1316-R1326.

Rummel C, Inoue W, Sachot C, Poole S, Hubschle T, Luheshi GN. 2008. Selective contribution of interleukin-6 and leptin to brain inflammatory signals induced by systemic LPS injection in mice. J Comp Neurol 511:373-395.

Rummel C, Inoue W, Poole S, Luheshi GN. 2009. Leptin regulates leukocyte recruitment into the brain following systemic LPS-induced inflammation. Mol Psychiatry (in press).

Saha S, Engstrom L, Mackerlova L, Jakobsson PJ, Blomqvist A. 2005. Impaired febrile responses to immune challenge in mice deficient in microsomal prostaglandin E synthase-1. Am J Physiol Regul Integr Comp Physiol 288: R1100-R1107.

Saito N, Pulford KA, Breton-Gorius J, Masse JM, Mason DY, Cramer EM. 1991. Ultrastructural localization of the CD68 macrophage-associated antigen in human blood neutrophils and monocytes. Am J Pathol 139:1053-1059.

Satriotomo I, Bowen KK, Vemuganti R. 2006. JAK2 and STAT3 activation contributes to neuronal damage following transient focal cerebral ischemia. J Neurochem 98:1353-1368.

Scammell TE, Elmquist JK, Griffin JD, Saper CB. 1996. Ventromedial preoptic prostaglandin E2 activates fever-producing autonomic pathways. J Neurosci 16:6246-6254.

Schiltz JC, Sawchenko PE. 2003. Signaling the brain in systemic inflammation: the role of perivascular cells. Front Biosci 8:s1321-1329.

Stephanou A, Okosi A, Knight RA, Chowdrey HS, Latchman DS. 1997. C/EBP activates the human corticotropin-releasing hormone gene promoter. Mol Cell Endocrinol 134: 41-50.

Stemeck E, Johnson PF. 1998. CCAAT/enhancer binding protein beta is a neuronal transcriptional regulator activated by nerve growth factor receptor signaling. J Neurochem 70:2424-2433.

Sugawara I, Mizuno S, Yamada H, Matsumoto M, Akira S. 2001. Disruption of nuclear factor-interleukin-6, a transcription factor, results in severe mycobacterial infection. Am J Pathol 158:361-366.

Summy-Long JY, Hu S. 2009. Peripheral osmotic stimulation inhibits the brain's innate immune response to microdialysis of acidic perfusion fluid adjacent to supraoptic nucleus. Am J Physiol Regul Integr Comp Physiol 297: R1532-R1545.

Sun W, Choi SH, Park SK, Kim SJ, Noh MR, Kim EH, Kim HJ, Kim H. 2007. Identification and characterization of novel activity-dependent transcription factors in rat cortical neurons. J Neurochem 100:269-278.

Sung HY, Francis SE, Crossman DC, Kiss-Toth E. 2006. Regulation of expression and signalling modulator function of mammalian tribbles is cell-type specific. Immunol Lett 104: 171-177.

Takahashi Y, Smith P, Ferguson A, Pittman QJ. 1997. Circumventricular organs and fever. Am J Physiol 273: R1690-R1695.

Tanaka N, Hoshino Y, Gold J, Hoshino S, Martiniuk F, Kurata T, Pine R, Levy D, Rom WN, Weiden M. 2005. Interleukin-10 induces inhibitory C/EBPbeta through STAT-3 and represses HIV-1 transcription in macrophages. Am J Respir Cell Mol Biol 33:406-411.

Tanaka T, Akira S, Yoshida K, Umemoto M, Yoneda Y, Shirafuji N, Fujiwara H, Suematsu S, Yoshida N, Kishimoto T. 1995. Targeted disruption of the NF-IL6 gene discloses its essential role in bacteria killing and tumor cytotoxicity by macrophages. Cell 80:353-361.

Taubenfeld SM, Milekic MH, Monti B, Alberini CM. 2001. The consolidation of new but not reactivated memory requires hippocampal C/EBPbeta. Nat Neurosci 4:813-818.

Tazawa R, Xu XM, Wu KK, Wang LH. 1994. Characterization of the genomic structure, chromosomal location and

promoter of human prostaglandin H synthase-2 gene. Biochem Biophys Res Commun 203:190–199.

Uematsu S, Matsumoto M, Takeda K, Akira S. 2002. Lipopolysaccharide-dependent prostaglandin E(2) production is regulated by the glutathione-dependent prostaglandin E(2) synthase gene induced by the Toll-like receptor 4/MyD88/NF-IL6 pathway. J Immunol 168:5811–5816.

Vallières L, Rivest S. 1997. Regulation of the genes encoding interleukin-6, its receptor, and gp130 in the rat brain in response to the immune activator lipopolysaccharide and the proinflammatory cytokine interleukin-1beta. J Neurochem 69:1668–1683.

Wong ML, Bongiorno PB, Rettori V, McCann SM, Licinio J. 1997. Interleukin (IL) 1beta, IL-1 receptor antagonist, IL-10, and IL-13 gene expression in the central nervous system and anterior pituitary during systemic inflammation: pathophysiological implications. Proc Natl Acad Sci U S A 94:227–232.

Wu CT, Eiserich JP, Ansari AA, Coppel RL, Balasubramanian S, Bowlus CL, Gershwin ME, Van De Water J. 2003. Myeloperoxidase-positive inflammatory cells participate in bile duct damage in primary biliary cirrhosis through nitric oxide-mediated reactions. Hepatology 38:1018–1025.

Wuchert F, Ott D, Rafalzik S, Roth J, Gerstberger R. 2009. Tumor necrosis factor-alpha, interleukin-1beta and nitric oxide induce calcium transients in distinct populations of cells cultured from the rat area postrema. J Neuroimmunol 206:44–51.

Yamagata K, Matsumura K, Inoue W, Shiraki T, Suzuki K, Yasuda S, Sugiura H, Cao C, Watanabe Y, Kobayashi S. 2001. Coexpression of microsomal-type prostaglandin E synthase with cyclooxygenase-2 in brain endothelial cells of rats during endotoxin-induced fever. J Neurosci 21:2669–2677.

Yamamoto K, de Waard V, Fearns C, Loskutoff DJ. 1998. Tissue distribution and regulation of murine von Willebrand factor gene expression in vivo. Blood 92:2791–2801.

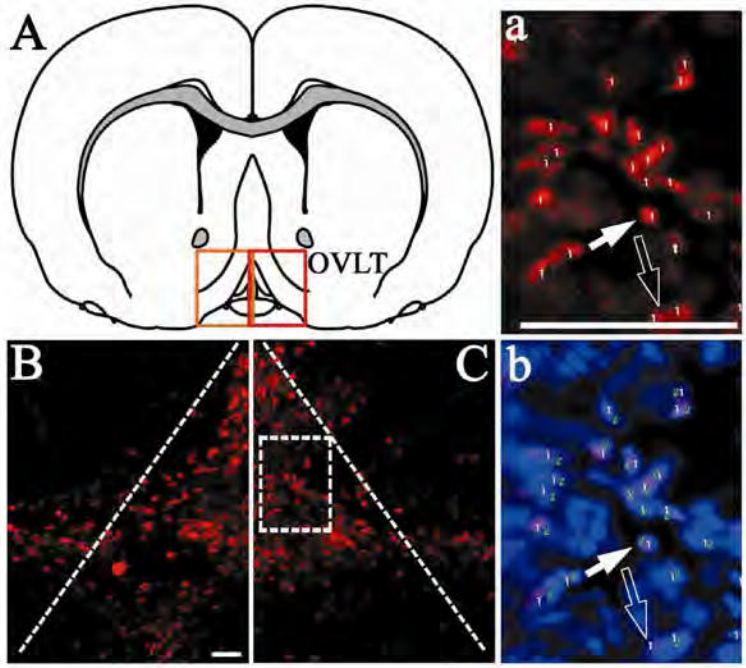
Yamamoto M, Uematsu S, Okamoto T, Matsuura Y, Sato S, Kumar H, Satoh T, Saitoh T, Takeda K, Ishii KJ, Takeuchi O, Kawai T, Akira S. 2007. Enhanced TLR-mediated NF-IL6 dependent gene expression by Trib1 deficiency. J Exp Med 204:2233–2239.

Yi JH, Park SW, Kapadia R, Vemuganti R. 2007. Role of transcription factors in mediating post-ischemic cerebral inflammation and brain damage. Neurochem Int 50:1014–1027.

Yukawa K, Tanaka T, Tsuji S, Akira S. 1998. Expressions of CCAAT/enhancer-binding proteins beta and delta and their activities are intensified by cAMP signaling as well as Ca^{2+}/calmodulin kinases activation in hippocampal neurons. J Biol Chem 273:31345–31351.

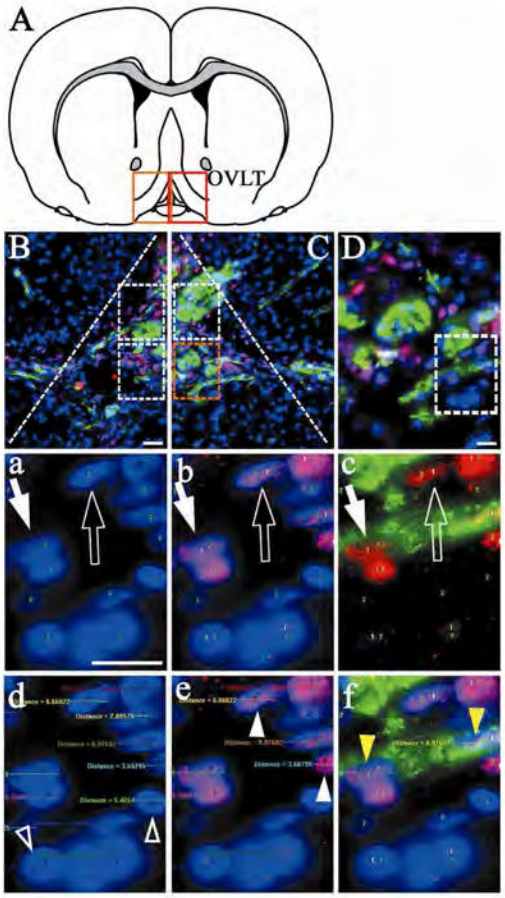
Zhang Y, Rom WN. 1993. Regulation of the interleukin-1 beta (IL-1 beta) gene by mycobacterial components and lipopolysaccharide is mediated by two nuclear factor-IL6 motifs. Mol Cell Biol 13:3831–3837.

Supporting Information



Supporting Figure 1: Counting of NF-IL6 immunoreactive cell nuclei in the vascular organ of the lamina terminalis 8 hours after systemic challenge with 100µg/kg LPS. The overview (A) illustrates the region of interest; the orange and the red squares indicate the areas from which two 40 fold microphotographs were used for counting. The respective microphotographs are shown in B and C. Dashed white lines (triangles) depict the counting area to which the obtained density of nuclear NF-IL6 signals refers to in Fig. 3. All possible nuclear NF-IL6 signals (red) were labeled with "1", as shown here for a small fraction (a) of the counting area (C), the level of which is indicated by a dashed white square. Red NF-IL6-signals that co-localized with the blue DAPI counterstain are labeled with "2" (white arrows in a and b). Please note that possible

staining artifacts were identified (open arrows in a and b), which were omitted from the counting analyses. Microphotographs with labeling for cell counting (a-b) are cutouts of screen shots of pictures that were used for the actual counting procedure. These pictures could not be exported in a compatible file format from the image editing software MetaMorph to Photoshop and therefore appear at lower resolution than they were used for actual counting. Scale bars = 25µm in B (applies to C) and a (applies to b).



Supporting Figure 2: Quantification of different NF-IL6 immunoreactive (IR) cell phenotypes in the OVLT. 2 to 4 100fold (immersion oil) microphotographs (dashed squares in B and C) were taken from the triangular counting area that was defined using two 40fold images (dashed white lines in B and C). The counting procedure was performed in 100fold microphotographs. A cutout (a – c) of the microphotograph (D) derived from the area within the orange square (C) is represented by a dashed white square in D and shown for better visualization of the Microscopical counting procedure at high magnification. (a) All DAPI stained nuclei were counted and labeled with "2", (b) followed by the identification and counting of co-localization of NF-IL6 and DAPI (blue) positive nuclei, which were labeled with "1". To identify the portion of NF-IL6 positive nuclei belonging to the respective cell phenotype (in this case endothelial cells, labeled with von Willebrand factor, vW) we counted vW-positive cell bodies that could be assigned to an NF-IL6 positive nucleus. Those were labeled with "3". White arrows in a – c indicate an NF-IL6 signal within the nucleus of an endothelial cell, while open arrows show signals in the nuclei of other cell phenotypes. The same microphotographs (cutout as in a – c) were used to measure the horizontal diameter of DAPI stained nuclei (diameter and respective distance in µm are shown in d – f). These measurements were done to correct cell counts for oversampling of large cells. Open arrowheads demonstrate examples of nuclei that did not show NF-IL6 IR, while NF-IL6 positive nuclei are indicated by white and those being assigned to endothelial cells with yellow arrowheads. Microphotographs with labeling for cell counting (a-f) are cutouts of screen shots of pictures that were used for the actual counting procedure. These pictures could not be exported in a compatible file format from the image editing software MetaMorph to Photoshop and therefore appear at lower resolution than they were used for actual counting. Scale bars = 25µm in B (applies to C); 10µm in a (applies to b - f).

1.6. „Peripheral and central cyclooxygenase (COX) products may contribute to the manifestation of brain controlled sickness responses during localized inflammation induced by macrophage-activating lipopeptide-2 (MALP-2)“

Knorr C., Marks D., Gerstberger R., Mühlradt PF., Roth J., **Rummel C.**
Neurosci Lett (2010) 479: 107-11.

Impakt Faktor: 2,055

Eigener Anteil an der Publikation:

- Initiative: wesentlich (50 %)
- Projektplanung: wesentlich (50 %)
- Durchführung der Versuche: unterstützend (30 %)
- Auswertung der Experimente: wesentlich (50 %)
- Erstellung der Publikation: wesentlich (50 %)

Neuroscience Letters 479 (2010) 107–111

Contents lists available at ScienceDirect

Neuroscience Letters

journal homepage: www.elsevier.com/locate/neulet

Peripheral and central cyclooxygenase (COX) products may contribute to the manifestation of brain-controlled sickness responses during localized inflammation induced by macrophage-activating lipopeptide-2 (MALP-2)

Carolin Knorr[a], Doreen Marks[a], Rüdiger Gerstberger[a], Peter F. Mühlradt[b], Joachim Roth[a], Christoph Rummel[a,*]

[a] Department of Veterinary-Physiology, Justus-Liebig-University Giessen, Frankfurter Strasse 100, D-35392 Giessen, Germany
[b] Wound Healing Research Group, BioTec Gründerzentrum, Inhoffenstrasse 7, D-38124 Braunschweig, Germany

ARTICLE INFO

Article history:
Received 18 March 2010
Received in revised form 10 May 2010
Accepted 11 May 2010

Keywords:
Immune-to-brain communication
Prostaglandins
Fever
Transcription factors

ABSTRACT

We investigated whether an inflammation-dependent activation of the brain occurs in response to systemic intraperitoneal (i.p.) or local injections of macrophage-activating lipopeptide-2 (MALP-2) into a subcutaneous (s.c.) air pouch, and whether local (peripheral) or central cyclooxygenase (COX)-2-dependent formations of prostaglandin E_2 (PGE_2) are involved in MALP-2-induced illness responses. Body temperature, activity, food and water intake were measured telemetrically. Local (s.c.) and circulating levels of PGE_2 were measured by an ELISA. Inflammatory activation of the brain in response to MALP-2 was determined by immunohistochemical detection of the transcription factors NFκB and STAT3 in cell nuclei as well as the appearance of COX-2 at the same sites. S.c. treatment with the preferential COX-2 inhibitor meloxicam attenuated, but not abolished fever induced by local injections of MALP-2 into the pouch. Local MALP-2-induced formation of PGE_2 was blunted by treatment with meloxicam. In the brain, i.p. stimulation with MALP-2-induced nuclear STAT3- and NFκB-translocation in the vasculature and the sensory circumventricular organs, which was accompanied by an increase in COX-2 immunoreactivity (IR) in endothelial cells. Local MALP-2-treatment induced a moderate STAT3 activation and a small but significant increase in COX-2 IR while no NFκB-activation could be observed in the brains of these animals. We demonstrated that the activation of the brain STAT3 (NFκB)-COX-2 singling cascade seems to be involved in the manifestation of brain-controlled illness symptoms induced by systemic and local inflammatory stimulation with MALP-2. The present data further suggest a contribution of peripherally produced PGE_2 to MALP-2-induced activation of brain sites implicated in fever.

© 2010 Elsevier Ireland Ltd. All rights reserved.

The 2-kDa lipopeptide MALP-2 has been identified and characterized as the molecular pattern of the cell wall-less bacterium *Mycoplasma fermentans* that activates macrophages and other cells by interacting with the heterodimeric toll-like receptors (TLRs) 2 and 6 [12]. Brain-controlled illness responses such as fever, depressed motor activity, anorexia and adipsia are observed in rats after systemic (i.p.) injections of MALP-2 in a dose-dependent manner [8]. Interestingly, it was shown that intradermal administration of MALP-2 evokes local skin reactions [5] and has the capacity to accelerate the healing of skin wounds in mice after local treatment at the site of injury [4]. Thus, a localized treatment with MALP-2 has strong potential therapeutic capacities [4,18]. Therefore, it is of interest to investigate possible side effects of such a localized (i.e. subcutaneous) treatment with this substance on the whole organism including the brain, where a number of sickness responses are generated [3]. In a previous study [9] we used an established experimental model of a subcutaneous air pouch [11] to investigate a possible inflammatory activation of the brain in response to injections of MALP-2 into the pouch. At the subcutaneous site of injection we observed a pronounced formation of tumor necrosis factor-α (TNF), interleukin-6 (IL-6) and prostaglandin E_2 (PGE_2), which all are important afferent signal molecules in immune-to-brain communication pathways [1]. Moderate amounts of IL-6 and PGE_2 seemed to enter the systemic circulation of rats locally treated with MALP-2, and also a moderate IL-6-mediated activation of brain sites lacking a complete blood–brain barrier occurred [9]. The first goal of the present study was to elucidate whether the local subcutaneous formation of PGE_2 participates in the observed febrile response. We further aimed to characterize the activation of the rat brain during a localized (s.c.) as opposed to a systemic (i.p.) inflammatory stimulation with MALP-2, with special emphasis on the induction of COX-2 and the transcription factors NFκB and STAT3.

* Corresponding author. Tel.: +49 641 99 38850; fax: +49 641 99 38159.
E-mail address: Christoph.D.Rummel@vetmed.uni-giessen.de (C. Rummel).

0304-3940/$ – see front matter © 2010 Elsevier Ireland Ltd. All rights reserved.
doi:10.1016/j.neulet.2010.05.036

which both seem to be associated with a COX-2-dependent synthesis of PGE_2 in the brain, at least in response to an inflammatory challenge with bacterial lipopolysaccharide (LPS) [15].

Male Wistar rats with body weights (BW) in the range of 220–250 g were used for this study. All experiments were carried out in accordance with the local Ethics Committee (approval numbers GI 18/2 – Nr. 59/2003 and GI 18/2 – Nr. 15/2007). After surgery animals were housed individually in a temperature and humidity controlled climate chamber at 25 °C and 50% humidity under a 12:12 h day–night cycle with lights on from 7:00 a.m. to 7:00 p.m.

Abdominal temperature (T_{abd}) and motor activity were measured by use of biotelemetry transmitters (VM-FH-discs, Mini-Mitter) implanted 1 week before the experiment into the abdominal cavity of anesthetized animals (100 mg/kg ketamine hydrochloride and 4 mg/kg xylazin). Oral meloxicam (1 mg/kg, Boehringer Ingelheim, Germany) treatment was used 1 h before and 1 day after surgery for pain relief. Immediately after placement of a biotelemetry transmitter into the abdominal cavity a subcutaneous air pouch was formed. A volume of 20 ml of air, sterilized by passing through a 0.7 μm filter (BD Plastipak, Bechton-Dickinson, Heidelberg, Germany), was injected into the subcutaneous tissue of the dorsal midline, caudal to the scapulae. Three or two days prior to the experiment the air pouch was re-inflated with another 10 ml of sterile air. This model has been used to induce a localized inflammatory response in rats [11]. Food intake and drinking behavior were telemetrically monitored as previously described [9].

MALP-2 was donated as a sterile, lyophilised, endotoxin- and pyrogen-free powder (P.F. Mühlradt), which was then diluted in 10% Cremophor® EL–90% sterile phosphate buffered saline (PBS). Cremophor® EL is a non-ionic solubiliser and emulsifier designed for the *in vivo* use in human and veterinary pharmaceutical industry (BASF Aktiengesellschaft, Ludwigshafen, Germany). MALP-2 was used at a dose of 100 μg/kg body weight and dissolved at a concentration of 100 μg/ml. Control experiments were performed with 10% Cremophor® EL in 90% PBS (solvent). Cremophor® EL is tolerated extremely well; no toxic effects were observed after percutaneous application in rats of a volume that was 400 times higher than in the present study (4 ml/kg versus 10 μl/kg; manufacturers' datasheet). We did not detect any sign of inflammation in solvent treated animals containing 10% Cremophor® EL as monitored by STAT3, NFκB and COX-2 immunohistochemistry (Fig. 3, Table 1) of brains of these animals. From previous studies we further know that small concentrations of interleukin-6 or PGE_2, which can be measured in lavage collected from the pouch, are identical, irrespective of whether saline, water, or cremophor solution are used as solvent for a given drug. MALP-2 or solvent were administered in combination with the preferential COX-2 inhibitor meloxicam (5 mg/kg; Boehringer Ingelheim, Germany) or its solvent (10% ethanol in PBS). In additional experiments we tested whether the local subcutaneous formation of PGE_2 in response to MALP-2 was, indeed, depressed by the administration of meloxicam. For this purpose, lavage from the air pouch was collected [9] and assayed for PGE_2

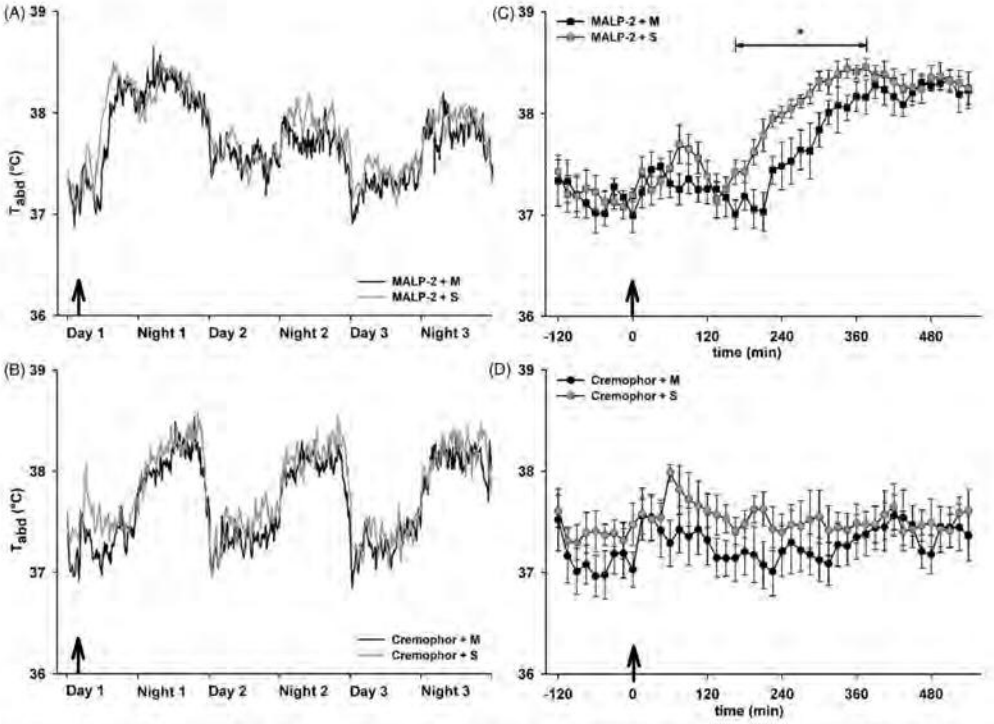


Fig. 1. Changes in abdominal temperature of rats in response to injections of 100 μg/kg MALP-2 or cremophor (10% cremophor in PBS) combined with metacam (5 mg/kg, M) or solvent (10% ethanol in PBS, S) into a subcutaneous air pouch over a period of 3 days and nights starting 2 h before the injection (A and B), and a detailed analysis of the thermal responses during the day of the respective injection (C and D). The arrow indicates the time of injection. Data are expressed as means (A and B), or means ± SEM (C and D). From 165 to 360 min after injection T_{abd} of MALP-2-injected rats was significantly reduced by metacam treatment ($^*p < 0.05$; $n = 6$ for each group).

Table 1
Qualitative analysis of COX-2 immunoreactivity in the rat brain.

Selected brain structures	COX-2 immunoreactivity			
	Cremophor		MALP-2	
	Pouch	i.p.	Pouch	i.p.
Circumventricular organs				
Vascular organ of the lamina terminalis			+	++
Subfornical organ	–	–	+	+++
Area postrema	–	–	±	+
Others				
Endothelial cells throughout the brain	–	–	+	++

Relative values of COX-2 immunoreactivity are given as estimates for the density of their respective labeling. Analyses of the rat brains were performed 3 h after i.p. or intra-pouch injection of MALP-2 (100 μg/kg) or cremophor (10% cremophor in PBS). A five-point scale was used to rate the data: +++ = high density of immunoreactivity; ++ = moderate density; + = low density; ± = single cells show COX-2 immunoreactivity in some cases; – = no immunoreactivity.

by a commercially available enzyme immunoassay (Assay designs, Ann Arbor, MI, USA).

In four groups of rats ($n = 4$ each), treated systemically (i.p.) or locally (intra-pouch) with MALP-2 or cremophor, COX-2, NFκB and STAT3 immunohistochemistry was performed on coronal cryostat sections (20 μm, model HM 500, Microm, Walldorf, Germany) which were prepared as described elsewhere [15,16]. A rabbit anti-COX-2 antibody (1:2000; cat no.: 160126; Cayman Chemical), a goat anti-NFκB antibody (1:500; cat no.: sc-372 G; Santa Cruz Biotechnology), and a rabbit anti-STAT3 antibody (1:4000; cat no.: sc-482; Santa Cruz Biotechnology) were used to detect the respective molecules. Specificity of each antibody was shown previously [7,13,21]. Brain endothelial cells represent the major cellular phenotype showing COX-2, NFκB, or STAT3 expression in response to inflammatory stimulation with lipopolysaccharide [15,16]. COX-2 induction in neurons and astrocytes occurs primarily after more severe inflammatory stimuli than used in the present study such as excitotoxic brain disease [20]. Therefore, we aimed to co-localize putative MALP-2-induced COX-2-, NFκB- or STAT3 immunoreactivity with the endothelial cell marker von Willebrand factor (sheep anti-rat anti-vWF antibody; 1:3000; SARTW-HRP, Affinity Biologicals, Essen, Germany). Brain sections were incubated with the respective primary antibody mixture at 4 °C for 36–48 h. COX-2 and STAT3 were visualized with CY3-conjugated anti-rabbit IgG (1:500), NFκB with CY3-conjugated anti-goat IgG, and vWF with FITC-conjugated anti-sheep IgG (1:500) as secondary antibodies (Jackson Immuno-Research, Dianova, Hamburg, Germany). Immunocytochemical analysis was further combined with the nuclear DAPI stain (Molecular Probes, MoBiTec GmbH, Göttingen, Germany) to verify nuclear localization of detected signals.

Sections were analyzed and documented with a conventional light/fluorescent Olympus BX50 microscope (Olympus Optical Co., Hamburg, Germany).

All data are presented as means ± SEM. T_{abd} of different groups of rats were compared by two-way repeated measures ANOVA followed by Scheffé's post hoc test. Cumulative motor activity, food and water intake and levels of PGE_2 in lavage fluid collected from the air pouch were compared by one-way ANOVA and Scheffé's test (StatView, Abacus concepts, Berkeley, USA).

In the left panels of Fig. 1(A and B), the continuous recording of T_{abd} is documented for a period of 3 days starting with the lights on period of the day of injection into the air pouch of 100 μg/kg MALP-2 together with 5 mg/kg meloxicam or solvent (Fig. 1A) or cremophor together with meloxicam or solvent (Fig. 1B). On the day of the respective injection both groups treated locally with MALP-2 developed a fever which was lower in rats co-

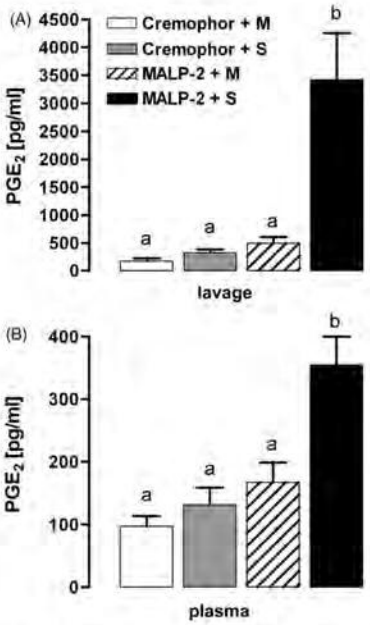


Fig. 2. Levels of immuno-reactive PGE2 in air pouch lavage fluid (A) and plasma (B) at 2 h after injection of 100 μg/kg MALP-2 or cremophor combined with metacam (5 mg/kg, M) or solvent (10% ethanol in PBS, S) into the pouch. Any columns with the same letter are not significantly different from each other, while any columns with different letters are significantly different ($p < 0.05$). Columns represent means ± SEM ($n = 5$ for each group).

injected with meloxicam (Fig. 1C). A detailed analysis revealed that intra-pouch injection of meloxicam significantly reduced MALP-2-induced fever from 165 to 360 min after its administration. This effect was predominantly due to a delay of the febrile increase of body temperature in rats treated with meloxicam along with MALP-2. Another effect of MALP-2 on T_{abd} relates to the circadian temperature changes over the following 2 days and nights. The amplitude of the circadian variations of T_{abd} was reduced by MALP-2 so that daytime temperature was higher and nighttime temperature lower than in the respective control groups, a phenomenon, which we also observed in previous studies [8,9]. In the control groups injected with cremophor, administration of meloxicam had no visible effect on T_{abd} (Fig. 1B and D).

Treatment with meloxicam had no significant effect on the moderate reductions of motor activity as well as food and water intake induced by subcutaneous injections of MALP-2 (data not shown).

The next experiment aimed to test, whether injection of meloxicam into the pouch was capable to depress localized formation of prostaglandins, namely PGE_2. Indeed, the significant rise of MALP-2-induced PGE_2 in lavage collected from the pouch (Fig. 2A) was completely abolished by the local administration of meloxicam. Consequently, the moderate increase of PGE_2 in plasma induced by local subcutaneous stimulation with MALP-2 also was depressed (Fig. 2B).

The data shown in Figs. 1 and 2 suggest that a localized subcutaneous formation of prostaglandins contributes to the fever, which develops after injection of MALP-2 into the air pouch. However, a portion of the MALP-2-induced febrile response could not be antagonized by local treatment with meloxicam.

In a last experiment we therefore tested the hypothesis that a localized inflammation, evoked by injection of MALP-2 into the subcutaneous air pouch, was capable to cause an inflammatory activation of the brain. For comparison, another group of rats received systemic (i.p.) injections of MALP-2, which are known to produce a robust systemic inflammatory response accompanied by pronounced circulating levels of pro-inflammatory cytokines [8]. I.p. injection of MALP-2 caused the appearance of COX-2, NFκB, and STAT3 immunoreactivity (IR) in endothelial cells of brain vessels 3 h after stimulation, as shown exemplarily for the subfornical organ (SFO), one of the sensory circumventricular organs (sCVO) lacking a tight blood–brain barrier (Fig. 3D, H, and L). COX-2 IR in the other sCVOs namely the vascular organ of the lamina terminalis (OVLT) and the area postrema (AP) was less pronounced or much weaker, respectively (Table 1, data not shown). The local injection of MALP-2 into the pouch induced a moderate STAT3 activation (Fig. 3K) and a small but constant increase in COX-2 IR (Fig. 3C) in brain endothelial cells of vessels in preoptic/hypothalamic and extrahypothalamic areas, while almost no NFκB-activation could be observed in the brains of this group of rats (Fig. 3G). Other

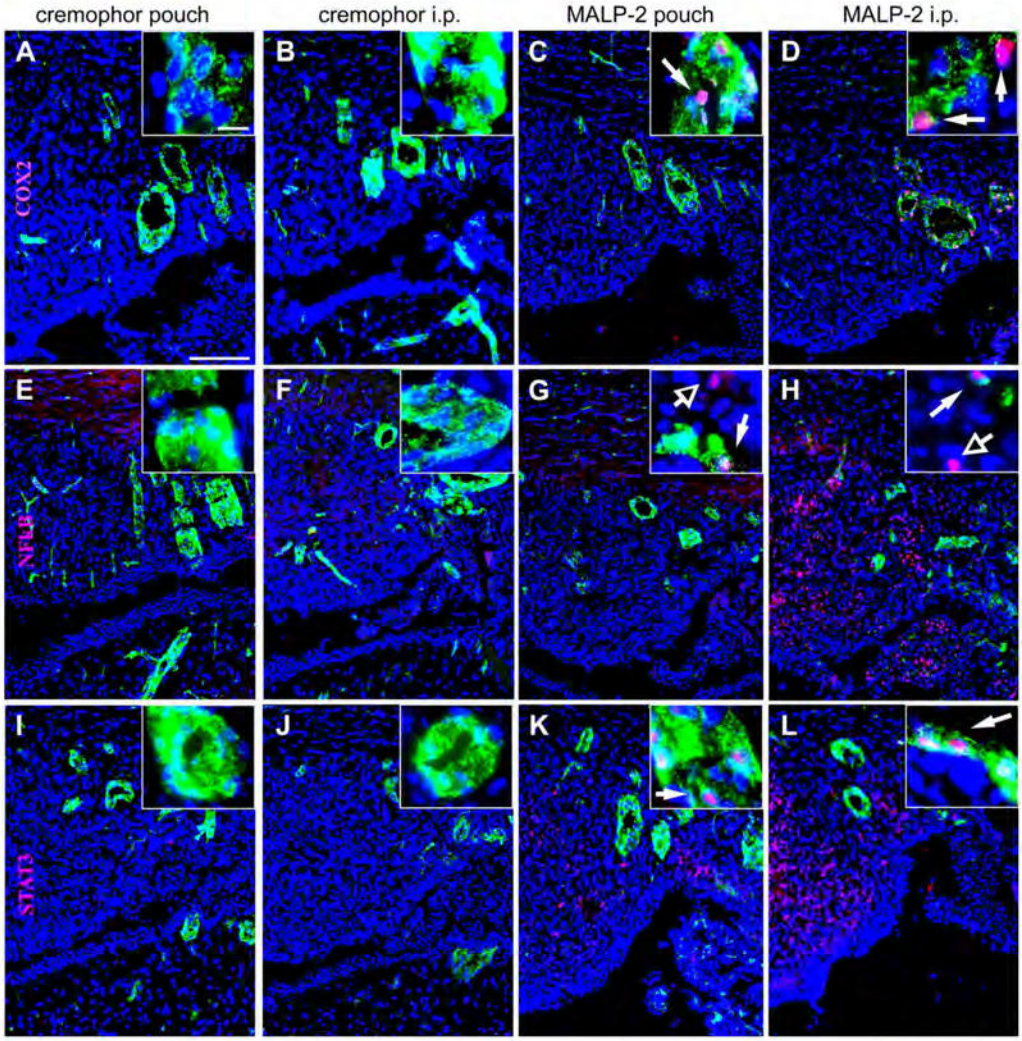


Fig. 3. Representative photomicrographs of the lateral portion from the rat subfornical organ (SFO) 3 h after injection of cremophor or 100 μg/kg MALP-2 into the abdominal cavity (i.p.) or into the subcutaneous air pouch (pouch). COX-2 (A–D)-, STAT3 (E–H)- and NFκB (I–L)-immunoreactivity (IR) is shown (red). Note that red IR co-localizes with von Willebrand factor-positive (green) endothelial cells. Nuclear DAPI stain was used to label cell nuclei and depict general neuroanatomy. Specific perinuclear COX-2 and nuclear STAT3/NFκB labeling induced by systemic (i.p.) or local subcutaneous (pouch) treatment with MALP-2 is shown at higher magnifications in the insets. White arrows indicate positive endothelial cells while other cell phenotypes are highlighted by open arrows. The scale bar in A represents 100 and 10 μm in the inset ($n = 4$ for each group). (For interpretation of the references to color in this figure legend, the reader is referred to the web version of the article.)

than for COX-2-, STAT3- and NFκB IR after local or i.p. injection of MALP-2 also appeared in other cell phenotypes than endothelial cells (Fig. 3G, H, K, and L), most likely including astrocytes as shown previously [16]. In rats, injected i.p. or s.c. (into the pouch) with cremophor, COX-2-, NFκB- and STAT3-IR remained absent in brain endothelial cells. The possibility can thus not be ruled out that the rather moderate COX-2-activation of the brain during a localized subcutaneous inflammation evoked by MALP-2 participates in the manifestation of the febrile response observed under these experimental conditions.

Local administration of MALP-2 to skin wounds, at doses similar to those used in our present study, accelerated wound healing in diabetic mice [4]. This effect was associated with a stimulated local expression of various chemokines and cytokines. This and other [18] beneficial effects of locally administered MALP-2 are indicative of potent therapeutic capacities of this substance. The investigation of how local treatment with MALP-2 affects the organism with special regard to classical non-specific illness responses seemed therefore warranted. The sickness responses which we observed in this study (i.e. fever, anorexia, adipsia and reduced activity) were rather moderate and restricted to the day when MALP-2 was administered into the pouch. Still, it seemed of interest to get some insight into putative mechanisms being responsible for the observed brain-controlled responses during the first day of a MALP-2-induced subcutaneous localized inflammatory response. With regard to fever, a portion of the increase in T_{abd} was mediated by a localized formation of prostaglandins, a moderate amount of which entered the peripheral circulation (Fig. 1). In both compartments, air pouch and bloodstream, the MALP-2-induced rise of PGE_2 could be antagonized by co-administration of the preferential COX-2 inhibitor meloxicam into the pouch, while fever was just attenuated but not completely abolished, indicating the existence of a second fever-inducing mechanism outside the pouch. The peripheral formation of PGE_2 at the subcutaneous site of inflammation might contribute to the initiation of fever, due to the observation that the depressed formation of PGE_2 by meloxicam delayed the increase of temperature by 1–2 h. Evidence for a role of peripherally generated PGE_2 in triggering the onset of LPS-induced fever, either via stimulation of sensory afferent nerves or via transport to the brain with the blood, has been elaborated within the last few years [2,19]. A participation of locally produced PGE_2 at the subcutaneous site of inflammation in the initiation of fever in response to MALP-2 is likely according to our data. On the other hand, an induced expression of COX-2 within the brain, namely in endothelial cells, is regarded as a crucial step in the manifestation of fever [10], and the major intracellular signaling pathway for COX-2- and thereby fever-induction is the activation and nuclear translocation of the transcription factor NFκB [14]. Indeed, we detected NFκB and COX-2 IR in the rat brain after systemic (i.p.) treatment with MALP-2. However, the local (s.c.) stimulation with MALP-2 resulted in the appearance of moderate amounts of COX-2 IR in brain endothelial cells while hardly any NFκB IR was detected (Fig. 3). A possible explanation for this discrepancy was provided by recent study, in which LPS was injected into the air pouch and COX-2 IR could be linked to the activation to an additional transcription factor in the brain, namely STAT3 [15]. Under inflammatory conditions, STAT3 activation in the brain is predominantly mediated by the cytokine IL-6 [6,17]. Small amounts of IL-6 have been shown to enter the circulation from the air pouch after MALP-2 injection and to cause a moderate STAT3 activation in the brain [9] (Fig. 3). We therefore suggest the following chain of events occurring after injection of MALP-2 into the air pouch. (i) Considerable concentrations of PGE_2 are generated at the s.c. site of localized inflammation which account for that part of the febrile response which can be blocked by injection of meloxicam into the pouch. (ii) Small amounts of IL-6 enter the circulation in response to s.c. injections of MALP-2 and cause a moderate induction of COX-2 in brain endothelial cells possibly linked to the observed activation of STAT3. Such a mechanism operating within the brain might account for that part of the febrile response which could not be blocked by administration of meloxicam into the air pouch.

Acknowledgements

Carolin Knorr was supported by a scholarship from the H. Wilhelm Schaumann Stiftung. We thank Jolanta Murgott for excellent technical assistance.

References

[1] H.O. Besedovsky, A. Del Rey, Immune-neuro-endocrine interactions: facts and hypotheses, Endocr. Rev. 17 (1996) 64–102.
[2] C.M. Blatteis, Endotoxic fever: new concepts of its regulation suggest new approaches to its management, Pharmacol. Ther. 111 (2006) 194–223.
[3] R. Dantzer, J.C. O'Connor, G.G. Freund, R.W. Johnson, K.W. Kelley, From inflammation to sickness and depression: when the immune system subjugates the brain, Nat. Rev. Neurosci. 9 (2008) 46–56.
[4] U. Deiters, J. Barsig, B. Tawil, P.F. Mühlradt, The macrophage-activating lipopeptide-2 accelerates wound healing in diabetic mice, Exp. Dermatol. 13 (2004) 731–739.
[5] C. Galanos, M. Gumenschneider, P.F. Mühlradt, E. Jirillo, M.A. Freudenberg, MALP-2, a *Mycoplasma* lipopeptide with classical endotoxic properties: end of an era of LPS monopoly? J. Endotoxin Res. 6 (2001) 471–476.
[6] E.M. Harré, J. Roth, U. Pehl, M. Kueth, R. Gerstberger, T. Hübschle, Selected contribution: role of IL-6 in LPS-induced nuclear translocation in sensory circumventricular organs during fever in rats, J. Appl. Physiol. 92 (2002) 2657–2666.
[7] T. Hübschle, E.M. Harré, W. Mayerhof, U. Pehl, J. Roth, R. Gerstberger, The central pyrogenic action of interleukin-6 is related to nuclear translocation of STAT3 in the anteroventral preoptic area of the rat brain, J. Therm. Biol. 26 (2001) 299–305.
[8] T. Hübschle, J. Mütze, P.F. Mühlradt, S. Korte, R. Gerstberger, J. Roth, Pyrexia, anorexia, adipsia, and depressed motor activity in rats during systemic inflammation induce by the Toll-like receptors-2 and -6 agonists MALP-2 and FSL-1, Am. J. Physiol. Regul. Integr. Comp. Physiol. 290 (2006) R180–R187.
[9] C. Knorr, T. Hübschle, J. Murgott, P.F. Mühlradt, R. Gesrtberger, J. Roth, Macrophage-activating lipopeptide-2 (MALP-2) induces a localized inflammatory response in rats resulting in activation of brain sites implicated in fever, Brain Res. 1205 (2008) 36–46.
[10] K. Matsumura, S. Kobayashi, Signaling the brain in inflammation: the role of endothelial cells, Front. Biosci. 9 (2004) 2819–2826.
[11] A. Miller, G.N. Luheshi, N.J. Rothwell, S.J. Hopkins, Local cytokine induction by LPS in the rat air pouch and its relationship to the febrile response, Am. J. Physiol. Regul. Integr. Comp. Physiol. 272 (1997) R857–R861.
[12] M. Morr, O. Takeuchi, S. Akira, M.M. Simon, P.F. Mühlradt, Differential recognition of structural details of bacterial lipopeptides by toll-like receptors, Eur. J. Immunol. 32 (2002) 3337–3347.
[13] A. Nadjar, C. Combe, S. Layé, V. Tridon, R. Dantzer, T. Amedee, P. Parnet, Nuclear factor κB nuclear translocation as a crucial marker of brain response to interleukin-1. A study in rat and interleukin-1 type I deficient mouse, J. Neurochem. 87 (2003) 1024–1036.
[14] A. Nadjar, V. Tridon, M.J. May, S. Ghosh, R. Dantzer, T. Amedee, P. Parnet, NFkappaB activates in vivo the synthesis of inducible COX-2 in the brain, J. Cereb. Blood Flow Metab. (2005) 1047–1059.
[15] C. Rummel, C. Sachot, S. Poole, G.N. Luheshi, Circulating interleukin-6 induces fever through a STAT3-linked activation of COX-2 in the brain, Am. J. Physiol. Regul. Integr. Comp. Physiol. 291 (2006) R1316–R1326.
[16] C. Rummel, T. Voss, K. Matsumura, S. Korte, R. Gerstberger, J. Roth, T. Hübschle, Nuclear STAT3 translocation in guinea pig and rat brain endothelium during systemic challenge with lipopolysaccharide and interleukin-6, J. Comp. Neurol. 491 (2005) 1–14.
[17] C. Rummel, W. Inoue, C. Sachot, S. Poole, T. Hübschle, G.N. Luheshi, Selective contribution of interleukin-6 and leptin to brain inflammatory signals induced by systemic LPS injection in mice, J. Comp. Neurol. 511 (2008) 373–395.
[18] J. Schmidt, T. Welsch, D. Jäger, P.F. Mühlradt, M.W. Büchler, A. Märten, Intratumoral injection of the toll-like receptor-2/6 agonist 'macrophage-activating lipopeptide-2' in patients with pancreatic carcinoma: a phase I/II trial, Br. J. Cancer 97 (2007) 598–604.
[19] A.A. Steiner, A.J. Ivanov, J. Serrats, H. Hosokawa, A.N. Phayre, J.R. Robbins, J.L. Roberts, S. Kobayashi, K. Matsumura, P.E. Sawchenko, A.A. Romanovsky, Cellular and molecular basis of the initiation of fever, PLoS Biol. 4 (2006) 1517–1524.
[20] T. Takemiya, K. Matsumura, K. Yamagata, Roles of prostaglandin synthesis in excitotoxic brain diseases, Neurochem. Int. 51 (2007) 112–120.
[21] K. Yamagata, K. Matsumura, W. Inoue, T. Shiraki, K. Suzuki, S. Yasuda, H. Sugiura, C. Cao, Y. Watanabe, S. Kobayashi, Coexpression of microsomal-type prostaglandin E synthase with cyclooxygenase-2 in brain endothelial cells of rats during endotoxin-induced fever, J. Neurosci. 21 (2001) 2669–2677.

1.7. „Leptin regulates neutrophil recruitment into the brain following severe systemic LPS-induced inflammation“

Reprinted by permission from Macmillan Publishers Ltd: [Mol Psychiatry], advance online publication, 22 September 2009 (doi: 10.1038/mp.2009.98.)

Rummel C., Inoue W., Poole S., Luheshi GN.
Mol Psychiatry (2010) 15: 523-34.

Impakt Faktor: 15,470

Eigener Anteil an der Publikation:

- Initiative: weitgehend eigenständig (80 %)
- Projektplanung: wesentlich (50 %)
- Durchführung der Versuche: wesentlich (50 %)
- Auswertung der Experimente: wesentlich (50 %)
- Erstellung der Publikation: weitgehend eigenständig (80 %)

Molecular Psychiatry (2009), 1–12
© 2009 Nature Publishing Group All rights reserved 1359-4184/09 $32.00
www.nature.com/mp

ORIGINAL ARTICLE

Leptin regulates leukocyte recruitment into the brain following systemic LPS-induced inflammation

C Rummel[1,3,4], W Inoue[1,4], S Poole[2] and GN Luheshi[1]

[1]Douglas Mental Health University Institute, Department of Psychiatry, McGill University, Montreal, Quebec, Canada and [2]Department of Endocrinology, National Institute for Biological Standards and Control, Potters Bar, UK

The appetite suppressing hormone leptin has emerged as an important modulator of immune function and is now considered to be a critical link between energy balance and host defense responses to pathogens. These 'adaptive' responses can, in situations of severe and sustained systemic inflammation, lead to adverse effects including brain damage that is partly mediated by neutrophil recruitment into the brain. We examined the contribution of leptin to this process in leptin-deficient (*ob/ob*), -resistant (*db/db*) and wild-type (WT) mice injected intraperitoneally with a septic dose of lipopolysaccharide (LPS). This treatment induced a dramatic increase in the number of neutrophils entering the brain of WT mice, an effect that was almost totally abolished in the mutant mice and correlated with a significant reduction in the mRNA levels of interleukin-1β, intracellular adhesion molecule-1 and neutrophil-specific chemokines. These effects were reversed with leptin replenishment in *ob/ob* mice leading to recovery of neutrophil recruitment into the brain. Moreover, 48 h food deprivation in WT mice, which decreased circulating leptin levels, attenuated the LPS-induced neutrophil recruitment as did a single injection of an anti-leptin antiserum 4 h before LPS treatment in WT mice. These results provide the first demonstration that leptin has a critical role in leukocyte recruitment to the brain following severe systemic inflammation with possible implications for individuals with altered leptin levels such as during obesity or starvation.
Molecular Psychiatry advance online publication, 22 September 2009; doi:10.1038/mp.2009.98

Keywords: inflammation; neutrophils; cytokines; chemokines; sepsis

Introduction

Leptin is an adipocyte-derived hormone whose primary function is to regulate energy balance by acting on hypothalamic neurons.[1] It is now known that this hormone can influence a multitude of physiological systems including immunity.[2,3] The importance of this cytokine-like mediator in immune function was clearly demonstrated in mice with genetic leptin deficiency (*ob/ob*) or resistance (*db/db*), which exhibit various signs of immunodeficiency,[4,5] are susceptible to bacterial infection[6,7] or resistant to autoimmune diseases.[8,9] The abnormalities exhibited by these mice are analogous to starvation-induced immunosuppression, which is accompanied by a dramatic reduction in circulating leptin levels and is reversible by leptin replenishment.[10,11] These observations led to the proposal that leptin represents a critical signal that links the nutritional status of the host to its ability to effectively respond to a pathogenic challenge. Our previous results[12,13] and those of others[14,15] supported this proposal by demonstrating that leptin acts as an important circulating mediator of systemic infection or inflammation by activating brain mechanisms responsible for sickness behaviors. This was based on results showing an acute rise in circulating leptin levels following systemic bacterial lipopolysaccharide (LPS) or other inflammatory agents,[16–18] as well as its ability to induce fever and appetite loss along with brain interleukin (IL)-1β and prostaglandin synthesis,[12–14,19,20] and the attenuation of LPS-induced sickness behaviors by a neutralizing antiserum against leptin.[13,15] In a recent study,[21] we characterized the sites of leptin's action on the brain during systemic LPS inflammation and found that it acts predominantly on the leptomeningis, cerebral fissures and vasculatures, which collectively form the barrier-related structures of the brain. These structures were shown to express leptin receptors,[22–24] and brain macrophages residing in them were reported to exhibit IL-1β expression following leptin or LPS

Correspondence: Dr GN Luheshi, Douglas Mental Health University Institute, Department of Psychiatry, McGill University, 6875 Boulevard LaSalle, Montreal, Quebec, Canada H4H 1R3.
E-mail: giamal.luheshi@mcgill.ca
[3]Current address: Department of Veterinary-Physiology, Justus-Liebig-University Giessen, Frankfurter Strasse 100, Giessen D-35392, Germany.
[4]These authors contributed equally to the work.
Received 30 April 2009; revised 7 July 2009; accepted 18 August 2009

stimulation.[20,25,26] While these results reinforce the proposed link between leptin and brain IL-1β and the ensuing sickness behaviors, the location of this interaction is also indicative of potential pathological consequences in the case of unabated production of IL-1β during severe systemic inflammation. In fact, the same barrier-related structures form the site of primary contact for invading leukocytes, and it has been shown that sustained IL-1β action in the brain is a potent driver for the recruitment of these cells, in particular neutrophils.[27,28] Recently, we have provided preliminary evidence implicating leptin in this process by showing that it is involved in the increase of chemokine mRNA expression in the brain following peripheral LPS challenge.[21] Therefore, in this study we tested the hypothesis that leptin contributes to the induction of innate inflammatory mediators such as IL-1β and chemokines in the brain, and is also involved in circulating leukocyte recruitment, whereby it could potentially contribute to subsequent neuropathological conditions associated with severe systemic inflammation[29,30] and/or psychiatric conditions such as eating disorders that are linked to abnormal leptin levels[31] and brain inflammatory events.[32,33] To this end, we used a mouse model of sepsis induced by systemic injection of a high dose of LPS, which has previously been shown to trigger recruitment of neutrophils into the brain,[34] and examined brain expression of innate inflammatory mediators and neutrophil recruitment in wild–type (WT), *ob/ob* and *db/db* mice. To address the physiological relevance of leptin's involvement in this process, we also studied the impact of food deprivation, which dramatically decreases circulating leptin levels,[10,11] on the LPS-induced brain inflammatory responses. Finally, we examined the effects of transient leptin deficiency in otherwise normal (non-obese or -starved) animals by pharmacologically neutralizing endogenous leptin and assessing the LPS-induced brain inflammatory responses.

By demonstrating a link between leptin and leukocyte recruitment, we highlight in this study the importance of this hormone to an individual's ability to respond effectively to a pathogenic challenge, especially in situations of leptin deficiency such as during prolonged inflammation-induced anorexia.

Materials and methods

Animals

Adult male *ob/ob* (B6. V-*Lep*^{ob}/J) and *db/db* (B6.Cg-*m* +/+ *Lepr*^{db}/J) mice maintained on a C57BL/6J background were purchased from the Jackson Laboratories (Bar Harbor, ME, USA). In all studies 7-week-old animals (on the day of injection) were used, with a body weight of approximately 20 g for WT and 40 g for *ob/ob* and *db/db* mice. An age-dependent effect on the leukocyte recruitment to the brain has been reported in experimental models of brain inflammation;[35,36] therefore, animals were age-matched and mutant mice were heavier than control WT animals. All animals were housed in a controlled environment at an ambient temperature of 21 ± 2 °C on 12:12 h light–dark cycle (light on at 0830 hours) with free access to water and standard laboratory chow unless otherwise specified. The institutional Animal Care Committee pursuant to the Canadian Council of Animal Care guidelines approved all experimental procedures.

Treatment and experimental protocols

The appropriate conditions for investigating neutrophil recruitment to the brain during LPS-induced systemic inflammation were determined in a pilot study. Detailed protocols and results are available in 'supplementary information' at Molecular Psychiatry's website. On the basis of these results (Supplementary Figure S1), WT, *ob/ob* and *db/db* mice were injected with either LPS (*Escherichia coli* 0111:B4; cat: L-2630; Sigma, Ontario, Canada) at a dose of 2.5 mg kg^{-1} (intraperitoneally, i.p.) or with pyrogen-free saline, and their brains collected 24 h after the treatment. The dose of LPS was adjusted to the weight of the animals to account for possible confounding effects due to the higher body weight of *ob/ob* and *db/db* mice (average of 40 g) compared with their WT counterparts (average of 20 g). A separate group of *ob/ob* mice was treated with either murine leptin (1 μg μl^{-1}, 6 μg day^{-1}; PeproTec, Rocky Hill, NJ, USA) or saline delivered by Alzet miniosmotic pumps (0.25 μl h^{-1}; model 1002, Durect, Cupertino, CA, USA) implanted subcutaneously in the dorsal midline caudal to the scapulae of the animals under isoflurane anesthesia 10 days before the LPS treatment. To address the effect of the decline in leptin levels associated with acute starvation on the brain responses, additional groups of WT animals were fasted for 48 h with or without leptin replenishment (6 μg day^{-1}) using Alzet pumps before the LPS treatment. To test the effect of acute leptin deficiency in otherwise normal animals, additional groups of WT mice were treated with a neutralizing sheep anti-mouse leptin antiserum (LAS; S4159, NIBSC, Potters Bar, UK) or preimmune sheep serum (NIBSC) at 0.5 ml kg^{-1} i.p. 4 h before LPS or saline treatment. The volume and timing of LAS injections were determined in accordance with a previous study using the same antiserum.[21]

Animals were killed 24 h after LPS or saline treatment by terminal anesthesia (pentobarbital; 70 mg kg^{-1}, i.p.) and blood samples collected by cardiac puncture. Mice were then transcardially perfused with ice-cold saline with 5 IU ml^{-1} of heparin to flush-out any remaining blood from the brain. The brains were quickly removed, frozen in powdered dry ice and kept at −80 °C until analysis.

Tissue processing

For all studies, brain sections were collected from three levels (encompassing the anterior hypothalamus, bregma −0.1 to −0.82 mm; the posterior

hypothalamus, bregma −1.22 to −2.3 mm; and the brain stem, bregma −7.2 to −7.92 mm) using coordinates from the mouse brain atlas.[37]

To perform immunohistochemistry and reverse transcription (RT)-PCR on the same tissue taken from the same brain, 9–18 consecutive frozen sections were thaw-mounted on glass slides for immunohistochemistry, and the remainder of the serial brain sections from the forebrain (bregma −0.10 to −2.3 mm) were overlaid on a frozen glass slide, the hypothalamus dissected, and collected in a cryotube at −80 °C for RNA extraction.

Quantitative RT-PCR

Total RNA was extracted using TRIzol (Invitrogen, Ontario, Canada) according to the manufacturer's instructions. Following reverse transcription, quantitative RT-PCR was carried out in duplicate using pre-optimized primer/probe mixture (TaqMan Gene Expression Assays; Applied Biosystems, Ontario, Canada) and TaqMan universal PCR master mix (Applied Biosystems) on 7500 Real-Time PCR System (Applied Biosystems). The cDNA quantities between different reactions were normalized by using a housekeeping gene β-actin (cat: 4352341E, Applied Biosystems) as a reference. The sample values represent X-fold differences from a control sample (given a designated value of 1) within the same experiment. The assay ID for each gene is as follows: IL-1β (Mm00434228_m1), CD14 (Mm00438094_g1), intracellular adhesion molecule (ICAM)-1 (Mm00516024_g1), tissue inhibitor of metalloproteinase (TIMP)-1 (Mm00441818_m1), keratinocyte-derived chemokine (KC) (Mm01354329_g1), macrophage inflammatory protein (MIP)-2 (Mm00436450_m1).

Immunohistochemistry

Fresh-frozen sections were post-fixed in 2% paraformaldehyde, incubated with rat monoclonal anti-mouse neutrophil antibody (1:500 dilution; 7/4, cat: MCA771G, AbD Serotec, Oxford, UK) followed by CY3-conjugated donkey anti-rat immunoglobulin G (IgG) antibody (1:500 dilution; cat: 712-165-150, Jackson Immuno Research, West Grove, PA, USA). Cell nuclei were stained with 4,6-diamidino-2-phenylindole (1:4000 dilution in phosphate-buffered saline; Molecular Probes, Eugene, OR, USA). All antibodies were diluted in the blocking solution (10% normal donkey serum (Chemicon International, Temecula, CA, USA), 0.2% Triton-X100 in phosphate-buffered saline). ICAM-1 staining followed the same procedure with a few modifications; frozen sections were dipped in 100% ethanol, kept at −20 °C for 15 min, air-dried followed by paraformaldehyde fixation; the blocking solution contained 0.01% Triton-X100. Rat monoclonal anti-mouse ICAM-1 (1:200 dilution; cat: sc-52553, Santa Cruz Biotechnology, Santa Cruz, CA, USA) was used as a primary antibody.

For the double labeling of neutrophil/ICAM-1, the anti-neutrophil antibody was mixed with a goat anti-mouse ICAM-1 antibody (1:200 dilution; cat: sc-1511, Santa Cruz Biotechnology). All secondary antibodies were multiple labeling-grade, raised in donkey, and used at 1:500 dilution (Jackson Immuno Research): CY3-conjugated anti-rat IgG for neutrophil and anti-goat IgG (cat: 705-095-147) for ICAM-1. In control experiments, the sections were incubated with the primary antibody mixture in which the primary antibody was substituted with an IgG from a non-immunized animal (rat and goat IgG for 7/4 and ICAM-1, respectively; Jackson Immuno Research). Inappropriate crossreaction between antibodies was confirmed to be negligible (data not shown).

Assessment of neutrophil recruitment

Three different levels of the brain (at the levels of the subfornical organ, the arcuate nucleus and the area postrema) were analyzed. First, for each animal, three to four sections were analyzed at each brain level and the mean value was calculated. Second, the mean values from the three brain levels were summed to represent the total number of neutrophil. For each brain section, one image was taken with a ×2.5 magnification objective lens using a fixed exposure time, gain and offset for all sections. This low-magnification image covers more than 60% of the brain area at the levels of the hypothalamus and more than 80% of the area at the level of the brain stem. Representative images are shown in Supplementary Figure S2. The number of neutrophil-positive labeling as defined by size and light intensity was determined using an automatic counting procedure (Scion Image 4.0.2, Scion, Frederick, MD, USA). Obvious artifacts due to dust or air bubbles were manually excluded from the area of interest.

Cytokine enzyme-linked immunosorbent assay

Plasma levels of tumor necrosis factor (TNF), IL-1β and IL-6 were measured in duplicate using a mouse cytokine ELISA kit (Quantikine; R&D systems, Minneapolis, MN, USA) according to the manufacture's instruction. The detection limits of the assay were 10.2, 6.0, 6.0 pg ml^{-1} for TNF, IL-1β and IL-6, respectively. Plasma leptin levels were measured by a mouse leptin enzyme-linked immunosorbent assay (NIBSC), as described previously.[21] The detection limit of the assay was 156.2 pg ml^{-1}.

Data analysis

All data were presented as mean values ± s.e.m. Data were analyzed using a one-way analysis of variance followed by a Newman–Keuls multiple comparisons *post hoc* test. A parametric unpaired two-tailed Student's *t*-test was used to compare leptin-replaced groups of *ob/ob* animals. Values (*P*-value) less than 5% were deemed significant.

Results

Systemic LPS-induced neutrophil recruitment into the brain is leptin dependent

To examine the role of leptin-ObRb signaling in neutrophil recruitment, we compared the accumulation of neutrophils in the brain in WT, *ob/ob* and *db/db* mice 24 h after the LPS challenge (2.5 mg kg^{-1}, i.p.). The robust neutrophil accumulation observed in LPS-treated WT mice was almost completely abolished in *ob/ob* (Figure 1) or *db/db* (not shown) mice. Importantly, leptin replenishment in *ob/ob* mice clearly reversed the recruitment. The neutrophil numbers were quantified in coronal sections collected at three levels of the brain (at the level of the subfornical organ, the arcuate nucleus and the area postrema, see representative images in Supplementary Figure S2). The average total cell number from the three brain levels (3–4 sections per level × 3 levels, $n = 5$–6 per group) are shown in Figure 1b. The neutrophil accumulation in LPS-treated *ob/ob* or *db/db* mice was significantly lower than in WT counterparts ($P < 0.001$). Although LPS tended to increase neutrophil numbers in *ob/ob* and *db/db* mice, this effect was not statistically significant ($P > 0.05$, LPS vs saline). Leptin replenishment in *ob/ob* mice significantly reversed the attenuation of LPS-induced neutrophil accumulation ($P < 0.05$).

Leptin is involved in cerebral ICAM-1 upregulation during LPS-induced systemic inflammation

A previous study demonstrated that the adhesion molecule ICAM-1 has a crucial role in neutrophil recruitment into the brain associated with LPS-induced systemic inflammation.[34] Therefore, we next

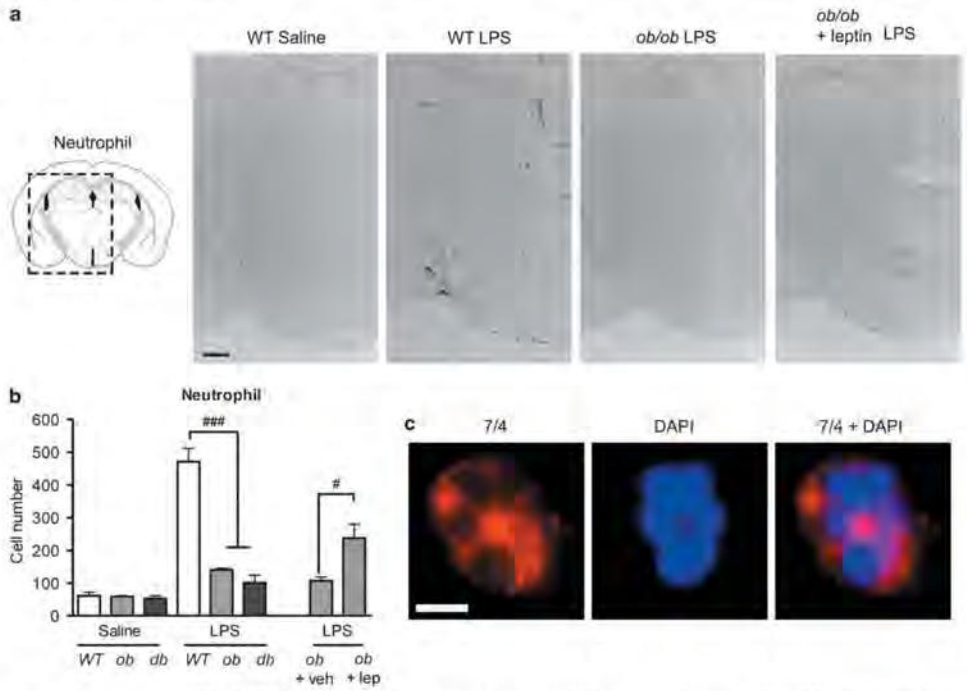


Figure 1 Lipopolysaccharide (LPS)-induced neutrophil recruitment to the brain of wild-type (WT), ob/ob and leptin-treated ob/ob mice. (**a**) Representative images depicting neutrophil distribution in coronal sections of the brain in the area shown by an atlas template. The fluorescent images are presented in brightfield for clarity of contrast at low magnification. In WT mice, LPS (2.5 mg kg^{-1}, intraperitoneally) dramatically increased neutrophil accumulation 24 h after stimulation. This response was abolished in *ob/ob* mice and was reversed by leptin treatment. Note that the distribution of neutrophils was prominent along the ventricles, the interhemispheric and hippocampal fissures, the leptomeningis and vasculatures. Scale bar = 400 μm. (**b**) Quantitative data for neutrophil recruitment. The neutrophil numbers were quantified in coronal sections collected at three levels of the brain (at the level of the subfornical organ, the arcuate nucleus and the area postrema). The average total cell number from the three brain levels (3–4 sections per level × 3 levels, $n = 5$–6 per group) are shown here. Values are presented as means ± s.e.m. *P*-values: $^{*} < 0.05$, $^{***} < 0.001$. (**c**) Images of a neutrophil at high magnification. 7/4-immunoreactivity (IR) (red) and its segmented nucleus characteristic of granulocyte neutrophils stained with 4,6-diamidino-2-phenylindole (DAPI) (blue). Scale bar = 5 μm.

asked whether leptin-ObRb signaling is important for cerebral ICAM-1 expression. ICAM-1 protein and mRNA expression were analyzed in the brains of WT, *ob/ob* and *db/db* mice 24 h after the LPS challenge. Figure 2a shows that, in WT mice, LPS treatment strongly increased ICAM-1-immunoreactivity (IR) along vasculature and in the leptomeningis, ependymal linings of the ventricles and the choroid plexus when compared with saline controls. The increase in ICAM-1-IR was clearly attenuated in both *ob/ob* (Figure 2a) and *db/db* mice (data not shown), and this effect was reversed by leptin replenishment in *ob/ob* mice. In saline-treated groups, a weak but clear ICAM-1-IR was observed along blood vessels and in the leptomeningis. This constitutive ICAM-1-IR was comparable between WT, *ob/ob* and *db/db* (not shown) mice, indicating that leptin is not critical for basal ICAM-1 expression in the brain under non-inflammatory conditions. Consistent with the protein expression profile, the LPS treatment induced a 20-fold increase of ICAM-1 mRNA expression in WT mice as measured by quantitative RT-PCR (Figure 2b). In *ob/ob* and *db/db* mice, the LPS-induced ICAM-1 mRNA expression was significantly attenuated ($P<0.001$, approximately 50% of the levels of WT counterparts), and the reduction was nearly completely reversed by leptin replenishment in *ob/ob* mice ($P<0.01$).

Double immunohistochemistry for ICAM-1 and 7/4 revealed that most, if not all, of the accumulating 7/4-IR neutrophils were closely associated with ICAM-1-IR structures (Figure 2c), an observation in line with the reported functional importance of ICAM-1 for neutrophil recruitment.[34] Interestingly, some 7/4-IR cells were found adhering to the abluminal (brain) side of the ICAM-1-IR vasculature-like structures.

Leptin-mediated neutrophil recruitment is associated with cerebral IL-1β and neutrophil chemokine upregulation

Systemic inflammation triggers *de novo* synthesis of various inflammatory mediators in the brain, some of which, in addition to ICAM-1, have key roles in

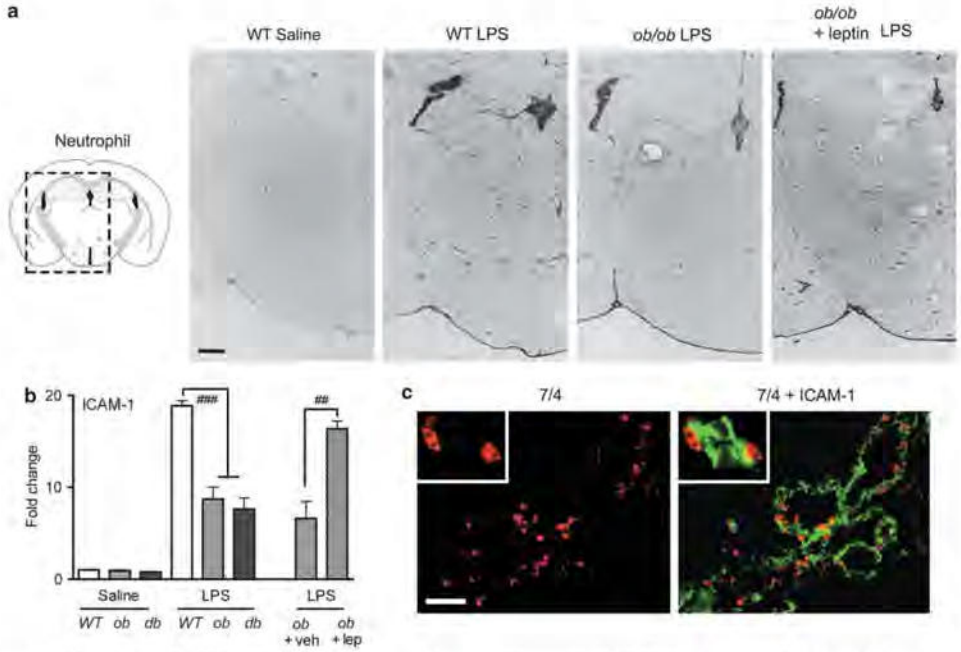


Figure 2 Lipopolysaccharide (LPS)-induced intracellular adhesion molecule-1 (ICAM-1) expression in the brain of wild-type (WT), ob/ob and leptin-treated ob/ob mice. (**a**) Representative images depicting ICAM-1 protein expression in coronal sections of the brain in the area shown by an atlas template. The fluorescent images are presented in brightfield for clarity of contrast at low magnification. LPS treatment (2.5 mg kg^{-1}, intraperitoneally) dramatically increased ICAM-1-immunoreactivity (IR) in the leptomeningis, cerebral vasculatures and fissures, and the choroid plexus in WT mice 24 h after the challenge. The increase of ICAM-1-IR was clearly attenuated in *ob/ob* mice and was reversed by leptin treatment in these animals. Scale bar = 400 μm. (**b**) ICAM-1 mRNA levels in the brain analyzed by using quantitative reverse transcription-PCR. Values are presented as means + s.e.m. ($n=5$–6). *P*-values: $^{\#\#}<0.01$, $^{\#\#\#}<0.001$. (**c**) Double immunohistochemistry for ICAM-1 and neutrophils (7/4 antigen) in the brain of LPS-treated WT mice. 7/4-IR (red) was closely associated with ICAM-1-IR (green). Scale bar = 50 μm.

cerebral recruitment of leukocytes. To examine the contributions of leptin-ObRb signaling to this brain response, mRNA levels of several innate inflammatory mediators were measured by using quantitative RT-PCR. The LPS treatment resulted in a 120-fold increase in IL-1β mRNA levels ($P<0.001$) in WT mice when compared with saline controls (Figure 3). This increase was dramatically attenuated in both *ob/ob* and *db/db* mice ($P<0.001$), and replenishment of leptin in *ob/ob* mice significantly reversed the attenuated IL-1β mRNA levels ($P<0.05$). Similarly, LPS-induced TNF mRNA levels were significantly reduced in *ob/ob* ($P<0.05$) and *db/db* ($P<0.05$) mice. However, unlike IL-1β, leptin replenishment in *ob/ob* mice did not reverse the attenuation of TNF. We in addition detected significant effects of leptin-ObRb signaling on the LPS-induced increases of the key neutrophil chemokines KC and MIP-2 (Figure 3). In contrast, the increase of CD14 mRNA, another LPS-inducible innate inflammatory gene,[38] was comparable between WT, *ob/ob* and *db/db* mice, and the increase of TIMP-1, an endogenous metalloproteinase inhibitor also implicated in leukocyte infiltration into the brain,[39] was enhanced in *ob/ob* ($P<0.05$) but not

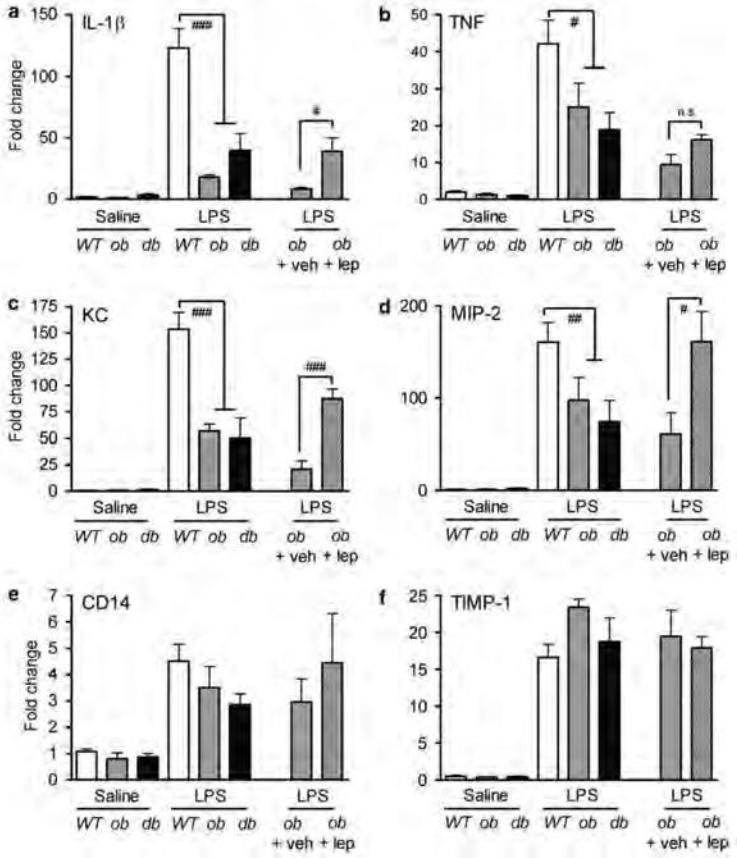


Figure 3 mRNA expression of innate inflammatory mediators in the brain following systemic lipopolysaccharide (LPS) challenge in wild-type (WT), ob/ob and db/db mice. mRNA levels in the brain were analyzed 24 h after LPS challenge (2.5 mg kg^{-1}, intraperitoneally) using quantitative RT-PCR. (**a–d**) LPS-induced mRNA levels of interleukin (IL)-1β, tumor necrosis factor (TNF), keratinocyte-derived chemokine (KC) and macrophage inflammatory protein (MIP)-2 were dramatically reduced in *ob/ob* and *db/db* mice when compared with WT controls. (**e** and **f**) The LPS-induced CD14 and tissue inhibitor of metalloproteinase (TIMP)-1 mRNA levels were similar between WT, *ob/ob* and *db/db* mice. Replenishment of leptin in *ob/ob* mice significantly increased the LPS-induced mRNA levels of IL-1β, KC and MIP-2, whereas it had no effect on TNF, CD14 and TIMP-1 mRNA increase, as compared with vehicle infusion. Values are presented as means + s.e.m. ($n=5–6$). *P*-values: $^{*}<0.05$, $^{**}<0.01$, $^{***}<0.001$; NS, not significant.

in *db/db* mice. These results indicate that the impaired mRNA induction of ICAM-1, IL-1β, KC and MIP-2 were not due to a general reduction of the inflammatory response in *ob/ob* or *db/db* mice but rather to a specific contribution of leptin-ObRb signaling to their gene regulation in the brain.

Genetic deficiency of leptin or ObRb may cause an abnormal systemic inflammatory response to LPS,[40,41] which in turn affects brain responses. To examine this possibility, plasma levels of cytokines (TNF, IL-1β and IL-6) were measured in the same groups of mice. The results are summarized in Supplementary Table S1, which shows that the levels of all cytokines were below the detection limit of the assay in saline-treated animals regardless of the genotypes. In WT mice, TNF and IL-6 levels were significantly elevated by LPS, whereas IL-1β levels, although detectable, were not statistically higher than the saline controls (which were assigned the value of the detection limit of the assay) 24 h after injection. In contrast to the apparent attenuation of brain inflammation (that is, neutrophil recruitment and inflammatory gene expressions), the LPS-induced elevations of TNF and IL-6 levels were significantly enhanced in *ob/ob* ($P<0.001$) and *db/db* ($P<0.001$) mice as compared with WT counterparts. Leptin replenishment in *ob/ob* mice significantly reversed the exaggerated IL-6 ($P<0.01$) but not TNF levels. IL-1β levels were not affected by leptin or ObRb signaling. Plasma leptin levels were not altered by LPS treatment in WT mice but were significantly increased in *db/db* animals ($P<0.001$). As expected, leptin was not detectable in *ob/ob* mice in any of the treatment groups and leptin infusion in *ob/ob* mice increased leptin levels ($P<0.001$).

Acute starvation suppresses the brain innate inflammatory response by a decrease in circulating leptin levels

Given leptin's role in linking nutritional status, immunity and the brain, we tested if the reduction in leptin levels during acute starvation will influence the inflammatory mechanisms linked to neutrophil trafficking into the brain. To this end, WT mice were fasted for 48 h with or without leptin replenishment before LPS administration (2.5 mg kg^{-1}, i.p.), and the inflammatory responses in the brain were assessed 24 h after the injection. The LPS-induced neutrophil accumulation was significantly attenuated by fasting without leptin infusion as compared with *ad lib* feeding ($P<0.01$), and leptin replenishment significantly reversed neutrophil accumulation ($P<0.05$, Figure 4a). Fasting impaired the LPS-induced innate inflammatory gene expression in the brain in a manner almost identical to leptin or leptin receptor genetic deficiency (Figures 4b–h). Briefly, fasted mice with vehicle infusion showed impaired LPS-induced increase in IL-1β ($P<0.001$), KC ($P<0.01$), MIP-2 ($P<0.05$) and ICAM-1 ($P<0.001$) mRNA levels while having comparable CD14 and TIMP-1 mRNA increases when compared with *ad lib*-fed counterparts. Leptin replenishment during fasting reversed the

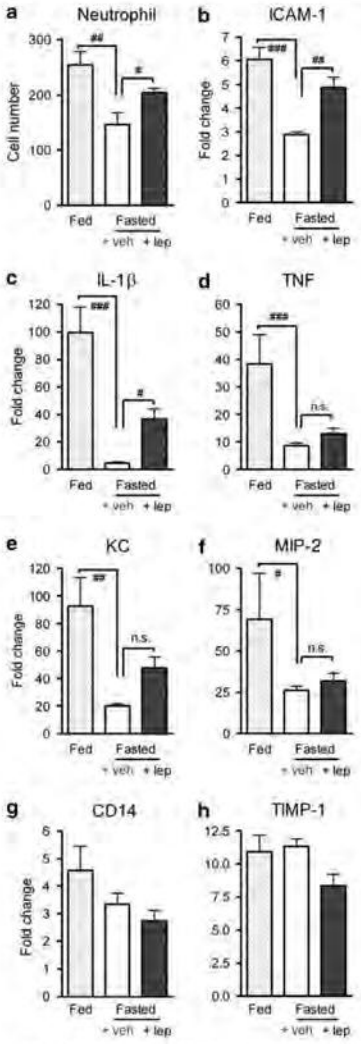


Figure 4 The effects of fasting and leptin replenishment on neutrophil recruitment and brain inflammatory gene expression during systemic LPS inflammation. (**a**) Mice were fed, fasted or fasted with leptin replenishment for 48 h before LPS treatment (2.5 mg kg^{-1}, intraperitoneally). Neutrophil recruitment was quantified 24 h after the LPS challenge. (**b–h**) The levels of mRNA expression in the brain were measured by quantitative reverse transcription (RT)-PCR in the same animals. Values are presented as means + s.e.m. ($n=5$). *P*-values: $^{*}<0.05$, $^{**}<0.01$, $^{***}<0.001$. NS, not significant.

induction of IL-1β ($P<0.05$) and ICAM-1 ($P<0.01$) mRNA levels. Although there was a tendency for KC mRNA levels to recover, this did not reach statistical

significance. MIP-2 mRNA levels were not affected by leptin replacement. In saline-treated groups, fasting with or without leptin did not alter neutrophil numbers (44.3 ± 3.7 and 44.0 ± 2.6 for vehicle and leptin, respectively) and inflammatory gene expressions in the brain (data not shown).

Supplementary Table S1 shows that neither fasting nor leptin infusion affected the plasma levels of TNF, IL-1β or IL-6, an observation in contrast to the case of genetic leptin deficiency. Fasting reduced plasma leptin levels below the detection limit of the assay, and leptin infusion in fasted mice increased leptin levels.

Transient neutralization of leptin alleviates neutrophil accumulation in the brain during systemic LPS inflammation

Given the significant role of leptin in LPS-induced neutrophil recruitment to the brain, which is potentially neurotoxic, it is important to elucidate whether a transient neutralization of leptin could be used as a potential tool for therapeutic intervention. To test this, WT mice received a single injection of LAS ($0.5\ ml\ kg^{-1}$, i.p.) or a control preimmune sheep serum 4 h before the administration of LPS ($2.5\ mg\ kg^{-1}$, i.p.) or saline, and the brains examined 24 h after LPS treatment. Figure 5a shows that LAS treatment significantly attenuated the LPS-induced neutrophil accumulation in the brain ($P<0.001$). Among the genes that were found to be regulated by leptin (in *ob/ob*, *db/db* or fasted mice) during LPS-induced inflammation, LAS-treatment attenuated only KC ($P<0.01$) and MIP-2 ($P<0.001$) mRNA induction, whereas it did not affect the induction of ICAM-1 and IL-1β mRNA (Figures 5b–h). In addition, LPS-induced TIMP-1 mRNA expression was attenuated by LAS ($P<0.01$).

Analysis of circulating cytokine levels in this experiment showed that LPS-induced increases in plasma TNF and IL-6 levels ($P<0.01$) were not affected by LAS treatment (Supplementary Table S1). Neither LPS not leptin altered IL-1β levels. The leptin levels both in the LAS–saline and LAS–LPS groups were below the detection limit of the assay, confirming the effectiveness of LAS treatment.

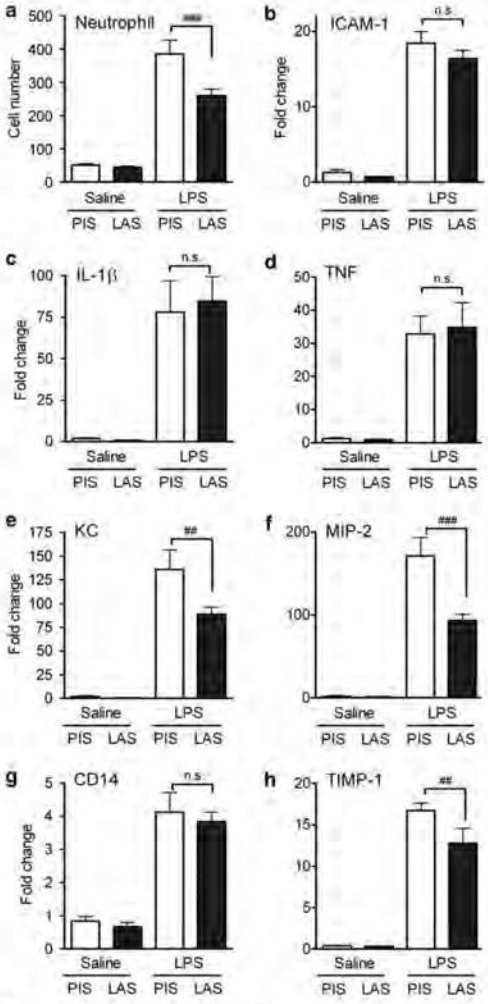


Figure 5 The effects of acute leptin neutralization on brain inflammatory gene expression and neutrophil recruitment during systemic lipopolysaccharide (LPS) inflammation. Mice were treated with either LAS ($0.5\ ml\ kg^{-1}$, intraperitoneally (i.p.)) or control preimmune sheep serum (PIS) 4 h before LPS ($2.5\ mg\ kg^{-1}$ i.p.) or saline injection. Brains were analyzed 24 h after the LPS/saline challenge. (**a**) Neutrophil recruitment. (**b–h**) mRNA levels measured by using quantitative reverse transcription (RT)-PCR. Values are presented as means + s.e.m. ($n=5$). *P*-values: $^{**}<0.01$, $^{***}<0.001$. NS, not significant.

Discussion

The main finding of this study is that leptin mediates the recruitment of neutrophils to the brain during severe systemic LPS inflammation by acting at the level of barrier-related structures that are involved in immune cell trafficking into the brain. Interestingly, the pattern of leptin activity demonstrated by us previously[21] exhibited remarkable similarity to the distribution of leptin-mediated neutrophil accumulation observed in this study (Figure 1 and Supplementary Figure S1).

The attenuation of LPS-induced neutrophil recruitment, as well as the accompanying gene expression, was comparable between *ob/ob* and *db/db* mice, the latter have intact short forms of ObR but lack the long form ObRb, indicating that these leptin-mediated processes were dependent primarily on ObRb. This observation in turn indicates that the neutrophil

recruitment and brain production of inflammatory mediators are independent of the reported direct actions of leptin on neutrophils (which only express the short form ObRs), in which this hormone has been shown to stimulate chemotaxis[42] or inhibit spontaneous apoptosis,[43] suggesting that its action on alternative targets including the brain is the major contributing factor to the leptin-mediated processes observed in this study.

Parallel to the suppression of the neutrophil recruitment, LPS-induced IL-1β mRNA upregulation was strongly blunted in the brains of *ob/ob*, *db/db* or fasted WT mice when compared with (*ad lib* fed) WT counterparts. IL-1β is rapidly induced in the brain by various inflammatory stimuli, and is a potent contributor to subsequent brain innate inflammatory responses.[44] IL-1β alone, when acting centrally, is sufficient to trigger recruitment of neutrophils to the brain,[27,26,45,46] whereas blockade of IL-1β actions by using IL-1 receptor antagonist or genetic deletion of its functional receptor IL-1R1 prevents the neutrophil recruitment associated with neuroinflammation.[47,48] In the context of this study, we and others have previously demonstrated that leptin administration, either centrally or systemically, induces brain IL-1β both at the mRNA and protein levels,[12,14,19,20] which localized mainly in macrophages in the meningis and perivascular spaces.[20] Interestingly, this is very similar to the pattern of expression induced by systemic injection of LPS where brain IL-1β production is known to emanate largely from brain macrophages primarily residing in perivascular spaces, as well as from parenchymal microglia.[25,26,49,50] These data favor our speculation that defective brain IL-1β production resulting from leptin (or ObRb) deficiency is one of the underlying mechanisms responsible for reduced neutrophil recruitment during systemic inflammation observed in this study.

Neutrophil attachment to brain endothelium is the prerequisite step for their eventual recruitment into the central nervous system. In this study, the replenishment of leptin in leptin-deficient *ob/ob* or fasted WT mice almost completely restored the attenuated ICAM-1 mRNA upregulation by LPS, indicating a significant influence of leptin on the LPS-induced brain ICAM-1 expression. Moreover, immunohistochemical approaches demonstrated that the leptin-mediated ICAM-1 expression was predominantly localized in the cerebrovasculature, the leptomeningis, cerebral fissures and the choroid plexus, all of which were primary sites of neutrophil accumulation (Figures 1 and 2). In fact, double-labeling studies clearly showed that the majority of neutrophils were closely associated with ICAM-1-IR cells, on both the luminal and abluminal sides of the vasculature-like structures (Figure 2c). As the brains examined in this study were well perfused with heparinized saline, we presume that this close contact may represent an integrin-mediated neutrophil arrest to the endothelium, the essential step for eventual neutrophil infiltration into the parenchyma. In fact, Bohatschek *et al*.[34] reported that neutrophil infiltration into the brain following peripheral LPS challenge was strongly reduced in ICAM-1-deficient mice to the levels below 50% of WT controls. The mechanism underlying leptin's regulation of ICAM-1 is not yet clear but IL-1β is likely to be an important factor. It is well established that, in the brain, IL-1R1 is constitutively, and indeed predominantly, expressed in the barrier-related structures (for example, vasculatures, the leptomeningis and the choroid plexus),[51,52] and IL-1β readily induces ICAM-1 in these structures.[46] Given that leptin induces IL-1β in perivascular and meningeal macrophages *in vivo*,[20] it is conceivable that leptin-induced IL-1β acts on the barrier-related structures in a paracrine manner and regulates leukocyte recruitment through ICAM-1.

A transient neutralization of leptin with LAS effectively attenuated neutrophil recruitment during LPS inflammation. This is an important observation with therapeutic potential for combating certain neuropathologies, such as cerebral ischemia, in which both neutrophil recruitment and systemic inflammation are linked with detrimental outcomes.[53,54] However, this approach also revealed some issues regarding the actions of leptin worth consideration. In contrast to other models (genetic deficiency or fasting), LAS treatment did not alter the LPS-induced IL-1β and ICAM-1 mRNA expression. The efficiency of neutralization is certainly a factor to be considered, however the plasma leptin levels in LAS-treated animals were verified at the end of the experiment and were all below the detection limit of the assay. Alternatively, this observation implies that the depletion of leptin signaling preceding, rather than in the course of inflammation, is critical for the attenuation of IL-1β and ICAM-1 levels. In contrast, LAS treatment was able to attenuate, similar to other models of leptin deficiency, the LPS-induced mRNA increase of KC and MIP-2, both of which are potent and well-characterized neutrophil chemoattractants in mice.[55] This indicates that although IL-1β has been demonstrated to be a powerful inducer of KC and MIP-2,[28,45] leptin could be an additional factor influencing their brain expression independent of IL-1β. In line with this rationale, it was previously demonstrated that, in the periphery, leptin directly stimulates the production of KC and MIP-2.[56] As these chemokines are essential for neutrophil recruitment to the brain even in the presence of IL-1β and ICAM-1,[28,56] their LAS-mediated attenuation explains the reduced neutrophil recruitment by LAS treatment without affecting the expression of either IL-1β or ICAM-1.

A number of studies have shown that replenishment of leptin in starved animals restores their abnormal host defense responses in various experimental models of inflammation,[10,57,58] highlighting the physiological importance of this hormone. This study demonstrated that acute starvation attenuates brain production of innate inflammatory mediators including IL-1β, ICAM-1 and KC in a leptin-dependent

manner, which was paralleled by the reduction in neutrophil recruitment during LPS-induced systemic inflammation. Importantly, these changes are specific to a certain facet of the brain inflammatory response and are not a result of a generalized insensitivity to LPS, as the expression of CD14 and TIMP-1 mRNA in the brain, which were also induced by LPS, were unaffected by fasting or leptin levels. Similarly, the reduction of leptin levels by fasting (as well as by LAS treatment) did not significantly affect plasma levels of TNF, IL-1β and IL-6 (measured as indicators for systemic inflammation) during LPS-induced inflammation, although a previous study[58] reported an exaggeration of plasma TNF in LPS-treated fasted mice (by using a different LPS dose and time points for cytokine measurements). Interestingly, the mutant *ob/ob* and *db/db* mice demonstrated exaggerated plasma TNF and IL-6 elevations in response to LPS. These results indicate that factor(s) unique to mutant mice (for example, a permanent leptin deficiency and/or excessive fat storage), rather than a transient leptin deficiency, have a significant impact on peripheral TNF and IL-6 production. Importantly, the increase in the levels of these cytokines in the circulation was dissociated from the attenuated brain inflammation observed in our studies, and therefore negates their influence on the observed changes in neutrophil recruitment and favors the direct action of leptin on the brain as reported in this study. Interestingly, leptin levels were not affected by the LPS treatment in our experiments (Supplementary Table S1), in agreement with some[59,60] but contrary to other[16–18] studies. The reason for this apparent discrepancy is currently unclear, but the relatively late time point chosen in this study (24 h) may have not been ideal for the detection of LPS-induced leptin increase. Regardless, our results favor the scenario that the deficiency of leptin, rather than the absence of its increase from baseline, impairs the inflammatory response in the brain during systemic LPS-induced inflammation.

In addition to the direct role of leptin in the recruitment of neutrophils, other facets of its actions need to be considered as possible contributors to the response observed in our study. In particular, this includes its role in mediating the temperature response to LPS reported previously by us,[13] and others.[15,61,62] Given the relatively high dose of LPS used in our study, it is likely that a mixture of hypothermia followed by a fever ensues following the injection as shown previously.[63,64] This temperature response could conceivably affect the integrity of the blood–brain barrier,[65] which in turn could potentially influence leukocyte entry into the brain.

In conclusion, this study, by demonstrating a significant contribution of leptin to neutrophil recruitment caused by severe systemic inflammation, suggests a potential role for this hormone in the development and/or progression of neuropathological conditions linked to leukocyte-mediated pathogenesis[54,55,66] and/or immune-to-brain communication by leukocytes involved in the generation of sickness behavior.[67] Our finding that leptin is integral to the brain's innate inflammatory response may have broad implications on how the abnormal nutritional status during starvation, obesity or eating disorders (for example, anorexia nervosa or binge-eating), all of which are associated with changes in circulating levels of leptin,[31] can impact the etiology of brain disease.

Acknowledgments

We thank Ms G Somay for excellent technical assistance. This study was supported by the Canadian Institute of Health Research and the Natural Sciences and Engineering Research Council of Canada (GNL). CR is a fellow of the Deutsche Forschungsgemeinschaft (DFG project RU 1397/1-1). WI is a recipient of a PhD scholarship from the Nakajima Foundation, Japan.

Conflict of interest

The authors declare no conflict of interest.

References

1 Friedman JM. Leptin, leptin receptors, and the control of body weight. *NutrRev* 1998; **56**(2 Part 2): s38–s46.
2 Faggioni R, Feingold KR, Grunfeld C. Leptin regulation of the immune response and the immunodeficiency of malnutrition. *FASEB J* 2001; **15**: 2565–2571.
3 La Cava A, Matarese G. The weight of leptin in immunity. *Nat Rev Immunol* 2004; **4**: 371–379.
4 Chandra RK. Cell-mediated immunity in genetically obese C57BL/6J ob/ob) mice. *Am J Clin Nutr* 1980; **33**: 13–16.
5 Fernandes G, Handwerger BS, Yunis EJ, Brown DM. Immune response in the mutant diabetic C57BL/Ks-dt + mouse. Discrepancies between *in vitro* and *in vivo* immunological assays. *J Clin Invest* 1978; **61**: 243–250.
6 Ikejima S, Sasaki S, Sashinami H, Mori F, Ogawa Y, Nakamura T *et al*. Impairment of host resistance to Listeria monocytogenes infection in liver of db/db and ob/ob mice. *Diabetes* 2005; **54**: 182–189.
7 Mancuso P, Gottschalk A, Phare SM, Peters-Golden M, Lukacs NW, Huffnagle GB. Leptin-deficient mice exhibit impaired host defense in Gram-negative pneumonia. *J Immunol* 2002; **168**: 4018–4024.
8 Matarese G, Di Giacomo A, Sanna V, Lord GM, Howard JK, Di Tuoro A *et al*. Requirement for leptin in the induction and progression of autoimmune encephalomyelitis. *J Immunol* 2001; **166**: 5909–5916.
9 Busso N, So A, Chobaz-Peclat V, Morard C, Martinez-Soria E, Talabot-Ayer D *et al*. Leptin signaling deficiency impairs humoral and cellular immune responses and attenuates experimental arthritis. *J Immunol* 2002; **168**: 875–882.
10 Lord GM, Matarese G, Howard JK, Baker RJ, Bloom SR, Lechler RI. Leptin modulates the T-cell immune response and reverses starvation-induced immunosuppression. *Nature* 1998; **394**: 897–901.
11 Howard JK, Lord GM, Matarese G, Vendetti S, Ghatei MA, Ritter MA *et al*. Leptin protects mice from starvation-induced lymphoid atrophy and increases thymic cellularity in ob/ob mice. *J Clin Invest* 1999; **104**: 1051–1059.
12 Luheshi GN, Gardner JD, Rushforth DA, Loudon AS, Rothwell NJ. Leptin actions on food intake and body temperature are mediated by IL-1. *Proc Natl Acad Sci USA* 1999; **96**: 7047–7052.

13 Sachot C, Poole S, Luheshi GN. Circulating leptin mediates lipopolysaccharide-induced anorexia and fever in rats. *J Physiol* 2004; **561**(Part 1): 263–272.
14 Hosoi T, Okuma Y, Nomura Y. Leptin regulates interleukin-1beta expression in the brain via the STAT3-independent mechanisms. *Brain Res* 2002; **949**: 139–146.
15 Harden LM, du Plessis I, Poole S, Laburn HP. Interleukin-6 and leptin mediate lipopolysaccharide-induced fever and sickness behavior. *Physiol Behav* 2006; **89**: 146–155.
16 Sarraf P, Frederich RC, Turner EM, Ma G, Jaskowiak NT, Rivet III DJ *et al*. Multiple cytokines and acute inflammation raise mouse leptin levels: potential role in inflammatory anorexia. *J Exp Med* 1997; **185**: 171–175.
17 Grunfeld C, Zhao C, Fuller J, Pollack A, Moser A, Friedman J *et al*. Endotoxin and cytokines induce expression of leptin, the ob gene product, in hamsters. *J Clin Invest* 1996; **97**: 2152–2157.
18 Faggioni R, Fantuzzi G, Fuller J, Dinarello CA, Feingold KR, Grunfeld C. IL-1 beta mediates leptin induction during inflammation. *Am J Physiol* 1998; **274**(1 Part 2): R204–R208.
19 Wisse BE, Ogimoto K, Morton GJ, Wilkinson CW, Frayo RS, Cummings DE *et al*. Physiological regulation of hypothalamic IL-1beta gene expression by leptin and glucocorticoids: implications for energy homeostasis. *Am J Physiol Endocrinol Metab* 2004; **287**: E1107–E1113.
20 Inoue W, Poole S, Bristow AF, Luheshi GN. Leptin induces cyclooxygenase-2 via an interaction with interleukin-1beta in the rat brain. *Eur J Neurosci* 2006; **24**: 2233–2245.
21 Rummel C, Inoue W, Sachot C, Poole S, Hubschle T, Luheshi GN. Selective contribution of interleukin-6 and leptin to brain inflammatory signals induced by systemic LPS injection in mice. *J Comp Neurol* 2008; **511**: 373–395.
22 Bjorbaek C, Elmquist JK, Michl P, Ahima RS, van Bueren A, McCall AL *et al*. Expression of leptin receptor isoforms in rat brain microvessels. *Endocrinology* 1998; **139**: 3485–3491.
23 Mutze I, Roth J, Gerstberger R, Matsumura K, Hubschle T. Immunohistochemical evidence of functional leptin receptor expression in neuronal and endothelial cells of the rat brain. *Neurosci Lett* 2006; **394**: 105–110.
24 Mercer JG, Hoggard N, Williams LM, Lawrence CB, Hannah LT, Trayhurn P. Localization of leptin receptor mRNA and the long form splice variant (Ob-Rb) in mouse hypothalamus and adjacent brain regions by *in situ* hybridization. *FEBS Lett* 1996; **387**: 113–116.
25 Van Dam A-M, Brouns M, Louisse S, Berkenbosch F. Appearance of interleukin-1 in macrophages and in ramified microglia in the brain of endotoxin-treated rats: a pathway for the induction of non-specific symptoms of sickness? *Brain Res* 1992; **588**: 291–296.
26 Quan N, Whiteside M, Herkenham M. Time course and localization patterns of interleukin-1beta messenger RNA expression in brain and pituitary after peripheral administration of lipopolysaccharide. *Neuroscience* 1998; **83**: 281–293.
27 Ferrari CC, Depino AM, Prada F, Muraro N, Campbell S, Podhajcer O *et al*. Reversible demyelination, blood-brain barrier breakdown, and pronounced neutrophil recruitment induced by chronic IL-1 expression in the brain. *Am J Pathol* 2004; **165**: 1827–1837.
28 Shaftel SS, Carlson TJ, Olschowka JA, Kyrkanides S, Matousek SB, O'Banion MK. Chronic interleukin-1beta expression in mouse brain leads to leukocyte infiltration and neutrophil-independent blood brain barrier permeability without overt neurodegeneration. *J Neurosci* 2007; **27**: 9301–9309.
29 Cunningham C, Wilcockson DC, Campion S, Lunnon K, Perry VH. Central and systemic endotoxin challenges exacerbate the local inflammatory response and increase neuronal death during chronic neurodegeneration. *J Neurosci* 2005; **25**: 9275–9284.
30 Semmler A, Hermann S, Mormann F, Weberpals M, Paxian SA, Okulla T *et al*. Sepsis causes neuroinflammation and concomitant decrease of cerebral metabolism. *J Neuroinflammation* 2008; **5**: 38.
31 Bluher S, Mantzoros CS. The role of leptin in regulating neuroendocrine function in humans. *J Nutr* 2004; **134**: 2469S–2474S.
32 Jimenez I, Sobrino T, Rodriguez-Yanez M, Pouso M, Cristobo I, Sabucedo M *et al*. High serum levels of leptin are associated with post-stroke depression. *Psychol Med* 2009; **39**: 1201–1209.
33 Terao S, Yilmaz G, Stokes KY, Ishikawa M, Kawase T, Granger DN. Inflammatory and injury responses to ischemic stroke in obese mice. *Stroke* 2008; **39**: 943–950.
34 Bohatschek M, Werner A, Raivich G. Systemic LPS injection leads to granulocyte influx into normal and injured brain: effects of ICAM-1 deficiency. *Exp Neurol* 2001; **172**: 137–152.
35 Lawson LJ, Perry VH. The unique characteristics of inflammatory responses in mouse brain are acquired during postnatal development. *Eur J Neurosci* 1995; **7**: 1584–1595.
36 Anthony DC, Bolton SJ, Fearn S, Perry VH. Age-related effects of interleukin-1 beta on polymorphonuclear neutrophil-dependent increases in blood-brain barrier permeability in rats. *Brain* 1997; **120**: 435–444.
37 Paxinos G, Franklin KBJ. *The Mouse Brain in Stereotaxic Coordinates*, 2nd edn. Academic Press: New York, 2001.
38 Lacroix S, Feinstein D, Rivest S. The bacterial endotoxin lipopolysaccharide has the ability to target the brain in upregulating its membrane CD14 receptor within specific cellular populations. *Brain Pathol* 1998; **8**: 625–640.
39 Crocker SJ, Whitmire JK, Frausto RF, Chertboonmuang P, Soloway PD, Whitton JL *et al*. Persistent macrophage/microglial activation and myelin disruption after experimental autoimmune encephalomyelitis in tissue inhibitor of metalloproteinase-1-deficient mice. *Am J Pathol* 2006; **169**: 2104–2116.
40 Faggioni R, Fantuzzi G, Gabay C, Moser A, Dinarello CA, Feingold KR *et al*. Leptin deficiency enhances sensitivity to endotoxin-induced lethality. *Am J Physiol* 1999; **276**(1 Part 2): R136–R142.
41 Steiner AA, Dogan MD, Ivanov AI, Patel S, Rudaya AY, Jennings DH *et al*. A new function of the leptin receptor: mediation of the recovery from lipopolysaccharide-induced hypothermia. *FASEB J* 2004; **18**: 1949–1951.
42 Montecucco F, Bianchi G, Gnerre P, Bertolotto M, Dallegri F, Ottonello L. Induction of neutrophil chemotaxis by leptin: crucial role for p38 and Src kinases. *Ann N Y Acad Sci* 2006; **1069**: 463–471.
43 Bruno A, Conus S, Schmid I, Simon HU. Apoptotic pathways are inhibited by leptin receptor activation in neutrophils. *J Immunol* 2005; **174**: 8090–8096.
44 Allan SM, Tyrrell PJ, Rothwell NJ. Interleukin-1 and neuronal injury. *Nat Rev Immunol* 2005; **5**: 629–640.
45 Anthony D, Dempster R, Fearn S, Clements J, Wells G, Perry VH *et al*. CXC chemokines generate age-related increases in neutrophil-mediated brain inflammation and blood-brain barrier breakdown. *Curr Biol* 1998; **8**: 923–926.
46 Proescholdt MG, Chakravarty S, Foster JA, Foti SB, Briley EM, Herkenham M. Intracerebroventricular but not intravenous interleukin-1beta induces widespread vascular-mediated leukocyte infiltration and immune signal mRNA expression followed by brain-wide glial activation. *Neuroscience* 2002; **112**: 731–749.
47 Ching S, He L, Lai W, Quan N. IL-1 type I receptor plays a key role in mediating the recruitment of leukocytes into the central nervous system. *Brain Behav Immun* 2005; **19**: 127–137.
48 Garcia JH, Liu KF, Relton JK. Interleukin-1 receptor antagonist decreases the number of necrotic neurons in rats with middle cerebral artery occlusion. *Am J Pathol* 1995; **147**: 1477–1486.
49 Eriksson C, Nobel S, Winblad B, Schultzberg M. Expression of interleukin 1 alpha and beta, and interleukin 1 receptor antagonist mRNA in the rat central nervous system after peripheral administration of lipopolysaccharides. *Cytokine* 2000; **12**: 423–431.
50 Garabedian BV, Lemaigre-Dubreuil Y, Mariani J. Central origin of IL-1beta produced during peripheral inflammation: role of meninges. *Brain Res Mol Brain Res* 2000; **75**: 259–263.
51 Konsman JP, Vigues S, Mackerlova L, Bristow A, Blomqvist A. Rat brain vascular distribution of interleukin-1 type-1 receptor immunoreactivity: relationship to patterns of inducible cyclooxygenase expression by peripheral inflammatory stimuli. *J Comp Neurol* 2004; **472**: 113–129.
52 Ericsson A, Liu C, Hart RP, Sawchenko PE. Type 1 interleukin-1 receptor in the rat brain: distribution, regulation, and relationship to sites of IL-1-induced cellular activation. *J Comp Neurol* 1995; **361**: 681–698.
53 McColl BW, Rothwell NJ, Allan SM. Systemic inflammatory stimulus potentiates the acute phase and CXC chemokine

responses to experimental stroke and exacerbates brain damage via interleukin-1- and neutrophil-dependent mechanisms. *J Neurosci* 2007; **27**: 4403–4412.
54 Spencer SJ, Mouihate A, Pittman QJ. Peripheral inflammation exacerbates damage after global ischemia independently of temperature and acute brain inflammation. *Stroke* 2007; **38**: 1570–1577.
55 Kielian T, Barry B, Hickey WF. CXC chemokine receptor-2 ligands are required for neutrophil-mediated host defense in experimental brain abscesses. *J Immunol* 2001; **166**: 4634–4643.
56 Fenton JI, Hursting SD, Perkins SN, Hord NG. Leptin induces an Apc genotype-associated colon epithelial cell chemokine production pattern associated with macrophage chemotaxis and activation. *Carcinogenesis* 2007; **28**: 455–464.
57 Mancuso P, Huffnagle GB, Olszewski MA, Phipps J, Peters-Golden M. Leptin corrects host defense defects after acute starvation in murine pneumococcal pneumonia. *Am J Respir Crit Care Med* 2006; **173**: 212–218.
58 Faggioni R, Moser A, Feingold KR, Grunfeld C. Reduced leptin levels in starvation increase susceptibility to endotoxic shock. *Am J Pathol* 2000; **156**: 1781–1787.
59 Gautron L, Mingam R, Meranis A, Combe C, Laye S. Influence of feeding status on neuronal activity in the hypothalamus during lipopolysaccharide-induced anorexia in rats. *Neuroscience* 2005; **134**: 933–946.
60 Spencer SJ, Mouihate A, Galic MA, Ellis SL, Pittman QJ. Neonatal immune challenge does not affect body weight regulation in rats. *Am J Physiol Regul Integr Comp Physiol* 2007; **293**: 581–589.
61 Rosenthal M, Roth J, Storr B, Zeisberger E. Fever response in lean (Fa/–) and obese (fa/fa) Zucker rats and its lack to repeated injections of LPS. *Physiol Behav* 1996; **59**: 787–793.
62 Steiner AA, Dogan MD, Ivanov AI, Patel S, Rudaya AY, Jennings DH *et al*. A new function of the leptin receptor: mediation of the recovery from lipopolysaccharide-induced hypothermia. *FASEB J* 2004; **18**: 1949–1951.
63 Kozak W, Kluger MJ, Soszynski D, Conn CA, Rudolph K, Leon LR *et al*. IL-6 and IL-1 beta in fever. Studies using cytokine-deficient (knockout) mice. *Ann N Y Acad Sci* 1998; **856**: 33–47.
64 Weiland TJ, Voudouris NJ, Kent S. CCK(2) receptor nullification attenuates lipopolysaccharide-induced sickness behavior. *Am J Physiol Regul Integr Comp Physiol* 2007; **292**: R112–R123.
65 Kiyatkin EA, Sharma HS. Permeability of the blood-brain barrier depends on brain temperature. *Neuroscience* 2009; **161**: 926–939.
66 Perry VH, Cunningham C, Holmes C. Systemic infections and inflammation affect chronic neurodegeneration. *Nat Rev Immunol* 2007; **7**: 161–167.
67 D'Mello C, Le T, Swain MG. Cerebral microglia recruit monocytes into the brain in response to tumor necrosis factoralpha signaling during peripheral organ inflammation. *J Neurosci* 2009; **29**: 2089–2102.

Supplementary Information accompanies the paper on the Molecular Psychiatry website (http://www.nature.com/mp)

Supplementary information

Determination of the LPS dose, the time point and important brain areas for investigating neutrophil recruitment during LPS-induced systemic inflammation.

To determine the appropriate dose of LPS, time points and potential brain areas of neutrophil recruitment during LPS-induced systemic inflammation, we first analyzed the brains of WT mice collected 3, 24 or 48 h after an i.p. injection of LPS at two different doses (50 µg/kg and 2.5 mg/kg). Every third serial coronal section (20 µm) from bregma 0.5 to -2.3 and -7.2 to -7.92 mm was processed for immunohistochemical detection of neutrophils. Sections prepared from saline-treated mice showed no, or very little 7/4-IR positive cells throughout the brain (Fig. S1). Following the higher dose of LPS (2.5 mg/kg), a few neutrophils were detected by 3 h along the leptomeningis and vasculature-like structures. By 24 h, a robust neutrophil recruitment was observed, which was mostly associated with the leptomeningis, cerebral fissures, ventricle walls and vasculature-like structures (Fig. S1A and B) and dispersed from the boundary of the brain to the parenchyma by 48 h (Fig. S1A and B). In response to the lower dose of LPS (50 µg/kg), only a few neutrophils were observed in the brain by 24 h after injection (Fig. S1A), or any other time points studied (3 and 48 h, data not shown), confirming a previous finding that the recruitment of neutrophils requires a relatively high systemic dose of LPS [34].

Supplementary figures and legends

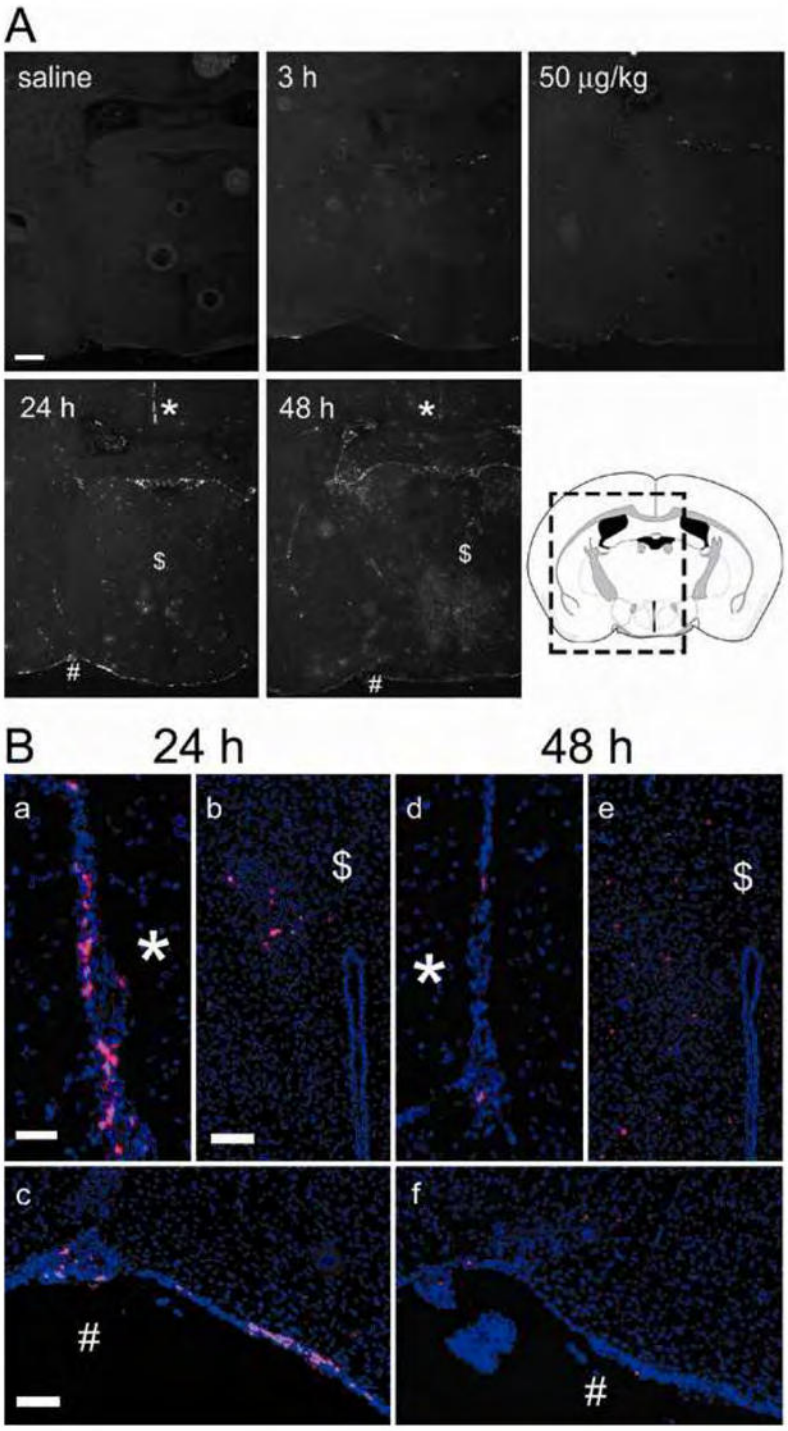

A
saline
3 h
50 µg/kg
24 h
48 h
B
24 h
48 h
a
b
d
e
c
f

Fig. S1. **Neutrophil recruitment to the brain during LPS-induced systemic inflammation.** *(A)* Immunohistochemical detection of granulocyte neutrophils (7/4 antigen) in coronal brain sections of mice treated with saline or LPS. Images show brain sections taken 3, 24 and 48 h after the higher dose of LPS (2.5 mg/kg) injection, and 24 h after saline or the lower dose of LPS (50 µg/kg). The higher LPS dose induced a robust recruitment of neutrophils by 24 h, which was sustained for 48 h. The lower dose of LPS resulted in minimal recruitment of neutrophils 24 h after injection. Scale bar, 400 µm. *(B)* Magnified images of the areas shown in *A* indicated with * (*a* and *d*), $ (*b* and *e*) and # (*c* and *f*) at 24 (*a-c*) and (*d-f*) 48 h after the high dose of LPS injection. Note that, neutrophils accumulated in the interhemispheric fissure (*a* and *d*), vasculature-like structures in the PVN (*b* and *e*) and the leptomeningis (*c* and *f*) at 24 h, and they dissipated by 48 h. Scale bars 50, 100 and 100 µm in *a*, *b* and *c*, respectively.

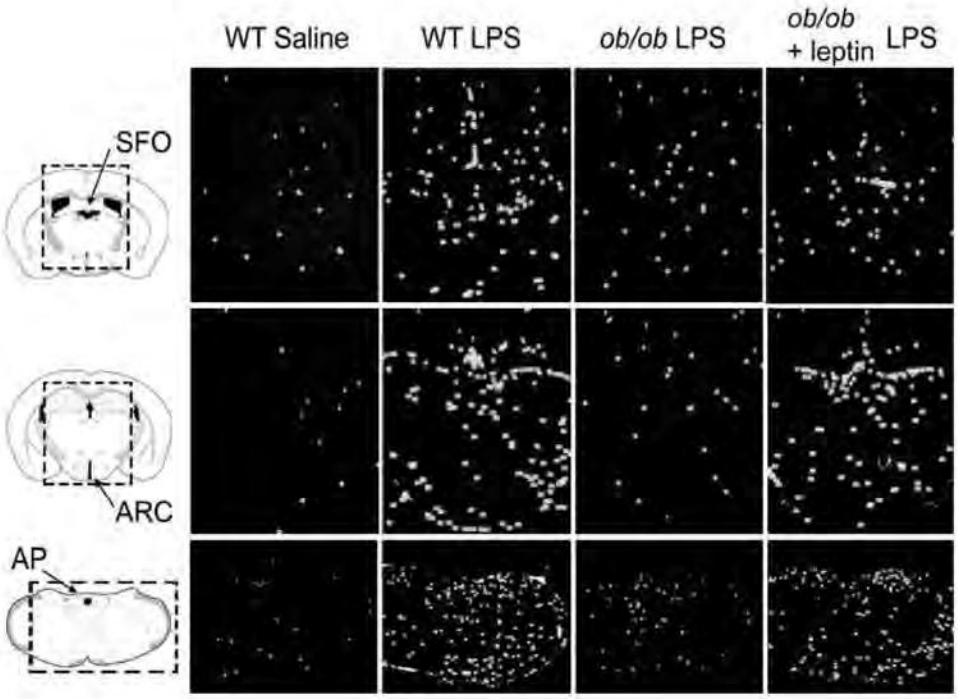


Fig. S2. **LPS-induced neutrophil recruitment to the brain of WT, *ob/ob* and leptin-treated *ob/ob* mice.** Neutrophil numbers were quantified in coronal sections of the brain at the level of the subfornical organ (SFO), the arcuate nucleus (ARC) and the area postrema (AP). For clarity, the actual neutrophil-IR was superimposed with white squares that were used for automatic quantification of cell numbers.

Table S3. **Cytokine plasma levels 24h after saline or LPS-stimulation.**

Table 1

A

	Saline			LPS			LPS	
	WT (3-5)	*ob/ob* (3-5)	*db/db* (3-5)	WT (5)	*ob/ob* (5)	*db/db* (5)	*ob/ob* + vehicle (5)	*ob/ob* + leptin (5)
TNF (pg/ml)	< DL (10.2)	< DL (10.2)	< DL (10.2)	32.3 ± 20.4 [a]	133.7 ± 9.9 [a,b]	99.6 ± 15.1 [a,b]	70.2 ± 11.2	61.3 ± 39.5
IL-1 (pg/ml)	< DL (6.0)	< DL (6.0)	< DL (6.0)	9.5 ± 1.6	10.2 ± 2.7	10.8 ± 1.4	20.6 ± 7.9	9.6 ± 2.9
IL-6 (pg/ml)	< DL (6.0)	< DL (6.0)	< DL (6.0)	41.0 ± 6.8 [a]	> DL (1000) [a,b]	> DL (1000) [a,b]	972.1 ± 27.9 [d]	314.3 ± 172.9 [c]
Leptin (ng/ml)	0.9 ± 0.1	< DL (0.2) [a]	27.4 ± 2.1 [a]	1.5 ± 0.8	< DL (0.2) [b]	80.5 ± 9.3 [a, b]	< DL (0.2)	12.5 ± 1.6

[a] Significantly different from saline-treated counterparts

[b] Significantly different from WT counterparts

[c] Significantly different from vehicle-treated counterparts

[d] 4 out of 5 samples were above the higher assay limit 1000 pg/ml

DL, detection limit of the assay

B

	Fed	Fasted	
	vehicle (4-5)	vehicle (4-5)	in (4-5)
TNF (pg/ml)	16.2 ± 1	< DL (10.2)	5 ± 6.7
IL-1 (pg/ml)	9.2 ± 1.6	< DL (6.0)	2 ± 2.5
IL-6 (pg/ml)	66 ± 6.3	95 ± 16.2	3 ± 53.4
Leptin (ng/ml)	2.1 ± 0.6	< DL (0.2)	) ± 2.1[a]

[a] Significantly different from vehicle-treated counterparts

DL, detection limit of the assay

C

	Saline		LPS	
	PIS (3	LAS (3-5)	PIS (4	LAS (4-5)
TNF (pg/ml)	< DL (	< DL (10.2)	19.9 ±	17.6 ± 2.8 [a]
IL-1 (pg/ml)	< DL (	< DL (6.0)	10.7 ±	10 ± 2.9
IL-6 (pg/ml)	< DL (	< DL (6.0)	76.4 ± 1	53.8 ± 12.6 [a]
Leptin (ng/ml)	1.2 ±	< DL (0.2) [b]	1.5 ±	< DL (0.2) [b]

[a] Significantly different from saline-treated counterparts

[b] Significantly different from PIS-treated counterparts

DL, detection limit of the assay

1.8. „Molecular aspects of fever and hyperthermia“

Roth J., **Rummel C**., Barth SW., Gerstberger R., Hübschle T.
Immunol Allergy Clin (2009) 29: 229-245.

Impakt Faktor: 2,959

Eigener Anteil an der Publikation:

- Durchführung der Versuche: unterstützend (20 %)
- Auswertung der Experimente: unterstützend (20 %)
- Erstellung der Publikation: unterstützend (20 %)

Molecular Aspects of Fever and Hyperthermia

Joachim Roth, PhD[a,*], Christoph Rummel, PhD, DVM[a], Stephan W. Barth, DVM[b], Rüdiger Gerstberger, PhD[a], Thomas Hübschle, PhD[a]

KEYWORDS

- Innate immunity • Pyrogens • Cytokines
- Immune-to-brain communication • Cyclooxygenase
- Prostaglandins

When heat production or heat gain exceeds heat dissipation or heat loss, the body core temperature rises above its range specified for the normal active state of the species.[1,2] Such a thermal imbalance leads to a state of hyperthermia. This imbalance can occur for several reasons: an increase in metabolic heat production, an impairment of heat-dissipating effector mechanisms, a decrease in heat-absorbing mechanisms by the environment under hot external conditions, or a response to a drug. Usually, an overwhelming of the mechanisms for temperature control causes the resulting hyperthermia.

Fever is a state that also is characterized by an elevation of body temperature, but there is no overwhelming of thermoregulatory control mechanisms. In contrast, the thermoregulatory control system is adjusted to increase body temperature to match a higher set point (ie, the higher body temperature actively is established and defended by the operation of heat-producing and heat-conserving thermoeffectors).[1]

Persons who are hyperthermic have increased skin blood flow to improve convective heat loss and sweat to dissipate heat by evaporation of water. In contrast, at least during the rising phase of fever, skin blood flow is reduced and persons who are febrile do not sweat but rather shiver to increase metabolic heat production. These thermoregulatory effector mechanisms are supported by appropriate behavior. Although a hyperthermic organism seeks a cool environment, the state of fever is characterized

---

This article is a version of an article previously published in *Neurologic Clinics*: Roth J, Rummel C, Barth SW, Gerstberger R, Hübschle T. Molecular aspects of fever and hyperthermia. Neurol Clin 2006;24(3):421–39.

[a] Department of Veterinary Physiology, Faculty of Veterinary Medicine, Justus-Liebig-University Giessen, Frankfurter Strasse 100, D-35392 Giessen, Germany

[b] Department of Nutritional Physiology and Biochemistry, Federal Research Institute of Nutrition and Food, Haid-und-Neu Strasse 9, D-76131 Karlsruhe, Germany

* Corresponding author.

E-mail address: joachim.roth@vetmed.uni-giessen.de (J. Roth).

Immunol Allergy Clin N Am 29 (2009) 229–245
doi:10.1016/j.iac.2009.02.005 immunology.theclinics.com
0889-8561/09/$ – see front matter © 2009 Elsevier Inc. All rights reserved.

by huddling or by the search for warm environmental conditions.[3,4] The strategy to establish fever seems to depend on ambient temperature. In the cold, increased heat production is activated to achieve the febrile state, whereas in warm environments, a suppression of heat-loss mechanisms is typical.[5]

In summary, the rise in core temperature during fever usually is a result of change in the thermocontroller characteristics leading to an elevation of the set point of body temperature. Time course and extent of natural fevers vary, but an upper limit (41°C in humans) rarely is exceeded. At this upper limit, core temperature is maintained for some time and reduced when the set point of body temperature returns to its normal level. Although any rise in body temperature may result from fever, those rises that are not accompanied by supportive changes in thermoeffector activities are termed *hyperthermia*.[1]

FEVER AS A PART OF THE ACUTE-PHASE RESPONSE TO INFECTION OR SYSTEMIC INFLAMMATION

A strong association between fever and infection has been recognized for a long time, which is why fever is frequently called a hallmark of infection.[6] The manifestation of fever, however, is not restricted to infectious diseases of bacterial, viral, protozoal, fungal, or other origin. Fever also is observed in response to injury, such as injuries associated with surgery, trauma, chemicals, or thermal insults. In addition, fever frequently accompanies some endogenous mechanisms. Such mechanisms include autoimmune responses (eg, rheumatoid arthritis) and tumors. The question arises, therefore: What do all these situation that elicit fever have in common?

Inflammation is the general term for changes that may occur in vascularized tissues as part of the response to tissue damage, infection, or immunologic reactions. The aforementioned stimuli that can cause fever are identical to those capable of eliciting inflammatory responses (ie, infection, injury, and endogenous mechanisms). The functions of the inflammatory response include destruction or inactivation of the initiating irritant or agent and then the clearance of the area of debris so that healing can occur. Various cell types activated in the damaged or infected tissue release many soluble mediators, including growth factors, cytokines, chemokines, eicosanoids, kinis, biogenic amines, and neuropepdides. At the site of inflammation, these mediators exert vascular effects (vasodilation, vascular stasis, and increased capillary permeability), promote leukocyte migration from the circulation into the inflamed tissue, and coordinate the still-localized array of defense responses. Some of these mediators have the capacity to stimulate local sensory nerves (discussed later). In cases where the inflammatory response exceeds a certain strength, significant amounts of endogenous mediators and, in case of infection, microbes or microbial products enter the systemic circulation and are disseminated by blood flow to different organs. This results in a complex array of systemic reactions, collectively termed *the acute-phase response*, which is defined as the multifactorial stereotyped response of an organism to infection, injury, or trauma. The acute-phase response comprises changes in plasma concentrations of trace metals, liver proteins (acute-phase proteins), hormones, intermediary metabolism, neutrophilia, and a characteristic set of brain-controlled signs of illness, collectively termed *sickness behavior*.[1,7] Sickness behavior includes development of fever, loss of appetite, increased slow-wave sleep, decreased motor activity, reduced libido, and decreased allertness.[8]

The acute-phase response is considered an early, nonspecific host defense response and is triggered by the release of cytokines, such as interleukin (IL)-1, IL-6, tumor necrosis factor (TNF)-α, and interferons. These cytokines and other inflammatory

mediators, which may appear in the blood during infection, injury, or endogenous pathophysiologic reactions (discussed previously), are therefore implicated in fever. They are frequently called *endogenous pyrogens*.[3,6,9–12]

EXPERIMENTAL FEVER

Depending on the disease that causes clinical fever, febrile patterns are categorized into diagnostically valuable groups. A published report from a symposium summarizes clinical fever patterns:[13] sustained fevers of several days with only slight remissions (pneumonia, typhoid fever, or malaria), intermittent fevers with large fluctuations (sepsis), biphasic fevers with two phases lasting several days (many viral infections), weekly periods of fever with equally long afebrile periods and with repetition of this cycle (Hodgkin disease), and several other fever patterns.[13]

Current knowledge of molecular mechanisms of fever derives almost exclusively from experimental fever research performed in animals or, in rare cases, human volunteers. Experimental fever is induced by injection of an exogenous pyrogen, a fever-inducing microbial component or product. Bolus injections of a given exogenous pyrogen usually result in a generalized inflammatory response. In the majority of experimental fever studies, lipopolysaccharide (LPS) from gram-negative bacteria is used to induce a febrile response. Depending on dosage, ambient temperature, and route of administration, LPS, also known as bacterial endotoxin, evokes a stereotypic and reproducible fever that consists of several phases and lasts 6 to 8 hours.[14–17] **Fig. 1** shows the typical thermal responses of rats to intraperitoneal injections of a moderate or a high LPS dose compared with sterile saline at an ambient temperature of 24°C.

In rats, the injection procedure causes a transient stress-induced increase of abdominal temperature, which is measured continuously by means of an intra-abdominally implanted telemetry transmitter. In rats treated with 100 μg/kg LPS, this rise of body temperature is followed by a fever, which is absent in control animals

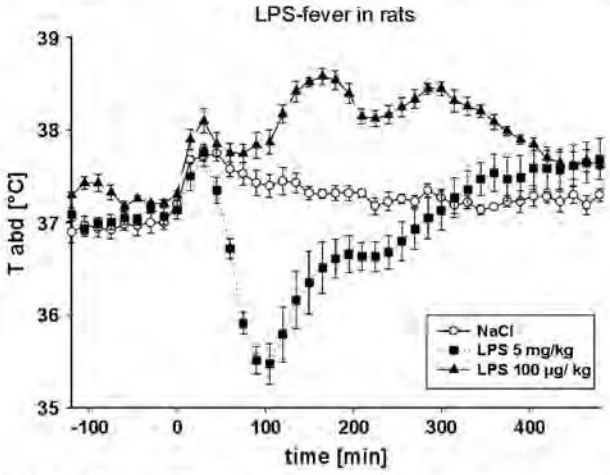


Fig. 1. Changes of abdominal temperature (T abd) in three groups of rats injected intraperitoneally with either sterile saline (NaCl), a moderate dose of 100 μg/kg LPS, or a high dose of 5 mg/kg LPS. Body temperature was recorded continuously by means of an intra-abdominally implanted temperature-sensitive transmitter (remote radiotelemetry) at an ambient temperature of 24°C. The moderate dose of LPS induced a biphasic fever, whereas the high LPS dose caused a septic shock–like state associated with severe hypothermia.

injected with sterile saline. Administration of 5 mg/kg LPS causes a septic shock–like state, characterized by the development of hypothermia rather than fever.

Because most knowledge of molecular aspects of fever is based on studies in which LPS is used as exogenous pyrogen, the majority of the findings presented in this article derive from the experimental model of LPS fever. However, many other products from various microorganisms (gram-positive bacteria, mycoplasmas, viruses, fungi, and parasites) are capable of inducing a pronounced febrile response. The question of whether or not there are common, or rather distinct, molecular mechanisms for the generation of experimental fever in response to all of these exogenous pyrogens is under investigation.[18,19] In addition to microbial products, experimental fever also can be induced by some nonmicrobial agents (different antigens, inflammatory agents, plant lectins, and alcaloids), synthetic products (polynucleotides, antitumor agents, and immunoadjuvants), or even some host-derived substances (destroyed tissue, antigen-antibody complexes, activated complement fragments, certain metabolites, and lymphocyte products). Because most of these fever-inducing pathogenic stimuli are derived from the body's external environment, they generally are termed *exogenous pyrogens*.[11,20]

EXOGENOUS PYROGENS CAUSE THE PRODUCTION OF ENDOGENOUS PYROGENS

The historical discovery of the "endogenous pyrogen" in 1948 led to the hypothesis that exogenous pyrogens do not directly cause fever.[21] This "endogenous pyrogen," obtained from isolated peritoneal macrophages, induced fever in noninfected rabbits. The substance was heat labile and was suggested, therefore, to be a protein. Later studies demonstrated that, after injection of an exogenous pyrogen, such as LPS, endogenous pyrogen appeared in the circulation of the LPS-stimulated animals.[20]

Intensive research has focused on the molecular identification and cloning of putative endogenous pyrogens. These molecules are members of the growing family of cytokines. The term *cytokine* is used as a generic name for a diverse group of soluble proteins acting as humoral regulators that modulate the functional activities of individual cells and tissues. In the context of this article, cytokines of particular interest are those associated with the inflammatory response. With regard to experimentally induced LPS fever (see **Fig. 1**), four sets of observations support a role for inflammatory cytokines in the manifestation of the observed febrile response.

The first set of observations relates to the appearance of several cytokines in the systemic circulation more or less in parallel to the development of fever. In response to injections of LPS, TNF-α is the first cytokine that appears in the bloodstream,[22–24] followed by traces of IL-1[24] and high amounts of IL-6.[23,25,26] From these three cytokines, considered the most important endogenous mediators of LPS fever, only IL-6 can be measured in significant quantities in the blood during the time course of fever, and circulating levels of IL-6 show the best correlation with the febrile changes of body temperature.[23,25,27]

The second body of evidence relates to the repeated observations that systemic injections or infusions of single proinflammatory cytokines can induce fever, as shown for IL-1,[28,29] TNF-α,[30,31] and IL-6.[32,33] In this context, the pyrogenic effects of peripherally administered IL-6 are moderate compared with those of IL-1 or TNF-α. It is a matter of debate whether or not the pyrogenic effects of systemic injections of these cytokines reflect the physiologic conditions induced by administration of LPS.[3]

The third set of observations derives from experimental procedures in which single LPS-induced cytokines were neutralized or antagonized in their biologic activity and a concomitant reduction of LPS fever was observed. Thus, treatments with IL-1

receptor antagonist,[12,26] a TNF-α–neutralizing synthetic form of the P55-soluble TNF-α receptor,[12,34] or IL-6–neutralizing IL-6 antibodies[35] resulted in a significant attenuation of the febrile response to LPS, indicating a role for these cytokines in the manifestation of LPS fever. However, such anticytokine strategies predominantly inhibited the late phases of LPS fever, and there seemed to be some species-specific differences in the role of TNF-α in the LPS-induced febrile response.[3,12,22,34]

Finally, the fourth set of observations derives from studies in cytokine-deficient knockout mice.[36] In IL-1 knockout mice, LPS fever is reduced although not abolished.[37,38] The investigators in these studies conclude that IL-1 contributes to, but is not essential for, the manifestation of a febrile response to LPS. Alternatively, fever in response to a moderate fever–inducing LPS dose is abolished in IL-6 knockout mice,[38,39] suggesting that IL-6 gene expression is essential for fever caused by a moderate LPS challenge.

Thus, a large body of evidence supports the view that the appearance of an exogenous pyrogen (LPS or others) in a host causes fever via the formation of endogenous pyrogens (cytokines). In recent years, our knowledge of how predominantly immune cells are stimulated by foreign molecules to produce a cascade of pyrogenic cytokines has improved substantially. The innate immune system, predominantly associated with neutrophils, monocytes, and macrophages, represents the first defense line against a variety of pathogens. The presence of a given pathogen within an infected host is recognized by endogenous receptors for so-called "pathogen-associated molecular patterns" (PAMPs). Members of the Toll-like receptor (TLR) family are identified as key receptors for the recognition of PAMPs. TLR signal transduction mechanisms in myeloid and possibly other cells finally leads to the production of inflammatory cytokines in the infected host.[19,40,41] LPS from gram-negative bacteria, the best-studied activator of the innate immune system, acts via the TLR4 receptor.[42] Meanwhile, several distinct microbe-associated PAMPs and several specific TLR subtypes recognizing those PAMPs are identified.[40,41] It seems that the activation of various TLRs finally results in similar circulating cascades of proinflammatory cytokines and, thereby, the manifestation of a febrile response.[18,19,34]

HOW DO CIRCULATING CYTOKINES CONVEY A PYROGENIC MESSAGE TO THE BRAIN?

The febrile shift of the thermoregulatory set point to a higher body temperature occurs within the preoptic-anterior hypothalamic area, the most important control center of thermoregulation. Accepting that circulating cytokines are important humoral mediators of fever, the question arises of how these large hydrophilic peptides with a molecular weight of 15 to 25 kd pass the relatively impermeable blood-brain barrier to stimulate the relevant hypothalamic thermoregulatory structures. Three mechanisms for immune-to-brain signaling by circulating pyrogenic cytokines are proposed. Cytokines transported by the bloodstream could act at sites lacking a tight blood-brain barrier, the so-called "circumventricular organs" (CVOs).[43] Alternatively, circulating cytokines could interact with their specific receptors on brain endothelial cells[44] or perivascular cells.[45] Finally, it is proposed that fever-promoting cytokines can pass the blood-brain barrier by active and saturable transport systems specific for individual cytokines.[46] An assumed manifestation of a febrile response by these mechanisms collectively is termed *humoral hypothesis of fever induction*. The article by Banks and colleagues elsewhere in this issue discusses the mechanisms of how endogenous pyrogens are transported from the blood to the brain. Here, a brief look is directed to both of the other humoral fever induction pathways.

INTERACTIONS OF ENDOGENOUS OR EXOGENOUS PYROGENS WITH SENSORY CIRCUMVENTRICULAR ORGANS

CVOs are brain structures that have cells in contact with the cerebroventricular system, have a dense vascularization, and lack a blood-brain barrier. A subgroup of the CVOs is called *sensory CVOs* and includes the vascular organ of the laminae terminalis (OVLT), the subfornical organ, and the area postrema. These brain structures have capillaries with fenestrated endothelia surrounded by perivascular spaces. The parenchyma of these structures is composed of not only glial cells, but also of neuronal soma, dendritic/axonal processes, and terminals that reveal multiple reciprocal connectivities to other hypothalamic and extra-hypothalamic nuclei. Because of the lack of a blood-brain barrier, the cells within the sensory CVOs are exposed directly to circulating signal molecules. The cells may be able to sense the signal molecules via specific receptors.[43] The OVLT and the subfornical organ are located within the anterior wall of the third ventricle, the lamina terminalis. The area postrema is a component of the dorsal vagal motor complex, a major viscerosensory and autonomic center of the medulla oblongata. The locations of the sensory (and other) CVOs are illustrated in **Fig. 2**.

Research suggests that, because of their properties as target structures for circulating inflammatory molecules, each of the three sensory CVOs participates in the manifestation of brain-controlled sickness responses. With regard to fever, the OVLT has special importance because of its location close to the preoptic area. This part of the anterior-preoptic hypothalamic structures, where fever is induced, is activated strongly after intravenous injection of LPS, as demonstrated by a high level of Fos immunoreactivity, which is a neuroanatomic marker for physiologically activated neurons (**Fig. 3**).[47] Because of its high sensitivity to pyrogenic stimulation, this part of the preoptic area is suggested as representing a pyrogenic zone of the brain.[48]

Lesion studies provided the first evidence for a role of the OVLT in the manifestation of fever. Large lesions of the lamina terminalis that completely included the OVLT prevented fever after systemic injections of bacterial LPS.[49,50] At the cellular and molecular levels, three prerequisites must be met for the OVLT to act as a sensor of circulating pyrogenic cytokines: (1) Cellular elements within the OVLT must possess

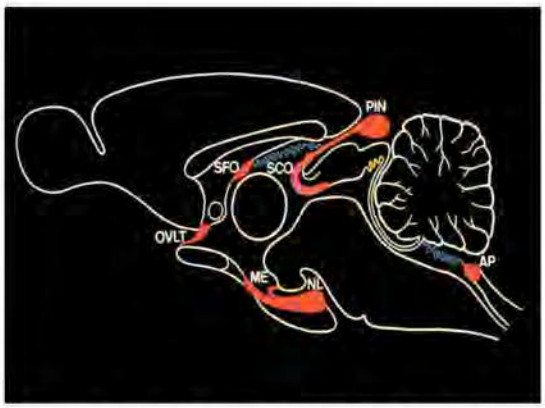


Fig. 2. A midsagittal section through the rat brain. Red indicates areas that lack a tight blood-brain barrier. Blue and yellow indicate parts of the choroid plexus. AP, area postrema; ME, median eminence; NL, neural lobe of the pituitary; PIN, pineal organ; SCO, subcomissural organ; SFO, subfornical organ.

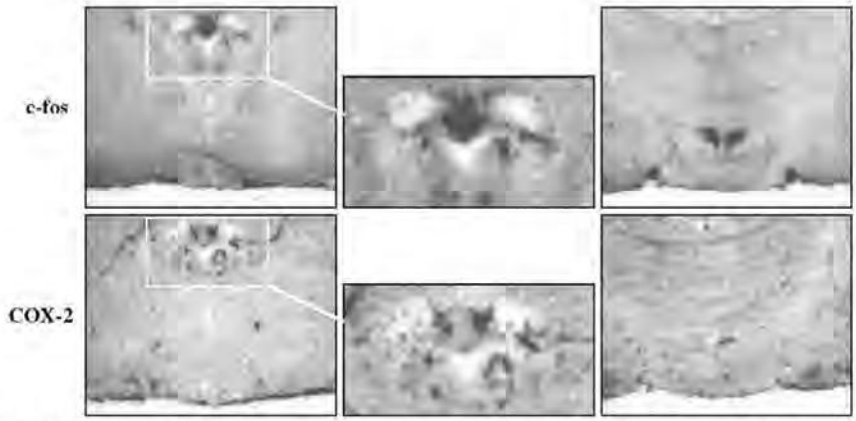


Fig. 3. Expression of the c-fos (*upper three panels*) and the COX-2 gene (*lower three panels*) in the rat brain after LPS treatment (2500 μg/kg) as determined by radioactive in situ hybridization. Strong hybridization signals specific for *c-fos* (*upper panels, left* and *middle*) and *COX-2* mRNA (*lower panels, left* and *middle*) are visible in form of black labeling in the subfornical organ, one of the sensory CVOs. Although *c-fos* signals accumulate in the core region of the subfornical organ, *COX-2*–specific signals are located in the lateral part of the subfornical organ and extend into vascular signals in the surrounding tissue. The paraventricular nucleus shows a strong *c-fos* up-regulation (*upper panels, right*), whereas only scarce vascular *COX-2* signals appear in this region (*lower panels, right*). *COX-2* signals are hardly detectable in control animals injected with sterile saline instead of LPS (not shown).

receptors for IL-1,[51] IL-6,[52] and TNF-α;[53] (2) neurons located in the OVLT must change their firing rate under the influence of pyrogenic cytokines[54] (such electrical activity changes affect adjacent thermosensitive neurons transsynaptically and thereby contribute to the generation of fever), and (3) a direct genomic activation of cellular elements within the OVLT must occur in response to circulating cytokines as revealed by the expression of the c-fos gene[43] or by the nuclear translocation of cytokine-specific transcription factors into the nuclei of cytokine-stimulated cells, such as the acute phase response factor, signal-transducer and activator of transcription 3 (STAT3).[17,33] Thus, much evidence indicates that the OVLT may act as a sensor for circulating endogenous pyrogens and, thus, might be able to transfer febrile signals to the preoptic-hypothalamic structures situated nearby.

In addition to receptors for pyrogenic cytokines, several TLRs are expressed within the sensory CVOs.[41] Consequently, circulating PAMPs (ie, LPS and others) can be sensed by these specialized brain structures even before a peripheral formation of proinflammatory cytokines. We recently reported microglial cells, located in sensory CVOs, directly respond to LPS stimulation with fast transient rises in intracellular calcium concentration and a localized formation of pyrogenic cytokines.[55] This direct and rapid response of brain sites with an incomplete blood-brain barrier, which are implicated in the manifestation of fever, to circulating PAMPs can be interpreted as an alternative possibility for transmission of febrile signals to the brain.

INTERACTIONS OF ENDOGENOUS PYROGENS WITH BRAIN ENDOTHELIAL CELLS AND PERIVASCULAR CELLS

Several lines of arguments support the view that not only sensory CVOs but also the entire brain endothelium is a major target for circulating cytokines implicated in fever.

One such argument points to clear evidence that brain endothelial cells constitutively express receptors for TNF-α[53] and IL-1.[56] Namely, the IL-1 receptor type 1 seems to be predominantly expressed in endothelial cells of brain venules but not in those of arterioles.[56] The accessory signal transduction molecule for the IL-6 receptor, glycoprotein 130, also is expressed constitutively in brain endothelial cells, whereas the expression of the IL-6 receptor itself is induced in these cells under inflammatory conditions.[52] An IL-6–activated signal transduction in the brain endothelium also can be achieved by circulating soluble IL-6 receptors in connection with their ligand (IL-6) and the glycoprotein 130 signal transducer located in the membranes of endothelial cells within the brain.

A genomic activation of the brain endothelium by IL-1[57] or IL-6[58] recently has been demonstrated. IL-1 and IL-6 induce a pronounced nuclear translocation of the transcription factors, nuclear factor κB (NF-κB) (activated by IL-1) or STAT3 (activated by IL-6), in endothelial cells all over the brain.[57,58] **Fig. 4** shows an example from the authors' experiments for IL-6–stimulated brain endothelial cells showing nuclear STAT3 activation.

At least the IL-1 receptor type 1 and its stimulation under inflammatory stimulation also is demonstrated in perivascular cells,[56] a subset of bone marrow–derived brain macrophages. The final response of such a genomic activation of brain endothelial and perivascular cells is the expression of enzymes, which are responsible for the formation of prostaglandin E2 (PGE2). PGE2 is regarded as a key mediator of fever. In this context, there seems to be a critical role for perivascular and endothelial cells in monitoring circulating cytokines. With regard to the capacity of both cell types to respond to such signals with the production of prostaglandins, perivascular cells seem to exhibit an even greater sensitivity to inflammatory stimuli.[45]

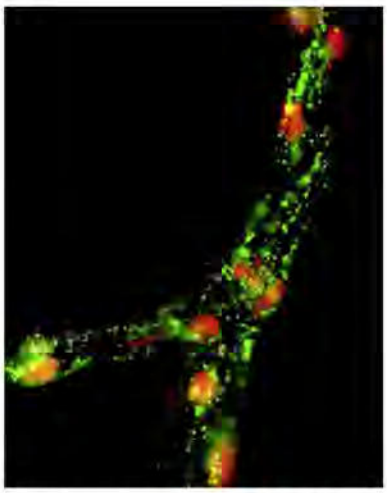


Fig. 4. Guinea pig brain endothelial cells respond to stimulation with bacterial LPS (30 μg/kg, intraperitoneal injection) with a nuclear translocation of the transcription factor STAT3 at 90 minutes after LPS injection. Immunoreactive nuclear STAT3 signals (*red*) are surrounded by immunohistochemically detected von Willebrand factor (*green*), a marker protein of endothelial cells. Nuclear STAT3 activation in brain endothelial cells is detected in LPS-stimulated animals but not in controls injected with sterile saline (not shown).

A CRUCIAL ROLE FOR PROSTAGLANDIN E2 WITHIN THE CENTRAL NERVOUS SYSTEM

Whether or not pyrogenic cytokines are interacting with cells in sensory CVOs or with brain endothelial/perivascular cells or whether or not they are transported into the brain, they have to cause production or release of the final mediators of fever within the preoptic-anterior hypothalamus. For the following reasons, PGE2 traditionally is regarded as the key fever mediator in the brain and as the biologic agent finally responsible for the febrile upward shift of the thermoregulatory set point: (1) Prostaglandins evoke fever when injected into cerebral ventricles,[59] even in very small amounts into the most PGE2-sensitive site within the preoptic-anterior hypothalamic area;[48] (2) the levels of PGE2 in the blood[60] and in the brain[61] rise parallel to the febrile changes of body temperature; and (3) drugs that block prostaglandin synthesis also effectively inhibit fever.[11,12,60] **Fig. 5** shows an example from the authors' experiments on the effects of inhibitors of PGE2 synthesis on LPS-induced fever in rats. Systemic treatments with a nonselective cyclooxygenase (COX) inhibitor (diclofenac) or with a preferential COX-2 inhibitor (meloxicam), which blocks formation of PGE2, result in significant and similar attenuations of LPS-induced fever in rats.

PGE2 is a derivative of arachidonic acid, which is cleaved from membrane phospholipids by phospholipase A2. In a second step, arachidonic acid is converted to prostaglandin H2 by COX enzymes. Finally, prostaglandin H2 is isomerized to PGE2 by prostaglandin E synthase (PGES).[44,62] Several isoenzymes exist for each of these catalytic steps. COX-2 and microsomal PGES-1 (mPGES-1) are inducible enzymes regulated transcriptionally by NF-κB, a transcription factor activated by LPS, IL-1, or TNF-α (ie, under inflammatory conditions).[63] During LPS fever, the expressions of COX-2 and mPGES-1 are up-regulated strongly by pyrogenic cytokines,[64] and the

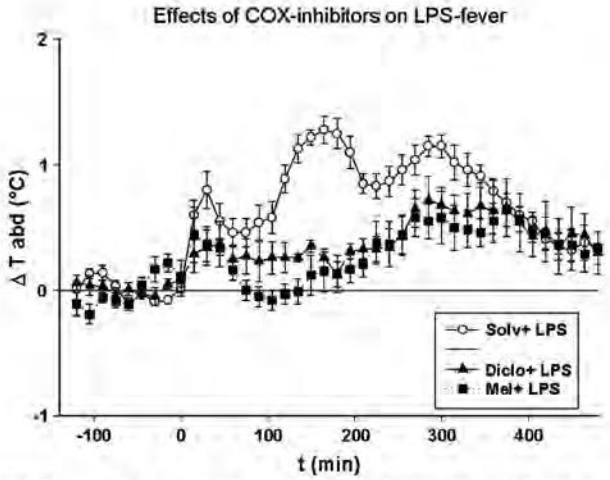


Fig. 5. Changes of abdominal temperature (T abd) in three groups of rats, injected intraperitoneally with 100 μg/kg LPS alone (Solv+ LPS); with 100 μg/kg LPS along with 5 mg/kg of the nonselective COX-inhibitor diclofenac (Diclo+ LPS); or with 100 μg/kg LPS along with 5 mg/kg of the preferential COX-2 inhibitor meloxicam (Mel+ LPS). Body temperature was recorded continuously by means of an intra-abdominally implanted temperature-sensitive transmitter (radiotelemetry). Treatment with both COX-inhibitors (nonselective versus preferential COX-2 inhibitor) resulted in a similar attenuation of LPS-induced fever. t (min), time in minutes.

colocalized expressions of COX-2 and mPGES-1 are suggested as the major source for PGE2 biosynthesis in the brain during fever.[44,63,64] Predominantly brain endothelial cells and perivascular cells express COX-2 under the influence of inflammatory cytokines.[44,45] A strong expression of COX-2 in response to a fever-inducing systemic treatment with LPS occurs in the OVLT and the subfornical organ. An example from the authors' experiments demonstrates this for the subfornical organ (see **Fig. 3**). In contrast, systemic treatment with LPS does not cause a pronounced induction of COX-2 in the hypothalamic paraventricular nucleus, which is known to activate during fever,[47] as shown by the pronounced LPS-induced expression of the c-fos gene (see **Fig. 3**).

The fact that an up-regulation of COX-2/mPGES-1 is observed during LPS fever alone is not proof of a critical role of these inducible enzymes in the manifestation of the febrile response. There is, however, more experimental support for such a hypothesis. Several reports have found that selective COX-2–specific inhibitors block LPS-induced fever.[64–66] Further supporting evidence has come from studies in knockout mice deficient in either COX-2[67,68] or mPGES-1.[69,70] In both cases, the febrile response is depressed. It seems, therefore, that the synthesis of COX-2/mPGES-1 in the brain, which is induced by pyrogenic cytokines, is critical for the brain-intrinsic formation of PGE2 during fever.

PGE2 seems to evoke fever via activation of the prostaglandin receptor subtype EP3, as suggested from studies in knockout mice deficient in this receptor, in which fever in response to LPS is strongly impaired.[71,72] It is suggested that an efferent fever-inducing pathway arises from activated EP3 receptors located in the preoptic-anterior hypothalamic area, namely in the medial preoptic nucleus[73,74] close to the OVLT. Using the viral tracing technique combined with immunocytochemical detection of the EP3 receptor, a complete efferent fever pathway starting from the medial preoptic area and ending finally in the thermogenic brown adipose tissue of the rat is demonstrated neuroanatomically.[75] A colocalization of virus protein with the EP3 receptor also is found in some neurons of the OVLT itself.[75] This neuronal chain thus might be regarded as the efferent part of the thermoregulatory reflexes, which are activated by interactions of circulating endogenous pyrogens with cells located within the OVLT and the adjacent medial preoptic area.

AN ALTERNATIVE AND RAPID MECHANISM OF PYROGENIC SIGNAL TRANSMISSION FROM THE PERIPHERY TO THE BRAIN

This article has described a complete chain of events leading to the genesis of fever, starting with the LPS-induced formation of endogenous pyrogens (cytokines), their interactions with relevant targets in the brain (CVOs and brain endothelial cells), the induction of enzymes responsible for the formation of PGE2 (COX-2 and mPGES-1), the activation of descending neuronal pathways via the EP3 receptor, and the stimulation of thermogenesis via this pathway to support the febrile shift of the thermoregulatory set point. Is this the end of the story? One recent challenge to this hypothesis focuses on the initial or "early" phase of LPS-induced fever (see **Figs. 1** and **5**).[76] The objections to the prevailing view are based mainly on the observation that, at least under some specific experimental conditions, the first phase of LPS-induced fever seems to be initiated before the appearance of cytokines in the blood. Therefore, an alternative and rapid signal pathway for the induction of the early phase of LPS fever is suggested.[77]

Within the past 10 years, several published studies indicate that the humoral hypothesis (described previously) does not represent the only and exclusive pathway

by which inflammatory signals from the periphery are transported to the brain. Some evidence suggests that the stimulation of afferent nerves, namely afferents from the vagus nerve but also possibly cutaneous afferent sensory nerves,[78] might participate in the manifestation of brain-controlled sickness responses under specific experimental conditions. Initially, this evidence derived from the observation that such signs of illness, which are regulated by the brain, can be attenuated or even abrogated by surgical section of the abdominal trunks of the vagus nerve.[8,11,12,79,80] In addition to arguments based on these effects of subdiaphragmatic vagotomy, additional arguments support a role of the vagus nerve as a pathway for transmission of immune signals to those parts of the brain where fever, anorexia, or sickness behavior are induced. Injection of IL-1 into the portal vein is shown to increase the firing rate of the vagal hepatic afferent nerve branch[81] and, in primary afferent neurons of the vagus nerve, immediate early genes seem to be activated by cytokines.[82] The role of the vagus nerve in the manifestation of fever is controversial, mainly because studies of vagotomized animals have led to somewhat conflicting results.[83]

Based on several experimental studies, Blatteis[76,77,80] suggests a novel hypothesis, including afferent parts of the vagus nerve. This hypothesis could account for a rapid induction of the early phase of LPS-induced fever before the release of larger amounts of cytokines into the bloodstream. Under some conditions, those larger amounts of cytokines might be involved in the maintenance rather than in the initiation of fever. According to this hypothesis, the febrigenic process is initiated by the arrival of LPS in the liver and its uptake by Kupffer cells, causing an immediate activation of complement. The complement component C5a, in turn, seems to stimulate the Kupffer cells to a rapid release of PGE2, which is suggested as activating local sensory vagal terminals that project to the medulla oblongata of the brainstem. From the medulla, this vagally transmitted excitation is believed to be transmitted to the preoptic-anterior hypothalamic area via the ventral noradrenergic bundle. An intra-hypothalamic release of norepinephrine might cause immediate neuronal activity changes via stimulation of α-adrenoreceptors, which are capable of activating efferent fever-promoting pathways. The aforementioned role for intrahypothalamic COX-2/mPGES-1–dependent release of PGE2 in the manifestation of fever thus might operate only for the longer second phase (see **Figs. 1** and **5**) of the LPS-induced febrile response.[76,77] A critical role for TLR4-bearing hepatic (and pulmonary) macrophages in triggering the earliest phase of LPS fever has also been suggested by Romanovsky and colleagues,[84] who reported a rapid formation of peripheral PGE2 by these cells coinciding with the onset of the febrile response.

In summary, it seems possible that the brain is informed by inflammatory processes in the periphery by rapid neuronal signals and, with some delay, by humoral signals. The combination of both types of signals might allow the brain to better identify the nature of the inflammatory challenge and thereby activate a more appropriate defense strategy. Fever, as a part of many successful defense strategies, thus may be a beneficial component of the acute-phase response, which helps to optimize the responses of the immune system against an infectious insult.

MOLECULAR ASPECTS OF HYPERTHERMIA

As discussed, hyperthermia occurs when temperature regulation against overheating is active as a consequence of the temporary or permanent imbalance between heat load and the capacity to dissipate heat. Molecular aspects of hyperthermia include the description of molecular changes, which occur in the heat-stressed brain and,

in some cases, the molecular mechanisms, which are the specific causes for a developing hyperthermia.

MALIGNANT HYPERTHERMIA

Malignant hyperthermia is caused by a rare, genetically fixed mutation of the ryanodine receptor, or calcium release channel, in the sarcoplasmatic reticulum of the striated muscles. Some inhalation anesthetics, such as halothane or isofluorane, cause excessive release of calcium from the sarcoplasmatic reticulum in genetically susceptible subjects. Also, the muscle relaxant succinylcholine or high circulating levels of stress hormones can act as triggering agents. As a consequence, uncoordinated muscle contractions with a tremendous rise in oxygen consumption and metabolic rate induce a severe hyperthermia accompanied by acidosis, tachycardia, or cardiac arrhythmias. The often-fatal hyperthermia is supported by the limitations of active heat dissipation during anesthesia.[1,2]

DRUG-INDUCED HYPERTHERMIA

The use of amphetamine-type stimulants can induce a pronounced and sometimes lethal increase in body temperature. Intoxication with 3,4-methylenedioxymethamphetamine (ecstasy), as a consequence of its worldwide recreational use, results in increasing numbers of hospital cases and deaths.[85] In most cases, lethality results from persistent hyperthermia, which leads to a breakdown of skeletal muscles (rhabdomyolysis) and renal failure. Ecstasy-induced hyperthermia seems to result from a strong activation of the sympathetic nervous system and the hypothalamic-pituitary thyroid/adrenal axes.[86] The excessive release of norepinephrine causes pronounced heat generation via β3-adrenergic activation of uncoupling protein type 3 and α1-adrenergic suppression of heat dissipation resulting from sympathetically mediated vasoconstriction.[86] Ecstasy thus represents an impressive example of a drug-induced manifestation of hyperthermia.

THE HEAT STROKE SYNDROME

During prolonged hyperthermia, with a body temperature of 41°C or higher, the brain suffers severe damage, which frequently leads to death. Alterations in microvascular permeability cause the development of cerebral edema. Postmortem findings show microhemorrhages, tissue softening, and destruction of neurons. Victims exhibit disorientation, delirium, and convulsions. This syndrome is referred to popularly as heat stroke. The precise mechanisms that account for the manifestation of heat stroke are under investigation.[87,88] Several molecular changes that occur in the heat-stressed brain already have been identified.[89] The expression of several molecules is up-regulated in the brain under conditions of severe hyperthermia. Thus, the induction of a specific set of proteins, the so-called "heat-shock proteins," is related closely to damaged brain areas and thus can be used as markers of cell injury. There is some evidence that heat-shock proteins have neuroprotective properties.[89] Hyperthermic brain injury is accompanied further by an activation of glial cells (ie, astrocytes), as indicated by the expression of the cell marker protein, glial fibrillary acidic protein. Under pathologic conditions, such as brain hyperthermia, induction of this protein is associated with a breakdown of the blood-brain barrier and vasogenic edema.

Activation of the immune system during infection or inflammation is characterized not only by a systemic formation of cytokines but also by the expression of cytokines in the brain.[3,90] There is evidence that an increased expression of IL-1 within the

central nervous system is associated with brain injury. An increased production of IL-1 in the damaged brain accompanies heat stroke–induced cerebral ischemia and neuronal damage. The survival time of rats can be prolonged by treatment with an IL-1 receptor antagonist. This indicates a role for IL-1 and possibly other cytokines in the manifestation of the heat stroke syndrome.[91] In this context, it recently has been reported that elevated cytokine concentrations occur in human heat stroke and in experimental animal heat stroke models.[87,88] The precise role of the stimulated formation of cytokines in heat stroke, as opposed to fever, still has to be elucidated. It is anticipated that a more detailed understanding of the putative roles of cytokines in the modifications of body core temperature in experimental heat stroke models will provide important insight into the role of these substances in the complex etiology of the long-term consequences of this syndrome.[88]

REFERENCES

1. International Union of Physiological Sciences, Commission for Thermal Physiology. Glossary of terms for thermal physiology. 3rd edition. Jpn J Physiol 2001;51:245–80.
2. Roth J. Hyperthermia. In: Fink G, editor. Encyclopedia of stress, vol. 2. San Diego (CA): Academic Press; 2000. p. 431–8.
3. Kluger MJ. Fever: role of pyrogens and cryogens. Physiol Rev 1991;71:93–127.
4. Moltz H. Fever: causes and consequences. Neurosci Biobehav Rev 1993;17: 237–69.
5. Hellon R, Townsend Y, Laburn H, et al. Mechanisms of fever. In: Schönbaum E, Lomax P, editors. Thermoregulation: pathology, pharmacology and therapy. New York: Pergamon Press; 1991. p. 19–54.
6. Blatteis CM. Fever: pathological or physiological, injurious or beneficial? J Therm Biol 2003;28:1–13.
7. Gabay C, Kushner J. Acute-phase proteins and other systemic responses to inflammation. N Engl J Med 1999;340:448–54.
8. Dantzer R. Cytokine-induced sickness behavior: where do we stand? Brain Behav Immun 2001;15:7–24.
9. Luheshi G, Rothwell NJ. Cytokines and fever. Int Arch Allergy Immunol 1996;109: 301–7.
10. Dinarello CA. Cytokines as endogenous pyrogens. J Infect Dis 1999;179(Suppl 2):S294–304.
11. Zeisberger E. From humoral fever to neuroimmunological control of fever. J Therm Biol 1999;24:287–326.
12. Roth J, de Souza GEP. Fever induction pathways: evidence from responses to systemic or local cytokine formation. Braz J Med Biol Res 2001;34:301–14.
13. Mackowiak PA, Bartlett JG, Borden EC, et al. Concepts of fever: recent advances and lingering dogma. Clin Infect Dis 1997;25:119–38.
14. Romanovsky AA, Szekely M. Fever and hypothermia: two adaptive thermoregulatory responses to systemic inflammation. Med Hypotheses 1998;50:219–26.
15. Rudaya AY, Steiner AA, Robbins JR, et al. Thermoregulatory responses to lipopolysaccharide in the mouse: dependence on the dose and ambient temperature. Am J Physiol 2005;289:R1244–52.
16. Cartmell T, Mitchell D, Lamond FJD, et al. Route of administration differentially affects fevers induced by gram-negative and gram-positive pyrogens in rabbits. Exp Physiol 2002;87(3):391–9.

Author's personal copy

17. Rummel C, Hübschle T, Gerstberger R, et al. Nuclear translocation of the transcription factor STAT3 in the guinea pig brain during systemic or localized inflammation. J Physiol 2004;557(2):671–87.
18. Fortier ME, Kent S, Ashdown H, et al. The viral mimic, polyinosinic: polycytidylic acid, induces fever in rats via an interleukin-1-dependent mechanism. Am J Physiol 2004;287:R759–66.
19. Hübschle T, Mütze J, Mühlradt PF, et al. Pyrexia, anorexia, adipsia and depressed motor activity in rats during systemic inflammation induced by the Toll-like receptor 2- and 6-agonists MALP-2 and FSL-1. Am J Physiol 2006;290:R180–7.
20. Cooper KE. Fever and antipyresis—the role of the nervous system. Cambridge: University Press; 1995.
21. Beeson PB. Temperature-elevating effect of a substance obtained from polymorphonuclear leucocytes. J Clin Invest 1948;27:524–48.
22. Long NC, Kunkel SL, Vander AL, et al. Antiserum against TNF enhances LPS fever in the rat. Am J Physiol 1990;258:R332–7.
23. Roth J, Conn CA, Kluger MJ, et al. Kinetics of systemic and intrahypothalamic IL-6 and tumor necrosis factor during endotoxin fever in guinea pigs. Am J Physiol 1993; 265:R653–8.
24. Jansky L, Vybiral S, Pospisilova D, et al. Production of systemic and hypothalamic cytokines during the early phase of endotoxin fever. Neuroendocrinology 1995; 62:55–61.
25. LeMay LG, Vander AJ, Kluger MJ. Role of interleukin-6 in fever in the rat. Am J Physiol 1990;258:R798–803.
26. Luheshi G, Miller AJ, Brouwer S, et al. Interleukin-1 receptor antagonist inhibits endotoxin fever and systemic interleukin-6 induction in the rat. Am J Physiol 1996;270:E91–5.
27. Roth J, McClellan JL, Kluger MJ, et al. Attenuation of fever and release of cytokines after repeated injections of lipopolysaccharide in guinea pigs. J Physiol 1994;477(1):177–85.
28. Anforth HR, Bluthe RM, Bristow A, et al. Biological activity and brain actions of recombinant rat interleukin-1α and interleukin-1β. Eur Cytokine Netw 1998;9:279–88.
29. Roth J, Störr B, Voigt K, et al. Inhibition of nitric oxide synthase results in a suppression of interleukin-1 beta-induced fever in rats. Life Sci 1998;62: PL345–50.
30. Dinarello CA, Cannon JG, Wolff SM, et al. Tumor necrosis factor (cachectin) is an endogenous pyrogen and induces production of interleukin-1. J Exp Med 1986; 163:1433–50.
31. Goldbach JM, Roth J, Störr B, et al. Repeated infusions of TNFα cause attenuation of the thermal response and influence LPS-fever in guinea pigs. Am J Physiol 1996;270:R749–54.
32. Blatteis CM, Quan N, Xin L, et al. Neuromodulation of acute phase responses to interleukin-6 in guinea pigs. Brain Res Bull 1990;25:895–901.
33. Harré EM, Roth J, Pehl U, et al. Selected contribution: role of IL-6 in LPS-induced nuclear STAT3 translocation in sensory circumventricular organs during fever in rats. J Appl Physiol 2002;92:2657–66.
34. Roth J, Martin D, Störr B, et al. Neutralization of bacterial pyrogen-induced circulating tumour necrosis factor by its type 1 soluble receptor in guinea pigs: effects on fever and endogenous formation of interleukin-6. J Physiol 1998;509(2): 267–75.
35. Cartmell T, Poole S, Turnbull AV, et al. Circulating interleukin-6 mediates the febrile response to localised inflammation in rats. J Physiol 2000;526(3):653–61.

Author's personal copy

36. Leon LR. Invited review: cytokine regulation of fever: studies using gene knockout mice. J Appl Physiol 2002;92:2648–55.
37. Kozak W, Zheng H, Conn CA, et al. Thermal and behavioural effects of lipopolysaccharide and influenza in interleukin-1β-deficient mice. Am J Physiol 1995;269:R969–77.
38. Kozak W, Kluger MJ, Soszynski D, et al. IL-6 and IL-1β in fever: studies using cytokine-deficient (knockout) mice. Ann N Y Acad Sci 1998;856:33–47.
39. Chai Z, Gatti S, Toniatti C, et al. Interleukin (IL)-6 gene expression in the central nervous system is necessary for fever in response to lipopolysaccharide or IL-1β: a study on IL-6-deficient mice. J Exp Med 1996;183:311–6.
40. Aderem A, Ulevich RJ. Toll-like receptors in the induction of the innate immune response. Nature 2000;406:782–7.
41. Rivest S. Molecular insights into the cerebral innate immune system. Brain Behav Immun 2003;17:13–9.
42. Poltorak A, Ricciardi-Castagnoli P, Citterio S, et al. Physical contact between LPS and Toll-like receptor 4 revealed by genetic complementation. Proc Natl Acad Sci U S A 2000;97:2163–7.
43. Roth J, Harré EM, Rummel C, et al. Signaling the brain in systemic inflammation: role of sensory circumventricular organs. Front Biosci 2004;9:290–300.
44. Matsumura K, Kobayashi S. Signaling the brain in inflammation: the role of endothelial cells. Front Biosci 2004;9:2819–26.
45. Schiltz JC, Sawchenko PE. Signaling the brain in systemic inflammation: the role of perivascular cells. Front Biosci 2003;8:s1321–9.
46. Banks WA, Kastin AJ, Broadwell RD. Passage of cytokines across the blood-brain barrier. Neuroimmunomodulation 1995;2:241–8.
47. Elmquist JK, Scammell TE, Jacobson CD, et al. Distribution of Fos-like immunoreactivity in the rat brain following intravenous lipopolysaccharide administration. J Comp Neurol 1996;371:85–103.
48. Scammell TE, Elmquist JK, Griffin JD, et al. Ventromedial preoptic prostaglandin E2 activates fever-producing autonomic pathways. J Neurosci 1996;16:6246–54.
49. Blatteis CM, Bealer SL, Hunter WS, et al. Suppression of fever after lesions of the anteroventral third ventricle in guinea pigs. Brain Res Bull 1983;11:519–26.
50. Blatteis CM, Hales JRS, McKinley MJ, et al. Role of the anteroventral third ventricle region in fever in sheep. Can J Physiol Pharmacol 1987;65:1255–60.
51. Ericsson A, Liu C, Hart RP, et al. Type 1 interleukin-1 receptor in the rat brain: distribution, regulation, and relationship to sites of IL-1-induced cellular activation. J Comp Neurol 1995;361:681–98.
52. Valliéres L, Rivest S. Regulation of the genes encoding interleukin-6, its receptor, and gp130 in the rat brain in response to immune activator lipopolysaccharide and the proinflammatory cytokine interleukin-1β. J Neurochem 1997;69:1668–83.
53. Nadeaux S, Rivest S. Effects of circulating tumor necrosis factor on the neuronal activity and expression of the genes encoding the tumor necrosis factor receptors (p55 and p75) in the rat brain: a view from the blood-brain barrier. Neuroscience 1999;93:1449–64.
54. Shibata M, Blatteis CM. Human recombinant tumor necrosis factor and interferon affect the activity of neurons in the organum vasculosum laminae terminalis. Brain Res 1991;562:323–6.
55. Wuchert F, Ott D, Murgott J, et al. Rat area postrema microglial cells act as sensors for the Toll-like receptor-4 agonist lipopolysaccharide. J Neuroimmunol 2008;204:66–74.
56. Konsman JP, Vigues S, Mackerlova L, et al. Rat brain vascular distribution of interleukin-1 type-1 receptor immunoreactivity: relationship to patterns of inducible

Author's personal copy

cyclooxygenase expression by peripheral inflammatory stimuli. J Comp Neurol 2004;472:113–29.
57. Nadjar A, Combe C, Layé S, et al. Nuclear factor κB nuclear translocation as a crucial marker of brain response to interleukin-1. A study in rat and interleukin-1 type I deficient mouse. J Neurochem 2003;87:1024–36.
58. Rummel C, Voss T, Matsumura K, et al. Nuclear STAT3 translocation in guinea pig and rat brain endothelium during systemic challenge with lipopolysaccharide and interleukin-6. J Comp Neurol 2005;491:1–14.
59. Milton AS, Wendlandt S. Effects on body temperature of prostaglandins of the A, E, and F series on injection into the third ventricle of unanaesthetized cats and rabbits. J Physiol 1971;218:325–36.
60. Milton AS. Prostaglandins and fever. Prog Brain Res 1998;115:129–39.
61. Sehic E, Szekely M, Ungar AL, et al. Hypothalamic prostaglandin E2 during lipopolysaccharide-induced fever in guinea pigs. Brain Res Bull 1996;39:391–9.
62. Ivanov AI, Romanovsky AA. Prostaglandin E2 as a mediator of fever: synthesis and catabolism. Front Biosci 2004;9:1977–93.
63. Turrin NP, Rivest S. Unraveling the molecular details involved in the intimate link between the immune and neuroendocrine systems. Exp Biol Med 2004;229: 996–1006.
64. Yamagata K, Matsumura K, Inoue W, et al. Coexpression of microsomal-type prostaglandin E synthase with cyclooxygenase-2 in brain endothelial cells of rats during endotoxin-induced fever. J Neurosci 2001;21:2669–77.
65. Cao C, Matsumura K, Yamagata K, et al. Involvement of cyclooxygenase-2 in LPS-induced fever and regulation of its mRNA by LPS in the rat brain. Am J Physiol 1997;272:R1712–25.
66. Zhang YH, Lu J, Elmquist JK, et al. Specific roles of cyclooxygenase-1 and cyclooxygenase-2 in lipopolysaccharide-induced fever and fos expression in rat brain. J Comp Neurol 2003;463:3–12.
67. Li S, Wang Y, Matsumura K, et al. The febrile response to lipopolysaccharide is blocked in cyclooxygenase-2−/−; but not in cyclooxygenase-1−/− mice. Brain Res 1999;825:86–94.
68. Steiner AA, Rudaya AY, Robbins JR, et al. Expanding the febrigenic role of cyclooxygenase-2 to the previously overlooked responses. Am J Physiol 2005;289:R1253–7.
69. Engblom D, Saha S, Engström L, et al. Microsomal prostaglandin E synthase-1 is the central switch during immune-induced pyresis. Nat Neurosci 2003;6:1137–8.
70. Saha S, Engström L, Mackerlova L, et al. Impaired febrile responses to immune challenge in mice deficient in microsomal prostaglandin E synthase-1. Am J Physiol 2005;288:R1100–7.
71. Ushikubi F, Segi E, Sugimoto Y, et al. Impaired febrile response in mice lacking the prostaglandin E subtype EP3. Nature 1998;395:281–4.
72. Oka T, Oka K, Kobayashi T, et al. Characteristics of thermoregulatory and febrile responses in mice deficient in prostaglandin EP1 and EP3 receptors. J Physiol 2003;551:945–54.
73. Nakamura K, Matsumura K, Kaneko T, et al. The rostral raphe pallidus nucleus mediates pyrogenic transmission from the preoptic area. J Neurosci 2002;22: 4600–10.
74. Lazarus M, Yoshida K, Coppari R, et al. EP3 prostaglandin receptors in the median preoptic nucleus are critical for fever response. Nat Neurosci 2007;10:1131–3.
75. Yoshida K, Nakamura K, Matsumura K, et al. Neurons of the rat preoptic area and the raphe pallidus nucleus innervating the brown adipose tissue express prostaglandin E receptor subtype EP3. Eur J Neurosci 2003;18:1848–60.

Author's personal copy

76. Blatteis CM. The cytokine-prostaglandin cascade in fever production: fact or fancy? J Therm Biol 2004;29:359–68.
77. Blatteis CM. Endotoxic fever: new concepts of its regulation suggest new approaches to its management. Pharm Therap 2006;111:194–223.
78. Ross G, Roth J, Störr B, et al. Afferent nerves are involved in the febrile response to injection of LPS into artificial subcutaneous chambers in guinea pigs. Physiol Behav 2000;71:305–13.
79. Watkins LR, Maier SF, Goehler LE. Cytokine-to-brain communication: a review & analysis of alternative mechanisms. Life Sci 1995;57:1011–26.
80. Blatteis CM, Sehic E. Fever: How may circulating cytokines signal the brain. News Physiol Sci 1997;12:1–9.
81. Niijima A. The afferent discharges from sensors for interleukin 1β in the hepato-portal system in the anesthetized rat. J Auton Nerv Syst 1996;61:287–91.
82. Goehler LE, Gaykema RPA, Hammack SE, et al. Interleukin-1 induces c-Fos immunoreactivity in primary afferent neurons of the vagus nerve. Brain Res 1998;804:306–10.
83. Romanovsky AA. Signaling the brain in the early sickness syndrome: Are sensory nerves involved? Front Biosci 2004;9:494–504.
84. Romanovsky AA, Steiner AA, Matsumura K. Cells that trigger fever. Cell Cycle 2006;5:e1–3.
85. Mills EM, Banks ML, Sprague JE, et al. Uncoupling the agony from ecstasy. Nature 2003;426:403–4.
86. Mills EM, Rusynak DE, Sprague JE. The role of the sympathetic nervous system and uncoupling proteins in the thermogenesis induced by 3,4-methylendioxy-metamphetamine. J Mol Med 2004;82:787–99.
87. Leon LR, Blaha MD, Dubose DA. Time course of cytokine, corticosterone and tissue injury responses in mice during heat strain recovery. J Appl Physiol 2006;100:1400–9.
88. Leon LR. The thermoregulatory consequences of heat stroke: are cytokines involved? J Therm Biol 2006;100:1400–9.
89. Sharma HS, Westman J. Brain function in hot environment. Amsterdam (Netherlands): Elsevier; 1998.
90. Layé S, Parnet P, Goujon E, et al. Peripheral administration of lipopolysaccharide induces the expression of cytokine transcripts in the brain and pituitary of mice. Brain Res Mol Brain Res 1994;27:157–62.
91. Rothwell NJ, Relton JK. Involvement of cytokines in acute neurodegeneration in the CNS. Neurosci Biobehav Rev 1993;17:217–27.

1.9. „Selective contribution of interleukin-6 and leptin to brain inflammatory signals induced by systemic LPS injection in mice“

Rummel C., Inoue W., Sachot C., Hübschle T., Poole S., Luheshi GN.
J Comp Neurol (2008) 511:373-395.

Impakt Faktor: 3,774

Eigener Anteil an der Publikation:

- Initiative: eigenständig (90 %)
- Projektplanung: eigenständig (90 %)
- Durchführung der Versuche: eigenständig (90 %)
- Auswertung der Experimente: eigenständig (90 %)
- Erstellung der Publikation: weitgehend eigenständig (80 %)

THE JOURNAL OF COMPARATIVE NEUROLOGY 511:373–395 (2008)

Selective Contribution of Interleukin-6 and Leptin to Brain Inflammatory Signals Induced by Systemic LPS Injection in Mice

CHRISTOPH RUMMEL,[1,2]* WATARU INOUE,[1] CHRISTELLE SACHOT,[1] STEPHEN POOLE,[3] THOMAS HÜBSCHLE,[2] AND GIAMAL N. LUHESHI[1]

[1]Douglas Mental Health University Institute, Department of Psychiatry, McGill University, Montreal, Quebec, H4H 1R3, Canada

[2]Department of Veterinary-Physiology, Justus-Liebig-University Giessen, D-35392 Giessen, Germany

[3]Department of Endocrinology, National Institute for Biological Standards and Control, Potters Bar, EN6 3QG, United Kingdom

ABSTRACT

This study aimed to address the relative contributions of the proinflammatory cytokine interleukin-6 (IL-6) and the cytokine-like hormone leptin to the genomic activation of brain cells during lipopolysaccharide (LPS)-induced systemic inflammation. Wildtype and IL-6KO mice were injected with LPS (50 μg/kg, intraperitoneally) and the brains analyzed by immunohistochemistry and reverse-transcriptase polymerase chain reaction (RT-PCR). LPS induced a pronounced nuclear translocation of the signal transducer and activator of transcription (STAT3) throughout the brains of wildtype mice, an effect that was significantly diminished, but not abolished, in the IL-6KOs. The remnant STAT3-activation, although still observed within some of the same areas activated by IL-6, was most intense in ependymal and meningial cells and along distinct blood vessels throughout the brain. This expression was almost totally abolished in the presence of an anti-leptin antiserum. Interestingly, the induction of cyclooxygenase 2 and microsomal prostaglandin E synthase (mPGES), the rate-limiting enzymes for synthesis of PGE2 by LPS, was diminished to a degree that correlated with the absence of IL-6 but not entirely with leptin. These results demonstrate that the induction of the inflammatory pathway in the brain is mediated by both IL-6 and leptin, which appear to work in tandem. Unlike IL-6, however, the contribution of leptin to this response was limited to distinct cell types/brain areas and STAT3-responsive target genes implicated in the brain-controlled sickness-type response. The physiological significance of leptin's action on meningeal and endothelial cells remains to be clarified but might reflect a role in LPS-induced immune cell infiltration into the brain. J. Comp. Neurol. 511: 373–395, 2008. © 2008 Wiley-Liss, Inc.

Indexing terms: Indexing terms: systemic inflammation; immune-to-brain communication; cytokines; circumventricular organs; endothelial cells

Research into mechanisms regulating immune-to-brain communication during systemic infection and inflammation has evolved significantly in the last two decades, with several signaling pathways being proposed and investigated (Langhans, 2000; Conti et al., 2004; Quan and Banks, 2007). Prominent among these is the humoral route of communication, which involves transmission of signals from the immune system to the brain via blood-borne mediators. Studies on fever have shown that these mediators belong mostly to the proinflammatory cytokine family, in particular interleukin (IL)-1β and IL-6 (Netea et al., 2000; Conti et al., 2004). Of these, only IL-6 rises consistently in the circulation (Miller et al., 1997; Cartmell et al., 2000; Cartmell et al., 2001) of febrile animals and we (Cartmell et al., 2000; Rummel et al., 2006) and others (Turnbull et al., 2003; Oka et al., 2007) have demonstrated that it is most likely the main circulating pyro-

Grant sponsor: Canadian Institute of Health Research and Natural Sciences and Engineering Research Council of Canada; Grant sponsor: Deutsche Forschungsgemeinschaft; Grant number: DFG project RU 1397/1-1 (to C.R.); Grant sponsor: Nakajima Foundation, Japan (PhD scholarship to W.I.).

*Correspondence to: Dr. Christoph Rummel, Department of Veterinary-Physiology, Justus-Liebig-University Giessen, Frankfurter Strasse 100, D-35392 Giessen, Germany.
E-mail: Christoph.D.Rummel@vetmed.uni-giessen.de

Received 27 March 2008; Revised 17 June 2008; Accepted 31 July 2008
DOI 10.1002/cne.21850
Published online in Wiley InterScience (www.interscience.wiley.com).

© 2008 WILEY-LISS, INC.

genic signal to the brain during inflammation. In the brain recent extensive studies have revealed new insights on the structures and cell types involved in mediating the fever response to IL-6 (Vallières and Rivest, 1999; Lebel et al., 2000; Harré et al., 2002, 2003; Rummel et al., 2005, 2006). These studies added clarity to the mechanisms and brain circuits/neuronal networks involved by monitoring the activation of a variety of signaling molecules and transcription factors such as the janus kinase (JAK)-signals transducer and activator of transcription (STAT)3 pathway (Akira, 1997). This is the main signaling pathway activated by IL-6, which results in the induction of nuclear translocation of STAT3, and ultimately regulates target gene expression. Using immunohistochemical detection of STAT3 in animals during systemic inflammation, several studies (Lebel et al., 2000; Hübschle et al., 2001b; Harré et al., 2002, 2003; Rummel et al., 2004, 2005, 2006) clearly demonstrated that IL-6 acts on the circumventricular organs (CVOs), brain structures with a "leaky" blood–brain barrier (BBB), endothelial cells, and other hypothalamic brain areas implicated in the induction of fever. In our recent studies we demonstrated for the first time that lipopolysaccharide (LPS)-induced STAT3-activation was almost entirely IL-6-dependent and accompanied by the induction of cyclooxygenase (COX)2, the rate-limiting enzyme for prostaglandin (PG) synthesis, and that the expression of this enzyme clearly colocalized with the nuclear STAT3 staining (Rummel et al., 2006). The colocalization was specific to endothelial cells lining the brain microvasculature and was spread throughout the brain including those regions important for fever regulation. These observations along with previous in vivo studies clearly support a significant role for IL-6 as a neuroimmune mediator in fever and other sickness-type behaviors (Turnbull et al., 2003; Harden et al., 2006; Rummel et al., 2006; Oka et al., 2007). However, while the role of IL-6 as the main mediator of STAT3-activation in the brain is established, preliminary results from the present study revealed a moderate but significant amount of remnant LPS-induced nuclear STAT3 translocation in the brains of IL-6-deficient mice (IL-6KO), confirming previous reports of others working on liver tissue (Yang et al., 2005) or the brain (Lebel et al., 2000) from IL-6KO animals treated systemically with LPS. This raised the question of whether a second mediator, other than IL-6, is involved in STAT3 activation of brain cells during systemic inflammation.

Recently, emerging evidence suggested that leptin, which mediates its main effects through STAT3-signaling, may be acting in a similar fashion to IL-6, for example, on endothelial cells (Mütze et al., 2006), and therefore could account for some of the observed IL-6-independent STAT3-activation in brains of LPS-stimulated IL-6KO mice. Leptin is an adipose-derived hormone known mainly as a regulator of energy balance that also fulfils some of the criteria for a circulating neuroimmune mediator (Lago et al., 2007). For instance, during systemic inflammation leptin, like IL-6, rises in the circulation (Sarraf et al., 1997; Berkowitz et al., 1998; Faggioni et al., 1998; Gomez-Ambrosi et al., 2004), induces COX2 in the brain (Inoue et al., 2006) or PG release from hypothalamic slices (Brunetti et al., 1999), and mediates fever (Luheshi et al., 1999; Sachot et al., 2004; Harden et al., 2006). The similarities of leptin with IL-6 also include the fact that the receptors for both belong to the class 1 cytokine family of receptors and that both signal through the STAT3 pathway. Given the similarities in the mechanisms and actions of the two cytokines, an earlier mapping study (Hübschle et al., 2001b) investigating STAT3-activation in the brain of animals following an intracerebroventricular (i.c.v.) injection of either leptin or IL-6 revealed distinct but partly overlapping distribution of leptin- versus IL-6-induced STAT3-activation.

Although interesting, this study did not address the role of the endogenous peptides and whether the same pattern of activation of brain regions will be observed following a systemic infectious stimulus, which would reflect more accurately the physiological role of both of these mediators. Thus, to characterize the involvement of endogenous leptin as a mediator of immune-to-brain communication, we sought to investigate the possibility that leptin, in addition to IL-6, mediates activation of brain structures / cell types during LPS-induced systemic inflammation by using immunohistochemical approaches for detecting nuclear STAT3 translocation. In designing these studies and given the substantial role played by IL-6 in triggering STAT3 in the brain (Rummel et al., 2005, 2006), we chose to utilize IL-6-deficient mice in order to study the contri-

Abbreviations

AP	Area postrema
ARC	Arcuate nucleus
BBB	Blood-brain barrier
COX2	Cyclooxygenase 2
CVOs	Circumventricular organs
DAPI	4′,6-diamidino-2-phenyl-indole dilactate
GAPDH	Glyceraldehyde 3-phosphate dehydrogenase
IκBα	Inhibitor of kappa B alpha
ICAM1	Intercellular adhesion molecule 1
IL-1β	Interleukin-1 beta
IL-6	Interleukin-6
i.p.	Intraperitoneal
KO	Deficient mouse
LAS	Mouse leptin antiserum
LPS	Lipopolysaccharide
MCP1	Monocyte chemotactic protein 1
ME	Median eminence
MIP2	Macrophage inflammatory protein 2
MnPO	Median preoptic nucleus
mPGES	Microsomal PGE_2 synthase
NF-κB	Nuclear factor kappa B
OBra	Leptin receptor a
OBrb	Leptin receptor b
OVLT	Vascular organ of the lamina terminalis
ox	Optic chiasm
PBS	Phosphate-buffered saline
Pe	Periventricular nucleus
PGE_2	Prostaglandin E 2
PVN	Paraventricular nucleus
RPa	Raphe pallidus nucleus
RT	Room temperature
SFO	Subfornical organ
SOCS3	Suppressor of cytokine signaling 3
Sol	Nucleus of the solitary tract
SON	Supraoptic nucleus
STAT3	Signal transducer and activator of transcription 3
TIMP1	Tissue inhibitor of metalloproteinase 1
VMPO	Ventromedial preoptic nucleus
vW	von Willebrand factor
V_{III}/V_{IV}	Third/fourth ventricle

bution of leptin to the STAT3-mediated inflammatory response in the brain in isolation. In these studies wildtype and IL-6KO animals were treated with LPS, with some IL-6KO mice coinjected with a mouse anti-leptin antiserum (LAS) to neutralize biological activities of endogenous leptin and to evaluate if, indeed, a portion of the LPS-induced STAT3 translocation in brain cells is leptin-mediated. In addition, using reverse-transcriptase polymerase chain reaction (RT-PCR), the expression of COX2 and another rate-limiting enzyme for PG synthesis microsomal PGE synthase (mPGES) mRNA as well as a number of other important markers of inflammation such as intercellular adhesion molecule (ICAM)1 (Wung et al., 2005) or monocyte chemotactic protein (MCP)1 (Chen et al., 2006) were investigated as putative functionally relevant gene products downstream of STAT3-activation. In order to dissect out the relative contribution to the induction of these target genes by the STAT3-signaling mediators IL-6 and leptin compared to the well-known role of NF-κB-signaling ones such as IL-1β (Cao et al., 1996; Thibeault et al., 2001), IL-1β mRNA expression and NF-κB-activation was also investigated in the hypothalamus of these animals.

MATERIALS AND METHODS

Animals

All animals used in the present study were purchased from the same source (Jackson laboratory, Saint Constant, Canada) at 6 weeks of age. These were housed in groups (n = 5) in a controlled environment at an ambient temperature of 21 ± 2°C on a 12:12-hour light-dark cycle (lights off at 8:30 PM) with free access to standard laboratory chow and water for 1 week until they reached a body weight of 19–24 g on the day of the experiment. Adult 7 weeks old male IL-6KO mice (strain name, B6.129S2-Il-6tmlkopf/j; stock number 002650) that were backcrossed to C57BL/6J and maintained as a congenic strain in the supplier's facility were used in all experiments. C57BL/6J mice (stock number, 000664) purchased from the same supplier were used as wildtype controls. None of the animals used in the study were bred in-house. The animals were handled extensively for at least 3 days prior to each experiment for habituation. The Animal Care Committee of McGill University pursuant to the Canadian Council of Animal Care guidelines approved all experimental procedures used in this study.

Preparation and characterization of LAS

A polyclonal sheep anti-leptin antiserum (LAS; cat. no. S4159, lot S05-13) against recombinant mouse leptin (cat. no. 498-OB, R&D Systems, Minneapolis, MN) representing the mature mouse leptin protein sequence (Zhang et al., 1994) combined with recombinant rat leptin (cat. no. 598-LP, R&D Systems) (Murakami and Shima, 1995) both expressed in *E. coli* was raised at the National Institute for Biological Standards and Control (NIBSC, Potters Bar, UK) using the immunization method described previously (Poole et al., 1989). Bleeds were taken 10 days after each boost, the serum filtered (0.22 μm), and stored at −80°C. The antiserum from the second boost was used in all experiments. The crude antiserum stains a single band of 17 kD molecular weight with both murine and rat recombinant leptin (R&D Systems) on Western blot (data not shown). The ability of the antiserum to effectively neutralize the bioactivity of endogenous leptin was tested in vivo. A single intraperitoneal (i.p.) injection of LAS (0.5 mL/mice) in wildtype mice significantly increased their body weight 24 hours after injection when compared to an injection of normal sheep serum (NSS; i.p., 0.5 mL/mice; data not shown). In addition, the same treatment dramatically reduced plasma leptin levels to concentrations below the detection limit as measured by enzyme-linked immunosorbent assay (ELISA) (Fig. 9A). A nonspecific inflammatory response caused by the injection of the relatively large volume of LAS was negligible when the expression of inflammatory genes was examined in the brain by RT-PCR or immunohistochemistry (IHC; Table 3; Figs. 2–4C,I,O, 5B, 6, 7, 10).

Further, IgG from sheep LAS was affinity-purified using a protein G column (ImmunoPure Immobilized Protein G; Pierce Biotechnology, Rockford, IL). The purified IgG was dialyzed (MWCO 8,000) against carbonate buffer (pH 8.2) and the concentration adjusted to 2.0 mg/mL and used as the coating antibody for a sandwich ELISA assay. A portion of dialyzed IgG was biotinylated using sulfo-N-hydroxysuccinimide esters of biotin (Sulfo-NHS-Biotin Reagents, Pierce Biotechnology) at a molar ratio of 1:80 followed by dialysis (MWCO 8,000) with carbonate buffer (pH 8.2) and used as the detection antibody for the ELISA. Importantly, no cross-reactivity with other cytokines such as TNF, IL-1β, IL-6, or IL-10 (data not shown) was observed using this leptin ELISA, further confirming the specificity of the LAS.

Treatment and experimental protocols

Male wildtype (C57BL/6J; n = 14 used for RT-PCR and IHC; n = 4 used only for IHC) and IL-6KO mice (IL-6KO; B6.129S2-IL-6tm1Kopf/j, Jackson Laboratory; n = 20 for RT-PCR and IHC; n = 6 for IHC only) were injected with a moderate dose of LPS (derived from *E. coli*, suspended in sterile pyrogen-free 0.9% saline; 0111:B4, lot 42k4120; L-2630, Sigma, St. Louis, MO) at a dose of 50 μg/kg i.p. (prepared as a 500 μg/mL solution, volume of 5 mL/kg) or an equivalent volume of vehicle (NaCl, 0.9% saline, 5 mL/kg). Injections were performed between 12 and 2 PM. The same dose and serotype of LPS was previously shown to induce fever in C57BL6 mice but not in IL-6KO mice and to significantly increase circulating IL-6 concentrations in C57BL6 mice (Kozak et al., 1998). Half of the LPS-stimulated and saline-treated IL-6KO mice were also pretreated (−4 hours) i.p. with 0.5 mL of a sheep anti-mouse leptin antiserum (LAS, n = 10). The volume and timing of LAS injections were determined in accordance with previous studies using cytokine-specific antisera (Turnbull et al., 2003; Rummel et al., 2006). In summary, we had six treatment groups as follows: wildtype animals treated with LPS or saline (LPS, NaCl), IL-6KO animals treated with LPS or saline (LPS IL-6KO, NaCl IL-6KO), and IL-6KO mice pretreated with LAS and stimulated with LPS or saline (LPS IL-6KO LAS, NaCl IL-6KO LAS).

Nuclear STAT3-activation in the mouse brain, commonly used as a marker of activation for JAK-STAT signaling molecules, was investigated 3 hours after LPS stimulation based on the findings of an earlier study showing that LPS-induced activated STAT3 levels in the hypothalamus peaked between 2–4 hours post-LPS treatment (Hosoi et al., 2004). At this time animals were euthanized by terminal anesthesia (pentobarbital; 70 μg/kg via i.p.

injection) and blood samples collected via cardiac puncture using a sterile heparinized syringe. Mice were then transcardially perfused with 50 mL ice-cold 0.9% NaCl solution, their brains quickly removed, frozen in powdered dry ice, and kept at −80°C until analysis. The brains of all animals were prepared for IHC as previously described (Rummel et al., 2005).

Leptin ELISA

Heparinized (10 IU/mL) blood samples were centrifuged (5,300*g*, 10 minutes, 4°C), the supernatant was collected, and stored at −80°C until assays were performed. Leptin levels were measured in duplicate using a sandwich leptin ELISA prepared as described above. The ELISA was performed according to a standard procedure described elsewhere (Rees et al., 1999) except for the blocking reagent that was substituted with 1% of nonfat dried milk (Bio-Rad, Hercules, CA) in washing buffer (0.01 M phosphate, 0.05 M NaCl, 0.1% Tween20, pH 7.2). Wells were coated with purified anti-leptin antiserum IgG (2 μg/mL in phosphate-buffered saline [PBS]) at 4°C overnight. Plasma samples (1:10, vol:vol) and standards were diluted in the blocking reagent. The biotinylated antibody was diluted (1:500) in blocking reagent. The detection limit of the assay was 62.5 pg/mL. Recovery of recombinant murine leptin (400 pg/mL) spiked in plasma samples was between 77%–96%. The intra- and interassay variations were less than 10% and 20%, respectively.

Tissue processing

Coronal cryostat sections (20 μm, prepared with a Leica CM 3050 S cryostat, Leica Microsystems, Nussloch, Germany) were prepared from several brain areas encompassing the hypothalamus (including the vascular organ of the lamina terminalis, OVLT; the ventromedial preoptic area, VMPO; the subfornical organ, SFO; the supraoptic nucleus, SON; periventricular nucleus, Pe; the arcuate nucleus, ARC; and the median eminence, ME; bregma 0.50 to −2.30 mm) and the brainstem (area postrema, AP; raphe pallidus nucleus, RPa; bregma −7.2 to −7.92 mm) according to the atlas of Paxinos and Franklin (2001). These brain areas were chosen according to a preliminary experiment where every third section of two animals of each treatment regimen (NaCl, LPS, NaCl IL6KO, LPS IL-6KO, NaCl IL-6KO LAS, and LPS IL-6KO LAS) was processed for STAT3 IHC. Every area of STAT3-activation in the hypothalamus and the brainstem of wildtype and KO mice was identified and used for further investigation of this study (data were included into the qualitative and quantitative assessment of nuclear STAT3 translocation for each treatment; see Table 3 and Fig. 5). In order to perform RT-PCR and IHC from the same brains, depending on the brain structure, 9–18 consecutive frozen sections were thaw-mounted on super frost glass slides. The remainders of the serial whole brain sections of the forebrain were collected (bregma 0.50 to −2.30 mm) and the hypothalamus dissected and used for RNA extraction.

Semiquantitative RT-PCR

Total RNA was extracted using TRIzol (Invitrogen, Burlington, Ontario) according to the manufacturer's instructions. The first-strand cDNA was synthesized from 1 μg total RNA using 200 units of Molony murine leukemia virus reverse transcriptase (Invitrogen), 5 μM of random hexamers (Applied Bioscience, Streetsville, Ontario), and 1 mM of dNTP mix (Sigma) in a total reaction volume of 20 μL. Following reverse transcription, the product was stored at −20°C. The cDNA product (0.9 μL) was added to 15 μL PCR reaction mix containing ReadyMix Taq PCR (Sigma) and 6 pmol of gene-specific primer sets for the suppressor of cytokine signaling 3 (SOCS3), cyclooxygenase (COX)2, microsomal prostaglandin E synthase (mPGES), IL-1β, inhibitor of kappa B alpha (IκBα), leptin receptor (OBr)a, OBrb, macrophage inflammatory protein 2 (MIP2), tissue inhibitor of metalloproteinase 1 (TIMP1), and glyceraldehyde 3-phosphate dehydrogenase (GAPDH) as the housekeeping gene. In each case amplification was performed with a thermal cycler (GeneAmp PCR system 9700; Applied Bioscience) using the following cycling parameters: 1) denaturing, 95°C for 5 minutes; 2) amplification cycle, 95°C for 30 seconds, annealing temperature for 30 seconds, and 72°C for 1 minute; 3) final extension, 72°C for 10 minutes. Primers were designed to span a sequence derived from different exons (separated by an intron in genomic DNA sequence) in order to minimize amplification from non-mRNA-derived templates. Inappropriate amplification from genomic DNA was negligible when amplification was performed with a template without reverse transcription. The gene accession numbers, primer sequences, annealing temperatures, and cycle numbers used are listed in Table 1. PCR products were separated by 2% agarose gel electrophoresis and visualized with ethidium bromide staining. The band density was obtained for quantification using GeneTool image analysis software (Syngene, Frederick, MD). To normalize the expression level of genes between different samples, the levels were estimated as the ratio of geneX/GAPDH. In a pilot experiment the amount of PCR product (on a log scale) versus the number of cycles was plotted, and the linear range of template amplification was determined for two samples from each treatment group. The cycle numbers were determined to be within the exponential phase of amplification for all treatment groups.

Immunohistochemistry

General procedure. On the day of the experiment the frozen brain sections were briefly air-dried at room temperature for 5 (for STAT3) or 10 (for COX2 and NF-κB) minutes and then immersion-fixed in 2% paraformaldehyde diluted in 0.1 M PBS (pH 7.4) for 10 minutes at room temperature (RT). Following three successive washes in PBS the sections were treated for 1 hour at RT with a blocking solution consisting of PBS, containing 10% normal donkey serum (NDS; Chemicon International, Temecula, CA) and depending on the type of applied antibodies, 0.1% or 0.25% Triton X-100. Details of the primary antibody concentrations and blocking procedures are shown in Table 2.

The sections were incubated with the primary antibodies for 24 hours at 4°C followed by three successive washes in PBS and visualization with CY3-conjugated antirabbit IgG (for STAT3 and COX2; 1:500 dilution; cat. no. 711-165-152) or CY3-conjugated antigoat IgG (for NF-κB; 1:500; cat. no. 705-165-147). All secondary antibodies were raised in donkey and all were multiple-labeling grade (Jackson ImmunoResearch, West Grove, PA). Sections were counterstained with the nuclear DAPI stain (Molecular Probes, Eugene, OR) for 15 minutes, using a 1:4,000 dilution in PBS to assess the nuclear localization of the STAT3 and NF-κB signals and to give better visualization

TABLE 1. Primer Sets and Conditions Used for RT-PCR

Primer Sets	Primer Sequences: Sense, Antisense	Annealing Temperatures and Cycle Numbers	Gene Accession Number
SOCS3	5'-CTTACGACCGCTGTCTCTCC-3' 5'-GGTACTCGCTTTTGGAGCTG-3'	61°C, 36	NM_007707
COX2	5'-AGCCAGGCAGCAAATCCT-3' 5'-GGGGTCAGGGATGAACTCTC-3'	57°C, 36	NM_011198
mPGES	5'-TTTCTGCTCTGCAGCACACT-3' 5'-GAGAACTGGGCCAGGACATA-3'	62°C, 34	NM_023415
IL-1α	5'-GTTGACGGACCCAAAAGAT-3' 5'-GGGTGTGCCGTCTTTCATTA-3'	57°C, 32	NM_008361
IκBα	5'-AGACTCGTTCCTGACCTT-GG-3' 5'-AGGTATGCGTCAAGACTGCT-3'	60°C, 40	NM_010907
OBra	5'-ACACTGTTAATTTCACACCAGAG-3' 5'-AGTCATTCAAACCATAGTTTAGG-3'	59°C, 36	AF304191
OBrb	5'-ACACTGTTAATTTCACACCAGAG-3' 5'-TTCCAAAAGCTCATCCAACCC-3'	59°C, 36	NM_012596
GAPDH	5'-ACTCCACTCACGGCAAATTC-3' 5'-GGATGCAGGGATGATGTTCT-3'	57°C, 28	NM_008084
ICAM1	5'-CCTGCAATGGCTTCAACC-3' 5'-CACTCTCCGGAAACGAATACA-3'	60°C, 32	NM_010493
MCP1	5'-GCCTCAGCCAGATGCAGT-3' 5'-GCTGAAGACCTTAGGGCAGA-3'	60°C, 32	NM_011333
MIP2	5'-GAAGTCATAGCCACTCTCAAGG-3' 5'-CAACATCTGCGCAATGGA-3'	60°C, 36	NM_009140
TIMP1	5'-AACTCGGACCTGGTCATAAGG-3' 5'-AAGAAGCTGCAGGCACTGAT-3'	60°C, 36	NM_011593

TABLE 2. Conditions for the Primary Antibodies Used for Immunohistochemistry

Antigen	Immunogen	Blocking /Triton X-100	Species, Type (Dilution Used, Catalog Number, Manufacturer)
STAT3	Synthetic peptide, aa 750-769, C-terminus, mouse origin	0.1%	Rabbit polyclonal IgG (1:9000; cat. sc-482; Santa Cruz Biotechnology, CA)
COX2	Corresponding to aa 584-598 of mouse origin COX2	0.25%	Rabbit polyclonal IgG (1:2000; cat. 160126; Cayman Chemical, Ann Arbor, MI)
NF-κB	Synthetic peptide, aa 531-550, C-terminus, human origin	0.1%	Goat polyclonal IgG (1:500 cat. sc-372 G; Santa Cruz Biotechnology, CA)
vW	Purified rat plasma von Willebrand factor	0.1, 0.25%	Sheep polyclonal IgG (1:5000; cat. SARTW-IG; Affinity Biologicals, Ancaster, Ontario, Canada)
vW	Purified human plasma von Willebrand factor	0.1%	Rabbit polyclonal IgG (1:3000; cat. A0082; Dako Canada, Inc., Mississauga, Ontario, Canada)

of the tissue surrounding the signal. Finally, all sections were coverslipped using an equal mix of glycerol/phosphate buffer solution and stored at 4°C until microscopic analysis was performed.

STAT3. A rabbit anti-STAT3 antibody was used to detect STAT3 signals in the mouse brain. This antibody was raised against C-terminus of the STAT3 polypeptide (Matthews et al., 2007) and recognizes both the phosphorylated (activated) and the nonphosphorylated (constitutive) forms of the transcription factor. This antibody was previously demonstrated to be specific in the rat and guinea pig brain (Hübschle et al., 2001a; Rummel et al., 2004) with an almost identical staining pattern as described for mice in the present study. Obtained results on the STAT3 distribution pattern in the mouse brain using this antibody are further substantiated by another study using in situ hybridization of SOCS3. This is a major endproduct of the STAT3 signaling pathway, which is involved in autoregulatory feedback for activated STAT3 and is broadly used as a marker for STAT3-activation (Lebel et al., 2000). Western blot analyses using the same antiserum for rat brain tissue (Gautron et al., 2006) or a mouse cell line (manufacturer's datasheet) revealed a single band at 85/86 kD, respectively.

COX2. The rabbit anti-COX2 antibody was raised against a peptide of murine COX2 (Table 2, manufacturer's datasheet). The antibody shows specific staining of this enzyme as seen in the present study typically at a perinuclear subcellular localization in the rat and mouse brain but not in brains of mice deficient in COX2 (Li et al., 1999; Yamagata et al., 2001). The COX2 antiserum recognizes a single band on Western blot of the rat brain (Mouihate and Pittman, 2003) or a mouse cell line (72 kD, manufacturer's datasheet).

NF-κB. As for STAT3, the goat anti-NF-κB antibody used in our studies recognizes both cytoplasmic (inactive) and nuclear (active) forms of the peptide (see Table 2 for sequence) (Dejardin et al., 1999). Specifically, this antibody targets the inactive p65 subunit in the cytoplasm (bound to p50 and IκB) as well as the active monomeric or dimeric form in the nucleus. Using IHC it shows a specific staining pattern of cytoplasmic and activated nuclear immunoreactivity (IR) in the rat and mouse brain including endothelial cells identical to what was observed in the present study (Nadjar et al., 2003; Rummel et al., 2006). This antiserum recognizes a single 65-kD band on Western blots of the mouse brain (Nadjar et al., 2003).

Specificity of each antibody in the present study (STAT3, COX2, and NF-κB) was confirmed by preabsorption with the respective blocking peptides (data not shown).

von Willebrand factor

Both specific cell marker antibodies against von Willebrand factor (vW; A 0082, SARTW-IG) have been extensively used for characterization of endothelial cell phenotypes in mice, guinea pigs, and rats and produce a cytoplasmatic staining pattern with the classic morphol-

ogy and distribution of brain endothelial cells that is identical to the vW-IR observed in the present study (Yamamoto et al., 1998; Konsman et al., 2004; Rummel et al., 2005). The antiserum A 0082 (Dako, Carpinteria, CA) shows one precipitate by crossed immunoelectrophoresis against human plasma and cross-reacts with the mouse equivalent of vW by IHC (manufacturer's datasheet). In situ hybridization of vW mRNA expression in the mouse brain confirmed the characteristic staining pattern observed by IHC (Yamamoto et al., 1998). Specificity of the SARTW-IG antiserum (Affinity Biologicals, Ancaster, Ontario) was demonstrated for rat vW by immunoelectrophoresis and ELISA (manufacturer's datasheet).

Colocalization studies

To identify endothelial cells, double IHC was performed using vW. Virtually every section used for qualitative and quantitative analyses of STAT3-activation and COX2- or NF-κB-staining was colocalized with vW. However, for clarity double-staining and DAPI counterstain is not shown in Figures 2–4 in all cases, as it would have masked the overall effect, which would have made it difficult to discern any differences between the treatment groups on STAT3-activation. The antibodies for STAT3/COX2 or NF-κB were mixed with a sheep antirat vW factor antibody (1:3,000; Cat. no. SARTW-IG; Affinity Biologicals) or a rabbit antihuman vW factor antibody (1:3,000; Cat. no. A0082; Dako Canada, Mississauga, Ontario), respectively, and brain sections were incubated with the primary antibodies at 4°C for 36–48 hours. STAT3/COX2 or NF-κB were visualized with CY3-conjugated antirabbit IgG or CY3-conjugated antigoat IgG (1:500 dilution each; Cat. no. 705-165-147 or 711-165-152) and vW with FITC-conjugated antisheep IgG (1:500 dilution; Cat. no. 713-095-147) as secondary antibodies. In control experiments the sections were incubated with the primary antibody mixture in which one of the primary antibodies was substituted with nonimmunized animal IgG (rabbit IgG for STAT3, vW and COX2, goat IgG for NF-κB, sheep IgG for vW). Inappropriate cross-reaction between antibodies was confirmed to be negligible.

Microscopic analysis

Sections were analyzed using a conventional light/fluorescent Zeiss-Axioplan microscope (Nussdorf, Germany) equipped with the appropriate filter sets to detect the fluorescent conjugates Cy3, FITC, and DAPI. Images were taken with a black-and-white digital camera (Retiga Mono Digital 1300 CCD). Image editing software (Northern Eclipse, Empix Imaging, Mississauga, Ontario; Adobe Photoshop 5.5, San Jose, CA) was used to adjust brightness and contrast and to combine the individual images into the RGB color figure plates. Digital mouse brain maps were arranged by adjustment of corresponding mouse brain levels taken from the digital mouse brain map atlas of Paxinos and Franklin (2001).

The quantitative data are presented as means ± SEM for the cortex, meninges, ependyma, the sensory CVOs (OVLT, SFO, AP), the VMPO, SON, and RPa (Fig. 5). In accordance with previous qualitative and quantitative STAT3 data published by our group in the rat and guinea pig brain (Rummel et al., 2005, 2006), nuclear STAT3 signals were either very sporadic or nondetectable in the structures of saline-treated control animals and are therefore, for representation purposes, set to the level of 1 for

TABLE 3. Qualitative Analysis of Nuclear STAT3 Translocation in the Mouse Brain

Selected Brain Structures	Nuclear STAT3 Expression					
	NaCl	LPS	NaCl	LPS	NaCl	LPS
	Wildtype		IL-6KO		IL-6KO LAS	
Hypothalamus and preoptic area						
Ventromedial preoptic nucleus	-	++	-	++	-	+
Supraoptic nucleus	-	+++	-	++	-	+
Periventricular nucleus		+++	-	+		+
Median preoptic nucleus		+	-	-	-	
Paraventricular nucleus	-	+	+	+	-	-
Arcuate nucleus	+	++	±	+	-	+
Circumventricular organs						
Vascular organ of the lamina terminalis	-	+++	-	++	-	+
Subfornical organ	-	++	-	++	-	++
Area postrema	±	+	-	+	-	+
Median eminence	±	+	±	+	-	-
Brainstem						
Nucleus of the solitary tract	-	+	-	-	-	-
Raphe pallidus nucleus	-	+++	-	++	-	±
Others						
Meninges	-	+++	±	+++	-	+
Endothelial cells capillaries	±	+++	-	±	-	+
large vessels	-	+++	-	++	-	+
Ependymal lining of ventricles	-	+++	-	++	-	+
Choroid plexus	-	+++	-	-	-	-

Relative values of nuclear STAT3 immunoreactivity are given as estimates for the density of their respective labeling. Analyses were performed 3 hours after i.p. injection of LPS (50 μg/kg) or saline (5 mL/kg, NaCl) in wildtype (n = 9), IL-6KO (n = 7), and IL-6KO mice treated with leptin antiserum (LAS, n = 7) in the forebrain and the brainstem.

A five-point scale was used to rate the data: +++ = high density of nuclear signals, ++ = moderate density, + = low density, ± = single nuclear signals in some cases, - = no nuclear signals.

Figure 5 (see also Table 3). Cell counts were performed on photomicrographs that were taken with a 20-fold (for the cortex) or 40-fold (for all other brain areas) objective lens using the Northern Eclipse imaging software. These photomicrographs were taken of brain areas at corresponding localizations as indicated in the overviews of Figures 2–4 and represented adequate cutouts of the respective brain region with the same size. Two to four sections per animal were analyzed for each of the three LPS-treated groups (each n = 4–7). Thus, the final data represent means (n = 2–4) of the means (n = 4–7) ± SEM. The number of all spot-like nuclear STAT3 signals defined by their size and light intensity was determined using an automatic counting facility of Scion Image (NIH image analyses software, 4.0.2 of Scion Image, Scion, Frederick, MD) within the photomicrographical frame. In addition, the counting area was outlined when counting meningeal and ependymal cells to demarcate these brain areas / cell types from surrounding neuropil. Obvious artifacts due to dust or air bubbles were excluded from the area for automatic counting.

Data analysis

Circulating levels of leptin, semiquantitative data on nuclear STAT3 translocation and the relative density of SOCS3, COX2, mPGES, IL-1β, IκBα, OBra, OBrb, MIP2, and TIMP1 expression in the hypothalamus were compared separately between the experimental groups (NaCl,

LPS, NaCl KO, LPS KO, NaCl KO LAS, and LPS KO LAS) by one-way analysis of variance (ANOVA) followed by Newman–Keuls multiple comparisons post-hoc test. We also investigated potential correlations (Pearson) between individual values of the respective relative density of the RNA signals COX2/mPGES to SOCS3/IκBα in the hypothalamus (n = 34 for each correlated gene). GraphPad Prism 4 software (San Diego, CA) was used for all statistical analyses. *P*-values less than 5% were deemed significant. All data are presented as mean values ± SEM.

RESULTS

IL-6 and leptin contribute to LPS-induced nuclear STAT3 translocation in a distinct manner

As previously shown for the rat and the guinea pig (Rummel et al., 2005), LPS (50 μg/kg i.p.) induced a dramatic increase of nuclear STAT3 translocation 3 hours after injection widely distributed throughout the brains of wildtype mice (Table 3; Fig. 1A,D,G,J). The majority of STAT3-expressing cells in the brain parenchyma was observed along large vessels and capillaries, as indicated with black line drawings in Figure 1 (see also Fig. 2D,d). These structures were found to be almost entirely vW-positive endothelial cells, an observation that confirmed our earlier reports in guinea pigs and rats (Rummel et al., 2005). An exception was observed along larger blood vessels where some STAT3-positive IR were vW-negative (Fig. 2d). This most likely constitutes STAT3-activated astrocytes surrounding blood vessels as shown previously (Rummel et al., 2005). In addition to these structures, STAT3-signals were observed in several specific brain areas. Strong nuclear STAT3 translocation was found in cells of the meninges, some, but not all, of which were in endothelial cells (Fig. 2j). In addition, the Pe showed robust STAT3-activation in vW-negative ependymal cells that were defined by their morphology and their neuroanatomical localization lining the ventricles (Fig. 2P,p). Other activated regions included the sensory CVOs, namely, the OVLT, the SFO, and the AP, as well as other structures such as the VMPO, the SON, and the RPa (Fig. 3-4,D,J,P). In these structures (OVLT, SFO, AP, VMPO, SON, and RPa), only ≈20% of STAT3-postive cells were also vW-positive. Similar results were obtained in our previous study in guinea pigs (Rummel et al., 2005). In this study, in addition we observed that astrocytes constituted 20% of all STAT3-responsive cells in the OVLT and SFO and 80% in the AP, suggesting that astrocytes might also contribute to the LPS-induced STAT3-activation in the present investigation for the respective brain structures in mice (OVLT, SFO, AP, VMPO, SON, and RPa), as suggested previously by others using rats (Gautron et al., 2002).

The LPS-induced nuclear STAT3 translocation observed in wildtype animals was dramatically attenuated in IL-6KO mice (Table 3; Fig. 1), confirming the major role of IL-6 in mediating LPS-induced brain STAT3 activation (Rummel et al., 2006). Surprisingly, however, a significant amount of remnant STAT3 activation was still observed in IL-6KO mice. In addition, the reduction of STAT3 activation in IL-6KO mice varied depending on the brain structure. STAT3 activation in capillaries of the brain parenchyma, for example, almost entirely disappeared in IL-6KOs (Figs. 1, 2D,E,J,K). Brain area/structure-specific qualitative analysis revealed that STAT3 activation was dramatically decreased in IL-6KOs compared to wildtype mice in the SON, the Pe, the median preoptic nucleus (MnPO), paraventricular nucleus (PVN), the ARC, the OVLT, the nucleus of the solitary tract (Sol), the RPa, large vessels, ependymal lining of ventricles, and the choroid plexus (Table 3; Figs. 1, 2E,Q, 3E, 4K,Q). The reduction was relatively smaller but significant in the SFO and the VMPO (Figs. 3K, 4E, 5E,G). In contrast, IL-6KO mice showed, both quantitatively and qualitatively, almost intact STAT3 activation in the AP, ME, and cells in meninges (wildtype vs. IL-6KO; Table 3; Figs. 2J,K, 3P,Q). In addition to these areas, remnant STAT3 expression in IL-6KO animals was observed in large blood vessels and the ependymal lining of the cerebral ventricles (Fig. 2E,Q). The distribution of nuclear STAT3 translocation in the large blood vessels of these animals followed a very specific pattern surrounding the third ventricles and the cortical bifurcation of the two brain hemispheres as documented in Figure 1.

We then examined if the remnant STAT3 activation in IL-6KO mice is mediated by leptin, by neutralizing its action in vivo with a specific antiserum. LAS treatment in LPS-stimulated IL-6KO mice significantly attenuated or, in some cases, abolished the remaining STAT3 activation. As with IL-6 the contribution of leptin to this response (LPS-induced STAT3-activation) was brain area/structure-specific and included large blood vessels, cells in meninges, the ependymal linings of all ventricles (Fig. 1, right column; Fig. 2F,L,R) as well as the OVLT, the VMPO, the SON, and the RPa (Figs. 3F, 4F,L,R). However, only a weak contribution of leptin to the LPS-induced STAT3-activation was detected in the ARC and capillaries in the cerebral cortex (Table 3) and very little or no activation in the PVN, the MnPO, the SFO, the AP, the ME, the Sol, and the choroid plexus (Table 3; Figs. 1E,F,K,L, 3K,L,Q,R). Saline-injected controls only exhibited cytoplasmic (inactive) STAT3 or occasionally very few nuclear STAT3-positive cells in the ARC or the ME (Table 3; Figs. 2–4).

Figure 5 shows the results of semiquantitative analysis for the amount of STAT3 translocation in different brain structures of wildtype, IL-6KO, and IL-6KO mice treated with LAS. Overall, the results confirm the qualitative data described above (Table 3; Figs. 1–4); leptin, as well as IL-6, contributed to the LPS-induced nuclear STAT3 translocation in specific brain structures/areas. IL-6 deficiency significantly diminished the nuclear STAT3 translocation in most of the structures/areas analyzed (cortex, ependyma, OVLT, SFO, VMPO, SON, and RPa), while having no affect on STAT3 activation in the meninges and the AP. Neutralization of leptin in IL-6KO mice further attenuated nuclear STAT3 translocation in all the structures/areas where IL-6 deficiency affected this response, except for the SFO. Interestingly, in the meningis, leptin blockade combined with IL-6 deficiency, but not IL-6 deficiency alone, almost totally abolished STAT3 translocation. Lastly, in the AP, nuclear STAT3 translocation was not affected by either IL-6 deficiency or leptin blockade in IL-6KO animals.

Using semiquantitative RT-PCR we were, in addition, able to confirm the contribution of IL-6 and leptin to the LPS-induced activation of the JAK-STAT pathway by measuring the change in expression of SOCS3 mRNA

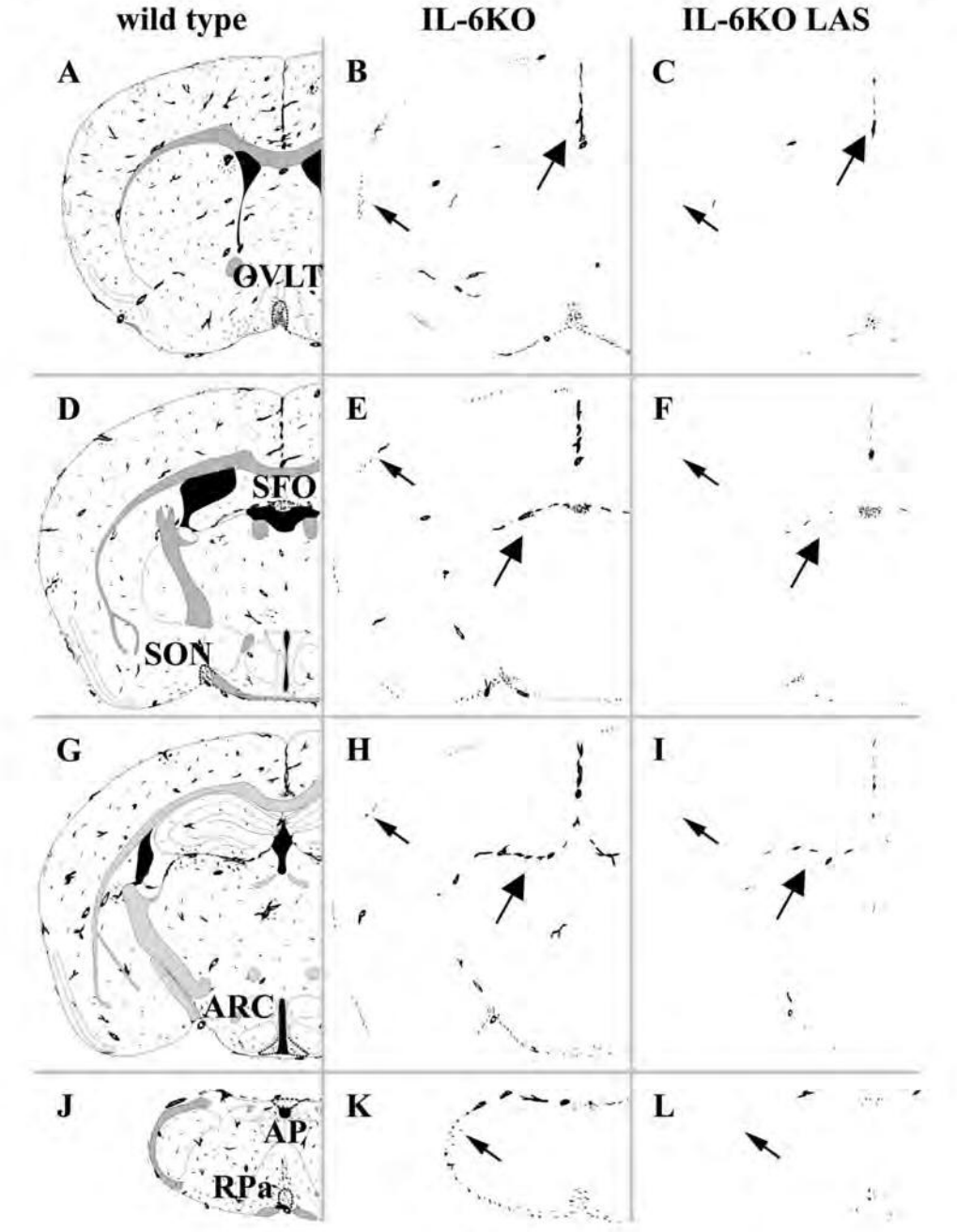

wild type
IL-6KO
IL-6KO LAS
A
B
C
OVLT
D
E
F
SFO
SON
G
H
I
ARC
J
K
L
AP
RPa

Figure 1

(Fig. 5J; $P < 0.01$). Interestingly, saline-treated IL-6KO animals presented a lower basal level expression of SOCS3 mRNA compared to their wildtype counterparts (Fig. 5J; $P < 0.01$). LAS did not modify this effect any further.

LPS-induced hypothalamic COX2 and mPGES but not IL-1β/IκBα mRNA expression is attenuated in IL-6KO mice

As expected, LPS induced a significant increase of COX2 and mPGES mRNA expression in the hypothalamus of wildtype animals (Fig. 6A,B; $P < 0.001$) as well as IHC staining of COX2 protein (Fig. 7D). In the LPS-stimulated IL-6KO mice COX2 and mPGES mRNA levels were significantly reduced, thus confirming our earlier published observation linking endogenous IL-6 with COX2, although no clear reduction of COX2-IR could be detected in the present study (Fig. 7D,E). This, however, may be due to the different route of LPS injection used in the present study (i.p.) compared to a localized (intrapouch) one in our earlier experiments (Rummel et al., 2006). Treatment of the IL-6KO animals with LAS did not reduce COX2-IR, at least not dramatically (Fig. 7F), and had no significant effect on COX2 mRNA expression (Fig. 6A). COX2-IR was absent in control animals (Fig. 7A–C).

It is known that other than the STAT3-signaling mediators IL-6 and leptin, NF-κB-signaling cytokines such as IL-1β play an important role in the induction of COX2 and mPGES (Nadjar et al., 2005; Pecchi et al., 2006). In order to investigate the contribution of IL-1β to the induction of COX2 and mPGES mRNA expression we performed RT-PCR for IL-1β and for IκBα mRNA, which is used as a marker for the activation of the NF-κB signaling pathway (Laflamme and Rivest, 1999). Administration of LPS resulted in a significant induction of IL-1β/IκBα mRNA in the hypothalamus (Fig. 6C,D; $P < 0.01$). Neither IL-1β nor IκBα was altered in IL-6KO mice or by LAS treatment in comparison to their wildtype counterpart controls. This observation was further confirmed using IHC, as nuclear NF-κB translocation was not significantly different between the three LPS-treated groups (Fig. 7J–L). Nuclear translocation of NF-κB was absent in control animals (Fig. 7G–I), where only cytoplasmic (inactive) NF-κB-IR was observed.

We further studied the correlation between COX2/mPGES with that of SOCS3/IκBα mRNA expression (Fig. 8A–D). Analyses of these data indicated a clear and significant correlation of both signaling pathways with the two rate-limiting enzymes of the prostaglandin synthesis pathway. Possibly, SOCS3 represents a better indicator (Fig. 8A,B) than IκBα (Fig. 8C,D), in particular for mPGES-induction in the hypothalamus (Fig. 8B). This observation provides additional support for the link between the transcription factor STAT3 and the production of PG in concert with the well-known role of NF-κB in this effect.

LAS abrogates circulating leptin levels, significantly upregulates OBra, but has no effect on OBRb mRNA expression in the mouse hypothalamus

Previously it was reported that circulating leptin levels rise during LPS-induced systemic inflammation in mice (Sarraf et al., 1997; Berkowitz et al., 1998; Faggioni et al., 1998; Gomez-Ambrosi et al., 2004). In the present study we observed a small but significant (2-fold) increase in plasma leptin concentrations in wildtype animals 3 hours after LPS treatment (Fig. 9A; 1.550 ± 0.314 ng/mL) compared to their saline-injected controls (0.767 ± 0.119 ng/mL, $P < 0.01$). Similar levels were reached after LPS stimulation in IL-6KO animals (1.641 ± 0.266 ng/mL). However, no significant induction of plasma leptin concentrations were detected in the IL-6KO mice. This was probably due to the fact that respective saline-treated IL-6KO animals appeared to have higher plasma leptin concentrations (1.236 ± 0.199 ng/mL) than in wildtype animals. LAS treatment completely abolished circulating leptin levels (Fig. 9A).

Proinflammatory cytokines such as IL-6 are well known for their capacity to rise dramatically during systemic inflammation. This is usually accompanied by an upregulation of its receptor expression, which has been reported to help facilitate the response of brain cells to this cytokine (Vallières and Rivest, 1997). In line with this observation, we investigated the expression of the long (OBrb, Fig. 9B) and the short form (OBra, Fig. 9C) of the leptin receptor in the hypothalamus 3 hours after LPS stimulation. The expression of these genes was not altered in LPS-stimulated wildtype or IL-6KO mice. However, LAS treatment in IL-6KO mice resulted in a significant increase of OBra expression in both the saline-treated as well as (although less pronounced) the LPS-stimulated animal groups (Fig. 9C; $P < 0.001$ or $P < 0.01$, respectively).

IL-6 and leptin selectively contribute to LPS-induced hypothalamic mRNA expression of molecules implicated in cell invasion processes

Mapping leptin and IL-6-mediated activation of cells in the mouse brain during LPS-induced systemic inflammation revealed a specific pattern and distribution of nuclear STAT3 translocations in cells belonging largely to the interface of the periphery to the brain (Fig. 1). This included large and small blood vessels, cells in meninges, and the sCVOs known to have a leaky BBB, in total

Fig. 1. Representative mouse brain maps, illustrating the distribution of nuclear STAT3 translocation that occurs in cells lining large and small blood vessels/cells in meninges and specific structures such as the vascular organ of the lamina terminalis (OVLT; **A–C**), the subfornical organ (SFO; **D–F**), the supraoptic nucleus (SON; D–F), the arcuate nucleus (ARC; **G–I**), the area postrema (AP; **J–L**) and the raphe pallidus nucleus (RPa; J–L) after pyrogenic LPS challenge (50 μg/kg i.p.) in wildtype (left column), IL-6KO (middle column), and IL-6KO mice (right column) pretreated with a leptin antiserum (LAS, −4 hours, 0.5 mL/mouse, i.p.). Specific brain areas showing a significant nuclear STAT3 translocation in wildtype mice are labeled and surrounded by a dashed line. The location of STAT3-responsive brain cells is schematically indicated by black line drawings onto digital mouse brain maps (A,D,G,J) as seen in 20-μm thick coronal brain section used for IHC analysis (LPS 50 μg/kg i.p., 3 hours). Note that brain endothelium is positive for STAT3-activation throughout the entire brain with no obvious prevalence for distinct brain nuclei in wildtype mice. IL-6KO mice show some remnant LPS-induced STAT3-activation in the brain along primarily large and some small blood vessels (thick black arrows), in meningeal cells (thin black arrows) and specific brain structures as indicated in the left column for wildtype mice; this response follows a specific and characteristic distribution pattern and is drastically reduced by LAS treatment in almost all areas excluding the SFO, the ARC, and the AP.

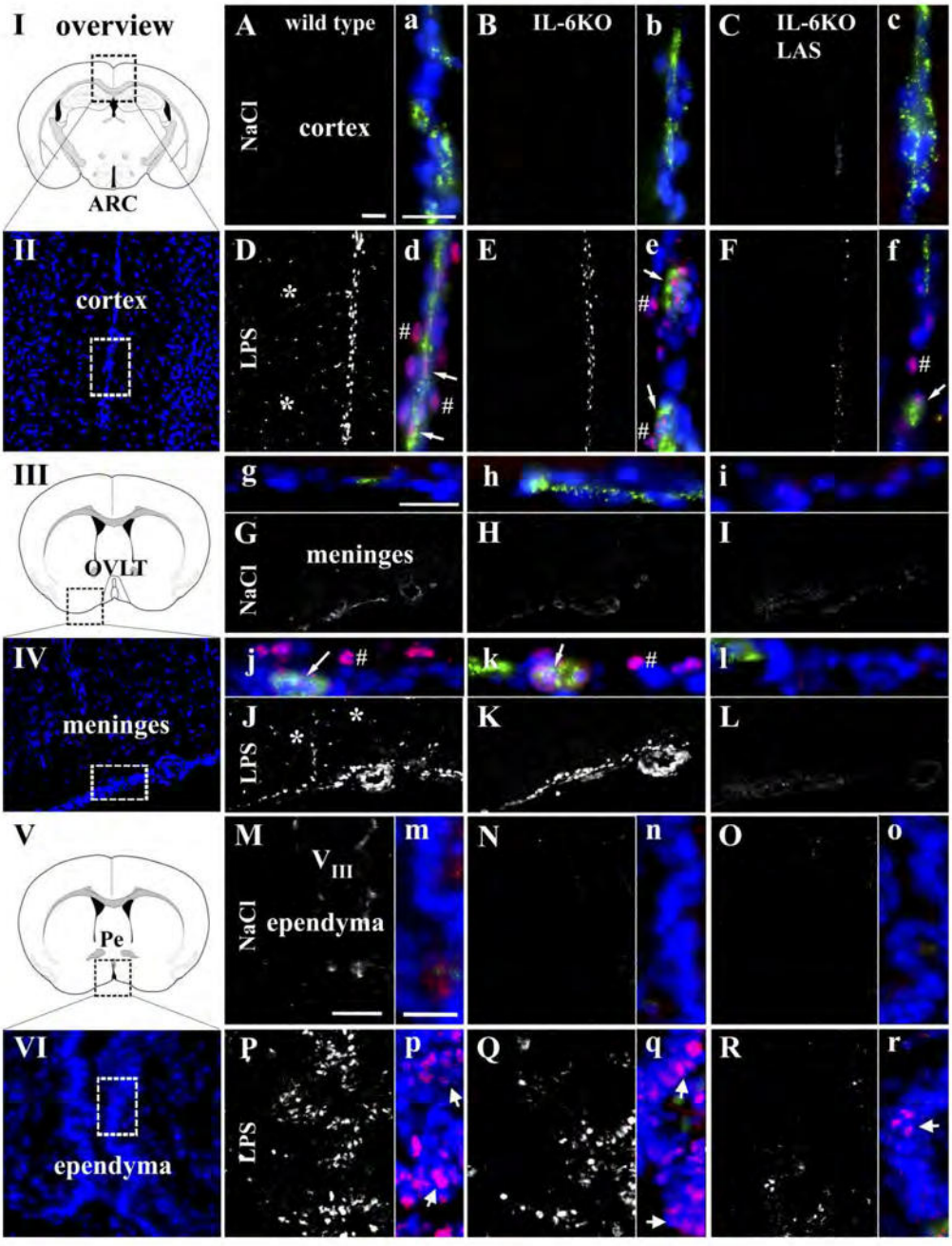

I overview
ARC
A wild type
NaCl
cortex
a
B IL-6KO
b
C IL-6KO
LAS
c
II
cortex
D
LPS
d
E
e
F
f
III
OVLT
g
h
i
G
meninges
NaCl
H
I
IV
meninges
j
k
l
J
LPS
K
L
V
Pe
M
V_{III}
NaCl
ependyma
m
N
n
O
o
VI
ependyma
P
LPS
p
Q
q
R
r

Figure 2

representing a very large surface. Functionally very important, this interface between the peripheral circulation and the brain parenchyma plays a key role in governing any type of cell trafficking or invasion from the periphery into the brain. In order to assess the contribution of IL-6 and leptin to the functional processes known to occur in this area we studied the expression of several genes known to be involved in brain invasion by immune cells. These included monocyte chemotactic protein-1 (MCP1) and the macrophage inflammatory protein 2 (MIP2), implicated in the attraction of macrophages and neutrophil granulocytes, intercellular adhesion molecule 1 (ICAM1), an important adhesion molecule for these cell types, and tissue inhibitor of metalloproteinase 1 (TIMP1), a factor regulating tissue penetration of immune cells. The analyses of mRNA expression of these four genes revealed a dramatic and significant increase 3 hours after LPS-stimulation in all treatment groups (Fig. 10A–D). For ICAM1, MCP1, and MIP2 the expression after LPS injection was significantly higher in IL-6KO animals than in their wildtype counterparts. Interestingly, only TIMP1 mRNA expression in the hypothalamus seemed to be partly IL-6-mediated, as IL-6KO mice exhibited a lower expression of this chemokine compared to wildtype animals during LPS-induced systemic inflammation (Fig. 10D). The selective contribution of leptin to this response appeared to be different from that of IL-6 for the chemokines MCP1 and MIP2, since LAS treatment significantly reduced LPS induced increases of the mRNA of both in IL-6KO mice (Fig. 10B,C). Interestingly, the LAS treatment significantly increased ICAM1 mRNA expression and decreased TIMP1 mRNA expression in IL-6KO mice (Fig. 10A,D).

DISCUSSION

In the present study we characterize for the first time the relative contribution of endogenous IL-6 and leptin in LPS-induced activation of cells in the brain of mice during systemic inflammation. We show that the role of IL-6 in immune-to-brain communication involves the activation of the STAT3-COX2-mPGES-pathway in the brain, as demonstrated previously by ourselves and others (Rummel et al., 2006; Oka et al., 2007). The contribution of leptin to this response appears to be limited to distinct areas of the brain and to specific cell types such as the OVLT, VMPO, SON, RPa, meningeal, ependymal, and endothelial cells and does not appear to involve COX2 and mPGES induction. We further provide evidence for a role of IL-6 in inducing the metalloproteinase inhibitor TIMP1, while leptin seems to contribute to the induction of TIMP1 as well as the chemokines MIP2 and MCP1. Collectively, these results indicate that IL-6 and leptin are both important players in mediating brain-controlled illness responses and do so with both overlapping and distinct mechanisms of action.

Technical considerations

Nuclear STAT3 translocation as assessed by IHC is now widely used as a method for monitoring the action of leptin and IL-6 in the brain (Hübschle et al., 2001b; Gautron et al., 2002; Harré et al., 2002; Hosoi et al., 2002; Münzberg et al., 2003; Huo et al., 2004; Münzberg et al., 2004; Rummel et al., 2004, 2005, 2006; Mütze et al., 2006). However, JAK STAT3 signaling, while constituting the main signaling pathway triggered by these immune-mediators, it is not the only one. For instance, IL-6 has been shown to activate NF-IL6 (Akira, 1997), and leptin has been reported to stimulate the mitogen-activated protein kinase cascade (MAPK), the phosphoinositide 3-kinase (PI3K), or the AMP-activated protein kinase (AMPK) pathways (Frühbeck, 2006). Thus, in the present study it is possible that these cytokines were acting on additional brain structures / cell types via pathways distinct from JAK STAT3; however, these actions are likely to be minimal compared to those involving the activation of JAK STAT.

In these studies we have, for technical reasons, opted for using genetically modified animals as the most efficient way of studying the activity of leptin in the absence of the influence of IL-6, which given its wider activity would have masked any distinct actions of leptin, especially since leptin acts on the same areas as IL-6 but to a significantly lower extent (e.g., along large blood vessels). As a consequence, and as with most studies using genetically modified animals, the results have to be treated with some caution. For example, in the present study possible compensatory changes in circulating cytokine levels in IL-6KO mice as compared to their wildtype counterpart controls have to be taken into consideration. Several reports have shown that IL-6KO mice have higher circulating tumor necrosis factor alpha (TNFα) levels after systemic stimulation with a high dose of LPS (Fattori et al., 1994; Kozak et al., 1998) and increased TNFα, IL-1β, and IL-10 plasma concentrations in a model of septic inflammation by cecal ligation (Wang et al., 2001). However, in the present study we used a moderate pyrogenic dose of LPS (50 μg/kg i.p.), and although we did not measure any of the cytokines reported to increase in the earlier studies, we did assess changes in the NF-κB signaling pathway in the hypothalamus. This was clearly not altered between the two animal strains, indicating no dramatic change in circulating cytokines such as IL-1β and TNFα, both of which activate NF-κB. Moreover, plasma leptin levels in IL-6KO mice were not significantly different from those of wildtype animals,

Fig. 2. Black-and-white pictures of the cortex **(A–F)**, the meninges **(G–L)**, and ependymal cells **(M–R)** from coronal sections at the respective level as indicated in brain maps with a dashed square in overviews I, III, and V show IHC staining of STAT3. For better visualization of the tissue surrounding the signals, one representative DAPI counterstained (blue) microphotograph for each brain structure is illustrated in overviews II, IV, and VI. LPS-induced nuclear STAT3 translocation (white spot-like pattern) 3 hours after injection in capillaries scattered throughout the parenchyma (D), along grouped capillaries (white asterisks), and larger blood vessels (D,J), meningeal (J), and ependymal cells (P) of wildtype animals; in IL-6KO mice a few remnant STAT3-stainings are observed in cells lining some small and large blood vessels (E,K), cells in meninges (K), and ependymal cells (Q), which is significantly reduced (F,R) or almost completely abolished (L) by leptin antiserum pretreatment (LAS, −4 hours, 0.5 ml/mouse, i.p.). STAT3-accumulation (red) within cell nuclei (blue DAPI stain) can be clearly depicted at high magnification (insets of d–f and j–k) in part in von Willebrand factor (vW)-positive (green) endothelial cells (thin white arrows). The locations of areas used for high magnification are indicated by a dashed square in overviews II, IV, and VI, respectively. Note that some nuclear STAT3-staining is observed in cells that do not colocalize with vW in the cortex and meninges (indicated by "#"; d–f and j–k) or do not colocalize at all with vW like in the ependyma (p–r, thick white arrow). Saline treatment (NaCl i.p.; A–C, G–I and M–O) does not induce nuclear STAT3 translocation 3 hours after the injection. ARC, arcuate nucleus; OVLT, vascular organ of the lamina terminalis; Pe, periventricular nucleus; V_{III}, third ventricle. Scale bars = 50 μm in A,M (applies to A–L or M–R); 25 μm in insets (each applies to the following high magnifications).

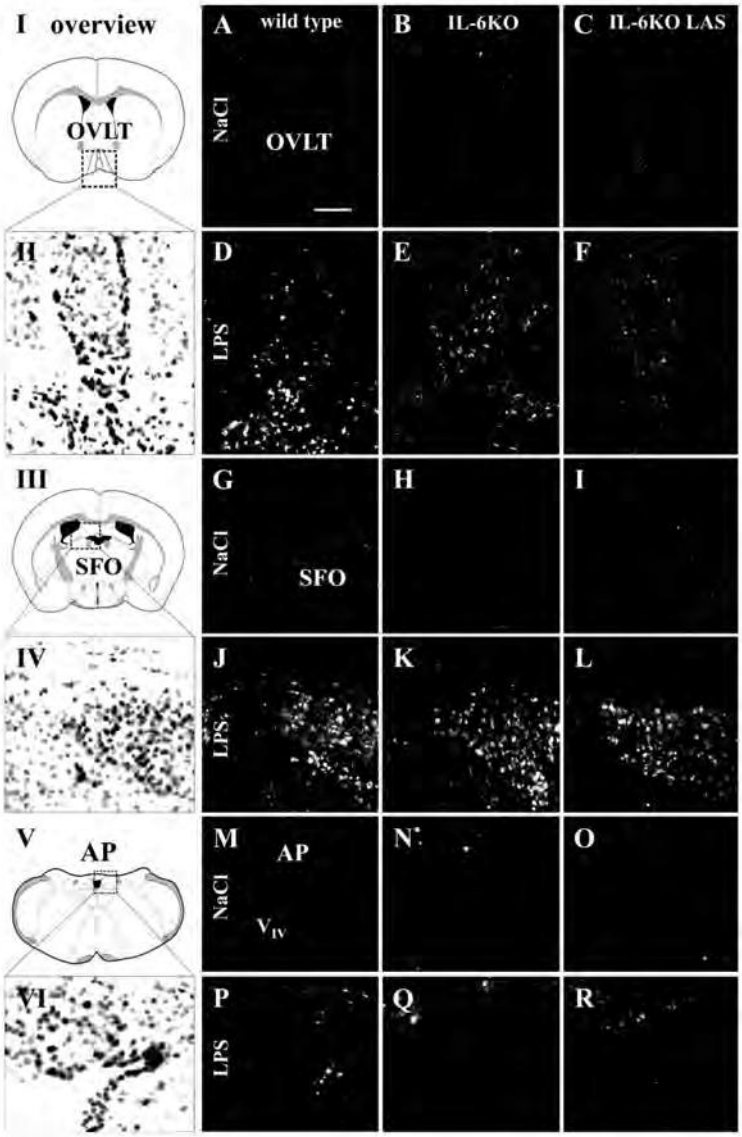


Fig. 3. Black-and-white pictures of the sensory circumventricular organs (vascular organ of the lamina terminalis, OVLT; caudal portion of the subfornical organ, SFO; cranial portion of the area postrema, AP) from coronal sections at the respective level as indicated in brain maps with a dashed square in overviews I, III, and V show IHC staining of STAT3. For better visualization of the tissue surrounding the signals, one representative DAPI-counterstained (presented in brightfield) microphotograph for each brain structure is illustrated in overviews II, IV, and VI. LPS (50 μg/kg, i.p.; **D,J,P**) induces nuclear STAT3 translocation 3 hours after injection in these brain structures of wildtype animals (white spot-like pattern); in IL-6KO mice STAT3-staining is significantly reduced in the OVLT **(E)** and further diminished by leptin antiserum (LAS, −4 hours, 0.5 mL/mouse, i.p.) pretreatment **(F)**. No obvious qualitative changes were observed between the treatment groups of LPS-stimulated animals at the level of the SFO or the AP **(J–L,P–R)**. Note that 3 hours after stimulation only very few nuclear STAT3 translocations can be depicted in the latter brain structure (P–R). NaCl-treated animals do not show nuclear STAT3 translocation **(A–C,G–I,M–O)**; occasionally, some negligible staining could be seen. V_{IV}, fourth ventricle. Scale bar = 50 μm.

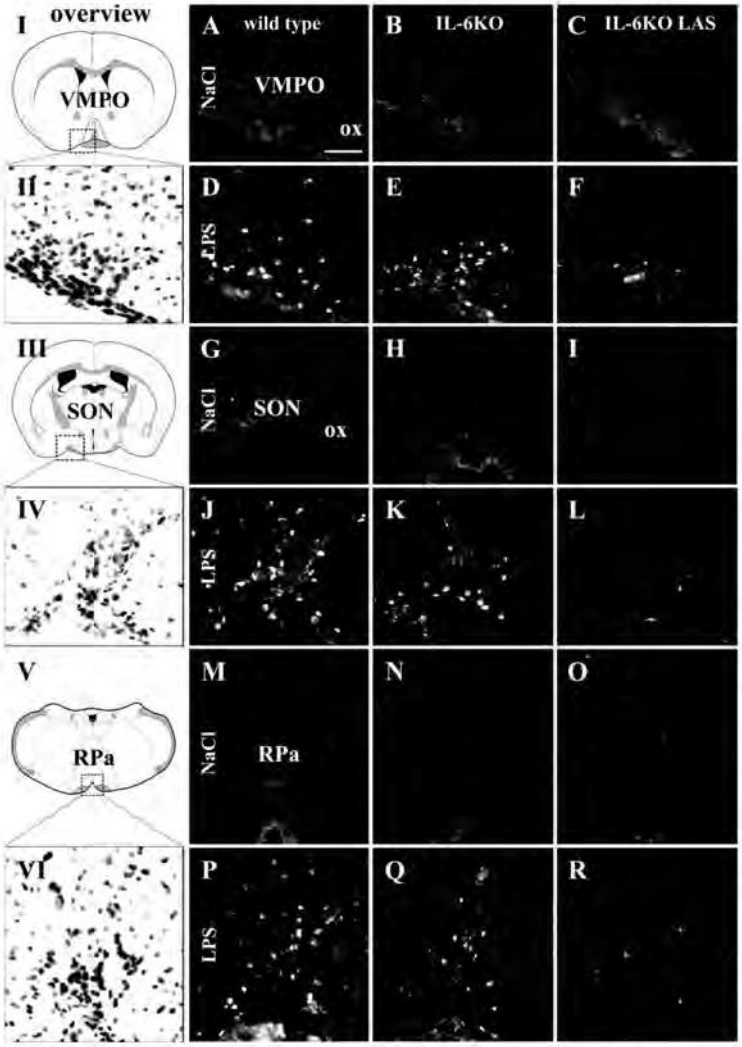


Fig. 4. Black-and-white pictures of the ventromedial preoptic area (VMPO), the supraoptic nucleus (SON), and the raphe pallidus nucleus (RPa) from coronal sections at the respective level as indicated in brain maps with a dashed square in overviews I, III, and V show IHC staining of STAT3. DAPI-counterstained (presented in bright-field) microphotographs illustrate each brain structure in overviews II, IV, and VI for better visualization of the tissue surrounding the signals. LPS (50 μg/kg, i.p.; **D,J,P**) induces nuclear STAT3 translocation 3 hours after injection in these brain structures of wildtype animals (white spot-like pattern); in IL-6KO mice STAT3-staining is reduced **(E,K,Q)** and further decreased by leptin antiserum (LAS, −4 hours, 0.5 mL/mouse, i.p.) pretreatment **(F,L,R)**. NaCl-treated animals occasionally displayed some negligible primarily cytoplasmatic staining **(A–C,G–I,M–O)**. ox, optic chiasm. Scale bar = 50 μm.

which could have significantly influenced the outcome of the present study. We therefore believe that our results were not notably influenced by compensatory changes during the inflammatory response in IL-6KO animals. There are in addition other concerns that accompany the use of genetically modified animals when investigating circulating mediators of brain STAT3-signaling. Depending on the type of KO animals, both IL-6 and leptin can become redundant. This

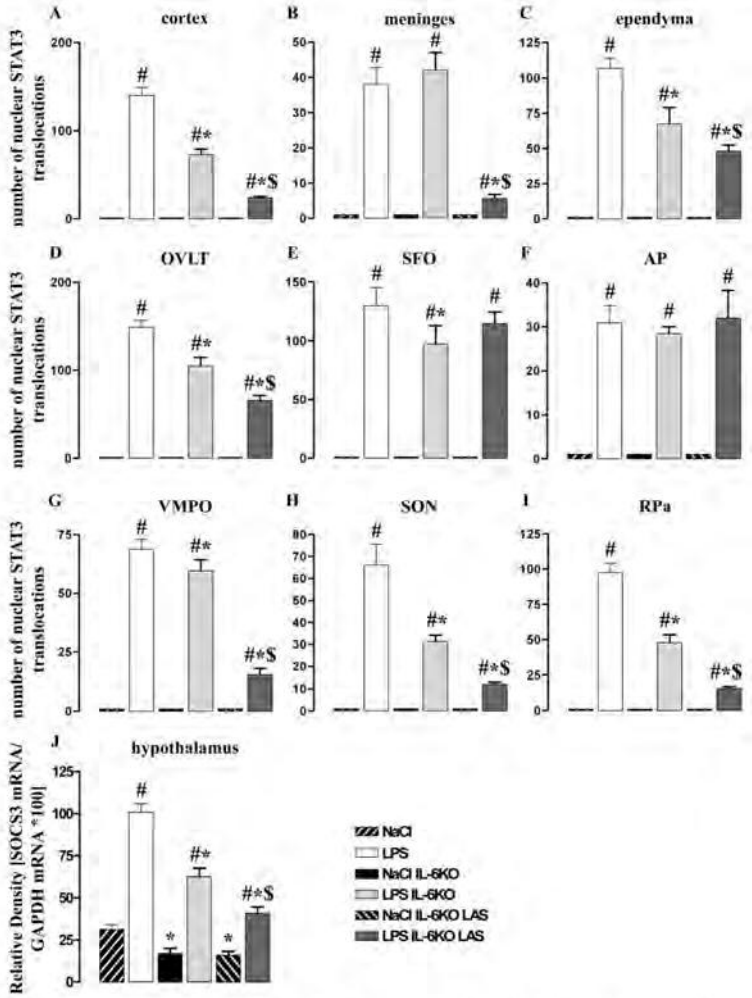


Fig. 5. **A–I:** Quantification of nuclear STAT3-immune reactivity (IR) in the cortex, meninges, ependyma, the vascular organ of the lamina terminalis (OVLT), the subfornical organ (SFO), the area postrema (AP), the ventromedial preoptic area (VMPO), the supraoptic nucleus (SON), and the raphe pallidus nucleus (RPa) of 2–4 sections per animal (each n = 4–7) per group (taken with a 20/40× objective as shown in the overview by a dashed line of Figs. 2–4) shows a significant increase in LPS (50 μg/kg, i.p.) treated animals 3 hours after stimulation. With the exception of meninges (B) and the AP (F), this response was reduced in IL-6KO mice. Remnant STAT3-activation in IL-6KO mice was further decreased after leptin antiserum (LAS, −4 hours, 0.5 mL/mouse, i.p.) treatment in every brain structure but the SFO and the AP. Occasionally, NaCl treatment resulted in very few STAT3-IR positive nuclei. For better presentation purposes, the values of these control animals were set by default as one. **J:** Injection of LPS (50 μg/kg, i.p.) induced a significant increase of SOCS-3 mRNA expression in the hypothalamus of wildtype mice 3 hours after stimulation compared to NaCl-treated controls. This response was partially and significantly reduced in IL-6KO mice and further decreased by administration of LAS. Note that saline-injected IL-6KO animals also displayed an attenuated expression of SOCS3 relative to saline-injected wildtype mice. Values are presented as means ± SEM and statistical significance was considered as $P < 0.05$. #Different from saline-treated counterpart (e.g., LPS vs. NaCl); *different from WT mice counterpart (e.g., LPS IL-6KO vs. LPS); $different from IL-6KO mice counterpart without LAS (e.g., LPS IL-6KO LAS vs. LPS IL-6KO).

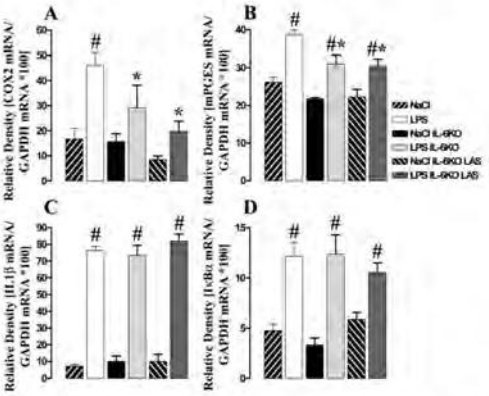


Fig. 6. Injection of LPS (50 μg/kg i.p.) induced a significant increase of COX2 **(A)**/mPGES **(B)** and IL-1β **(C)**/IκBα mRNA **(D)** expression in the hypothalamus of wildtype mice 3 hours after the injection. This induction was significantly attenuated in IL-6KO mice for COX2/mPGES. Note, leptin antiserum pretreatment (LAS, −4 hours, 0.5 mL/mouse, i.p.) in these mice did not significantly reduce COX2 or mPGES mRNA expression (A,B). IL-1β/IκBα mRNA expression was not effected in IL-6-deficient mice or by LAS treatment relative to wildtype animals (B,C). Values are presented as means ± SEM and statistical significance was considered as $P < 0.05$. #Different from saline-treated counterpart (e.g., LPS vs. NaCl); *different from WT mice counterpart (e.g., LPS IL-6KO vs. LPS).

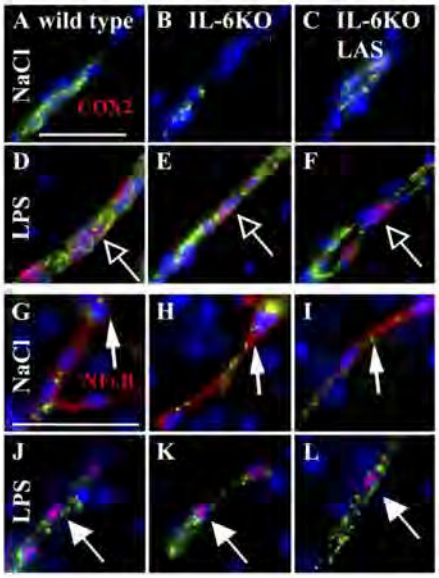


Fig. 7. LPS (50 μg/kg i.p.) induced the expression of COX2-immunoreactivity (IR) within blood vessels **(D–F)**. Strong perinuclear COX2-IR (red) is observed in von Willebrand factor (vW) positive (green) capillary endothelial cells of wildtype animals 3 hours after LPS challenge (D). This staining was still present in IL-6KO mice (E) and in IL-6KO mice treated with leptin antiserum (LAS, −4 hours, 0.5 mL/mouse, i.p.; F). Open arrows indicate COX2-positive cells. Saline treated control animals do not show any COX2-IR **(A–C)**. LPS treatment also resulted in nuclear translocation of NF-κB (p65) within blood vessels **(J–L,** large white arrows), which was not significantly different in between IL-6KO mice (K) and IL-6KO animals treated with LAS (L) relative to wildtype animals (J) 3 hours after stimulation. NF-κB accumulation (red) within cell nuclei (blue DAPI stain) can be clearly seen in vW positive (green) capillary endothelial cells. Cytoplasmic (inactive, red)-IR is observed in control animals **(G–I,** thin white arrows). Scale bars = 25 μm.

was demonstrated, for example, in macrophages of leptin-deficient animals *(obob)*, which exhibited increased IL-6 expression (Lee et al., 1999) and increased levels of circulating IL-6 in a model of zymosan-induced arthritis (Bernotiene et al., 2004). These observations suggest that the use of *obob* mice as opposed to LAS in studies such as ours may be difficult to interpret since circulating IL-6 in the *obob* mice will more than likely compensate for the absence of leptin when mediating LPS-induced STAT3 activation in the brain. Another complication associated with the use of leptin or leptin receptor *(dbdb)* deficient mice is the fact that they develop a number of metabolic phenotypes that might significantly alter the immune response to infection and inflammation (Ikejima et al., 2005; Palmer et al., 2006).

Given these concerns, the use of acute neutralization with antisera, we believe, affords a better strategy for isolating the contribution of leptin in the absence of IL-6. Even though unknown serum factors (binding proteins or low levels of IL-6) may modify the immune response of the host, we believe that these are minimal, and indeed we have no evidence showing that this was the case in our study, as mice treated with LAS alone exhibited no obvious signs of inflammation.

IL-6 contributes to LPS-induced STAT3 translocation during immune-to-brain communication

We confirmed the findings of our group and others on LPS- (Gautron et al., 2002; Harré et al., 2002; Rummel et al., 2004, 2005) and IL-6- (Harré et al., 2002; Rummel et al., 2005) induced STAT3-activation in rats and guinea pigs for the mouse brain 3 hours after systemic stimulation in various structures and cell types. There are, however, some differences between data obtained with previous approaches and the results from the present study, but these are most likely due to timepoints, species used, and routes of LPS injection. Using a model of localized inflammation, we previously reported that LPS-induced nuclear STAT3 translocation appeared to be almost entirely mediated by circulating IL-6 (Rummel et al., 2006), whereas in the present study during systemic LPS-stimulated inflammation in IL-6KO mice we observed a significant amount of remnant STAT3-activation in several brain structures / cell types (meningeal cell, cells lining the vasculature, some ependymal cells, the sCVO, the VMPO, SON, Pe, ARC, and RPa). Notably, the same observation was previously made for JAK STAT3-activation in the liver (Alonzi et al., 1998). The authors of that study showed that in another model of localized inflammation, turpentine-induced STAT3-activation was absent in IL-6KO mice but only slightly altered when LPS was injected systemically. Interestingly, LPS does not

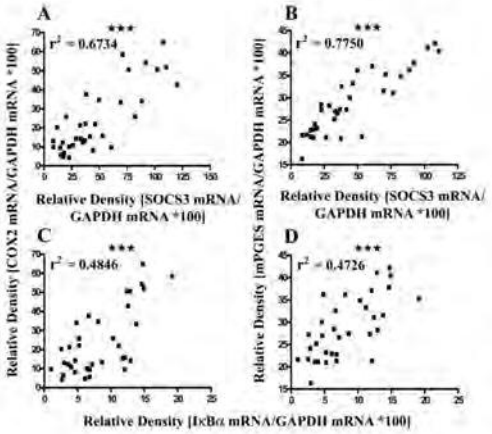


Fig. 8. Correlation analysis was performed for COX2/mPGES mRNA with SOCS3/IκBα mRNA expression in the mouse hypothalamus. LPS treatment (50 μg/kg, i.p.) induced a rise of COX2/mPGES mRNA expression, which correlates significantly with SOCS3/IκBα mRNA expression in the hypothalamus from all individual pairs of values ($n = 34$, black squares) of mice 3 hours after the injection **(A–D)**. Note that the two enzymes COX2 and mPGES, implicated in the prostaglandin synthesis pathway, are more closely related to the JAK-STAT signaling pathway as indicated by SOCS3 mRNA expression (A,B) than to the NF-κB signaling pathway (illustrated by IκBα mRNA expression, C,D), which is well known to be the main intracellular pathway for the transcription of these enzymes. ($^{***}P < 0.001$, r^2 = coefficient of correlation).

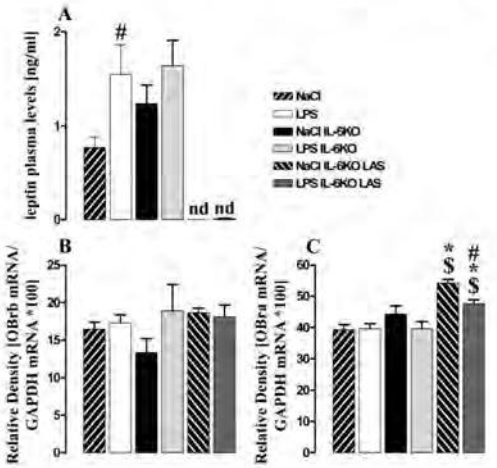


Fig. 9. **A:** Leptin levels measured using ELISA 3 hours after injection of LPS (50 μg/kg i.p.) in plasma are shown in wildtype mice compared with IL-6KO animals relative to IL-6KO animals treated with leptin antiserum (LAS, −4 hours, 0.5 mL/mouse, i.p.) or respective saline controls. A significant increase of circulating leptin was only observed in wildtype mice after LPS challenge. Note that LAS treatment abolished plasma leptin levels to values beneath the detection limit (not detected, n.d.). The mRNA expression of the long form (**B,** OBrb) and the short form (**C,** OBra) of the leptin receptor was not altered by LPS treatment or in the absence of IL-6 (IL-6KO). LAS treatment resulted in an overall increase of OBra but not OBrb mRNA expression. This effect was significantly attenuated by LPS-stimulation. Values are presented as means ± SEM and statistical significance was considered as $P < 0.05$. *Different from saline-treated counterpart (e.g., LPS vs. NaCl); #different from WT mice counterpart (e.g., LPS IL-6KO vs. LPS); $different from IL-6KO mice counterpart without LAS (e.g., LPS IL-6KO LAS vs. LPS IL-6KO).

reach the circulation in the airpouch model and is not readily detected in febrile animals from models of localized inflammation induced by turpentine nor after systemic IL-6 treatment (Cartmell et al., 2000, 2001; Ross et al., 2003; Turnbull et al., 2003). This is in contrast to the present study, where LPS was injected systemically and therefore LPS itself can reach the brain through the humoral route. Thus, direct activation by LPS could account for some of the remaining STAT3 activation in the brain that was observed in the present study. Although the main effects of LPS are predominantly mediated through the NF-κB signaling pathway, some evidence supports the idea for a direct activation of JAK STAT (Bode et al., 1999; Dalpke et al., 2003; Shoenfelt and Fenton, 2006). The receptor transcripts for LPS are present on cells within the sCVOs, endothelial cells, and meninges (Laflamme and Rivest, 2001; Chakravarty and Herkenham, 2005). A direct action of LPS on brain cells, however, seems to occur primarily at later stages of systemic inflammation than investigated in the present study (Chakravarty and Herkenham, 2005). In addition to this, LPS could be inducing other potential molecules employing the JAK STAT3 signaling pathway, such as leukemia inhibitory factor (LIF), ciliary neurotrophic factor (CNTF), which in turn could propagate this effect.

To our knowledge, this is the first neuroanatomical mapping study in mice that characterizes the general pattern of STAT3-activation in the brain during systemic inflammation. Previous studies of this kind were limited to investigating SOCS3 mRNA expression in the mouse brain, which was used as an indicator for JAK STAT3-activation (Lebel et al., 2000). Using in situ hybridization, those workers compared the overall distribution of SOCS3 mRNA-staining between wildtype and IL-6KO animals after i.p. injection of a high dose of LPS. The authors of that study concluded that IL-6 mediates LPS-induced SOCS3 transcription specifically in cells along the microvasculature and the ventricle ependyma, and among other brain structures contributes to the activation of the sCVO. These observations are in general agreement with the IHC data obtained in the present study as well as our results on SOCS3 mRNA expression in the hypothalamus. Interestingly, we also observed a reduction of SOCS3 mRNA expression in saline-treated IL-6KO compared to wildtype animals, indicating a contribution of basal IL-6 levels to a constitutive activation of the JAK STAT3 signaling pathway in the brain in the absence of any stimuli.

Contribution of leptin to LPS-induced nuclear STAT3 translocation in the brain

The remnant nuclear STAT3 translocation and SOCS3 mRNA expression in the brains of the LPS-treated IL-6KO mice suggested strongly that a second mediator is

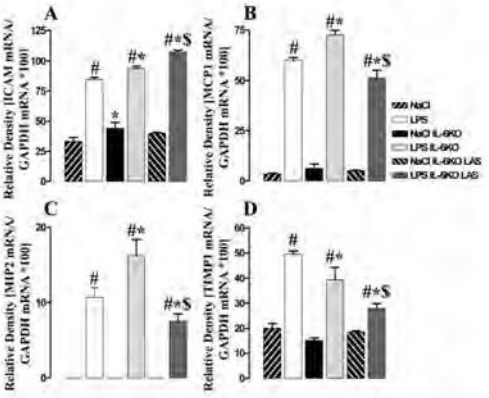


Fig. 10. LPS-injection (50 μg/kg i.p.) induced a dramatic increase of the intercellular adhesion molecule 1 (ICAM1, **A**), monocyte chemotactic protein 1 (MCP1, **B**), the macrophage inflammatory protein 2 (MIP2, **C**), and the tissue inhibitor of metalloproteinase 1 (TIMP1, **D**) mRNA expression in the hypothalamus of wildtype, IL-6KO, and IL-6KO mice treated with leptin antiserum (LAS, −4 hours, 0.5 mL/ mouse, i.p.) 3 hours after stimulation. Absence of IL-6 increased LPS-induced ICAM1, MCP1, MIP2 but decreased TIMP1 mRNA expression significantly in comparison to wildtype animals. In the IL-6KO LAS group of mice only ICAM1 expression increased but MCP1, MIP2, and TIMP1 mRNA expression was significantly attenuated relative to IL-6KO and wildtype mice. Values are presented as means ± SEM and statistical significance was considered as $P < 0.05$. [#]Different from saline-treated counterpart (e.g., LPS vs. NaCl); [*]different from WT mice counterpart (e.g., LPS IL-6KO vs. LPS); [$]different from IL-6KO mice counterpart without LAS (e.g., LPS IL-6KO LAS vs. LPS IL-6KO).

involved. A number of circulating mediators are known to signal through this pathway, including those that act via the gp130 receptor family to mediate acute phase responses during infection and inflammation. These include LIF, CNTF, oncostatin (OSM), and IL-11 and, of course, leptin, all of which have been shown to be induced by LPS or other LPS-inducible cytokines (Sarraf et al., 1997; Berkowitz et al., 1998; Heinrich et al., 1998; Gomez-Ambrosi et al., 2004). Investigating the contribution of leptin to this response was one of the main aims of the present study based on the observations that systemic injections of high doses of exogenous leptin (1–5 mg/kg) were shown to induce strong STAT3-activation in the caudobasal hypothalamus and the brain stem of rodents (Hosoi et al., 2002; Münzberg et al., 2003; Mütze et al., 2006) in a similar fashion as observed after i.c.v. injection of this hormone (Hübschle et al., 2001b; Stepanyan et al., 2003). In the present study we were able to show, for the first time, that endogenous leptin induces nuclear STAT3-activation in cells lining the brain vasculature, cells in meninges, ependymal cells, and specific brain structures, namely, the VMPO, SON, ARC, OVLT, and RPa following a moderate dose of LPS. Interestingly, these are the same areas activated by IL-6, suggesting that the two appear to work in concert. There were, however, some exceptions. Leptin, for example, seemed to exclusively target the VMPO, while IL-6 activated the Pe, MnPO, PVN, and Sol. For the SON, OVLT, and RPa this was the first report of a leptin-induced STAT3-activation in these areas, which appear to be targeted by both IL-6 and leptin. Notably, injection of exogenous leptin did not show nuclear STAT3-IR in cells of these brain structures (Hübschle et al., 2001b; Mütze et al., 2006), suggesting a similar explanation as already proposed for IL-6. For instance, cells in these brain areas might have been primed by LPS or other proinflammatory cytokines to become responsive to leptin, possibly by changes in receptor expression. The alternative spliced forms of the leptin receptor (OBr) are designated OBra, OBrb, OBrc, OBrd, OBre, and OBrf (Lee et al., 1996; Wang et al., 1996). Among these receptor subtypes, only the long form (OBrb) is supposed to fully induce STAT3-activation (Bjorbaek et al., 1997; Myers, 2004), the short forms seem to participate in the degradation or the transport of leptin across the BBB (Golden et al., 1997; Bjorbaek et al., 1998; Uotani et al., 1999). Results from our study indicated clearly that, unlike what was previously reported for the IL-6 receptor (Vallières and Rivest, 1997; Lebel et al., 2000), no such increase of receptor expression had occurred in the hypothalamus for OBrb, at least not at the mRNA level. In contrast however, OBra mRNA expression was significantly higher after LAS treatment, confirming an observations made in an earlier study showing increased OBr expression after fasting (Lin and Huang, 1997), a procedure that drastically decreases endogenous circulating leptin levels and thereby reflects the LAS treatment used in our study (Hardie et al., 1996). The functional relevance of this finding still has to be characterized but might involve an increased transport of leptin across the BBB to compensate for the reduced circulating levels. Participation of other STAT3-signaling candidates in the remaining STAT3-activation after LAS treatment in IL-6KO mice remains to be determined. CNTF would be a good candidate for this, especially as its action on ependymal cells, meningeal cells, along blood vessels, and the CVOs has been recently documented (Kelly et al., 2004).

Importantly, we discovered that the pattern of the remaining STAT3-activation in IL-6KO mice (cf. Fig. 1) matches the specific distribution of OBr as observed by in situ hybridization using a probe that recognizes all isoforms of the leptin receptor (Schwartz et al., 1996; Guan et al., 1997) as well as sites of leptin binding in the brain (Corp et al., 1998; Baskin et al., 1999; Carlo et al., 2007). This observation adds strong support to the notion that endogenous leptin contributes to LPS-induced STAT3-activation in these brain structures.

Anatomical and functional implications for IL-6 and leptin acting on specific brain structures / cell types during LPS-induced inflammation

The present work was based on previous studies showing that the exact same LPS treatment (serotype, dose, and route of injection) failed to induce fever in IL-6KO mice (Kozak et al., 1998). Thus, the reduction of LPS-induced STAT3-signaling in brain areas associated with fever such as the OVLT, MnPO, RPa, and VMPO (Nakamura et al., 2004; Roth et al., 2004; Lazarus, 2006) and the decrease in COX2 mRNA expression in the hypothalamus might constitute a mechanism by which these mice become resistant to fever. Previously, we reported that leptin contributes to LPS-induced COX2 induction in the

brain of rats (Inoue et al., 2006). Here, and in spite of an observed tendency for reduced COX2 expression in the presence of LAS, the difference was not significant. In any case, the physiological significance of a contribution of leptin to this response remains questionable, as IL-6KO animals are known not to mount a fever response to systemic inflammation (Chai et al., 1996; Kozak et al., 1998), making the addition of LAS to gauge the contribution of leptin to this response redundant. Nevertheless, COX2-IR in endothelial cells and mPGES mRNA expression in the hypothalamus remained significantly increased in all LPS-treated groups (wildtype, IL-6KO, and IL-6KO LAS).

In addition to fever, the activation of the prostaglandin synthesis pathway could alternatively be related to the anorexia associated with infection and inflammation, as suggested previously (Langhans et al., 1989; Johnson et al., 2002; Lugarini et al., 2002; Naoi et al., 2006). However, leptin-induced loss of appetite during inflammation is not solely mediated via COX2-induction in the brain, as this hormone has been shown to decrease food intake even in the presence of a COX inhibitor (Luheshi et al., 1999).

ARC. Unlike IL-6 (Vallières and Rivest, 1999), exogenously administrated leptin stimulates cells in the ARC, a brain structure well known for its role in appetite regulation (Elias et al., 2000; Hübschle et al., 2001b; Faouzi et al., 2007). However, we observed that IL-6 contributes to LPS-induced STAT3-activation in this brain area to a greater extent than leptin. This result was rather unexpected, as it was previously shown that LPS induces a similar decrease in food intake in IL-6KO and wildtype mice (Fattori et al., 1994). However, the anorectic dose of LPS used by Fattori et al. was much higher (in the mg range) and was shown to increase core body temperature in IL-6KO mice (Kozak et al., 1998), in contrast to the smaller, moderate dose of LPS used in the present study. Therefore, IL-6KO mice may also be resistant to some degree, in terms of food intake response, to this smaller dose of LPS. Support for this notion is further provided by the fact that during localized turpentine-induced inflammation the anorexic effects are decreased in the absence of IL-6 (Fattori et al., 1994; Kozak et al., 1997) and by the obese phenotype, which develops with age in these genetically modified animals (Wallenius et al., 2002).

OVLT/VMPO/MnPO. The action of IL-6 on the OVLT (Vallières et al., 1997; Hübschle et al., 2001b; Harré et al., 2002) and its contribution to LPS-induced activation of cells within this brain area is well established (Vallières and Rivest, 1999; Lebel et al., 2000; Rummel et al., 2006). We are, however, the first to show that leptin directly or indirectly activates nuclear STAT3 translocation in the OVLT, which is supported by the presence of OBr-IR in this brain area (Meister and Hakansson, 2001). The OVLT is situated in close vicinity to the VMPO, and together these two brain structures seem to form a functional unit and have been hypothesized to represent a key site for the initiation of fever during systemic inflammation (Elmquist et al., 1996). This area shows a high density of the prostanoid receptor EP4R (Oka et al., 2000), through which PGE2 might activate fever-producing autonomic pathways (Ranels and Griffin, 2003, 2005). A prominent role for fever induction pathways was recently demonstrated for the MnPO and EP3R (Lazarus, 2006; Lazarus et al., 2007). Here we observed that this particular brain structure was exclusively activated by IL-6, confirming our previous data that IL-6 contributes to COX2-induction in the MnPO (Rummel et al., 2006).

RPa. In the brainstem the RPa appeared to be the only specific brain area showing a respective contribution of leptin and IL-6 in LPS-induced STAT3-activation. This brain structure is known to contain sympathetic premotor neurons that project to the intermediolateral cell column in the spinal cord mediating efferent signals to effector organs such as brown adipose tissue (BAT) from higher autonomic centers implicated in the control of various homeostatic functions such as fever (Nakamura et al., 2002, 2004). Interestingly, i.c.v injection of IL-6 has been shown to enhance thermogenesis in BAT, an important heat-producing effector organ in rodents during fever (Li et al., 2002). Moreover, i.v. leptin injection also stimulated BAT thermogenesis and induced a cardiovascular response resulting, in increased heart rate and arterial blood pressure, which could be restored to control levels by inhibition of serotonergic neurons in the RPa (Morrison, 2004), some of which have been demonstrated to express OBr-IR (Hay-Schmidt et al., 2001). Thus, leptin and IL-6 might act in concert on this brain structure downstream of the preoptic area to directly or indirectly modulate the febrile response to LPS. For example, it is possible that this action is mediated via the induction of prostaglandins, since two-thirds of RPa neurons that project postsynaptically to BAT express EP3R (Yoshida et al., 2003).

SON. LPS activates oytoxinergic and vasopressinergic (AVP) neurons in the SON (Matsunaga et al., 2000) and is known to alter fluid homeostasis by the release of the antidiuretic hormone AVP, which results in water retention (Giusti-Paiva et al., 2003). Whereas the activation of cells in the SON by IL-6 has been shown previously in various species (Vallières et al., 1997; Vallières and Rivest, 1999; Hübschle et al., 2001b; Rummel et al., 2004), this is the first report of leptin activity in this region. A recent study did, however, demonstrate leptin-induced STAT5-activation in neurons of the SON after systemic stimulation (Mütze et al., 2007), supporting earlier results showing OBr-IR staining in this region (Hakansson et al., 1998; Meister and Hakansson, 2001). Moreover, centrally administered leptin increased the secretion of AVP (Yamamoto et al., 1999), although its effect on the electric activity of this brain structure was found to be primarily inhibitory (Honda et al., 2002). Similarly, IL-6 has been shown to increase AVP release after its systemic injection or during LPS-induced inflammation (Mastorakos et al., 1994; Palin et al., 2008). Thus, IL-6 and leptin might act in unison on the SON to contribute to an alteration of fluid homeostasis during LPS-induced inflammation and merits further investigation.

Cell types. LPS-induced nuclear STAT3 translocation has been demonstrated to occur in a variety of different cell types. Here, we confirmed our earlier results (Rummel et al., 2005, 2006) and showed that during LPS-induced inflammation STAT3 activation attributed to endogenous IL-6 was observed with a distinct preference in capillaries throughout the brain parenchyma. Leptin's action on endothelial cells reported previously (Mütze et al., 2006) was found in the present study to occur in vW-positive and -negative cells along the vasculature around the lateral ventricles, the bifurcation of the two hemispheres, and the ventrobasal lining of the hypothalamus following LPS treatment. In addition to endothelial cells, we observed IL-6- and leptin-stimulated nuclear STAT3-IR in what

appeared to be perivascular macrophages and astrocytes, which along with endothelial cells have previously been reported to respond to systemic LPS treatment with similar nuclear morphology and distribution seen in the present study (Elmquist et al., 1997; Gautron et al., 2002; Schiltz and Sawchenko, 2002; Rummel et al., 2005). The proportional contribution of each cell type to LPS-induced activation in the brain remains to be determined; however, our current observations based on COX2-IR and nuclear STAT3-IR show that endothelial cells constitute a major target for the action of IL-6 in the brain, at least at the timepoint (3 hours) investigated in our study. Leptin's effect on endothelial cells is supported by the fact that OBrb mRNA expression can be found on these cells throughout the entire brain (Bjorbaek et al., 1998) and that OBr-IR was detected in cultured endothelial cell lines (Sierra-Honigmann et al., 1998) as well as in models of vascular lesions (Schroeter et al., 2007). The action of leptin on endothelial cells is further substantiated by the fact that several studies have reported an angiogenic function for this cytokine-like hormone (Sierra-Honigmann et al., 1998; Park et al., 2001; Jin et al., 2003; Suganami et al., 2004). Interestingly, studies in mice with conditional STAT3 deletion in the endothelium (Kano et al., 2003) unexpectedly exacerbated the inflammatory response to a septic dose of LPS, resulting in increased lethality, suggesting a protective, antiinflammatory role for STAT3. However, in that study Kano et al. (2003) used a model of endotoxic shock, which might involve mechanisms different from those triggered during the moderate inflammation induced by the lower dose of LPS in the present study.

The vast majority of leptin-activated and a portion of IL-6-activated STAT3-responsive cells in specific brain structures are known to be of neuronal origin, as shown by a colocalization experiment with the neuron-specific nuclear protein (NeuN) (Mütze et al., 2006) or with c-fos mRNA expression and IR (Vallières et al., 1997; Vallières and Rivest, 1999; Hübschle et al., 2001b). In the present study, cellular analyses of some areas where leptin appeared to contribute significantly to the LPS-induced STAT3 activation such as the VMPO, the SON, the OVLT, and the RPa revealed that the cell types involved were mostly vW-negative. In these brain structures it is likely that some of the LPS-induced leptin-mediated nuclear STAT3 translocations occurred in neurons. In addition, we observed that leptin and IL-6 were acting on ependymal cells lining the ventricles, confirming previous observations by others (Lebel et al., 2000; Hübschle et al., 2001b). Interestingly, STAT3-activation in cells of the meninges appeared to be primarily mediated by leptin, which was previously reported following i.c.v. administration of leptin in a similar distribution as observed in the present study, especially at ventral sites of the hypothalamus (Hübschle et al., 2001b). The contribution of IL-6 to this response was negligible in our study, although IL-6 was previously demonstrated to activate this cell type (Harré et al., 2002). In guinea pigs we recently revealed a significant contribution of blood vessels and astrocytes to nuclear STAT3 translocation in meninges (Rummel et al., 2005), which combined with our present data showing vW-positive and -negative STAT3-activated cells in the meninges, suggests that leptin most likely acts on these two cell types in this brain structure. The significance of the action of leptin and IL-6 on ependymal cells and cells in the meninges might involve the induction of secondary mediators such as PGE2 (Wu et al., 2007), but thus far remains to be determined.

Physiological significance of IL-6 and leptin's actions on the brain during LPS-induced inflammation

We previously reported that COX2 induction is most likely regulated by STAT3 following a systemic challenge with LPS, IL-6, or leptin as indicated by colocalization of both signals (Inoue et al., 2006; Rummel et al., 2006). The results of the present study confirm that IL-6 contributes to LPS-induced activation of the prostaglandin synthesis pathway in the hypothalamus, as reported previously (Rummel et al., 2006; Oka et al., 2007). We recently demonstrated that, like IL-6, leptin contributes to LPS-induced COX2 induction in the hypothalamus of rats (Inoue et al., 2006). However, here, when using mice, we were not able to confirm this response. In addition, our present data suggest that leptin was not involved in mPGES-induction. This is an important finding, indicating that if leptin was involved in the induction of the PG synthesis pathway it might not be sufficient to activate the whole enzyme cascade. Moreover, LPS-induced COX2-IR was still present in the absence of IL-6 and leptin, suggesting that other factors are involved in the transcription of this enzyme. This is especially interesting as the major intracellular signaling pathway for COX2-induction is believed to be NF-κB (Nadjar et al., 2005; Kozak et al., 2006). While this is still valid, it most likely reflects the involvement of other pyrogenic mediators, such as IL-1β, which induces COX2 through an NF-κB-dependent mechanism (Nadjar et al., 2005). However, neither IL-1β mRNA expression nor the activation of the NF-κB signaling pathway appeared to be significantly altered by LAS in the present study. At the same time, LPS-stimulated JAK STAT3-activation was dramatically reduced, showing a strong correlation with the reduced COX2 and mPGES mRNA expression. Interestingly, although not significantly altered in IL-6KO mice or by LAS and to a much weaker extent than SOCS3, IκBα mRNA expression also significantly correlated with the expression of these two enzymes. This may be suggestive of a functional network ("cross-talk") between the STAT3-signaling cytokines IL-6 and leptin with NF-κB signaling mediators such as IL-1β and LPS (Agrawal et al., 2003; Yoshida et al., 2004) involved in regulating the transcription of the target gene COX2, as suggested recently (Rummel et al., 2006).

In addition to COX2, LPS-induced STAT3-activation may regulate other genes. Since we observed nuclear STAT3 translocation in endothelial, meningeal, and ependymal cells and the OVLT, structures that represent a gateway for immune cells involved in neuroimmune communication during severe inflammatory insults, we explored the possibility that the STAT3-activating mediators leptin and IL-6 are implicated in the expression of genes involved in cell invasion into the brain. Both of these mediators have previously been shown to induce neutrophil recruitment and chemotaxis (Romano et al., 1997; Montecucco et al., 2006) probably via the JAK STAT3 pathway (Jones et al., 2006; Panopoulos et al., 2006; Saxena et al., 2007) in organ systems other than the brain. Therefore, we decided to investigate the expression of the adhesion molecule ICAM1, the chemokines MIP2 and MCP1, as well as the metalloprotease inhibitor

TIMP1, all of which are involved in cell trafficking of neutrophil granulocytes and macrophages. As expected, we observed a significant increase in mRNA expression of all of these molecules in the hypothalamus, confirming findings from others after systemic injection of LPS or proinflammatory cytokines like IL-1β and TNFα (Cao et al., 1996; Rovai et al., 1998; Pagenstecher et al., 2000; Thibeault et al., 2001). Previously, ICAM expression was shown to be induced by IL-6 via a STAT3- and by TNFα via an NF-κB-dependent pathway (Wung et al., 2005). However, in the present study LPS-induced ICAM mRNA expression in the hypothalamus increased in IL-6KO mice compared to wildtype animals and the LPS-stimulated ICAM-IR did not change significantly in the absence of IL-6 and leptin (unpubl. obs.). Leptin and IL-6 therefore seemed to inhibit rather than stimulate ICAM1-induction via a STAT3-dependent mechanism. The reason for this discrepancy is not clear but indicates that other than STAT3, NF-κB signaling might be more important for the regulation of the ICAM promoter, at least after LPS stimulation (Ledebur and Parks, 1995). The expression of MCP1 and MIP2 increased in the absence of IL-6 but decreased in IL-6KO animals treated with LAS. This finding indicates that there might be a more complex regulation of these target genes dependent on factors other than those investigated. Nevertheless, NF-κB appears to be important and, unlike IL-6, leptin is involved in the LPS-induced increase of these chemokines, an observation that falls in line with previous reports (Thibeault et al., 2001; Yamagishi et al., 2001). Finally, we were able to show for the first time that both IL-6 and leptin mediate the vast majority of LPS-induced TIMP1 mRNA expression in the hypothalamus. These data are strongly supported by the fact that the TIMP1 promoter contains a STAT3-responsive element and by others' findings that show that both IL-6 and leptin induce TIMP1 expression in peripheral tissues (Bugno et al., 1995; Lin et al., 2006). These results strongly suggest that cell invasion into the brain, following a systemic (Bohatschek et al., 2001) or intracranial (Andersson et al., 1992; Lawson and Perry, 1995) injection of LPS may be modulated by IL-6 and leptin.

In conclusion, the data from the present study confirm our previous findings describing the roles played by leptin and IL-6 in mediating immune signals to the brain during inflammation. Beyond this, we provide new and important evidence for the specific action and the functional significance of these circulating endogenous cytokines. Our results suggest that the two mediators appear to be working synergistically on the JAK STAT3 signaling pathway to alter target gene expression in the brain during systemic inflammation. However, the contribution of each appeared to depend on the brain structure, cell type, and target gene.

ACKNOWLEDGMENT

We thank Ms. G. Somay for excellent technical assistance.

LITERATURE CITED

Agrawal A, Cha-Molstad H, Samols D, Kushner I. 2003. Overexpressed nuclear factor-kappaB can participate in endogenous C-reactive protein induction, and enhances the effects of C/EBPbeta and signal transducer and activator of transcription-3. Immunology 108:539–547.

Akira S. 1997. IL-6-regulated transcription factors. Int J Biochem Cell Biol 29:1401–1418.

Alonzi T, Fattori E, Cappelletti M, Ciliberto G, Poli V. 1998. Impaired Stat3 activation following localized inflammatory stimulus in IL-6-deficient mice. Cytokine 10:13–18.

Andersson PB, Perry VH, Gordon S. 1992. The acute inflammatory response to lipopolysaccharide in CNS parenchyma differs from that in other body tissues. Neuroscience 48:169–186.

Baskin DG, Breininger JF, Bonigut S, Miller MA. 1999. Leptin binding in the arcuate nucleus is increased during fasting. Brain Res 828:154–158.

Berkowitz DE, Brown D, Lee KM, Emala C, Palmer D, An Y, Breslow M. 1998. Endotoxin-induced alteration in the expression of leptin and beta3-adrenergic receptor in adipose tissue. Am J Physiol 274:E992–997.

Bernotiene E, Palmer G, Talabot-Ayer D, Szalay-Quinodoz I, Aubert ML, Gabay C. 2004. Delayed resolution of acute inflammation during zymosan-induced arthritis in leptin-deficient mice. Arthritis Res Ther 6:R256–263.

Bjorbaek C, Uotani S, da Silva B, Flier JS. 1997. Divergent signaling capacities of the long and short isoforms of the leptin receptor. J Biol Chem 272:32686–32695.

Bjorbaek C, Elmquist JK, Michl P, Ahima RS, van Bueren A, McCall AL, Flier JS. 1998. Expression of leptin receptor isoforms in rat brain microvessels. Endocrinology 139:3485–3491.

Bode JG, Nimmesgern A, Schmitz J, Schaper F, Schmitt M, Frisch W, Haussinger D, Heinrich PC, Graeve L. 1999. LPS and TNFalpha induce SOCS3 mRNA and inhibit IL-6-induced activation of STAT3 in macrophages. FEBS Lett 463:365–370.

Bohatschek M, Werner A, Raivich G. 2001. Systemic LPS injection leads to granulocyte influx into normal and injured brain: effects of ICAM-1 deficiency. Exp Neurol 172:137–152.

Brunetti L, Orlando G, Michelotto B, Ragazzoni E, Vacca M. 1999. Leptin stimulates prostaglandin E2 and F2alpha, but not nitric oxide production in neonatal rat hypothalamus. Eur J Pharmacol 369:299–304.

Bugno M, Graeve L, Gatsios P, Koj A, Heinrich PC, Travis J, Kordula T. 1995. Identification of the interleukin-6/oncostatin M response element in the rat tissue inhibitor of metalloproteinases-1 (TIMP-1) promoter. Nucleic Acids Res 23:5041–5047.

Cao C, Matsumora K, Yamagata K, Watanabe Y. 1996. Endothelial cells of the rat brain vasculature express cyclooxygenase-2 mRNA in response to systemic interleukin-1 beta: a possible site of prostaglandin synthesis responsible for fever. Brain Res 733:263–272.

Carlo AS, Meyerhof W, Williams LM. 2007. Early developmental expression of leptin receptor gene and [125I]leptin binding in the rat forebrain. J Chem Neuroanat 33:155–163.

Cartmell T, Poole S, Turnbull AV, Rothwell NJ, Luheshi GN. 2000. Circulating interleukin-6 mediates the febrile response to localised inflammation in rats. J Physiol 526:653–661.

Cartmell T, Luheshi GN, Hopkins SJ, Rothwell NJ, Poole S. 2001. Role of endogenous interleukin-1 receptor antagonist in regulating fever induced by localised inflammation in the rat. J Physiol 531:171–180.

Chai Z, Gatti S, Toniatti C, Poli V, Bartfai T. 1996. Interleukin (IL)-6 gene expression in the central nervous system is necessary for fever response to lipopolysaccharide or IL-1 beta: a study on IL-6-deficient mice. J Exp Med 183:311–316.

Chakravarty S, Herkenham M. 2005. Toll-like receptor 4 on nonhematopoietic cells sustains CNS inflammation during endotoxemia, independent of systemic cytokines. J Neurosci 25:1788–1796.

Chen SC, Chang YL, Wang DL, Cheng JJ. 2006. Herbal remedy magnolol suppresses IL-6-induced STAT3 activation and gene expression in endothelial cells. Br J Pharmacol 148:226–232.

Conti B, Tabarean I, Andrei C, Bartfai T. 2004. Cytokines and fever. Front Biosci 9:1433–1449.

Corp ES, Conze DB, Smith F, Campfield LA. 1998. Regional localization of specific [125I]leptin binding sites in rat forebrain. Brain Res 789:40–47.

Dalpke AH, Eckerle S, Frey M, Heeg K. 2003. Triggering of Toll-like receptors modulates IFN-gamma signaling: involvement of serine 727 STAT1 phosphorylation and suppressors of cytokine signaling. Eur J Immunol 33:1776–1787.

Dejardin E, Deregowski V, Chapelier M, Jacobs N, Gielen J, Merville MP, Bours V. 1999. Regulation of NF-kappaB activity by I kappaB-related proteins in adenocarcinoma cells. Oncogene 18:2567–2577.

Elias CF, Kelly JF, Lee CE, Ahima RS, Drucker DJ, Saper CB, Elmquist

JK. 2000. Chemical characterization of leptin-activated neurons in the rat brain. J Comp Neurol 423:261–281.

Elmquist JK, Scammell TE, Jacobson CD, Saper CB. 1996. Distribution of Fos-like immunoreactivity in the rat brain following intravenous lipopolysaccharide administration. J Comp Neurol 371:85–103.

Elmquist JK, Breder CD, Sherin JE, Scammell TE, Hickey WF, Dewitt D, Saper CB. 1997. Intravenous lipopolysaccharide induces cyclooxygenase 2-like immunoreactivity in rat brain perivascular microglia and meningeal macrophages. J Comp Neurol 381:119–129.

Faggioni R, Fantuzzi G, Fuller J, Dinarello CA, Feingold KR, Grunfeld C. 1998. IL-1 beta mediates leptin induction during inflammation. Am J Physiol 274:R204–208.

Faouzi M, Leshan R, Bjornholm M, Hennessey T, Jones J, Munzberg H. 2007. Differential accessibility of circulating leptin to individual hypothalamic sites. Endocrinology 148:5414–5423.

Fattori E, Cappelletti M, Costa P, Sellitto C, Cantoni L, Carelli M, Faggioni R, Fantuzzi G, Ghezzi P, Poli V. 1994. Defective inflammatory response in interleukin 6-deficient mice. J Exp Med 180:1243–1250.

Frühbeck G. 2006. Intracellular signalling pathways activated by leptin. Biochem J 393:7–20.

Gautron L, Lafon P, Chaigniau M, Tramu G, Laye S. 2002. Spatiotemporal analysis of signal transducer and activator of transcription 3 activation in rat brain astrocytes and pituitary following peripheral immune challenge. Neuroscience 112:717–729.

Gautron L, De Smedt-Peyrusse V, Laye S. 2006. Characterization of STAT3-expressing cells in the postnatal rat brain. Brain Res 1098:26–32.

Giusti-Paiva A, Ruginsk SG, de Castro M, Elias LL, Carnio EC, Antunes-Rodrigues J. 2003. Role of nitric oxide in lipopolysaccharide-induced release of vasopressin in rats. Neurosci Lett 346:21–24.

Golden PL, Maccagnan TJ, Pardridge WM. 1997. Human blood-brain barrier leptin receptor. Binding and endocytosis in isolated human brain microvessels. J Clin Invest 99:14–18.

Gomez-Ambrosi J, Becerril S, Oroz P, Zabalza S, Rodriguez A, Muruzabal FJ, Archanco M, Gil MJ, Burrell MA, Fruhbeck G. 2004. Reduced adipose tissue mass and hypoleptinemia in iNOS deficient mice: effect of LPS on plasma leptin and adiponectin concentrations. FEBS Lett 577:351–356.

Guan XM, Hess JF, Yu H, Hey PJ, van der Ploeg LH. 1997. Differential expression of mRNA for leptin receptor isoforms in the rat brain. Mol Cell Endocrinol 133:1–7.

Hakansson ML, Brown H, Ghilardi N, Skoda RC, Meister B. 1998. Leptin receptor immunoreactivity in chemically defined target neurons of the hypothalamus. J Neurosci 18:559–572.

Harden LM, du Plessis I, Poole S, Laburn HP. 2006. Interleukin-6 and leptin mediate lipopolysaccharide-induced fever and sickness behavior. Physiol Behav 89:146–155.

Hardie LJ, Rayner DV, Holmes S, Trayhurn P. 1996. Circulating leptin levels are modulated by fasting, cold exposure and insulin administration in lean but not Zucker (fa/fa) rats as measured by ELISA. Biochem Biophys Res Commun 223:660–665.

Harré EM, Roth J, Pehl U, Kueth M, Gerstberger R, Hübschle T. 2002. Selected contribution: role of IL-6 in LPS-induced nuclear STAT3 translocation in sensory circumventricular organs during fever in rats. J Appl Physiol 92:2657–2666.

Harré EM, Roth J, Gerstberger R, Hübschle T. 2003. Interleukin-6 mediates lipopolysaccharide-induced nuclear STAT3 translocation in astrocytes of rat sensory circumventricular organs. Brain Res 980:151–155.

Hay-Schmidt A, Helboe L, Larsen PJ. 2001. Leptin receptor immunoreactivity is present in ascending serotonergic and catecholaminergic neurons of the rat. Neuroendocrinology 73:215–226.

Heinrich PC, Behrmann I, Muller-Newen G, Schaper F, Graeve L. 1998. Interleukin-6-type cytokine signalling through the gp130/Jak/STAT pathway. Biochem J 334(Pt 2):297–314.

Honda K, Narita K, Murata T, Higuchi T. 2002. Leptin affects the electrical activity of neurones in the hypothalamic supraoptic nucleus. Brain Res Bull 57:721–725.

Hosoi T, Kawagishi T, Okuma Y, Tanaka J, Nomura Y. 2002. Brain stem is a direct target for leptin's action in the central nervous system. Endocrinology 143:3498–3504.

Hosoi T, Okuma Y, Kawagishi T, Qi X, Matsuda T, Nomura Y. 2004. Bacterial endotoxin induces STAT3 activation in the mouse brain. Brain Res 1023:48–53.

Hübschle T, Harré EM, Meyerhof W, Pehl U, Roth J, Gerstberger R. 2001a. The central pyrogenic action of interleukin-6 is related to nuclear translocation of STAT3 in the anteroventral preoptic area of the rat brain. J Therm Biol 26:299–305.

Hübschle T, Thom E, Watson A, Roth J, Klaus S, Meyerhof W. 2001b. Leptin-induced nuclear translocation of STAT3 immunoreactivity in hypothalamic nuclei involved in body weight regulation. J Neurosci 21:2413–2424.

Huo L, Münzberg H, Nillni EA, Bjorbaek C. 2004. Role of signal transducer and activator of transcription 3 in regulation of hypothalamic trh gene expression by leptin. Endocrinology 145:2516–2523.

Ikejima S, Sasaki S, Sashinami H, Mori F, Ogawa Y, Nakamura T, Abe Y, Wakabayashi K, Suda T, Nakane A. 2005. Impairment of host resistance to Listeria monocytogenes infection in liver of db/db and ob/ob mice. Diabetes 54:182–189.

Inoue W, Poole S, Bristow AF, Luheshi GN. 2006. Leptin induces cyclooxygenase-2 via an interaction with interleukin-1beta in the rat brain. Eur J Neurosci 24:2233–2245.

Jin X, Fukuda N, Su J, Takagi H, Lai Y, Lin Z, Kanmatsuse K, Wang ZW, Unger RH. 2003. Effects of leptin on endothelial function with OB-Rb gene transfer in Zucker fatty rats. Atherosclerosis 169:225–233.

Johnson PM, Vogt SK, Burney MW, Muglia LJ. 2002. COX-2 inhibition attenuates anorexia during systemic inflammation without impairing cytokine production. Am J Physiol Endocrinol Metab 282:E650–656.

Jones MR, Quinton LJ, Simms BT, Lupa MM, Kogan MS, Mizgerd JP. 2006. Roles of interleukin-6 in activation of STAT proteins and recruitment of neutrophils during Escherichia coli pneumonia. J Infect Dis 193:360–369.

Kano A, Wolfgang MJ, Gao Q, Jacoby J, Chai GX, Hansen W, Iwamoto Y, Pober JS, Flavell RA, Fu XY. 2003. Endothelial cells require STAT3 for protection against endotoxin-induced inflammation. J Exp Med 198:1517–1525.

Kelly JF, Elias CF, Lee CE, Ahima RS, Seeley RJ, Bjorbaek C, Oka T, Saper CB, Flier JS, Elmquist JK. 2004. Ciliary neurotrophic factor and leptin induce distinct patterns of immediate early gene expression in the brain. Diabetes 53:911–920.

Konsman JP, Vigues S, Mackerlova L, Bristow A, Blomqvist A. 2004. Rat brain vascular distribution of interleukin-1 type-1 receptor immunoreactivity: relationship to patterns of inducible cyclooxygenase expression by peripheral inflammatory stimuli. J Comp Neurol 472:113–129.

Kozak W, Poli V, Soszynski D, Conn CA, Leon LR, Kluger MJ. 1997. Sickness behavior in mice deficient in interleukin-6 during turpentine abscess and influenza pneumonitis. Am J Physiol 272:R621–630.

Kozak W, Kluger MJ, Soszynski D, Conn CA, Rudolph K, Leon LR, Zheng H. 1998. IL-6 and IL-1 beta in fever. Studies using cytokine-deficient (knockout) mice. Ann N Y Acad Sci 856:33–47.

Kozak W, Wrotek S, Kozak A. 2006. Pyrogenicity of CpG-DNA in mice: role of interleukin-6, cyclooxygenases, and nuclear factor-kappaB. Am J Physiol Regul Integr Comp Physiol 290:R871–880.

Laflamme N, Rivest S. 1999. Effects of systemic immunogenic insults and circulating proinflammatory cytokines on the transcription of the inhibitory factor kappaB alpha within specific cellular populations of the rat brain. J Neurochem 73:309–321.

Laflamme N, Rivest S. 2001. Toll-like receptor 4: the missing link of the cerebral innate immune response triggered by circulating gram-negative bacterial cell wall components. FASEB J 15:155–163.

Lago F, Dieguez C, Gomez-Reino J, Gualillo O. 2007. Adipokines as emerging mediators of immune response and inflammation. Nat Clin Pract Rheumatol 3:716–724.

Langhans W. 2000. Anorexia of infection: current prospects. Nutrition 16:996–1005.

Langhans W, Harlacher R, Scharrer E. 1989. Verapamil and indomethacin attenuate endotoxin-induced anorexia. Physiol Behav 46:535–539.

Lawson LJ, Perry VH. 1995. The unique characteristics of inflammatory responses in mouse brain are acquired during postnatal development. Eur J Neurosci 7:1584–1595.

Lazarus M. 2006. The differential role of prostaglandin E2 receptors EP3 and EP4 in regulation of fever. Mol Nutr Food Res 50:451–455.

Lazarus M, Yoshida K, Coppari R, Bass CE, Mochizuki T, Lowell BB, Saper CB. 2007. EP3 prostaglandin receptors in the median preoptic nucleus are critical for fever responses. Nat Neurosci 10:1131–1133.

Lebel É, Vallières L, Rivest S. 2000. Selective involvement of interleukin-6 in the transcriptional activation of the suppressor of cytokine signaling-3 in the brain during systemic immune challenges. Endocrinology 141:3749–3763.

Ledebur HC, Parks TP. 1995. Transcriptional regulation of the intercellular adhesion molecule-1 gene by inflammatory cytokines in human

endothelial cells. Essential roles of a variant NF-kappa B site and p65 homodimers. J Biol Chem 270:933–943.

Lee GH, Proenca R, Montez JM, Carroll KM, Darvishzadeh JG, Lee JI, Friedman JM. 1996. Abnormal splicing of the leptin receptor in diabetic mice. Nature 379:632–635.

Lee FY, Li Y, Yang EK, Yang SQ, Lin HZ, Trush MA, Dannenberg AJ, Diehl AM. 1999. Phenotypic abnormalities in macrophages from leptin-deficient, obese mice. Am J Physiol 276:C386–394.

Li S, Wang Y, Matsumura K, Ballou LR, Morham SG, Blatteis CM. 1999. The febrile response to lipopolysaccharide is blocked in cyclooxygenase-2(-/-), but not in cyclooxygenase-1(-/-) mice. Brain Res 825:86–94.

Li G, Klein RL, Matheny M, King MA, Meyer EM, Scarpace PJ. 2002. Induction of uncoupling protein 1 by central interleukin-6 gene delivery is dependent on sympathetic innervation of brown adipose tissue and underlies one mechanism of body weight reduction in rats. Neuroscience 115:879–889.

Lin S, Huang XF. 1997. Fasting increases leptin receptor mRNA expression in lean but not obese (ob/ob) mouse brain. Neuroreport 8:3625–3629.

Lin S, Saxena NK, Ding X, Stein LL, Anania FA. 2006. Leptin increases tissue inhibitor of metalloproteinase 1 (TIMP-1) gene expression by a specificity protein 1/signal transducer and activator of transcription 3 mechanism. Mol Endocrinol 20:3376–3388.

Lugarini F, Hrupka BJ, Schwartz GJ, Plata-Salamm CR, Langhans W. 2002. A role for cyclooxygenase-2 in lipopolysaccharide-induced anorexia in rats. Am J Physiol Regul Integr Comp Physiol 283:R862–868.

Luheshi GN, Gardner JD, Rushforth DA, Loudon AS, Rothwell NJ. 1999. Leptin actions on food intake and body temperature are mediated by IL-1. Proc Natl Acad Sci U S A 96:7047–7052.

Mastorakos G, Weber JS, Magiakou MA, Gunn H, Chrousos GP. 1994. Hypothalamic-pituitary-adrenal axis activation and stimulation of systemic vasopressin secretion by recombinant interleukin-6 in humans: potential implications for the syndrome of inappropriate vasopressin secretion. J Clin Endocrinol Metab 79:934–939.

Matsunaga W, Miyata S, Takamata A, Bun H, Nakashima T, Kiyohara T. 2000. LPS-induced Fos expression in oxytocin and vasopressin neurons of the rat hypothalamus. Brain Res 858:9–18.

Matthews JR, Watson SM, Tevendale MC, Watson CJ, Clarke AR. 2007. Caspase-dependent proteolytic cleavage of STAT3alpha in ES cells, in mammary glands undergoing forced involution and in breast cancer cell lines. BMC Cancer 7:29.

Meister B, Hakansson ML. 2001. Leptin receptors in hypothalamus and circumventricular organs. Clin Exp Pharmacol Physiol 28:610–617.

Miller AJ, Luheshi GN, Rothwell NJ, Hopkins SJ. 1997. Local cytokine induction by LPS in the rat air pouch and its relationship to the febrile response. Am J Physiol 272:R857–861.

Montecucco F, Bianchi G, Guerre P, Bertolotto M, Dallegri F, Ottonello L. 2006. Induction of neutrophil chemotaxis by leptin: crucial role for p38 and Src kinases. Ann N Y Acad Sci 1069:463–471.

Morrison SF. 2004. Activation of 5-HT1A receptors in raphe pallidus inhibits leptin-evoked increases in brown adipose tissue thermogenesis. Am J Physiol Regul Integr Comp Physiol 286:R832–837.

Mouihate A, Pittman QJ. 2003. Neuroimmune response to endogenous and exogenous pyrogens is differently modulated by sex steroids. Endocrinology 144:2454–2460.

Münzberg H, Huo L, Nillni EA, Hollenberg AN, Bjorbaek C. 2003. Role of signal transducer and activator of transcription 3 in regulation of hypothalamic proopiomelanocortin gene expression by leptin. Endocrinology 144:2121–2131.

Münzberg H, Flier JS, Bjorbaek C. 2004. Region-specific leptin resistance within the hypothalamus of diet-induced obese mice. Endocrinology 145:4880–4889.

Murakami T, Shima K. 1995. Cloning of rat obese cDNA and its expression in obese rats. Biochem Biophys Res Commun 209:944–952.

Mütze J, Roth J, Gerstberger R, Matsumura K, Hübschle T. 2006. Immunohistochemical evidence of functional leptin receptor expression in neuronal and endothelial cells of the rat brain. Neurosci Lett 394:105–110.

Mütze J, Roth J, Gerstberger R, Hübschle T. 2007. Nuclear translocation of the transcription factor STAT5 in the rat brain after systemic leptin administration. Neurosci Lett 417:286–291.

Myers MG Jr. 2004. Leptin receptor signaling and the regulation of mammalian physiology. Recent Prog Horm Res 59:287–304.

Nadjar A, Combe C, Layé S, Tridon V, Dantzer R, Amedee T, Parnet P. 2003. Nuclear factor kB nuclear translocation as a crucial marker of brain response to interleukin-1. A study in rat and interleukin-1 type I deficient mouse. J Neurochem 87:1024–1036.

Nadjar A, Tridon V, May MJ, Ghosh S, Dantzer R, Amedee T, Parnet P. 2005. NFkappaB activates in vivo the synthesis of inducible Cox-2 in the brain. J Cereb Blood Flow Metab 25:1047–1059.

Nakamura K, Matsumura K, Kaneko T, Kobayashi S, Katoh H, Negishi M. 2002. The rostral raphe pallidus nucleus mediates pyrogenic transmission from the preoptic area. J Neurosci 22:4600–4610.

Nakamura K, Matsumura K, Hubschle T, Nakamura Y, Hioki H, Fujiyama F, Boldogkoi Z, Konig M, Thiel HJ, Gerstberger R, Kobayashi S, Kaneko T. 2004. Identification of sympathetic premotor neurons in medullary raphe regions mediating fever and other thermoregulatory functions. J Neurosci 24:5370–5380.

Naoi K, Kogure S, Saito M, Hamazaki T, Watanabe S. 2006. Differential effects of selective cyclooxygenase (COX)-1 and COX-2 inhibitors on anorexic response and prostaglandin generation in various tissues induced by zymosan. Biol Pharm Bull 29:1319–1324.

Netea MG, Kullberg BJ, Van der Meer JW. 2000. Circulating cytokines as mediators of fever. Clin Infect Dis 31(Suppl 5):S178–184.

Oka T, Oka K, Scammell TE, Lee C, Kelly JF, Nantel F, Elmquist JK, Saper CB. 2000. Relationship of EP(1-4) prostaglandin receptors with rat hypothalamic cell groups involved in lipopolysaccharide fever responses. J Comp Neurol 428:20–32.

Oka Y, Ibuki T, Matsumura K, Namba M, Yamazaki Y, Poole S, Tanaka Y, Kobayashi S. 2007. Interleukin-6 is a candidate molecule that transmits inflammatory information to the CNS. Neuroscience 145:530–538.

Pagenstecher A, Stalder AK, Kincaid CL, Volk B, Campbell IL. 2000. Regulation of matrix metalloproteinases and their inhibitor genes in lipopolysaccharide-induced endotoxemia in mice. Am J Pathol 157:197–210.

Palin K, Moreau ML, Orcel H, Duvoid-Guillou A, Rabie A, Kelley KW, Moos F. 2008. Age-impaired fluid homeostasis depends on the balance of IL-6/IGF-I in the rat supraoptic nuclei. Neurobiol Aging (in press).

Palmer G, Aurrand-Lions M, Contassot E, Talabot-Ayer D, Ducrest-Gay D, Vesin C, Chobaz-Peclat V, Busso N, Gabay C. 2006. Indirect effects of leptin receptor deficiency on lymphocyte populations and immune response in db/db mice. J Immunol 177:2899–2907.

Panopoulos AD, Zhang L, Snow JW, Jones DM, Smith AM, El Kasmi KC, Liu F, Goldsmith MA, Link DC, Murray PJ, Watowich SS. 2006. STAT3 governs distinct pathways in emergency granulopoiesis and mature neutrophils. Blood 108:3682–3690.

Park HY, Kwon HM, Lim HJ, Hong BK, Lee JY, Park BE, Jang Y, Cho SY, Kim HS. 2001. Potential role of leptin in angiogenesis: leptin induces endothelial cell proliferation and expression of matrix metalloproteinases in vivo and in vitro. Exp Mol Med 33:95–102.

Paxinos G, Franklin KBJ. 2001. The mouse brain in stereotaxic coordinates, 2nd ed. Amsterdam: Elsevier.

Pecchi E, Dallaporta M, Thirion S, Salvat C, Berenbaum F, Jean A, Troadec JD. 2006. Involvement of central microsomal prostaglandin E synthase-1 in IL-1beta-induced anorexia. Physiol Genomics 25:485–492.

Poole S, Bristow AF, Selkirk S, Rafferty B. 1989. Development and application of radioimmunoassays for interleukin-1 alpha and interleukin-1 beta. J Immunol Methods 116:259–264.

Quan N, Banks WA. 2007. Brain-immune communication pathways. Brain Behav Immun 21:727–735.

Ranels HJ, Griffin JD. 2003. The effects of prostaglandin E2 on the firing rate activity of thermosensitive and temperature insensitive neurons in the ventromedial preoptic area of the rat hypothalamus. Brain Res 964:42–50.

Ranels HJ, Griffin JD. 2005. Effects of prostaglandin E2 on the electrical properties of thermally classified neurons in the ventromedial preoptic area of the rat hypothalamus. BMC Neurosci 6:14.

Rees GS, Ball C, Ward HL, Gee CK, Tarrant G, Mistry Y, Poole S, Bristow AF. 1999. Rat interleukin 6: expression in recombinant Escherichia coli, purification and development of a novel ELISA. Cytokine 11:95–103.

Romano M, Sironi M, Toniatti C, Polentarutti N, Fruscella P, Ghezzi P, Faggioni R, Luini W, van Hinsbergh V, Sozzani S, Bussolino F, Poli V, Ciliberto G, Mantovani A. 1997. Role of IL-6 and its soluble receptor in induction of chemokines and leukocyte recruitment. Immunity 6:315–325.

Ross G, Hübschle T, Pehl U, Braun HA, Voigt K, Gerstberger R, Roth J. 2003. Fever induction by localized subcutaneous inflammation in

guinea pigs: the role of cytokines and prostaglandins. J Appl Physiol 94:1395–1402.

Roth J, Harré EM, Rummel C, Gerstberger R, Hübschle T. 2004. Signaling the brain in systemic inflammation: role of sensory circumventricular organs. Front Biosci 9:290–300.

Rovai LE, Herschman HR, Smith JB. 1998. The murine neutrophil-chemoattractant chemokines LIX, KC, and MIP-2 have distinct induction kinetics, tissue distributions, and tissue-specific sensitivities to glucocorticoid regulation in endotoxemia. J Leukoc Biol 64:494–502.

Rummel C, Hübschle T, Gerstberger R, Roth J. 2004. Nuclear translocation of the transcription factor STAT3 in the guinea pig brain during systemic or localised inflammation. J Physiol 557:671–687.

Rummel C, Voss T, Matsumura K, Korte S, Gerstberger R, Roth J, Hübschle T. 2005. Nuclear STAT3 translocation in guinea pig and rat brain endothelium during systemic challenge with lipopolysaccharide and interleukin-6. J Comp Neurol 491:1–14.

Rummel C, Sachot C, Poole S, Luheshi GN. 2006. Circulating interleukin-6 induces fever through a STAT3-linked activation of COX-2 in the brain. Am J Physiol Regul Integr Comp Physiol 291:R1316–1326.

Sachot C, Poole S, Luheshi GN. 2004. Circulating leptin mediates lipopolysaccharide-induced anorexia and fever in rats. J Physiol 561: 263–272.

Sarraf P, Frederich RC, Turner EM, Ma G, Jaskowiak NT, Rivet DJ 3rd, Flier JS, Lowell BB, Fraker DL, Alexander HR. 1997. Multiple cytokines and acute inflammation raise mouse leptin levels: potential role in inflammatory anorexia. J Exp Med 185:171–175.

Saxena NK, Sharma D, Ding X, Lin S, Marra F, Merlin D, Anania FA. 2007. Concomitant activation of the JAK/STAT, PI3K/AKT, and ERK signaling is involved in leptin-mediated promotion of invasion and migration of hepatocellular carcinoma cells. Cancer Res 67:2497–2507.

Schiltz JC, Sawchenko PE. 2002. Distinct brain vascular cell types manifest inducible cyclooxygenase expression as a function of the strength and nature of immune insults. J Neurosci 22:5606–5618.

Schroeter MR, Schneiderman J, Schumann B, Gluckermann R, Grimmas P, Buchwald AB, Tirilomis T, Schondube FA, Konstantinides SV, Schafer K. 2007. Expression of the leptin receptor in different types of vascular lesions. Histochem Cell Biol 128:323–333.

Schwartz MW, Seeley RJ, Campfield LA, Burn P, Baskin DG. 1996. Identification of targets of leptin action in rat hypothalamus. J Clin Invest 98:1101–1106.

Shoenfelt JL, Fenton MJ. 2006. TLR2- and TLR4-dependent activation of STAT1 serine phosphorylation in murine macrophages is protein kinase C-delta-independent. J Endotoxin Res 12:231–240.

Sierra-Honigmann MR, Nath AK, Murakami C, Garcia-Cardena G, Papapetropoulos A, Sessa WC, Madge LA, Schechner JS, Schwabb MB, Polverini PJ, Flores-Riveros JR. 1998. Biological action of leptin as an angiogenic factor. Science 281:1683–1686.

Stepanyan Z, Kocharyan A, Pyrski M, Hubschle T, Watson AM, Schulz S, Meyerhof W. 2003. Leptin-target neurones of the rat hypothalamus express somatostatin receptors. J Neuroendocrinol 15:822–830.

Suganami E, Takagi H, Ohashi H, Suzuma K, Suzuma I, Oh H, Watanabe D, Ojima T, Suganami T, Fujio Y, Nakao K, Ogawa Y, Yoshimura N. 2004. Leptin stimulates ischemia-induced retinal neovascularization: possible role of vascular endothelial growth factor expressed in retinal endothelial cells. Diabetes 53:2443–2448.

Thibeault I, Laflamme N, Rivest S. 2001. Regulation of the gene encoding the monocyte chemoattractant protein 1 (MCP-1) in the mouse and rat brain in response to circulating LPS and proinflammatory cytokines. J Comp Neurol 434:461–477.

Turnbull AV, Prehar S, Kennedy AR, Little RA, Hopkins SJ. 2003. Interleukin-6 is an afferent signal to the hypothalamo-pituitary-adrenal axis during local inflammation in mice. Endocrinology 144: 1894–1906.

Uotani S, Bjorbaek C, Tornoe J, Flier JS. 1999. Functional properties of leptin receptor isoforms: internalization and degradation of leptin and ligand-induced receptor downregulation. Diabetes 48:279–286.

Vallières L, Rivest S. 1997. Regulation of the genes encoding interleukin-6, its receptor, and gp130 in the rat brain in response to the immune activator lipopolysaccharide and the proinflammatory cytokine interleukin-1beta. J Neurochem 69:1668–1683.

Vallières L, Rivest S. 1999. Interleukin-6 is a needed proinflammatory cytokine in the prolonged neural activity and transcriptional activation of corticotropin-releasing factor during endotoxemia. Endocrinology 140:3890–3903.

Vallières L, Lacroix S, Rivest S. 1997. Influence of interleukin-6 on neural activity and transcription of the gene encoding corticotrophin-releasing factor in the rat brain: an effect depending upon the route of administration. Eur J Neurosci 9:1461–1472.

Wallenius V, Wallenius K, Ahren B, Rudling M, Carlsten H, Dickson SL, Ohlsson C, Jansson JO. 2002. Interleukin-6-deficient mice develop mature-onset obesity. Nat Med 8:75–79.

Wang MY, Zhou YT, Newgard CB, Unger RH. 1996. A novel leptin receptor isoform in rat. FEBS Lett 392:87–90.

Wang Q, Fang CH, Hasselgren PO. 2001. Intestinal permeability is reduced and IL-10 levels are increased in septic IL-6 knockout mice. Am J Physiol Regul Integr Comp Physiol 281:R1013–1023.

Wu Z, Hayashi Y, Zhang J, Nakanishi H. 2007. Involvement of prostaglandin E2 released from leptomeningeal cells in increased expression of transforming growth factor-beta in glial cells and cortical neurons during systemic inflammation. J Neurosci Res 85:184–192.

Wung BS, Ni CW, Wang DL. 2005. ICAM-1 induction by TNFalpha and IL-6 is mediated by distinct pathways via Rac in endothelial cells. J Biomed Sci 12:91–101.

Yamagata K, Matsumura K, Inoue W, Shiraki T, Suzuki K, Yasuda S, Sugiura H, Cao C, Watanabe Y, Kobayashi S. 2001. Coexpression of microsomal-type prostaglandin E synthase with cyclooxygenase-2 in brain endothelial cells of rats during endotoxin-induced fever. J Neurosci 21:2669–2677.

Yamagishi SI, Edelstein D, Du XL, Kaneda Y, Guzman M, Brownlee M. 2001. Leptin induces mitochondrial superoxide production and monocyte chemoattractant protein-1 expression in aortic endothelial cells by increasing fatty acid oxidation via protein kinase A. J Biol Chem 276:25096–25100.

Yamamoto K, de Waard V, Fearns C, Loskutoff DJ. 1998. Tissue distribution and regulation of murine von Willebrand factor gene expression in vivo. Blood 92:2791–2801.

Yamamoto S, Morimoto I, Kai K, Arao T, Fujihira T, Morita E, Kannan H, Eto S. 1999. Centrally administered murine leptin stimulates plasma arginine-vasopressin secretion and increases the level of mRNA expression in the supraoptic nucleus of conscious rats. Neuroendocrinology 70:207–212.

Yang XP, Schaper F, Teubner A, Lammert F, Heinrich PC, Matern S, Siewert E. 2005. Interleukin-6 plays a crucial role in the hepatic expression of SOCS3 during acute inflammatory processes in vivo. J Hepatol 43:704–710.

Yoshida K, Nakamura K, Matsumura K, Kanosue K, Konig M, Thiel HJ, Boldogkoi Z, Toth I, Roth J, Gerstberger R, Hubschle T. 2003. Neurons of the rat preoptic area and the raphe pallidus nucleus innervating the brown adipose tissue express the prostaglandin E receptor subtype EP3. Eur J Neurosci 18:1848–1860.

Yoshida Y, Kumar A, Koyama Y, Peng H, Arman A, Boch JA, Auron PE. 2004. Interleukin 1 activates STAT3/nuclear factor-kappaB cross-talk via a unique TRAF6- and p65-dependent mechanism. J Biol Chem 279:1768–1776.

Zhang Y, Proenca R, Maffei M, Barone M, Leopold L, Friedman JM. 1994. Positional cloning of the mouse obese gene and its human homologue. Nature 372:425–432.

1.10. „The role of the vagus nerve in mediating the long-term anorectic effects of leptin“

Sachot C., **Rummel C**., Bristow AF., Luheshi GN.

J Neuroendocrinol (2007) 19: 250-261.

Impakt Faktor: 4,650

Eigener Anteil an der Publikation:

- Initiative: unterstützend (30 %)
- Projektplanung: unterstützend (30 %)
- Durchführung der Versuche: unterstützend (30 %)
- Auswertung der Experimente: wesentlich (50 %)
- Erstellung der Publikation: unterstützend (30 %)

Journal of Neuroendocrinology **19**, 250–261
© 2007 The Authors. Journal Compilation © 2007 Blackwell Publishing Ltd

ORIGINAL ARTICLE

The Role of the Vagus Nerve in Mediating the Long-Term Anorectic Effects of Leptin

C. Sachot,* C. Rummel,* A. F. Bristow† and G. N. Luheshi*

**Douglas Hospital Research Centre, Department of Psychiatry, McGill University, Montreal, Quebec, Canada.*
†National Institutes of Biological Standards and Control, Potters Bar, UK.

Journal of Neuroendocrinology

Leptin, the product of the *obese (ob)* gene, is mainly known for its regulatory role of energy balance by direct activation of hypothalamic receptors. Recently, its function in the acute control of food intake was additionally attributed to activation of the vagus nerve to regulate meal termination. Whether vagal afferent neurones are involved in longer term effects of leptin on food intake, however, remains undetermined. Using vagotomised (VGX) rats, we sought to clarify the contributions of vagal afferents in mediating the long-lasting effect of leptin on appetite suppression. Intraperitoneal (i.p.) injection of leptin (3.5 mg/kg) attenuated food intake at 4, 6, 8 and 24 h and body weight at 24 h postinjection in SHAM-operated rats; however, this response was not abrogated by vagotomy. In a separate study using immunohistochemistry, we observed leptin-induced Fos expression in the nucleus tractus solitarii, a brain structure where vagal afferent fibres terminate. This signal was not attenuated in VGX animals compared to the SHAM group. Moreover, leptin treatment led to a similar level of nuclear STAT3 translocation, a marker of leptin signalling, in the hypothalami of SHAM and VGX animals. In addition to the effects of leptin, vagotomy surgery itself resulted in a decrease of 24 h food intake. Analyses of brains from saline-treated VGX animals revealed a significant induction of Fos in the nucleus tractus solitarii and changes in agouti-related peptide and pro-opiomelanocortin mRNA expression in the hypothalamus compared to their SHAM counterparts, indicating that the vagotomy surgery itself induced a modification of brain activity in areas involved in regulating appetite. Collectively, our data suggest that vagal afferents do not constitute a major route of mediating the regulatory effect of leptin on food intake over a period of several hours.

Key words: vagus nerve, food intake, NTS, Fos, hypothalamus.

doi: 10.1111/j.1365-2826.2006.01528.x

Correspondence to:
Dr Giamal N. Luheshi, Douglas Hospital Research Centre, McGill University, 6875 Boulevard LaSalle, Verdun, Quebec, H4H 1R3, Canada (e-mail: giamal.luheshi@mcgill.ca).

Leptin is a 16-kDa peptide, which is produced primarily by adipocytes and released into the circulation in proportion to body mass (1). From the circulation, leptin gains access to the central nervous system (CNS) and acts principally on its hypothalamic receptors (2) following entry to the brain via a specific transport mechanism (3) to regulate energy balance by suppressing appetite and increasing energy expenditure. Recent studies have demonstrated that the action of leptin on food intake is not limited to the CNS, thus suggesting another route through which the leptin-mediated signal could be transmitted to the brain, namely neural afferents. This is supported by a number of reports demonstrating leptin receptor expression on the vagal trunk (4) and leptin activation of vagal afferents innervating the intestines of cats (5), as well as the stomach and duodenum of rats (6, 7). More importantly, Peters *et al.* (8) reported that a transient and localised injection of leptin via the intraceliac artery can reduce meal size without affecting 24 h food intake and that this response was attenuated by vagotomy surgery. This elegant study was designed to mimic the local release of gastric leptin, which is synthesised and secreted from cells within the celiac arterial perfusion bed (9). However, vagal afferents may also be exposed over a longer period to circulating adipose-derived leptin, which may affect food intake for more than one meal. Indeed administration of exogenous leptin is known to suppress appetite for several hours resulting in loss of body weight (10–14). It is probable that this more prolonged anorectic action of leptin similar to its short-term effects may also be relayed to the brain by vagal afferents innervating the gastrointestinal tract in a manner similar to the effect of leptin on its brain receptors.

Recently, the physiological role of leptin as a regulator of energy has been increasingly associated with immune function and was expanded to include the reduction of food intake that accompanies infection/inflammation. This is supported by studies demonstrating that leptin is produced in the circulation during inflammation (15–18) and that it interacts significantly with cytokines, important immunomodulatory mediators (19–23). Our previous observations strongly suggest that leptin is a circulating mediator involved in the anorexia of inflammation (24) and acts as a pyrogen when administered exogenously at a dose that also decreases food intake (22). This suppression of appetite during inflammation is part of the generalised host defence reaction termed 'acute phase response', which is beneficial in overcoming invading pathogens and involves immune-to-brain communication (25). The vagus nerve has actually been shown to partly mediate the central response to peripheral tissue damage or infection (26) and to constitute a possible route for relaying the signal responsible for decreased food intake associated with inflammation (27). Particularly, interleukin (IL)-1β, a member of the cytokine family and important mediator of inflammation-induced anorexia (28, 29), has been demonstrated to trigger the activation of vagal afferents (30–32). We therefore hypothesised that leptin, similar to IL-1β, may also activate the vagus nerve to signal from the periphery to the brain during inflammation. However, it has been reported that selective surgical transection of all subdiaphragmatic vagal sensory axons failed to block the appetite-suppressive effects of IL-1β (33). This remains to be determined for leptin.

In the present study, we aimed to test whether the long-lasting anorectic response induced by leptin in a physiological situation and during inflammation could be mediated through the action of this hormone on its vagal receptors. To test this hypothesis, we assessed changes in food intake and body weight in subdiaphragmatically vagotomised (VGX) rats after systemic administration of leptin. We further performed neuroanatomical mapping studies to examine the association between changes in food intake with modification of brain signals known to be triggered specifically by leptin and/or by stimulation of the vagus nerve.

Materials and methods

Animals

Adult male Sprague-Dawley rats (250–275 g; Charles River, Saint Constant, Quebec, Canada) were used in all experiments. Animal care was provided according to protocols and guidelines approved by McGill University and the Canadian Council of Animal Care. Animals were housed individually in a controlled environment at an ambient temperature of 21 ± 2 °C. Observations were carried out under a 12 : 12 h light/dark cycle (lights on 09.00 h) or a 12 : 12 h reverse light/dark cycle (lights on 21.00 h). All animals had free access to food and water and were handled extensively for at least 2 days prior to the start of each experiment.

Surgery

Animals were food deprived for 24 h prior to surgery and randomly assigned to vagotomy or SHAM operations, as previously described (34). Briefly, animals were anaesthetised [ketamin (50 mg/kg), xylazin (5 mg/kg), acetopromazin (0.5 mg/kg); i.p. injection], and 1 cm of the main ventral and dorsal trunks of the vagus nerve were transected immediately caudal to the diaphragm. This procedure ensures that all subdiaphragmatic vagal innervations including the hepatic branch are removed. SHAM-operated rats that underwent the same surgical procedures except the transection of the vagus nerve were used as controls. The animals were allowed to recover for 3–4 weeks. During the first week post-surgery, both SHAM and VGX animals were provided with sweetened milk diet because it has previously been shown to improve recovery by reducing body weight loss (35). VGX animals (25–30%) that did not regain weight were excluded from the study.

The completeness of the vagotomy surgery was assessed in two ways. Post-mortem stomachs (together with its contents) were collected at the end of each experiment and weighed, as transection of the gastric vagal branches causes food retention in the stomach (36) (Fig. 1A). In addition, the brains were collected for immunohistochemical analyses, and vagotomy was verified as previously described (37). High isolectin I-B4 (cat: L5391, Sigma-Aldrich, St Louis, MO, USA) binding is found in the nucleus tractus solitarii (NTS) of SHAM animals, a brain structure where vagal afferent fibres termin-

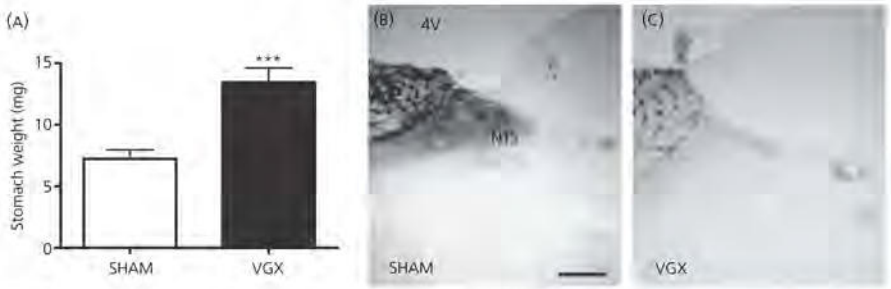


Fig. 1. Verification of the vagotomy surgery. The stomachs of vagotomised (VGX) animals weighed significantly more (13.45 ± 1.16 g) than those of SHAM-operated ones (7.24 ± 0.73 g; SHAM versus VGX; $t(56) = 4.607$, $P < 0.001$) (A). Isolectin I-B4 binding (black staining) in the nucleus tractus solitarii (NTS) of SHAM animals (B) was highly reduced in the NTS of VGX animals (C). 4V, Fourth ventricle; AP, area postrema. Scale bar = 100 μm.

ate (Fig. 1B). This labelling is highly reduced in the NTS of VGX animals if the surgery was effective (Fig. 1C).

Treatments

In all studies, the animals received a single i.p. injection of recombinant murine leptin (NIBSC, Potters Bar, UK) at a dose of 3.5 mg/kg. This dose was based on observations made in our previous study (22) and by other groups (10–14), and on preliminary dose/response experiments demonstrating that a lower dose (1 mg/kg) did not reduce food intake consistently and that a higher dose (5 mg/kg) did not further decrease food intake (data not shown). Control animals received the same volume of sterile physiological saline.

Measurement of food consumption and body weight

The importance of the vagus nerve as a target of leptin activity in appetite regulation was tested by assessing changes in food intake and body weight in VGX compared to SHAM animals. For accurate measurements of food consumption, powdered food was placed in special dispensers (PFF16D jar; Allentown, NJ, USA) inside the cage and the normal pellet food removed from the top of the cage. The food dispensers are designed to avoid spillage during feeding and therefore provide an accurate method of assessing food consumed by each animal. These studies were conducted under reverse light cycle during the active phase of the animals. Animals were previously habituated to powdered food and food measurement (powdered 5012, Ralston Purina, Ottawa, Ontario, Canada) for 2 days prior to the day of treatment. On the day of experiment, animals were separated into four treatment groups: (i) leptin SHAM; (ii) leptin VGX; (iii) saline SHAM; and (iii) saline VGX ($n = 14–15$ per group) and the appropriate treatment administered using i.p. injection of 1 ml/kg. Changes in food consumption were measured by weighing the container (including the food) prior to treatments and at 4, 6, 8 and 24 h post-treatment using a top pan balance (Scout, VWR international, Ville Mont-Royal, Quebec, Canada) accurate to 0.1 g. In the same study, changes in body weight were monitored by weighing animals immediately before injections and again 24 h post-treatment.

Tissue processing

To determine whether the changes in food consumption and body weight were associated with modification of brain activity, rats were assigned to immunohistochemistry (IHC, $n = 4–5$ per group) or semiquantitative reverse transcriptase-polymerase chain reaction (RT-PCR, $n = 5$ per group) studies. For this purpose, SHAM and VGX animals ($n = 5$ per group) were sacrificed 2 h after treatment using a lethal i.p. dose of anaesthetic. An additional group of animals ($n = 5$ per group) receiving the same treatment were sacrificed 1 h following the injection to assess time dependent changes in some of the immunohistochemical signals being investigated. For IHC studies, rats were transcardially perfused with 100 ml of heparinised saline, followed by 300 ml of ice-cold (4 °C) phosphate buffered paraformaldehyde solution (PFA 4% in PB, 0.1 M pH 7.4). Brains were removed, immersed for 3–5 h in the same fixative at 4 °C, cryoprotected by immersion over night in 20% sucrose in PBS (0.1 M pH 7.4), and frozen in cold-isopentane. Coronal serial free-floating sections (20 μm, prepared with a Leica CM 3050 S cryostat; Leica, Nussloch, Germany) were collected in a cryoprotective solution (PBS 0.05 M pH 7.4, 30% ethylene glycol, 20% glycerol) and stored at −20 °C until use. For RT-PCR, animals were transcardially perfused with ice-cold (4 °C) diethyl pyrocarbonate-treated saline. Brains were quickly removed and the hypothalami were microdissected and then frozen on powdered dry ice. This tissue was stored at −80 °C until analysis.

IHC

Fos and phospho-(P) signal transducer and activator of transcription (STAT)3 IHC

Fos immunoreactivity (IR) was investigated in the NTS as a marker of cellular activity, which may be induced after leptin action via the vagus nerve. The expression of the active form of STAT3, PSTAT3, was assessed in the NTS and hypothalamus as a marker for a direct action of leptin on its receptor (38, 39). Fos (40) and PSTAT3 (41) IHC protocols were performed as described previously with some modifications. Between each step, brain sections were rinsed in PBS (0.1 M, pH 7.4).

For Fos IHC, brain stem sections were first incubated for 30 min in 0.3% hydrogen peroxide in PBS to neutralise endogenous peroxidases. For PSTAT3, brain stem and hypothalamic sections were pretreated with 3% hydrogen peroxide in methanol for 40 min, followed by successive incubations in 0.3% glycine-PBS for 25 min and in 0.03% sodium dodecyl sulphate for 25 min. Sections were then treated for 1 h at room temperature with blocking solution, composed of PBS, 10% normal donkey serum (NDS; Chemicon International Inc., Temecula, CA, USA) and 0.3% or 0.4% Triton-X100, respectively, for detection of Fos or PSTAT3. The blocking solutions were also used for diluting the various antibodies used for the detection process. The tissue was incubated with a rabbit polyclonal primary antibody raised against the N-terminal domain of Fos (1 : 20000, cat: Ab-5; PC38T, Calbiochem, San Diego, CA, USA) overnight at room temperature or raised against the phosphorylated peptide corresponding to residues around Tyr705 of mouse PSTAT3 (1 : 500, cat: 9131; Cell Signalling, Beverly, MA, USA) overnight at 4 °C. The sections were then incubated in biotinylated donkey anti-rabbit Immunoglobulin G (IgG) (1 : 1000 for Fos, 1 : 500 for PSTAT3, cat:11-065-152, Jackson ImmunoResearch, West Grove, PA, USA) and in an avidin-biotin solution (1 : 1000 in PBS; kit ABC Vectastin Elite, Vector, Burlingame, CA, USA) 2 h at room temperature for each treatment. After an additional rinse in a 0.1 M sodium acetate (NaAc, pH 6.0) solution, sections were incubated in a 0.05% 3,3′-diaminobenzidine tetrahydrochloride (DAB, Sigma-Aldrich), 1.25% or 2.5% nickel ammonium sulphate, respectively, for Fos and PSTAT3, 0.02% hydrogen peroxide mixed in NaAc. The reaction was stopped after 5–7 min with successive washes of NaAc and PBS. Sections were then mounted onto gelatin-coated slides, air-dried over night, immersed in xylene and cover-slipped with DEPEX mounting medium (Fluka, Buchs, Switzerland).

Controls for the specificity of anti-Fos and PSTAT3 antibodies used in the current study were described previously and the antibodies reported to be specific (40, 41). In addition, some sections were included in our analyses with the primary antibody omitted, which resulted in the abolishment of the labelling thus confirming the specificity of the Fos and PSTAT3 IR (data not shown).

Fos and leptin receptor (ObR) colocalisation

Double-immunostaining studies for Fos and ObR were performed to investigate whether leptin can induce Fos directly in the NTS. For these experiments, sections were pretreated for 1 h at room temperature with the same blocking solution as previously described for Fos. The same solution was also used for antibody dilutions. The sections were incubated over night at 4 °C with a rabbit anti-Fos antibody (1 : 5000) mixed with a goat polyclonal anti-ObR antibody (1 : 500, cat: GT15012; Neuromics, Northfield, MN, USA) raised against the extracellular domain of murine ObR (amino acids 1–839). Primary antibodies were visualised with donkey CY3-conjugated anti-rabbit IgG (for PSTAT, 1 : 500; cat: 711-165-152 Jackson ImmunoResearch) and donkey Alexa Fluor 488-conjugated antigoat IgG (for ObR; 1 : 500; A11055, Invitrogen, Burlington, Ontario, Canada). The specificity of ObR staining was

confirmed by preincubation of the antibody with recombinant murine leptin receptor protein (0.02 μM; Neuromics, data not shown). Sections were mounted in an aqueous medium containing the nuclear counter stain, 4′6-diamidino-2-phenylindole (DAPI, Vector) and cover-slipped. In control experiments, the sections were incubated with the primary antibody mixture in which one of the primary antibodies was substituted with non-immunised rabbit IgG. Inappropriate cross-reaction between antibodies was confirmed to be negligible (data not shown).

Microscopy

Sections were analysed with a Zeiss-Axioplan microscope (Nussdorf, Germany). Digital black and white images were captured (Retiga Mono Digital 1300 CCD) and fluorescent pictures coloured using Northern Eclipse Software (Empix Imaging Inc., Mississauga, Ontario, Canada).

The number of Fos positive cells visualised after DAB staining was evaluated in the caudal NTS (bregma: −14.30 to −14.08 mm) and in the medial NTS (bregma: −13.80 mm to −13.68 mm coordinates from a rat brain atlas) (42). In each rat, one side of the NTS from three to four sections of each of the two areas investigated were analysed. A circle of the same area was drawn on every section using Northern Eclipse software and the number of Fos positive cells was manually counted within this area at ×10 magnification. The position of the circle within each brain region was delineated using anatomical landmarks. All counts were performed blind to treatment conditions. Similarly, the number of PSTAT3-immunreactive cells was measured in the arcuate nucleus, ventromedial hypothalamic nucleus (VMH) and dorsomedial hypothalamic nucleus (DMH) (bregma: −3.14 mm to −3.30 mm).

RT-PCR

Hypothalamic mRNA expression of the suppressor of cytokine signalling 3 (SOCS3) was assessed using semiquantitative RT-PCR as a measure of the Janus Kinase (JAK)/STAT pathway activation. In addition to SOCS3, we also measured mRNA expression of agouti-related peptide (AgRP) and pro-opiomelanocortin (POMC) to evaluate whether leptin and vagotomy-induced changes in food intake may be associated with modification of the hypothalamic signals known to regulate energy balance. Total RNA was extracted using TRIzol (Invitrogen) according to the manufacturer's instructions. The first-strand cDNA was synthesised from 1 μg of total RNA using 200 units of Molony murine leukaemia virus reverse transcriptase (Invitrogen), 5 μM of random hexamers (Applied Bioscience, Streetsville, Ontario, Canada), and 1 mM of dNTP mix (Sigma-Aldrich) in a total reaction volume of 20 μl. Following reverse transcription, the product was stored at −20 °C. The cDNA product (0.9 μl) was added to 15 μl PCR reaction mix containing ReadyMix Taq PCR (Sigma-Aldrich) and 6 pmol of gene-specific primer sets for SOCS-3, AgRP, POMC and β-actin. Amplification was performed with a thermal cycler (GeneAmp PCR system 9700; Applied Bioscience) using the following cycling parameters: (i) denaturing, 94 °C for 5 min; (ii) amplification cycle, 94 °C for 30 s, 1 min for POMC, annealing temperature, 60 °C for 30 s, 1 min for POMC and 72 °C for 1 min, 2 min for POMC and (ii) final extension, 72 °C for 10 min. Primers were designed to span a sequence derived from different exons (separated by introns in genomic DNA sequence) to minimise amplification from non-mRNA-derived templates. Inappropriate amplification from genomic DNA was negligible when amplification was performed with a template without reverse transcription. The gene accession numbers, primer sequences and cycle numbers used are listed as following: SOCS-3 (NM_053565) sense 5′-CCAGCCGCCACTTCTTCAC-3′, antisense 5′-GTGGAGCATCATACTGGTCC-3′, 40 cycles; AgRP (XM_001075738) sense 5′-AGAGTTCTCAGGTCTAAGTCT-3′, antisense, 5′-CTTGAAGAAGCGGCAGTAG-CAC-3′, 33 cycles; POMC (NM_139326) sense, 5′-CCCGAGAAACAGCAG-CAGTG-3′ antisense, 5′-AGGGGGCCTTGGAGTGAGAA-3′, 28 cycles; β-actin (NM_031144) sense 5′-GCCGTCTTCCCCTCCATCGTG-3′, antisense 5′-TAC-GACCAGAGGCATACAGGGACAAC-3′, 26 cycles. PCR products were separated by 2% agarose gel electrophoresis and visualised with ethidium bromide staining. The band density was obtained for quantification using GeneTool image analysis software (Syngene, Frederick, MD, USA). To normalise the expression level of genes between different samples, the levels were estimated as the ratio of gene*X*/β-actin. In a pilot experiment, the amount of PCR product (on a log scale) versus the number of cycles was plotted, and the linear range of template amplification was determined for two samples from each treatment group. The cycle numbers were determined within the exponential phase of amplification for all treatment groups.

Statistical analysis

All data are presented as the mean ± SEM and were analysed using Datasim software (Desktop Press, Lewiston, ME, USA). Cumulative food intake (4, 6, 8 and 24 h) and change in body weight, IHC quantification and PCR data were analysed individually by parametric two-way ANOVA with treatment (saline/leptin) and surgery (SHAM/VGX) as two between-factors. Stomach weight data were analysed using a parametric unpaired two-tailed t-test. In all cases, values less than 5% were deemed statistically significant.

Results

Subdiaphragmatic vagotomy does not alter leptin-induced loss of appetite and body weight

The role of vagal afferent fibres as a target of leptin activity in appetite regulation was tested by assessing changes in food intake and body weight in VGX compared to SHAM animals at different time points after leptin injection. As expected leptin (3.5 mg/k, i.p.) resulted in a significant reduction in the amount of food consumed by both SHAM and VGX animals at 4 h [ANOVA: $F(1,54) = 14.83$, $P < 0.001$], 6 h [$F(1,54) = 13.87$, $P < 0.001$], 8 h [$F(1,54) = 11.98$, $P < 0.01$] and 24 h [$F(1,54) = 25.06$, $P < 0.0001$] after the injection compared to their saline-treated counterparts (Fig. 2A). The anorectic effect of leptin was not affected by the vagotomy surgery at any time point as indicated by the absence of significant interaction between surgery and treatment [ANOVA: 4 h, $F(1,54) = 1.158$; 6 h, $F(1,54) = 0.440$; 8 h, $F(1,54) = 0.0003$; 24 h, $F(1,54) = 0.005$]. Interestingly however, the vagotomy surgery itself resulted in a slight decrease of food intake at 24 h [ANOVA: $F(1,54) = 6.967$, $P < 0.05$] compared to the SHAM animals, independent of treatment (Fig. 2A).

In addition to monitoring changes of food consumption, the body weight of the same animals was recorded at 0 h (prior to treatment) then at 24 h following injections (Fig. 2B). Control animals injected with saline gained 3.21 ± 0.93 g for the SHAM group and 3.28 ± 1.24 g for the VGX animals. As with food intake, treatment with leptin (3.5 mg/k, i.p.) prevented this gain of weight both in SHAM and VGX animals [ANOVA: $F(1,54) = 6.973$, $P < 0.05$]. This effect remained intact in VGX animals compared to the SHAM group as illustrated by the absence of significant interaction between surgery and treatment [ANOVA: $F(1,54) = 0.137$]. However, the vagotomy surgery itself did not affect 24 h change in body weight [ANOVA: $F(1,54) = 0.188$] compared to the SHAM-operated animals.

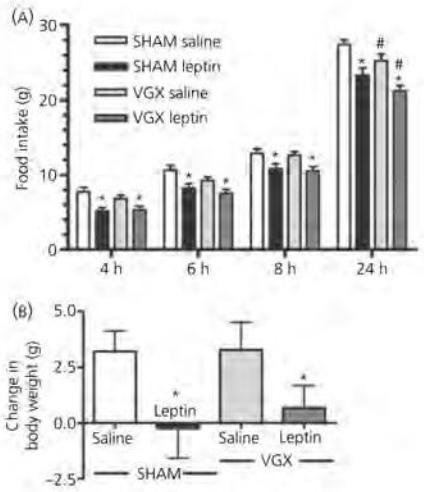


Fig. 2. Vagotomy surgery did not reverse the leptin-induced reduction in food intake and body weight. Leptin treatment (3.5 mg/kg, i.p.) significantly attenuated cumulative food intake at 4, 6, 8 and 24 h (A) in SHAM operated-rats. This response was not abrogated by vagotomy. In addition, vagotomised (VGX) animals ate less over 24 h independent of treatment with saline or leptin treatment (*leptin versus saline food intake: 4 h, $P < 0.001$; 6 h, $P < 0.001$; 8 h, $P < 0.01$; 24 h, $P < 0.0001$, #vagotomy versus SHAM surgery food intake: 24 h, $P < 0.05$). Leptin treatment prevented the gain in body weight observed in the saline-treated groups regardless of surgery. In addition, the vagotomy surgery did not affect 24 h change in body weight of the VGX animals compared to their SHAM-operated counterparts (B) (*leptin versus saline body weight 24 h, $P < 0.05$).

Leptin and vagotomy induced Fos in the NTS

To determine whether changes in food consumption and body weight were associated with modification of brain activity, Fos IR was investigated as a marker of cellular activity in the NTS, a brain structure involved in food intake regulation where vagal afferent fibres terminate. Leptin induced Fos expression 2 h post-treatment in the part of the NTS caudal to the area postrema (AP) of SHAM and VGX animals (Fig. 3D,F and Fig. 3B) [ANOVA: $F(1,14) = 6.851$, $P < 0.05$], mainly in the medial subnucleus, compared to their saline-treated counterparts (SHAM, Fig. 3C; VGX, Fig. 3E). The absence of significant interaction between surgery and treatment (Fig. 3B) [ANOVA: $F(1,14) = 0.131$] revealed that leptin-induced Fos IR in the SHAM animals (Fig. 3D) was not diminished by the subdiaphragmatic vagotomy (leptin VGX; Fig. 3F). However, similar to the food intake observations, the vagotomy surgery itself induced Fos expression in the caudal NTS [ANOVA: $F(1,14) = 9.052$, $P < 0.01$], an effect that can particularly be observed by comparing the VGX saline-treated animals (Fig. 3E) with their SHAM counterpart controls (Fig. 3C). As previously reported (34, 43, 44), Fos expression as a consequence of this surgery can also be found in the medial NTS at the level of the AP from VGX animals (saline, Fig. 3K; leptin, Fig. 3L) compared to SHAM-operated controls (saline, Fig. 3I; leptin, Fig. 3J). A two-way ANOVA on the number of Fos positive cells in this part of the NTS (Fig. 3H) confirmed a significant effect of surgery [ANOVA: $F(1,14) = 33.60$, $P < 0.0001$]. However, leptin did not induce Fos expression in the medial NTS [ANOVA: $F(1,14) = 0.179$] in either surgical group (SHAM, Fig. 3J; VGX, Fig. 3L) compared to their saline-treated counterparts (SHAM, Fig. 3I; VGX, Fig. 3K). This restricted induction of Fos localised in the caudal NTS following leptin treatment has previously been reported in other studies (40, 45).

Leptin acts directly in the NTS and the hypothalamus

Our observation that VGX surgery did not inhibit leptin-induced Fos in the caudal NTS suggests a direct action of leptin on these cells. Previous studies showing the presence of leptin receptor mRNA and leptin-stimulated nuclear STAT3 translocation in the NTS of rats (38, 39, 46) support this hypothesis. Therefore, we investigated whether leptin action on the NTS could be mediated through a direct activation of its receptor by assessing first the colocalisation of Fos and ObR IR and then the expression of PSTAT3 in this area of the brain.

Using double-IHC for Fos and ObR, we observed ObR IR in the brain stem and specifically in the entire NTS (e.g. caudal NTS: saline SHAM animal, Fig. 4A; other levels of the NTS, not shown). In leptin-treated SHAM animals, the ObR IR was found to clearly colocalise with Fos (Fig. 4B). Similar observations were made in the brains of VGX saline and leptin-treated animals where surgery and/or leptin-induced Fos colocalised with ObR both in the caudal and the medial part of the NTS (e.g. caudal NTS: saline VGX, Fig. 4C; leptin VGX, Fig. 4D).

In a second study, injection of leptin (3.5 mg/kg, i.p.) induced PSTAT3 in the caudal (Fig. 3M) and medial (Fig. 3O) NTS 1 h but not 2 h (caudal, Fig. 3N; medial, Fig. 3P) post-treatment in SHAM animals compared to the saline group (data not shown). Leptin-induced PSTAT3 in the caudal NTS was seen to be mainly located in the medial subnucleus, similar to Fos, but with a different pattern (for comparison, see Fig. 3O,M). In addition, the two signals were expressed at different times: 1 h for PSTAT3 and 2 h for Fos in the caudal NTS. Interestingly, PSTAT3 was also expressed 1 h after leptin treatment in the medial NTS. However, unlike that observed in the caudal NTS, this was not followed by Fos induction 2 h post-treatment (for comparison, see Fig. 3J,O).

To further assess the humoral action of leptin, we examined PSTAT3 expression in the hypothalamus, the main site of action of leptin in the regulation of energy balance (47). As expected (46, 48), leptin induced PSTAT3 2 h after injection in the arcuate nucleus, VMH and DMH in the SHAM group (Fig. 5E) compared to the saline-treated animals (Fig. 5C). Leptin treatment resulted in the same pattern of PSTAT3 IR in the hypothalamus of the VGX animals (Fig. 5F). Vagotomy surgery (Fig. 5D) did not affect the basal PSTAT3 expression observed in the arcuate nucleus of SHAM animals (Fig. 5C) after saline treatment. The absence of a surgery effect on PSTAT3 expression was confirmed by the quantification of PSTAT3 positive cells in each of the three nuclei in our four treatment groups (data not shown).

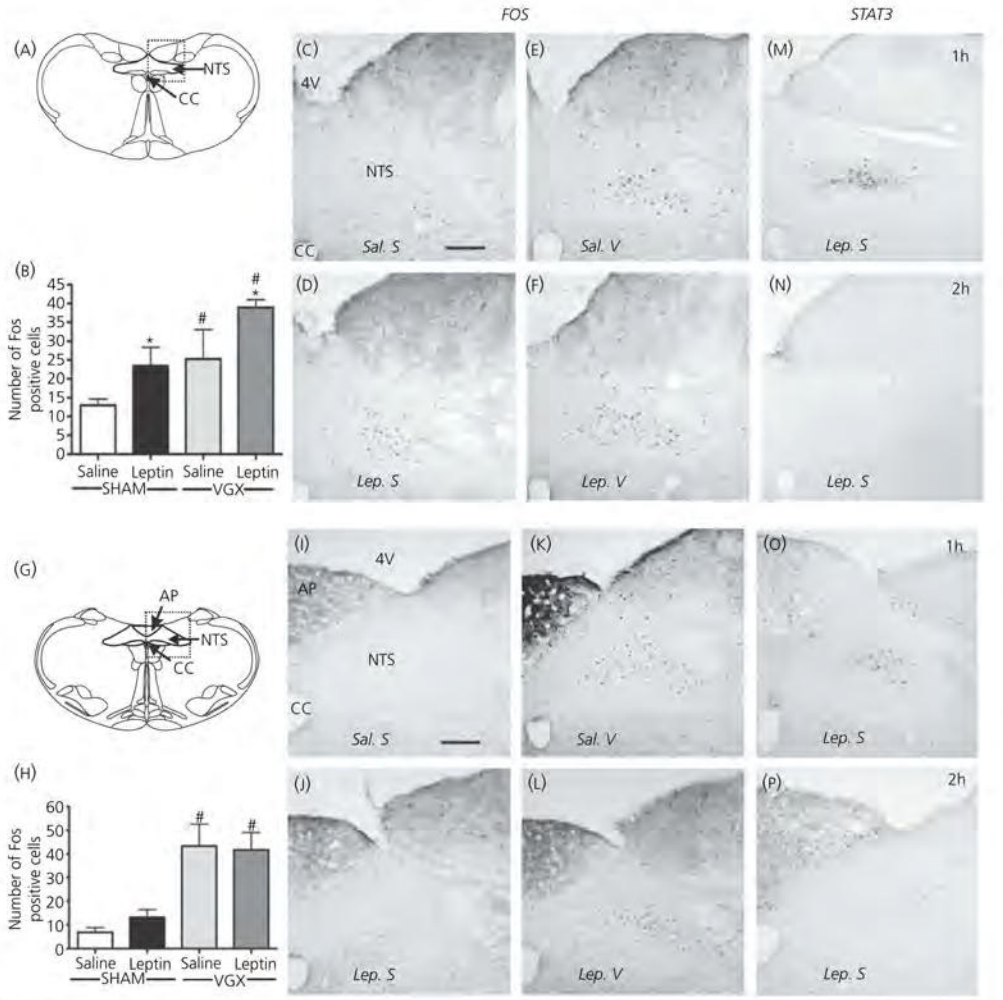


Fig. 3. Fos and PSTAT3 induction in the nucleus of the nucleus tractus solitarii (NTS) after leptin treatment in vagotomised (VGX) and SHAM animals. The left panel shows a brain map overview representation (adapted from Paxinos and Watson; 42) of the caudal (A) and medial (G) NTS where Fos quantification was processed (caudal NTS, B; medial NTS, H). The number of Fos positive cells are expressed per section counted (four sections per animal with $n = 4$–5 animals per group; *leptin versus saline caudal NTS, $P < 0.05$; #vagotomy versus SHAM surgery NTS, caudal part $P < 0.01$, medial part $P < 0.0001$). The middle panel shows representative sections of Fos IR. Leptin injection (3.5 mg/kg, i.p.) led to an increase of Fos expression in the caudal NTS of SHAM (D) and VGX (F) animals compared to their saline-treated counterpart SHAM (C) and VGX (E) 2 h post-treatment. Leptin-induced Fos IR in the SHAM animals (D) was not diminished by subdiaphragmatic vagotomy (F), which itself resulted in Fos expression at this level of the NTS (saline VGX, E). Similarly, VGX animals (saline, K; leptin, L) exhibited a higher level of Fos expression in the medial NTS compared to the SHAM-operated group (saline, I; leptin, J). However, leptin did not induce Fos expression in this part of the NTS (SHAM, J) compared to the caudal part (SHAM, D). The right panels represent PSTAT3 IR at each level of the NTS investigated. Injection of leptin (i.p.) induced PSTAT3 in the caudal (M) and medial (O) NTS 1 h post-treatment of SHAM animals. PSTAT3 IR disappeared 2 h after treatment (caudal NTS, N; medial NTS, P). Sal.S, Saline SHAM; Sal.V, saline VGX; Lep.S, leptin SHAM; Lep.V, leptin VGX. Scale bar = 100 μm.

To monitor more precisely the magnitude of STAT3 activation after leptin, we measured changes in SOCS3 mRNA expression in the hypothalamus by using semiquantitative RT-PCR. SOCS3 is a major end product of the STAT3 signalling pathway, which is involved in auto-regulatory feedback for activated STAT3 and is broadly used as a marker for STAT3 activation (49). This was

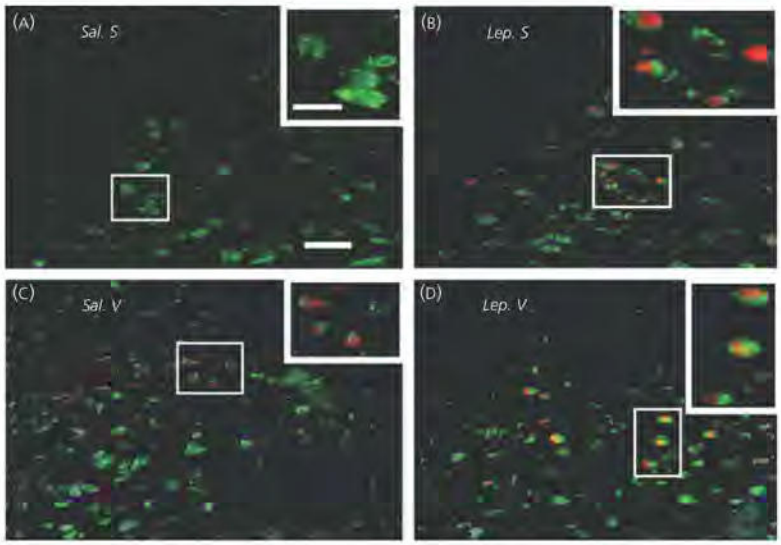


Fig. 4. Leptin receptors colocalise with Fos IR. Leptin receptor (ObR) IR was observed in the nucleus tractus solitarii (NTS; green labelling; saline SHAM, A), and found to colocalises with leptin-induced Fos (red labelling) in SHAM animals (B). Fos positive-cells also expressed the ObR in the NTS of saline vagotomised (VGX) (C) and leptin VGX (D) animals. Insets represent higher magnification of the white squares. Sal.S, Saline SHAM; Sal.V, saline VGX; Lep.S, leptin SHAM; Lep.V, leptin VGX. Scale bar = 50 μm. Inset scale bar = 30 μm.

confirmed in the present study by the significant induction of SOCS3 mRNA levels in the hypothalami of leptin-treated SHAM and VGX animals compared to their saline counterpart controls [ANOVA: $F(1,15) = 6.029$, $P < 0.05$] (Fig. 5B). No significant effects of surgery [$F(1,15) = 0.247$] were noted on this paradigm.

Effect of the vagotomy surgery on the hypothalamic mRNA expression of AgRP and POMC

The effect of surgery on the food intake paradigm observed in the current study was interesting and one that was previously described by others (50, 51). To investigate some of the factors that might contribute to this effect, we studied changes in the levels of hypothalamic neuropeptides such as AgRP and POMC, which are closely associated with appetite regulation (52) and are known to be regulated by leptin (53–55). The vagotomy surgery significantly increased, in a similar manner AgRP mRNA levels in the hypothalami of saline and leptin-treated animals compared to their SHAM counterparts [ANOVA: $F(1,15) = 4.926$, $P < 0.05$] (Fig. 6A). The opposite effect was observed for POMC, the levels of which were decreased in VGX animals regardless of treatment. However, these changes were not significant [$F(1,15) = 3.568$, $P = 0.07$] (Fig. 6B). The expression of neither neuropeptide was affected by leptin treatment [AgRP: $F(1,15) = 1.076$ (Fig. 6A); POMC: $F(1,15) = 0.290$ (Fig. 6B)] 2 h after the injection compared to the saline-treated group.

Discussion

Vagal afferent neurones are now known to constitute a target for appetite regulating peptides such as leptin as a route for propagating peripheral signals to the appetite controlling centres in the brain. Indeed, the regulatory effect of leptin on short-term food intake has been shown to be mediated via this route (8). In the present study, we show that i.p. injection of leptin (3.5 mg/kg) does not act principally through the neural pathway but preferentially uses the humoral route to propagate anorexigenic signals to the brain. Specifically, our data show that the leptin-induced decrease of food intake is not affected in the absence of a vagal input to the brain. This is also based on our observation that leptin treatment led to the induction of nuclear STAT3 translocation in the caudobasal hypothalamus in both SHAM and VGX animals in nuclei reported to have strong constitutive expression of the functional leptin receptor such as the arcuate nucleus, VMH and DMH (2). These findings are consistent with the fact that leptin regulates appetite principally via direct activation of the JAK/STAT pathway after binding to its functional receptor in the hypothalamus (2, 56). Given the relatively high dose of leptin used in these studies, the question of specificity may be a factor that needs to be considered when interpreting some of the results obtained. That these observations were due to the activity of leptin on its receptors, rather than a general side-effect was confirmed by our immunohistochemical data. These studies showed that the distribution of PSTAT3 was

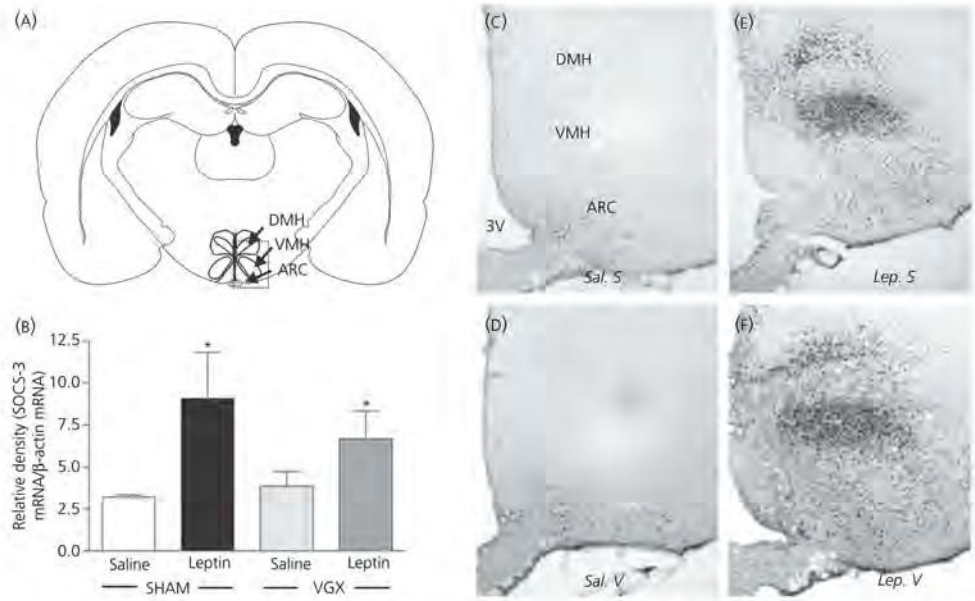


Fig. 5. Leptin induced PSTAT3 in the hypothalamus of SHAM and vagotomised (VGX) animals. The left panel shows an overview representation of the caudo-basal hypothalamus (adapted from Paxinos and Watson, 42) (A). Leptin treatment (3.5 mg/kg) induced comparable levels of PSTAT3 in the arcuate nucleus (ARC), ventromedial hypothalamic nucleus (VMH) and dorsomedial hypothalamic nucleus (DMH) of SHAM (E) and VGX (F) groups compared to the saline-treated SHAM (C) and VGX (D) animals 2 h after injection. Basal PSTAT3 expression was observed in the arcuate nucleus of the saline SHAM (C) and VGX animals (D). Leptin treatment significantly increased SOCS3 mRNA levels in the hypothalami of SHAM and VGX animals compared to their saline counterpart (B) (*leptin versus saline, $P < 0.05$). Sal.S, Saline SHAM; Sal.V, saline VGX; Lep.S, leptin SHAM; Lep.V, leptin VGX. Scale bar = 100 μm.

comparable to the one described in a different study using a dose of 1 mg/kg (39). Additionally, the anatomic pattern of Fos-positive cell expression in the brains of leptin-treated animals was similar after administration of leptin at doses of 1.0 mg/kg and 5.0 mg/kg (57). The authors of this study also reported no significant differences in the relative number of leptin-activated cells (40).

However, it is possible that the relatively high dose of leptin used in the present study may have masked the action of this hormone on the vagus nerve. Therefore, the failure of subdiaphragmatic vagotomy to alter leptin-induced anorexia does not rule out a role for the sensory gut-brain neuroaxis in mediating leptin effects on food intake. Peters *et al.* (8) reported that a more localised intraceliac injection of leptin (10 μg/rat) reduced 15 min intake of sucrose and that this response was attenuated by vagotomy surgery. The effect of leptin in this case was relatively rapid, leading to the conclusion that this route of gut-to-brain communication is involved in mediating leptin-induced acute reduction of meal size. Based on our previous observations (22) and those of others (10–14), as well as dose/response studies conducted as part of the current investigation (data not shown), we administered a 3.5 mg/kg dose of leptin to induce a significant and long-lasting suppression of food intake. Interestingly, from the perspective of the current study, a similar dose of leptin was shown to increase circulating leptin levels for at least 3 h post-injection (58) and, consequently, the time of exposure for vagal afferents. Taken together, these data suggest that the vagal afferent neurones do not constitute a major route of mediating the sustained effects of leptin on food intake and body weight and only participate in the termination of individual meals (8). This is in contrast to the observation made in a recent study showing that the acute effect of leptin on food intake required the integrity of the vagus nerve (59). It is difficult to reconcile these data with our current results; however, the difference in the source of leptin (Amgen Biological versus NIBSC), the species (mice versus rat), the vendors (Harlan laboratorie versus Charles River) (60) and the feeding state of the animals (food deprived versus *ad libitum*) may be responsible for this discrepancy. To avoid the consequences of exogenously administrated leptin, it would be interesting to investigate in future studies the role of endogenous, circulating, adipose-derived leptin and, more particularly, its possible action at the level of the vagus nerve to regulate food intake.

Despite these observations, we cannot totally exclude the notion that leptin may act on other areas of vagal afferent neurones that are located anterior to the diaphragm. For example, the direct action of leptin on the nodose ganglion, which contains the cell bodies of the vagus nerve, would not have been altered by

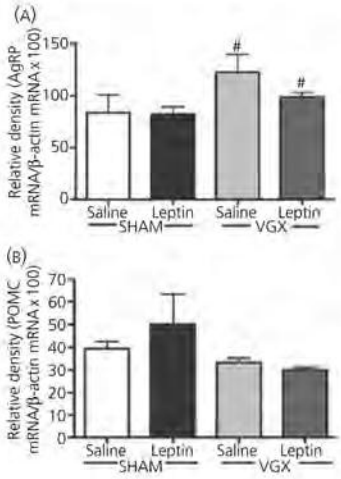


Fig. 6. Vagotomy surgery altered agouti-related peptide (AgRP) and pro-opiomelanocortin (POMC) mRNA expression in the hypothalamus. The vagotomy surgery led to an increase of AgRP mRNA levels in the hypothalami of saline and leptin-treated animals compared to their SHAM counterparts. Leptin treatment (3.5 mg/kg) did not modify AgRP mRNA of SHAM and vagotomised (VGX) animals compared to the saline control 2 h after the injection (A). The surgery also decreased POMC mRNA expression in the hypothalami of saline and leptin-treated animals compared to the SHAM groups although this was not statistically significant ($P = 0.07$). Leptin had no effect on POMC mRNA expression 2 h post-treatment (B) (#vagotomy versus SHAM surgery, $P < 0.05$).

subdiaphragmatic vagotomy. The presence of functional leptin receptors at this level (4, 61, 62) and the fact that leptin was shown to depolarise cultured nodose neurones (7) both support this hypothesis. A direct action of leptin on the nodose ganglion is further strengthened by our observation that subdiaphragmatic vagotomy did not reduce leptin-induced Fos expression in the caudal NTS. Other than the nodose ganglion, however, leptin-induced Fos expression in the NTS could also be due to an action of leptin on the forebrain, which is neuroanatomically connected to the brain stem via various projections (52). Such an effect would not have been altered by the vagotomy procedure. Indeed, several studies have already demonstrated that leptin action on the hypothalamus may result in descending signals that modulate neural processing of meal-related inputs of vagal afferents that originate from the gut (63–65). More specifically, one of these studies (64) showed that intracerebroventricular injection of leptin led to increases in CCK-induced Fos expression at the same level of the NTS where we observed Fos after i.p. leptin injection in our present work.

Thus, leptin-induced responses in the NTS could have been due to activation of the nodose ganglion and/or descending projection from the hypothalamus. Alternatively, it is possible that, given the induction of Fos in the NTS of VGX animals, the surgical procedure itself may have masked the vagal action of leptin because subdiaphragmatic vagotomy includes the transection of both afferent and efferent fibres of the vagus nerve, which may result in long-term consequences on homeostatic function. Consistent with this hypothesis, we found that VGX animals consumed significantly less than SHAM-operated ones over a 24 h time period. In support of this finding, previous studies have reported that body weight of VGX animals was consistently lower than that of SHAM animals although the animals were kept on a liquid diet (50, 51). Moreover, it was suggested (51) that the change in body weight might reflect altered intake of the first meal size but not metabolic efficiency. The behavioural modifications were also associated with an increase in neuropeptide Y (NPY) levels in the arcuate nucleus of VGX animals (50). Other than NPY, neuropeptides such as AgRP and POMC are important regulators of energy balance, as was shown in food deprivation studies in rats in which hypothalamic AgRP mRNA expression was up-regulated and POMC mRNA expression down-regulated, collectively leading to appetite stimulation (66). Interestingly, in the present study, the VGX surgery, in absence of any treatment, led to an increase in AgRP and a trend toward a reduction of POMC mRNA expression in the hypothalamus, which could reflect the change in body weight between the VGX (383.67 ± 6.97 g) and the SHAM animals (407.38 ± 4.44 g) observed at the time of injection [$t(56) = 2.908$, $P < 0.01$]. However, food intake remained reduced in VGX animals compared to the SHAM animals despite these changes, which would normally stimulate the drive to eat. These observations suggest that removal of the vagus nerve not only results in a loss of satiety regulation but also in the suppression of the hunger promoting signal, an effect that was described earlier by others (50). Surprisingly, we did not observe an effect of leptin on either AgRP or POMC expression, which seems contrary to many studies showing that it regulates the synthesis of these neuropeptides. However, these observations were made in fasted, obese animals or in animals chronically treated with leptin (53–55, 67), and not in fed, lean ones, such as those used in our present work.

The results from our current study and previous findings of others (34, 43, 44) showing Fos expression in the NTS induced by vagotomy surgery itself provide a possible brain mechanism associated with the change of food intake of VGX animals. Most of the hypothalamic nuclei involved in energy balance regulation receive inputs from the NTS (68). Therefore, it is possible that this aforementioned unexpected Fos expression leads to a modification of hypothalamic signals resulting in a lower level of ingestion. A possible mechanism of this surgery-induced Fos in the NTS could involve glutamatergic and GABAergic neurones, which are widely expressed within the NTS (69, 70). Despite discrepant findings between different studies, it has been suggested that glutamate may be the transmitter used by vagal afferents to signal satiety to the NTS (71). It is feasible that, if the GABAergic neurones present in the NTS receive a tonic excitatory glutamatergic input, it will be disrupted in the absence of a vagal stimulus. This could result in the GABA-innervated neurones losing the inhibitory signal, consequently resulting in cell excitation and, subsequently, in Fos induction. This mechanism has already been proposed in a study showing that fourth ventricular infusion of MK-801, a

noncompetitive antagonist of NMDA glutamate receptors resulted in a significant induction of Fos expression in the NTS (72).

It is possible that the vagotomy surgery could have masked the effects of leptin-mediated NTS activation via the vagus nerve. In this respect, the induction of Fos in the caudal NTS of the SHAM animals by leptin constitutes, in the present study, the only evidence supporting its action through the vagus nerve to communicate with the brain. This is supported by the observation that Fos expression appears to be independent of a direct action of leptin on its receptor. Although Fos and leptin receptors colocalise in the caudal NTS, the pattern of leptin receptor expression is not confined only to this area. Similarly, the nuclear translocation of STAT3 as a marker for direct action of leptin on its receptor is more widely distributed in the NTS compared to the very caudal Fos expression observed in the leptin SHAM group. Therefore, direct action of leptin through its receptor in the NTS would probably have induced Fos in a less restricted area than the caudal NTS. In addition, it has been shown that only a small percentage of vagal fibres respond to leptin (7). The fact that leptin induced only a small number of Fos positive cells in our study is consistent with this idea, and reinforces the possibility, that this Fos expression may be due to an action of leptin at the subdiaphragmatic level of the vagus nerve.

Interestingly, we observed a difference in the time window during which PSTAT3 is detected in the NTS and the hypothalamus. As previously reported in other studies (46), STAT3 phosphorylation was present in the NTS 1 h, but not 2 h, following leptin injection, whereas PSTAT3 was present in the hypothalamus 2 h post-treatment. This may be a reflection of the different properties of the blood–brain barrier (BBB) around these two areas of the brain. It has been shown that leptin mainly gains access to the hypothalamus from the circulation via a specific transport mechanism (3). However, the presence of circum ventricular organs (CVOs), brain structures with a 'leaky' BBB, could constitute another route for leptin to enter the brain. Interestingly, fenestrated capillaries are abundant not only in the area postrema, a CVO localised in close vicinity to the NTS, but also directly in this particular brain structure itself (73, 74). This could allow circulating leptin access to the NTS more rapidly compared to the hypothalamus, thus possibly explaining the time difference observed.

The rapid action of leptin in the NTS may be involved in mediating its effect on food intake and body weight through activation of vagal efferent nerve fibres. Indeed, our current work and studies by others show that PSTAT3 and leptin receptor immunoreactive cells are located in the NTS and in the dorsal motor nucleus of the vagus (DMV) in the brain stem, which receives projections from the NTS (38, 41). Neurones of the DMV provide the parasympathetic motor output to the subdiaphragmatic viscera via the efferent vagal fibres. Interestingly, the cholinergic neurones of the DMV that directly control the viscera contain the functional leptin receptor and cytoplasmatic STAT3 (4). In addition, fourth ventricle administration or microinjection of leptin into the NTS is sufficient to suppress appetite and weight gain (38). Collectively, these data suggest that leptin action in the brain stem may result in an activation of the parasympathetic motor output and contribute to energy balance regulation. However, there is no direct evidence to suggest that this action of leptin stimulates the activity of the vagal efferent fibres or the release of acetylcholine from the terminal nerve endings.

One study has proposed a mechanism aimed at reconciling how the vagus nerve could mediate both the action of leptin on appetite as a normal regulator of energy balance and as a neuroimmune circulating mediator in disease (75). These workers found two types of leptin sensitive vagal fibres; an IL-1β dependent type 1 and an IL-1β independent type 2. This led the authors to suggest a dual role for leptin through these two distinct vagal fibres: type 1 units could control food intake during inflammation, whereas type 2 units could generate acute physiological satiety signals.

In conclusion, our data suggest that administration of exogenous leptin leading to a reduction of food intake within hours and a loss of body weight acts principally through the humoral pathway to target the brain. This experiment also suggests that vagal fibre neurones are not involved in relaying this effect of leptin but may be important in regulating the drive to eat. However, we cannot exclude a role for vagal afferents in mediating endogenous leptin-induced long-term effects on homeostasis.

Acknowledgements

This work was supported by the Canadian Institutes of Health Research and Natural Sciences and Engineering Research Council of Canada.

Accepted 14 December 2006

References

1 Maffei M, Halaas J, Ravussin E, Pratley RE, Lee GH, Zhang Y, Fei H, Kim S, Lallone R, Ranganathan S. Leptin levels in human and rodent: measurement of plasma leptin and ob RNA in obese and weight-reduced subjects. *Nat Med* 1995; **1**: 1155–1161.

2 Elmquist JK, Bjorbaek C, Ahima RS, Flier JS, Saper CB. Distributions of leptin receptor mRNA isoforms in the rat brain. *J Comp Neurol* 1998; **395**: 535–547.

3 Banks WA, Kastin AJ, Huang W, Jaspan JB, Maness LM. Leptin enters the brain by a saturable system independent of insulin. *Peptides* 1996; **17**: 305–311.

4 Buyse M, Ovesjo ML, Goiot H, Guilmeau S, Peranzi G, Moizo L, Walker F, Lewin MJ, Meister B, Bado A. Expression and regulation of leptin receptor proteins in afferent and efferent neurons of the vagus nerve. *Eur J Neurosci* 2001; **14**: 64–72.

5 Gaige S, Abysique A, Bouvier M. Effects of leptin on cat intestinal vagal mechanoreceptors. *J Physiol* 2002; **543**: 679–689.

6 Wang YH, Tache Y, Sheibel AB, Go VL, Wei JY. Two types of leptin-responsive gastric vagal afferent terminals: an in vitro single-unit study in rats. *Am J Physiol* 1997; **273**: R833–R837.

7 Peters JH, Ritter RC, Simasko SM. Leptin and CCK selectively activate vagal afferent neurons innervating the stomach and duodenum. *Am J Physiol Regul Integr Comp Physiol* 2006; **290**: R1544–R1549.

8 Peters JH, McKay BM, Simasko SM, Ritter RC. Leptin-induced satiation mediated by abdominal vagal afferents. *Am J Physiol Regul Integr Comp Physiol* 2005; **288**: R879–R884.

9 Bado A, Levasseur S, Attoub S, Kermorgant S, Laigneau JP, Bortoluzzi MN, Moizo L, Lehy T, Guerre-Millo M, Marchand-Brustel Y, Lewin MJ. The stomach is a source of leptin. *Nature* 1998; **394**: 790–793.

10 Halaas JL, Gajiwala KS, Maffei M, Cohen SL, Chait BT, Rabinowitz D, Lallone RL, Burley SK, Friedman JM. Weight-reducing effects of the plasma protein encoded by the obese gene. *Science* 1995; **269**: 543–546.

11 Campfield LA, Smith FJ, Guisez Y, Devos R, Burn P. Recombinant mouse OB protein: evidence for a peripheral signal linking adiposity and central neural networks. *Science* 1995; **269**: 546–549.

12 Campfield LA, Smith FJ, Burn P. The OB protein (leptin) pathway – a link between adipose tissue mass and central neural networks. *Horm Metab Res* 1996; **28**: 619–632.

13 Pelleymounter MA, Cullen MJ, Baker MB, Hecht R, Winters D, Boone T, Collins F. Effects of the obese gene product on body weight regulation in ob/ob mice. *Science* 1995; **269**: 540–543.

14 Harris RB, Zhou J, Redmann SM Jr, Smagin GN, Smith SR, Rodgers E, Zachwieja JJ. A leptin dose-response study in obese (ob/ob) and lean (+/?) mice. *Endocrinology* 1998; **139**: 8–19.

15 Berkowitz DE, Brown D, Lee KM, Emala C, Palmer D, An Y, Breslow M. Endotoxin-induced alteration in the expression of leptin and beta3-adrenergic receptor in adipose tissue. *Am J Physiol* 1998; **274**: E992–E997.

16 Grunfeld C, Zhao C, Fuller J, Pollock A, Moser A, Friedman J, Feingold KR. Endotoxin and cytokines induce expression of leptin, the *ob* gene product, in hamsters. A role for leptin in the anorexia of infection. *J Clin Invest* 1996; **97**: 2152–2157.

17 Mastronardi CA, Yu WH, Srivastava VK, Dees WL, McCann SM. Lipopolysaccharide-induced leptin release is neurally controlled. *Proc Natl Acad Sci USA* 2001; **98**: 14720–14725.

18 Sarraf P, Frederich RC, Turner EM, Ma G, Jaslowiak NT, Rivet DJ, IIIFlier JS , Lowell BB, Fraker DL, Alexander HR. Multiple cytokines and acute inflammation raise mouse leptin levels: potential role in inflammatory anorexia. *J Exp Med* 1997; **185**: 171–175.

19 Faggioni R, Fantuzzi G, Fuller J, Dinarello CA, Feingold KR, Grunfeld C. IL-1 beta mediates leptin induction during inflammation. *Am J Physiol* 1998; **274**: R204–R208.

20 Finck BN, Kelley KW, Dantzer R, Johnson RW. In vivo and in vitro evidence for the involvement of tumor necrosis factor-alpha in the induction of leptin by lipopolysaccharide. *Endocrinology* 1998; **139**: 2278–2283.

21 Loffreda S, Yang SQ, Lin HZ, Karp CL, Brengman ML, Wang DJ, Klein AS, Bulkley GB, Bao C, Noble PW, Lane MD, Diehl AM. Leptin regulates pro-inflammatory immune responses. *FASEB J* 1998; **12**: 57–65.

22 Luheshi GN, Gardner JD, Rushforth DA, Loudon AS, Rothwell NJ. Leptin actions on food intake and body temperature are mediated by IL-1. *Proc Natl Acad Sci USA* 1999; **96**: 7047–7052.

23 Zarkesh-Esfahani H, Pockley AG, Wu Z, Hellewell PG, Weetman AP, Ross RJ. Leptin indirectly activates human neutrophils via induction of TNF-alpha. *J Immunol* 2004; **172**: 1809–1814.

24 Sachot C, Poole S, Luheshi GN. Circulating leptin mediates lipopolysaccharide-induced anorexia and fever in rats. *J Physiol* 2004; **561**: 263–272.

25 Hart BL. Biological basis of the behavior of sick animals. *Neurosci Biobehav Rev* 1988; **12**: 123–137.

26 Konsman JP, Luheshi GN. CNS responses to peripheral insults. In: Rothwell, N, Loddick, SA, eds. *Immune and Inflammatory Responses in the Nervous System*. Oxford: Oxford University Press, 2002: 51–69.

27 Schwartz GJ. Neural-immune gut-brain communication in the anorexia of disease. *Nutrition* 2002; **18**: 528–533.

28 Bluthe RM, Laye S, Michaud B, Combe C, Dantzer R, Parnet P. Role of interleukin-1beta and tumour necrosis factor-alpha in lipopolysaccharide-induced sickness behaviour: a study with interleukin-1 type I receptor-deficient mice. *Eur J Neurosci* 2000; **12**: 4447–4456.

29 Laye S, Gheusi G, Cremona S, Combe C, Kelley K, Dantzer R, Parnet P. Endogenous brain IL-1 mediates LPS-induced anorexia and hypothalamic cytokine expression. *Am J Physiol Regul Integr Comp Physiol* 2000; **279**: R93–R98.

30 Bret-Dibat JL, Bluthe RM, Kent S, Kelley KW, Dantzer R. Lipopolysaccharide and interleukin-1 depress food-motivated behavior in mice by a vagal-mediated mechanism. *Brain Behav Immun* 1995; **9**: 242–246.

31 Goehler LE, Gaykema RP, Hammack SE, Maier SF, Watkins LR. Interleukin-1 induces c-Fos immunoreactivity in primary afferent neurons of the vagus nerve. *Brain Res* 1998; **804**: 306–310.

32 Kurosawa M, Uvnas-Moberg K, Miyasaka K, Lundeberg T. Interleukin-1 increases activity of the gastric vagal afferent nerve partly via stimulation of type A CCK receptor in anesthetized rats. *J Auton Nerv Syst* 1997; **62**: 72–78.

33 Schwartz GJ, Plata-Salaman CR, Langhans W. Subdiaphragmatic vagal deafferentation fails to block feeding-suppressive effects of LPS and IL-1 beta in rats. *Am J Physiol* 1997; **273**: R1193–R1198.

34 Konsman JP, Luheshi GN, Bluthe RM, Dantzer R. The vagus nerve mediates behavioural depression, but not fever, in response to peripheral immune signals; a functional anatomical analysis. *Eur J Neurosci* 2000; **12**: 4434–4446.

35 Kraly FS, Jerome C, Smith GP. Specific postoperative syndromes after total and selective vagotomies in the rat. *Appetite* 1986; **7**: 1–17.

36 Simons CT, Kulchitsky VA, Sugimoto N, Homer LD, Szekely M, Romanovsky AA. Signaling the brain in systemic inflammation: which vagal branch is involved in fever genesis? *Am J Physiol* 1998; **275**: R63–R68.

37 Li H, Nomura S, Mizuno N. Binding of the isolectin I-B4 from Griffonia simplicifolia to the general visceral afferents in the vagus nerve: a 1. *Neurosci Lett* 1997; **222**: 53–56.

38 Grill HJ, Schwartz MW, Kaplan JM, Foxhall JS, Breininger J, Baskin DG. Evidence that the caudal brainstem is a target for the inhibitory effect of leptin on food intake. *Endocrinology* 2002; **143**: 239–246.

39 Munzberg H, Huo L, Nillni EA, Hollenberg AN, Bjorbaek C. Role of signal transducer and activator of transcription 3 in regulation of hypothalamic proopiomelanocortin gene expression by leptin. *Endocrinology* 2003; **144**: 2121–2131.

40 Elias CF, Kelly JF, Lee CE, Ahima RS, Drucker DJ, Saper CB, Elmquist JK. Chemical characterization of leptin-activated neurons in the rat brain. *J Comp Neurol* 2000; **423**: 261–281.

41 Hosoi T, Kawagishi T, Okuma Y, Tanaka J, Nomura Y. Brain stem is a direct target for leptin's action in the central nervous system. *Endocrinology* 2002; **143**: 3498–3504.

42 Paxinos G, Watson C. *The Rat Brain in Stereotaxic Coordinates*, 4th edn. San Diego, CA: Academic Press, 1998.

43 Traub RJ, Sengupta JN, Gebhart GF. Differential c-fos expression in the nucleus of the solitary tract and spinal cord following noxious gastric distention in the rat. *Neuroscience* 1996; **74**: 873–884.

44 Yang ZJ, Rao ZR, Ju G. Evidence for the medullary visceral zone as a neural station of neuroimmunomodulation. *Neurosci Res* 2000; **38**: 237–247.

45 Wang L, Martinez V, Barrachina MD, Tache Y. Fos expression in the brain induced by peripheral injection of CCK or leptin plus CCK in fasted lean mice. *Brain Res* 1998; **791**: 157–166.

46 Mutze J, Roth J, Gerstberger R, Matsumura K, Hubschle T. Immunohistochemical evidence of functional leptin receptor expression in neuronal and endothelial cells of the rat brain. *Neurosci Lett* 2006; **394**: 105–110.

47 Friedman JM, Halaas JL. Leptin and the regulation of body weight in mammals. *Nature* 1998; **395**: 763–770.

48 Hubschle T, Thom E, Watson A, Roth J, Klaus S, Meyerhof W. Leptin-induced nuclear translocation of STAT3 immunoreactivity in hypothalamic

nuclei involved in body weight regulation. *J Neurosci* 2001; **21**: 2413–2424.
49 Myers MG Jr. Leptin receptor signaling and the regulation of mammalian physiology. *Recent Prog Horm Res* 2004; **59**: 287–304.
50 Furness JB, Koopmans HS, Robbins HL, Clerc N, Tobin JM, Morris MJ. Effects of vagal and splanchnic section on food intake, weight, serum leptin and hypothalamic neuropeptide Y in rat. *Auton Neurosci* 2001; **92**: 28–36.
51 Phillips RJ, Baronowsky EA, Powley TL. Long-term regeneration of abdominal vagus: efferents fail while afferents succeed. *J Comp Neurol* 2003; **455**: 222–237.
52 Broberger C. Brain regulation of food intake and appetite: molecules and networks. *J Intern Med* 2005; **258**: 301–327.
53 Mizuno TM, Mobbs CV. Hypothalamic agouti-related protein messenger ribonucleic acid is inhibited by leptin and stimulated by fasting. *Endocrinology* 1999; **140**: 814–817.
54 Mizuno TM, Kleopoulos SP, Bergen HT, Roberts JL, Priest CA, Mobbs CV. Hypothalamic pro-opiomelanocortin mRNA is reduced by fasting and [corrected] in ob/ob and db/db mice, but is stimulated by leptin. *Diabetes* 1998; **47**: 294–297.
55 Schwartz MW, Seeley RJ, Woods SC, Weigle DS, Campfield LA, Burn P, Baskin DG. Leptin increases hypothalamic pro-opiomelanocortin mRNA expression in the rostral arcuate nucleus. *Diabetes* 1997; **46**: 2119–2123.
56 Gao Q, Wolfgang MJ, Neschen S, Morino K, Horvath TL, Shulman GI, Fu XY. Disruption of neural signal transducer and activator of transcription 3 causes obesity, diabetes, infertility, and thermal dysregulation. *Proc Natl Acad Sci USA* 2004; **101**: 4661–4666.
57 Elmquist JK, Ahima RS, Elias CF, Flier JS, Saper CB. Leptin activates distinct projections from the dorsomedial and ventromedial hypothalamic nuclei. *Proc Natl Acad Sci USA* 1998; **95**: 741–746.
58 Ahima RS, Prabakaran D, Mantzoros C, Qu D, Lowell B, Maratos-Flier E, Flier JS. Role of leptin in the neuroendocrine response to fasting. *Nature* 1996; **382**: 250–252.
59 Barrachina MD, Martinez V, Wang L, Wei JY, Tache Y. Synergistic interaction between leptin and cholecystokinin to reduce short-term food intake in lean mice. *Proc Natl Acad Sci USA* 1997; **94**: 10455–10460.
60 Pecoraro N, Ginsberg AB, Warne JP, Gomez F, la Fleur SE, Dallman MF. Diverse basal and stress-related phenotypes of Sprague Dawley rats from three vendors. *Physiol Behav* 2006; **89**: 598–610.
61 Burdyga G, Spiller D, Morris R, Lal S, Thompson DG, Saeed S, Dimaline R, Varro A, Dockray GJ. Expression of the leptin receptor in rat and human nodose ganglion neurones. *Neuroscience* 2002; **109**: 339–347.
62 Peiser C, Springer J, Groneberg DA, McGregor GP, Fischer A, Lang RE. Leptin receptor expression in nodose ganglion cells projecting to the rat gastric fundus. *Neurosci Lett* 2002; **320**: 41–44.
63 Blevins JE, Schwartz MW, Baskin DG. Evidence that paraventricular nucleus oxytocin neurons link hypothalamic leptin action to caudal brain stem nuclei controlling meal size. *Am J Physiol Regul Integr Comp Physiol* 2004; **287**: R87–R96.
64 Emond M, Schwartz GJ, Ladenheim EE, Moran TH. Central leptin modulates behavioral and neural responsivity to CCK. *Am J Physiol* 1999; **276**: R1545–R1549.
65 Morton GJ, Blevins JE, Williams DL, Niswender KD, Gelling RW, Rhodes CJ, Baskin DG, Schwartz MW. Leptin action in the forebrain regulates the hindbrain response to satiety signals. *J Clin Invest* 2005; **115**: 703–710.
66 Mizuno TM, Makimura H, Silverstein J, Roberts JL, Lopingco T, Mobbs CV. Fasting regulates hypothalamic neuropeptide Y, agouti-related peptide, and proopiomelanocortin in diabetic mice independent of changes in leptin or insulin. *Endocrinology* 1999; **140**: 4551–4557.
67 Korner J, Savontaus E, Chua SC Jr, Leibel RL, Wardlaw SL. Leptin regulation of Agrp and Npy mRNA in the rat hypothalamus. *J Neuroendocrinol* 2001; **13**: 959–966.
68 Ter Horst GJ, de Boer P, Luiten PG, van Willigen JD. Ascending projections from the solitary tract nucleus to the hypothalamus. A *Phaseolus vulgaris* lectin tracing study in the rat. *Neuroscience* 1989; **31**: 785–797.
69 Fong AY, Stornetta RL, Foley CM, Potts JT. Immunohistochemical localization of GAD67-expressing neurons and processes in the rat brainstem: subregional distribution in the nucleus tractus solitarius. *J Comp Neurol* 2005; **493**: 274–290.
70 Qian M, Johnson AE, Kallstrom L, Carrer H, Sodersten P. Cholecystokinin, dopamine D2 and N-methyl-D-aspartate binding sites in the nucleus of the solitary tract of the rat: possible relationship to ingestive behavior. *Neuroscience* 1997; **77**: 1077–1089.
71 Treece BR, Covasa M, Ritter RC, Burns GA. Delay in meal termination follows blockade of N-methyl-D-aspartate receptors in the dorsal hindbrain. *Brain Res* 1998; **810**: 34–40.
72 Zheng H, Kelly L, Patterson LM, Berthoud HR. Effect of brain stem NMDA-receptor blockade by MK-801 on behavioral and fos responses to vagal satiety signals. *Am J Physiol* 1999; **277**: R1104–R1111.
73 Gross PM, Wall KM, Wainman DS, Shaver SW. Subregional topography of capillaries in the dorsal vagal complex of rats. II. Physiological properties. *J Comp Neurol* 1991; **306**: 83–94.
74 Gross PM, Wall KM, Pang JJ, Shaver SW, Wainman DS. Microvascular specializations promoting rapid interstitial solute dispersion in nucleus tractus solitarius. *Am J Physiol* 1990; **259**: R1131–R1138.
75 Gaige S, Abou E, Abysique A, Bouvier M. Effects of interactions between interleukin-1beta and leptin on cat intestinal vagal mechanoreceptors. *J Physiol* 2004; **555**: 297–310.

© 2007 The Authors. Journal Compilation © 2007 Blackwell Publishing Ltd,

1.11. „STAT3 and COX-2 activation in the guinea-pig brain during fever induced by the Toll-like receptor-3 agonist polyinosinic:polycytidylic acid“

Springer Cell Tissue Res, article title (see above), volume 328, year of publication 2007, pages 549-561, names of authors (see below), "With permission of Springer"

Voss T., Barth SW., **Rummel C**., Gerstberger R., Hübschle T., Roth J.
Cell Tissue Res (2007) 328 :549-561.

Impakt Faktor: 2,804

Eigener Anteil an der Publikation:

- Initiative: unterstützend (10 %)
- Projektplanung: unterstützend (20 %)
- Durchführung der Versuche: unterstützend (35 %)
- Auswertung der Experimente: unterstützend (30 %)
- Erstellung der Publikation: unterstützend (10 %)

Cell Tissue Res (2007) 328:549–561
DOI 10.1007/s00441-007-0386-6

REGULAR ARTICLE

STAT3 and COX-2 activation in the guinea-pig brain during fever induced by the Toll-like receptor-3 agonist polyinosinic:polycytidylic acid

Thilo Voss · Stephan W. Barth · Christoph Rummel · Rüdiger Gerstberger · Thomas Hübschle · Joachim Roth

Received: 25 August 2006 / Accepted: 26 January 2007 / Published online: 8 March 2007
© Springer-Verlag 2007

Abstract Intra-arterial injections of synthetic double-stranded RNA (polyinosinic:polycytidylic acid, PIPC) at a dose of 500 μg/kg evoked pronounced fever in guinea-pigs. PIPC-induced fever could be antagonized by treatment with the non-selective cyclooxygenase (COX) inhibitor diclofenac and was, in part, attenuated by the administration of the selective COX-2-inhibitor nimesulide (dose: 5 mg/kg for both COX inhibitors). We further investigated whether direct activation of brain cells during PIPC-induced fever could be demonstrated. Using radioactive in situ hybridization, we demonstrated that treatment with PIPC resulted in an upregulation of COX-2 and interleukin-1β mRNA in the guinea-pig brain. Thus, COX-2-specific hybridization signals seemed to be mainly associated with brain blood vessels. Intra-arterial injections of PIPC further induced the pronounced nuclear translocation of the transcription factor STAT3 in the endothelium of various fore- and hindbrain areas and in the meninges. In brain structures that lacked a tight blood-brain barrier, i.e. the sensory circumventricular organs (area postrema, vascular organ of laminae terminalis, subfornical organ), the astrocytes and a population of still undetermined cellular phenotype also showed marked STAT3 activation in response to PIPC. The Toll-like receptor-3 agonist PIPC therefore caused a similar activation of brain cells as that reported for other experimental models of systemic inflammation.

Keywords Fever · Systemic inflammation · Toll-like receptors · Cytokines · Cyclooxygenase · Transcription factors · Guinea-pig (male)

This study was supported by the Deutsche Forschungsgemeinschaft (DFG project RO 896/5-2).

T. Voss · C. Rummel · R. Gerstberger · T. Hübschle · J. Roth (✉)
Institut für Veterinär-Physiologie,
Justus-Liebig-Universität Giessen,
Frankfurter Strasse 100,
35392 Giessen, Germany
e-mail: Joachim.Roth@vetmed.uni-giessen.de

S. W. Barth
Federal Research Centre for Nutrition and Food,
Karlruhe, Germany

Introduction

Double-stranded RNA is produced as a side-product of viral replication and is able to evoke cellular responses (Jacobs and Langland 1996). Therefore, polyinosinic:polycytidylic acid (PIPC), a synthetic analogue of double-stranded RNA, has been used as a model of viral infection (Fortier et al. 2004; Traynor et al. 2004). The properties of PIPC as a fever-inducing agent, a so-called "exogenous pyrogen", have repeatedly been demonstrated in rabbits (Absher and Stinebring 1969; Kimura et al. 1994; Rotondo et al. 1988; Soszynski et al. 1991; Won and Lin 1988), rats (Chuang et al. 1990; Fortier et al. 2004; Ellis et al. 2006), mice (Traynor et al. 2004) and guinea-pigs (Cooper et al. 1988; Li et al. 2000; Voss et al. 2006). Responses to PIPC in vivo and in vitro are mediated by activation of toll-like receptor (TLR)-3 signalling pathways (Alexopoulou et al. 2001). Members of the TLR family have been identified as key receptors for so-called "pathogen-associated molecular patterns" (PAMPs) and represent a crucial component of the innate immune system.

In vivo, the activation of TLR3 by systemic treatment of experimental animals with PIPC causes elevated levels of pyrogenic cytokines in the blood (Fortier et al. 2004; Voss et al. 2006); this is also the case in response to treatments

with other pathogen-associated molecules that activate TLR-2, TLR-6, TLR-4 or TLR9 (Roth et al. 1997; Hübschle et al. 2006; Kozak et al. 2006). Thus, distinct activators of the innate immune system probably evoke fever and other brain-controlled signs of illness via similar brain-intrinsic mechanisms. Such brain-intrinsic mechanisms include the activation of transcription factors (Gautron et al. 2002; Harré et al. 2002; Nadjar et al. 2003; Hosoi et al. 2004; Rummel et al. 2004, 2005b; Sako et al. 2005) and the induction of cytokines, such as interluekin-1β (IL-1β), and of the inducible form of the cyclooxygenases, viz. COX-2 (Breder and Saper 1996; Cao et al. 1997; Fortier et al. 2004; Konsman et al. 2004; Rummel et al. 2005a). The goals of this study have therefore been to investigate whether systemic treatment with the TLR-3 agonist PIPC results in the expression of IL-1β and COX-2 in the guinea-pig brain and whether PIPC-induced fever is modified by injections of a non-selective COX inhibitor (diclofenac) or a selective COX-2 inhibitor (nimesulide). We have further been interested to determine whether a nuclear translocation of the transcription factor STAT3 (signal transducer and activator of transcription 3) is present in the brain of PIPC-treated guinea-pigs and whether this transcription factor can thus be used as a marker of brain-cell activation in response to peripheral TLR3-stimulation.

Materials and methods

Animals

This study was performed on male guinea-pigs (*Cavia aperea porcellus*) with a body weight of about 400 g at the beginning of the experiments (day of surgery). The animals were housed in individual cages at 22°C under a 12:12 h light-dark cycle (lights off at 7.00 p.m.) and had access to food and water *ad libitum*. Twice a week, the reservoirs were filled with fresh pelleted food and water and, at the same time, the cages were cleaned. About 10 days before the experiment, the guinea-pigs were prepared surgically (see below) and habituated at least twice to the experimental handling procedures. National guidelines for experiments with vertebrate animals were followed and local ethics committee approval was obtained from the regional government for the experimental protocols (reference number GI 18/2-42/00).

Substances

PIPC (Sigma-Aldrich, Taufkirchen, Germany) was suspended in sterile pyrogen-free saline at a concentration of 500 μg/ml. The drug was intra-arterially (i.a.) injected at a dose of 500 μg/kg based on data from a previous study (Voss et al. 2006). According to the manufacturer's information, this synthetic compound does not contain measurable amounts of endotoxin.

Diclofenac-sodium (Calbiochem, LaJolla, Calif.) was dissolved at 5 mg/ml in a vehicle consisting of 95% sterile saline and 5% ethanol and administered at a dose of 5 mg/kg i.a. with PIPC or saline.

Nimesulide (Cayman Chemical Company, Ann Arbor, Mich.) was dissolved at 5 mg/ml in a vehicle consisting of 90% sterile saline and 10% dimethylsulphoxide and administered at a dose of 5 mg/kg i.a. with PIPC or saline. For each experiment, the solution was freshly prepared and sonicated for 5 min immediately prior to injection.

Surgery

The animals received oral administration of 200 μg/kg meloxicam as an analgesic (Boehringer Ingelheim Vetmedica, Ingelheim, Germany), prior to surgery, and a prophylactic injection of the antibiotic enrofloxacin (10 mg/kg, subcutaneous injection; Bayer Health Care, Leverkusen, Germany), immediately after surgery. Guinea-pigs were chronically implanted with intra-arterial catheters for injections and intra-abdominal radiotransmitters for the measurement of body core temperature. Briefly, the guinea-pigs were anaesthetized with 0.25 mg/kg medetomidine hydrochloride (Pfitzer, Karlsruhe, Germany) injected intra-muscularly into the thigh muscle, followed by intraperitoneal injection of 100 mg/kg ketamine hydrochloride (Pharmacia Upjohn, Erlangen, Germany). Under aseptic conditions, a polyethylene catheter (Portex, Kent, UK; 0.4-mm inner diameter, 0.8-mm outer diameter) was inserted through the left carotid artery until it reached the aortic arch. Slow aspiration of blood with a syringe indicated the correct positioning of the catheter, which was then fixed with two sutures. The distal end of the catheter was tunneled subcutaneously to the interscapular region of the back where it was exteriorized and again fixed with two sutures. The muscle layer and the skin were closed separately with sutures. Thereafter, the catheter was flushed with sterile heparinized saline and sealed by heating. Finally, a midline laparotomy was performed in each animal for implantation of a free-floating temperature transmitter into the peritoneal cavity. Muscle layer and skin were sutured separately to close the abdominal incision.

Experimental protocols

Experiment 1: detection of COX-2 and IL-1β mRNA in the guinea-pig brain after treatment with PIPC

Using radioactive in situ hybridization (see below), we studied the expression of COX-2 and IL-1β in the guinea-

pig brain in response to i.a. injections of PIPC (n=4) or sterile saline (n=2). COX-2 expression was determined 180 min after the respective injections. This time point was chosen according to our previous study (Rummel et al. 2005a).

Experiment 2: effects of COX inhibitors on PIPC-induced fever

Eight groups of guinea-pigs were used for this experiment. In the first four groups, the effect of diclofenac on PIPC-induced fever was tested. The animals were i.a. injected either with PIPC + diclofenac (n=8), PIPC + solvent (n=7), saline + diclofenac (n=7) or saline + solvent (n=7). The other four groups received i.a. injections of PIPC + nimesulide (n=6), PIPC + solvent (n=5), saline + nimesulide (n=4) or saline + solvent (n=4). Injections were performed between 10.00 and 10.30 a.m. Body temperature was evaluated and documented from 2 h before until 24 h after the respective injections.

Experiment 3: preparation of brains for immunohistochemistry on free-floating sections

This pilot experiment was performed to determine those brain areas in which nuclear STAT3 signals appeared in response to stimulation with PIPC. Two groups of guinea-pigs were i.a. injected either with PIPC (n=5) or an equivalent volume of sterile saline (n=3). The brains of all animals were prepared for STAT3 immunohistochemistry 2 h after injection. Guinea-pigs were deeply anaesthetized with sodium pentobarbital (60–100 mg/kg; Narcoren, Merial, Hallbergmoos, Germany) and transcardially perfused with 400 ml 0.9% NaCl solution followed by 500 ml fixative containing 4% paraformaldehyde in 0.1 M phosphate buffer (pH 7.2). Brains were removed and postfixed in the same fixative for 1 h at room temperature. The tissue was cryoprotected in 20% sucrose in phosphate buffer overnight at 4°C and cut the following day.

Experiment 4: preparation of brains for fluorescent immunohistochemical colocalization studies

Two groups of guinea-pigs were i.a. injected either with PIPC (n=4) or an equivalent volume of sterile saline (n=3). For immunohistochemical colocalization studies, a modified postfixation protocol for freshly frozen brain sections was applied to enable the detection of STAT3 additionally in endothelial cells (Rummel et al. 2005b). Briefly, guinea-pigs were deeply anaesthetized with sodium pentobarbital as described above and transcardially perfused with 400 ml 0.9% NaCl solution at room temperature to remove blood and blood cells. The brains were quickly removed and shock-frozen on powdered dry ice and then stored at −70°C until sectioned. Coronal 20-μm-thick brain sections were cut on a cryostat (model HM 500, Microm, Walldorf, Germany), thaw-mounted onto poly-L-lysine-coated glass slides, immersion-fixed in 2% paraformaldehyde diluted in 0.1 M phosphate buffer (pH 7.2) for 10 min at room temperature and washed three times with phosphate buffer before the immunohistochemical procedure.

Measurement of body temperature

Abdominal temperature was measured by use of the intra-abdominally implanted biotelemetry transmitters (PDT-4000 E-mitter; Mini-Mitter, Sunriver, Ore.). Output (frequency in Hz) was monitored by an antenna placed under each cage (ER-4000 radioreceivers, Mini-Mitter). A data acquisition system (Vital View, Mini Mitter) was used for automatic control of data collection and analysis. Body temperature was monitored and recorded at 5-min intervals. For analysis and graphical documentation, temperature data were used at time intervals of 15 min.

COX-2 and IL-1β in situ hybridization

Animals were decapitated 180 min after local or systemic injections of PIPC or 0.9% NaCl (controls) and the brains were removed quickly, frozen on dry ice and stored at −70°C until further use. For COX-2 and IL-1β mRNA hybridization, coronal cryostat sections (20 μm; HM 500-O, Microm) were obtained from brain regions containing the subfornical organ (SFO) and from other hypothalamic and extrahypothalamic brain areas. Sections were mounted and processed as previously described (Barth et al. 2004; Rummel et al. 2005a). For hybridization, consecutive sections were hybridized with a cocktail of oligodeoxynucleotide probes complementary to the guinea-pig COX-2 cDNA (nt932-nt888, nt1049-nt1005, nt1321-nt1277; GenBank accession no. Y07896.1) or IL-1β cDNA (nt181-nt225, nt431-nt475, nt641-nt685; GenBank accession no. AF119622), respectively. The specificity of the probe sequences for complementarity exclusively with COX-2 or IL-1β cDNAs was checked versus GenBank by blastN (National Centre for Biotechnology Information). The probe labelling and high-stringency hybridization procedure followed that of Barth et al. (2004) with 50 μl/section of an equimolar mixture with one of the cocktails of three oligodeoxynucleotide probes and a final probe concentration of $7.5–10\times10^5$ cpm/μl hybridization buffer. For autoradiographical detection, X-ray films (Kodak Biomax MR) were exposed to hybridized sections for 13 days (COX-2) or 18 days (IL-1β).

STAT3 immunohistochemistry

To detect STAT3 signals in the guinea-pig brain, free-floating sections were incubated with a rabbit anti-STAT3 antibody (sc-482; Santa Cruz Biotechnology, Heidelberg, Germany). Previous studies investigating STAT3 distribution in the rat or guinea-pig brain had shown that amplification procedures were a helpful tool to investigate STAT3 immunoreactivity (Strömberg et al. 2000; Hübschle et al. 2001; Rummel et al. 2004). Therefore, a commercial tyramide amplification kit (NEL700, NEN Life Science Products, Cologne, Germany), based on the catalysed reporter deposition amplification method, was used. Controls for STAT3 immunoreactivity included processing sections without the primary antibody or incubating sections with rabbit pre-immune serum instead of rabbit anti-STAT3 antiserum. In both cases, no STAT3 immunoreactivity was found in any brain area. Finally, the specificity of the STAT3 immunohistochemistry was established by pre-adsorbing the primary antibodies with the antigen (Rummel et al. 2004).

Coronal 40-µm-thick brain sections were cut on a freezing microtome (model 1205, Jung, Heidelberg, Germany). Tyramide amplification staining was performed according to the kit description, but in a phosphate buffer system (pH 7.2). In detail, sections were placed into 10% normal horse serum, 0.3% Triton X-100 in phosphate buffer for 1 h at room temperature and then transferred to 0.5% blocking powder to block unspecific tyramine-binding sites. Primary STAT3 antibody incubation (dilution 1:12,000) was performed for 36-48 h at 4°C. The STAT3 antibody was subsequently detected with a secondary biotinylated anti-rabbit antibody (1:200, Vector BA-1000, Linaris Biologische Produkte, Wertheim-Bettingen, Germany) for 1 h at room temperature. After amplification, immunohistochemical processing was completed with an avidin-biotin-horseradish-peroxidase complex (Vector Elite Kit, Linaris Biologische Produkte), which was visualized by the diaminobenzidine hydrochloride (DAB, Sigma Chemicals) reaction in the presence of hydrogen peroxide. Finally, sections were counterstained with cresyl violet and coverslipped with Entellan (Merck, Darmstadt, Germany) for light-microscopic analysis (Olympus Optical, Hamburg, Germany).

For fluorescent immunohistochemical colocalization studies, coronal 20-µm-thick sections of frozen brains were cut on a cryostat (HM500, Microm), thaw-mounted on poly-L-lysine-coated glass slides and immersion-fixed in 2% paraformaldehyde diluted in 0.1 M phosphate buffer (pH 7.2) for 10 min at room temperature. After three washes in phosphate buffer, the immunohistochemical procedure was started by incubating the sections with phosphate buffer containing 10% normal horse serum and 0.3% Triton-X for 1 h. The aforementioned anti-STAT3 antibody (see above) was used for this procedure at a dilution of 1:4,000. STAT3 was visualized with Cy3-conjugated streptavidin (1:800; Jackson ImmunoResearch 016-160-084, Dianova, Hamburg, Germany) and colocalized with the nuclear DAPI (4,6-diamidino-2-phenylindole) stain (Molecular Probes D3751, MoBiTec, Göttingen, Germany), at a dilution of 1:800 in phosphate buffer, in order to judge the nuclear localization of the STAT3 signals (Hübschle et al. 2001; Rummel et al. 2005b). To determine further the cellular phenotypes of those cells responding with a PIPC-induced nuclear STAT3 translocation, STAT3 analysis was combined with the immunohistochemical detection of cell-specific marker proteins in colocalization studies. Putative responding neurons were assessed with a mouse monoclonal anti-neuron-specific nuclear protein antibody (1:100; anti-NeuN; MAB 377, Calbiochem, VWR-Deutschland, Darmstadt, Germany). Astrocytes were analysed by using a mouse monoclonal anti-glial fibrillary acidic protein antibody (1:2,000; anti-GFAP; MAB 3402, MoBiTec) and brain endothelium was stained with a sheep polyclonal anti-rat von Willebrand factor antibody (1:3000; anti-vW; SARTW-HRP, Affinity Biolocicals, Essen, Germany). The final fluorescent visualization of these primary antibodies was undertaken with Alexa Fluor-488-conjugated secondary antibodies (Molecular Probes) used at dilutions of 1:500 (goat anti-mouse) and 1:400 (donkey anti-sheep) in phosphate buffer, respectively. Finally, all sections were coverslipped with a glycerol/phosphate buffer solution and stored at 4°C until analysed microscopically by means of a conventional light/fluorescent Olympus BX50 microscope (Olympus Optical, Hamburg, Germany) equipped with the appropriate filter sets to detect the fluorescent conjugates Alexa Fluor 488, Cy3 and DAPI.

Evaluation and statistics

In graphs of the thermal responses to injections of PIPC or sterile saline, the mean abdominal temperature was plotted against time and expressed as means (±SEM) at each time point. Abdominal temperatures of different groups of guinea-pigs were compared by two-way repeated measures ANOVA followed by Scheffé's *post hoc* test. All calculations were carried out on an Apple Macintosh computer with the software package StatView (Abacus Concepts, Berkeley, Calif.).

Results

Experiment 1: detection of COX-2 and IL-1β mRNA in the guinea-pig brain after treatment with PIPC

This experiment was performed to determine whether injection of PIPC stimulates the expression of COX-2

mRNA in the guinea-pig brain, as recently demonstrated for the first time after treatment of this animal species with bacterial lipopolysaccharide (LPS; Rummel et al. 2005a). In addition, we studied the induction of IL-1β mRNA for the first time in guinea-pigs. Using radioactive in situ hybridization, we analysed COX-2 and IL-1β expression in the guinea-pig brain 180 min after i.a. injections of 500 μg/kg PIPC or sterile saline.

Although the resolution of X-ray autoradiograms is limited compared with that of high resolution nuclear trac emulsion, the pattern of COX-2-specific hybridization signals throughout the entire brain strongly suggests that COX-2 mRNA signals are mainly associated with blood vessels in animals treated with PIPC, as shown for the SFO as an example (Fig. 1a). In some brain areas, including the area around the SFO, IL-1β mRNA appeared together with COX-2-specific hybridization signals (Fig. 1d). However, in the choroid plexus (CP), COX-2-specific hybridization signals were absent (Fig. 1b), whereas IL-1β signals appeared in the CP of guinea-pigs treated with PIPC (Fig. 1e). In animals injected with sterile saline, COX-2-spcific (Fig. 1c) and IL-1β-specific (Fig. 1f) hybridization signals were hardly detectable throughout the brain, as shown for the SFO in Fig. 1c,f.

Experiment 2: effects of COX inhibitors on PIPC-induced fever

Because of the capacity of PIPC to induce COX-2 expression in the brain, we tested the effects of a non-selective COX inhibitor (diclofenac, Fig. 2) and a COX-2-selective inhibitor (nimesulide, Fig. 3) on PIPC-induced fever.

Administration of PIPC together with the solvent for diclofenac immediately induced fever with a peak of about 41°C, which was reached 3 h after injection. In agreement with our recent report (Voss et al. 2006), i.a. injection of PIPC evoked a febrile response lasting for about 24 h in guinea-pigs. Administration of 5 mg/kg diclofenac completely abolished PIPC-induced fever ($F=266.5$; $P<0.001$ from 60–1,200 min after injection of PIPC plus solvent versus PIPC plus diclofenac; Fig. 1a). Administration of diclofenac with sterile saline (vehicle for PIPC) caused no alterations in body temperature when compared with the thermal responses to treatment with saline and solvent for diclofenac (Fig. 2b).

Administration of 5 mg/kg of the COX-2-inhibitor nimesulide together with PIPC significantly reduced fever from 90–240 min after injection when compared with the febrile response of guinea-pigs treated with PIPC and the vehicle for nimesulide ($F=24.1$; $P=0.0027$; Fig. 3a). From 660–1,080 min after injection, fever tended to be higher in

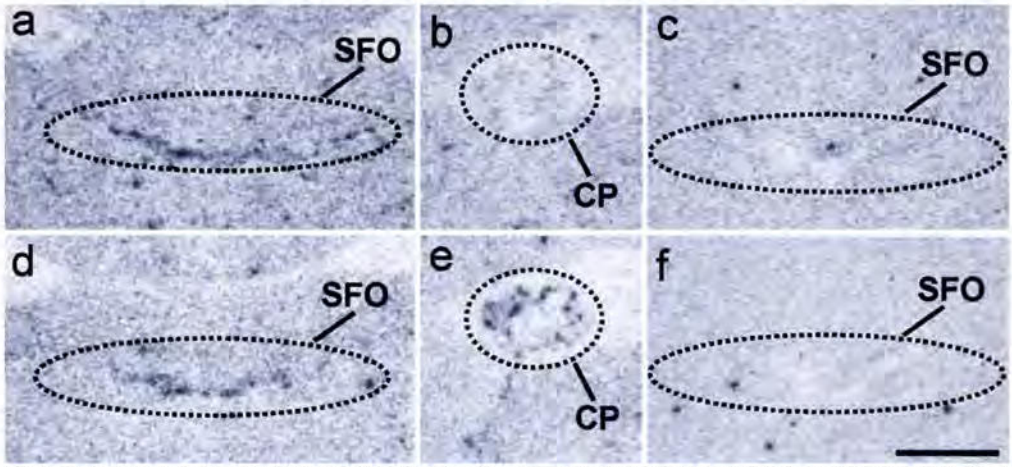


Fig. 1 mRNA expression for cyclooxygenase-2 (COX-2: **a**–**c**) and interleukin-1β (IL-1β: **d**–**f**) within guinea-pig brain after treatment with PIPC; bright-field micrographs of emulsion-coated sections. **a**, **d** Black labelling represents autoradiographically visualized radioactive in situ hybridization signals for mRNA specific to COX-2 (**a**) or IL-1β (**d**) around the area of the subfornical organ (*SFO*) of guinea-pigs 3 h after injection of PIPC intra-arterially (i.a.). **b**, **e** Black labelling represents expression of IL-1β mRNA (**e**) within the choroid plexus (*CP*) of PIPC-treated guinea-pigs. COX-2-specific hybridization signals are absent in this brain area 3 h after injection of PIPC (**b**). **c**, **f** Radioactive in situ hybridization signals for mRNA specific to COX-2 (**c**) and IL-1β (**f**) are infrequent in guinea-pigs injected with sterile saline. *Bar* 1 mm

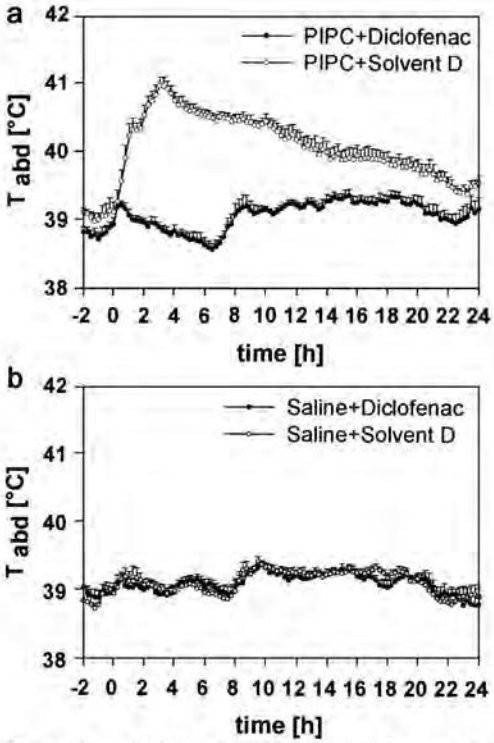


Fig. 2 **a** Changes in abdominal temperatures (*T abd*) of two groups of guinea-pigs injected i.a. with 500 µg/kg PIPC plus 5 mg/kg diclofenac (*PIPC + Diclofenac*; diclofenac is a non-selective COX inhibitor; $n=8$) or with 500 µg/kg PIPC plus solvent for diclofenac (*PIPC + Solvent D*; $n=7$). From 60–1,200 min from the time of injection, treatment with diclofenac caused a significant depression of PIPC-induced fever ($P<0.001$). **b** Changes in abdominal temperatures (*T abd*) of two groups of guinea-pigs injected i.a. with sterile saline plus 5 mg/kg diclofenac (*Saline + Diclofenac*; $n=4$) or with sterile saline plus solvent for diclofenac (*Saline + Solvent D*; $n=6$). No significant differences were seen between the *T abd* of these two groups

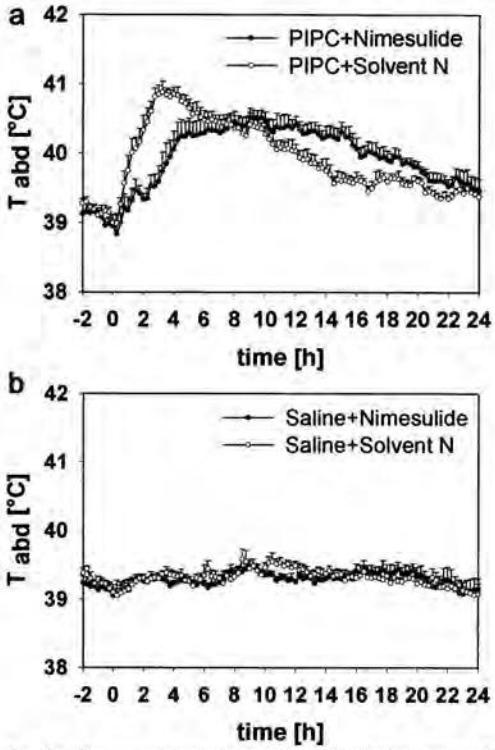


Fig. 3 **a** Changes in abdominal temperatures (*T abd*) of two groups of guinea-pigs injected i.a. with 500 µg/kg PIPC plus 5 mg/kg nimesulide (*PIPC + Nimesulide*; nimesulide is a preferential COX-2 inhibitor; $n=6$) or with 500 µg/kg PIPC plus solvent for nimesulide (*PIPC + Solvent N*; $n=5$). From 90–240 min from the time of injection, treatment with nimesulide caused a significant attenuation of PIPC-mduced fever ($P<0.01$). **b** Changes in abdominal temperatures (*T abd*) of two groups of guinea-pigs injected i.a. with sterile saline plus 5 mg/kg nimesulide (*Saline + Nimesulide*; $n=4$) or with sterile saline plus solvent for nimesulide (*Saline + Solvent N*; $n=4$). No significant differences were seen between the *T abd* of these two groups

the control group. However, there was no significant difference between body temperatures of both groups during this period ($F=3.34$; $P=0.1175$).

Experiment 3: determination of PIPC-responsive sites in the guinea-pig brain by using STAT3-immunohistochemistry

Immunohistochemical detection of the nuclear translocation of the transcription factor STAT3 has repeatedly been used to demonstrate brain activation after systemic challenge with PAMPs, such as LPS (Gautron et al. 2002; Harré et al. 2002) or bacterial DNA (Sako et al. 2005). In this pilot experiment, we have used DAB-STAT3 immunohistochemistry to determine the activated brain sites in response to treatment with PIPC.

At 2 h after injection of PIPC, nuclear STAT3 immunoreactivity was observed in the cell nuclei of brain areas that lacked a tight blood-brain barrier, the so-called sensory circumventricular organs (sCVOs), such as the area postrema (AP), the vascular organ of the lamina terminalis (OVLT) and SFO. After i.a. injection of sterile saline, hardly any nuclear STAT3 signal was observed at the corresponding time. Some additional nuclear STAT3 signals were observed in the meninges of PIPC-treated guinea-pigs. Systemic treatment with the TLR-3 activator PIPC thus

resulted in an activation of brain areas implicated in fever (Roth et al. 2004), at least in part.

Experiment 4: immunohistochemical demonstration of the colocalization of nuclear STAT3 signals with markers of astrocytes and endothelial cells in brain of PIPC-treated guinea-pigs

This experiment was performed to determine the phenotype of those cells in which nuclear STAT3 activation was observed after systemic treatment with PIPC. From a previous study (Rummel et al. 2005b), we knew that the immunoreactivity of signal molecules in brain endothelial cells was strongly impaired by the perfusion fixation technique; STAT3 signals in brain endothelial cells almost disappeared in perfusion-fixed brains. Therefore, the post-fixation method was applied to fresh-frozen brain sections for a detailed immunohistochemical analysis according to our previous studies (Rummel et al. 2005b; Mütze et al. 2006). I.a. injection of 500 μg/kg PIPC, as opposed to sterile saline, induced the appearance of numerous nuclear STAT3 signals in cells of the AP (Fig. 4), OVLT (Fig. 5) and SFO (Fig. 6).

To demonstrate that PIPC-induced STAT3 signals were located in cell nuclei, we combined the immunohistochemical detection of STAT3 (red) with the nuclear DAPI stain (blue; Figs. 4, 5, 6, 7). Nuclear STAT3 signals could therefore be detected in pink. We evaluated the phenotype of PIPC-responsive brain cells immunohistochemically (green) by using the endothelial marker vWF (Figs. 4, 5, 6a, 7), the astrocytic marker GFAP (Figs. 4, 5, 6b,d) and the neuronal marker NeuN (Figs. 4, 5, 6c).

At 2 h after i.a. injections of 500 μg/kg PIPC, we could demonstrate that generally two cell types, viz. endothelial cells (Figs. 4, 5, 6a) and astrocytes (Figs. 4, 5, 6b) formed a distinct subpopulation of STAT3-activated cells in all of the three sensory CVOs. On the other hand, we failed to detect STAT3-positive neurons (Figs. 4, 5, 6c) within the AP, OVLT and SFO. In the respective areas of saline-treated animals, hardly any nuclear STAT3 signal occurred (Figs. 4, 5, 6d). In the AP of guinea-pigs treated with PIPC, the nuclear STAT3 signals in medial aspects of this CVO were frequently clustered in a V-shaped arrangement towards the border of the nucleus of the solitary tract (Fig. 4). In addition to single endothelial cells and a substantial number of astrocytes, we found a population of cells with STAT3-

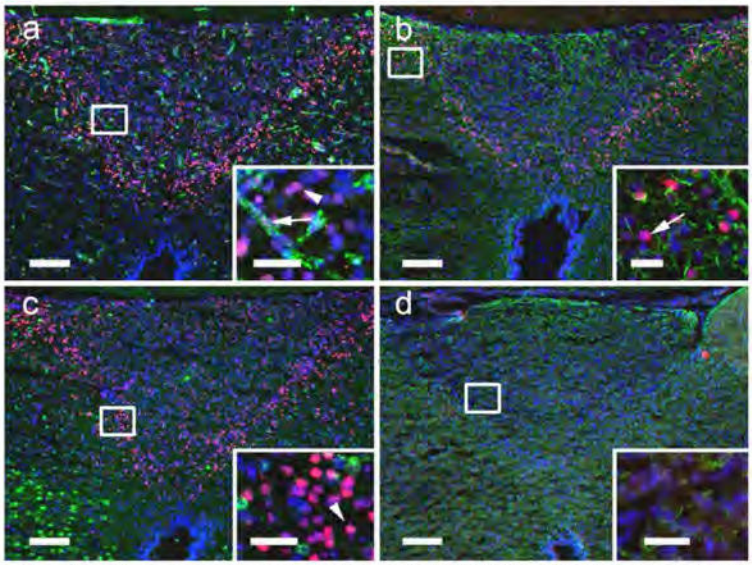


Fig. 4 Endothelial cells and astrocytes, as opposed to neurons, within the area postrema (AP) respond to pyrogenic challenge with PIPC (500 μg/kg, i.a.) by nuclear translocation of the transcription factor STAT3, 2 h after injection. Nuclear STAT3 immunoreactivity (*red*) colocalizes with the nuclear DAPI stain (*blue*) resulting in *pink* signals. In addition, antibodies against the endothelial van Willebrand factor (vWF, **a**), against the astrocyte glial fibrillary acidic protein (GFAP, **b**) or against the neuron-specific nuclear protein (NeuN, **c**) were used to demonstrate the phenotype of cells (*green*) showing nuclear STAT3 activation. STAT3-positive endothelial cells (**a**) and astrocytes (**b**) were observed in cells within the AP. No STAT3-positive neurons (**c**) were detected on any cell within the AP. In control animals injected with sterile saline only, single or even no nuclear STAT3 signals occurred (**d**). Brain sections of the controls (**d**) were stained with anti-GFAP antibodies. *Arrows* indicate nuclear STAT3 signals co-localized with specific cell markers, whereas *arrowheads* indicate nuclear STAT3 signals not co-localized with specific cell markers. *Bars* 100 μm (*overviews*), 25 μm (*insets*)

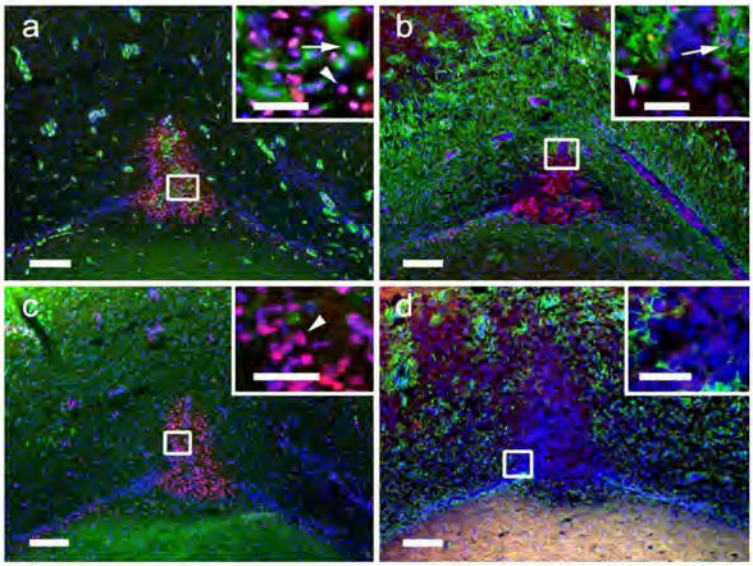


Fig. 5 Endothelial cells and astrocytes, as opposed to neurons, within the organum vasculosum of the lamina terminalis (OVLT) respond to pyrogenic challenge with PIPC (500 μg/kg, i.a.) by nuclear translocation of the transcription factor STAT3, 2 h after injection. Nuclear STAT3 immunoreactivity (*red*) colocalizes with the nuclear DAPI stain (*blue*) resulting in *pink* signals. In addition, antibodies against the endothelial vWF (**a**), against the astrocyte GFAP (**b**) or against NeuN (**c**) were used to demonstrate the phenotype of cells (*green*) showing nuclear STAT3 activation. STAT3-positive endothelial cells (**a**) and astrocytes (**b**) were observed in cells within the OVLT. No STAT3-positive neurons (**c**) were detected on any cell within the OVLT. In control animals injected with sterile saline only, single or even no nuclear STAT3 signals occurred (**d**). Brain sections of the controls (**d**) were stained with anti-GFAP antibodies. *Arrows* indicate nuclear STAT3 signals co-localized with specific cell markers, whereas *arrowheads* indicate nuclear STAT3 signals not co-localized with specific cell markers. *Bars* 100 μm (*overviews*), 25 μm (*insets*)

positive nuclei but we could not determine their cellular phenotype.

Single STAT3-positive endothelial cells were also observed within the OVLT and SFO (Figs. 5a, 6a). In both of these sCVOs, STAT3-positive astrocytes were mainly present in the border regions (Figs. 5b, 6b). The large wall of astrocytes surrounding both the OVLT and SFO did not contain nuclear STAT3 signals. In the core regions of the OVLT and SFO, large numbers of nuclear STAT3 signals were observed but, in the majority of cells, no co-localization was found with vWF and GFAP. In no single case could co-localization of nuclear STAT3 signals with the neuronal marker NeuN be established for the sensory CVOs (Figs. 4, 5, 6c).

In PIPC-treated animals, endothelial cells with nuclear STAT3 signals were observed not only within the sCVOs, but also in the entire brain vasculature as shown for blood vessels in the cortex (Fig. 7a). A clear co-localization of nuclear STAT3 signals with endothelial vWF was detected along the brain vasculature pathways. In control animals injected with sterile saline, endothelial cells of brain blood vessels hardly showed any nuclear STAT3 signals (Fig. 7b).

In summary, endothelial cells within the entire brain vasculature, astrocytes and a population of cells of still undetermined phenotype within the sensory CVOs (AP, OVLT, SFO) and the meninges revealed nuclear STAT3 activation in response to i.a. injections of PIPC.

Discussion

PIPC as an activator of innate immunity

Double-stranded RNA has fever-inducing capacities, as has been known for a number of decades (Absher and Stinebring 1969). However, the precise mechanisms of the way that PIPC, a synthetic double-stranded RNA, might evoke fever remained poorly understood until the discovery and characterization of the TLR family. TLRs represent an important component of the innate immune response and are capable of recognizing a variety of so called PAMPs. For example, LPS from gram-negative bacteria, the most frequently used agent to induce experimental fever, is recognized by TLR4 (Polotrak et al. 1998; Chow et al.

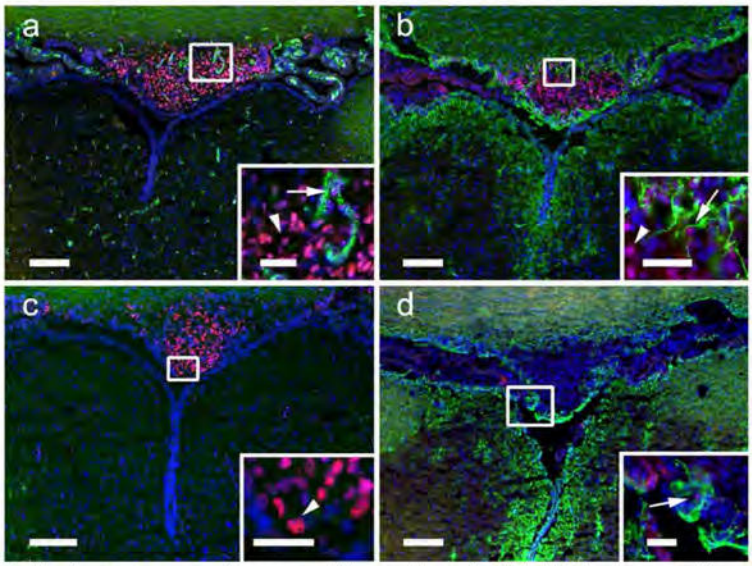


Fig. 6 Endothelial cells and astrocytes as opposed to neurons within the subfornical organ SFO respond to pyrogenic challenge with PIPC (500 μg/kg, i.a.) by nuclear translocation of the transcription factor STAT3, 2 h after injection. Nuclear STAT3 immunoreactivity (*red*) colocalizes with the nuclear DAPI stain (*blue*) resulting in *pink* signals. In addition, antibodies against the endothelial vWF (**a**), against the astrocyte GFAP (**b**) or against NeuN (**c**) were used to demonstrate the phenotype of cells (*green*) showing nuclear STAT3 activation. STAT3-positive endothelial cells (**a**) and astrocytes (**b**) were observed in cells within the SFO. No STAT3-positive neurons (**c**) were detected on any cell within the SFO. In control animals injected with sterile saline only, single or even no nuclear STAT3 signals occurred (**d**). Brain sections of the controls (**d**) were stained with anti-GFAP antibodies. *Arrows* indicate nuclear STAT3 signals co-localized with specific cell markers, whereas *arrowheads* indicate nuclear STAT3 signals not co-localized with specific cell markers. *Bars* 100 μm (*overviews*), 25 μm (*insets*)

1998) and all phases of LPS-induced fever have been recently shown to depend on TLR4 signalling (Steiner et al. 2006). TLR3 is the receptor that recognizes double-stranded RNA, such as PIPC. Binding of PIPC to TLR3 induces the activation of a transcription factor, viz. nuclear factor kappa B, and thereby the production of cytokines, such as the interferons, IL-6 and tumor necrosis factor α (Alexopoulou et al. 2001), which belong to the group of endogenous pyrogens (Kluger 1991; Luheshi and Rothwell 1996). Within the last few years, some attempts have been made to characterize the pyrogenic properties of various PAMPs and to compare their fever-inducing mechanisms

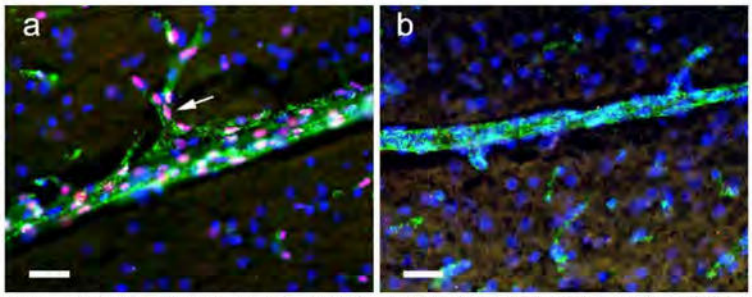


Fig. 7 STAT3-activated endothelial cells were not only detected within the sensory CVOs, but also in blood vessels distributed throughout the brain of guinea-pigs treated with PIPC (**a**) as opposed to those injected with sterile saline (**b**). As an example, in endothelial cells of blood vessels located within the cortex, nuclear STAT3 activation (*red*) colocalizes with the nuclear DAPI stain (*blue*) resulting in *pink* signals in vessels of PIPC-treated guinea-pigs. Antibodies against endothelial vWF were used (*green*). Nuclear STAT3 activation is absent in blood vessels of control animals (**b**). *Arrow* in **a** indicates a typical nuclear STAT3 signal co-localized with vWF. *Bars* 25 μm

and pathways with those employed by bacterial LPS, which is used as a standard in experimental fever research (Fortier et al. 2004; Hübschle et al. 2006; Kozak et al. 2006). One central goal of this study has been to document a putative activation of brain cells in response to treatment with PIPC in guinea-pigs and to compare our observations with pyrogenic brain activation induced by other PAMPs, such as bacterial LPS (Rummel et al. 2004, 2005a,b) or bacterial DNA (Sako et al. 2005).

Role of COX in PIPC-induced fever

Traditionally, prostaglandin E2 (PGE2) is regarded as the key fever mediator in the brain and as the biological agent finally responsible for the manifestation of the febrile response (Ivanov and Romanovsky 2004; Roth et al. 2006). COX is one of the key enzymes for the synthesis of PGE2 from arachidonic acid. Two COX isoforms exist: COX-1 and COX-2. COX-1 is constitutively expressed and its products mainly mediate physiological functions. COX-2 is predominantly inducible under conditions of inflammation but basal levels of COX-2 are present in the brain (for a review, see Botting 2006). The use of selective COX-2 inhibitors (Cao et al. 1997; Steiner et al. 2001; Zhang et al. 2003; Fabricio et al. 2004) or of COX-2-deficient ("knockout") mice (Li et al. 1999; Steiner et al. 2005) suggest a critical role for COX-2 as a mediator of fever induced by bacterial LPS.

The first experimental evidence for a role of PGE2 in the febrile response evoked by PIPC in rabbits was derived from the observation that fever and the concomitant rise in circulating PGE2 were both blocked by ketoprofen, a non-selective inhibitor of both COX isoforms (Rotondo et al. 1988). However, the effects of selective COX-2 inhibitors on PIPC-induced fever has not previously been investigated. We have therefore compared the effects of a non-selective COX inhibitor (diclofenac) with those of a selective COX-2-inhibitor (nimesulide) on PIPC-induced fever. Both of these drugs have successfully been used in guinea-pigs to elucidate the role of COX enzymes in LPS fever in this species (Steiner et al. 2001; Roth et al. 2002). PIPC (500 μg/kg, i.a.) induces a strong and long-lasting fever that is completely depressed by co-administration of 5 mg/kg diclofenac (Fig. 2). This observation is in agreement with our previous studies showing that diclofenac is a highly potent antipyretic drug in guinea-pigs, when LPS is used as a fever-inducing agent (Roth et al. 2002; Rummel et al. 2005a). The result shown in Fig. 2 confirms the critical role of PGE2 in the manifestation of PIPC-induced fever. The COX-2-selective inhibitor nimesulide has been shown to attenuate LPS fever in guinea-pigs, the later stages of fever being more affected than the early phase of the febrile response (Steiner et al. 2001). To our surprise, treatment with 5 mg/kg nimesulide (the highest recommended dose of this drug for in vivo studies) selectively attenuates the early stage of PIPC-induced fever (90–240 min after injection of PIPC; Fig. 3). We have observed COX-2 mRNA signals at 3 h after injection of PIPC (Fig. 1), i.e. at the same time when there is a maximum of COX-2 mRNA after an inflammatory challenge with LPS (Cao et al. 1995; Rummel et al. 2005a). Although the induction of IL-1β and COX-2 in brain seems to participate in the manifestation of PIPC-induced fever (Fortier et al. 2004), it is questionable that these events are related to the early onset fever, which we have observed as rapidly as 30 min after i.a. injection of this pyrogen (Figs. 2, 3). A quick and rapid signal, possibly generated in the periphery and transmitted to the brain either via a humoral or even via a neuronal afferent pathway, might be responsible for the initiation of PIPC-induced fever within 30 min. Such a mechanism has been proposed and experimentally substantiated for LPS fever in guinea-pigs (for a review, see Blatteis 2006). Whether a similar mechanism operates for the initiation of PIPC-induced fever remains to be determined. In this context, the time courses and the pyrogenic mechanisms responsible for PIPC-induced and LPS-induced fevers are not identical (Li et al. 2000).

The up-regulation of the COX-2 enzyme may start earlier than 3 h after administration of PIPC. A significant increase of COX-2 mRNA, as detected with reverse transcription/polymerase chain reaction in whole hypothalamic tissue homogenates, is measurable in rats at 2 h after stimulation with a fever-inducing dose of PIPC (Fortier et al. 2004). The induction of COX-2 mRNA may even start within 30 min after inflammatory stimulation (Ivanov and Romanovsky 2004). With regard to the finding of constitutive expression of COX-2 in the brain (Botting 2006), the inhibition of COX-2 by nimesulide might account for the attenuation of PIPC-induced fever during an early stage of the febrile response (90–240 min after injection). This observation is in agreement with a recent study showing that even the early phase of LPS fever is absent in COX-2-deficient mice (Steiner et al. 2005). Nevertheless, an adequate reason for nimesulide being so much less effective in suppressing PIPC-fever in guinea-pigs when compared with diclofenac remains elusive. A plausible explanation may be the weaker capacity of nimesulide to inhibit COX when compared with other nonsteroid anti-inflammatory drugs (Botting 2004). The different kinetic profiles of diclofenac and nimesulide in blood and brain, their distinct diffusibility into and distribution within the brain, their dissimilar modes of binding to COX-2 and their differing effective antipyretic concentrations might also be responsible for the observed effects of both drugs on PIPC-induced fever. The attenuation of the early phase of the PIPC-

induced fever by nimesulide and by diclofenac could also be attributable to the antioxidant activity of these drugs at the dose used in our experiments, since the inhibition of oxygen radical formation by aspirin-like and other drugs has been shown to prevent fever (Riedel et al. 2003). Namely nimesulide has the capacity to inhibit LPS-induced production of superoxide anions (Krishan et al. 2006).

Nevertheless, our observations of COX-2 expression in the brain of PIPC-treated guinea-pigs and of COX inhibitors attenuating (nimesulide) or depressing (diclofenac) PIPC-induced fever clearly indicate that the formation of COX products within the brain participates in the manifestation of the febrile response to double-stranded RNA.

Nuclear STAT3 activation in brain of PIPC-treated guinea-pigs

Immunohistochemical investigation of the nuclear translocation of the transcription factor STAT3 has been used to demonstrate the activation of brain cells after peripheral inflammatory stimulation with bacterial LPS (Gautron et al. 2002; Harré et al. 2002; Hosoi et al. 2004; Rummel et al. 2004, 2005b) or with bacterial DNA (Sako et al. 2005). For the first time, nuclear STAT3 activation has been used in this study to show the activation of brain cells in response to i.a. injections of PIPC, a stimulator of TLR3 (Figs. 4, 5, 6, 7). The nuclear STAT3 activation that we have observed in distinct brain areas and structures is probably not mediated by circulating PIPC directly but rather by cytokines produced in response to TLR3 activation. One family of cytokines signals through a common receptor subunit named gp130 and includes IL-6, IL-11, leukemia inhibitory factor, ciliary neurotrophic factor, leptin and others. Binding of these cytokines to their specific membrane receptor leads to the dimerization of gp130, followed by the activation of a janus kinase (JAK), which in turn phosphorylates cytoplasmic STAT3 (Heinrich et al. 1998; Takeda and Akira 2000). Phosphorylated STAT3 dimerizes and translocates into the nucleus of the activated cell, where it can be detected immunohistochemically. Of all the aforementioned cytokines, IL-6 is the likely candidate for being responsible, at least in part, for the observed nuclear STAT3 activation in the brain of PIPC-treated animals, since a significant increase of IL-6 occurs in the blood 2 h after systemic injections of PIPC (Fortier et al. 2004; Voss et al. 2006).

The so-called sCVOs (AP, OVLT, SFO) are those brain structures that respond with pronounced nuclear STAT3 activation (Figs. 4, 5, 6). Because of the lack of a tight blood-brain barrier, the cells within the sCVOs are directly exposed to circulating signal molecules and can thus act as sensors for chemical messengers transported by the blood stream. Receptors for various fever-inducing cytokines and even for PAMPs have been identified within the sCVOs (for a review, see Roth et al. 2004). The observed nuclear STAT3 activation within these specialized brain structures is thus in agreement with their proposed role as the port of entry into the brain for inflammatory signal molecules. As a result of the co-localization of nuclear STAT3 signals with GFAP, distinct populations of astrocytes have been identified, in all of the three sCVOs, as cells responding to systemic injections of PIPC. This finding corresponds to previous studies in which the activation of brain cells has been investigated after inflammatory stimulation with LPS (Harré et al. 2003; Rummel et al. 2005b). Using a modified method of tissue preparation (postfixation of freshly frozen brain sections), we have been able to identify endothelial cells of blood vessels distributed throughout the brain as a second population of brain cells responding to inflammatory stimulation with PIPC (Fig. 7). In a previous paper (Rummel et al. 2005b), we have discussed possible reasons that the immunohistochemical detection of signal or marker molecules in endothelial cells is disturbed by use of the traditional perfusion fixation technique. In addition to the sensory CVOs, the entire brain endothelium can thus be regarded as a sensor for inflammatory signal molecules after treatment with PIPC. This observation is in agreement with the described expression of receptors for various cytokines in brain endothelial cells (Lebel et al. 2000; Konsman et al. 2004) and with the subsequent induction of COX-2 expression in these cells.

The phenotype of at least a third population of cells showing STAT3 activation after stimulation with PIPC, e.g. the STAT3-positive cells in the core regions of the OVLT and SFO in PIPC-treated guinea-pigs (Figs. 5, 6), will have to be characterized in future studies. Despite having tested antibodies directed to other cellular markers, we have failed to identify the phenotype of these cells. Another open question of interest relates to the functional relevance of nuclear STAT3 activation in the brain of PIPC-treated animals, since recent evidence has been presented for the protective (anti-inflammatory) genomic action of STAT3 during systemic inflammation (Kano et al. 2003).

Concluding remarks

In this study, we have demonstrated that peripheral administration of the TLR3 activator PIPC results in a pattern of brain-cell activation resembling that induced by bacterial LPS. Thus, the activation of distinct receptors of the innate immune system seems to result finally in the manifestation of similar brain-intrinsic mechanisms that may be responsible for the stereotypic pattern of brain-controlled illness responses, including fever. Once more, nuclear STAT3 signals have been shown to serve as useful markers of inflammatory brain activation.

Acknowledgements The skillful technical assistance of Jolanta Murgott is gratefully acknowledged.

References

Absher M, Stinebring WR (1969) Toxic properties of a synthetic double-stranded RNA: pyrogenicity of Poly I:Poly C in rabbits. Nature 223:715–717

Alexopoulou L, Holt AC, Medzhitov R, Flavell RA (2001) Recognition of double-stranded RNA and activation of NF-κB by Toll-like receptor 3. Nature 413:732–738

Barth SW, Riediger T, Lutz TA, Rechkemmer G (2004) Peripheral amylin activates circumventricular organs expressing calcitonin receptor a/b subtypes and receptor activity modifying proteins in the rat. Brain Res 997:97–102

Blatteis CM (2006) Endotoxic fever: new concepts of its regulation suggest new approaches to its management. Pharmacol Ther 111:194–223

Botting R (2004) Antipyretic therapies. Front Biosci 9:956–966

Botting RM (2006) Cyclooxygenase: past, present and future. A tribute to John R. Vane (1927–2004). J Therm Biol 31:208–219

Breder CD, Saper CB (1996) Expression of inducible cyclooxygenase mRNA in the mouse brain after systemic administration of bacterial lipopolysaccharide. Brain Res 713:64–69

Cao C, Matsumura K, Yamagata K, Watanabe Y (1995) Induction by lipopolysaccharide of cyclooxygenase-2 mRNA in rat brain: its possible role in febrile response. Brain Res 613:331–336

Cao C, Matsumura K, Yamagata K, Watanabe Y (1997) Involvement of cyclooxygenase-2 in LPS-induced fever and regulation of its mRNA by LPS in the rat brain. Am J Physiol Regul Integr Comp Physiol 287:R1712–R1725

Chow JC, Young DW, Golenbock DT, Christ WJ, Gusovsky F (1998) Toll-like receptor-4 mediates lipopolysaccharide-induced signal transduction. J Biol Chem 274:10689–10692

Chuang J, Lin MT, Chan SA, Won SJ (1990) Febrile effects of polyriboinosinic: polyribocytidylic acid and interferon: relationship to somatostatin in rat hypothalamus. Pflügers Arch Eur J Physiol 415:606–610

Cooper KE, Blähser S, Malkinson TJ, Merker G, Roth J, Zeisberger E (1988) Changes in body temperature and vasopressin content of brain neurons, in pregnant and non-pregnant guinea pigs, during fevers produced by Poly I:Poly C. Pflügers Arch Eur J Physiol 412:292–296

Ellis S, Mouihate A, Pittman QJ (2006) Neonatal programming of the rat neuroimmune response: stimulus specific changes elicited by bacterial and viral mimetics. J Physiol (Lond) 571:695–701

Fabricio ASC, Veiga FH, Cristofoletti R, Navarra P, Souza GEP (2004) The effects of selective and nonselective cyclooxygenase inhibitors on endothelin-1-induced fever in rats. Am J Physiol Regul Integr Comp Physiol 288:R671–R677

Fortier ME, Kent S, Ashdown H, Poole S, Boksa P, Luheshi GN (2004) The viral mimic, polyinosinic:polycytidylic acid, induces fever in rats via an interleukin-1-dependent mechanisms. Am J Physiol Regul Integr Comp Physiol 287:R759–R766

Gautron L, Lafon P, Chaigniau M, Tramu G, Layé S (2002) Spatiotemporal analysis of signal transducer and activator of transcription 3 activation in rat brain astrocytes and pituitary following peripheral immune stimulation. Neuroscience 112:717–729

Harré EM, Roth J, Gerstberger R, Hübschle T (2003) Interleukin-6 mediates lipopolysaccharide-induced nuclear STAT3 translocation in astrocytes of rat sensory circumventricular organs. Brain Res 980:151–155

Harré EM, Roth J, Pehl U, Kueth M, Gerstberger R, Hübschle T (2002) Selected contribution: role of IL-6 in LPS-induced nuclear STAT3 translocation in sensory circumventricular organs during fever in rats. J Appl Physiol 92:2657–2666

Heinrich P, Behrmann C, Müller-Newen J, Schaper GF, Graeve L (1998) Interleukin-6-type cytokine signalling through the gp130/Jak/STAT pathway. Biochem J 334:297–314

Hosoi T, Okuma Y, Kawagishi T, Qi X, Matsuda T, Nomura Y (2004) Bacterial endotoxin induces STAT3 activation in the mouse brain. Brain Res 1023:48–53

Hübschle T, Thom E, Watson A, Roth J, Klaus S, Meyerhof W (2001) Leptin-induced nuclear translocation of STAT3 immunoreactivity in hypothalamic nuclei involved in body weight regulation. J Neurosci 21:2413–2424

Hübschle T, Mütze J, Mühlradt PF, Korte S, Gerstberger R, Roth J (2006) Pyrexia, anorexia, adipsia, and depressed motor activity in rats during systemic inflammation induced by the Toll-like receptors-2 and -6 agonists MALP-2 and FSL-1. Am J Physiol Regul Integr Comp Physiol 290:R180–R187

Ivanov AI, Romanovsky AA (2004) Prostaglandin E2 as a mediator of fever: synthesis and catabolism. Front Biosci 9:1977–1993

Jacobs BL, Langland JQ (1996) When two strands are better than one: the mediators and modulators of the cellular responses to double stranded RNA. Virology 219:339–349

Kano A, Wolfgang MJ, Gao Q, Jacobi J, Chai GX, Hansen W, Iwamoto Y, Pober JS, Flavell RA, Fu XY (2003) Endothelial cells require STAT3 for protection against endotoxin-induced inflammation. J Exp Med 198:1517–1525

Kimura M, Toth LA, Agostini H, Cady AB, Majde JA, Krueger JM (1994) Comparison of acute phase responses induced in rabbits by lipopolysaccharide and double stranded RNA. Am J Physiol Regul Integr Comp Physiol 267:R1596–R1605

Kluger MJ (1991) Fever: role of pyrogens and cryogens. Physiol Rev 71:93–127

Konsman JP, Vigues S, Mackerlova L, Bristow A, Blomqvist A (2004) Rat brain vasculature distribution of interleukin-1 type-1 receptor immunoreactivity: relationship to patterns of inducible cyclooxygenase expression by peripheral inflammatory stimuli. J Comp Neurol 472:113–129

Kozak W, Wrotek S, Kozak A (2006) Pyrogenicity of CpG-DNA in mice: role of interleukin-6, cyclooxygenases, and nuclear factor-κB. Am J Physiol Regul Integr Comp Physiol 290:R871–R880

Krishan KL, Sohi KK, Pathak CM, Kaushik G (2006) Nimesulide inhibits lipopolysaccharide-induced production of superoxide anions and nitric oxide and iNOS expression in alveolar macrophages. Life Sci 78:1662–1669

Lebel E, Vallières L, Rivest S (2000) Selective involvement of interleukin-6 in the transcriptional activation of the suppressor of cytokine signalling-3 in the brain during systemic immune challenges. Endocrinology 141:3749–3763

Li S, Wang Y, Matsumura K, Ballou LR, Morham SG, Blatteis CM (1999) The febrile response to lipopolysaccharide is blocked in cyclooxygenase-$2^{-/-}$, but not cyclooxygenase-$1^{-/-}$ mice. Brain Res 825:86–94

Li S, Sehic E, Ungar AL, Blatteis CM (2000) Complement does not mediate the febrile responses of guinea pigs to muramyl dipeptide and polyriboinosinic-polyribocycytidylic acid. J Therm Biol 25:51–58

Luheshi GN, Rothwell NJ (1996) Cytokines and fever. Int Arch Allergy Immunol 109:301–307

Mütze J, Roth J, Gerstberger R, Matsumura K, Hübschle T (2006) Immunohistochemical evidence of functional leptin receptor expression in neuronal and endothelial cells of the rat brain. Neurosci Lett 394:105–110

Nadjar A, Combe C, Layé S, Tridon V, Dantzer R, Amedee T, Parnet P (2003) Nuclear factor κB nuclear translocation as a crucial

marker of brain response to interleukin-1. A study in rat and interleukin-1 type I deficient mouse. J Neurochem 87:1024–1036
Polotrak A, He X, Smirnova I, Liu MY, Van Huffel C, Du X, Birdwell D, Alejos E, Silva M, Galanos C, Freudenberg M, Ricciardi-Castagnoli P, Layton B, Beutler B (1998) Defective LPS signalling in C3H/HeJ and C57BL/10ScCr mice: mutations in Tlr4 gene. Science 282:2085–2088
Riedel W, Lang U, Oetjen U, Schlapp U, Shibata M (2003) Inhibition of oxygen radical formation by methylene blue, aspirin, or a-lipoic acid prevents bacterial-lipopolysaccharide-induced fever. Mol Cell Biochem 247:83–94
Roth J, Aslan T, Störr B, Zeisberger E (1997) Lack of cross tolerance between LPS and muramyl dipeptide in induction of circulating TNF-α and IL-6 in guinea pigs. Am J Physiol Regul Integr Comp Physiol 273:R1529–R1533
Roth J, Hübschle T, Pehl U, Ross G, Gerstberger R (2002) Influence of systemic treatment with cyclooxygenase inhibitors on lipopolysaccharide-induced fever and circulating levels of cytokines and cortisol in guinea pigs. Pflügers Arch Eur J Physiol 412:292–296
Roth J, Harré EM, Rummel C, Gerstberger R, Hübschle T (2004) Signaling the brain in systemic inflammation: role of sensory circumventricular organs. Front Biosci 9:290–300
Roth J, Rummel C, Barth SW, Gerstberger R, Hübschle T (2006) Molecular aspects of fever and hyperthermia. Neurol Clin 24:421–439
Rotondo D, Abul HT, Milton AS, Davidson J (1988) Pyrogenic immunomodulators increase the level of prostaglandin E2 in the blood simultaneously with the onset of fever. Eur J Pharmacol 154:145–152
Rummel C, Hübschle T, Gerstberger R, Roth J (2004) Nuclear translocation of the transcription factor STAT3 in the guinea pig brain during systemic or localized inflammation. J Physiol (Lond) 557:671–687
Rummel C, Barth SW, Voss T, Korte S, Gerstberger R, Hübschle T, Roth J (2005a) Localized vs. systemic inflammation in guinea pigs: a role for prostaglandins at distinct points of the fever induction pathways? Am J Physiol Regul Integr Comp Physiol 289:340–347
Rummel C, Voss T, Matsumura K, Korte S, Gerstberger R, Roth J, Hübschle T (2005b) Nuclear STAT3 translocation in guinea pig and rat brain endothelium during systemic challenge with lipopolysaccharide and interleukin-6. J Comp Neurol 491:1–14
Sako K, Okuma Y, Hosoi T, Nomura Y (2005) STAT3 activation and c-FOS expression in the brain following peripheral administration of bacterial DNA. J Neuroimmunol 158:40–49
Soszynski D, Kozak W, Szewczenko M (1991) Course of fever response to repeated administration of sublethal doses of lipopolysaccharides, polyinosinic:polycytidylic acid and muramyl dipeptide to rabbits. Experientia 47:43–47
Steiner AA, Li S, Llanos-Q J, Blatteis CM (2001) Differential inhibition by nimesulide of the early and late phases of intravenous- and intracerebroventricular-LPS-induced fever in guinea pigs. Neuroimmunomodulation 9:263–275
Steiner AA, Rudaya AY, Robbins JR, Dragic AS, Langenbach R, Romanovsky AA (2005) Expanding the role of cyclooxygenase-2 to the previously overlooked responses. Am J Physiol Regul Integr Comp Physiol 289:R1253–R1257
Steiner AA, Chakravarty S, Rudaya AY, Herkenham M, Romanovsky AA (2006) Bacterial lipopolysaccharide fever is initiated via Toll-like receptor 4 on hematopoietic cells. Blood 107:4000–4002
Strömberg H, Svensson SP, Hermanson O (2000) Distribution of the transcription factor signal transducer and activator of transcription 3 in the rat central nervous system and dorsal root ganglia. Brain Res 853:105–114
Takeda K, Akira S (2000) STAT family of of transcription factors in cytokine-mediated biological responses. Cytokine Growth Factors Rev 11:199–211
Traynor TN, Majde JA, Bohnet SG, Krueger JM (2004) Intratracheal double-stranded RNA plus interferon-γ: a model for analysis of the acute phase response to respiratory viral infections. Life Sci 74:2563–2576
Voss T, Rummel C, Gerstberger R, Hübschle T, Roth J (2006) Fever and circulating cytokines induced by double stranded RNA in guinea pigs: dependence on the route of administration and effects of repeated injections. Acta Physiol 187:379–389
Won SJ, Lin MT (1988) Pyrogenicity of interferon and its inducer in rabbits. Am J Physiol Regul Integr Comp Physiol 254:340–347
Zhang YH, Lu J, Elmquist JK, Saper CB (2003) Specific roles of cyclooxygenase-1 and cyclooxygenase-2 in lipopolysaccharide-induced fever and Fos expression in rat brain. J Comp Neurol 463:3–12

1.12. „Circulating interleukin-6 induces fever through a STAT3-linked activation of COX-2 in the brain“

Rummel C., Sachot C., Poole S., Luheshi GN.
Am J Physiol (2006) 291:R1316-R1326.

Impakt Faktor: 3,284

Eigener Anteil an der Publikation:

- Initiative: eigenständig (90 %)
- Projektplanung: weitgehend eigenständig (80 %)
- Durchführung der Versuche: eigenständig (90 %)
- Auswertung der Experimente: eigenständig (90 %)
- Erstellung der Publikation: weitgehend eigenständig (75 %)

Am J Physiol Regul Integr Comp Physiol 291: R1316–R1326, 2006.
First published June 29, 2006; doi:10.1152/ajpregu.00301.2006.

Circulating interleukin-6 induces fever through a STAT3-linked activation of COX-2 in the brain

Christoph Rummel,[1] Christelle Sachot,[1] Stephen Poole,[2] and Giamal N. Luheshi[1]

[1]*Douglas Hospital Research Centre, Department of Psychiatry, McGill University, Montreal, Quebec, Canada; and*
[2]*Department of Endocrinology, National Institute for Biological Standards and Control, Potters Bar, United Kingdom*

Submitted 5 May 2006; accepted in final form 27 June 2006

Rummel, Christoph, Christelle Sachot, Stephen Poole, and Giamal N. Luheshi. Circulating interleukin-6 induces fever through a STAT3-linked activation of COX-2 in the brain. *Am J Physiol Regul Integr Comp Physiol* 291: R1316–R1326, 2006. First published June 29, 2006; doi:10.1152/ajpregu.00301.2006.—Interleukin (IL)-6 is an important humoral mediator of fever following infection and inflammation and satisfies a number of criteria for a circulating pyrogen. However, evidence supporting such a role is diminished by the moderate or even absent ability of the recombinant protein to induce fever and activate the cyclooxygenase-2 (COX-2) pathway in the brain, a prerequisite step in the initiation and maintenance of fever. In the present study, we investigated the role of endogenous circulating IL-6 in a rodent model of localized inflammation, by neutralizing its action using a specific antiserum (IL-6AS). Rats were injected with LPS (100 μg/kg) or saline into a preformed air pouch in combination with an intraperitoneal injection of either normal sheep serum or IL-6AS (1.8 ml/rat). LPS induced a febrile response, which was accompanied by a significant rise in plasma IL-6 and nuclear STAT3 translocation in endothelial cells throughout the brain 2 h after treatment, including areas surrounding the sensory circumventricular organs and the median preoptic area (MnPO), important regions in mediating fever. These responses were abolished in the presence of the IL-6AS, which also significantly inhibited the LPS-induced upregulation of mRNA expression or immunoreactivity (IR) of the inducible form of COX, the rate-limiting enzyme for PGE_2-synthesis. Interestingly, nuclear signal transducer and activator of transcription (STAT)3-positive cells colocalized with COX-2-IR, signifying that IL-6-activated cells are directly involved in PGE_2 production. These observations suggest that IL-6 is an important circulating pyrogen that activates the COX-2-pathway in cerebral microvasculature, most likely through a STAT3-dependent pathway.

local inflammation; cytokines; nuclear factor-κB; prostaglandins; circumventricular organs

FEVER IS A BRAIN-REGULATED sickness response, which can be triggered by a multitude of peripheral signaling pathways (46), including circulating endogenous pyrogens (15). These humoral mediators, which belong primarily to the cytokine family, are induced in the periphery following systemic infection or inflammation, and gain entry to the brain where they act on specific receptors. A number of proinflammatory cytokines have been shown to fit the criteria proposed for circulating pyrogens (26), such as IL-1, IL-6, and TNF-α. Of these, only IL-6 was demonstrated to consistently increase in the circulation of febrile animals (8, 10, 38) and humans (42) in a manner that correlates significantly with the magnitude and duration of the fever response to exogenous pathogens, such as LPS (34, 47, 49). Furthermore, absence of endogenous IL-6 activity following neutralization with a specific antiserum (10) or in IL-6-deficient mice (11, 28) demonstrated unequivocally that IL-6 is essential for the fever response following infection. Conversely, administration of recombinant IL-6 in different species of rodents and using different routes of administration resulted in rather moderate (3, 16, 22, 23, 52) or absent (10, 34, 59) increases in body temperature.

These apparent discrepancies are further confounded by observations, showing that exogenously systemically administered IL-6, unlike IL-1β, does not trigger PGE production in the brain as measured by the induction of cyclooxygenase (COX)-2 (30, 58), the rate-limiting enzyme in PGE_2 synthesis (35, 66). The induction of COX-2 and PGs in the brain represents a critical step in the generation of fever and is an important criterion for the definition of a circulating pyrogen. The major intracellular signaling pathway for COX-2 (40, 56) and fever (29, 33, 59) induction is believed to be NF-κB. Unlike IL-1β, which signals through this transcription factor, IL-6 triggers a different signaling pathway, namely JAK-signal transducer and activator of transcription (STAT)3 (2). Recent evidence, however, suggests that COX-2 induction, at least in peripheral tissue, such as the myocardium, can indeed be activated through this pathway (63). In the brain, studies have now shown that systemically administered IL-6 can induce nuclear STAT3 translocation in structures implicated in the fever response (22, 51), namely endothelial cells lining the vasculature within the blood-brain barrier (BBB) and the sensory circumventricular organs (sCVOs), which lack an intact BBB. The same studies, however, did not address the precise functional consequence of IL-6-mediated genomic activation of these structures, including whether this humoral mediator can trigger PG synthesis.

The aim of the present study, therefore, was to address the question of whether circulating IL-6 can trigger the brain mechanisms associated with the fever response by assessing whether it induces COX-2 expression in the brain. For this, we targeted the contribution of the endogenous circulating protein by using a specific neutralizing antiserum in rodents treated with LPS, a potent pyrogen and activator of systemic IL-6 and COX-2 in the brain.

MATERIALS AND METHODS

Animals

Adult male Sprague-Dawley rats (Charles River, Saint Constant, Canada) with a body weight of 290–320 g on the day of experiment

Address for reprint requests and other correspondence: G. N. Luheshi, Douglas Hospital Research Centre, Dept. of Psychiatry, McGill Univ., 6875 Blvd. LaSalle, Verdun, Montreal, QC, H4H 1R3, Canada (e-mail: giamal.luheshi@mcgill.ca).

The costs of publication of this article were defrayed in part by the payment of page charges. The article must therefore be hereby marked "*advertisement*" in accordance with 18 U.S.C. Section 1734 solely to indicate this fact.

0363-6119/06 $8.00 Copyright © 2006 the American Physiological Society

Downloaded from ajpregu.physiology.org on April 15, 2010

were used in all studies. Animals were housed individually in a controlled environment at an ambient temperature of 21 ± 2°C on 12:12-h light-dark cycle (lights off at 7:00 PM) with free access to standard laboratory chow and water. All animals were handled extensively for at least 2 days before each experiment for habituation. The Animal Care Committee of McGill University pursuant to the Canadian Council of Animal Care guidelines approved all experimental procedures.

Surgery and Measurement of Body Temperature

Rats were anesthetized with ketamine/xylazine/acepromazine (50, 5, and 0.5 mg/kg, respectively) via intramuscular injection and implanted with intra-abdominal temperature-sensitive radiotransmitters. During the same procedure, each animal received 20 ml of sterile air injected into the subcutaneous tissue of the dorsal midline at the level of the scapulae to form an "air pouch" for administering the inflammatory agent, as previously described (10, 17). Three days before the experiment, animals were briefly reanesthetized (3% isoflurane in oxygen) until they demonstrated complete areflexia and the air pouches reinflated with 10 ml of sterile air to maintain the cavities. On *day 6* following the initial surgery, injections were performed between 1:00 and 2:00 PM directly into the subcutaneous air pouches in lightly restrained (hand-held), conscious animals. Changes in core body temperature were monitored in these animals using remote biotelemetry (Data Sciences, St. Paul, MN), as described earlier (9).

Treatment and Experimental Protocols

All animals including controls were pretreated (−4 h) either intraperitoneally with 1.8 ml normal sheep serum (NSS: $n = 19$; Sigma) or 1.8 ml of sheep anti-rat IL-6 serum [$n = 5$; IL-6 antiserum (AS); National Institute for Biological Standards and Control (NIBSC) Potters Bar, UK]. The IL-6AS serum recognizes both recombinant (*Escherichia coli*-derived) and natural rat IL-6, but does not cross react with rat recombinant (rr)IL-1α, IL-1β, or TNF-α (45). In a previous study, we reported that pretreatment with the same IL-6AS had no effect on body temperature in saline-treated animals (10). Some animals ($n = 10$) were injected subcutaneously with bacterial LPS (derived from *E. coli*, suspended in sterile pyrogen-free 0.9% saline; 0111:B4, Lot 42k4120; L-2630; Sigma) at 100 μg/kg (prepared as 100 μg/ml solution). This dose of LPS was previously shown to induce fever and to significantly increase circulating IL-6 concentrations in rats (9). Another group of rats ($n = 4$) received an intraperitoneal injection of rrIL-6 (*E. coli*-derived, nonglycosylated, specific activity 250,000 IU/μg as measured in a B9 mouse hybridoma bioassay; NIBSC) at a dose of 45 μg/kg and a volume of 1 ml/kg diluted in sterile 0.9% saline. Equivalent volumes of the vehicle (0.9% saline, 1 ml/kg, each $n = 5$) were injected subcutaneously or intraperitoneally, respectively, in control groups. In all cases, core body temperature was continuously monitored for 12 h before treatment and for 2 h after treatment. The final time point was based on our earlier studies showing that LPS-induced (100 μg/kg) plasma IL-6 levels in the air pouch model peak at 2 h posttreatment (10). At this time, animals were euthanized by using terminal anesthesia (ketamine/xylazine/acepromazine; 100, 10, and 1 mg/kg ip, respectively), blood samples were collected via cardiac puncture, and lavage fluid was collected from each air pouch by injecting, then quickly withdrawing 1 ml saline using a sterile syringe. Following the fluid collection, rats were transcardially perfused with 150 ml ice-cold 0.9% NaCl solution; their brains were quickly removed, frozen in powdered dry ice, and kept at −80°C until analysis. The brains of all animals were prepared for immunohistochemistry as previously described (51).

IL-6 ELISA

To determine IL-6 concentration, heparinized (10 IU/ml) blood and lavage samples were centrifuged (5,300 *g*, 10 min, 4°C), the supernatant was collected and stored at −80°C until assays were performed. IL-6 levels were measured in duplicates using a two-site, rat-specific ELISA (NIBSC) as described previously (45).

Tissue Processing

Coronal cryostat sections (20 μm, prepared with a model CM 3050 S cryostat; Leica Microsystems, Nussloch, Germany) were prepared from two brain areas encompassing the forebrain [including the vascular organ of the lamina terminalis (OVLT), the subfornical organ (SFO), and the median eminence (ME); bregma 0.5 to −3.5 mm] and the brain stem [area postrema (AP) and surrounding tissue, bregma −14.28 to −12.28 mm] according to the atlas of Paxinos and Watson (44). To perform RT-PCR and immunohistochemistry from the same brain, every third consecutive frozen section was thaw-mounted on poly-L-lysine-coated glass slides for immunohistochemistry and stored at −80°C until processing. The remainder of the serial whole brain sections were collected for RNA extraction and stored in a cryotube at −80°C for mRNA extraction. Because IL-6 was recently shown to activate endothelial cells throughout the entire brain, including the cortex (51), whole brain sections were used for RT-PCR analyses.

Semiquantitative RT-PCR

Total RNA was extracted using Trizol (Invitrogen, Burlington, ON, Canada) according to the manufacturer's instructions. The first-strand cDNA was synthesized from 1 μg total RNA using 200 units of Molony murine leukemia virus RT (Invitrogen), 5 μM of random hexamers (Applied Biosciences, Streetsville, ON, Canada), and 1 mM of deoxyribonucleotide triphosphate mix (Sigma) in a total reaction volume of 20 μl. Following RT, the product was stored at −20°C. The cDNA product (0.9 μl) was added to 15 μl PCR reaction mix containing ReadyMix Taq PCR (Sigma) and 6 pmol of gene-specific primer sets for COX-2 and suppressor of cytokine signaling 3 (SOCS3) and β-actin. In each case, amplification was performed with a thermal cycler (GeneAmp PCR System 9700; Applied Biosciences) using the following cycling parameters: *1*) denaturing, 95°C for 5 min; *2*) amplification cycle, 95°C for 30 s, annealing temperature for 30 s and 72°C for 1 min; and *3*) final extension, 72°C for 10 min. Primers were designed to span a sequence derived from different exons (separated by an intron in genomic DNA sequence) to minimize amplification from non-mRNA-derived templates. Inappropriate amplification from genomic DNA was negligible when amplification was performed with a template without RT. The gene accession numbers, primer sequences, annealing temperatures, and cycle numbers used are listed as follows: COX-2 (NM_017232) sense 5′-TGATAGGAGAGACGATCAAGA-3′, anti-sense 5′-ATGGTAGAGGGCTTTCAACT-3′, 57°C, 32 cycles; SOCS3 (NM_053565) sense 5′-CCAGCGCCACTTCTTCAC-3′, anti-sense 5′-GTGGAGCATCATACTGGTCC-3′, 60°C, 40 cycles; β-actin (NM_031144) sense 5′-GCCGTCTTCCCCTCCATCGTG-3′, anti-sense 5′-TACGACCAGAGGCATACAGGGACAAC-3′, 60°C, 20 cycles. PCR products were separated by 2% agarose gel electrophoresis and visualized with ethidium bromide staining. The band density was obtained for quantification using GeneTool image analysis software (Syngene, Frederick, MD). To normalize the expression level of genes between different samples, the levels were estimated as the ratio of geneX/β-actin. In a pilot experiment, the amount of PCR product (on a log scale) vs. the number of cycles was plotted, and the linear range of template amplification was determined for two samples from each treatment group. The cycle numbers were determined to be within the exponential phase of amplification for all treatment groups.

Immunohistochemistry

General procedure. On the day of the experiment, the frozen brain sections were air dried at room temperature for 10 min and then

Downloaded from ajpregu.physiology.org on April 15, 2010

immersion fixed in 2% paraformaldehyde diluted in 0.1 M PBS (pH 7.4) for 10 min at room temperature. After three successive washes in PBS, the sections were treated for 1 h at room temperature with a blocking solution consisting of PBS containing 10% normal donkey serum (NDS; Chemicon International, Temecula, CA) and depending on the type of applied antibodies, 0.1% or 0.25% Triton X-100. Details of the primary antibody concentrations as well as fixation and blocking procedures are shown in Table 1.

The sections were incubated with the primary antibodies for 36–48 h at 4°C followed by visualization with CY3-conjugated anti-rabbit IgG (for STAT3 and COX-2; 1:500 dilution; cat. no. 711–165-152) or CY3-conjugated anti-goat IgG (for NF-κB; 1:500; cat. no. 705–165-147). All secondary antibodies were raised in donkey and all were multiple labeling-grade (Jackson ImmunoReaserch, West Grove, PA). Sections were counterstained with the nuclear 4,6-diamidino-2-phenylindole (DAPI) stain (Molecular Probes, Eugene, OR) for 15 min, using a 1:4,000 dilution in PBS to assess the nuclear localization of the STAT3 signals and to give better visualization of the tissue surrounding the signal. Finally, all sections were cover slipped using an equal mix of glycerol/PBS and stored at 4°C until microscopic analysis was performed.

STAT3. A rabbit anti-STAT3 antibody was used to detect STAT3 signals in rat brain. This antibody was raised to detect both the phosphorylated (activated) and the nonphosphorylated (constitutive) forms of the transcription factor and was previously demonstrated to be specific for both (25). In some studies (colocalization), a specific antibody (rabbit polyclonal anti-phopho-STAT3 antibody) was used for the detection of the phosphorylated (P) form of STAT3.

COX-2. The rabbit anti-COX-2 antibody was raised against a peptide of murine COX-2. The antibody shows specific staining of this enzyme typically at a perinuclear subcellular localization.

NF-κB. As for STAT3, the goat anti-NF-κB antibody used in our studies recognizes both cytoplasmic (inactive) and nuclear (active) forms of the peptide. Specifically, this antibody targets the inactive p65 subunit in the cytoplasm (bound to p50 and inhibitor κB), as well as the active monomeric or dimeric form in the nucleus.

Specificity of each antibody was shown previously [STAT3, (25); COX-2, (64); NF-κB, (39)] and was confirmed by preabsorption with respective blocking peptides (data shown only for NF-κB, see Fig. 8, *O–P*).

Colocalization studies. In studies involving double immunostaining for PSTAT + COX-2 and PSTAT + NF-κB, the rabbit anti-PSTAT antibody (see Table 1) was mixed with a goat COX-2 antibody (dilution 1:2,000, raised against the COOH terminus of murine COX-2; cat. no. sc-1747; Santa Cruz Biotechnology, Santa Cruz, CA) or the goat anti-NF-κB antibody (see Table 1), respectively. Primary antibodies were visualized with CY3-conjugated anti-rabbit IgG (for PSTAT, 1:500 dilution; cat. no. 711–165-152) and FITC-conjugated anti-goat IgG (for COX-2 and NF-κB; 1:500 dilution). The specificity of the COX-2 staining was confirmed by preincubation of the antibody with the specific blocking peptide (10-fold excess; cat. no. sc-1747 P, Santa Cruz Biotechnology). In control experiments, the sections were incubated with the primary antibody mixture in which one of the primary antibodies was substituted with noniinmunized animal IgG (rabbit IgG for STAT3, PSTAT, and COX-2). Inappropriate cross-reaction between antibodies was confirmed to be negligible.

To identify endothelial cells, double immunohistochemistry was performed using the specific cell marker antibodies against von Willebrand (vW) factor. The antibodies for STAT3, PSTAT, or COX-2 were mixed with a sheep anti-rat vW factor antibody (1:3,000; cat. no. SARTW-IG; Affinity Biologicals, Ancaster, ON, Canada), and brain sections were incubated with the primary antibodies at 4°C for 36 to 48 h. STAT3, PSTAT, and COX-2 were visualized with CY3-conjugated anti-rabbit IgG (1:500 dilution) and vW with FITC-conjugated anti-sheep IgG (1:500 dilution; cat. no. 713–095-147) as secondary antibodies.

Data Analysis

Temperature data were analyzed using a two-way repeated measures ANOVA followed by Newman-Keuls multiple comparisons post hoc test to compare treatment groups and controls. Circulating levels of IL-6 and the relative density of SOCS3 and COX-2 expression in the forebrain and the brain stem were compared separately between the experimental groups (LPS, LPS + IL-6AS) by one-way ANOVA followed by Newman-Keuls multiple comparisons post hoc test. A parametric unpaired two-tailed Student's *t*-test was used to compare IL-6 and vehicle-treated groups. We also investigated potential correlations between individual values of plasma IL-6 and the respective relative density of mRNA signals in the brain. Each brain area (forebrain, brain stem) was evaluated separately, with an $n = 9$ (IL-6 vs. NaCl; $n = 4/5$), respectively. Datasim software (Desktop Press, Lewiston, ME) was used for two-way ANOVA analysis and GraphPad Prism (GraphPad Software, San Diego, CA) was used for the other statistical analyses. $P < 5\%$ was deemed significant. All data are presented as means ± SE.

RESULTS

IL-6-AS Significantly Inhibits LPS-Induced Fever and Circulating IL-6 Levels

LPS (100 μg/kg) induced a significant increase (90–120 min, $P < 0.005$ vs. saline) in body temperature, which peaked at 110 min after injection (LPS sc, NSS ip; 38.19 ± 0.13°C; see Fig. 1*A*). IL-6AS (ip) pretreatment completely abolished this response. The mean IL-6 levels in the blood and lavage were 0.16 and 0.15 ng/ml, respectively, in saline-treated animals. LPS treatment induced a 50-fold increase of IL-6 in the lavage and a threefold increase in plasma IL-6 (lavage: 3.36 ± 0.69 ng/ml; plasma: 0.53 ± 0.10 ng/ml; see Fig. 1, *B* and *C*).

Table 1. *Conditions for the antibodies used for immunohistochemistry*

	Postfixation	Blocking/Triton X-100	One Antibody
STAT3	PFA 2	0.1	Rabbit polyclonal IgG (1:9000; cat no.: sc-482; Santa Cruz Biotechnology, Santa Cruz, CA)
COX-2	PFA 2	0.25	Rabbit IgG (1:2000; cat no.: 160126; Cayman Chemical, Ann Arbor, MI)
NF-κB, p65	PFA 2	0.1	Goat polyclonal IgG (1:500 cat no.: sc-372 G; Santa Cruz Biotechnology)
PSTAT	PFA 2	0.1	Rabbit polyclonal IgG (1:500; cat no.: 9131; Cell Signaling, Beverly, MA)
vW factor	PFA 2	0.1, 0.25	Sheep polyclonal IgG (1:300; cat no.: SARTW-IG; Affinity Biologicals, Ancaster, Ontario, CA)

Values are in percent. STAT3, signal transducer and activator of transcription-3; COX-2, cyclooxygenase-2; PSTAT, phospho-STAT3; vW, von Willebrand.

Downloaded from ajpregu.physiology.org on April 15, 2010

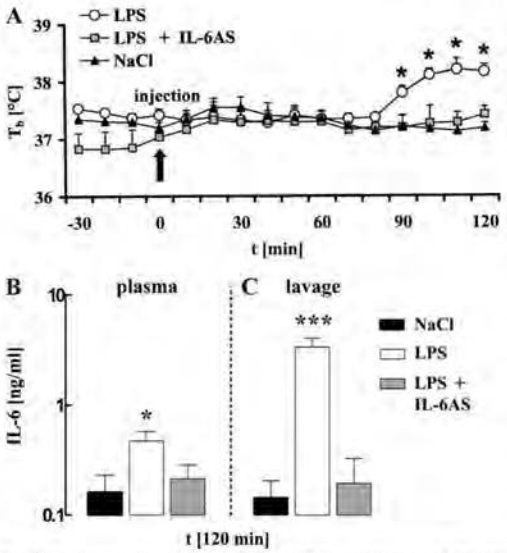


Fig. 1. *A*: changes of core body temperature (T_b) after injection of LPS (100 μg/kg sc; $n = 5$) or LPS + IL-6AS (100 μg/kg sc + 1.8 ml ip; $n = 5$) are shown with the respective saline control ($n = 5$ each). The arrow depicts the time of LPS or vehicle injection. Either normal sheep serum (NSS; 1.8 ml/kg ip) or IL-6 antiserum (IL-6AS) were injected 4 h before LPS or saline (0 h). IL-6 levels measured using ELISA 2 h after injection of LPS (100 μg/kg sc) in plasma (*B*) and at the site of injection (lavage; *C*) are shown compared with an LPS + IL-6AS treatment (IL-6AS, 1.8 ml/kg ip) or respective saline controls (1 ml/kg; $^*P < 0.05$, $^{***}P < 0.001$) on a logarithmic scale. Values are presented as means ± SE.

In both cases, this was significantly attenuated in the presence of IL-6AS ($P = 0.0172$ for plasma; $P < 0.0001$ for the lavage).

Exogenous administration of rat recombinant IL-6 (45 μg/kg ip) induced a significant rise (40–50 and 70–80 min, $P < 0.05$ vs. saline) in body temperature, which peaked 40 min after treatment (IL-6 ip, NSS ip; 37.99 ± 0.17°C; see Fig. 2*A*). rrIL-6 treatment was accompanied with a fourfold significant rise of circulating IL-6 2 h after injection (0.57 ± 0.13 ng/ml, $P = 0.0081$; Fig. 2*B*).

IL-6-AS Significantly Inhibited LPS-Induced Nuclear STAT3 Translocation and SOCS3 mRNA Expression in Sensory CVOs and Brain Endothelial Cells

LPS induced a dramatic increase in nuclear STAT3 translocation in the brain 2 h after treatment (Table 2). Double immunohistochemical studies revealed that the majority of this staining was localized in vW factor positive endothelial cells throughout the entire brain (see Fig. 5*M* for example), including fever-relevant areas, such as the MnPO (data not shown). One exception was observed in the sCVOs in which nuclear STAT3-positive IR was detected in other cell types in addition to the endothelial cells (OVLT, SFO, AP; Fig. 3, *B*, *E*, and *H*). This response was almost totally abolished in the presence of IL-6AS in the forebrain and the brain stem (data not shown), including all three structures of the sCVOs (Fig. 3, *C*, *F*, and *I*), although a few remnant STAT3 nuclear-positive cells could still be seen in the SFO (Fig. 3*F*). Saline-treated controls (Fig. 3, *A*, *D*, and *G*) only exhibited cytoplasmic (inactive) STAT3.

To further assess the contribution of IL-6 to the activation of this pathway by LPS, we measured the change in expression of SOCS3. This is a major end product of the STAT3 signaling pathway, which is involved in autoregulatory feedback for activated STAT3 and is broadly used as a marker for STAT3 activation (32). Changes in the levels of SOCS3 were measured by semiquantitative RT-PCR on mRNA obtained from two different regions of the brain: forebrain (including the OVLT, SFO, and ME; bregma 0.5 to −3.5 mm) and the brain stem (including the AP and surrounding tissue, bregma −14.28 to −12.28 mm). LPS treatment significantly increased SOCS3 mRNA levels in both of these regions, a change that was significantly inhibited by IL-6AS (Fig. 4*A*, forebrain, $P = 0.0053$; Fig. 4*B*, brain stem, $P = 0.0002$).

In a separate experiment, systemic (45 μg/kg ip) rrIL-6 treatment alone induced STAT3 translocation in endothelial cells (data not shown) throughout the entire brain (Table 2) and SOCS3 mRNA expression both in the forebrain (Fig. 4*C*, $P = 0.0141$) and in the brain stem (Fig. 4*D*, $P = 0.0019$).

IL-6-AS significantly inhibited LPS-induced COX-2 mRNA expression in the brain and COX-2-IR within brain endothelial cells.

Constitutive, neuronal COX-2-IR, was detected in the brains taken from all treatment groups (Fig. 5, *A–D*), as previously reported by others (5, 7, 27). LPS treatment clearly induced COX-2-IR in blood vessels throughout the entire brain, including the cortex (see Fig. 5*B* for an example) and structures implicated in fever, such as the MnPO (Fig. 5*F*) or the sCVOs (see Fig. 5*J*, SFO for example). For practical reasons, only examples for this broad and consistent effect throughout the brain are shown. Double immunolabeling with vW factor-IR indicated that this staining was localized to endothelial cells

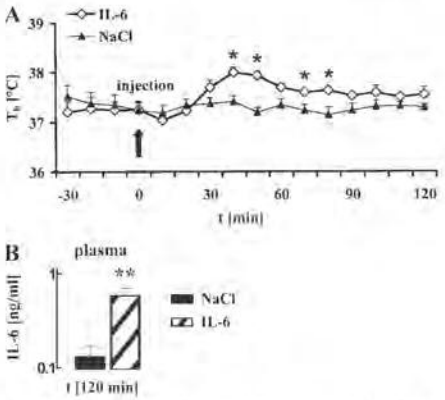


Fig. 2. *A*: changes of T_b after injection of rat recombinant IL-6 (rrIL-6; 45 μg/kg ip; $n = 4$) are shown with respective saline controls ($n = 5$ each). The arrow depicts the time of rrIL-6 or vehicle injection. NSS (1.8 ml/kg ip) was injected at −4 h. *B*: immunoreactive IL-6 levels measured 2 h after injection of rrIL-6 (45 μg/kg ip) in plasma are shown compared with respective saline controls (1 ml/kg; $^*P < 0.05$, $^{**}P < 0.01$) on a logarithmic scale. Values are presented as means ± SE.

Downloaded from ajpregu.physiology.org on April 15, 2010

Table 2. *Qualitative analysis of nuclear STAT3/NF-κB translocation and COX-2-IR*

	NaCl, sc	LPS, sc	LPS + IL-6AS, sc + ip	NaCl, ip	IL-6, ip
Nuclear STAT3	±	+++	+	±	++
COX-2	±	++	±	+	++
Nuclear NF-κB	−	+	+	−	−

Relative values of nuclear STAT3/NF-κB and perinuclear COX-2 immunoreactivity are given as estimates of the density of their respective labeling. Analyses were performed 2 h after local subcutaneous (sc) injection of LPS (100 μg/kg; $n = 5$), LPS/IL-6-anti serum (AS) (100 μg/kg + 1.8 ml ip; $n = 5$), and saline (1 ml/kg; $n = 5$) or systemic intro peritoneal (ip) injection of rat recombinant IL-6 (45 μg/kg; $n = 4$) and saline (1 ml/kg; $n = 5$) in the forebrain and the brain stem. IR, immunoreactivity. A five-point scale was used to rate the data: +++, high density of nuclear/perinuclear signals; ++, moderate density; +, low density; ±, single nuclear/perinuclear signals in some cases; −, no nuclear/perinuclear signals.

(Fig. 5, *B*, *F*, and *J*). Coadministration of IL-6AS (Fig. 5, *C*, *G*, and *K*) almost completely abolished this response to a comparable level seen in saline-treated animals (Fig. 5, *A*, *E*, and *I*).

In a separate experiment, exogenous administration of rrIL-6 (45 μg/kg ip) was followed by a similar induction of COX-2 in the brain. COX-2-IR could be clearly seen throughout the brain (Fig. 5, *D*, *H*, and *L*), including areas in close proximity to the sCVOs (Fig. 5*L*, SFO, for example) and the MnPO (Fig. 5*H*). Colocalization studies with vW factor-IR indicated that this was specific to endothelial cells (Fig. 6, *D*, *H*, and *L*). In general, control saline-treated animals did not show significant induction of COX-2-IR; however, in some cases, single COX-2-IR positive cells were detected in endothelial cells, most likely reflecting constitutive expression of this enzyme (data not shown).

The levels of COX-2 mRNA were measured by semiquantitative RT-PCR. LPS treatment significantly increased COX-2 levels only in the brain stem, but not in the forebrain. The LPS-induced rise in COX-2 mRNA in this brain area was attenuated by IL-6AS (Fig. 6*B*, $P = 0.0112$). Similarly, exogenous administration of rrIL-6 resulted in a significant induction of COX-2 mRNA in the brain stem (Fig. 6*D*, $P = 0.0296$). The lack of significant change in COX-2 mRNA expression between the control and treated groups in the forebrain is most likely due to the very high constitutive expression of COX-2 in cortical neurons (see Fig. 5, *A–D*), which probably masked any intricate changes that were detected with the immunohistochemical analysis of this brain region.

PSTAT-IR Colocalizes with COX-2-IR After rrIL-6 or LPS Stimulation

On the basis of the observation that both PSTAT (Fig. 5*M*) and COX-2 (Fig. 5, *B*, *D*, *F*, *H*, *J*, and *L*) were induced in endothelial cells after LPS or rrIL-6 stimulation, colocalization of PSTAT and COX-2 was examined in these animals by double immunohistochemistry. LPS-induced perinuclear COX-2-IR was found to clearly colocalize with PSTAT-IR in blood vessel-like structures in the cortex (Fig. 5*N*) and other areas (data not shown). Similar observations were made in the brains of rrIL-6-treated animals (Fig. 5, *O–T*).

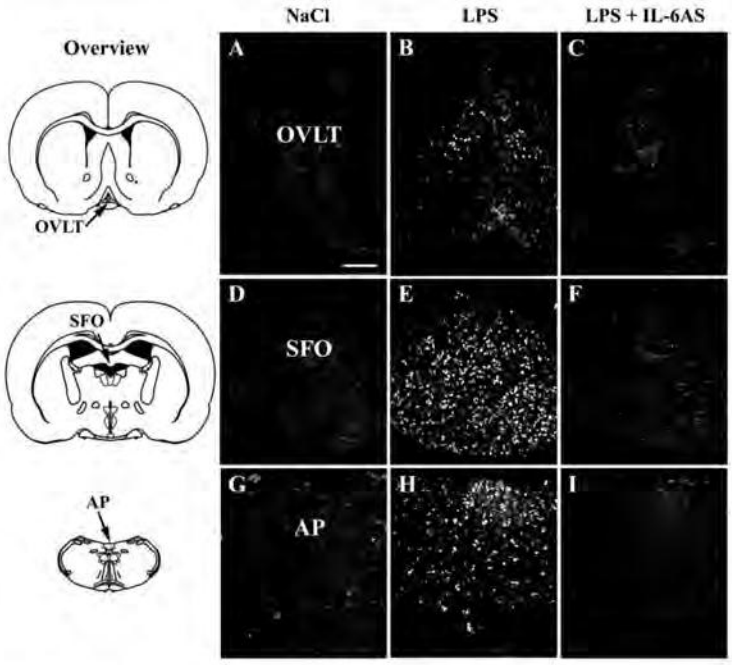


Fig. 3. LPS (*B*, *E*, and *H*; 100 μg/kg sc) induces nuclear STAT3 translocation 2 h after injection in the sensory circumventricular organs (sCVOs; white spot-like pattern), which is almost completely abolished by IL-6AS pretreatment [*C*, *F*, and *I*; 1.8 ml/kg ip; gray background is cytoplasmic staining representing the inactive form of signal transducer and activator of transcription-3 (STAT3)]. Constitutive cytoplasmic expression of STAT3 is observed in the sCVOs of the control group (*A*, *D*, and *G*). Scale bar in *A* represents 50 μm and applies to *A–I*; OVLT, vascular organ of the lamina terminalis; SFO, subfornical organ; AP, area postrema.

Downloaded from ajpregu.physiology.org on April 15, 2010

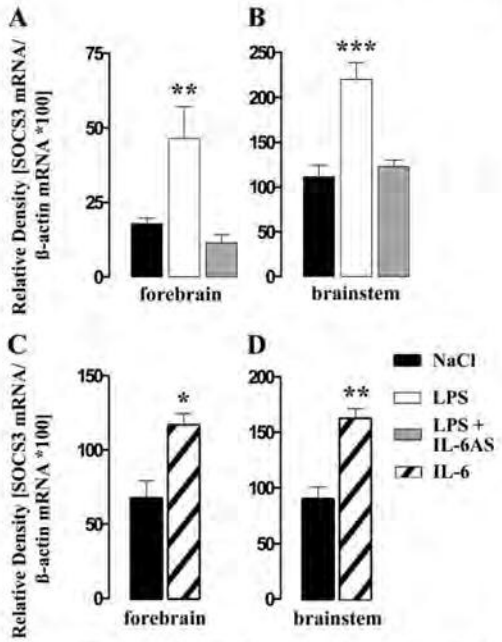


Fig. 4. Injection of LPS (100 μg/kg sc) induces a significant increase of suppressor of cytokine signaling-3 (SOCS3) mRNA expression in the forebrain (*A*) and the brain stem (*B*) of rats 2 h after injection compared with controls (NaCl; 1 ml/kg sc). These responses are totally abolished by administration of IL-6AS (1.8 ml/kg ip). In addition, rrIL-6 treatment (45 μg/kg ip) induces a rise of SOCS3 mRNA expression in the forebrain (*C*) and the brain stem (*D*) of rats 2 h after the injection (*$P < 0.05$, **$P < 0.01$, ***$P < 0.001$). Values are presented as means ± SE.

rrIL-6-Induced SOCS3 Correlates with COX-2 Expression

To further clarify the relationship between IL-6 activity in the brain and the induction of COX-2, we studied the correlation between SOCS3 mRNA induction as a measure of cellular action of IL-6 and COX-2 mRNA expression. The analysis of these data indicated a clear and significant correlation between the two in the brain stem (Fig. 7*B*; $r^2 = 0.8642$, $P = 0.006$), but not in the forebrain (Fig. 7*A*; $r^2 = 0.1693$, $P = 0.6632$). This provides additional support for the hypothesis that exogenous rrIL-6 directly activates the COX-2-pathway within the rat brain through a STAT3-related mechanism.

LPS-Induced Transcription Factor NF-κB Is not Affected by IL-6-AS Treatment

Nuclear translocation of p65, a subunit of NF-κB, was investigated to monitor its activation within immunostained rat brain sections 2 h after stimulation. LPS injection (Fig. 8, *G* and *H*, *cortex* for example) induced nuclear translocation of NF-κB within endothelial-like cells throughout the entire brain. Coadministration of IL-6AS did not affect this response (Fig. 8, *C* and *D*). Nuclear translocation was absent in control animals (Fig. 8, *A* and *B*) and in those treated with rrIL-6 alone (Fig. 8, *E* and *F*), where only cytoplasmic (inactive) NF-κB-IR was observed (Table 2). Interestingly, nuclear translocation of NF-κB in LPS-treated animals was seen to colocalize with PSTAT (Fig. 8, *I–N*), indicating a possible association of these two different intracellular signaling pathways.

DISCUSSION

The results of the current study confirm our earlier observations (10) and those of others (6, 11, 28, 34), demonstrating that IL-6 is an important neuroimmune mediator in fever following infection or inflammation. An important aspect of the role of IL-6 in fever that some studies (10, 11, 28) did not address and others did not show (30, 58) was a direct link between the circulating cytokine and the activation of the COX pathway, a critical step in the generation of fever. In the present study, we provide evidence demonstrating that circulating IL-6 does indeed activate this pathway. This is in agreement with an earlier study demonstrating that COX-2 induction was absent in the brains of IL-6 knockout mice injected with turpentine (a potent inflammatory agent) (57). Other studies using recombinant IL-6 administered systemically in rats failed to demonstrate COX-2 induction in the brain and had no effect on core body temperature (30, 58). The discrepancy between these observations and ours from the present study is most likely because of the bioactivity of the different recombinant protein used, whether as a result of species difference, i.e., human as opposed to rat (10, 30), or amounts injected (10, 58). In our experiments, we used a dose of 45 μg/kg of rrIL-6, which reflects better biological concentrations found in the circulation of rats in response to a systemic injection of LPS (21) and thus enough to reach a threshold concentration necessary for inducing fever. This was confirmed by our recent study showing that nuclear STAT3 translocation following LPS treatment in guinea pigs occurs only after plasma concentrations of IL-6 reach a critical level (50), also suggesting that LPS-induced STAT3 activation is IL-6 dependent. We have now confirmed these observations and those of others (19, 22, 24, 51) by demonstrating unequivocally that this is indeed the case. Most importantly, the present study showed that STAT3 activation using the paradigms described occurred in endothelial cells lining the vasculature of the brain, adding support to previous observations that these cells constitute important targets for circulating pyrogens (36). We also observed IL-6-induced STAT3 activation in the sCVOs, in cells other than endothelial cells. Although previously identified as important areas in fever, based primarily on lesion studies (48), the significance of a direct action of IL-6 on nonendothelial cells within the sCVOs in fever remains undetermined. One possibility is that IL-6 could be acting on thermoregulatory neurons, especially in the SFO in a similar manner to IL-1β, which was previously shown to trigger the firing of isolated neurons in this area (14). Other than nuclear STAT3 translocation, however, we have no evidence indicating that IL-6 is acting directly on this area to induce fever, especially since the only COX-2-IR we detected in this region was in endothelial cells in close proximity to this area of the brain. Thus, the most likely contribution of this brain region to the fever response remains to be that of a gateway for circulating pyrogens to access their targets in the brain through a "leaky" BBB. In contrast, the action of endogenous pyrogens on endothelial cells is well documented, and

Downloaded from ajpregu.physiology.org on April 15, 2010

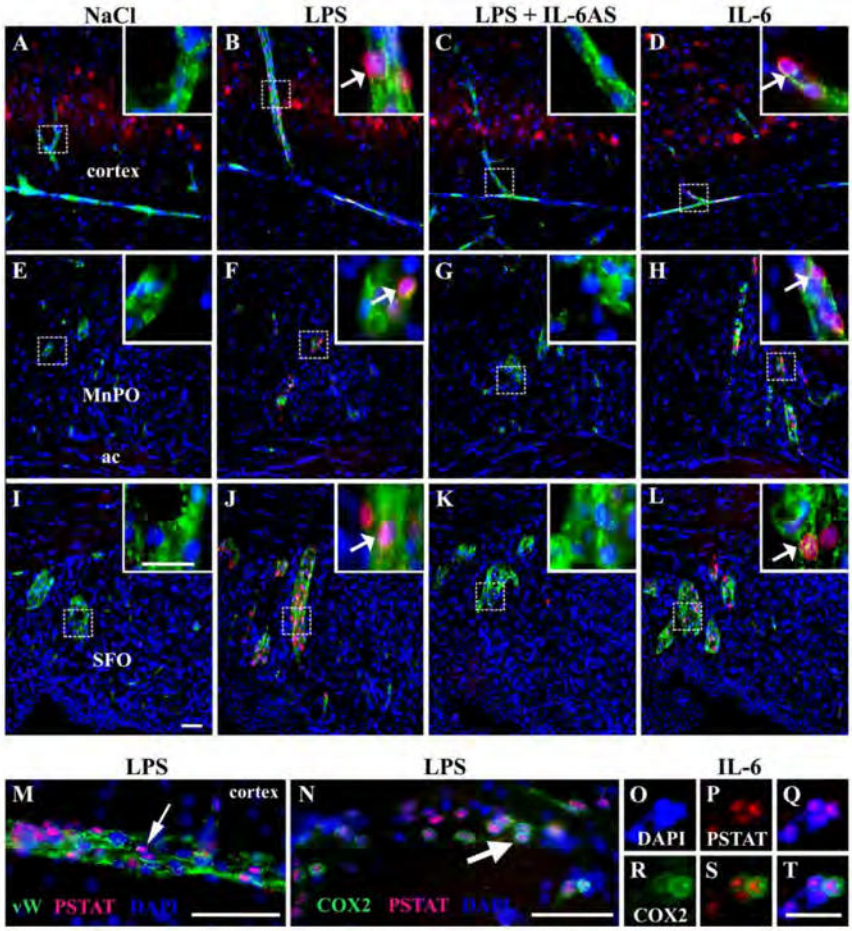


Fig. 5. LPS (*B*, *F*, and *J*; 100 μg/kg sc) and rrIL-6 (*D*, *H*, and *L*; 45 μg/kg ip) treatment lead to a robust induction of cycloxygenase-2 (COX-2) immunoreactivity (COX-2-IR; red) 2 h after the injection within von Willebrand factor (vW; green)-positive endothelial cells of the entire brain including the cortex (*B* and *D*) and brain structures important in fever, such as the median preoptic nucleus (MnPO; *F* and *H*; microphotographs of the upper part of caudal sections are shown) and the sCVOs [*J* and *L*; subfornical organ (SFO); microphotographs of half-medial sections are shown]. IL-6AS (*C*, *G*, and *K*; 1.8 ml/kg ip) attenuates LPS-induced COX-2-IR to a level comparable to that observed in the brain of control animals (*A*, *E*, and *I*; NaCl; 1 ml/kg sc). White arrows depict colocalization of vW with COX-2-IR as indicated, respectively, in the *inset* of each microphotograph. *Insets* represent higher magnification of dashed squares. The perinuclear [blue nucleus, 4,6-diamino-2-phenylindole (DAPI)] staining of COX-2 can be clearly identified at high magnification (*B*, *D*, *F*, *H*, *J*, and *L*; white arrow). In the cortex, constitutive neuronal COX-2-IR (red spot-like pattern in the upper part of microphotograph *A–D*) is present in all treatment groups. In the lower panel (microphotographs *M–T*), colocalization of nuclear (DAPI-stain, blue) phosphorylated STAT-IR (PSTAT-IR; red) and COX-2-IR (green) or vW-IR (green only for *M*) is shown 2 h after rrIL-6 (*O–T*, 45 μg/kg) or LPS (*M* and *N*, 100 μg/kg sc) treatment. The photomicrograph color composition of the triple labeling in *N* and *T* is demonstrated in *O–T*. The individual color channels are shown in *O–P* and *R* and dual and triple overlays within the images of *Q* and *S–T*. Note that the structural similarity to a blood vessel can be clearly depicted between microphotograph *M* and *N*. White arrows indicate colocalization as shown with color-coded labeling of *M* and *N*. Scale bars in *I* (applies to *A–L*), *M* and *N* represent 50 μm; 25 μm in the *inset* of *I* (applies to insets of *A–L*) and *T* (applies to *O–T*); anterior commissure, ac.

these cells are known to be the major source of PGE_2 in the brain (36). Our study, however, is the first to document that systemic circulating IL-6 can act on these cells to induce COX-2, confirming findings of an earlier study in which this cytokine was injected directly into the brain (6). Other than endothelial cells, we also observed COX-2-IR in perivascular macrophage-like cells, which, along with endothelial cells (27), have previously been reported to express the inducible form of COX after inflammatory stimuli (55). The proportional contribution of each cell type to PGE_2 production in the brain

Downloaded from ajpregu.physiology.org on April 15, 2010

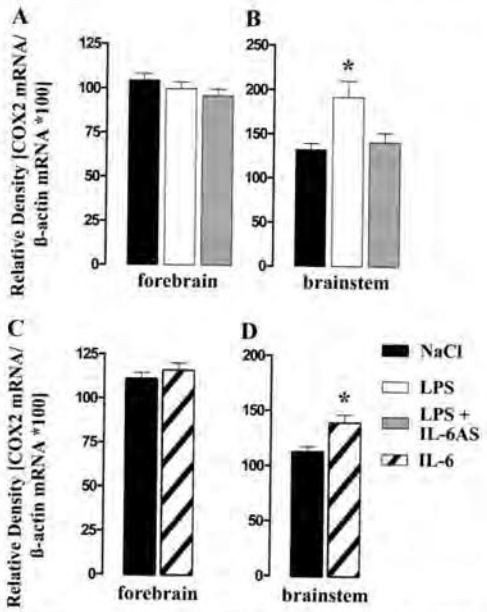


Fig. 6. Injection of LPS (100 μg/kg sc) induces a significant increase of COX-2 mRNA expression in the brain stem (*B*) but not in the forebrain (*A*) of rats 2 h after the injection. This induction was significantly attenuated by administration of IL-6AS (B; 1.8 ml/kg ip). rrIL-6 treatment (45 μg/kg ip) induces a significant upregulation of COX-2 mRNA expression in the brain stem (*D*) but not in the forebrain (*C*) of rats 2 h after the injection (*$P < 0.05$). Values are presented as means ± SE.

remains undetermined; however, our current observations based on COX-2-IR show that endothelial cells are by far the major source, at least at the time point (2 h) investigated in our study.

Furthermore, our results show that circulating IL-6-mediated COX-2-induction in endothelial cells occurred throughout the entire brain. However, PGE receptors, especially the EP3 receptor (EP3R) subtype are mainly expressed in specific brain structures, such as the MnPO (18), in which PG binding was reported to be highest (37), an observation that corresponds with the importance of this region in fever (31, 43). In addition, using Fos immunohistochemistry, Oka et al. (43) showed that activated neurons during LPS-induced fever within this brain structure colocalized with prostaglandin E receptors. This and other studies (53, 54, 60) demonstrated that despite PG production throughout the brain, the action of PGE in fever is limited to specific thermoregulatory hypothalamic nuclei. In the present study, by demonstrating that IL-6 induces COX-2 production in the MnPO, we provide strong evidence that this cytokine is involved in triggering the COX pathway in the hypothalamic regions mostly associated with regulating the febrile response. This is further supported by observations made in another study, in which the number of LPS-activated (Fos-IR positive) cells in the preoptic area was significantly reduced in IL-6 knockout mice (58).

Our investigation of the link between the IL-6-triggered signaling pathway, namely JAK-STAT and COX-2 induction, revealed a close association between the two. This was indicated by the significant correlation between circulating rrIL-6-induced SOCS3 mRNA and COX-2 mRNA levels (Fig. 7*B*). In addition, we show clear colocalization of COX-2-IR with PSTAT-IR, thus supporting a functional link between STAT3 and COX-2 induction. Our observations point to a somewhat unexpected, but possible role of the JAK-STAT pathway in COX-2 gene regulation. The difficulty with this rationale is that, to our knowledge, there is no consensus region reported for STAT3 in the COX-2 promoter region pointing to the possibility that IL-6-activated transcription factors other than STAT3 could play a role. A plausible candidate for this could be NF-IL-6, which along with STAT3, has been reported to mediate IL-6 signaling, also by phosphorylation followed by nuclear translocation (41). The role of this transcription factor in COX-2 expression was previously reported with several studies demonstrating its activation following different inflammatory stimuli (61). However, the majority of these studies were conducted in vitro to assess cell-specific molecular mechanisms in COX-2 induction, for example, in LPS-stimulated macrophages or in fibroblasts (20, 62), but to our knowledge not in brain endothelial cells and not in vivo. In the present study, using immunohistochemistry we failed to detect LPS- or

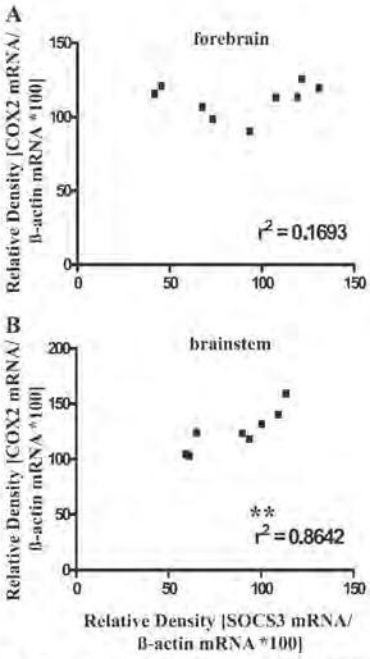


Fig. 7. rrIL-6 treatment (45 μg/kg, ip) induces a rise of COX-2 mRNA expression, which correlates significantly to SOCS3 mRNA expression in the brain stem (*B*) but not in the forebrain (*A*) from all individual pairs of values ($n = 9$, black squares) of rats 2 h after the injection. (**$P < 0.01$; r^2, coefficient of correlation).

Downloaded from ajpregu.physiology.org on April 15, 2010

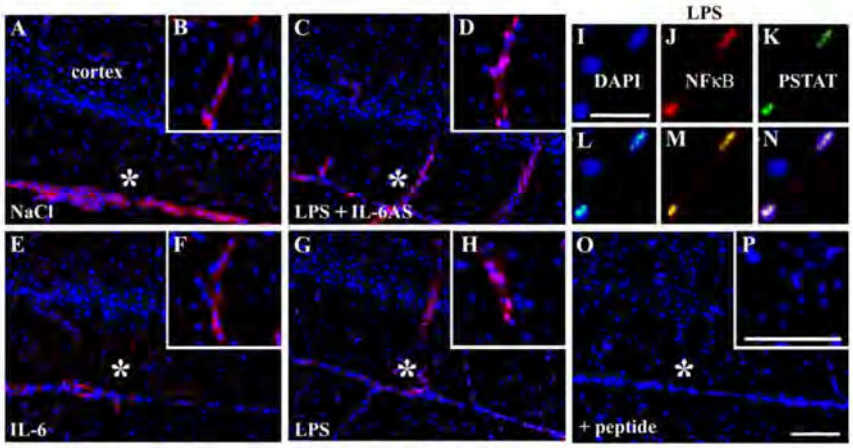


Fig. 8. LPS (*G* and *H*; 100 μg/kg sc) treatment led to nuclear translocation of NF-κB within blood vessel-like structures, which was not affected by IL-6AS (*C* and *D*; 1.8 ml/kg ip) 2 h after the injection. NF-κB accumulation (red) within cell nuclei (*I*; blue DAPI stain) can be clearly seen at high magnification (*D*, *H*, *I*, *J*, and *N*). rrIL-6 (*E* and *F*; 45 μg/kg ip) had no effect on nuclear NF-κB translocation 2 h after the injection, similar to what was observed in brains of control animals (*A* and *B*; NaCl, 1 ml/kg). In both cases, cytoplasmic (inactive)-IR can be clearly seen at high magnification (*B* and *F*). LPS induced NF-κB (*J*; red) and PSTAT-IR (*K*; green) are clearly seen to colocalize (*M*; yellow). PSTAT (green) accumulation within cell nuclei (*I*; blue, DAPI) is represented in *L* (turquoise). The photomicrograph color composition of these triple-labeling experiments (DAPI, PSTAT, and NF-κB) is demonstrated in *N* (bright spots). Specificity of the NF-κB antibodies was confirmed by preabsorption with a 10-fold excess of a rat NF-κB blocking peptide (*O–P*). White asterisks (*) depict cells of cortical blood vessels. Scale bars in *O* (applies to *A*, *C*, *E*, *G*, and *O*) and *P* (applies to *B*, *D*, *F*, *H*, and *P*) represent 50 μm; 25 μm in *I* (applies to *I–N*).

IL-6-induced NF-IL6 activity in any of the brain regions and cell types analyzed at the 2-h time point, indicating that its importance during the early febrile response is questionable (data not shown).

Our proposed hypothesis that JAK-STAT is involved in COX-2 induction, contradicts the established dogma that the activation of the transcription factor NF-κB is the main intracellular pathway for fever induction (29, 33). Although this is still valid, it most likely reflects the involvement of other pyrogenic mediators such as IL-1β, which induces COX-2 through an NF-κB-dependent mechanism (40). However, unlike IL-6, IL-1β is not detected in the circulation of febrile animals (8, 38), at least not in models of localized inflammation, such as the one used in our current study. The other possibility is TNF-α, which like IL-1β also signals via NF-κB but unlike IL-1β is readily detectable in the circulation of LPS-treated animals. A role for this cytokine in fever is, however, still a subject of some debate with evidence for and against its role as a pyrogen (12). Nevertheless, although NF-κB was clearly induced in our studies, its activation was not affected in the presence of IL-6AS in clear contrast to STAT3, suggesting that the COX-2 induction observed in our experiments is independent of the NF-κB-pathway. Interestingly, however, we did detect PSTAT-IR with activated NF-κB-IR in blood vessel-like structures an observation that offers basis for some speculation. A recently described functional network between transcription factors ("crosstalk") suggests that STAT3, NF-κB, and NF-IL-6 physically interact with one another. They mediate synergistic effects for instance by stabilizing their respective binding to genomic DNA or even transactivate promotors in proximity (1, 65). In line with these findings, COX-2 induction in myocardial preconditioning was identified to be both STAT3- and NF-κB-dependent (4). Interestingly, these authors also suggested that COX-2 can be upregulated via an IL-6 activated, JAK-STAT-dependent pathway in the myocardium (13, 63), a similar conclusion to ours in the brain.

In summary, we provided new and strong evidence demonstrating that IL-6 is directly involved in the activation of at least some components of the COX pathway in fever. Our findings do not, however, preclude the synergistic actions of this cytokine with other mediators working through different signaling pathways; indeed, our observations add insight into mechanisms of complex cytokine networks that may be operating at the level of transcription factors.

GRANTS

This work was supported by the Canadian Institutes of Health Research and Natural Sciences and Engineering Research Council of Canada.

REFERENCES

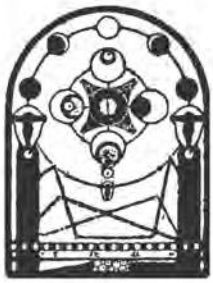
1. **Agrawal A, Cha-Molstad H, Samols D, and Kushner I.** Overexpressed nuclear factor-kappaB can participate in endogenous C-reactive protein induction, and enhances the effects of C/EBPbeta and signal transducer and activator of transcription-3. *Immunology* 108: 539–547, 2003.
2. **Akira S.** IL-6-regulated transcription factors. *Int J Biochem Cell Biol* 29: 1401–1418, 1997.
3. **Blatteis CM, Quan N, Xin L, and Ungar AL.** Neuromodulation of acute-phase responses to interleukin-6 in guinea pigs. *Brain Res Bull* 25: 895–901, 1990.
4. **Bolli R, Dawn B, and Xuan YT.** Role of the JAK-STAT pathway in protection against myocardial ischemia/reperfusion injury. *Trends Cardiovasc Med* 13: 72–79, 2003.
5. **Breder CD, Dewitt D, and Kraig RP.** Characterization of inducible cyclooxygenase in rat brain. *J Comp Neurol* 355: 296–315, 1995.

Downloaded from ajpregu.physiology.org on April 15, 2010

6. **Cao C, Matsumura K, Shirakawa N, Maeda M, Jikihara I, Kobayashi S, and Watanabe Y.** Pyrogenic cytokines injected into the rat cerebral ventricle induce cyclooxygenase-2 in brain endothelial cells and also upregulate their receptors. *Eur J Neurosci* 13: 1781–1790, 2001.
7. **Cao C, Matsumura K, Yamagata K, and Watanabe Y.** Cyclooxygenase-2 is induced in brain blood vessels during fever evoked by peripheral or central administration of tumor necrosis factor. *Brain Res Mol Brain Res* 56: 45–56, 1998.
8. **Cartmell T, Luheshi GN, Hopkins SJ, Rothwell NJ, and Poole S.** Role of endogenous interleukin-1 receptor antagonist in regulating fever induced by localised inflammation in the rat. *J Physiol* 531: 171–180, 2001.
9. **Cartmell T, Luheshi GN, and Rothwell NJ.** Brain sites of action of endogenous interleukin-1 in the febrile response to localized inflammation in the rat. *J Physiol* 518: 585–594, 1999.
10. **Cartmell T, Poole S, Turnbull AV, Rothwell NJ, and Luheshi GN.** Circulating interleukin-6 mediates the febrile response to localised inflammation in rats. *J Physiol* 526: 653–661, 2000.
11. **Chai Z, Gatti S, Toniatti C, Poli V, and Bartfai T.** Interleukin (IL)-6 gene expression in the central nervous system is necessary for fever response to lipopolysaccharide or IL-1 beta: a study on IL-6-deficient mice. *J Exp Med* 183: 311–316, 1996.
12. **Conti B, Tabarean I, Andrei C, and Bartfai T.** Cytokines and fever. *Front Biosci* 9: 1433–1449, 2004.
13. **Dawn B, Xuan YT, Guo Y, Rezazadeh A, Stein AB, Hunt G, Wu WJ, Tan W, and Bolli R.** IL-6 plays an obligatory role in late preconditioning via JAK-STAT signaling and upregulation of iNOS and COX-2. *Cardiovasc Res* 64: 61–71, 2004.
14. **Desson SE and Ferguson AV.** Interleukin 1beta modulates rat subfornical organ neurons as a result of activation of a non-selective cationic conductance. *J Physiol* 550: 113–122, 2003.
15. **Dinarello CA.** Cytokines as endogenous pyrogens. *J Infect Dis* 179, *Suppl* 2: S294–S304, 1999.
16. **Dinarello CA, Cannon JG, Mancilla J, Bishai I, Lees J, and Coceani F.** Interleukin-6 as an endogenous pyrogen: induction of prostaglandin E2 in brain but not in peripheral blood mononuclear cells. *Brain Res* 562: 199–206, 1991.
17. **Edwards JC, Sedgwick AD, and Willoughby DA.** The formation of a structure with the features of synovial lining by subcutaneous injection of air: an in vivo tissue culture system. *J Pathol* 134: 147–156, 1981.
18. **Ek M, Arias C, Sawchenko P, and Ericsson-Dahlstrand A.** Distribution of the EP3 prostaglandin E(2) receptor subtype in the rat brain: relationship to sites of interleukin-1-induced cellular responsiveness. *J Comp Neurol* 428: 5–20, 2000.
19. **Gautron L, Lafon P, Chaigniau M, Tranu G, and Layé S.** Spatiotemporal analysis of signal transducer and activator of transcription 3 activation in rat brain astrocytes and pituitary following peripheral immune challenge. *Neuroscience* 112: 717–729, 2002.
20. **Gorgoni B, Caivano M, Arizmendi C, and Poli V.** The transcription factor C/EBPbeta is essential for inducible expression of the cox-2 gene in macrophages but not in fibroblasts. *J Biol Chem* 276: 40769–40777, 2001.
21. **Harré EM, Roth J, Gerstberger R, and Hübschle T.** Interleukin-6 mediates lipopolysaccharide-induced nuclear STAT3 translocation in astrocytes of rat sensory circumventricular organs. *Brain Res* 980: 151–155, 2003.
22. **Harré EM, Roth J, Pehl U, Kueth M, Gerstberger R, and Hübschle T.** Selected contribution: role of IL-6 in LPS-induced nuclear STAT3 translocation in sensory circumventricular organs during fever in rats. *J Appl Physiol* 92: 2657–2666, 2002.
23. **Helle M, Brakenhoff JP, De Groot ER, and Aarden LA.** Interleukin 6 is involved in interleukin 1-induced activities. *Eur J Immunol* 18: 957–959, 1988.
24. **Hosoi T, Okuma Y, Kawagishi T, Qi X, Matsuda T, and Nomura Y.** Bacterial endotoxin induces STAT3 activation in the mouse brain. *Brain Res* 1023: 48–53, 2004.
25. **Hübschle T, Harré EM, Meyerhof W, Pehl U, Roth J, and Gerstberger R.** The central pyrogenic action of interleukin-6 is related to nuclear translocation of STAT3 in the anteroventral preoptic area of the rat brain. *J Therm Biol* 26: 299–305, 2001.
26. **Kluger MJ.** Fever: role of pyrogens and cryogens. *Physiol Rev* 71: 93–127, 1991.
27. **Konsman JP, Vigues S, Mackerlova L, Bristow A, and Blomqvist A.** Rat brain vascular distribution of interleukin-1 type-1 receptor immunoreactivity: relationship to patterns of inducible cyclooxygenase expression by peripheral inflammatory stimuli. *J Comp Neurol* 472: 113–129, 2004.
28. **Kozak W, Kluger MJ, Soszynski D, Conn CA, Rudolph K, Leon LR, and Zheng H.** IL-6 and IL-1 beta in fever. Studies using cytokine-deficient (knockout) mice. *Ann NY Acad Sci* 856: 33–47, 1998.
29. **Kozak W, Wrotek S, and Kozak A.** Pyrogenicity of CpG-DNA in mice: role of interleukin-6, cyclooxygenases, and nuclear factor-kappaB. *Am J Physiol Regul Integr Comp Physiol* 290: R871–R880, 2006.
30. **Lacroix S and Rivest S.** Effect of acute systemic inflammatory response and cytokines on the transcription of the genes encoding cyclooxygenase enzymes (COX-1 and COX-2) in the rat brain. *J Neurochem* 70: 452–466, 1998.
31. **Lazarus M.** The differential role of prostaglandin E2 receptors EP3 and EP4 in regulation of fever. *Mol Nutr Food Res* 50: 451–455, 2006.
32. **Lebel É, Vallères L and Rivest S.** Selective involvement of interleukin-6 in the transcriptional activation of the suppressor of cytokine signaling-3 in the brain during systemic immune challenges. *Endocrinology* 141: 3749–3763, 2000.
33. **Lee JJ, Huang WT, Shao DZ, Liao JF, and Lin MT.** Blocking NF-kappaB activation may be an effective strategy in the fever therapy. *Jpn J Physiol* 53: 367–375, 2003.
34. **LeMay LG, Vander AJ, and Kluger MJ.** Role of interleukin 6 in fever in rats. *Am J Physiol Regul Integr Comp Physiol* 258: R798–R803, 1990.
35. **Li S, Wang Y, Matsumura K, Ballou LR, Morham SG, and Blatteis CM.** The febrile response to lipopolysaccharide is blocked in cyclooxygenase-2(−/−), but not in cyclooxygenase-1 (−/−) mice. *Brain Res* 825: 86–94, 1999.
36. **Matsumura K and Kobayashi S.** Signaling the brain in inflammation: the role of endothelial cells. *Front Biosci* 9: 2819–2826, 2004.
37. **Matsumura K, Watanabe Y, Onoe H, and Hayaishi O.** High density of prostaglandin E2 binding sites in the anterior wall of the 3rd ventricle: a possible site of its hyperthermic action. *Brain Res* 533: 147–151, 1990.
38. **Miller AJ, Luheshi GN, Rothwell NJ, and Hopkins SJ.** Local cytokine induction by LPS in the rat air pouch and its relationship to the febrile response. *Am J Physiol Regul Integr Comp Physiol* 272: R857–R861, 1997.
39. **Nadjar A, Combe C, Layé S, Tridon V, Dantzer R, Amedee T, and Parnet P.** Nuclear factor κB nuclear translocation as a crucial marker of brain response to interleukin-1. A study in rat and interleukin-1 type I deficient mouse. *J Neurochem* 87: 1024–1036, 2003.
40. **Nadjar A, Tridon V, May MJ, Ghosh S, Dantzer R, Amedee T, and Parnet P.** NFkappaB activates in vivo the synthesis of inducible Cox-2 in the brain. *J Cereb Blood Flow Metab* 25: 1047–1059, 2005.
41. **Nakajima T, Kinoshita S, Sasagawa T, Sasaki K, Naruto M, Kishimoto T, and Akira S.** Phosphorylation at threonine-235 by a ras-dependent mitogen-activated protein kinase cascade is essential for transcription factor NF-IL6. *Proc Natl Acad Sci USA* 90: 2207–2211, 1993.
42. **Nijsten MW, de Groot ER, ten Duis HJ, Klasen HJ, Hack CE, and Aarden LA.** Serum levels of interleukin-6 and acute phase responses. *Lancet* 2: 921, 1987.
43. **Oka T, Oka K, Scammell TE, Lee C, Kelly JF, Nantel F, Elmquist JK, and Saper CB.** Relationship of EP(1–4) prostaglandin receptors with rat hypothalamic cell groups involved in lipopolysaccharide fever responses. *J Comp Neurol* 428: 20–32, 2000.
44. **Paxinos G and Watson C.** *The Rat Brain in Stereotaxic Coordinates* (4th ed.). San Diego, CA: Academic, 1998.
45. **Rees GS, Ball C, Ward HL, Gee CK, Tarrant G, Mistry Y, Poole S, and Bristow AF.** Rat interleukin 6: expression in recombinant *Escherichia coli*, purification and development of a novel ELISA. *Cytokine* 11: 95–103, 1999.
46. **Romanovsky A, Almeida MC, Aronoff DM, Ivanov AI, Konsman JP, Steiner AA, and Turek VF.** Fever and hypothermia in systemic inflammation: recent discoveries and revisions. *Front Biosci* 10: 2193–2216, 2005.
47. **Roth J, Conn CA, Kluger MJ, and Zeisberger E.** Kinetics of systemic and intrahypothalamic IL-6 and tumor necrosis factor during endotoxin fever in guinea pigs. *Am J Physiol Regul Integr Comp Physiol* 265: R653–R658, 1993.
48. **Roth J, Harré EM, Rummel C, Gerstberger R, and Hübschle T.** Signaling the brain in systemic inflammation: role of sensory circumventricular organs. *Front Biosci* 9: 290–300, 2004.
49. **Roth J, McClellan JL, Kluger MJ, and Zeisberger E.** Attenuation of fever and release of cytokines after repeated injections of lipopolysaccharide in guinea-pigs. *J Physiol* 477: 177–185, 1994.

Downloaded from ajpregu.physiology.org on April 15, 2010

50. **Rummel C, Hübschle T, Gerstberger R, and Roth J.** Nuclear translocation of the transcription factor STAT3 in the guinea pig brain during systemic or localised inflammation. *J Physiol* 557: 671–687, 2004.
51. **Rummel C, Voss T, Matsumura K, Korte S, Gerstberger R, Roth J, and Hübschle T.** Nuclear STAT3 translocation in guinea pig and rat brain endothelium during systemic challenge with lipopolysaccharide and interleukin-6. *J Comp Neurol* 491: 1–14, 2005.
52. **Sakata Y, Morimoto A, Long NC, and Murakami N.** Fever and acute-phase response induced in rabbits by intravenous and intracerebroventricular injection of interleukin-6. *Cytokine* 3: 199–203, 1991.
53. **Scammel TE, Griffin JD, Elmquist JK, and Saper CB.** Microinjection of a cyclooxygenase inhibitor into the anteroventral preoptic region attenuates LPS fever. *Am J Physiol Regul Integr Comp Physiol* 274: R783–R789, 1998.
54. **Scammell TE, Elmquist JK, Griffin JD, and Saper CB.** Ventromedial preoptic prostaglandin E2 activates fever-producing autonomic pathways. *J Neurosci* 16: 6246–6254, 1996.
55. **Schiltz JC and Sawchenko PE.** Distinct brain vascular cell types manifest inducible cyclooxygenase expression as a function of the strength and nature of immune insults. *J Neurosci* 22: 5606–5618, 2002.
56. **Tamura M, Sebastian S, Yang S, Gurates B, Fang Z, and Bulun SE.** Interleukin-1beta elevates cyclooxygenase-2 protein level and enzyme activity via increasing its mRNA stability in human endometrial stromal cells: an effect mediated by extracellularly regulated kinases 1 and 2. *J Clin Endocrinol Metab* 87: 3263–3273, 2002.
57. **Turnbull AV, Prehar S, Kennedy AR, Little RA, and Hopkins SJ.** Interleukin-6 is an afferent signal to the hypothalamo-pituitary-adrenal axis during local inflammation in mice. *Endocrinology* 144: 1894–1906, 2003.
58. **Vallières L and Rivest S.** Interleukin-6 is a needed proinflammatory cytokine in the prolonged neural activity and transcriptional activation of corticotropin-releasing factor during endotoxemia. *Endocrinology* 140: 3890–3903, 1999.
59. **Wang J, Ando T, and Dunn AJ.** Effect of homologous interleukin-1, interleukin-6 and tumor necrosis factor-alpha on the core body temperature of mice. *Neuroimmunomodulation* 4: 230–236, 1997.
60. **Williams JW, Rudy TA, Yaksh TL, and Viswanathan CT.** An extensive exploration of the rat brain for sites mediating prostaglandin-induced hyperthermia. *Brain Res* 120: 251–262, 1977.
61. **Wu KK.** Control of cyclooxygenase-2 transcriptional activation by pro-inflammatory mediators. *Prostaglandins Leukot Essent Fatty Acids* 72: 89–93, 2005.
62. **Wu KK, Liou JY, and Cieslik K.** Transcriptional Control of COX-2 via C/EBPbeta. *Arterioscler Thromb Vasc Biol* 25: 679–685, 2005.
63. **Xuan YT, Guo Y, Zhu Y, Han H, Langenbach R, Dawn B, and Bolli R.** Mechanism of cyclooxygenase-2 upregulation in late preconditioning. *J Mol Cell Cardiol* 35: 525–537, 2003.
64. **Yamagata K, Matsumura K, Inoue W, Shiraki T, Suzuki K, Yasuda S, Sugiura H, Cao C, Watanabe Y, and Kobayashi S.** Coexpression of microsomal-type prostaglandin E synthase with cyclooxygenase-2 in brain endothelial cells of rats during endotoxin-induced fever. *J Neurosci* 21: 2669–2677, 2001.
65. **Yoshida Y, Kumar A, Koyama Y, Peng H, Arman A, Boch JA, and Auron PE.** Interleukin 1 activates STAT3/nuclear factor-kappaB cross-talk via a unique TRAF6- and p65-dependent mechanism. *J Biol Chem* 279: 1768–1776, 2004.
66. **Zhang YH, Lu J, Elmquist JK, and Saper CB.** Specific roles of cyclooxygenase-1 and cyclooxygenase-2 in lipopolysaccharide-induced fever and Fos expression in rat brain. *J Comp Neurol* 463: 3–12, 2003.



Downloaded from ajpregu.physiology.org on April 15, 2010

1.13. „Fever and circulating cytokines induced by double-stranded RNA in guinea pigs: dependence on the route of administration and effects of repeated injections“

Voss T., **Rummel C**., Gerstberger R., Hübschle T., Roth J.

Acta Physiol (Oxf) (2006) 187: 379-389.

Impakt Faktor: 3,138

Eigener Anteil an der Publikation:

- Durchführung der Versuche: wesentlich (40 %)
- Auswertung der Experimente: unterstützend (30 %)
- Erstellung der Publikation: unterstützend (20 %)

Acta Physiol 2006, **187**, 379–389

Fever and circulating cytokines induced by double-stranded RNA in guinea pigs: dependence on the route of administration and effects of repeated injections

T. Voss, C. Rummel, R. Gerstberger, T. Hübschle and J. Roth
Institut für Veterinär-Physiologie, Justus-Liebig-Universität Giessen, Giessen, Germany

Received 30 January 2006, revision requested 19 February 2006, revision received 16 March 2006, accepted 23 March 2006
Correspondence: J. Roth, Institut für Veterinär-Physiologie, Justus-Liebig-Universität Giessen, Frankfurter Strasse 100, D-35392 Giessen, Germany.
E-mail: joachim.roth@vetmed.uni-giessen.de

Abstract

Aims: The aim of this study was to characterize the properties of synthetic double-stranded RNA to induce fever and circulating cytokines in guinea pigs with special emphasis on the route of administration and on a putative development of tolerance to this pyrogen.

Methods: Changes in abdominal temperature were recorded in unrestrained animals by use of intra-abdominally implanted radiotransmitters. Circulating concentrations of tumour necrosis factor-α (TNF-α) and interleukin-6 (IL-6) were measured by use of specific bioassays.

Results: The pyrogenic effect of double-stranded RNA at a dose of 500 μg kg^{-1} depended on the route of its administration. Intra-arterial (i.a.) or intraperitoneal injections of double-stranded RNA induced pronounced fevers and strong elevations of circulating TNF-α and IL-6. Intramuscular injections of the synthetic pyrogen caused rather moderate febrile and cytokine responses. Administration of synthetic RNA into artificial subcutaneously implanted Teflon chambers had no pyrogenic and cytokine-inducing effects. I.a. injections of double-stranded RNA, repeated five times at intervals of 3 days, resulted in fevers of similar shape and duration and similar cytokine response patterns. However, the strength of fever and cytokine formation was significantly reduced, although not abolished, in response to the repeated injections compared with the first injection, indicating a partial development of tolerance.

Conclusions: The modulation of the strength of RNA-induced fever, dependent on the route of administration, or the state of partial tolerance to this pyrogen, may thus be related to the formation of pyrogenic cytokines.

Keywords fever, interleukin-6, pyrogenic tolerance, radiotelemetry, systemic inflammation, Toll-like receptors, tumour necrosis factor.

Polyinosinic : polycytidylic acid (PIPC) is a synthetic analogue of double-stranded RNA, which is produced as a replication side-product by many viruses (Jacobs & Langland 1996). Traditionally, PIPC is regarded as a stimulator of interferon production (Field *et al.* 1967), and this substance has been used as a model of viral infection (Katafuchi *et al.* 2003, Fortier *et al.* 2004, Traynor *et al.* 2004). The properties of PIPC as an exogenous pyrogen were repeatedly demonstrated in rabbits (Rotondo *et al.* 1987, Soszynski *et al.* 1991, Kimura *et al.* 1994), rats (Chuang *et al.* 1990, Fortier *et al.* 2004), mice (Traynor *et al.* 2004) and guinea pigs (Cooper *et al.* 1988, Li *et al.* 2000).

Within the last years strong research efforts have been directed to the identification and characterization of the recognition system of the innate immune system for various pathogen-associated molecular patterns. Toll-like receptors (TLRs) represent an initial and important component of this recognition system (Aderem & Ulevitch 2000), and TLR-3 is the mammalian receptor

© 2006 Scandinavian Physiological Society, doi: 10.1111/j.1748-1716.2006.01587.x

activated by double-stranded RNA and thus also by PIPC (Alexopoulou *et al.* 2001). Stimulation of macrophages with PIPC *in vitro* causes increased release of interleukin-6 (IL-6) and tumour necrosis factor-α (TNF-α) into the supernatant (Alexopoulou *et al.* 2001). Both of these cytokines are constantly elevated in the blood during the febrile response induced by bacterial lipopolysaccharide (LPS) and have therefore been implicated in the regulation of fever (Kluger 1991, Luheshi & Rothwell 1996, Roth & DeSouza 2001). Interestingly, it has been reported recently that treatment of rats with PIPC, like LPS, also causes a rise of TNF-α and IL-6 in plasma, 2 h after its injection almost parallel to the onset of fever (Fortier *et al.* 2004). The authors of this study suggested that the mechanisms for the manifestation of LPS- and PIPC-induced fevers might be rather similar (Fortier *et al.* 2004).

A number of open questions remain concerning the febrile response to PIPC when compared to LPS-fever. We (Rummel *et al.* 2004, 2005) and others (Cartmell *et al.* 2002) reported that the route of administration of LPS and other pyrogens differentially affects fever. We therefore tested different routes of administration of PIPC to induce systemic or localized inflammatory responses in guinea pigs to compare the resulting pyrogenic effects in relation to circulating TNF-α and IL-6. Another question of interest relates to the development of tolerance to repeated administrations of exogenous pyrogens. Fever and other components of the acute-phase response are progressively attenuated when LPS is administered repeatedly in short-term intervals. This phenomenon is called LPS-tolerance or endotoxin-tolerance and strongly correlates with a down-regulation of the LPS-induced formation of cytokines (Roth *et al.* 1994, 1997a, Zeisberger & Roth 1998). Whether a similar mechanism operates for repeated injections of PIPC is not clear (Cooper *et al.* 1988, Soszynski *et al.* 1991). We therefore tested the effects of several administrations of PIPC and compared fever and systemic production of TNF-α and IL-6 in response to each of these injections.

Materials and methods

Animals

This study was performed in male guinea pigs (*Cavia aperea porcellus*) with a body weight of 385–410 g at the beginning of the experiments (day of surgery). The animals were housed in individual cages at 22 °C and a 12 : 12 h light dark cycle (light off at 7:00 p.m.). The animals had access to food and water *ad libitum*. Twice a week the reservoirs were filled with fresh pelleted food and water and at the same time the cages were changed. About 10 days before the experiment, the animals were prepared surgically (see below) and habituated at least twice to the experimental handling procedures. The national guidelines for experiments with vertebrate animals were followed and local ethics committee approval was obtained from the regional government for the experimental protocols (reference number GI 18/2-42/00).

Surgery

Guinea pigs were chronically implanted with intra-arterial (i.a.) catheters for blood sampling and injections as well as intra-abdominal radiotransmitters for the measurement of body core temperature. Some animals were additionally implanted with artificial subcutaneous (s.c.) Teflon (polytetrafluoroethene) chambers equipped with catheters for injections. Briefly, the guinea pigs were anaesthetized with 0.25 mg kg^{-1} medetomidine hydrochloride (Pfitzer GmbH, Karlsruhe, Germany) injected intramuscularly (i.m.), followed by intraperitoneal (i.p.) injection of 100 mg kg^{-1} ketamine hydrochloride (Pharmacia Upjohn, Erlangen, Germany). A polyethylene catheter (0.4 mm inner diameter, 0.8 mm outer diameter; Portex, Kent, UK) was inserted through the left carotid artery until it reached the aortic arch. Slow aspiration of blood with a syringe indicated the correct position of the catheters. The catheter was then fixed with two sutures. The distal end of the catheter was tunnelled s.c. to the interscapular region of the back where it was exteriorized and again fixed with two sutures. The muscle layer and the skin were closed separately with sutures. Finally, the catheter was flushed with sterile heparinized saline and sealed by heating.

For one experiment Teflon chambers were implanted into s.c. cavities which were formed with a cylindrical Plexiglas stick after a cutaneous incision. The cavities which existed after removing the Plexiglas stick had about the same diameter and size as the artificial s.c. chamber which was open at both ends. The open sides of the cylindrical chambers with an inner diameter of 10 mm had close contact to the skin tissue. The s.c. chamber was placed laterally to the dorsal midline, caudally to the scapulae of the anaesthetized guinea pigs. The chambers were equipped with catheters for administration of drugs, which were also tunnelled s.c. to the interscapular region of the back, caudally to the arterial catheter and sealed by heating. Then the skin was closed with sutures. Details about size and shape of the s.c. chambers have been described and documented elsewhere (Ross *et al.* 2000, 2003).

Finally, a midline laparotomy was performed in each animal for implantation of a free floating temperature transmitter into the peritoneal cavity. Muscle layer and skin were sutured separately to close the abdominal incision.

 © 2006 Scandinavian Physiological Society, doi: 10.1111/j.1748-1716.2006.01587.x

Sampling of blood plasma

During the acute experiment single blood samples (0.4–0.5 mL) were slowly (within 1 min) drawn via the implanted catheter into heparinized sterile syringes (heparin-sodium-25 000; Merckle GmbH, Blaubeuren, Germany) by aspiration, put into chilled polypropylene tubes and immediately centrifuged. The catheter was flushed with saline and closed by heating. The blood plasma was stored at −70 °C for later determination of cytokines. Within the week before the experiment, the animals were accustomed to the blood sampling procedure once or twice, which then did not cause excitement during experiments.

Measurement of body temperature

Abdominal temperature was measured by use of the intra-abdominally implanted biotelemetry transmitters (PDT-4000 E-mitter; Mini-Mitter Co., Sunriver, OR, USA). Output (frequency in Hz) was monitored by an antenna placed under each cage (ER-4000 radioreceivers; Mini-Mitter). A data acquisition system (Vital View; Mini Mitter) was used for automatic control of data collection and analysis. Body temperature was monitored and recorded at 5-min intervals. For the analysis and graphical documentation, temperature data at time intervals of 15 min were used.

Bioassays for TNF-α and IL-6

Determination of TNF-α was performed by a bioassay based on the cytotoxic effect of TNF-α on the mouse fibrosarcoma cell line WEHI 164 subclone 13 (Espevic & Nissen-Meyer 1986). The assay was performed in sterile, 96-well microtitre plates. Serial dilutions of biological samples or different concentrations of a murine TNF-α-standard (code 88/532, National Institute for Biological Standards and Control, South Mimms, UK) were incubated for 24 h in wells that had been seeded with 50 000 actinomycin D-treated WEHI cells. The number of surviving cells after 24 h was measured by use of the dimethylthiazol-diphenyl tetrazolium bromide (MTT) colorimetric assay (Holt *et al.* 1991). Plasma samples were pre-diluted so that serial dilution of samples and standard dilution curves were parallel. The detection limit of the assay, after considering the dilution of samples into the assays, was 6 pg mL^{-1} TNF-α.

Determination of IL-6 was performed by a bioassay based on the dose-dependent growth stimulation of IL-6 on the B9 hybridoma cell line (Aarden *et al.* 1987). The assay was performed in sterile, 96-well microtitre plates. In each well, 5000 B9 cells were incubated for 72 h with serial dilutions of biological samples or with different concentrations of a human IL-6 standard (code 89/548, National Institute for Biological Standards and Control, South Mimms, UK). The number of cells in each well was measured by use of the MTT assay (see above). The detection limit of the assay, after considering the dilution of samples into the assays, was 3 international units (IU) IL-6 mL^{-1}.

Experimental protocols

Experiment 1. This experiment was performed to test the capacity of PIPC to induce fever and circulating TNF-α and IL-6 when administered via different routes of administration. PIPC (Sigma-Aldrich, Taufkirchen, Germany) was dissolved in sterile pyrogen-free saline at concentrations of 500, or 1000 μg mL^{-1}. According to the manufacturers' information this synthetic compound does not contain measurable amounts of endotoxin. For this experiment eleven groups of guinea pigs were used. In three groups of animals ($n = 3$ in each group) PIPC at doses of 500, or 1000 μg kg^{-1}, corresponding to an injection volume of 1 mL kg^{-1}, or an equivalent volume of sterile saline were s.c. injected into the implanted Teflon chambers. Another three groups of guinea pigs received i.m. injections of 500 μg kg^{-1} ($n = 6$), or 1000 μg kg^{-1} ($n = 3$) PIPC, or vehicle ($n = 6$) into the thigh muscle. The next three groups were injected i.p. with 500 μg kg^{-1} ($n = 4$), or 1000 μg kg^{-1} ($n = 6$) PIPC, or with sterile saline ($n = 6$). Finally, two groups of animals received i.a. injections of 500 μg kg^{-1} PIPC ($n = 9$), or solvent ($n = 8$). The higher dose of PIPC (1000 μg kg^{-1}) was tested for the i.a. route of administration in just two guinea pigs. The higher dose of PIPC did not induce a further increase of fever irrespective of the route of its administration meaning that the smaller dose used (500 μg kg^{-1}) is already maximal when it comes to fever production. Therefore, only the responses to the lower dose of 500 μg kg^{-1} PIPC were illustrated.

From all animal groups blood samples were collected at selected intervals from the time of injection and assayed for bioactive TNF-α and IL-6. All injections were performed between 10:45 and 11 a.m.

Experiment 2. This experiment was performed to investigate whether tolerance to repeated i.a. injections of 500 μg kg^{-1} PIPC develops in guinea pigs with regard to the fever and response and the endogenous PIPC-induced formation of circulating cytokines. This experiment was performed in eight animals. The injections of PIPC were repeated five times, at 3-day intervals, always between 10 and 11 a.m. Blood samples for determination of TNF-α and IL-6 were taken 60, 120, or 240 min after each of the five consecutive injections of PIPC. In some animals blood was collected

© 2006 Scandinavian Physiological Society, doi: 10.1111/j.1748-1716.2006.01587.x

also 60 min before the respective injection. A comparable schedule had been used in some of our previous studies for the investigation of the development of tolerance to other exogenous pyrogens (Roth *et al.* 1994, 1997b).

Evaluation and statistics

In graphs of the thermal responses to injections of PIPC or sterile saline, the mean abdominal temperatures were plotted against time and expressed as mean ± SEM at each time point. Abdominal temperatures of different groups of guinea pigs were compared by two-way repeated measures ANOVA followed by Scheffé's *post hoc* test. The fever index as the integrated area under the fever curve was further used to compare the strength of the febrile responses to repeated injections of PIPC during the light-time period of the day of injection and calculated for 8 h. The mean of all temperatures measured at 15 min intervals over the 2 h before injection of PIPC was used as the baseline temperature for the calculation of each individual fever index. Fever indices were compared by one-way ANOVA followed by Scheffé's *post hoc* test. Circulating levels of TNF-α or IL-6 were also compared by one-way ANOVA and Scheffé-test. Because the values for cytokine concentrations are not normally distributed, a log-transformation of the cytokine values was performed prior to the statistical calculation. All calculations were carried out on an Apple Macintosh computer using the software package STATVIEW (Abacus Concepts, Berkeley, CA, USA).

Results

Experiment 1: Manifestation of PIPC-induced fever depends on the route of its administration

Injections of PIPC into s.c. chambers Teflon chambers did not evoke fever when compared with the respective control animals treated with sterile saline (Fig. 1a, upper panel). Corresponding to the lack of thermal response there was no increase of TNF-α or IL-6 in plasma in response to s.c. injections of PIPC. TNF-α was not detected in any plasma sample, bioactive IL-6 in plasma did not exceed the baseline values of 25–60 IU mL^{-1}.

Intramuscular injections of PIPC at a dose of 500 $\mu g\ kg^{-1}$ caused a rather moderate fever in guinea pigs, which started with a delay of about 120 min from the time of PIPC administration. Mean body temperatures of PIPC treated animals were significantly elevated from 150 to 360 min after injection when compared with the respective control group injected i.m. with sterile saline ($P = 0.012$; two-way repeated measures ANOVA, Scheffé-test). Bioactive TNF-α could not be detected at any time after administration of 500 $\mu g\ kg^{-1}$ PIPC. The baseline level of IL-6 (40 ± 15 IU mL^{-1}) slightly increased to a mean value of 127 ± 34 IU mL^{-1}) at 2 h after injection of PIPC and further to 210 ± 118 IU mL^{-1} another 2 h later. This moderate increase was, however, not statistically significant when compared with corresponding values of control animals.

In the next experimental groups we tested the i.p. route of administration. I.p. injections of PIPC induced robust fevers with significantly elevated body core temperatures during the entire light time period of the day of injection ($P < 0.001$; 60–480 min from the injection time), when compared with the control group (upper panel of Fig. 1b). I.p. administration of PIPC induced fever within 45 min with a peak of about 40.5 °C at 3 h after the time of PIPC administration. The corresponding control group injected i.p. with sterile saline showed an increase of body temperature of about 0.4 °C during the night-time ('light-off' period). I.p. administration of 500 $\mu g\ kg^{-1}$ PIPC, as opposed to administration of solvent, caused the appearance of bioactive TNF-α in plasma at 120 min after the time of injection. At this time circulating concentrations of 233 ± 64 pg mL^{-1} ($n = 3$) were detected in plasma of guinea pigs. At the same time levels of bioactive IL-6 in plasma rose from baseline values of 20–40 IU mL^{-1} to mean concentrations of 1918 ± 524 IU mL^{-1}. The most pronounced fever in response to PIPC was induced via the i.a. route of administration. I.a. injections of 500 $\mu g\ kg^{-1}$ PIPC evoked fever with a peak of 40.8 °C at 3 h after injection and a duration of about 20 h. From 60 to 480 min after the time of injection ('light on' period) as well as during the entire following 'night-time' period (480–1200 min after injection) mean abdominal temperatures of PIPC-treated guinea pigs were significantly elevated in comparison with the controls ($P < 0.001$ for both periods). For the i.a. injection of 500 $\mu g\ kg^{-1}$ PIPC, which was determined to be used for the further experiment (see below), a more complete kinetics of circulating TNF-α and IL-6 in plasma was investigated during the early stages of the pronounced febrile response. The results of the cytokine measurements are summarized in Figure 2.

One hour prior to the i.a. injection of 500 $\mu g\ kg^{-1}$ PIPC or solvent (sterile saline) bioactive TNF-α in plasma was not detected. Within 60 min from the time of injection, treatment with PIPC induced the appearance of high levels of TNF-α (4593 ± 1401 pg mL^{-1}) in the systemic circulation of guinea pigs. This value rapidly declined to a mean level 325 ± 59 pg mL^{-1} within the following hour in those plasma samples, in which TNF-α was detected. In four of nine samples bioactive TNF-α was even below the detection limit at 120 min after injection of PIPC. Another 2 h later TNF-α was not detectable at all.

 © 2006 Scandinavian Physiological Society, doi: 10.1111/j.1748-1716.2006.01587.x

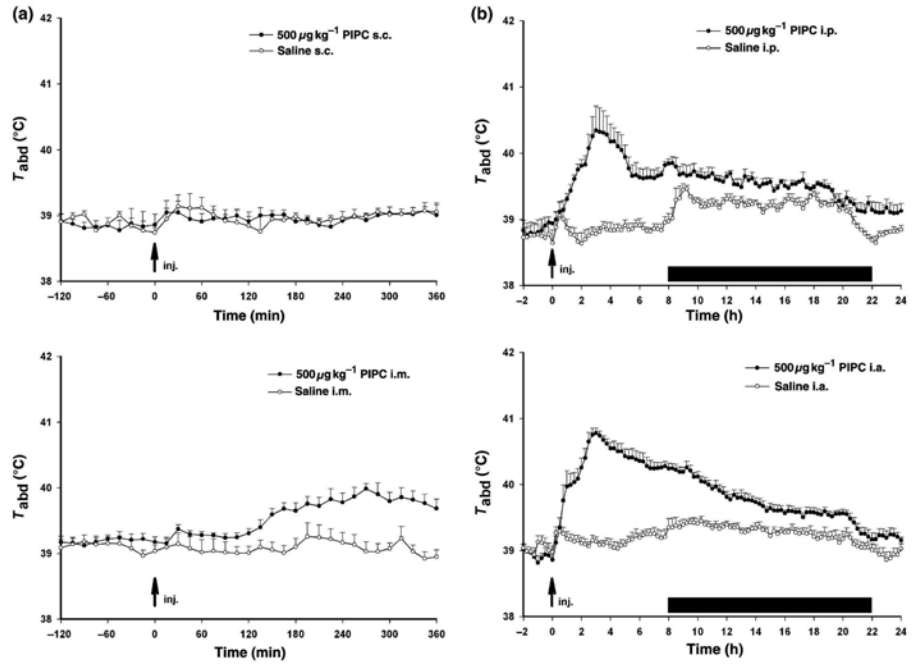


Figure 1 (a) Febrile responses of guinea pigs injected subcutaneously (s.c.) or intramuscularly (i.m.) with polyinosinic : polycytidylic acid (PIPC) or vehicle. Upper panel: Changes in abdominal temperatures (T_{abd}) of two groups of guinea pigs ($n = 3$ in each group) in response to injections of 500 μg kg^{-1} PIPC, or sterile saline into s.c. implanted Teflon chambers. Lower panel: Changes in abdominal temperatures of two groups of guinea pigs injected i.m. with 500 μg kg^{-1} PIPC ($n = 6$), or with sterile saline ($n = 6$). From 150–360 min from the time of injection treatment with PIPC caused a significant elevation of T_{abd} ($P < 0.05$). (b) Febrile responses of guinea pigs injected intraperitoneally (i.p.) or intra-arterially (i.a.) with PIPC or vehicle. Upper panel: Changes in abdominal temperatures (T_{abd}) of two groups of guinea pigs injected i.p. with 500 μg kg^{-1} PIPC ($n = 4$), or with sterile saline ($n = 6$). From 60 to 480 min from the time of injection treatment with PIPC caused a significant elevation of T_{abd} ($P < 0.001$). Lower panel: Changes in abdominal temperatures of two groups of guinea pigs injected i.a. with 500 μg kg^{-1} ($n = 9$), or with sterile saline ($n = 8$). From 60 to 480 min (day-time) and from 480 to 1200 min (night-time) after injection, PIPC caused a significant elevation of T_{abd} ($P < 0.001$ for both periods). The black horizontal bars indicate the night-time ('light-off' period).

One hour prior to the injections of PIPC or vehicle, mean levels of IL-6 in plasma were in the range of 10–60 IU mL^{-1} in both groups. In saline-treated animals similar baseline values were measured at all investigated time points after the injection. When compared with the corresponding values of the controls, i.a. injections of PIPC caused a significant elevation of IL-6 in plasma to 662 ± 258 IU mL^{-1} at 60 min, to 6283 ± 2318 IU mL^{-1} at 120 min and to 2957 ± 1321 IU mL^{-1} at 240 min after the treatment with PIPC. Figure 3 summarizes the peak values of TNF-α (upper panel) and IL-6 (lower panel) dependent on the distinct routes of administration of PIPC.

The TNF-α-peak in guinea pigs injected i.a. occurred 60 min after the time of injection of PIPC. At the corresponding time we failed to detect bioactive TNF-α in i.p.-treated animals, in which moderate amounts (significantly lower than in i.a. injected guinea pigs; $P < 0.05$) of circulating bioactive TNF-α were observed 1 h later. At 120 min from the time of injection we observed the highest levels of IL-6 in i.a. and i.p. injected guinea pigs. Again, circulating concentrations of bioactive IL-6 were significantly higher in i.a. when compared with i.p.-treated animals. At the corresponding time significantly lower levels of IL-6 in plasma were measured in guinea pigs injected i.m. or s.c. with PIPC. These values were not significantly higher than in corresponding controls.

As a result of the fact that i.a. injection of PIPC was most effective with regard to the induction of fever and

© 2006 Scandinavian Physiological Society, doi: 10.1111/j.1748-1716.2006.01587.x

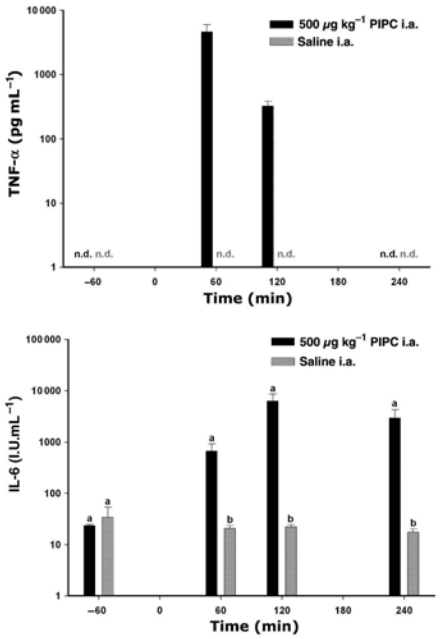


Figure 2 Circulating cytokines in guinea pigs injected intra-arterial (i.a.) with polyinosinic : polycytidylic acid (PIPC) or vehicle. Time course of concentrations of bioactive tumour necrosis factor α (upper panel), and interleukin-6 in plasma in response to i.a. administration of 500 μg kg^{-1} PIPC or sterile saline. For each time point, any columns with the same letter are not significantly different from each other, while any columns with different letters are significantly different ($P < 0.05$).

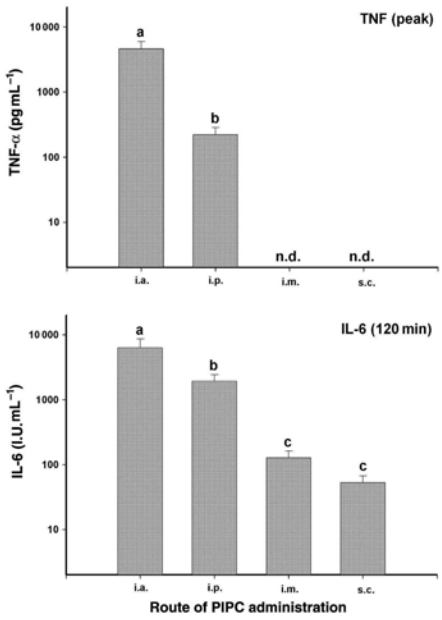


Figure 3 Comparison of tumour necrosis factor-α (TNF-α) (upper panel) and interleukin-6 (IL-6) peak values in dependence of the route of administration of polyinosinic : polycytidylic acid (PIPC). The TNF-α-peaks were observed 60 min after intra-arterial (i.a.) and 120 min after intraperitoneal (i.p.) injections of PIPC. IL-6 peaks of i.a.- and i.p.-treated guinea pigs were measured 120 min after administration of PIPC. Values from the corresponding time-point of intramuscular (i.m.)- and s.c.-injected animals are shown for comparison. I.m. and s.c. injections of PIPC did not cause significant elevations of circulating IL-6 when compared with values of the respective control animals. Any columns with the same letter are not significantly different from each other, while any columns with different letters are significantly different ($P < 0.05$).

of circulating cytokines, we used this route of administration to test the responses of guinea pigs to repeated stimulations with this pyrogen.

Experiment 2: Effects of repeated i.a. injections of PIPC on fever and circulating cytokines

The febrile responses of another group of guinea pigs injected i.a. with 500 μg kg^{-1} PIPC repeated five times at intervals of 3 days are summarized in Figure 4. In the upper and lower panel of Figure 4, the febrile responses to the second and third (upper panel), or to the fourth and fifth injections (lower panel) of PIPC were always compared with the fever induced by the first injection.

Shape and duration of fever curves were similar in response to each of the five consecutive injections of PIPC. Within the first 150 min of each of the five fevers induced by repeated injections of PIPC there were no significant differences between the febrile responses ($P > 0.05$ for all calculated comparisons; two-way repeated-measures ANOVA followed by Scheffé-test). However, starting with the second injection of PIPC, there was a significant attenuation of the febrile rises of body temperature from 180 min after injection until the end of the day-time period (480 min after injection) and during the entire following night-time period (510–1200 min after injection; $P < 0.05$, two-way repeated-measures ANOVA followed by Scheffé-test) in comparison to the response to the first injection. Fevers induced by the second, third, fourth and fifth injections of PIPC were not statistically different from each other.

The febrile responses of guinea pigs to repeated administrations of PIPC were further evaluated by calculation of the fever indices for 8 h from the time of pyrogen-treatment during the 'light-on' period of the

 © 2006 Scandinavian Physiological Society, doi: 10.1111/j.1748-1716.2006.01587.x

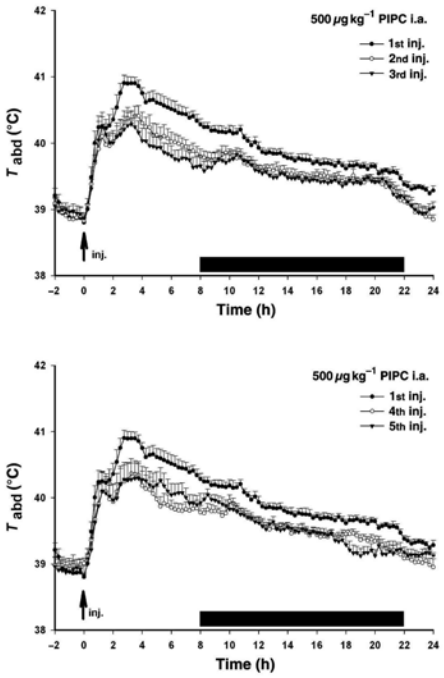


Figure 4 Fever response to repeated injections of polyinosinic : polycytidylic acid (PIPC). Upper panel: febrile responses of guinea pigs ($n = 8$) to the first compared with the second and third intra-arterial (i.a.) injections of 500 μg kg^{-1} PIPC. From 180 to 480 min (day-time) and from 480 to 1200 min (night-time) after injection, the second and third treatments with PIPC caused significantly smaller elevations of T_{abd} compared with the response of naïve guinea pigs ($P < 0.05$ for both periods). Lower panel: febrile responses of guinea pigs ($n = 8$) to the first compared with the fourth and fifth i.a. injections of 500 μg kg^{-1} PIPC. From 180 to 480 min (day-time) and from 480 to 1200 min (night-time) after injection, the fourth and fifth injections of PIPC caused significantly smaller elevations of T_{abd} compared with the response of naïve guinea pigs ($P < 0.05$ for both periods). The responses to the second, third, fourth and fifth injections of PIPC were not different from each other ($P > 0.05$ for all comparisons). The black horizontal bars indicate the night-time ('light-off' period).

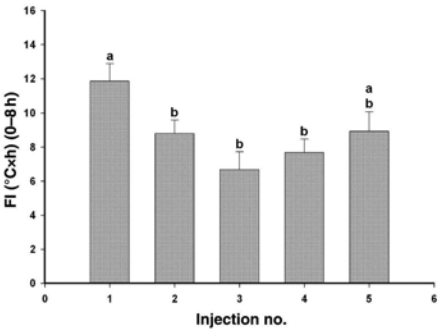


Figure 5 Fever indices calculated from the day-time temperatures for all repeated administrations of polyinosinic : polycytidylic acid (PIPC). Mean integrated area of the febrile responses calculated from the time of injection until the end of the daytime period (0–8 h) for all of the five repeated treatments with PIPC. Any columns with the same letter are not significantly different from each other, while any columns with different letters are significantly different ($P < 0.05$).

day of injection. The results of these calculations are summarized in Figure 5.

Compared with the fever index of the first thermal response to PIPC, the mean fever-indices of the second, third and fourth PIPC-induced febrile responses were significantly reduced ($P < 0.05$; one-way ANOVA and Scheffé-test). The integrated febrile response to the fifth injection narrowly missed the level of significance compared with the first fever probably due to a slightly higher variation of the body temperature data. The integrated areas under the second, third, fourth and fifth fever curves were not significantly different from each other.

Amounts of bioactive TNF-α and IL-6 in plasma at selected times after each of the five injections of PIPC are summarized in Figure 6.

One hour after the first injection of PIPC 1831 ± 400 pg mL^{-1} TNF-α were measured. This value was significantly reduced to 392 ± 115 pg mL^{-1} measured 1 h after the second injection and to 371 ± 134 pg mL^{-1} detected 1 h after the third treatment with PIPC ($P < 0.05$, one-way ANOVA followed by Scheffe-test). In contrast, the corresponding circulating levels of bioactive TNF-α after the fourth (982 ± 419 pg mL^{-1}) and fifth (583 ± 312 pg mL^{-1}) injections were not significantly different from the TNF-α response of naïve guinea pigs (first injection of PIPC, upper panel of Figure 5). Just in two out of eight animals we detected small amounts of bioactive TNF-α (45 and 109 pg mL^{-1} respectively) 120 min after the first administration of PIPC. In the other samples collected at this time point, including all samples from treatments two to five, TNF-α in plasma was below its detection limit.

Levels of bioactive IL-6 in plasma were progressively attenuated in response to five consecutive treatments with PIPC. At least 1 or 4 h after the respective injections a significant difference to the responses of naïve animals was already reached in the second experiment. At 2 h after the respective pyrogen-treatments, a significant difference to the response to the first

© 2006 Scandinavian Physiological Society, doi: 10.1111/j.1748-1716.2006.01587.x

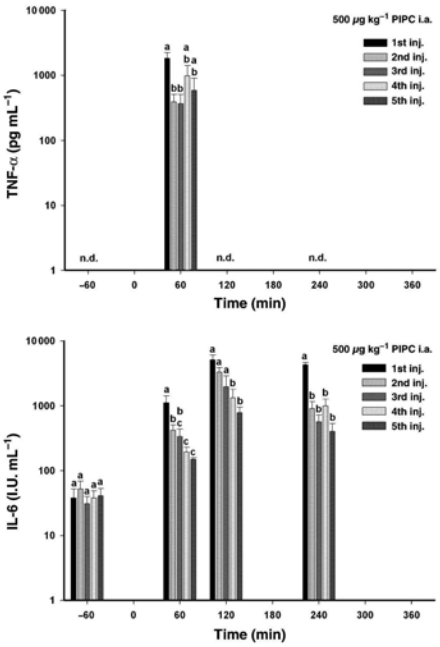


Figure 6 Circulating cytokines in guinea pigs repeatedly injected intra-arterial (i.a.) with polyinosinic : polycytidylic acid (PIPC) or vehicle. Time course of concentrations of bioactive tumour necrosis factor α (upper panel), and interleukin-6 in plasma in response to each of five i.a. administrations of 500 μg kg^{-1} PIPC or sterile saline. For each time point, any columns with the same letter are not significantly different from each other, while any columns with different letters are significantly different ($P < 0.05$).

injection was reached just in the fourth and fifth experiment, because of larger variations of IL-6-values at this time point. It thus seems that the significant attenuation of fever in response to repeated injections of PIPC in guinea pigs is accompanied by a corresponding reduction of PIPC-induced circulating IL-6 (lower level of Fig. 5).

Discussion

As double-stranded RNA is a by-product of viral replication, treatment of experimental animals with PIPC has frequently been considered as an *in vivo* model to mimic the acute-phase response to viral infections (Fortier *et al.* 2004, Traynor *et al.* 2004) and is accompanied by the induction of interferons (Katafuchi *et al.* 2003, Pruett *et al.* 2003). Already one of the first observations that PIPC is capable of causing fever in man and rabbits (Absher & Stinernbring 1969) stimulated the authors of that report to name PIPC a molecule with 'endotoxin-like properties'. Data presented in a recent study in rats, indeed, support the view that LPS- and PIPC-induced fevers are mediated by rather similar mechanisms and seem to be characterized by rather similar features (Fortier *et al.* 2004). (i) I.p. injections of LPS or PIPC both induce the appearance of increased levels of TNF-α and IL-6 in the blood (Long *et al.* 1990, Smith & Kluger 1992, Luheshi *et al.* 1996, Fortier *et al.* 2004). (ii) I.p. injections of LPS or PIPC both induce the expression of IL-1 and COX-2 in the brain (Layé *et al.* 1994, Cao *et al.* 1997, Fortier *et al.* 2004). (iii) LPS- and PIPC-induced fever, in part, seem to depend on IL-1 and COX-2 (Rotondo *et al.* 1987, Smith & Kluger 1992, Luheshi *et al.* 1996, Cao *et al.* 1997, Roth & DeSouza 2001, Fortier *et al.* 2004).

The results of the present study clearly show that the pyrogenic properties of PIPC depend on the route of its administration and that, in this respect, there are some striking differences to LPS-induced fever. For example, injections of LPS into artificial s.c. chambers evoke pronounced fever (Ross *et al.* 2000, 2003, Rummel *et al.* 2004, 2005), while injection of PIPC s.c. had no pyrogenic effect at all in guinea pigs (Fig. 1a). Likewise i.m. injections of LPS cause pronounced fever and high circulating levels of TNF-α and IL-6 (Roth *et al.* 1994), while administration of PIPC via the i.m. route induces a rather moderate fever (Fig. 1a) which is hardly accompanied by a rise in circulating cytokines. Pronounced fever and substantial amounts of cytokines in the blood are induced in guinea pigs by i.p. or i.a. injections of both, LPS (Rummel *et al.* 2004) or PIPC (Figs 1b and 2). The reasons for these discrepancies may be a limited access of PIPC to cells bearing TLR-3 receptors after its s.c. or i.m. administration, i.e. the missing ability of this synthetic molecule to leave the s.c. chamber or the i.m. space into the systemic circulation to be able to cause the formation of pronounced circulating levels of pyrogenic cytokines. On the other hand, the i.p. and especially the i.a. route of administration might have enabled access of PIPC to cells bearing TLR-3 receptors, so that a substantial production of pyrogenic cytokines and thereby fever were stimulated. Similar observations were made for *Staphylococcus aureus* cell walls as an exogenous pyrogen (Cartmell *et al.* 2002). Similar to PIPC in our study this pyrogen was hardly effective when administered via s.c., i.m. and even i.p. routes in rabbits. The route of administration thus seems to be a very important criterion for the characterization of fever-inducing properties of a given exogenous pyrogen.

One of the most striking differences between experimental fevers induced by bacterial LPS on the one hand and PIPC on the other hand, is the finding that PIPC

 © 2006 Scandinavian Physiological Society, doi: 10.1111/j.1748-1716.2006.01587.x

injected into s.c. chambers does not, in contrast to LPS (Ross *et al.* 2000, 2003, Rummel *et al.* 2005), evoke fever at all (Fig. 1a). This observation indicates that both exogenous pyrogens might activate distinct afferent signaling pathways. For LPS, a complete signaling pathway for the initiation of fever has been elaborated within the last years (Blatteis *et al.* 2004, Blatteis 2006). According to this hypothesis, the fever inducing process is started by the arrival of LPS in the liver and its uptake by Kupffer cells, causing an immediate activation of the complement system and the formation of the complement factor C5a, which in turn stimulates the Kupffer cells to release PGE2 as an afferent fever-promoting signal (Perlik *et al.* 2005, Li *et al.* 2006). In context to the present study, it seems that complement factors are not involved in fever induced by PIPC (Li *et al.* 2000). A localized activation of complement within the area of the s.c. chamber might thus readily occur in response to injections of LPS as opposed to PIPC and explain the distinct capacity of both pyrogens to evoke fever when injected into the s.c. chamber. The precise mechanisms of how the febrigenic process is triggered by PIPC has thus still to be explored. The cytokine data elaborated in this study suggest that TNF-α and/or IL-6 may participate in the maintenance of fever after the first 150 min of the febrile response, at least to i.a. injections of PIPC. The initial phase of PIPC-induced fever, however, seems to develop independently from circulating TNF-α and/or IL-6 as the reduced formation of both cytokines in response to repeated administrations of this pyrogen did not cause an attenuation of the initial phase of fever (see Fig. 5). The precise contribution of both cytokines in the maintenance of PIPC-induced fever might be assessed by successful neutralization or pharmacological blockade of TNF-α or IL-6.

Pyrogenic tolerance represents a transient state of diminished responsiveness to various bioactivities of pyrogens. This phenomenon has traditionally been ascribed to LPS and occurs in response to repeated or continuous administration of this pyrogen (Zeisberger & Roth 1998). In guinea pigs LPS-tolerance is associated with a reduced formation of cytokines (TNF-α, IL-6) after repeated confrontation with this pyrogen. Indeed, it could be demonstrated that fever and the endogenous formation of TNF-α and IL-6 are strongly correlated during the development of LPS-tolerance (Roth *et al.* 1994). There is some controversy, if febrile tolerance develops in response to repeated administration of PIPC in short-term intervals (Cooper *et al.* 1988, Soszynski *et al.* 1991). The comparatively novel evidence for the PIPC-inducible formation of TNF-α and IL-6 via TLR-3 receptor activation offered new possibilities to study the development of tolerance to PIPC. Using i.a. injections of PIPC with an identical time schedule as previously performed with LPS (Roth *et al.* 1994, 1997a), we tested the febrile responses and the concomitant circulating levels of TNF-α and IL-6. The results of this experiment again showed that the attenuation of fever starting with the second injection of PIPC is accompanied by a corresponding reduction of PIPC-induced IL-6 in plasma. This cytokine is generally regarded as an endogenous pyrogen (Kluger 1991, Luheshi & Rothwell 1996, Roth & DeSouza 2001) and thus IL-6 may also participate in the manifestation of PIPC-induced fever. There is, however, a striking difference between the development of tolerance to LPS or PIPC. The attenuation of fever and circulating cytokines in response to repeated injections of LPS in guinea pigs is progressive and finally leading to an almost complete lack of any response to this pyrogen (Roth *et al.* 1994, 1997a, Zeisberger & Roth 1998). In contrast, there is a rather moderate, but still significant reduction of fever starting with the second injection of PIPC, which is constantly maintained at the same level in all of the further experiments meaning without a stronger and progressive attenuation of fever in response to the third, fourth, or fifth injection. The reason may be the still manifest formation of pyrogenic cytokines (i.e. IL-6), which is sufficient to keep PIPC-induced fever at a constant level, which is just reduced but not abolished when compared with the febrile responses of naïve guinea pigs. In summary, it is concluded that i.a. injections of 500 μg kg^{-1} PIPC repeated five times at intervals of 3 days cause the manifestation of a partial tolerance with regard to fever and the concomitant endogenous formation of putative endogenous pyrogens.

Conflict of interest

None.

This study was supported by the Deutsche Forschungsgemeinschaft (DFG project RO 896/5–2). We thank Dr Stephen Hopkins (University of Manchester, UK) for providing us with the WEHI 164 subclone 13 and the B9 cell lines and informing us about important details of the TNF- and IL-6-assays. Skilful technical assistance of Jolanta Murgott is gratefully acknowledged.

References

Aarden, L.A., DeGroot, E.R., Schaap, O.L. & Landsdorp, P.M. 1987. Production of hybridoma growth factors by human monocytes. *Eur J Immunol* **17**, 1411–1416.

Absher, M. & Stinernbring, W.R. 1969. Endotoxin-like properties of Poly I : Poly C an interferon stimulator. *Nature* **223**, 715–717.

Aderem, A. & Ulevitch, R.J. 2000. Toll-like receptors in the induction of the innate immune response. *Nature* **406**, 782–787.

© 2006 Scandinavian Physiological Society, doi: 10.1111/j.1748-1716.2006.01587.x

Alexopoulou, L., Czopic Holt, A., Medzhitov, R. & Flavell, R.A. 2001. Recognition of double-stranded RNA and activation of NF-*k*B by Toll-like receptor 3. *Nature* **413**, 732–738.

Blatteis, C.M. 2006. Endotoxic fever: new concepts of its regulation suggest new approaches to its management. *Pharmacol Therap* in press Epub ahead of print PMID 16460809.

Blatteis, C.M., Feleder, C., Perlik, V. & Li, S. 2004. Possible sequence of pyrogenic afferent processing in the POA. *J Therm Biol* **29**, 391–400.

Cao, C., Matsumura, K., Yamagata, K. & Watanabe, Y. 1997. Involvement of cyclooxygenase-2 in LPS-induced fever and regulation of its mRNA by LPS in the rat brain. *Am J Physiol Regul Integr Comp Physiol* **287**, R1712–R1725.

Cartmell, T., Mitchell, D., Lamond, F.J.D. & Laburn, H.P. 2002. Route of administration differentially affects fevers induced by Gram-negative and Gram-positive pyrogens in rabbits. *Exp Physiol* **87.3**, 391–399.

Chuang, J., Lin, M.T., Chan, S.A. & Won, S.J. 1990. Febrile effects of polyriboinosinic: polyribocytidylic acid and interferon: relationship to somatostatin in rat hypothalamus. *Pflügers Arch – Eur J Physiol* **415**, 606–610.

Cooper, K.E., Blähser, S., Malkinson, T.J., Merker, G., Roth, J. & Zeisberger, E. 1988. Changes in body temperature and vasopressin content of brain neurons, in pregnant and non-pregnant guinea pigs, during fevers produced by Poly I : Poly C. *Pflügers Arch – Eur J Physiol* **412**, 292–296.

Espevic, T. & Nissen-Meyer, J. 1986. A highly sensitive cell line, WEHI 164 clone 13, for measuring cytotoxic factor/tumor necrosis factor from human monocytes. *J Immunol Methods* **95**, 99–105.

Field, A.K., Tytell, A.A., Lampson, G.P. & Hilleman, M.R. 1967. Inducers of interferon and host resistance. II. Multistranded synthetic polynucleotide complexes. *Proc Natl Acad Sci U S A* **58**, 1004–1010.

Fortier, M.E., Kent, S., Ashdown, H., Poole, S., Boksa, P. & Luheshi, G.N. 2004. The viral mimic, polyinosinic: polycytidylic acid, induces fever in rats via an interleukin-1-dependent mechanisms. *Am J Physiol Regul Integr Comp Physiol* **287**, R759–R766.

Holt, I., Cooper, R.G. & Hopkins, S.J. 1991. Relationship between local inflammation, interleukin-6 concentration and the acute phase response in arthritic patients. *Eur J Clin Invest* **21**, 479–484.

Jacobs, B.L. & Langland, J.Q. 1996. When two strands are better than one: the mediators and modulators of the cellular responses to double stranded RNA. *Virology* **219**, 339–349.

Katafuchi, T., Kondo, T., Yasaka, T., Kubo, K., Take, S. & Yoshimura, M. 2003. Prolonged effects of polyriboinosinic: polyribocytidylic acid on spontaneous running wheel activity and brain interferon-a mRNA in rats: a model for immunologically induced fatigue. *Neuroscience* **120**, 837–845.

Kimura, M., Toth, L.A., Agostini, H., Cady, A.B., Majde, J.A. & Krueger, J.M. 1994. Comparison of acute phase responses induced in rabbits by lipopolysaccharide and double stranded RNA. *Am J Physiol Regul Integr Comp Physiol* **267**, R1596–R1605.

Kluger, M.J. 1991. Fever: Role of pyrogens and cryogens. *Physiol Rev* **71**, 93–127.

Layé, S., Parnet, P., Goujon, E. & Dantzer, R. 1994. Peripheral administration of lipopolysaccharide induces the expression of cytokine transcripts in the brain and pituitary of mice. *Mol Brain Res* **27**, 157–162.

Li, S., Sehic, E., Ungar, A.L. & Blatteis, C.M. 2000. Complement does not mediate the febrile responses of guinea pigs to muramyl dipeptide and polyriboinosinic-polyribocycytidylic acid. *J Therm Biol* **25**, 51–58.

Li, S., Perlik, V., Feleder, C., Tang, Y. & Blatteis, C.M. 2006. Kupffer cell-generated PGE2 triggers the febbrile response of guinea pigs to intravenously injected LPS. *Am J Physiol Regul Integr Comp Physiol* **290**, R1262–R1270.

Long, N.J., Kunkel, S.L., Vander, A.J. & Kluger, M.J. 1990. Antiserum against tumor necrosis factor enhances lipopolysaccharide fever in rats. *Am J Physiol Regul Integr Comp Physiol* **258**, R332–R337.

Luheshi, G. & Rothwell, N. 1996. Cytokines and fever. *Int Arch Allergy Immunol* **109**, 301–307.

Luheshi, G., Miller, A.J., Brouwer, S., Dascombe, M.J., Rothwell, N.J. & Hopkins, S.J. 1996. Interleukin-1 receptor antagonist inhibits endotoxin fever and systemic interleukin-6 induction in the rat. *Am J Physiol Endocrinol Metab* **270**, E91–E95.

Perlik, V., Li, S., Goorha, S., Ballou, L.R. & Blatteis, C.M. 2005. LPS-activated complement, not LPS per se, triggers the early release of PGE2 by Kupffer cells. *Am J Physiol Regul Integr Comp Physiol* **289**, R332–R339.

Pruett, S.B., Fan, R. & Zheng, Q. 2003. Acute ethanol administration profoundly alters poly I:C-induced cytokine expression in mice by a mechanism that is not dependent on corticosterone. *Life Sci* **72**, 1825–1839.

Ross, G., Roth, J., Störr, B., Voigt, K. & Zeisberger, E. 2000. Afferent nerves are involved in the febrile response to injection of LPS into artificial subcutaneous chambers in guinea pigs. *Physiol Behav* **71**, 305–313.

Ross, G., Hübschle, T., Pehl, U., Braun, H.A., Voigt, K., Gerstberger, R. & Roth, J. 2003. Fever induction by localized subcutaneous inflammation in guinea pigs: the role of cytokines and prostaglandins. *J Appl Physiol* **94**, 1395–1402.

Roth, J. & DeSouza, G.E.P. 2001. Fever induction pathways: evidence from responses to systemic or local cytokine formation. *Braz J Med Biol Res* **34**, 301–314.

Roth, J., McClellan, J.L., Kluger, M.J. & Zeisberger, E. 1994. Attenuation of fever and release of cytokines after repeated injections of lipopolysaccharide in guinea pigs. *J Physiol* **477.1**, 177–185.

Roth, J., Aslan, T., Störr, B. & Zeisberger, E. 1997a. Lack of cross tolerance between LPS and muramyl dipeptide in induction of circulating TNF-α and IL-6 in guinea pigs. *Am J Physiol Regul Integr Comp Physiol* **273**, R1529–R1533.

Roth, J., Hopkins, S.J., Hoadley, M.E., Tripp, A., Aslan, T., Störr, B., Luheshi, G.N. & Zeisberger, E. 1997b. Fever and production of cytokines in response to repeated injections of muramyl dipeptide in guinea pigs. *Pflügers Archiv – Eur J Physiol* **434**, 525–533.

Rotondo, D., Abul, H.T., Milton, A.S. & Davidson, J. 1987. The pyrogenic actions of the interferon-inducer,

 © 2006 Scandinavian Physiological Society, doi: 10.1111/j.1748-1716.2006.01587.x

polyinosinic: polycytidylic acid are antagonised by ketoprofen. *Eur J Pharmacol* **154**, 257–260.

Rummel, C., Hübschle, T., Gerstberger, R. & Roth, J. 2004. Nuclear translocation of the transcription factor STAT3 in the guinea pig brain during systemic or localized inflammation. *J Physiol* **557.2**, 671–687.

Rummel, C., Barth, S.W., Voss, T., Korte, S., Gerstberger, R., Hübschle, T. & Roth, J. 2005. Localized vs. Systemic inflammation in guinea pigs: a role for prostaglandins at distinct points of the fever induction pathways? *Am J Physiol Regul Integr Comp Physiol* **289**, 340–347.

Smith, B. & Kluger, M.J. 1992. Human IL-1 receptor antagonist partially suppresses fever but not plasma levels of IL-6 in Fischer rats. *Am J Physiol Regul Integr Comp Physiol* **263**, R653–R655.

Soszynski, D., Kozak, W. & Szewczenko, M. 1991. Course of fever response to repeated administration of sublethal doses of lipopolysaccharides, polyinosinic: polycytidylic acid and muramyl dipeptide to rabbits. *Experientia* **47**, 43–47.

Traynor, T.N., Majde, J.A., Bohnet, S.G. & Krueger, J.M. 2004. Intratracheal double-stranded RNA plus interferon-γ: a model for analysis of the acute phase response to respiratory viral infections. *Life Sci* **74**, 2563–2576.

Zeisberger, E. & Roth, J. 1998. Tolerance to pyrogens. *Ann NY Acad Sci* **856**, 116–131.

© 2006 Scandinavian Physiological Society, doi: 10.1111/j.1748-1716.2006.01587.x

2. Manuskripte in Vorbereitung

2.1. „AG490 potentiates LPS-induced fever while reversing LPS-induced lethargy and adipsia“

2.2. „The role of IL-10 in the brain and periphery of LPS-induced septic like inflammation“

2.3. “Intraperitoneal and subcutaneous injections of the TLR9 agonist ODN-1668 in rats: brain inflammatory responses are rather related to peripheral IL-6 than interferons”

2.4. „The inflammatory transcription factor NF-IL6 is linked to the activation of the hypothalamic-pituitary-adrenal stress axis in rats“

2.5. “Age dependant effects of the PPAR-y agonist rosiglitazone on the brain and periphery during systemic LPS-induced inflammation in rats”

VI. ABKÜRZUNGEN

ACTH .....Adrenocorticotropes-Hormon
AgRP.....agouti-related peptide
AP .....*Area postrema*
ARC .....*Nucleus arcuatus hypothalami*
AVP .....Vasopressin
BAT .....braunes Fettgewebe
BBB .....Blood-Brain-Barrier
.....(Blut-Hirn-Schranke)
cAMP.....zyklisches
.....Adenosinmonophosphat
CART.....cocain amphetamin related
.....peptide
CD36.....cluster of differentiation 36
c-FOS.....FOS-Protein
.....Transkriptionsfaktor,
.....Onkogenprodukt
cGMP.....zyklisches Guanosin-
.....Monophosphat
CNTF.....ciliary neurotrophic factor
COX.....Zyklooxygenase
CpG-DNA.....Bakterielle DNA
CVOs .....zirkumventrikulären Organe
DAMPs .....danger-associated molecular
.....patterns
db/db .....Leptin Rezeptor defiziente
.....Mäuse (besitzen noch ObRa)
DMH.....*Nucleus dorsomediales*
.....*hypothalami*
DNA .....Desoxyribonukleinsäure
Egr1.....early growth response 1
ELISA.....enzyme-linked immunosorbent
.....assay
EP(1-4)R .....Prostaglandin E-
.....Rezeptorsubtyp 1-4
FOS.....FOS-Protein
gp130 .....Glykoprotein 130
HMGB1 .....high-mobility group box 1
HPA-Achse.....Hypothalamo-Hypophysen-
.....Nebennierenrinden-Achse
i.a. .....intraarteriell
ICAM.....intercellular adhesion molecule
i.c.v. .....intracerebroventrikulär
IFN.....Interferon
IκB..... Inhibitorischer Faktor κB
IL-(x)..... Interleukin-(x)
IL-1 ..... Interleukin-1
IL-1ß ..... Interleukin-1 beta
IL-6 ..... Interleukin-6
IL-6AS ..... IL-6 Antiserum
IL-1R..... Interleukin-1 Rezeptor
IL-6R..... Interleukin-6 Rezeptor
IL-1ra IL-1-Rezeptor-Antagonist
iNOS ..... induzierbare NO-Synthase
i.m. ..... intramuscular
Imiquimod..... TLR7-Agonist
i.p. ..... intraperitoneal
IRF ..... interferon regulatory factor
i.v. ..... intravenös
JAK ..... Janus-Kinase
KC..... keratinocyte derived chemokine
kDa. ..... Kilo Dalton
KO..... knockout
LAP..... liver –enriched activating
..... protein (active NF-IL6 Form)
LAS..... Leptin Antiserum
LIF..... leukemia inhibiting factor
LIP..... liver-enriched inhibitory protein
..... (hemmende NF-IL6 Form)
LPS..... Lipopolysaccharid
MALP-2 ..... Makrophagen-aktivierendes
..... Lipopeptid-2
MC4R..... Melanokortin 4 Rezeptor
MCP1 ..... monocyte chemoattractant
..... protein 1
ME..... *Eminentia mediana*
min. ..... Minute
MIP ..... Makrophagen-
..... Inflammatorisches-Protein
MMP ..... Matrix-Metalloproteinasen
MnPO ..... *Nucleus medianus praeopticus*
mPGES..... mikrosomale
..... Prostaglandin-E-Synthase
mRNA ..... messenger Ribonukleinsäure
MSH..... Melanozyten stimulierendes
..... Hormon
MyD88 ..... Adaptermolekül des IL-1R

NaCl.....Isotone Natriumchloridlösung
NF-IL6 .....nuclear factor-IL-6
NF-κB .....nuclear factor κB
NG.....neutrophiler Granulozyt
NLR .....nucleotide-binding domain and
.....leucin-rich repeat containing
.....Rezeptoren
NO.....Stickstoffmonoxid
NOS .....Stickstoffmonoxid-Synthase
NPY .....Neuropeptid Y
NRF1.....nuclear respiratory factor 1
NSAIDs.....nicht steroidalen
.....Entzündungshemmer
NTS.....*Nucleus tractus solitarius*
N. vagus .....*Nervus vagus*
ob/ob .....Leptin defiziente Mäuse
OBR .....Leptin Rezeptor
ObRa .....kurze Form des OBR
ObRb.....lange Form des OBR
OSM.....oncostatin M
OVLT .....*Organum vasculosum*
.....*laminae terminalis*
P .....Parthenolid
PAMPs.....pathogen-associated
.....molecular patterns
Pe .....*Nucleus periventricularis*
PG .....Prostaglandin
PGC1α .....(PPAR)γ coactivator (PGC)1α
PGE_2 .....Prostaglandin-E_2
PNS .....peripheres Nervensystem
POA .....*Area praeoptica hypothalami*
.....(Präoptische Region)
PIPC.....Polyinosinic : polycytidylic acid
POMC.....Proopiomelanocortin
PPAR .....Proliferator-activated receptor
PVN .....*Nucleus paraventricularis*
RPa.....*Nucleus raphe pallidus*
s.c. ..... subkutan
sCVOs..... senorischen CVOs
SFO ..... Subfornikalorgan
..... (*Organum subfornicale*)
SHR..... spontan hypertensiver
..... Rattenstamm (CD36 defizient)
SNS ..... Sympathisches Nervensystem
SOCS..... supressor of cytokine signaling
SON .....*Nucleus supraopticus*
STAT ..... Signalübersetzer und Aktivator
..... der Transkription
..... (engl: signal transducer and
..... activator of transcription)
STAT3 ..... STAT-Transkriptionsfaktor 3
TFAM ..... mitochondrial transcription
..... factor A
TIMP1 ..... tissue inhibitors of MMPs
TIR ..... Toll-interleukin-1 receptor
..... domain
TIRAP ..... TIR domain containing adaptor
..... protein
TLR ..... Toll-like-Rezeptor
TNF ..... Tumor-Nekrose-Faktor
TNF-α..... Tumor-Nekrose-Faktor-alpha
Trib..... serin/threonin kinase like protein
VMPO .....*Nucleus ventromedialis*
.....*praeopticus*
..... präoptische Region
vW ..... von-Willebrand-Faktor
..... Zellmarker für Endothelzellen
WKY ..... Wistar Kyoto Rattenstamm
ZNS ..... Zentralnervensystem

VII. LITERATURVERZEICHNIS

Abbud RA, Kelleher R, Melmed S. 2004. Cell-specific pituitary gene expression profiles after treatment with leukemia inhibitory factor reveal novel modulators for proopiomelanocortin expression. Endocrinology 145(2):867-880.

Aggarwal BB. 2010. Targeting inflammation-induced obesity and metabolic diseases by curcumin and other nutraceuticals. Annu Rev Nutr 30:173-199.

Agrawal A, Cha-Molstad H, Samols D, Kushner I. 2003. Overexpressed nuclear factor-kappaB can participate in endogenous C-reactive protein induction, and enhances the effects of C/EBPbeta and signal transducer and activator of transcription-3. Immunology 108(4):539-547.

Ahima RS, Prabakaran D, Mantzoros C, Qu D, Lowell B, Maratos-Flier E, Flier JS. 1996. Role of leptin in the neuroendocrine response to fasting. Nature 382(6588):250-252.

Ahren B. 2000. Diurnal variation in circulating leptin is dependent on gender, food intake and circulating insulin in mice. Acta Physiol Scand 169(4):325-331.

Ajami B, Bennett JL, Krieger C, Tetzlaff W, Rossi FM. 2007. Local self-renewal can sustain CNS microglia maintenance and function throughout adult life. Nat Neurosci 10(12):1538-1543.

Akarsu ES, Mamuk S. 2007. Escherichia coli lipopolysaccharides produce serotype-specific hypothermic response in biotelemetered rats. Am J Physiol Regul Integr Comp Physiol 292(5):R1846-1850.

Akira S. 1992. NF-IL6 and gene regulation. Res Immunol 143(7):734-736.

Akira S, Isshiki H, Sugita T, Tanabe O, Kinoshita S, Nishio Y, Nakajima T, Hirano T, Kishimoto T. 1990. A nuclear factor for IL-6 expression (NF-IL6) is a member of a C/EBP family. EMBO J 9(6):1897-1906.

Akira S, Kishimoto T. 1992. IL-6 and NF-IL6 in acute-phase response and viral infection. Immunol Rev 127:25-50.

Akira S, Uematsu S, Takeuchi O. 2006. Pathogen recognition and innate immunity. Cell 124(4):783-801.

Alexopoulou L, Holt AC, Medzhitov R, Flavell RA. 2001. Recognition of double-stranded RNA and activation of NF-kappaB by Toll-like receptor 3. Nature 413(6857):732-738.

Almeida MC, Steiner AA, Branco LG, Romanovsky AA. 2006. Neural substrate of cold-seeking behavior in endotoxin shock. PLoS One 1:e1.

Alves JD, Marinho A, Serra MJ. 2011. Tocilizumab: is there life beyond anti-TNF blockade? Int J Clin Pract 65(4):508-513.

Anderson KN, Bejcek BE. 2008. Parthenolide induces apoptosis in glioblastomas without affecting NF-kappaB. J Pharmacol Sci 106(2):318-320.

Andersson PB, Perry VH, Gordon S. 1992a. The acute inflammatory response to lipopolysaccharide in CNS parenchyma differs from that in other body tissues. Neuroscience 48(1):169-186.

Andersson PB, Perry VH, Gordon S. 1992b. Intracerebral injection of proinflammatory cytokines or leukocyte chemotaxins induces minimal myelomonocytic cell recruitment to the parenchyma of the central nervous system. J Exp Med 176(1):255-259.

Andrews DM, Matthews VB, Sammels LM, Carrello AC, McMinn PC. 1999. The severity of murray valley encephalitis in mice is linked to neutrophil infiltration and inducible nitric oxide synthase activity in the central nervous system. J Virol 73(10):8781-8790.

Anthony D, Dempster R, Fearn S, Clements J, Wells G, Perry VH, Walker K. 1998. CXC chemokines generate age-related increases in neutrophil-mediated brain inflammation and blood-brain barrier breakdown. Curr Biol 8(16):923-926.

Anthony DC, Bolton SJ, Fearn S, Perry VH. 1997. Age-related effects of interleukin-1 beta on polymorphonuclear neutrophil-dependent increases in blood-brain barrier permeability in rats. Brain 120 (Pt 3):435-444.

Anthony DC, Couch Y, Losey P, Evans MC. 2012. The systemic response to brain injury and disease. Brain Behav Immun 26(4):534-540.

Arsenijevic D, Garcia I, Vesin C, Vesin D, Arsenijevic Y, Seydoux J, Girardier L, Ryffel B, Dulloo A, Richard D. 2000. Differential roles of tumor necrosis factor-alpha and interferon-gamma in mouse hypermetabolic and anorectic responses induced by LPS. Eur Cytokine Netw 11(4):662-668.

Asarian L, Langhans W. 2010. A new look on brain mechanisms of acute illness anorexia. Physiol Behav 100(5):464-471.

Banks WA. 2004. The many lives of leptin. Peptides 25(3):331-338.

Banks WA, Farr SA, Morley JE. 2002. Entry of blood-borne cytokines into the central nervous system: effects on cognitive processes. Neuroimmunomodulation 10(6):319-327.

Banks WA, Kastin AJ, Huang W, Jaspan JB, Maness LM. 1996. Leptin enters the brain by a saturable system independent of insulin. Peptides 17(2):305-311.

Barker CF, Billingham RE. 1977. Immunologically privileged sites. Adv Immunol 25:1-54.

Barnes MJ, Rogers RC, Van Meter MJ, Hermann GE. 2010. Co-localization of TRHR1 and LepRb receptors on neurons in the hindbrain of the rat. Brain Res 1355:70-85.

Bartfai T, Conti B. 2010. Fever. ScientificWorldJournal 10:490-503.

Baskin DG, Breininger JF, Bonigut S, Miller MA. 1999. Leptin binding in the arcuate nucleus is increased during fasting. Brain Res 828(1-2):154-158.

Basu S, Haghiac M, Surace P, Challier JC, Guerre-Millo M, Singh K, Waters T, Minium J, Presley L, Catalano PM, Hauguel-de Mouzon S. 2011. Pregravid obesity associates with increased maternal endotoxemia and metabolic inflammation. Obesity (Silver Spring) 19(3):476-482.

Bechmann I, Galea I, Perry VH. 2007. What is the blood-brain barrier (not)? Trends Immunol 28(1):5-11.

Belevych N, Buchanan K, Chen Q, Bailey M, Quan N. 2010. Location-specific activation of the paraventricular nucleus of the hypothalamus by localized inflammation. Brain Behav Immun 24(7):1137-1147.

Beray-Berthat V, Palmier B, Plotkine M, Margaill I. 2003. Neutrophils do not contribute to infarction, oxidative stress, and NO synthase activity in severe brain ischemia. Exp Neurol 182(2):446-454.

Berkowitz DE, Brown D, Lee KM, Emala C, Palmer D, An Y, Breslow M. 1998. Endotoxin-induced alteration in the expression of leptin and beta3-adrenergic receptor in adipose tissue. Am J Physiol 274(6 Pt 1):E992-997.

Besedovsky HO, del Rey A. 2011. Central and peripheral cytokines mediate immune-brain connectivity. Neurochem Res 36(1):1-6.

Beutler B. 2004. Innate immunity: an overview. Mol Immunol 40(12):845-859.

Billack B, Heck DE, Mariano TM, Gardner CR, Sur R, Laskin DL, Laskin JD. 2002. Induction of cyclooxygenase-2 by heat shock protein 60 in macrophages and endothelial cells. Am J Physiol Cell Physiol 283(4):C1267-1277.

Bjorbaek C, Elmquist JK, El-Haschimi K, Kelly J, Ahima RS, Hileman S, Flier JS. 1999. Activation of SOCS-3 messenger ribonucleic acid in the hypothalamus by ciliary neurotrophic factor. Endocrinology 140(5):2035-2043.

Bjorbaek C, Elmquist JK, Michl P, Ahima RS, van Bueren A, McCall AL, Flier JS. 1998. Expression of leptin receptor isoforms in rat brain microvessels. Endocrinology 139(8):3485-3491.

Bjorbaek C, Uotani S, da Silva B, Flier JS. 1997. Divergent signaling capacities of the long and short isoforms of the leptin receptor. J Biol Chem 272(51):32686-32695.

Blasius AL, Beutler B. 2010. Intracellular toll-like receptors. Immunity 32(3):305-315.

Blatteis CM. 1986. Fever: is it beneficial? Yale J Biol Med 59(2):107-116.

Blatteis CM, Quan N, Xin L, Ungar AL. 1990. Neuromodulation of acute-phase responses to interleukin-6 in guinea pigs. Brain Res Bull 25(6):895-901.

Bluher S, Mantzoros CS. 2004. The role of leptin in regulating neuroendocrine function in humans. J Nutr 134(9):2469S-2474S.

Bluthé RM, Laye S, Michaud B, Combe C, Dantzer R, Parnet P. 2000. Role of interleukin-1beta and tumour necrosis factor-alpha in lipopolysaccharide-induced sickness behaviour: a study with interleukin-1 type I receptor-deficient mice. Eur J Neurosci 12(12):4447-4456.

Bluthé RM, Michaud B, Kelley KW, Dantzer R. 1996. Vagotomy blocks behavioural effects of interleukin-1 injected via the intraperitoneal route but not via other systemic routes. Neuroreport 7(15-17):2823-2827.

Bode JG, Nimmesgern A, Schmitz J, Schaper F, Schmitt M, Frisch W, Haussinger D, Heinrich PC, Graeve L. 1999. LPS and TNFalpha induce SOCS3 mRNA and inhibit IL-6-induced activation of STAT3 in macrophages. FEBS Lett 463(3):365-370.

Boghossian S, Ueno N, Dube MG, Kalra P, Kalra S. 2007. Leptin gene transfer in the hypothalamus enhances longevity in adult monogenic mutant mice in the absence of circulating leptin. Neurobiol Aging 28(10):1594-1604.

Bohatschek M, Werner A, Raivich G. 2001. Systemic LPS injection leads to granulocyte influx into normal and injured brain: effects of ICAM-1 deficiency. Exp Neurol 172(1):137-152.

Boivin N, Sergerie Y, Rivest S, Boivin G. 2008. Effect of pretreatment with toll-like receptor agonists in a mouse model of herpes simplex virus type 1 encephalitis. J Infect Dis 198(5):664-672.

Bojanowska E, Nowak A. 2007. Interactions between leptin and exendin-4, a glucagon-like peptide-1 agonist, in the regulation of food intake in the rat. J Physiol Pharmacol 58(2):349-360.

Bolli R, Dawn B, Xuan YT. 2003. Role of the JAK-STAT pathway in protection against myocardial ischemia/reperfusion injury. Trends Cardiovasc Med 13(2):72-79.

Borner T, Pinkernell S, Lutz TA, Riediger T. 2012. Lipopolysaccharide inhibits ghrelin-excited neurons of the arcuate nucleus and reduces food intake via central nitric oxide signaling. Brain Behav Immun.

Borovikova LV, Ivanova S, Zhang M, Yang H, Botchkina GI, Watkins LR, Wang H, Abumrad N, Eaton JW, Tracey KJ. 2000. Vagus nerve stimulation attenuates the systemic inflammatory response to endotoxin. Nature 405(6785):458-462.

Borsutzky S, Fiorelli V, Ebensen T, Tripiciano A, Rharbaoui F, Scoglio A, Link C, Nappi F, Morr M, Butto S, Cafaro A, Muhlradt PF, Ensoli B, Guzman CA. 2003. Efficient mucosal delivery of the HIV-1 Tat protein using the synthetic lipopeptide MALP-2 as adjuvant. Eur J Immunol 33(6):1548-1556.

Boulton M, Flessner M, Armstrong D, Mohamed R, Hay J, Johnston M. 1999. Contribution of extracranial lymphatics and arachnoid villi to the clearance of a CSF tracer in the rat. Am J Physiol 276(3 Pt 2):R818-823.

Brain SD, Williams TJ. 1988. Substance P regulates the vasodilator activity of calcitonin gene-related peptide. Nature 335(6185):73-75.

Bret-Dibat JL, Bluthe RM, Kent S, Kelley KW, Dantzer R. 1995. Lipopolysaccharide and interleukin-1 depress food-motivated behavior in mice by a vagal-mediated mechanism. Brain Behav Immun 9(3):242-246.

Broberger C. 2005. Brain regulation of food intake and appetite: molecules and networks. J Intern Med 258(4):301-327.

Broomfield SA, van der Most RG, Prosser AC, Mahendran S, Tovey MG, Smyth MJ, Robinson BW, Currie AJ. 2009. Locally administered TLR7 agonists drive systemic antitumor immune responses that are enhanced by anti-CD40 immunotherapy. J Immunol 182(9):5217-5224.

Brownlie R, Zhu J, Allan B, Mutwiri GK, Babiuk LA, Potter A, Griebel P. 2009. Chicken TLR21 acts as a functional homologue to mammalian TLR9 in the recognition of CpG oligodeoxynucleotides. Mol Immunol 46(15):3163-3170.

Brun P, Castagliuolo I, Di Leo V, Buda A, Pinzani M, Palu G, Martines D. 2007. Increased intestinal permeability in obese mice: new evidence in the pathogenesis of nonalcoholic steatohepatitis. Am J Physiol Gastrointest Liver Physiol 292(2):G518-525.

Bruno A, Conus S, Schmid I, Simon HU. 2005. Apoptotic pathways are inhibited by leptin receptor activation in neutrophils. J Immunol 174(12):8090-8096.

Bruunsgaard H, Pedersen BK. 2003. Age-related inflammatory cytokines and disease. Immunol Allergy Clin North Am 23(1):15-39.

Brynskikh A, Warren T, Zhu J, Kipnis J. 2008. Adaptive immunity affects learning behavior in mice. Brain Behav Immun 22(6):861-869.

Buller KM. 2001. Role of circumventricular organs in pro-inflammatory cytokine-induced activation of the hypothalamic-pituitary-adrenal axis. Clin Exp Pharmacol Physiol 28(7):581-589.

Burton MD, Johnson RW. 2011. Interleukin-6 trans-signaling in the senescent mouse brain is involved in infection-related deficits in contextual fear conditioning. Brain Behav Immun.

Burton MD, Sparkman NL, Johnson RW. 2011. Inhibition of interleukin-6 trans-signaling in the brain facilitates recovery from lipopolysaccharide-induced sickness behavior. J Neuroinflammation 8:54.

Busso N, So A, Chobaz-Peclat V, Morard C, Martinez-Soria E, Talabot-Ayer D, Gabay C. 2002. Leptin signaling deficiency impairs humoral and cellular immune responses and attenuates experimental arthritis. J Immunol 168(2):875-882.

Butchi NB, Du M, Peterson KE. 2010. Interactions between TLR7 and TLR9 agonists and receptors regulate innate immune responses by astrocytes and microglia. Glia 58(6):650-664.

Campbell SJ, Anthony DC, Oakley F, Carlsen H, Elsharkawy AM, Blomhoff R, Mann DA. 2008. Hepatic nuclear factor kappa B regulates neutrophil recruitment to the injured brain. J Neuropathol Exp Neurol 67(3):223-230.

Campbell SJ, Perry VH, Pitossi FJ, Butchart AG, Chertoff M, Waters S, Dempster R, Anthony DC. 2005. Central nervous system injury triggers hepatic CC and CXC chemokine expression that is associated with leukocyte mobilization and recruitment to both the central nervous system and the liver. Am J Pathol 166(5):1487-1497.

Campfield LA, Smith FJ, Guisez Y, Devos R, Burn P. 1995. Recombinant mouse OB protein: evidence for a peripheral signal linking adiposity and central neural networks. Science 269(5223):546-549.

Campisi J, Hansen MK, O'Connor KA, Biedenkapp JC, Watkins LR, Maier SF, Fleshner M. 2003. Circulating cytokines and endotoxin are not necessary for the activation of the sickness or corticosterone response produced by peripheral E. coli challenge. J Appl Physiol 95(5):1873-1882.

Cao C, Matsumura K, Yamagata K, Watanabe Y. 1996. Endothelial cells of the rat brain vasculature express cyclooxygenase-2 mRNA in response to systemic interleukin-1 beta: a possible site of prostaglandin synthesis responsible for fever. Brain Res 733(2):263-272.

Cao C, Matsumura K, Yamagata K, Watanabe Y. 1997. Involvement of cyclooxygenase-2 in LPS-induced fever and regulation of its mRNA by LPS in the rat brain. Am J Physiol Regul Integr Comp Physiol 272(6):R1712-1725.

Capuron L, Miller AH. 2011. Immune system to brain signaling: Neuropsychopharmacological implications. Pharmacol Ther.

Cardinaux JR, Allaman I, Magistretti PJ. 2000. Pro-inflammatory cytokines induce the transcription factors C/EBPbeta and C/EBPdelta in astrocytes. Glia 29(1):91-97.

Cardinaux JR, Magistretti PJ. 1996. Vasoactive intestinal peptide, pituitary adenylate cyclase-activating peptide, and noradrenaline induce the transcription factors CCAAT/enhancer binding protein (C/EBP)-beta and C/EBP delta in mouse cortical astrocytes: involvement in cAMP-regulated glycogen metabolism. J Neurosci 16(3):919-929.

Carlo AS, Meyerhof W, Williams LM. 2007. Early developmental expression of leptin receptor gene and [125I]leptin binding in the rat forebrain. J Chem Neuroanat 33(3):155-163.

Cartmell T, Luheshi GN, Hopkins SJ, Rothwell NJ, Poole S. 2001. Role of endogenous interleukin-1 receptor antagonist in regulating fever induced by localised inflammation in the rat. J Physiol 531(Pt 1):171-180.

Cartmell T, Mitchell D, Lamond FJ, Laburn HP. 2002. Route of administration differentially affects fevers induced by Gram-negative and Gram-positive pyrogens in rabbits. Exp Physiol 87(3):391-399.

Cartmell T, Poole S, Turnbull AV, Rothwell NJ, Luheshi GN. 2000. Circulating interleukin-6 mediates the febrile response to localised inflammation in rats. J Physiol 526 Pt 3:653-661.

Casanova JL, Abel L, Quintana-Murci L. 2011. Human TLRs and IL-1Rs in host defense: natural insights from evolutionary, epidemiological, and clinical genetics. Annu Rev Immunol 29:447-491.

Casey LC, Lee WM. 2012. Hepatitis C therapy update. Curr Opin Gastroenterol 28(3):188-192.

Chai Z, Gatti S, Toniatti C, Poli V, Bartfai T. 1996. Interleukin (IL)-6 gene expression in the central nervous system is necessary for fever response to lipopolysaccharide or IL-1 beta: a study on IL-6-deficient mice. J Exp Med 183(1):311-316.

Chakravarty S, Herkenham M. 2005. Toll-like receptor 4 on nonhematopoietic cells sustains CNS inflammation during endotoxemia, independent of systemic cytokines. J Neurosci 25(7):1788-1796.

Chandra RK. 1980. Cell-mediated immunity in genetically obese C57BL/6J ob/ob) mice. Am J Clin Nutr 33(1):13-16.

Chen J, Ivashkiv LB. 2010. IFN-gamma abrogates endotoxin tolerance by facilitating Toll-like receptor-induced chromatin remodeling. Proc Natl Acad Sci U S A 107(45):19438-19443.

Chikuma T, Yoshimoto T, Ohba M, Sawada M, Kato T, Sakamoto T, Hiyama Y, Hojo H. 2009. Interleukin-6 induces prostaglandin E(2) synthesis in mouse astrocytes. J Mol Neurosci 39(1-2):175-184.

Chuang J, Lin MT, Chan SA, Won SJ. 1990. Febrile effects of polyriboinosinic acid: polyribocytidylic acid and interferon: relationship to somatostatin in rat hypothalamus. Pflugers Arch 415(5):606-610.

Considine RV, Considine EL, Williams CJ, Hyde TM, Caro JF. 1996a. The hypothalamic leptin receptor in humans: identification of incidental sequence polymorphisms and absence of the db/db mouse and fa/fa rat mutations. Diabetes 45(7):992-994.

Considine RV, Sinha MK, Heiman ML, Kriauciunas A, Stephens TW, Nyce MR, Ohannesian JP, Marco CC, McKee LJ, Bauer TL, et al. 1996b. Serum immunoreactive-leptin concentrations in normal-weight and obese humans. N Engl J Med 334(5):292-295.

Conti B, Tabarean I, Andrei C, Bartfai T. 2004. Cytokines and fever. Front Biosci 9:1433-1449.

Cooper MD, Alder MN. 2006. The evolution of adaptive immune systems. Cell 124(4):815-822.

Corp ES, Conze DB, Smith F, Campfield LA. 1998. Regional localization of specific [125I]leptin binding sites in rat forebrain. Brain Res 789(1):40-47.

Cortes-Canteli M, Aguilar-Morante D, Sanz-Sancristobal M, Megias D, Santos A, Perez-Castillo A. 2011. Role of C/EBPbeta transcription factor in adult hippocampal neurogenesis. PLoS One 6(10):e24842.

Cortes-Canteli M, Luna-Medina R, Sanz-Sancristobal M, Alvarez-Barrientos A, Santos A, Perez-Castillo A. 2008. CCAAT/enhancer binding protein beta deficiency provides cerebral protection following excitotoxic injury. J Cell Sci 121(Pt 8):1224-1234.

Cortes-Canteli M, Wagner M, Ansorge W, Perez-Castillo A. 2004. Microarray analysis supports a role for ccaat/enhancer-binding protein-beta in brain injury. J Biol Chem 279(14):14409-14417.

Cowell RM, Blake KR, Russell JW. 2007. Localization of the transcriptional coactivator PGC-1alpha to GABAergic neurons during maturation of the rat brain. J Comp Neurol 502(1):1-18.

Creely SJ, McTernan PG, Kusminski CM, Fisher M, Da Silva NF, Khanolkar M, Evans M, Harte AL, Kumar S. 2007. Lipopolysaccharide activates an innate immune system response in human adipose tissue in obesity and type 2 diabetes. Am J Physiol Endocrinol Metab 292(3):E740-747.

Crocker SJ, Whitmire JK, Frausto RF, Chertboonmuang P, Soloway PD, Whitton JL, Campbell IL. 2006. Persistent macrophage/microglial activation and myelin disruption after experimental autoimmune encephalomyelitis in tissue inhibitor of metalloproteinase-1-deficient mice. Am J Pathol 169(6):2104-2116.

Currier RW, Steele JH. 2011. One health-one medicine: unifying human and animal medicine within an evolutionary paradigm. Ann N Y Acad Sci 1230:4-11.

D'Mello C, Le T, Swain MG. 2009. Cerebral microglia recruit monocytes into the brain in response to tumor necrosis factoralpha signaling during peripheral organ inflammation. J Neurosci 29(7):2089-2102.

Dadds MR, Bovbjerg DH, Redd WH, Cutmore TR. 1997. Imagery in human classical conditioning. Psychol Bull 122(1):89-103.

Dagon Y, Avraham Y, Magen I, Gertler A, Ben-Hur T, Berry EM. 2005. Nutritional status, cognition, and survival: a new role for leptin and AMP kinase. J Biol Chem 280(51):42142-42148.

Dalpke AH, Opper S, Zimmermann S, Heeg K. 2001. Suppressors of cytokine signaling (SOCS)-1 and SOCS-3 are induced by CpG-DNA and modulate cytokine responses in APCs. J Immunol 166(12):7082-7089.

Dantzer R, Kelley KW. 2007. Twenty years of research on cytokine-induced sickness behavior. Brain Behav Immun 21(2):153-160.

Dantzer R, Konsman JP, Bluthe RM, Kelley KW. 2000. Neural and humoral pathways of communication from the immune system to the brain: parallel or convergent? Auton Neurosci 85(1-3):60-65.

Dantzer R, O'Connor JC, Freund GG, Johnson RW, Kelley KW. 2008. From inflammation to sickness and depression: when the immune system subjugates the brain. Nat Rev Neurosci 9(1):46-56.

Davatelis G, Wolpe SD, Sherry B, Dayer JM, Chicheportiche R, Cerami A. 1989. Macrophage inflammatory protein-1: a prostaglandin-independent endogenous pyrogen. Science 243(4894 Pt 1):1066-1068.

de Oliveira AC, Candelario-Jalil E, Bhatia HS, Lieb K, Hull M, Fiebich BL. 2008. Regulation of prostaglandin E2 synthase expression in activated primary rat microglia: evidence for uncoupled regulation of mPGES-1 and COX-2. Glia 56(8):844-855.

Deiters U, Barsig J, Tawil B, Muhlradt PF. 2004. The macrophage-activating lipopeptide-2 accelerates wound healing in diabetic mice. Exp Dermatol 13(12):731-739.

Denes A, Ferenczi S, Kovacs KJ. 2011. Systemic inflammatory challenges compromise survival after experimental stroke via augmenting brain inflammation, blood- brain barrier damage and brain oedema independently of infarct size. J Neuroinflammation 8:164.

Denes A, Humphreys N, Lane TE, Grencis R, Rothwell N. 2010. Chronic systemic infection exacerbates ischemic brain damage via a CCL5 (regulated on activation, normal T-cell expressed and secreted)-mediated proinflammatory response in mice. J Neurosci 30(30):10086-10095.

Derecki NC, Cardani AN, Yang CH, Quinnies KM, Crihfield A, Lynch KR, Kipnis J. 2010. Regulation of learning and memory by meningeal immunity: a key role for IL-4. J Exp Med 207(5):1067-1080.

Descombes P, Schibler U. 1991. A liver-enriched transcriptional activator protein, LAP, and a transcriptional inhibitory protein, LIP, are translated from the same mRNA. Cell 67(3):569-579.

Desson SE, Ferguson AV. 2003. Interleukin 1beta modulates rat subfornical organ neurons as a result of activation of a non-selective cationic conductance. J Physiol 550(Pt 1):113-122.

Dinarello CA. 1983. Molecular mechanisms in endotoxin fever. Agents Actions 13(5-6):470-486.

Dinarello CA. 2009. Immunological and inflammatory functions of the interleukin-1 family. Annu Rev Immunol 27:519-550.

Dinarello CA. 2010. IL-1: discoveries, controversies and future directions. Eur J Immunol 40(3):599-606.

Dinarello CA, Cannon JG, Mancilla J, Bishai I, Lees J, Coceani F. 1991. Interleukin-6 as an endogenous pyrogen: induction of prostaglandin E2 in brain but not in peripheral blood mononuclear cells. Brain Res 562(2):199-206.

Dinkel K, Dhabhar FS, Sapolsky RM. 2004. Neurotoxic effects of polymorphonuclear granulocytes on hippocampal primary cultures. Proc Natl Acad Sci U S A 101(1):331-336.

Dogan MD, Ataoglu H, Akarsu ES. 2000. Effects of different serotypes of Escherichia coli lipopolysaccharides on body temperature in rats. Life Sci 67(19):2319-2329.

Domenech A, Miro G, Collado VM, Ballesteros N, Sanjose L, Escolar E, Martin S, Gomez-Lucia E. 2011. Use of recombinant interferon omega in feline retrovirosis: from theory to practice. Vet Immunol Immunopathol 143(3-4):301-306.

Dudaronek JM, Barber SA, Clements JE. 2007. CUGBP1 is required for IFNbeta-mediated induction of dominant-negative CEBPbeta and suppression of SIV replication in macrophages. J Immunol 179(11):7262-7269.

Eastman HB, Fawcett TW, Udelsman R, Holbrook NJ. 1996. Effects of perturbations of the hypothalamic-pituitary-adrenal axis on the acute phase response: altered C/EBP and acute phase response gene expression in lipopolysaccharide-treated rats. Shock 6(4):286-292.

Eder K, Baffy N, Falus A, Fulop AK. 2009. The major inflammatory mediator interleukin-6 and obesity. Inflamm Res 58(11):727-736.

Ejarque-Ortiz A, Medina MG, Tusell JM, Perez-Gonzalez AP, Serratosa J, Saura J. 2007. Upregulation of CCAAT/enhancer binding protein beta in activated astrocytes and microglia. Glia 55(2):178-188.

Ek M, Arias C, Sawchenko P, Ericsson-Dahlstrand A. 2000. Distribution of the EP3 prostaglandin E(2) receptor subtype in the rat brain: relationship to sites of interleukin-1-induced cellular responsiveness. J Comp Neurol 428(1):5-20.

Elias CF, Kelly JF, Lee CE, Ahima RS, Drucker DJ, Saper CB, Elmquist JK. 2000. Chemical characterization of leptin-activated neurons in the rat brain. J Comp Neurol 423(2):261-281.

Elmquist JK, Bjorbaek C, Ahima RS, Flier JS, Saper CB. 1998. Distributions of leptin receptor mRNA isoforms in the rat brain. 395(4):535-547.

Elmquist JK, Scammell TE, Jacobson CD, Saper CB. 1996. Distribution of Fos-like immunoreactivity in the rat brain following intravenous lipopolysaccharide administration. J Comp Neurol 371(1):85-103.

Emerich DF, Dean RL, 3rd, Bartus RT. 2002. The role of leukocytes following cerebral ischemia: pathogenic variable or bystander reaction to emerging infarct? Exp Neurol 173(1):168-181.

Engelhardt B. 2006. Molecular mechanisms involved in T cell migration across the blood-brain barrier. J Neural Transm 113(4):477-485.

Engelhardt B, Wolburg H. 2004. Mini-review: Transendothelial migration of leukocytes: through the front door or around the side of the house? Eur J Immunol 34(11):2955-2963.

Engineer DR, Garcia JM. 2012. Leptin in anorexia and cachexia syndrome. Int J Pept 2012:287457.

Faggioni R, Fantuzzi G, Fuller J, Dinarello CA, Feingold KR, Grunfeld C. 1998. IL-1 beta mediates leptin induction during inflammation. Am J Physiol 274(1 Pt 2):R204-208.

Fantuzzi G. 2009. Three questions about leptin and immunity. Brain Behav Immun 23(4):405-410.

Faouzi M, Leshan R, Bjornholm M, Hennessey T, Jones J, Munzberg H. 2007. Differential accessibility of circulating leptin to individual hypothalamic sites. Endocrinology 148(11):5414-5423.

Farooqi IS, Matarese G, Lord GM, Keogh JM, Lawrence E, Agwu C, Sanna V, Jebb SA, Perna F, Fontana S, Lechler RI, DePaoli AM, O'Rahilly S. 2002. Beneficial effects of

leptin on obesity, T cell hyporesponsiveness, and neuroendocrine/metabolic dysfunction of human congenital leptin deficiency. J Clin Invest 110(8):1093-1103.

Fattori E, Cappelletti M, Costa P, Sellitto C, Cantoni L, Carelli M, Faggioni R, Fantuzzi G, Ghezzi P, Poli V. 1994. Defective inflammatory response in interleukin 6-deficient mice. J Exp Med 180(4):1243-1250.

Fenton JI, Hursting SD, Perkins SN, Hord NG. 2007. Leptin induces an Apc genotype-associated colon epithelial cell chemokine production pattern associated with macrophage chemotaxis and activation. Carcinogenesis 28(2):455-464.

Ferguson AV, Li Z. 1996. Whole cell patch recordings from forebrain slices demonstrate angiotensin II inhibits potassium currents in subfornical organ neurons. Regul Pept 66(1-2):55-58.

Fernandes G, Handwerger BS, Yunis EJ, Brown DM. 1978. Immune response in the mutant diabetic C57BL/Ks-dt+ mouse. Discrepancies between in vitro and in vivo immunological assays. J Clin Invest 61(2):243-250.

Fernandes G, Yunis EJ, Good RA. 1976. Influence of diet on survival of mice. Proc Natl Acad Sci U S A 73(4):1279-1283.

Fernandez-Martos CM, Gonzalez P, Rodriguez FJ. 2012. Acute leptin treatment enhances functional recovery after spinal cord injury. PLoS One 7(4):e35594.

Finck BN, Kelley KW, Dantzer R, Johnson RW. 1998. In vivo and in vitro evidence for the involvement of tumor necrosis factor-alpha in the induction of leptin by lipopolysaccharide. Endocrinology 139(5):2278-2283.

Fortier M-E, Kent S, Ashdown H, Poole S, Boksa P, Luheshi GN. 2004. The viral mimic, polyinosinic:polycytidylic acid, induces fever in rats via an interleukin-1-dependent mechanism. Am J Physiol Regul Integr Comp Physiol 287(4):R759-766.

Franchimont D, Kino T, Galon J, Meduri GU, Chrousos G. 2003. Glucocorticoids and Inflammation Revisited: The State of the Art. NIH Clinical Staff Conference. Neuroimmunomodulation 10(5):247-260.

Francis J, MohanKumar PS, MohanKumar SM, Quadri SK. 1999. Systemic administration of lipopolysaccharide increases plasma leptin levels: blockade by soluble interleukin-1 receptor. Endocrine 10(3):291-295.

Friedman JM. 2002. The function of leptin in nutrition, weight, and physiology. Nutr Rev 60(10 Pt 2):S1-14; discussion S68-84, 85-17.

Furness JB, Koopmans HS, Robbins HL, Clerc N, Tobin JM, Morris MJ. 2001. Effects of vagal and splanchnic section on food intake, weight, serum leptin and hypothalamic neuropeptide Y in rat. Auton Neurosci 92(1-2):28-36.

Gaetano L, Watanabe K, Barogi S, Coceani F. 2010. Cyclooxygenase-2/microsomal prostaglandin E synthase-1 complex in the preoptic-anterior hypothalamus of the mouse: involvement through fever to intravenous lipopolysaccharide. Acta Physiol (Oxf) 200(4):315-324.

Gaige S, Abysique A, Bouvier M. 2002. Effects of leptin on cat intestinal vagal mechanoreceptors. J Physiol 543(Pt 2):679-689.

Gainsford T, Willson TA, Metcalf D, Handman E, McFarlane C, Ng A, Nicola NA, Alexander WS, Hilton DJ. 1996. Leptin can induce proliferation, differentiation, and functional activation of hemopoietic cells. Proc Natl Acad Sci U S A 93(25):14564-14568.

Galic MA, Riazi K, Henderson AK, Tsutsui S, Pittman QJ. 2009. Viral-like brain inflammation during development causes increased seizure susceptibility in adult rats. Neurobiol Dis 36(2):343-351.

Gautron L, Elmquist JK. 2011. Sixteen years and counting: an update on leptin in energy balance. J Clin Invest 121(6):2087-2093.

Gautron L, Lafon P, Chaigniau M, Tramu G, Laye S. 2002. Spatiotemporal analysis of signal transducer and activator of transcription 3 activation in rat brain astrocytes and pituitary following peripheral immune challenge. Neuroscience 112(3):717-729.

Gautron L, Lafon P, Tramu G, Laye S. 2003. In vivo activation of the interleukin-6 receptor/gp130 signaling pathway in pituitary corticotropes of lipopolysaccharide-treated rats. Neuroendocrinology 77(1):32-43.

Gautron L, Mingam R, Moranis A, Combe C, Laye S. 2005. Influence of feeding status on neuronal activity in the hypothalamus during lipopolysaccharide-induced anorexia in rats. Neuroscience 134(3):933-946.

Gaykema RP, Dijkstra I, Tilders FJ. 1995. Subdiaphragmatic vagotomy suppresses endotoxin-induced activation of hypothalamic corticotropin-releasing hormone neurons and ACTH secretion. Endocrinology 136(10):4717-4720.

German AJ. 2006. The growing problem of obesity in dogs and cats. J Nutr 136(7 Suppl):1940S-1946S.

German AJ, Ryan VH, German AC, Wood IS, Trayhurn P. 2010. Obesity, its associated disorders and the role of inflammatory adipokines in companion animals. Vet J 185(1):4-9.

Giusti-Paiva A, Ruginsk SG, de Castro M, Elias LL, Carnio EC, Antunes-Rodrigues J. 2003. Role of nitric oxide in lipopolysaccharide-induced release of vasopressin in rats. Neurosci Lett 346(1-2):21-24.

Goebel MU, Trebst AE, Steiner J, Xie YF, Exton MS, Frede S, Canbay AE, Michel MC, Heemann U, Schedlowski M. 2002. Behavioral conditioning of immunosuppression is possible in humans. Faseb J 16(14):1869-1873.

Goehler LE, Gaykema RP, Hammack SE, Maier SF, Watkins LR. 1998. Interleukin-1 induces c-Fos immunoreactivity in primary afferent neurons of the vagus nerve. Brain Res 804(2):306-310.

Goldbach JM, Roth J, Zeisberger E. 1997. Fever suppression by subdiaphragmatic vagotomy in guinea pigs depends on the route of pyrogen administration. Am J Physiol 272(2 Pt 2):R675-681.

Golden PL, Maccagnan TJ, Pardridge WM. 1997. Human blood-brain barrier leptin receptor. Binding and endocytosis in isolated human brain microvessels. J Clin Invest 99(1):14-18.

Gomez-Ambrosi J, Becerril S, Oroz P, Zabalza S, Rodriguez A, Muruzabal FJ, Archanco M, Gil MJ, Burrell MA, Fruhbeck G. 2004. Reduced adipose tissue mass and hypoleptinemia in iNOS deficient mice: effect of LPS on plasma leptin and adiponectin concentrations. FEBS Lett 577(3):351-356.

Greenhill CJ, Rose-John S, Lissilaa R, Ferlin W, Ernst M, Hertzog PJ, Mansell A, Jenkins BJ. 2011. IL-6 trans-signaling modulates TLR4-dependent inflammatory responses via STAT3. J Immunol 186(2):1199-1208.

Greis A, Murgott J, Gerstberger R, Hubschle T, Roth J. 2009. Effects of repeated injections of fibroblast-stimulating lipopeptide-1 on fever, formation of cytokines, and on the responsiveness to endotoxin in guinea-pigs. Acta Physiol (Oxf) 197(1):35-45.

Grill HJ, Schwartz MW, Kaplan JM, Foxhall JS, Breininger J, Baskin DG. 2002. Evidence that the caudal brainstem is a target for the inhibitory effect of leptin on food intake. Endocrinology 143(1):239-246.

Grunfeld C, Zhao C, Fuller J, Pollack A, Moser A, Friedman J, Feingold KR. 1996. Endotoxin and cytokines induce expression of leptin, the ob gene product, in hamsters. J Clin Invest 97(9):2152-2157.

Guan XM, Hess JF, Yu H, Hey PJ, van der Ploeg LH. 1997a. Differential expression of mRNA for leptin receptor isoforms in the rat brain. Mol Cell Endocrinol 133(1):1-7.

Guan XM, Yu H, Van der Ploeg LH, Smith RG. 1997b. Preparation of functionally active [35S]leptin for mapping its receptors in the brain. Anal Biochem 247(1):175-177.

Guerrero MD, Aquino M, Bruno I, Riccio R, Terencio MC, Paya M. 2009. Anti-inflammatory and analgesic activity of a novel inhibitor of microsomal prostaglandin E synthase-1 expression. Eur J Pharmacol 620(1-3):112-119.

Guevara R, Valle A, Gianotti M, Roca P, Oliver J. 2008. Gender-dependent differences in serum profiles of insulin and leptin in caloric restricted rats. Horm Metab Res 40(1):38-43.

Hakansson ML, Brown H, Ghilardi N, Skoda RC, Meister B. 1998. Leptin receptor immunoreactivity in chemically defined target neurons of the hypothalamus. J Neurosci 18(1):559-572.

Halaas JL, Gajiwala KS, Maffei M, Cohen SL, Chait BT, Rabinowitz D, Lallone RL, Burley SK, Friedman JM. 1995. Weight-reducing effects of the plasma protein encoded by the obese gene. Science 269(5223):543-546.

Halterman MW, De Jesus C, Rempe DA, Schor NF, Federoff HJ. 2008. Loss of c/EBP-beta activity promotes the adaptive to apoptotic switch in hypoxic cortical neurons. Mol Cell Neurosci 38(2):125-137.

Hanisch UK. 2002. Microglia as a source and target of cytokines. Glia 40(2):140-155.

Harden LM, du Plessis I, Poole S, Laburn HP. 2006. Interleukin-6 and leptin mediate lipopolysaccharide-induced fever and sickness behavior. Physiol Behav 89(2):146-155.

Harden LM, du Plessis I, Roth J, Loram LC, Poole S, Laburn HP. 2011. Differences in the relative involvement of peripherally released interleukin (IL)-6, brain IL-1beta and prostanoids in mediating lipopolysaccharide-induced fever and sickness behavior. Psychoneuroendocrinology 36(5):608-622.

Harré EM, Roth J, Gerstberger R, Hübschle T. 2003. Interleukin-6 mediates lipopolysaccharide-induced nuclear STAT3 translocation in astrocytes of rat sensory circumventricular organs. Brain Res 980(1):151-155.

Harré EM, Roth J, Pehl U, Kueth M, Gerstberger R, Hubschle T. 2002. Selected contribution: role of IL-6 in LPS-induced nuclear STAT3 translocation in sensory circumventricular organs during fever in rats. J Appl Physiol 92(6):2657-2666.

Harris AK, Ergul A, Kozak A, Machado LS, Johnson MH, Fagan SC. 2005. Effect of neutrophil depletion on gelatinase expression, edema formation and hemorrhagic transformation after focal ischemic stroke. BMC Neurosci 6:49.

Harris RB, Zhou J, Redmann SM, Jr., Smagin GN, Smith SR, Rodgers E, Zachwieja JJ. 1998. A leptin dose-response study in obese (ob/ob) and lean (+/?) mice. Endocrinology 139(1):8-19.

Hart BL. 1988. Biological basis of the behavior of sick animals. Neurosci Biobehav Rev 12(2):123-137.

Hashimoto M, Ueno T, Iriki M. 1994. What roles does the organum vasculosum laminae terminalis play in fever in rabbits? Pflugers Arch 429(1):50-57.

Hawn TR, Verbon A, Lettinga KD, Zhao LP, Li SS, Laws RJ, Skerrett SJ, Beutler B, Schroeder L, Nachman A, Ozinsky A, Smith KD, Aderem A. 2003. A common dominant TLR5 stop codon polymorphism abolishes flagellin signaling and is associated with susceptibility to legionnaires' disease. J Exp Med 198(10):1563-1572.

Hay-Schmidt A, Helboe L, Larsen PJ. 2001. Leptin receptor immunoreactivity is present in ascending serotonergic and catecholaminergic neurons of the rat. Neuroendocrinology 73(4):215-226.

Hayashi T, Cottam HB, Chan M, Jin G, Tawatao RI, Crain B, Ronacher L, Messer K, Carson DA, Corr M. 2008. Mast cell-dependent anorexia and hypothermia induced by

mucosal activation of Toll-like receptor 7. Am J Physiol Regul Integr Comp Physiol 295(1):R123-132.

Hayes MR, Skibicka KP, Leichner TM, Guarnieri DJ, DiLeone RJ, Bence KK, Grill HJ. 2010. Endogenous leptin signaling in the caudal nucleus tractus solitarius and area postrema is required for energy balance regulation. Cell Metab 11(1):77-83.

Heinrich PC, Behrmann I, Muller-Newen G, Schaper F, Graeve L. 1998. Interleukin-6-type cytokine signalling through the gp130/Jak/STAT pathway. Biochem J 334 (Pt 2):297-314.

Helle M, Brakenhoff JP, De Groot ER, Aarden LA. 1988. Interleukin 6 is involved in interleukin 1-induced activities. Eur J Immunol 18(6):957-959.

Hertel M, Braun S, Durka S, Alzheimer C, Werner S. 2002. Upregulation and activation of the Nrf-1 transcription factor in the lesioned hippocampus. Eur J Neurosci 15(10):1707-1711.

Hoebe K, Georgel P, Rutschmann S, Du X, Mudd S, Crozat K, Sovath S, Shamel L, Hartung T, Zahringer U, Beutler B. 2005. CD36 is a sensor of diacylglycerides. Nature 433(7025):523-527.

Holmes JE, Miller NE. 1963. Effects of Bacterial Endotoxin on Water Intake, Food Intake, and Body Temperature in the Albino Rat. J Exp Med 118:649-658.

Hopkins PA, Sriskandan S. 2005. Mammalian Toll-like receptors: to immunity and beyond. Clin Exp Immunol 140(3):395-407.

Hosoi T, Kawagishi T, Okuma Y, Tanaka J, Nomura Y. 2002a. Brain stem is a direct target for leptin's action in the central nervous system. Endocrinology 143(9):3498-3504.

Hosoi T, Okuma Y, Nomura Y. 2002b. Leptin regulates interleukin-1beta expression in the brain via the STAT3-independent mechanisms. Brain Res 949(1-2):139-146.

Howard JK, Lord GM, Matarese G, Vendetti S, Ghatei MA, Ritter MA, Lechler RI, Bloom SR. 1999. Leptin protects mice from starvation-induced lymphoid atrophy and increases thymic cellularity in ob/ob mice. J Clin Invest 104(8):1051-1059.

Hua F, Ma J, Ha T, Kelley J, Williams DL, Kao RL, Kalbfleisch JH, Browder IW, Li C. 2008. Preconditioning with a TLR2 specific ligand increases resistance to cerebral ischemia/reperfusion injury. J Neuroimmunol 199(1-2):75-82.

Hübschle T, Harré EM, Meyerhof W, Pehl U, Roth J, Gerstberger R. 2001a. The central pyrogenic action of interleukin-6 is related to nuclear translocation of STAT3 in the anteroventral preoptic area of the rat brain. J Therm Biol 26:299-305.

Hubschle T, Mutze J, Muhlradt PF, Korte S, Gerstberger R, Roth J. 2006. Pyrexia, anorexia, adipsia, and depressed motor activity in rats during systemic inflammation induced by the Toll-like receptors-2 and -6 agonists MALP-2 and FSL-1. Am J Physiol Regul Integr Comp Physiol 290(1):R180-187.

Hübschle T, Thom E, Watson A, Roth J, Klaus S, Meyerhof W. 2001b. Leptin-induced nuclear translocation of STAT3 immunoreactivity in hypothalamic nuclei involved in body weight regulation. J Neurosci 21(7):2413-2424.

Hummel KP, Dickie MM, Coleman DL. 1966. Diabetes, a new mutation in the mouse. Science 153(3740):1127-1128.

Iida M, Watanabe K, Tsurufuji M, Takaishi K, Iizuka Y, Tsurufuji S. 1992. Level of neutrophil chemotactic factor CINC/gro, a member of the interleukin-8 family, associated with lipopolysaccharide-induced inflammation in rats. Infect Immun 60(4):1268-1272.

Ikejima S, Sasaki S, Sashinami H, Mori F, Ogawa Y, Nakamura T, Abe Y, Wakabayashi K, Suda T, Nakane A. 2005. Impairment of host resistance to Listeria monocytogenes infection in liver of db/db and ob/ob mice. Diabetes 54(1):182-189.

Ingalls AM, Dickie MM, Snell GD. 1950. Obese, a new mutation in the house mouse. J Hered 41(12):317-318.

Inoue H, Yokoyama C, Hara S, Tone Y, Tanabe T. 1995. Transcriptional regulation of human prostaglandin-endoperoxide synthase-2 gene by lipopolysaccharide and phorbol ester in vascular endothelial cells. Involvement of both nuclear factor for interleukin-6 expression site and cAMP response element. J Biol Chem 270(42):24965-24971.

Inoue W, Matsumura K, Yamagata K, Takemiya T, Shiraki T, Kobayashi S. 2002. Brain-specific endothelial induction of prostaglandin E(2) synthesis enzymes and its temporal relation to fever. Neurosci Res 44(1):51-61.

Inoue W, Poole S, Bristow AF, Luheshi GN. 2006. Leptin induces cyclooxygenase-2 via an interaction with interleukin-1beta in the rat brain. Eur J Neurosci 24(8):2233-2245.

Inoue W, Somay G, Poole S, Luheshi GN. 2008. Immune-to-brain signaling and central prostaglandin E2 synthesis in fasted rats with altered lipopolysaccharide-induced fever. Am J Physiol Regul Integr Comp Physiol.

Inyushkin AN, Inyushkina EM, Merkulova NA. 2009. Respiratory responses to microinjections of leptin into the solitary tract nucleus. Neurosci Behav Physiol 39(3):231-240.

Ishihara Y, White CL, Kageyama H, Kageyama A, York DA, Bray GA. 2004. Effects of diet and time of the day on serum and CSF leptin levels in Osborne-Mendel and S5B/Pl rats. Obes Res 12(7):1067-1076.

Ivanov AI, Romanovsky AA. 2004. Prostaglandin E2 as a mediator of fever: synthesis and catabolism. Front Biosci 9:1977-1993.

Jiang N, Moyle M, Soule HR, Rote WE, Chopp M. 1995. Neutrophil inhibitory factor is neuroprotective after focal ischemia in rats. Ann Neurol 38(6):935-942.

Johnson RW. 2002. The concept of sickness behavior: a brief chronological account of four key discoveries. Vet Immunol Immunopathol 87(3-4):443-450.

Jovanovic Z, Yeo GS. 2010. Central leptin signalling: beyond the arcuate nucleus. Auton Neurosci 156(1-2):8-14.

Kano A, Wolfgang MJ, Gao Q, Jacoby J, Chai GX, Hansen W, Iwamoto Y, Pober JS, Flavell RA, Fu XY. 2003. Endothelial cells require STAT3 for protection against endotoxin-induced inflammation. J Exp Med 198(10):1517-1525.

Kapadia R, Tureyen K, Bowen KK, Kalluri H, Johnson PF, Vemuganti R. 2006. Decreased brain damage and curtailed inflammation in transcription factor CCAAT/enhancer binding protein beta knockout mice following transient focal cerebral ischemia. J Neurochem 98(6):1718-1731.

Kaplin A, Bartner S. 2005. Reciprocal communication between the nervous and immune systems: crosstalk, back-talk and motivational speeches. Int Rev Psychiatry 17(6):439-441.

Katafuchi T, Kondo T, Yasaka T, Kubo K, Take S, Yoshimura M. 2003. Prolonged effects of polyriboinosinic:polyribocytidylic acid on spontaneous running wheel activity and brain interferon-alpha mRNA in rats: a model for immunologically induced fatigue. Neuroscience 120(3):837-845.

Kawai T, Akira S. 2011. Toll-like receptors and their crosstalk with other innate receptors in infection and immunity. Immunity 34(5):637-650.

Kawasaki BT, Hurt EM, Kalathur M, Duhagon MA, Milner JA, Kim YS, Farrar WL. 2009. Effects of the sesquiterpene lactone parthenolide on prostate tumor-initiating cells: An integrated molecular profiling approach. Prostate 69(8):827-837.

Kelicen P, Tindberg N. 2004. Lipopolysaccharide induces CYP2E1 in astrocytes through MAP kinase kinase-3 and C/EBPbeta and -delta. J Biol Chem 279(16):15734-15742.

Kent S, Bluthe RM, Kelley KW, Dantzer R. 1992. Sickness behavior as a new target for drug development. Trends Pharmacol Sci 13(1):24-28.

Kerfoot SM, D'Mello C, Nguyen H, Ajuebor MN, Kubes P, Le T, Swain MG. 2006. TNF-alpha-secreting monocytes are recruited into the brain of cholestatic mice. Hepatology 43(1):154-162.

Kielian T. 2006. Toll-like receptors in central nervous system glial inflammation and homeostasis. J Neurosci Res 83(5):711-730.

Kielian T, Barry B, Hickey WF. 2001. CXC chemokine receptor-2 ligands are required for neutrophil-mediated host defense in experimental brain abscesses. J Immunol 166(7):4634-4643.

Kim JB, Sig Choi J, Yu YM, Nam K, Piao CS, Kim SW, Lee MH, Han PL, Park JS, Lee JK. 2006. HMGB1, a novel cytokine-like mediator linking acute neuronal death and delayed neuroinflammation in the postischemic brain. J Neurosci 26(24):6413-6421.

Kim KS. 2003. Pathogenesis of bacterial meningitis: from bacteraemia to neuronal injury. Nat Rev Neurosci 4(5):376-385.

Kim OY, Chae JS, Paik JK, Seo HS, Jang Y, Cavaillon JM, Lee JH. 2012. Effects of aging and menopause on serum interleukin-6 levels and peripheral blood mononuclear cell cytokine production in healthy nonobese women. Age (Dordr) 34(2):415-425.

Kirschning CJ, Wesche H, Merrill Ayres T, Rothe M. 1998. Human toll-like receptor 2 confers responsiveness to bacterial lipopolysaccharide. J Exp Med 188(11):2091-2097.

Kisseleva T, Bhattacharya S, Braunstein J, Schindler CW. 2002. Signaling through the JAK/STAT pathway, recent advances and future challenges. Gene 285(1-2):1-24.

Kitz R, Rose MA, Placzek K, Schulze J, Zielen S, Schubert R. 2008. LPS inhalation challenge: a new tool to characterize the inflammatory response in humans. Med Microbiol Immunol 197(1):13-19.

Kiyatkin EA, Sharma HS. 2009. Permeability of the blood-brain barrier depends on brain temperature. Neuroscience 161(3):926-939.

Kluger MJ. 1991. Fever: role of pyrogens and cryogens. Physiol Rev 71(1):93-127.

Kluger MJ, Rothenburg BA. 1979. Fever and reduced iron: their interaction as a host defense response to bacterial infection. Science 203(4378):374-376.

Kluger MJ, Vaughn LK. 1978. Fever and survival in rabbits infected with Pasteurella multocida. J Physiol 282:243-251.

Knorr C, Hubschle T, Murgott J, Muhlradt P, Gerstberger R, Roth J. 2008. Macrophage-activating lipopeptide-2 (MALP-2) induces a localized inflammatory response in rats resulting in activation of brain sites implicated in fever. Brain Res 1205:36-46.

Kong Y, Le Y. 2011. Toll-like receptors in inflammation of the central nervous system. Int Immunopharmacol 11(10):1407-1414.

Könner AC, Bruning JC. 2011. Toll-like receptors: linking inflammation to metabolism. Trends Endocrinol Metab 22(1):16-23.

Konsman JP, Kelley K, Dantzer R. 1999. Temporal and spatial relationships between lipopolysaccharide-induced expression of Fos, interleukin-1beta and inducible nitric oxide synthase in rat brain. Neuroscience 89(2):535-548.

Konsman JP, Luheshi GN, Bluthe RM, Dantzer R. 2000. The vagus nerve mediates behavioural depression, but not fever, in response to peripheral immune signals; a functional anatomical analysis. Eur J Neurosci 12(12):4434-4446.

Konsman JP, Vigues S, Mackerlova L, Bristow A, Blomqvist A. 2004. Rat brain vascular distribution of interleukin-1 type-1 receptor immunoreactivity: relationship to patterns of inducible cyclooxygenase expression by peripheral inflammatory stimuli. J Comp Neurol 472(1):113-129.

Kopelman PG. 2000. Obesity as a medical problem. Nature 404(6778):635-643.

Kozak W, Kluger MJ, Soszynski D, Conn CA, Rudolph K, Leon LR, Zheng H. 1998. IL-6 and IL-1 beta in fever. Studies using cytokine-deficient (knockout) mice. Ann N Y Acad Sci 856:33-47.

Kozak W, Poli V, Soszynski D, Conn CA, Leon LR, Kluger MJ. 1997. Sickness behavior in mice deficient in interleukin-6 during turpentine abscess and influenza pneumonitis. Am J Physiol 272(2 Pt 2):R621-630.

Kozak W, Wrotek S, Kozak A. 2006. Pyrogenicity of CpG-DNA in mice: role of interleukin-6, cyclooxygenases, and nuclear factor-kappaB. Am J Physiol Regul Integr Comp Physiol 290(4):R871-880.

Kugel D, Kochs G, Obojes K, Roth J, Kobinger GP, Kobasa D, Haller O, Staeheli P, von Messling V. 2009. Intranasal administration of alpha interferon reduces seasonal influenza A virus morbidity in ferrets. J Virol 83(8):3843-3851.

Kukulski F, Ben Yebdri F, Bahrami F, Levesque SA, Martin-Satue M, Sevigny J. 2010. The P2 receptor antagonist PPADS abrogates LPS-induced neutrophil migration in the murine air pouch via inhibition of MIP-2 and KC production. Mol Immunol 47(4):833-839.

Kurosawa M, Uvnas-Moberg K, Miyasaka K, Lundeberg T. 1997. Interleukin-1 increases activity of the gastric vagal afferent nerve partly via stimulation of type A CCK receptor in anesthetized rats. J Auton Nerv Syst 62(1-2):72-78.

Kyrkanides S, Tallents RH, Miller JN, Olschowka ME, Johnson R, Yang M, Olschowka JA, Brouxhon SM, O'Banion MK. 2011. Osteoarthritis accelerates and exacerbates Alzheimer's disease pathology in mice. J Neuroinflammation 8:112.

La Cava A, Matarese G. 2004. The weight of leptin in immunity. Nat Rev Immunol 4(5):371-379.

Lacroix S, Rivest S. 1998. Effect of acute systemic inflammatory response and cytokines on the transcription of the genes encoding cyclooxygenase enzymes (COX-1 and COX-2) in the rat brain. J Neurochem 70(2):452-466.

Laflamme N, Lacroix S, Rivest S. 1999. An essential role of interleukin-1beta in mediating NF-kappaB activity and COX-2 transcription in cells of the blood-brain barrier in response to a systemic and localized inflammation but not during endotoxemia. J Neurosci 19(24):10923-10930.

Laflamme N, Rivest S. 1999. Effects of systemic immunogenic insults and circulating proinflammatory cytokines on the transcription of the inhibitory factor kappaB alpha within specific cellular populations of the rat brain. J Neurochem 73(1):309-321.

Laflamme N, Rivest S. 2001. Toll-like receptor 4: the missing link of the cerebral innate immune response triggered by circulating gram-negative bacterial cell wall components. Faseb J 15(1):155-163.

Laflamme N, Soucy G, Rivest S. 2001. Circulating cell wall components derived from gram-negative, not gram-positive, bacteria cause a profound induction of the gene-encoding Toll-like receptor 2 in the CNS. J Neurochem 79(3):648-657.

Lafrance V, Inoue W, Kan B, Luheshi GN. 2010. Leptin modulates cell morphology and cytokine release in microglia. Brain Behav Immun 24(3):358-365.

Landman RE, Puder JJ, Xiao E, Freda PU, Ferin M, Wardlaw SL. 2003. Endotoxin stimulates leptin in the human and nonhuman primate. J Clin Endocrinol Metab 88(3):1285-1291.

Landschulz WH, Johnson PF, Adashi EY, Graves BJ, McKnight SL. 1988. Isolation of a recombinant copy of the gene encoding C/EBP. Genes Dev 2(7):786-800.

Langhans W, Hrupka B. 1999. Interleukins and tumor necrosis factor as inhibitors of food intake. Neuropeptides 33(5):415-424.

Langhans W, Savoldelli D, Weingarten S. 1993. Comparison of the feeding responses to bacterial lipopolysaccharide and interleukin-1 beta. Physiol Behav 53(4):643-649.

Lawson LJ, Perry VH. 1995. The unique characteristics of inflammatory responses in mouse brain are acquired during postnatal development. Eur J Neurosci 7(7):1584-1595.

Layé S, Gheusi G, Cremona S, Combe C, Kelley K, Dantzer R, Parnet P. 2000. Endogenous brain IL-1 mediates LPS-induced anorexia and hypothalamic cytokine expression. Am J Physiol Regul Integr Comp Physiol 279(1):R93-98.

Layé S, Parnet P, Goujon E, Dantzer R. 1994. Peripheral administration of lipopolysaccharide induces the expression of cytokine transcripts in the brain and pituitary of mice. Brain Res Mol Brain Res 27(1):157-162.

Lazarus M. 2006. The differential role of prostaglandin E2 receptors EP3 and EP4 in regulation of fever. Mol Nutr Food Res 50(4-5):451-455.

Lazarus M, Yoshida K, Coppari R, Bass CE, Mochizuki T, Lowell BB, Saper CB. 2007. EP3 prostaglandin receptors in the median preoptic nucleus are critical for fever responses. Nat Neurosci 10(9):1131-1133.

Le Tulzo Y, Shenkar R, Kaneko D, Moine P, Fantuzzi G, Dinarello CA, Abraham E. 1997. Hemorrhage increases cytokine expression in lung mononuclear cells in mice: involvement of catecholamines in nuclear factor-kappaB regulation and cytokine expression. J Clin Invest 99(7):1516-1524.

Lebel E, Vallieres L, Rivest S. 2000. Selective involvement of interleukin-6 in the transcriptional activation of the suppressor of cytokine signaling-3 in the brain during systemic immune challenges. Endocrinology 141(10):3749-3763.

Lee ES, Zhou H, Henderson AJ. 2001. Endothelial cells enhance human immunodeficiency virus type 1 replication in macrophages through a C/EBP-dependent mechanism. J Virol 75(20):9703-9712.

Lee GH, Proenca R, Montez JM, Carroll KM, Darvishzadeh JG, Lee JI, Friedman JM. 1996. Abnormal splicing of the leptin receptor in diabetic mice. Nature 379(6566):632-635.

Lee J, Chuang TH, Redecke V, She L, Pitha PM, Carson DA, Raz E, Cottam HB. 2003a. Molecular basis for the immunostimulatory activity of guanine nucleoside analogs: activation of Toll-like receptor 7. Proc Natl Acad Sci U S A 100(11):6646-6651.

Lee JJ, Huang WT, Shao DZ, Liao JF, Lin MT. 2003b. Blocking NF-kappaB activation may be an effective strategy in the fever therapy. Jpn J Physiol 53(5):367-375.

Lee WY, Allison MA, Kim DJ, Song CH, Barrett-Connor E. 2007. Association of interleukin-6 and C-reactive protein with subclinical carotid atherosclerosis (the Rancho Bernardo Study). Am J Cardiol 99(1):99-102.

Lehrer P, Karavidas MK, Lu SE, Coyle SM, Oikawa LO, Macor M, Calvano SE, Lowry SF. 2010. Voluntarily produced increases in heart rate variability modulate autonomic effects of endotoxin induced systemic inflammation: an exploratory study. Appl Psychophysiol Biofeedback 35(4):303-315.

Lehrer PM, Vaschillo E, Vaschillo B, Lu SE, Eckberg DL, Edelberg R, Shih WJ, Lin Y, Kuusela TA, Tahvanainen KU, Hamer RM. 2003. Heart rate variability biofeedback increases baroreflex gain and peak expiratory flow. Psychosom Med 65(5):796-805.

Lehrer PM, Vaschillo E, Vaschillo B, Lu SE, Scardella A, Siddique M, Habib RH. 2004. Biofeedback treatment for asthma. Chest 126(2):352-361.

LeMay LG, Vander AJ, Kluger MJ. 1990. Role of interleukin 6 in fever in rats. Am J Physiol Regul Integr Comp Physiol 258(3):R798-803.

Letiembre M, Hao W, Liu Y, Walter S, Mihaljevic I, Rivest S, Hartmann T, Fassbender K. 2007. Innate immune receptor expression in normal brain aging. Neuroscience 146(1):248-254.

Leulier F, Lemaitre B. 2008. Toll-like receptors--taking an evolutionary approach. Nat Rev Genet 9(3):165-178.

Levy RM, Mollen KP, Prince JM, Kaczorowski DJ, Vallabhaneni R, Liu S, Tracey KJ, Lotze MT, Hackam DJ, Fink MP, Vodovotz Y, Billiar TR. 2007. Systemic inflammation and remote organ injury following trauma require HMGB1. Am J Physiol Regul Integr Comp Physiol 293(4):R1538-1544.

Li G, Klein RL, Matheny M, King MA, Meyer EM, Scarpace PJ. 2002a. Induction of uncoupling protein 1 by central interleukin-6 gene delivery is dependent on sympathetic innervation of brown adipose tissue and underlies one mechanism of body weight reduction in rats. Neuroscience 115(3):879-889.

Li S, Wang Y, Matsumura K, Ballou LR, Morham SG, Blatteis CM. 1999. The febrile response to lipopolysaccharide is blocked in cyclooxygenase-2(-/-), but not in cyclooxygenase-1(-/-) mice. Brain Res 825(1-2):86-94.

Li Y, Karlin A, Loike JD, Silverstein SC. 2002b. A critical concentration of neutrophils is required for effective bacterial killing in suspension. Proc Natl Acad Sci U S A 99(12):8289-8294.

Lim G, Wang S, Zhang Y, Tian Y, Mao J. 2009. Spinal leptin contributes to the pathogenesis of neuropathic pain in rodents. J Clin Invest 119(2):295-304.

Liu S, Croniger C, Arizmendi C, Harada-Shiba M, Ren J, Poli V, Hanson RW, Friedman JE. 1999. Hypoglycemia and impaired hepatic glucose production in mice with a deletion of the C/EBPbeta gene. J Clin Invest 103(2):207-213.

Lobbes MB, Lutgens E, Heeneman S, Cleutjens KB, Kooi ME, van Engelshoven JM, Daemen MJ, Nelemans PJ. 2006. Is there more than C-reactive protein and fibrinogen? The prognostic value of soluble CD40 ligand, interleukin-6 and oxidized low-density lipoprotein with respect to coronary and cerebral vascular disease. Atherosclerosis 187(1):18-25.

Loffreda S, Yang SQ, Lin HZ, Karp CL, Brengman ML, Wang DJ, Klein AS, Bulkley GB, Bao C, Noble PW, Lane MD, Diehl AM. 1998. Leptin regulates proinflammatory immune responses. Faseb J 12(1):57-65.

Long NC, Kunkel SL, Vander AJ, Kluger MJ. 1990. Antiserum against tumor necrosis factor enhances lipopolysaccharide fever in rats. Am J Physiol Regul Integr Comp Physiol 258(2):R332-337.

Lord GM, Matarese G, Howard JK, Baker RJ, Bloom SR, Lechler RI. 1998. Leptin modulates the T-cell immune response and reverses starvation-induced immunosuppression. Nature 394(6696):897-901.

Lorton D, Lubahn CL, Estus C, Millar BA, Carter JL, Wood CA, Bellinger DL. 2006. Bidirectional communication between the brain and the immune system: implications for physiological sleep and disorders with disrupted sleep. Neuroimmunomodulation 13(5-6):357-374.

Lu D, Willard D, Patel IR, Kadwell S, Overton L, Kost T, Luther M, Chen W, Woychik RP, Wilkison WO, et al. 1994. Agouti protein is an antagonist of the melanocyte-stimulating-hormone receptor. Nature 371(6500):799-802.

Lu H, Wagner WM, Gad E, Yang Y, Duan H, Amon LM, Van Denend N, Larson ER, Chang A, Tufvesson H, Disis ML. 2010. Treatment failure of a TLR-7 agonist occurs due to self-regulation of acute inflammation and can be overcome by IL-10 blockade. J Immunol 184(9):5360-5367.

Lu YC, Kim I, Lye E, Shen F, Suzuki N, Suzuki S, Gerondakis S, Akira S, Gaffen SL, Yeh WC, Ohashi PS. 2009. Differential role for c-Rel and C/EBPbeta/delta in TLR-mediated induction of proinflammatory cytokines. J Immunol 182(11):7212-7221.

Lucin KM, Wyss-Coray T. 2009. Immune activation in brain aging and neurodegeneration: too much or too little? Neuron 64(1):110-122.

Luheshi G, Hopkins SJ, Lefeuvre RA, Dascombe MJ, Ghiara P, Rothwell NJ. 1993. Importance of brain IL-1 type II receptors in fever and thermogenesis in the rat. Am J Physiol 265(4 Pt 1):E585-591.

Luheshi GN, Bluthe RM, Rushforth D, Mulcahy N, Konsman JP, Goldbach M, Dantzer R. 2000. Vagotomy attenuates the behavioural but not the pyrogenic effects of interleukin-1 in rats. Auton Neurosci 85(1-3):127-132.

Luheshi GN, Gardner JD, Rushforth DA, Loudon AS, Rothwell NJ. 1999. Leptin actions on food intake and body temperature are mediated by IL-1. Proc Natl Acad Sci U S A 96(12):7047-7052.

Luheshi GN, Rummel C. 2007. Is programming of weight regulation immune to neonatal inflammation? Am J Physiol Regul Integr Comp Physiol 293(2):R578-580.

Luheshi GN, Stefferl A, Turnbull AV, Dascombe MJ, Brouwer S, Hopkins SJ, Rothwell NJ. 1997. Febrile response to tissue inflammation involves both peripheral and brain IL-1 and TNF-alpha in the rat. Am J Physiol 272(3 Pt 2):R862-868.

Lumeng CN, Saltiel AR. 2011. Inflammatory links between obesity and metabolic disease. J Clin Invest 121(6):2111-2117.

Lutz TA. 2010. The role of amylin in the control of energy homeostasis. Am J Physiol Regul Integr Comp Physiol 298(6):R1475-1484.

Ma F, Zhang J, Zhang C. 2010. The TLR7 agonists imiquimod and gardiquimod improve DC-based immunotherapy for melanoma in mice. Cell Mol Immunol 7(5):381-388.

Machado RR, Soares DM, Proudfoot AE, Souza GE. 2007. CCR1 and CCR5 chemokine receptors are involved in fever induced by LPS (E. coli) and RANTES in rats. Brain Res 1161:21-31.

Mackowiak PA, Browne RH, Southern PM, Jr., Smith JW. 1980. Polymicrobial sepsis: an analysis of 184 cases using log linear models. Am J Med Sci 280(2):73-80.

Maeda T, Kiguchi N, Kobayashi Y, Ikuta T, Ozaki M, Kishioka S. 2009. Leptin derived from adipocytes in injured peripheral nerves facilitates development of neuropathic pain via macrophage stimulation. Proc Natl Acad Sci U S A 106(31):13076-13081.

Maffei M, Halaas J, Ravussin E, Pratley RE, Lee GH, Zhang Y, Fei H, Kim S, Lallone R, Ranganathan S, et al. 1995. Leptin levels in human and rodent: measurement of plasma leptin and ob RNA in obese and weight-reduced subjects. Nat Med 1(11):1155-1161.

Maffei M, Stoffel M, Barone M, Moon B, Dammerman M, Ravussin E, Bogardus C, Ludwig DS, Flier JS, Talley M, et al. 1996. Absence of mutations in the human OB gene in obese/diabetic subjects. Diabetes 45(5):679-682.

Maier SF, Goehler LE, Fleshner M, Watkins LR. 1998. The role of the vagus nerve in cytokine-to-brain communication. Ann N Y Acad Sci 840:289-300.

Majoie HJ, Rijkers K, Berfelo MW, Hulsman JA, Myint A, Schwarz M, Vles JS. 2011. Vagus nerve stimulation in refractory epilepsy: effects on pro- and anti-inflammatory cytokines in peripheral blood. Neuroimmunomodulation 18(1):52-56.

Malvar Ddo C, Soares DM, Fabricio AS, Kanashiro A, Machado RR, Figueiredo MJ, Rae GA, de Souza GE. 2011. The antipyretic effect of dipyrone is unrelated to inhibition of PGE(2) synthesis in the hypothalamus. Br J Pharmacol 162(6):1401-1409.

Mancuso P, Gottschalk A, Phare SM, Peters-Golden M, Lukacs NW, Huffnagle GB. 2002. Leptin-deficient mice exhibit impaired host defense in Gram-negative pneumonia. J Immunol 168(8):4018-4024.

Marvel FA, Chen CC, Badr N, Gaykema RP, Goehler LE. 2004. Reversible inactivation of the dorsal vagal complex blocks lipopolysaccharide-induced social withdrawal and c-Fos expression in central autonomic nuclei. Brain Behav Immun 18(2):123-134.

Mastorakos G, Weber JS, Magiakou MA, Gunn H, Chrousos GP. 1994. Hypothalamic-pituitary-adrenal axis activation and stimulation of systemic vasopressin secretion by recombinant interleukin-6 in humans: potential implications for the syndrome of inappropriate vasopressin secretion. J Clin Endocrinol Metab 79(4):934-939.

Matarese G, Di Giacomo A, Sanna V, Lord GM, Howard JK, Di Tuoro A, Bloom SR, Lechler RI, Zappacosta S, Fontana S. 2001. Requirement for leptin in the induction and progression of autoimmune encephalomyelitis. J Immunol 166(10):5909-5916.

Matarese G, Moschos S, Mantzoros CS. 2005. Leptin in immunology. J Immunol 174(6):3137-3142.

Matsumura K, Kobayashi S. 2004. Signaling the brain in inflammation: the role of endothelial cells. Front Biosci 9:2819-2826.

Matsumura K, Watanabe Y, Onoe H, Hayaishi O. 1990. High density of prostaglandin E2 binding sites in the anterior wall of the 3rd ventricle: a possible site of its hyperthermic action. Brain Res 533(1):147-151.

Matsunaga W, Miyata S, Takamata A, Bun H, Nakashima T, Kiyohara T. 2000. LPS-induced Fos expression in oxytocin and vasopressin neurons of the rat hypothalamus. Brain Res 858(1):9-18.

Matsuo Y, Onodera H, Shiga Y, Nakamura M, Ninomiya M, Kihara T, Kogure K. 1994. Correlation between myeloperoxidase-quantified neutrophil accumulation and ischemic brain injury in the rat. Effects of neutrophil depletion. Stroke 25(7):1469-1475.

Mayer K, Kiessling A, Ott J, Schaefer MB, Hecker M, Henneke I, Schulz R, Gunther A, Wang J, Wu L, Roth J, Seeger W, Kang JX. 2009. Acute lung injury is reduced in fat-1 mice endogenously synthesizing n-3 fatty acids. Am J Respir Crit Care Med 179(6):474-483.

McAllister AK, van de Water J. 2009. Breaking boundaries in neural-immune interactions. Neuron 64(1):9-12.

McColl BW, Allan SM, Rothwell NJ. 2009. Systemic infection, inflammation and acute ischemic stroke. Neuroscience 158(3):1049-1061.

McColl BW, Rothwell NJ, Allan SM. 2007. Systemic inflammatory stimulus potentiates the acute phase and CXC chemokine responses to experimental stroke and exacerbates brain damage via interleukin-1- and neutrophil-dependent mechanisms. J Neurosci 27(16):4403-4412.

McGettrick AF, O'Neill LA. 2007. Toll-like receptors: key activators of leucocytes and regulator of haematopoiesis. Br J Haematol 139(2):185-193.

McKay LI, Cidlowski JA. 1999. Molecular control of immune/inflammatory responses: interactions between nuclear factor-kappa B and steroid receptor-signaling pathways. Endocr Rev 20(4):435-459.

McKinley MJ, Allen AM, Burns P, Colvill LM, Oldfield BJ. 1998. Interaction of circulating hormones with the brain: the roles of the subfornical organ and the organum vasculosum of the lamina terminalis. Clin Exp Pharmacol Physiol Suppl 25:S61-67.

Medawar PB. 1948. Immunity to homologous grafted skin; the fate of skin homografts transplanted to the brain, to subcutaneous tissue, and to the anterior chamber of the eye. Br J Exp Pathol 29(1):58-69.

Meister B, Hakansson ML. 2001. Leptin receptors in hypothalamus and circumventricular organs. Clin Exp Pharmacol Physiol 28(7):610-617.

Meuth SG, Gobel K, Wiendl H. 2012. Immune Therapy of Multiple Sclerosis - Future Strategies. Curr Pharm Des.

Mildner A, Schmidt H, Nitsche M, Merkler D, Hanisch UK, Mack M, Heikenwalder M, Bruck W, Priller J, Prinz M. 2007. Microglia in the adult brain arise from Ly-6ChiCCR2+ monocytes only under defined host conditions. Nat Neurosci 10(12):1544-1553.

Miller AJ, Luheshi GN, Rothwell NJ, Hopkins SJ. 1997. Local cytokine induction by LPS in the rat air pouch and its relationship to the febrile response. Am J Physiol 272(3 Pt 2):R857-861.

Miller RL, Meng TC, Tomai MA. 2008. The antiviral activity of Toll-like receptor 7 and 7/8 agonists. Drug News Perspect 21(2):69-87.

Miyaji EN, Carvalho E, Oliveira ML, Raw I, Ho PL. 2011. Trends in adjuvant development for vaccines: DAMPs and PAMPs as potential new adjuvants. Braz J Med Biol Res 44(6):500-513.

Miyamoto H, Ogawa M, Maruta K, Nikaido Y, Yamamoto C, Taniguchi H, Yoshida S. 1995. Temperature effects on Legionella pneumophila killing by and multiplication in phagocytes of guinea pigs. Microbiol Immunol 39(9):647-654.

Moldawer LL, Georgieff M, Lundholm K. 1987. Interleukin 1, tumour necrosis factor-alpha (cachectin) and the pathogenesis of cancer cachexia. Clin Physiol 7(4):263-274.

Montecucco F, Bianchi G, Gnerre P, Bertolotto M, Dallegri F, Ottonello L. 2006. Induction of neutrophil chemotaxis by leptin: crucial role for p38 and Src kinases. Ann N Y Acad Sci 1069:463-471.

Morimoto A, Murakami N, Takada M, Teshirogi S, Watanabe T. 1987. Fever and acute phase response induced in rabbits by human recombinant interferon-gamma. J Physiol 391:209-218.

Morr M, Takeuchi O, Akira S, Simon MM, Muhlradt PF. 2002. Differential recognition of structural details of bacterial lipopeptides by toll-like receptors. Eur J Immunol 32(12):3337-3347.

Morrison SF. 2004. Activation of 5-HT1A receptors in raphe pallidus inhibits leptin-evoked increases in brown adipose tissue thermogenesis. Am J Physiol Regul Integr Comp Physiol 286(5):R832-837.

Moyse E, Bedard K, Segura S, Mahaut S, Tardivel C, Ferland G, Lebrun B, Gaudreau P. 2012. Effects of aging and caloric restriction on brainstem satiety center signals in rats. Mech Ageing Dev 133(2-3):83-91.

Muhammad S, Barakat W, Stoyanov S, Murikinati S, Yang H, Tracey KJ, Bendszus M, Rossetti G, Nawroth PP, Bierhaus A, Schwaninger M. 2008. The HMGB1 receptor RAGE mediates ischemic brain damage. J Neurosci 28(46):12023-12031.

Muller DM, Pender MP, Greer JM. 2005. Blood-brain barrier disruption and lesion localisation in experimental autoimmune encephalomyelitis with predominant cerebellar and brainstem involvement. J Neuroimmunol 160(1-2):162-169.

Münzberg H, Huo L, Nillni EA, Hollenberg AN, Bjorbaek C. 2003. Role of signal transducer and activator of transcription 3 in regulation of hypothalamic proopiomelanocortin gene expression by leptin. Endocrinology 144(5):2121-2131.

Murray MJ, Murray AB. 1979. Anorexia of infection as a mechanism of host defense. Am J Clin Nutr 32(3):593-596.

Mütze J, Roth J, Gerstberger R, Hübschle T. 2007. Nuclear translocation of the transcription factor STAT5 in the rat brain after systemic leptin administration. Neurosci Lett 417(3):286-291.

Mütze J, Roth J, Gerstberger R, Matsumura K, Hübschle T. 2006. Immunohistochemical evidence of functional leptin receptor expression in neuronal and endothelial cells of the rat brain. Neurosci Lett 394(2):105-110.

Myers MG, Cowley MA, Munzberg H. 2008. Mechanisms of leptin action and leptin resistance. Annu Rev Physiol 70:537-556.

Myers MG, Jr. 2004. Leptin receptor signaling and the regulation of mammalian physiology. Recent Prog Horm Res 59:287-304.

Myers MG, Jr., Leibel RL, Seeley RJ, Schwartz MW. 2010. Obesity and leptin resistance: distinguishing cause from effect. Trends Endocrinol Metab 21(11):643-651.

Nadeau S, Hein P, Fernandes KJ, Peterson AC, Miller FD. 2005. A transcriptional role for C/EBP beta in the neuronal response to axonal injury. Mol Cell Neurosci 29(4):525-535.

Nadeau S, Rivest S. 1999. Effects of circulating tumor necrosis factor on the neuronal activity and expression of the genes encoding the tumor necrosis factor receptors (p55 and p75) in the rat brain: a view from the blood-brain barrier. Neuroscience 93(4):1449-1464.

Nadjar A, Bluthe RM, May MJ, Dantzer R, Parnet P. 2005a. Inactivation of the cerebral NFkappaB pathway inhibits interleukin-1beta-induced sickness behavior and c-Fos expression in various brain nuclei. Neuropsychopharmacology 30(8):1492-1499.

Nadjar A, Combe C, Layé S, Tridon V, Dantzer R, Amedee T, Parnet P. 2003. Nuclear factor κB nuclear translocation as a crucial marker of brain response to interleukin-1. A study in rat and interleukin-1 type I deficient mouse. J Neurochem 87(4):1024-1036.

Nadjar A, Tridon V, May MJ, Ghosh S, Dantzer R, Amedee T, Parnet P. 2005b. NFkappaB activates in vivo the synthesis of inducible Cox-2 in the brain. J Cereb Blood Flow Metab 25(8):1047-1059.

Nakamura K. 2011. Central circuitries for body temperature regulation and fever. Am J Physiol Regul Integr Comp Physiol 301(5):R1207-1228.

Navarro-Millan I, Singh JA, Curtis JR. 2012. Systematic review of tocilizumab for rheumatoid arthritis: a new biologic agent targeting the interleukin-6 receptor. Clin Ther 34(4):788-802 e783.

Nijsten MW, de Groot ER, ten Duis HJ, Klasen HJ, Hack CE, Aarden LA. 1987. Serum levels of interleukin-6 and acute phase responses. Lancet 2(8564):921.

Nilsberth C, Elander L, Hamzic N, Norell M, Lonn J, Engstrom L, Blomqvist A. 2009a. The role of interleukin-6 in lipopolysaccharide-induced fever by mechanisms independent of prostaglandin E2. Endocrinology 150(4):1850-1860.

Nilsberth C, Hamzic N, Norell M, Blomqvist A. 2009b. Peripheral lipopolysaccharide administration induces cytokine mRNA expression in the viscera and brain of fever-refractory mice lacking microsomal prostaglandin E synthase-1. J Neuroendocrinol 21(8):715-721.

Nimmerjahn A, Kirchhoff F, Helmchen F. 2005. Resting microglial cells are highly dynamic surveillants of brain parenchyma in vivo. Science 308(5726):1314-1318.

Oka Y, Ibuki T, Matsumura K, Namba M, Yamazaki Y, Poole S, Tanaka Y, Kobayashi S. 2007. Interleukin-6 is a candidate molecule that transmits inflammatory information to the CNS. Neuroscience 145(2):530-538.

Oliff A, Defeo-Jones D, Boyer M, Martinez D, Kiefer D, Vuocolo G, Wolfe A, Socher SH. 1987. Tumors secreting human TNF/cachectin induce cachexia in mice. Cell 50(4):555-563.

Olson JK, Miller SD. 2004. Microglia initiate central nervous system innate and adaptive immune responses through multiple TLRs. J Immunol 173(6):3916-3924.

Ott D, Murgott J, Rafalzik S, Wuchert F, Schmalenbeck B, Roth J, Gerstberger R. 2010. Neurons and glial cells of the rat organum vasculosum laminae terminalis directly respond to lipopolysaccharide and pyrogenic cytokines. Brain Res 1363:93-106.

Ozaki K, Leonard WJ. 2002. Cytokine and cytokine receptor pleiotropy and redundancy. J Biol Chem 277(33):29355-29358.

Ozata M, Ozdemir IC, Licinio J. 1999. Human leptin deficiency caused by a missense mutation: multiple endocrine defects, decreased sympathetic tone, and immune system dysfunction indicate new targets for leptin action, greater central than peripheral resistance to the effects of leptin, and spontaneous correction of leptin-mediated defects. J Clin Endocrinol Metab 84(10):3686-3695.

Ozinsky A, Underhill DM, Fontenot JD, Hajjar AM, Smith KD, Wilson CB, Schroeder L, Aderem A. 2000. The repertoire for pattern recognition of pathogens by the innate immune system is defined by cooperation between toll-like receptors. Proc Natl Acad Sci U S A 97(25):13766-13771.

Pagenstecher A, Stalder AK, Kincaid CL, Volk B, Campbell IL. 2000. Regulation of matrix metalloproteinases and their inhibitor genes in lipopolysaccharide-induced endotoxemia in mice. Am J Pathol 157(1):197-210.

Pahan K, Jana M, Liu X, Taylor BS, Wood C, Fischer SM. 2002. Gemfibrozil, a lipid-lowering drug, inhibits the induction of nitric-oxide synthase in human astrocytes. J Biol Chem 277(48):45984-45991.

Palin K, Bluthe RM, McCusker RH, Moos F, Dantzer R, Kelley KW. 2007. TNFalpha-induced sickness behavior in mice with functional 55 kD TNF receptors is blocked by central IGF-I. J Neuroimmunol 187(1-2):55-60.

Palin K, Moreau ML, Orcel H, Duvoid-Guillou A, Rabie A, Kelley KW, Moos F. 2008. Age-impaired fluid homeostasis depends on the balance of IL-6/IGF-I in the rat supraoptic nuclei. Neurobiol Aging.

Pandey DK, Rajkumar R, Mahesh R, Radha R. 2008. Depressant-like effects of parthenolide in a rodent behavioural antidepressant test battery. J Pharm Pharmacol 60(12):1643-1650.

Papadimitriou A, Priftis KN. 2009. Regulation of the hypothalamic-pituitary-adrenal axis. Neuroimmunomodulation 16(5):265-271.

Patel M, Xu D, Kewin P, Choo-Kang B, McSharry C, Thomson NC, Liew FY. 2005. TLR2 agonist ameliorates established allergic airway inflammation by promoting Th1 response and not via regulatory T cells. J Immunol 174(12):7558-7563.

Pecchi E, Dallaporta M, Jean A, Thirion S, Troadec JD. 2009. Prostaglandins and sickness behavior: old story, new insights. Physiol Behav 97(3-4):279-292.

Perez-Capote K, Saura J, Serratosa J, Sola C. 2006. Expression of C/EBPalpha and C/EBPbeta in glial cells in vitro after inducing glial activation by different stimuli. Neurosci Lett 410(1):25-30.

Perlstein RS, Whitnall MH, Abrams JS, Mougey EH, Neta R. 1993. Synergistic roles of interleukin-6, interleukin-1, and tumor necrosis factor in the adrenocorticotropin response to bacterial lipopolysaccharide in vivo. Endocrinology 132(3):946-952.

Perry VH, Cunningham C, Holmes C. 2007. Systemic infections and inflammation affect chronic neurodegeneration. Nat Rev Immunol 7(2):161-167.

Peters JH, McKay BM, Simasko SM, Ritter RC. 2005. Leptin-induced satiation mediated by abdominal vagal afferents. Am J Physiol Regul Integr Comp Physiol 288(4):R879-884.

Peters JH, Ritter RC, Simasko SM. 2006. Leptin and CCK selectively activate vagal afferent neurons innervating the stomach and duodenum. Am J Physiol Regul Integr Comp Physiol 290(6):R1544-1549.

Pintado C, Revilla E, Vizuete ML, Jimenez S, Garcia-Cuervo L, Vitorica J, Ruano D, Castano A. 2011. Regional difference in inflammatory response to LPS-injection in the brain: role of microglia cell density. J Neuroimmunol 238(1-2):44-51.

Pinteaux E, Inoue W, Schmidt L, Molina-Holgado F, Rothwell NJ, Luheshi GN. 2007. Leptin induces interleukin-1beta release from rat microglial cells through a caspase 1 independent mechanism. J Neurochem.

Pollmächer T, Haack M, Schuld A, Reichenberg A, Yirmiya R. 2002. Low levels of circulating inflammatory cytokines--do they affect human brain functions? Brain Behav Immun 16(5):525-532.

Pope RM, Lovis R, Mungre S, Perlman H, Koch AE, Haines GK, 3rd. 1999. C/EBP beta in rheumatoid arthritis: correlation with inflammation, not disease specificity. Clin Immunol 91(3):271-282.

Porter MH, Hrupka BJ, Langhans W, Schwartz GJ. 1998. Vagal and splanchnic afferents are not necessary for the anorexia produced by peripheral IL-1beta, LPS, and MDP. Am J Physiol 275(2 Pt 2):R384-389.

Potes CS, Lutz TA. 2010. Brainstem mechanisms of amylin-induced anorexia. Physiol Behav 100(5):511-518.

Proescholdt MG, Chakravarty S, Foster JA, Foti SB, Briley EM, Herkenham M. 2002. Intracerebroventricular but not intravenous interleukin-1beta induces widespread vascular-mediated leukocyte infiltration and immune signal mRNA expression followed by brain-wide glial activation. Neuroscience 112(3):731-749.

Qin L, Wu X, Block ML, Liu Y, Breese GR, Hong JS, Knapp DJ, Crews FT. 2007. Systemic LPS causes chronic neuroinflammation and progressive neurodegeneration. Glia 55(5):453-462.

Quan N. 2008. Immune-to-brain signaling: how important are the blood-brain barrier-independent pathways? Mol Neurobiol 37(2-3):142-152.

Quan N, Whiteside M, Kim L, Herkenham M. 1997. Induction of inhibitory factor κBα mRNA in the central nervous system after peripheral lipopolysaccharide administration: an in situ hybridization histochemistry study in the rat. Proc Natl Acad Sci U S A 94(20):10985-10990.

Ramji DP, Foka P. 2002. CCAAT/enhancer-binding proteins: structure, function and regulation. Biochem J 365(Pt 3):561-575.

Ransohoff RM, Kivisakk P, Kidd G. 2003. Three or more routes for leukocyte migration into the central nervous system. Nat Rev Immunol 3(7):569-581.

Redd WH, Dadds MR, Futterman AD, Taylor KL, Bovbjerg DH. 1993. Nausea induced by mental images of chemotherapy. Cancer 72(2):629-636.

Rennie KL, Jebb SA. 2005. Prevalence of obesity in Great Britain. Obes Rev 6(1):11-12.

Rharbaoui F, Drabner B, Borsutzky S, Winckler U, Morr M, Ensoli B, Muhlradt PF, Guzman CA. 2002. The Mycoplasma-derived lipopeptide MALP-2 is a potent mucosal adjuvant. Eur J Immunol 32(10):2857-2865.

Riazi K, Galic MA, Kuzmiski JB, Ho W, Sharkey KA, Pittman QJ. 2008. Microglial activation and TNFalpha production mediate altered CNS excitability following peripheral inflammation. Proc Natl Acad Sci U S A 105(44):17151-17156.

Riedel W, Lang U, Oetjen U, Schlapp U, Shibata M. 2003. Inhibition of oxygen radical formation by methylene blue, aspirin, or alpha-lipoic acid, prevents bacterial-lipopolysaccharide-induced fever. Mol Cell Biochem 247(1-2):83-94.

Riediger T, Cordani C, Potes CS, Lutz TA. 2010. Involvement of nitric oxide in lipopolysaccharide induced anorexia. Pharmacol Biochem Behav 97(1):112-120.

Riediger T, Rauch M, Schmid HA. 1999. Actions of amylin on subfornical organ neurons and on drinking behavior in rats. Am J Physiol 276(2 Pt 2):R514-521.

Riediger T, Schmid HA, Lutz T, Simon E. 2001. Amylin potently activates AP neurons possibly via formation of the excitatory second messenger cGMP. Am J Physiol Regul Integr Comp Physiol 281(6):R1833-1843.

Rijkers K, Aalbers M, Hoogland G, van Winden L, Vles J, Steinbusch H, Majoie M. 2010. Acute seizure-suppressing effect of vagus nerve stimulation in the amygdala kindled rat. Brain Res 1319:155-163.

Rivest S. 1999. Activation of the nuclear factor kappa B (NF-kappaB) and cyclooxygenase-2 (COX-2) genes in cerebral blood vessels in response to systemic inflammation. Mol Psychiatry 4(6):500.

Rivest S. 2003. Molecular insights on the cerebral innate immune system. Brain Behav Immun 17(1):13-19.

Rivest S. 2009. Regulation of innate immune responses in the brain. Nat Rev Immunol 9(6):429-439.

Rock FL, Hardiman G, Timans JC, Kastelein RA, Bazan JF. 1998. A family of human receptors structurally related to Drosophila Toll. Proc Natl Acad Sci U S A 95(2):588-593.

Romanovsky AA. 2004. Signaling the brain in the early sickness syndrome: are sensory nerves involved? Front Biosci 9:494-504.

Romanovsky AA. 2007. Thermoregulation: some concepts have changed. Functional architecture of the thermoregulatory system. Am J Physiol Regul Integr Comp Physiol 292(1):R37-46.

Romanovsky AA, Shido O, Sakurada S, Sugimoto N, Nagasaka T. 1996. Endotoxin shock: thermoregulatory mechanisms. Am J Physiol 270(4 Pt 2):R693-703.

Ron-Harel N, Cardon M, Schwartz M. 2011. Brain homeostasis is maintained by "danger" signals stimulating a supportive immune response within the brain's borders. Brain Behav Immun 25(5):1036-1043.

Rosenberg GA, Estrada EY, Mobashery S. 2007. Effect of synthetic matrix metalloproteinase inhibitors on lipopolysaccharide-induced blood-brain barrier opening in rodents: Differences in response based on strains and solvents. Brain Res 1133(1):186-192.

Rosenspire AJ, Kindzelskii AL, Petty HR. 2002. Cutting edge: fever-associated temperatures enhance neutrophil responses to lipopolysaccharide: a potential mechanism involving cell metabolism. J Immunol 169(10):5396-5400.

Ross G, Hübschle T, Pehl U, Braun HA, Voigt K, Gerstberger R, Roth J. 2003. Fever induction by localized subcutaneous inflammation in guinea pigs: the role of cytokines and prostaglandins. J Appl Physiol 94(4):1395-1402.

Ross G, Hübschle, T., Bickenbach, A., Zeisberger, E., Gerstberger, R., Roth, J. 2001. Febrile and cortisol responses induced in guinea pigs by localized peripheral inflammatory stimulation. J Therm Biol 26:319-324.

Ross G, Roth J, Storr B, Voigt K, Zeisberger E. 2000. Afferent nerves are involved in the febrile response to injection of LPS into artificial subcutaneous chambers in guinea pigs. Physiol Behav 71(3-4):305-313.

Roth J, Aslan T, Storr B, Zeisberger E. 1997. Lack of cross tolerance between LPS and muramyl dipeptide in induction of circulating TNF-alpha and IL-6 in guinea pigs. Am J Physiol 273(4 Pt 2):R1529-1533.

Roth J, Conn CA, Kluger MJ, Zeisberger E. 1993. Kinetics of systemic and intrahypothalamic IL-6 and tumor necrosis factor during endotoxin fever in guinea pigs. Am J Physiol 265(3 Pt 2):R653-658.

Roth J, De Souza GE. 2001. Fever induction pathways: evidence from responses to systemic or local cytokine formation. Braz J Med Biol Res 34(3):301-314.

Roth J, Harré EM, Rummel C, Gerstberger R, Hübschle T. 2004a. Signaling the brain in systemic inflammation: role of sensory circumventricular organs. Front Biosci 9:290-300.

Roth J, Martin D, Storr B, Zeisberger E. 1998. Neutralization of pyrogen-induced tumour necrosis factor by its type 1 soluble receptor in guinea-pigs: effects on fever and interleukin-6 release. J Physiol 509 (Pt 1):267-275.

Roth J, McClellan J, Kluger M, Zeisberger E. 1994a. Attenuation of fever and release of cytokines after repeated injections of lipopolysaccharide in guinea-pigs. J Physiol (Lond) 477(1):177-185.

Roth J, McClellan JL, Kluger MJ, Zeisberger E. 1994b. Attenuation of fever and release of cytokines after repeated injections of lipopolysaccharide in guinea-pigs. J Physiol 477 (Pt 1):177-185.

Roth J, Rummel C, Barth SW, Gerstberger R, Hübschle T. 2006. Molecular aspects of fever and hyperthermia. Neurol Clin 24(3):421-439, v.

Roth J, Rummel C, Barth SW, Gerstberger R, Hübschle T. 2009. Molecular aspects of fever and hyperthermia. Immunol Allergy Clin North Am 29(2):229-245.

Roth J, Rummel C, Harré EM, Voss T, Mütze J, Gerstberger R, Hübschle T. 2004b. Is interleukin-6 the necessary pyrogenic cytokine? J Therm Biol 29(7-8):383-389.

Roth J, Rummel, C., Harré, E. M., Voss, T., Mütze, J., Gerstberger, R., Hübschle, T. 2004. Is interleukin-6 the necessary pyrogenic cytokine? Journal of Thermal Biology 29(7-8):383-389.

Roubos EW, Dahmen M, Kozicz T, Xu L. 2012. Leptin and the hypothalamo-pituitary-adrenal stress axis. Gen Comp Endocrinol 177(1):28-36.

Rovai LE, Herschman HR, Smith JB. 1998. The murine neutrophil-chemoattractant chemokines LIX, KC, and MIP-2 have distinct induction kinetics, tissue distributions, and tissue-specific sensitivities to glucocorticoid regulation in endotoxemia. J Leukoc Biol 64(4):494-502.

Rudaya AY, Steiner AA, Robbins JR, Dragic AS, Romanovsky AA. 2005. Thermoregulatory responses to lipopolysaccharide in the mouse: dependence on the dose and ambient temperature. Am J Physiol Regul Integr Comp Physiol 289(5):R1244-1252.

Rummel C, Barth SW, Voss T, Korte S, Gerstberger R, Hübschle T, Roth J. 2005a. Localized vs. systemic inflammation in guinea pigs: a role for prostaglandins at distinct points of the fever induction pathways? Am J Physiol Regul Integr Comp Physiol 289(2):R340-R347.

Rummel C, Hübschle T, Gerstberger R, Roth J. 2004. Nuclear translocation of the transcription factor STAT3 in the guinea pig brain during systemic or localised inflammation. J Physiol 557:671-687.

Rummel C, Voss T, Matsumura K, Korte S, Gerstberger R, Roth J, Hübschle T. 2005b. Nuclear STAT3 translocation in guinea pig and rat brain endothelium during systemic challenge with lipopolysaccharide and interleukin-6. J Comp Neurol 491(1):1-14.

Sachot C, Poole S, Luheshi GN. 2004. Circulating leptin mediates lipopolysaccharide-induced anorexia and fever in rats. J Physiol 561(Pt 1):263-272.

Saha S, Engstrom L, Mackerlova L, Jakobsson PJ, Blomqvist A. 2005. Impaired febrile responses to immune challenge in mice deficient in microsomal prostaglandin E synthase-1. Am J Physiol Regul Integr Comp Physiol 288(5):R1100-1107.

Sakata Y, Morimoto A, Long NC, Murakami N. 1991. Fever and acute-phase response induced in rabbits by intravenous and intracerebroventricular injection of interleukin-6. Cytokine 3(3):199-203.

Sako K, Okuma Y, Hosoi T, Nomura Y. 2005. STAT3 activation and c-FOS expression in the brain following peripheral administration of bacterial DNA. J Neuroimmunol 158(1-2):40-49.

Samuelsson B, Morgenstern R, Jakobsson PJ. 2007. Membrane prostaglandin E synthase-1: a novel therapeutic target. Pharmacol Rev 59(3):207-224.

Sanchez J, Oliver P, Pico C, Palou A. 2004. Diurnal rhythms of leptin and ghrelin in the systemic circulation and in the gastric mucosa are related to food intake in rats. Pflugers Arch 448(5):500-506.

Sarraf P, Frederich RC, Turner EM, Ma G, Jaskowiak NT, Rivet DJ, 3rd, Flier JS, Lowell BB, Fraker DL, Alexander HR. 1997. Multiple cytokines and acute inflammation raise mouse leptin levels: potential role in inflammatory anorexia. J Exp Med 185(1):171-175.

Scammell TE, Elmquist JK, Griffin JD, Saper CB. 1996. Ventromedial preoptic prostaglandin E2 activates fever-producing autonomic pathways. J Neurosci 16(19):6246-6254.

Schedlowski M, Pacheco-Lopez G. 2010. The learned immune response: Pavlov and beyond. Brain Behav Immun 24(2):176-185.

Schiltz JC, Sawchenko PE. 2003. Signaling the brain in systemic inflammation: the role of perivascular cells. Front Biosci 8:s1321-1329.

Schmidt J, Welsch T, Jager D, Muhlradt PF, Buchler MW, Marten A. 2007. Intratumoural injection of the toll-like receptor-2/6 agonist 'macrophage-activating lipopeptide-2' in patients with pancreatic carcinoma: a phase I/II trial. Br J Cancer 97(5):598-604.

Schwartz DA, Wohlford-Lenane CL, Quinn TJ, Krieg AM. 1999. Bacterial DNA or oligonucleotides containing unmethylated CpG motifs can minimize lipopolysaccharide-induced inflammation in the lower respiratory tract through an IL-12-dependent pathway. J Immunol 163(1):224-231.

Schwartz GJ. 2002. Neural-immune gut-brain communication in the anorexia of disease. Nutrition 18(6):528-533.

Schwartz GJ, Plata-Salaman CR, Langhans W. 1997. Subdiaphragmatic vagal deafferentation fails to block feeding-suppressive effects of LPS and IL-1 beta in rats. Am J Physiol 273(3 Pt 2):R1193-1198.

Schwartz MW, Seeley RJ, Campfield LA, Burn P, Baskin DG. 1996. Identification of targets of leptin action in rat hypothalamus. J Clin Invest 98(5):1101-1106.

Scott MM, Lachey JL, Sternson SM, Lee CE, Elias CF, Friedman JM, Elmquist JK. 2009. Leptin targets in the mouse brain. J Comp Neurol 514(5):518-532.

Seeley RJ, Drazen DL, Clegg DJ. 2004. The critical role of the melanocortin system in the control of energy balance. Annu Rev Nutr 24:133-149.

Sehic E, Blatteis CM. 1996. Blockade of lipopolysaccharide-induced fever by subdiaphragmatic vagotomy in guinea pigs. Brain Res 726(1-2):160-166.

Serrats J, Schiltz JC, Garcia-Bueno B, van Rooijen N, Reyes TM, Sawchenko PE. 2010. Dual roles for perivascular macrophages in immune-to-brain signaling. Neuron 65(1):94-106.

Sessler DI. 1993. Perianesthetic thermoregulation and heat balance in humans. Faseb J 7(8):638-644.

Shaftel SS, Carlson TJ, Olschowka JA, Kyrkanides S, Matousek SB, O'Banion MK. 2007. Chronic interleukin-1beta expression in mouse brain leads to leukocyte infiltration and neutrophil-independent blood brain barrier permeability without overt neurodegeneration. J Neurosci 27(35):9301-9309.

Shao DZ, Lee JJ, Huang WT, Liao JF, Lin MT. 2004. Inhibition of nuclear factor-kappa B prevents staphylococcal enterotoxin A-induced fever. Mol Cell Biochem 262(1-2):177-185.

Shechter R, London A, Varol C, Raposo C, Cusimano M, Yovel G, Rolls A, Mack M, Pluchino S, Martino G, Jung S, Schwartz M. 2009. Infiltrating blood-derived macrophages are vital cells playing an anti-inflammatory role in recovery from spinal cord injury in mice. PLoS Med 6(7):e1000113.

Shoenfelt JL, Fenton MJ. 2006. TLR2- and TLR4-dependent activation of STAT1 serine phosphorylation in murine macrophages is protein kinase C-delta-independent. J Endotoxin Res 12(4):231-240.

Simard AR, Rivest S. 2006. Neuroprotective properties of the innate immune system and bone marrow stem cells in Alzheimer's disease. Mol Psychiatry 11(4):327-335.

Skibicka KP, Grill HJ. 2009. Hindbrain leptin stimulation induces anorexia and hyperthermia mediated by hindbrain melanocortin receptors. Endocrinology 150(4):1705-1711.

Smith BK, Kluger MJ. 1993. Anti-TNF-alpha antibodies normalized body temperature and enhanced food intake in tumor-bearing rats. Am J Physiol 265(3 Pt 2):R615-619.

Smith KD, Andersen-Nissen E, Hayashi F, Strobe K, Bergman MA, Barrett SL, Cookson BT, Aderem A. 2003. Toll-like receptor 5 recognizes a conserved site on flagellin required for protofilament formation and bacterial motility. Nat Immunol 4(12):1247-1253.

Soares DM, Figueiredo MJ, Martins JM, Machado RR, Sorgi C, Faciolli LH, Alves-Filho JC, Cunha FQ, Souza GE. 2012. A crucial role for IL-6 in the CNS of rats during fever induced by the injection of live E. coli. Med Microbiol Immunol 201(1):47-60.

Soares DM, Machado RR, Yamashiro LH, Melo MC, Souza GE. 2008. Cytokine-induced neutrophil chemoattractant (CINC)-1 induces fever by a prostaglandin-dependent mechanism in rats. Brain Res 1233:79-88.

Sobota R, Szwed M, Kasza A, Bugno M, Kordula T. 2000. Parthenolide inhibits activation of signal transducers and activators of transcription (STATs) induced by cytokines of the IL-6 family. Biochem Biophys Res Commun 267(1):329-333.

Sonti G, Ilyin SE, Plata-Salaman CR. 1996. Anorexia induced by cytokine interactions at pathophysiological concentrations. Am J Physiol 270(6 Pt 2):R1394-1402.

Sorabji R. 1974. Body and Soul in Aristotle. Philosophy 49:63-89

Spencer SJ, Mouihate A, Galic MA, Ellis SL, Pittman QJ. 2007a. Neonatal immune challenge does not affect body weight regulation in rats. Am J Physiol Regul Integr Comp Physiol.

Spencer SJ, Mouihate A, Pittman QJ. 2007b. Peripheral inflammation exacerbates damage after global ischemia independently of temperature and acute brain inflammation. Stroke 38(5):1570-1577.

Steiner AA, Chakravarty S, Robbins JR, Dragic AS, Pan J, Herkenham M, Romanovsky AA. 2005a. Thermoregulatory responses of rats to conventional preparations of lipopolysaccharide are caused by lipopolysaccharide per se-- not by lipoprotein contaminants. Am J Physiol Regul Integr Comp Physiol 289(2):R348-R352.

Steiner AA, Chakravarty S, Rudaya AY, Herkenham M, Romanovsky AA. 2006a. Bacterial lipopolysaccharide fever is initiated via Toll-like receptor 4 on hematopoietic cells. Blood 107(10):4000-4002.

Steiner AA, Hunter JC, Phipps SM, Nucci TB, Oliveira DL, Roberts JL, Scheck AC, Simmons DL, Romanovsky AA. 2009. Cyclooxygenase-1 or -2--which one mediates lipopolysaccharide-induced hypothermia? Am J Physiol Regul Integr Comp Physiol 297(2):R485-494.

Steiner AA, Ivanov AI, Serrats J, Hosokawa H, Phayre AN, Robbins JR, Roberts JL, Kobayashi S, Matsumura K, Sawchenko PE, Romanovsky AA. 2006b. Cellular and molecular bases of the initiation of fever. PLoS Biol 4(9):e284.

Steiner AA, Li S, Llanos QJ, Blatteis CM. 2001. Differential inhibition by nimesulide of the early and late phases of intravenous- and intracerebroventricular-LPS-induced fever in guinea pigs. Neuroimmunomodulation 9(5):263-275.

Steiner AA, Rudaya AY, Robbins JR, Dragic AS, Langenbach R, Romanovsky AA. 2005b. Expanding the febrigenic role of cyclooxygenase-2 to the previously overlooked responses. Am J Physiol Regul Integr Comp Physiol 289(5):R1253-1257.

Steinhoff M, Vergnolle N, Young SH, Tognetto M, Amadesi S, Ennes HS, Trevisani M, Hollenberg MD, Wallace JL, Caughey GH, Mitchell SE, Williams LM, Geppetti P, Mayer EA, Bunnett NW. 2000. Agonists of proteinase-activated receptor 2 induce inflammation by a neurogenic mechanism. Nat Med 6(2):151-158.

Steinman L. 2004a. Elaborate interactions between the immune and nervous systems. Nat Immunol 5(6):575-581.

Steinman L. 2004b. Immune therapy for autoimmune diseases. Science 305(5681):212-216.

Stepanyan Z, Kocharyan A, Pyrski M, Hubschle T, Watson AM, Schulz S, Meyerhof W. 2003. Leptin-target neurones of the rat hypothalamus express somatostatin receptors. J Neuroendocrinol 15(9):822-830.

Stephanou A, Okosi A, Knight RA, Chowdrey HS, Latchman DS. 1997. C/EBP activates the human corticotropin-releasing hormone gene promoter. Mol Cell Endocrinol 134(1):41-50.

Sternberg EM. 2006. Neural regulation of innate immunity: a coordinated nonspecific host response to pathogens. Nat Rev Immunol 6(4):318-328.

Sterneck E, Johnson PF. 1998. CCAAT/enhancer binding protein beta is a neuronal transcriptional regulator activated by nerve growth factor receptor signaling. J Neurochem 70(6):2424-2433.

Stevens SL, Ciesielski TM, Marsh BJ, Yang T, Homen DS, Boule JL, Lessov NS, Simon RP, Stenzel-Poore MP. 2008. Toll-like receptor 9: a new target of ischemic preconditioning in the brain. J Cereb Blood Flow Metab 28(5):1040-1047.

Stowe RP, Peek MK, Cutchin MP, Goodwin JS. 2010. Plasma cytokine levels in a population-based study: relation to age and ethnicity. J Gerontol A Biol Sci Med Sci 65(4):429-433.

Straccia M, Gresa-Arribas N, Dentesano G, Ejarque-Ortiz A, Tusell JM, Serratosa J, Sola C, Saura J. 2011. Pro-inflammatory gene expression and neurotoxic effects of activated microglia are attenuated by absence of CCAAT/enhancer binding protein beta. J Neuroinflammation 8:156.

Straub RH. 2004. Complexity of the bi-directional neuroimmune junction in the spleen. Trends Pharmacol Sci 25(12):640-646.

Sun W, Choi SH, Park SK, Kim SJ, Noh MR, Kim EH, Kim HJ, Kim H. 2007. Identification and characterization of novel activity-dependent transcription factors in rat cortical neurons. J Neurochem 100(1):269-278.

Takahashi Y, Smith P, Ferguson A, Pittman QJ. 1997. Circumventricular organs and fever. Am J Physiol 273(5 Pt 2):R1690-1695.

Takeda K, Akira S. 2005. Toll-like receptors in innate immunity. Int Immunol 17(1):1-14.

Takeda K, Noguchi K, Shi W, Tanaka T, Matsumoto M, Yoshida N, Kishimoto T, Akira S. 1997. Targeted disruption of the mouse Stat3 gene leads to early embryonic lethality. Proc Natl Acad Sci U S A 94(8):3801-3804.

Tanaka N, Hoshino Y, Gold J, Hoshino S, Martiniuk F, Kurata T, Pine R, Levy D, Rom WN, Weiden M. 2005. Interleukin-10 induces inhibitory C/EBPbeta through STAT-3 and represses HIV-1 transcription in macrophages. Am J Respir Cell Mol Biol 33(4):406-411.

Tanaka T, Kishimoto T. 2012. Immunotherapeutic implication of IL-6 blockade. Immunotherapy 4(1):87-105.

Tartaglia LA. 1997. The leptin receptor. J Biol Chem 272(10):6093-6096.

Tartaglia LA, Dembski M, Weng X, Deng N, Culpepper J, Devos R, Richards GJ, Campfield LA, Clark FT, Deeds J, et al. 1995. Identification and expression cloning of a leptin receptor, OB-R. Cell 83(7):1263-1271.

Tasaki K, Ruetzler CA, Ohtsuki T, Martin D, Nawashiro H, Hallenbeck JM. 1997. Lipopolysaccharide pre-treatment induces resistance against subsequent focal cerebral ischemic damage in spontaneously hypertensive rats. Brain Res 748(1-2):267-270.

Tassorelli C, Greco R, Morazzoni P, Riva A, Sandrini G, Nappi G. 2005. Parthenolide is the component of tanacetum parthenium that inhibits nitroglycerin-induced Fos activation: studies in an animal model of migraine. Cephalalgia 25(8):612-621.

Taubenfeld SM, Milekic MH, Monti B, Alberini CM. 2001. The consolidation of new but not reactivated memory requires hippocampal C/EBPbeta. Nat Neurosci 4(8):813-818.

Thaler JP, Yi CX, Schur EA, Guyenet SJ, Hwang BH, Dietrich MO, Zhao X, Sarruf DA, Izgur V, Maravilla KR, Nguyen HT, Fischer JD, Matsen ME, Wisse BE, Morton GJ, Horvath TL, Baskin DG, Tschop MH, Schwartz MW. 2012. Obesity is associated with hypothalamic injury in rodents and humans. J Clin Invest 122(1):153-162.

Thayer JF, Sternberg EM. 2010. Neural aspects of immunomodulation: focus on the vagus nerve. Brain Behav Immun 24(8):1223-1228.

Thibeault I, Laflamme N, Rivest S. 2001. Regulation of the gene encoding the monocyte chemoattractant protein 1 (MCP-1) in the mouse and rat brain in response to circulating LPS and proinflammatory cytokines. J Comp Neurol 434(4):461-477.

Thorpe R. 2002. Chemokine/chemokine receptor nomenclature. J Immunol Methods 262(1-2):1-3.

Tracey KJ. 2007. Physiology and immunology of the cholinergic antiinflammatory pathway. J Clin Invest 117(2):289-296.

Tracey KJ, Wei H, Manogue KR, Fong Y, Hesse DG, Nguyen HT, Kuo GC, Beutler B, Cotran RS, Cerami A, et al. 1988. Cachectin/tumor necrosis factor induces cachexia, anemia, and inflammation. J Exp Med 167(3):1211-1227.

Trayhurn P. 2005. The biology of obesity. Proc Nutr Soc 64(1):31-38.

Trayhurn P, Wood IS. 2004. Adipokines: inflammation and the pleiotropic role of white adipose tissue. Br J Nutr 92(3):347-355.

Traynor TR, Majde JA, Bohnet SG, Krueger JM. 2004. Intratracheal double-stranded RNA plus interferon-gamma: a model for analysis of the acute phase response to respiratory viral infections. Life Sci 74(20):2563-2576.

Tsao N, Hsu HP, Wu CM, Liu CC, Lei HY. 2001. Tumour necrosis factor-alpha causes an increase in blood-brain barrier permeability during sepsis. J Med Microbiol 50(9):812-821.

Tschöp J, Nogueiras R, Haas-Lockie S, Kasten KR, Castaneda TR, Huber N, Guanciale K, Perez-Tilve D, Habegger K, Ottaway N, Woods SC, Oldfield B, Clarke I, Chua S, Jr., Farooqi IS, O'Rahilly S, Caldwell CC, Tschop MH. 2010. CNS leptin action modulates immune response and survival in sepsis. J Neurosci 30(17):6036-6047.

Turek VF, Trevaskis JL, Levin BE, Dunn-Meynell AA, Irani B, Gu G, Wittmer C, Griffin PS, Vu C, Parkes DG, Roth JD. 2010. Mechanisms of amylin/leptin synergy in rodent models. Endocrinology 151(1):143-152.

Turnbull AV, Prehar S, Kennedy AR, Little RA, Hopkins SJ. 2003. Interleukin-6 is an afferent signal to the hypothalamo-pituitary-adrenal axis during local inflammation in mice. Endocrinology 144(5):1894-1906.

Uematsu S, Matsumoto M, Takeda K, Akira S. 2002. Lipopolysaccharide-dependent prostaglandin E(2) production is regulated by the glutathione-dependent prostaglandin E(2) synthase gene induced by the Toll-like receptor 4/MyD88/NF-IL6 pathway. J Immunol 168(11):5811-5816.

Uotani S, Bjorbaek C, Tornoe J, Flier JS. 1999. Functional properties of leptin receptor isoforms: internalization and degradation of leptin and ligand-induced receptor downregulation. Diabetes 48(2):279-286.

Utagawa A, Truettner JS, Dietrich WD, Bramlett HM. 2008. Systemic inflammation exacerbates behavioral and histopathological consequences of isolated traumatic brain injury in rats. Exp Neurol 211(1):283-291.

Valente T, Mancera P, Tusell JM, Serratosa J, Saura J. 2011. C/EBPbeta expression in activated microglia in amyotrophic lateral sclerosis. Neurobiol Aging.

Vallières L, Rivest S. 1997. Regulation of the genes encoding interleukin-6, its receptor, and gp130 in the rat brain in response to the immune activator lipopolysaccharide and the proinflammatory cytokine interleukin-1beta. J Neurochem 69(4):1668-1683.

Vallières L, Rivest S. 1999. Interleukin-6 is a needed proinflammatory cytokine in the prolonged neural activity and transcriptional activation of corticotropin-releasing factor during endotoxemia. Endocrinology 140(9):3890-3903.

van Enckevort FH, Sweep CG, Span PN, Demacker PN, Hermsen CC, Hermus AR. 2001. Reduced adrenal response to bacterial lipopolysaccharide in interleukin-6-deficient mice. J Endocrinol Invest 24(10):786-795.

Villaran RF, Espinosa-Oliva AM, Sarmiento M, De Pablos RM, Arguelles S, Delgado-Cortes MJ, Sobrino V, Van Rooijen N, Venero JL, Herrera AJ, Cano J, Machado A. 2010. Ulcerative colitis exacerbates lipopolysaccharide-induced damage to the nigral dopaminergic system: potential risk factor in Parkinson`s disease. J Neurochem 114(6):1687-1700.

Vina J, Gomez-Cabrera MC, Borras C, Froio T, Sanchis-Gomar F, Martinez-Bello VE, Pallardo FV. 2009. Mitochondrial biogenesis in exercise and in ageing. Adv Drug Deliv Rev 61(14):1369-1374.

Wallenius V, Wallenius K, Ahren B, Rudling M, Carlsten H, Dickson SL, Ohlsson C, Jansson JO. 2002. Interleukin-6-deficient mice develop mature-onset obesity. Nat Med 8(1):75-79.

Walters JN, Bickford JS, Newsom KJ, Beachy DE, Barilovits SJ, Herlihy JD, Nick HS. 2012. Regulation of human microsomal prostaglandin E synthase-1 by IL-1beta requires a distal enhancer element with a unique role for C/EBPbeta. Biochem J 443(2):561-571.

Wang H, Yu M, Ochani M, Amella CA, Tanovic M, Susarla S, Li JH, Yang H, Ulloa L, Al-Abed Y, Czura CJ, Tracey KJ. 2003. Nicotinic acetylcholine receptor alpha7 subunit is an essential regulator of inflammation. Nature 421(6921):384-388.

Wang J, Ando T, Dunn AJ. 1997a. Effect of homologous interleukin-1, interleukin-6 and tumor necrosis factor-alpha on the core body temperature of mice. Neuroimmunomodulation 4(5-6):230-236.

Wang MY, Zhou YT, Newgard CB, Unger RH. 1996. A novel leptin receptor isoform in rat. FEBS Lett 392(2):87-90.

Wang Y, Beydoun MA. 2007. The Obesity Epidemic in the United States--Gender, Age, Socioeconomic, Racial/Ethnic, and Geographic Characteristics: A Systematic Review and Meta-Regression Analysis. Epidemiol Rev.

Wang YH, Tache Y, Sheibel AB, Go VL, Wei JY. 1997b. Two types of leptin-responsive gastric vagal afferent terminals: an in vitro single-unit study in rats. Am J Physiol 273(2 Pt 2):R833-837.

Watkins LR, Wiertelak EP, Goehler LE, Mooney-Heiberger K, Martinez J, Furness L, Smith KP, Maier SF. 1994a. Neurocircuitry of illness-induced hyperalgesia. Brain Res 639(2):283-299.

Watkins LR, Wiertelak EP, Goehler LE, Smith KP, Martin D, Maier SF. 1994b. Characterization of cytokine-induced hyperalgesia. Brain Res 654(1):15-26.

Wisse BE, Ogimoto K, Morton GJ, Wilkinson CW, Frayo RS, Cummings DE, Schwartz MW. 2004. Physiological regulation of hypothalamic IL-1beta gene expression by leptin and glucocorticoids: implications for energy homeostasis. Am J Physiol Endocrinol Metab 287(6):E1107-1113.

Wisse BE, Ogimoto K, Tang J, Harris MK, Jr., Raines EW, Schwartz MW. 2007. Evidence that lipopolysaccharide-induced anorexia depends upon central, rather than peripheral, inflammatory signals. Endocrinology 148(11):5230-5237.

Wolburg H, Wolburg-Buchholz K, Engelhardt B. 2005. Diapedesis of mononuclear cells across cerebral venules during experimental autoimmune encephalomyelitis leaves tight junctions intact. Acta Neuropathol 109(2):181-190.

Wrona D. 2006. Neural-immune interactions: an integrative view of the bidirectional relationship between the brain and immune systems. J Neuroimmunol 172(1-2):38-58.

Wuchert F, Ott D, Murgott J, Rafalzik S, Hitzel N, Roth J, Gerstberger R. 2008. Rat area postrema microglial cells act as sensors for the toll-like receptor-4 agonist lipopolysaccharide. J Neuroimmunol 204(1-2):66-74.

Wuchert F, Ott D, Rafalzik S, Roth J, Gerstberger R. 2009. Tumor necrosis factor-alpha, interleukin-1beta and nitric oxide induce calcium transients in distinct populations of cells cultured from the rat area postrema. J Neuroimmunol 206(1-2):44-51.

Wung BS, Hsu MC, Wu CC, Hsieh CW. 2005. Resveratrol suppresses IL-6-induced ICAM-1 gene expression in endothelial cells: effects on the inhibition of STAT3 phosphorylation. Life Sci 78(4):389-397.

Xing Z, Gauldie J, Cox G, Baumann H, Jordana M, Lei XF, Achong MK. 1998. IL-6 is an antiinflammatory cytokine required for controlling local or systemic acute inflammatory responses. J Clin Invest 101(2):311-320.

Yamagata K, Matsumura K, Inoue W, Shiraki T, Suzuki K, Yasuda S, Sugiura H, Cao C, Watanabe Y, Kobayashi S. 2001. Coexpression of microsomal-type prostaglandin E synthase with cyclooxygenase-2 in brain endothelial cells of rats during endotoxin-induced fever. J Neurosci 21(8):2669-2677.

Yamamoto M, Uematsu S, Okamoto T, Matsuura Y, Sato S, Kumar H, Satoh T, Saitoh T, Takeda K, Ishii KJ, Takeuchi O, Kawai T, Akira S. 2007. Enhanced TLR-mediated NF-IL6 dependent gene expression by Trib1 deficiency. J Exp Med 204(9):2233-2239.

Yamamoto S, Morimoto I, Kai K, Arao T, Fujihira T, Morita E, Kannan H, Eto S. 1999. Centrally administered murine leptin stimulates plasma arginine-vasopressin secretion and increases the level of mRNA expression in the supraoptic nucleus of conscious rats. Neuroendocrinology 70(3):207-212.

Yamawaki Y, Kimura H, Hosoi T, Ozawa K. 2010. MyD88 plays a key role in LPS-induced Stat3 activation in the hypothalamus. Am J Physiol Regul Integr Comp Physiol 298(2):R403-410.

Yang XP, Schaper F, Teubner A, Lammert F, Heinrich PC, Matern S, Siewert E. 2005. Interleukin-6 plays a crucial role in the hepatic expression of SOCS3 during acute inflammatory processes in vivo. J Hepatol 43(4):704-710.

Yi JH, Park SW, Kapadia R, Vemuganti R. 2007. Role of transcription factors in mediating post-ischemic cerebral inflammation and brain damage. Neurochem Int 50(7-8):1014-1027.

Yirmiya R, Weidenfeld J, Pollak Y, Morag M, Morag A, Avitsur R, Barak O, Reichenberg A, Cohen E, Shavit Y, Ovadia H. 1999. Cytokines, "depression due to a general medical condition," and antidepressant drugs. Adv Exp Med Biol 461:283-316.

Yoshida K, Li X, Cano G, Lazarus M, Saper CB. 2009. Parallel preoptic pathways for thermoregulation. J Neurosci 29(38):11954-11964.

Yoshida Y, Kumar A, Koyama Y, Peng H, Arman A, Boch JA, Auron PE. 2004. Interleukin 1 activates STAT3/nuclear factor-kappaB cross-talk via a unique TRAF6- and p65-dependent mechanism. J Biol Chem 279(3):1768-1776.

Yuan G, Wahlqvist ML, He G, Yang M, Li D. 2006. Natural products and anti-inflammatory activity. Asia Pac J Clin Nutr 15(2):143-152.

Zeisberger E. 1999. From humoral fever to neuroimmunological control of fever. Journal of Thermal Biology 24:287-326.

Zeisberger E, Roth J. 1998. Tolerance to pyrogens. Ann N Y Acad Sci 856:116-131.

Zhang H, Ching S, Chen Q, Li Q, An Y, Quan N. 2008. Localized inflammation in peripheral tissue signals the CNS for sickness response in the absence of interleukin-1 and cyclooxygenase-2 in the blood and brain. Neuroscience 157(4):895-907.

Zhang Y, Proenca R, Maffei M, Barone M, Leopold L, Friedman JM. 1994. Positional cloning of the mouse obese gene and its human homologue. Nature 372(6505):425-432.

Zhang YH, Lu J, Elmquist JK, Saper CB. 2003. Specific roles of cyclooxygenase-1 and cyclooxygenase-2 in lipopolysaccharide-induced fever and Fos expression in rat brain. J Comp Neurol 463(1):3-12.

VIII. ANHANG

1. Publikationen

1.1. Begutachtete Veröffentlichungen:

- 1) Damm J., Wiegand F., Harden LM., Gerstberger R., **Rummel C.** and Roth J. (***2012***) Fever, sickness behavior and expression of inflammatory genes in the hypothalamus after systemic and localized subcutaneous stimulation of rats with the TLR 7 agonist imiquimod. *Neuroscience*, 201:166-83. Impakt Faktor: 3, 215

- 2) Welsch J., Hübschle T., Murgott J., Kirschning C., **Rummel C.**, Gerstberger R. and Roth J. (***2012***) Fever induction by systemic stimulation with macrophage-activating lipopeptide-2 depends upon Toll-like receptor 2 but not CD36. *Innate Immun*, 18:541-559. Impakt Faktor: 3,283

- 3) **Rummel C.**, Gerstberger R., Roth J. and Hübschle T. (***2011***) Parthenolide attenuates LPS-induced fever, circulating cytokines and markers of brain inflammation in rats. *Cytokine*, 56:739-748. Impakt Faktor: 3,537

- 4) **Rummel C.**, Matsumura K. and Luheshi GN. (***2011***) Circulating IL-6 contributes to peripheral LPS-induced mPGES-1 expression in the rat brain. *Brain Res Bull*, 86:319–325. Impakt Faktor: 2,498

- 5) Damm J., Luheshi GN., Gerstberger R., Roth J. and **Rummel C.** (***2011***) Spatiotemporal nuclear factor interleukin 6 expression in the rat brain during LPS-induced fever is linked to sustained hypothalamic inflammatory target gene induction. *J Comp Neurol* 519:480-505. Impakt Faktor: 3,774

- 6) Knorr C., Marks D., Gerstberger R., Mühlradt PF., Roth J. and **Rummel C.** (***2010***) Peripheral and central cyclooxygenase (COX) products may contribute to the manifestation of brain controlled sickness responses during localized inflammation induced by macrophage-activating lipopeptide-2 (MALP-2). *Neurosci Lett* 479:107-111. Impakt Faktor: 2,055

- 7) **Rummel C.**, Inoue W., Poole S. and Luheshi GN. (***2010***) Leptin regulates neutrophil recruitment into the brain following severe systemic LPS-induced inflammation. *Mol Psychiatry* 15:523-534. Impakt Faktor: 15,470
- 8) Roth J., **Rummel C.**, Barth SW., Gerstberger R. and Hübschle T. (***2009***) Molecular aspects of fever and hyperthermia. *Immunol Allergy Clin* 29:229-245. Impakt Faktor: 2,959
- 9) **Rummel C.**, Sachot C., Inoue W., Hübschle T., Poole S. and Luheshi GN. (***2008***) Selective contribution of interleukin-6 and leptin to brain inflammatory signals induced by systemic LPS injection in mice. *J Comp Neurol* 511:373-395. Impakt Faktor: 3,774
- 10) Luheshi GN. and **Rummel C.** (***2007***) Is programming of weight regulation immune to neonatal inflammation? *Am J Physiol* 293:R578-R580. Impakt Faktor: 3,284
- 11) Sachot C., **Rummel C.**, Bristow AF. and Luheshi GN. (***2007***) The role of the vagus nerve in mediating the long-term anorectic effects of leptin. *J Neuroendocrinol* 19:250-261. Impakt Faktor: 4,65
- 12) Voss T., Barth SW., **Rummel C.**, Gerstberger R., Hübschle T. and Roth J. (***2007***) STAT3 and COX-2 activation in the guinea-pig brain during fever induced by the Toll-like receptor-3 agonist polyinosinic:polycytidylic acid. *Cell Tissue Res* 328:549-561. Impakt Faktor: 2,804
- 13) Roth J., **Rummel C.**, Barth SW., Gerstberger R. and Hübschle T. (***2006***) Molecular aspects of fever and hyperthermia. *Neurol Clin* 24:421-439, v. Impakt Faktor: 2,533
- 14) **Rummel C.**, Sachot C., Poole S. and Luheshi GN. (***2006***) Circulating interleukin-6 induces fever through a STAT3-linked activation of COX-2 in the brain. *Am J Physiol* 291:R1316-R1326. Impakt Faktor: 3,284

- 15) Voss T., **Rummel C.**, Gerstberger R., Hübschle T. and Roth J. (***2006***) Fever and circulating cytokines induced by double-stranded RNA in guinea pigs: dependence on the route of administration and effects of repeated injections. *Acta Physiol (Oxf)* 187:379-389. Impakt Faktor: 3,138

- 16) **Rummel C.**, Voss T., Matsumura K., Korte S., Gerstberger R., Roth J. and Hübschle T. (***2005***) Nuclear STAT3 translocation in guinea pig and rat brain endothelium during systemic challenge with lipopolysaccharide and interleukin-6. *J Comp Neurol* 491:1-14. Impakt Faktor: 3,774

- 17) **Rummel C.**, Barth S., Voss T., Korte S., Gerstberger R. Hübschle T. and Roth J. (***2005***) Systemic versus localized inflammation: a role for prostaglandins at distinct points of the fever-induction pathways? *Am J Physiol* 289:R340-R347. Impakt Faktor: 3,284

- 18) **Rummel C.**, Hübschle T., Gerstberger R. and Roth J. (***2004***) Nuclear translocation of the transcription factor STAT3 in the guinea pig brain during systemic or localized inflammation. *J Physiol* 557:671-687. Impakt Faktor: 5,139

- 19) Roth J., Harré E. M., **Rummel C.**, Gerstberger R. and Hübschle T. (***2004***) Signaling the brain in systemic inflammation: role of sensory circumventricular organs. *Front Biosci* 9:290-300. Impakt Faktor: 4,048

- 20) Roth J., **Rummel C.**, Harré E. M., Voss T., Mütze J., Gerstberger R. and Hübschle T. (***2004***) Is interleukin-6 the necessary pyrogenic cytokine? *J Therm Biol* 29:383-389. Impakt Faktor: 1,273

1.2. Nicht begutachtete Veröffentlichungen:

- 21) Fuchs F., Damm J., Gerstberger R., Roth J. and **Rummel C.** (***2012***) The inflammatory transcription factor NF-IL6 is linked to the activation of the hypothalamic-pituitary-adrenal stress axis in rats. *Brain Behav Immun* in press

- 22) Koenig S., Wenz T., Luheshi GN., Gerstberger R., Roth J. and **Rummel C.** (***2012***) Age dependant effects of the PPAR-y agonist rosiglitazone on the brain and periphery during systemic LPS-induced inflammation in rats. *Brain Behav Immun* in press

- 23) **Rummel C.**, Gerstberger R., Roth J. and Hübschle T. (***2011***) Systemic parthenolide treatment attenuates LPS-induced fever, circulating cytokines and markers of brain inflammation in rats. *Brain Behav Immun* 25 (Suppl. 1): s191-s192.

- 24) Damm J., Harden L., Gerstberger R., Roth J. and **Rummel C.** (***2011***) The putative JAK-STAT inhibitor AG490 exacerbates LPS-fever, reduces sickness behavior, and alters the expression of pro- and antiinflammatory genes in the rat brain. *Brain Behav Immun* 25 (Suppl. 1): s183-s184.

- 25) **Rummel C.**, Inoue W., Poole S. and Luheshi GN. (***2010***) Leptin and immune-to-brain communication: its role in leukocyte recruitment into the brain during systemic LPS-induced inflammation. *Brain Behav Immun* 24 (Suppl. 1): s1.

- 26) Damm J., Gerstberger R., Roth J., Luheshi GN. and **Rummel C.** (***2010***) Nuclear factor interleukin 6 is a new delayed early cell activation marker in the rat brain during the time course of LPS-induced systemic inflammation. *Brain Behav Immun* 24 (Suppl. 1): s5.

- 27) **Rummel C.**, Hübschle T., Gerstberger R., and Roth J. (***2010***) Parthenolide attenuates LPS-induced fever and circulating cytokines in rats. 19. *Tagung der DVG-Fachgruppe Physiologie und Biochemie*: p94.

- 28) Wiegand F., Damm J., Gerstberger R., **Rummel C.** and Roth J. (***2010***) The Toll-like receptor (TLR)-7 agonist imiquimod induces a localized subcutaneous inflammatory response in rats. *19. Tagung der DVG-Fachgruppe Physiologie und Biochemie*: p85.

- 29) Damm J., Luheshi GN., Gerstberger R, Roth J. and **Rummel C.** (***2010***) Neuroanatomical distribution of nuclear NF-IL6 immunoreactivity in the rat brain during the time course of systemic inflammation. *19. Tagung der DVG-Fachgruppe Physiologie und Biochemie*: p84.

- 30) Knorr C., Marks D., Gerstberger R., Mühlradt P., Roth J. and **Rummel C.** (***2010***) Peripheral and central cyclooxygenase (COX) products in the manifestation of brain-controlled sickness responses during localized inflammation induced by macrophage-activating lipopeptide-2 (MALP-2). *19. Tagung der DVG-Fachgruppe Physiologie und Biochemie*: p83.

- 31) **Rummel C.**, Inoue W., Poole S. and Luheshi GN. (***2010***) The recruitment of neutrophil granulocytes into the mouse brain during LPS-induced systemic inflammation is regulated by leptin. *19. Tagung der DVG-Fachgruppe Physiologie und Biochemie*: p22.

- 32) **Rummel C.**, Inoue W., Poole S. and Luheshi GN. (***2009***) Leptin modulates neuroinflammation and neutrophil recruitment into the brain of mice during severe LPS-induced systemic inflammation. *Acta Physiologica* 195 (Suppl. 669): s33.

- 33) Damm J., Luheshi GN., Gerstberger R, Roth J. and **Rummel C.** (***2009***) Spatiotemporal activation of the transcription factor NF-IL6 in the rat brain during systemic inflammation. *Acta Physiologica* 195 (Suppl. 669): s16.

- 34) **Rummel C.**, Sachot C., Inoue W., Poole S. and Luheshi GN. (***2007***) IL-6 and leptin differentially activate STAT3 and the COX2-mPGES-pathway in the brain during LPS-induced systemic inflammation in mice. *Can J Neurol Sci* 34 (Suppl. 3): s106.

- 35) Voss T., **Rummel C.**, Gerstberger R., Hübschle T. and Roth J. (***2005***) Fever and cytokine responses to single or repeated injections of double stranded RNA in guinea pigs. *Pflügers Arch – Eur J Physiol* 459 (Suppl.): s91.

- 36) **Rummel C.**, Barth S., Gerstberger R., Hübschle T. and Roth J. (***2005***) The role of prostaglandins in the induction of fever during localized as opposed to systemic inflammation. *Pflügers Arch – Eur J Physiol* 449 (Suppl.): s92.

- 37) **Rummel C.**, Hübschle T., Gerstberger R. and Roth J. (***2003***) Genomic activation of cellular elements within the brain during systemic or localized inflammation in guinea pigs. *Pflügers Arch – Eur J Physiol* 445 (Suppl.): s54.

- 38) **Rummel C.**, Gerstberger R., Roth J. and Hübschle T. (***2003***) Interleukin-6-induced genomic activation during systemic or localized inflammation in guinea pigs investigated with STAT3-immunohistochemistry. *Brain Behav Immun* 17 (Suppl.): s200.

1.3. Buchkapitel

- 39) **Rummel C.** (***2004***). Lyme-Borreliose - die häufigste durch Zecken übertragene Infektionskrankheit in der USA und Europa. In: Milzbrand, Pest, Pocken; Bedrohung durch alte und neue Krankheitserreger. pp. 19-38, *VVB Laufersweiler Verlag*, Wettenberg.

1.4. Doktorarbeit

- **Rummel C.** (***2005***). Charakterisierung der Bedeutung von Interleukin-6 und Prostaglandinen bei der Fieberentstehung nach systemischer oder lokaler Stimulation mit bakteriellem Lipopolysaccharid bei Meerschweinchen. In veterinarian Faculty. pp. 250, Justus-Liebig-Universität, Giessen, *VVB Laufersweiler Verlag*, Wettenberg.

2. Danksagung

Ich möchte mich hiermit herzlich bei allen Mitarbeitern der Veterinärphysiologie und der „Luheshi-family“ bedanken. Vor allem die tolle Atmosphäre und das konstruktive positive Zusammenarbeiten haben mir viel Freunde bereitet. Dies gilt auch für die außergewöhnlichen drei Jahre in Montreal in einem internationalen jungen Labor in dem wie in einer Familie Rückhalt und sehr lehrreicher wissenschaftlicher Austausch geboten wurde; merci mille fois Christelle et Wataru, thanks a million to the „Luheshi Family“ and of cause to my former supervisor and Kollaboration partner for ongoing projects Dr. Giamal Lusheshi.

Herrn Prof. Dr. Rüdiger Gerstberger danke ich für seine unermüdliche persönliche Unterstützung bei allen Fragen zur Lehre und Forschung, die ganz außergewöhnlich ist. Die von Ihm mir gewährten Freiheiten und die freundschaftliche Aufnahme in den Kreis der Physiologen hat mir erst ermöglicht, meine eigene Arbeitsgruppe aufbauen zu können. Mein ebenso immerwährender Dank gilt Prof. Dr. Joachim Roth, der mich auch nach Beendigung meiner Doktorandenzeit in vorbildlichster Weise mit Rat und Tat in produktiver Zusammenarbeit unterstützt hat. Beiden gilt mein Dank für das Vertrauen und ein Arbeitsklima, wie man es sich besser nicht wünschen kann. Weiterhin danke ich PD Dr. Thomas Hübschle für initiale und sehr prägende Unterweisung im neuroanatomischen Arbeiten, die mich seither stets als wichtiger Pfeiler meiner Forschungsarbeiten begleitet hat.

Vielen Dank auch an Doreen Marks, Daniela Ott, Jolanta Murgott und Bärbel Reuter für das Zusammenarbeiten nicht nur in technischen Fragen. Herzlichen Dank an meine erste eigene Doktorandin Jelena Damm, die mit mir Pioneerarbeit geleistet hat, um die kleinen Neuerungen für die Projekte zu etablieren. Großer Dank natürlich an meine Emmy Noether-Gruppe mit Franziska Fuchs, Sandy Koenig, Jenny Schneiders, Jelena Damm und Doreen Marks, die mir in für mich sehr lehrreichen Jahren viel Freude bereitet haben. Darüber hinaus danke ich Frau Pfeiff-Boschek für die Hilfe in allen administrativen Fragen, der Werkstadt

und allen, die sich um den Tierstall kümmern für die sehr gute Zusammenarbeit und allen anderen Mitarbeitern des Instituts, die dazu beigetragen haben, dass die Physiologie weiterhin ein derart angenehmer Arbeitsplatz für mich ist. Im Besonderen hat es mir viel Spaß gemacht mit allen Doktoranden aus den unterschiedlichen Perioden zusammen zu arbeiten. Ich war begeistert, dass ich neben der Arbeit das freitägliche Frühstücken und auch ansonsten so viele gesellige nationale und internationale Veranstaltungen miterleben durfte die durch Lois Harden und Denis Soares mir sehr lieb gewonnene neue Freundschaften geschaffen hat.

Ansonsten möchte ich dem „Rudel“ und meinen anderen Freunden und Bekannten für ihre seelische und ausgleichende Unterstützung danken!

Schließlich wäre das alles nicht möglich gewesen, wenn meine Eltern und meine Schwester nicht immer für mich da gewesen wären. Danke!

3. Erklärung nach §6 der Habilitationsordnung

„Hiermit erkläre ich, dass ich bisher an keiner anderen Stelle ein Habilitationsgesuch eingereicht habe und nicht vor Abschluss des Verfahrens an anderer Stelle ein Habilitationsgesuch einreichen werde."

Rummel

Gießen, den 31.05.2012 Dr. Christoph Rummel

„Ich habe die Habilitationsschrift selbständig und nur mit den Hilfen angefertigt, die ich in der Arbeit angegeben habe. Alle Textstellen, die wörtlich oder sinngemäß aus veröffentlichten oder nicht veröffentlichten Schriften entnommen sind, und alle Angaben, die auf mündlichen Auskünften beruhen, sind als solche kenntlich gemacht. Bei der Erstellung der Habilitationsschrift und bei den von mir durchgeführten und in der Arbeit erwähnten Untersuchungen habe ich die Grundsätze guter wissenschaftlicher Praxis, wie sie in der „Satzung der Justus-Liebig-Universität zur Sicherung guter wissenschaftlicher Praxis" umschrieben sind, eingehalten."

Rummel

Gießen, den 31.05.2012 Dr. Christoph Rummel